Descriptive Uranium Deposit and Mineral System Models

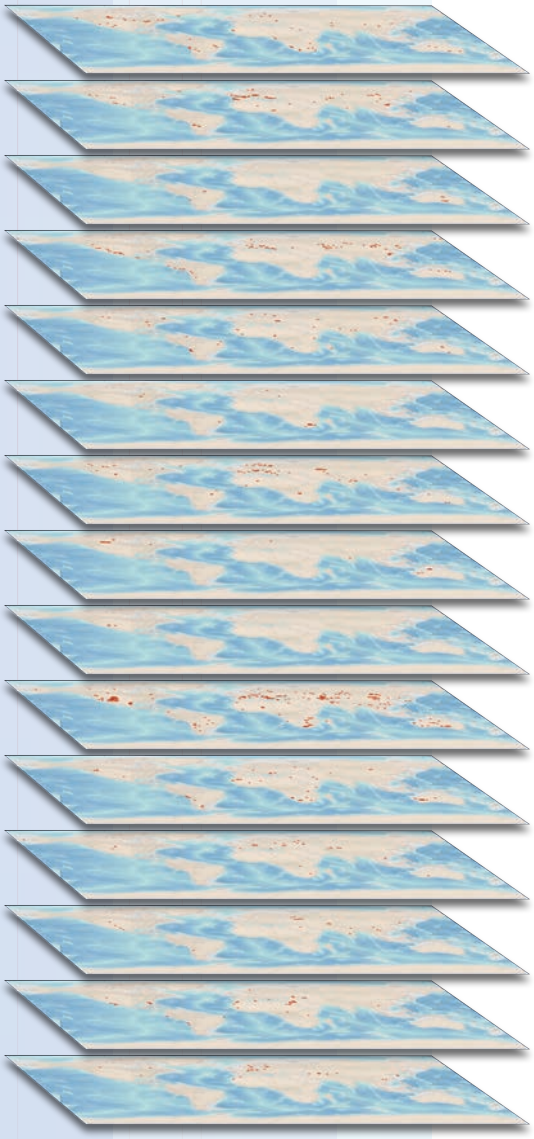

1. INTRUSIVE
2. GRANITE RELATED
3. POLYMETALLIC BRECCIA COMPLEX
4. VOLCANIC RELATED
5. METASOMATITE
6. METAMORPHITE
7. PROTEROZOIC UNCONFORMITY
8. COLLAPSE BRECCIA PIPE
9. SANDSTONE
10. PALEO QUARTZ–PEBBLE CONGLOMERATE
11. SURFICIAL
12. LIGNITE COAL
13. CARBONATE
14. PHOSPHATE
15. BLACK SHALE

IAEA
International Atomic Energy Agency

DESCRIPTIVE URANIUM DEPOSIT AND MINERAL SYSTEM MODELS

The following States are Members of the International Atomic Energy Agency:

AFGHANISTAN
ALBANIA
ALGERIA
ANGOLA
ANTIGUA AND BARBUDA
ARGENTINA
ARMENIA
AUSTRALIA
AUSTRIA
AZERBAIJAN
BAHAMAS
BAHRAIN
BANGLADESH
BARBADOS
BELARUS
BELGIUM
BELIZE
BENIN
BOLIVIA, PLURINATIONAL STATE OF
BOSNIA AND HERZEGOVINA
BOTSWANA
BRAZIL
BRUNEI DARUSSALAM
BULGARIA
BURKINA FASO
BURUNDI
CAMBODIA
CAMEROON
CANADA
CENTRAL AFRICAN REPUBLIC
CHAD
CHILE
CHINA
COLOMBIA
CONGO
COSTA RICA
CÔTE D'IVOIRE
CROATIA
CUBA
CYPRUS
CZECH REPUBLIC
DEMOCRATIC REPUBLIC OF THE CONGO
DENMARK
DJIBOUTI
DOMINICA
DOMINICAN REPUBLIC
ECUADOR
EGYPT
EL SALVADOR
ERITREA
ESTONIA
ESWATINI
ETHIOPIA
FIJI
FINLAND
FRANCE
GABON
GEORGIA
GERMANY
GHANA
GREECE
GRENADA
GUATEMALA
GUYANA
HAITI
HOLY SEE
HONDURAS
HUNGARY
ICELAND
INDIA
INDONESIA
IRAN, ISLAMIC REPUBLIC OF
IRAQ
IRELAND
ISRAEL
ITALY
JAMAICA
JAPAN
JORDAN
KAZAKHSTAN
KENYA
KOREA, REPUBLIC OF
KUWAIT
KYRGYZSTAN
LAO PEOPLE'S DEMOCRATIC REPUBLIC
LATVIA
LEBANON
LESOTHO
LIBERIA
LIBYA
LIECHTENSTEIN
LITHUANIA
LUXEMBOURG
MADAGASCAR
MALAWI
MALAYSIA
MALI
MALTA
MARSHALL ISLANDS
MAURITANIA
MAURITIUS
MEXICO
MONACO
MONGOLIA
MONTENEGRO
MOROCCO
MOZAMBIQUE
MYANMAR
NAMIBIA
NEPAL
NETHERLANDS
NEW ZEALAND
NICARAGUA
NIGER
NIGERIA
NORTH MACEDONIA
NORWAY
OMAN
PAKISTAN
PALAU
PANAMA
PAPUA NEW GUINEA
PARAGUAY
PERU
PHILIPPINES
POLAND
PORTUGAL
QATAR
REPUBLIC OF MOLDOVA
ROMANIA
RUSSIAN FEDERATION
RWANDA
SAINT LUCIA
SAINT VINCENT AND THE GRENADINES
SAN MARINO
SAUDI ARABIA
SENEGAL
SERBIA
SEYCHELLES
SIERRA LEONE
SINGAPORE
SLOVAKIA
SLOVENIA
SOUTH AFRICA
SPAIN
SRI LANKA
SUDAN
SWEDEN
SWITZERLAND
SYRIAN ARAB REPUBLIC
TAJIKISTAN
THAILAND
TOGO
TRINIDAD AND TOBAGO
TUNISIA
TURKEY
TURKMENISTAN
UGANDA
UKRAINE
UNITED ARAB EMIRATES
UNITED KINGDOM OF GREAT BRITAIN AND NORTHERN IRELAND
UNITED REPUBLIC OF TANZANIA
UNITED STATES OF AMERICA
URUGUAY
UZBEKISTAN
VANUATU
VENEZUELA, BOLIVARIAN REPUBLIC OF
VIET NAM
YEMEN
ZAMBIA
ZIMBABWE

The Agency's Statute was approved on 23 October 1956 by the Conference on the Statute of the IAEA held at United Nations Headquarters, New York; it entered into force on 29 July 1957. The Headquarters of the Agency are situated in Vienna. Its principal objective is "to accelerate and enlarge the contribution of atomic energy to peace, health and prosperity throughout the world''.

DESCRIPTIVE URANIUM DEPOSIT AND MINERAL SYSTEM MODELS

INTERNATIONAL ATOMIC ENERGY AGENCY
VIENNA, 2020

COPYRIGHT NOTICE

For further information on this publication, please contact:

Nuclear Fuel Cycle and Materials Section
International Atomic Energy Agency
Vienna International Centre
PO Box 100
1400 Vienna, Austria
Email: Official.Mail@iaea.org

Printed by the IAEA in Austria
May 2020

IAEA Library Cataloguing in Publication Data

Names: International Atomic Energy Agency.
Title: Descriptive uranium deposit and mineral system models / International Atomic Energy Agency.
Description: Vienna : International Atomic Energy Agency, 2020. | Includes bibliographical references.
Identifiers: IAEAL 20-01322 | ISBN 978–92–0–109220–5 (paperback : alk. paper)
ISBN 978–92–0–109320–2 (pdf)
Subjects: LCSH: Ores — Sampling and estimation. | Geology — Statistical methods. | Ore deposits.
Classification: UDC 553.041 | IAEA/DES/MOD

FOREWORD

Quantitative evaluation of mineral resources involves interpolation between and extrapolation from known data points at many different scales, from formalized ore body estimation to continental (or even global) scale assessments. These evaluations of potential mineralization are most robust when supported by a good understanding of the possible geological variations that constrain the calculated information between the known data points, both spatially and numerically.

In the case of resource estimation at the ore deposit scale, a robust geological or structural model, mainly from drilling data, constrains the geostatistical parameters used. In the case of larger scale evaluations of potential mineralization, drilling data are relatively sparse and regional scale information must be used to supplement the information at the local ore deposit scale. Regional scale inputs are often by necessity more conceptual in nature, but nevertheless should be linked with transparent and reproducible statistical data and data processes in order to produce the best possible large scale assessments of potential mineral endowment. Similar to geostatistical estimation of mineral resources at deposit scale, various techniques exist to assess the unsampled potential mineralization between data points at much larger scales. There have been numerous studies of spatial distribution of mineralization potential incorporating mineral potential modelling.

The most established technique used for quantitative aspects of mineral resources is that developed by the United States Geological Survey in the 1970s and since used in many quantitative mineral resource assessments worldwide, although relatively rarely for uranium. The ‘three part method’ of resource assessment generally relies on inputs controlled by good, internally consistent geological models for specific deposit types, comprehensive deposit statistics for grade and tonnage for these deposit types, and a good understanding of the probability of the occurrence of these deposit types in well defined areas or permissive geology (ideally using mineral potential modelling).

The IAEA has developed the necessary parameters for these modelling techniques, which are presented in various publications and databases issued in 2018 and 2019. This publication outlines deposit models that incorporate provinces (developed using a permissive area approach) and grade and tonnage parameters calculated from necessary final input grade tonnage models. The deposit models in the main text are simplified from the annex, available on-line as a separate supplementary file. The information is presented as a compendium of summary descriptive deposit (and broader mineral system) tables that are intended to be used as standalone ‘data sheets’ for each deposit type and deposit subtype. Because deposit subtypes are derivatives of deposit types, there is a necessary degree of repetition between them in order to achieve the desired standalone format. With these, Member States can assess the potential for remaining — or speculative — uranium resources for long term supply beyond identified resources in a consistent and reproducible manner. Because the time from commencement of exploration to discovery and through to development and production of uranium is many decades, and because current identified resources are not necessarily fully exploitable, these speculative resources are an important part of Member States’ long term energy planning strategy.

The IAEA officers responsible for this publication were M. Fairclough and K. Poliakovska of the Division of Nuclear Fuel Cycle and Waste Technology.

EDITORIAL NOTE

This publication has been prepared from the original material as submitted by the contributors and has not been edited by the editorial staff of the IAEA. The views expressed remain the responsibility of the contributors and do not necessarily represent the views of the IAEA or its Member States.

Neither the IAEA nor its Member States assume any responsibility for consequences which may arise from the use of this publication. This publication does not address questions of responsibility, legal or otherwise, for acts or omissions on the part of any person.

The use of particular designations of countries or territories does not imply any judgement by the publisher, the IAEA, as to the legal status of such countries or territories, of their authorities and institutions or of the delimitation of their boundaries.

The mention of names of specific companies or products (whether or not indicated as registered) does not imply any intention to infringe proprietary rights, nor should it be construed as an endorsement or recommendation on the part of the IAEA.

The IAEA has no responsibility for the persistence or accuracy of URLs for external or third party Internet web sites referred to in this publication and does not guarantee that any content on such web sites is, or will remain, accurate or appropriate.

CONTENTS

1. INTRODUCTION

1.1. BACKGROUND

The International Atomic Energy Agency (IAEA) has a long history of developing databases for global uranium deposits, focusing on statistical and spatial information [1-4]. In parallel, the IAEA has been developing uranium deposit models based on detailed geological descriptions as illustrated by [5, 6].

Collectively, the abovementioned databases and models form a basis for assessing the global distribution of uranium deposits and evaluating supply-demand scenarios. However, long term sustainability of uranium supply is contingent upon more reliable future undiscovered resource estimates beyond the currently identified quantities.

There are various techniques for assessing these speculative resources, ranging from mineral potential modelling to quantitative mineral resource assessments [7]. Supplying the statistical and spatial data and appropriate modelling techniques, along with relevant elements of the deposit classification systems, provides the complete range of inputs for Member States to generate predictive models for longer term uranium supply.

Mineral deposit models are fundamental to exploration decision making and the communication of geoscientific information and knowledge. Whilst commonly referred to as either empirical or conceptual, mineral deposit models typically include an array of observational and theoretical recognition criteria considered by the model authors as representative of a given mineral deposit or group of deposits [8, 9].

A descriptive mineral deposit model is a systematic arrangement of essential empirical and genetic geological attributes common to a group of similar deposits. Individual deposit descriptions form the foundation of a descriptive mineral deposit model. Deposit models can be broadly grouped into two types: comprehensive and synoptic. Comprehensive models provide a complete and detailed understanding of the deposit type. Synoptic models identify and summarize the essential deposit-type attributes, from which extraneous attributes may be excluded, and are particularly useful for quantitative assessment of undiscovered mineral resources and mineral prospectively mapping exploration applications.

In 2018, the IAEA published a revised classification scheme for the uranium deposit models recognised [5]. On the whole, the IAEA has classified global uranium deposits into 15 types, 37 subtypes and 14 classes (Table 1). Essentially an empirical system, the IAEA classification scheme categorises uranium deposits chiefly by host rock and/or structure. An exception to this rule is the process-based surficial deposit type that combines a diverse group of uranium ores in near-surface environments and formed by surficial earth processes.

As discussed in [10], whilst invaluable for communication, reference and learning, the 66 descriptive uranium deposit models covered by the IAEA classification scheme include many variations on a theme and comprise countless geological variables, many evident at the deposit scale only. In addition, the models are largely based on information from deposit-scale studies whilst input from camp, district and regional studies is limited. And so, these models should be viewed as a starting point of foundation for Member States to build upon.

1.2. OBJECTIVE

The main aim of this study was to translate the descriptive models covered by the IAEA classification scheme [5] into process-based uranium deposit models generated in the framework of a mineral systems approach [11-15] and converted according to methods described in [9, 10, 14]. Whilst based on an extensive literature review and first hand knowledge of certain deposit types, the uranium mineral systems models presented here should be regarded as preliminary, with future scrutiny by and input from subject matter experts expected to further strengthen the models.

A key intention with the uranium mineral systems models is the provision of an enhanced scheme in which uranium deposits are presented according to the critical genetic processes that shape them (cf. Table 5 in [15]). Such a scheme has greater predictive power and, thus, is better suited to studies concerned with the number, size and location of speculative uranium resources.

1.3. SCOPE

This publication provides a set of systematic descriptive models for each uranium deposit type, subtypes and class as explained in detail in [1] and Table 1, using a consistent approach to summarise the same types of information for each. Each model is intended to have a stand-alone capability, and so is presented as such, using a tabular style that is typical of informal mineral resource industry standards. Each deposit type model includes a map showing the distribution of deposits and (where defined) the uranium provinces hosting such deposits.

Each model also has a scatterplot showing the grade and tonnage distribution of that particular deposit type, subtype or class, and cumulative frequency (or probability) curves separately for grade and tonnage from which the median and mean value is derived. Thus, each of the deposit models comprises a standard 2–page summary and 2 pages of figures. In some cases, the subdivision of deposit types into classes results in insufficient data points to generate a statistically meaningful distribution curve from which to derive mean and median, and so the distribution curves for the subtype to which that class belongs are shown for context. In general, this is approximately where $N < 10$, and so means and medians are also not included in the deposit model text. It should also be noted that for each model, the uranium provinces listed are for the deposit type only, because subdivision of subtypes and classes into provinces is often not possible with information currently available.

1.4. STRUCTURE

The structure of this publication is led by a discussion on the Mineral Systems approach to mineral deposit modelling, followed by an explanation of this to the construction of deposit templates, including and example of a input to such models in the form of uranium provinces. The majority of the document is the actual resultant models themselves as 15 Appendices generated by O. Kreuzer which are a compendium of individual descriptive mineral system deposit models, each of which is independent of the other (but consistent in approach).

Each uranium deposit type is followed by its Subtypes (where defined) which both contain the common information with the parent Type as well as the differences. In order to achieve this, there is necessarily some degree of repetition between the types and the hierarchical subtypes. The ordering of Appendices is consistent with the IAEA numerical ordering of Types.

2. MINERAL SYSTEMS APPROACH

The adaptation in the early 1990s of the petroleum system approach [16] to mineral deposits [11, 12] came on the back of improved oil and gas discovery rates informed by a better understanding of the processes leading to hydrocarbon deposition.

Analogous to a petroleum system, a mineral system may be regarded as an expression of or adjunct to much larger geological processes that occasionally concentrate minerals to economic proportions. In this concept, mineral deposits symbolise focal points of earth systems processes that operate on a variety of temporal and spatial scales to focus mass and energy flux [13-15]. Quoting [11], a mineral system incorporates "all geological factors that control the generation and preservation of mineral deposits and stress the processes that are involved in mobilising ore components from a source, transporting and accumulating them in more concentrated form and then preserving them throughout the subsequent geological history" (Fig. 1).

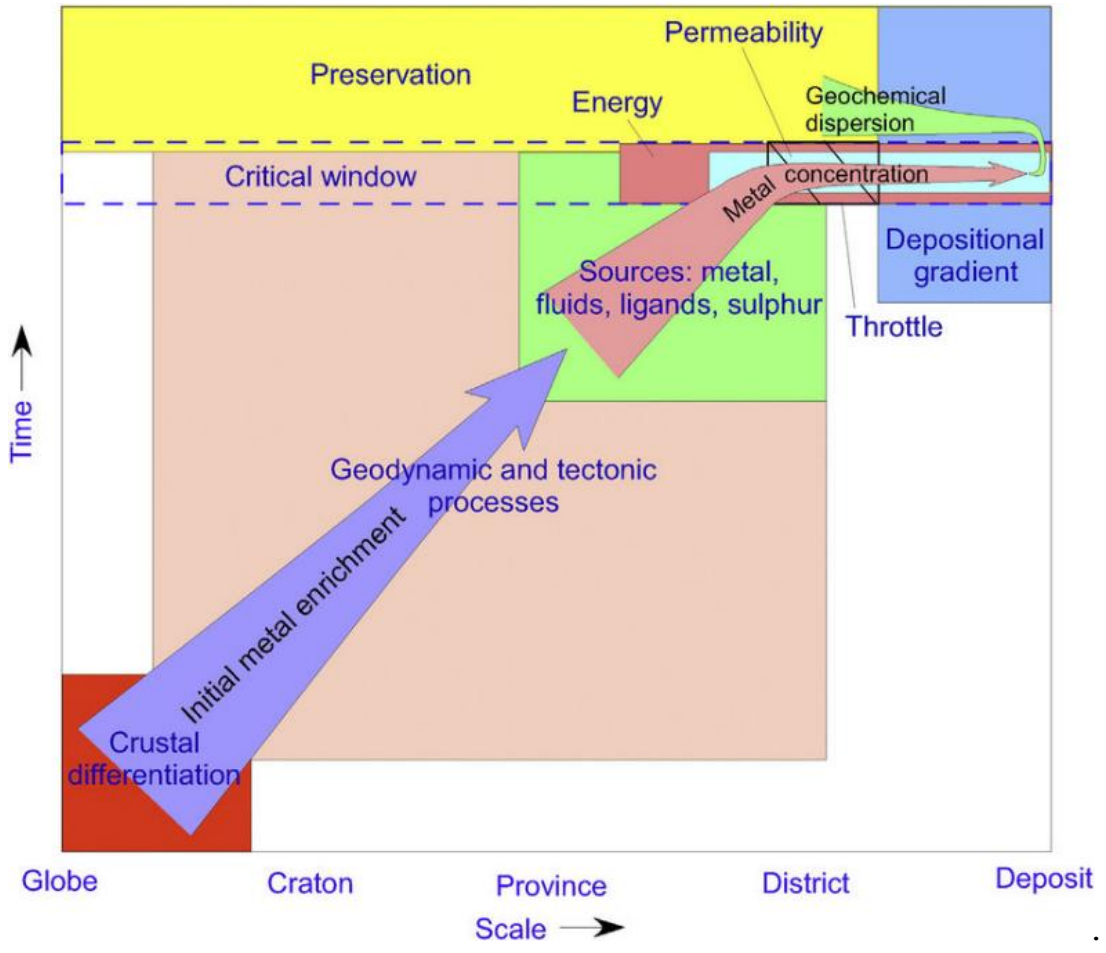

FIG. 1. Schematic representation of a mineral system, illustrating progressive metal concentration (indicated by arrows) and processes enabling this concentration from initial crustal differentiation to mineral deposit formation across space (scale) and time. The critical window represents the commonly short-lived conjunction in space and time of the critical processes and ingredients required to form a mineral system (Source: [17]).

Important implications of the mineral systems concept include the following [9, 11-15]:

- Mineral deposit formation is precluded where one or more of the critical processes are absent. This probabilistic aspect of the mineral systems concept has been harnessed for measuring exploration success and value, developing decision support and target ranking tools and the purpose of economic risk and prospectivity analysis;
- Different mineral deposit types may be created in a single mineral system, depending on, for example, crustal depth level of ore deposition, types of ore-forming fluids, host rock types or structural controls. As such, the mineral systems concept represents a unifying belief system, acknowledging the inherent natural variability among mineral deposits, emphasising common genetic processes and relating them in a predictable manner to their broader geodynamic framework;
- Whilst the critical processes are not observable or mappable in their own right, their expressions can be observed and mapped, for example, in outcrop, drillcore and geochemical and geophysical data. Focusing on identifying the critical processes of ore deposit formation and their mappable expressions, the mineral systems concept offers a framework for integration, organization and interrogation of multidisciplinary data at a variety of scales.

3. EXPLANATORY NOTES

Mineral systems models are traditionally presented as standalone summaries that, whilst self-contained, include references to broader sources of reference information from which the summary is drawn. The uranium mineral systems models developed as part of this study are presented here according to the nomenclature and order of the IAEA classification scheme [5] and the IAEA Uranium Deposits Database (UDEPO) [1], and both as generalised types and their constituent subtypes and classes (Table 1), despite there being some degree of overlap in the information.

The main reason for this approach was to provide a uniform format that: (i) is consistent with the existing IAEA classification scheme, and (ii) holds the information required for and is amenable to statistical modelling in the framework of the United States Geological Survey (USGS) three-part form of quantitative mineral resource assessments [18]. A critical assumption of such assessments is that specific mineral deposit types have specific log-normal grade-tonnage distributions that only hold if the underlying data are for a tightly constrained deposit model with minimal geological variation. For this reason, it is important to not use generalised deposit models (i.e., 'types'), unless there is insufficient data at the subtype or class level.

The UDEPO database contains approximately 3000 deposits. For the purposes of the database, a deposit is defined as an accumulation of uranium for which a statistical calculation exists indicating the amount of contained uranium. In most cases, this resource estimation is published, but is not necessarily compliant with national standards (for example JORC in Australia or NI-43 101 in Canada), because many historic values predate such standards. In exceptional cases, in particular for unconventional resources such as phosphate and black shale types, a secretarial estimate is made from sparse published average grades and volumes of mineralised rock to provide an order of magnitude assessment, but it is recognised that such calculations are approximate and coupled with the relatively few numbers of deposits, the statistical distribution has a low level of confidence. The spatial distribution of all UDEPO deposits is shown in Fig. 1 where the co-ordinates are known. The statistical distribution of all UDEPO deposits is shown in Fig. 2, where both the grade and tonnage is known. The logarithmic medians and means for all deposit types in UDEPO are shown in Figs 3 and 4 respectively.

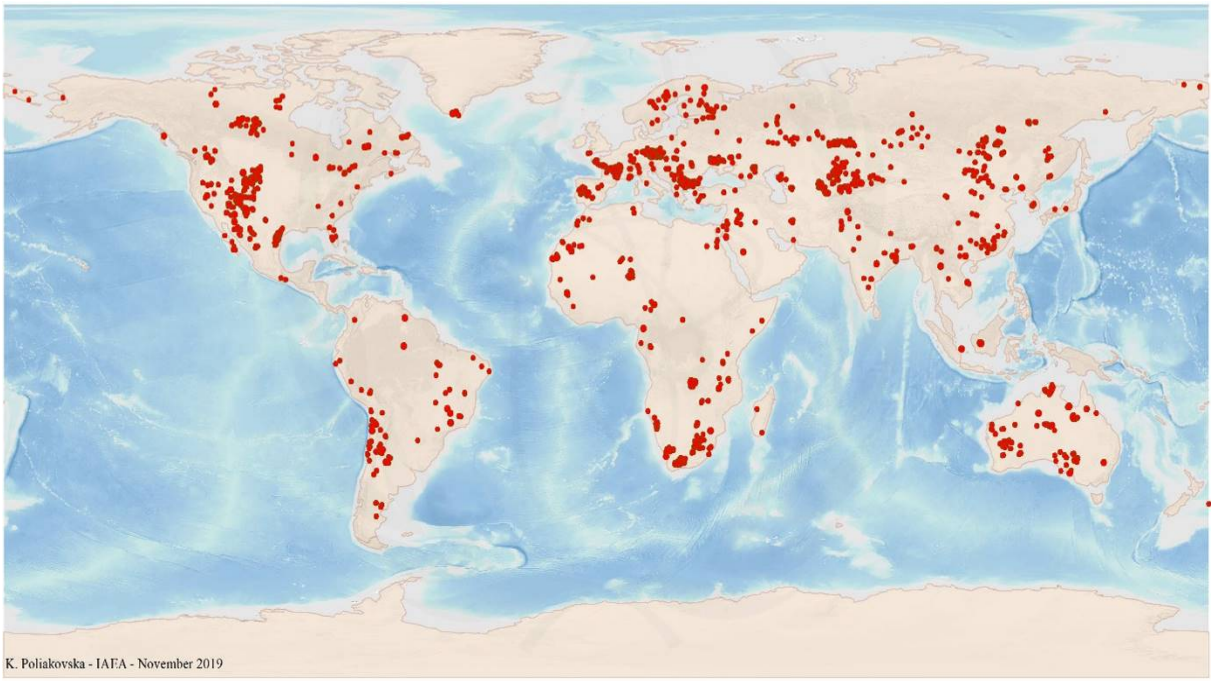

FIG. 2. Distribution of all deposits with coordinates in the UDEPO database.

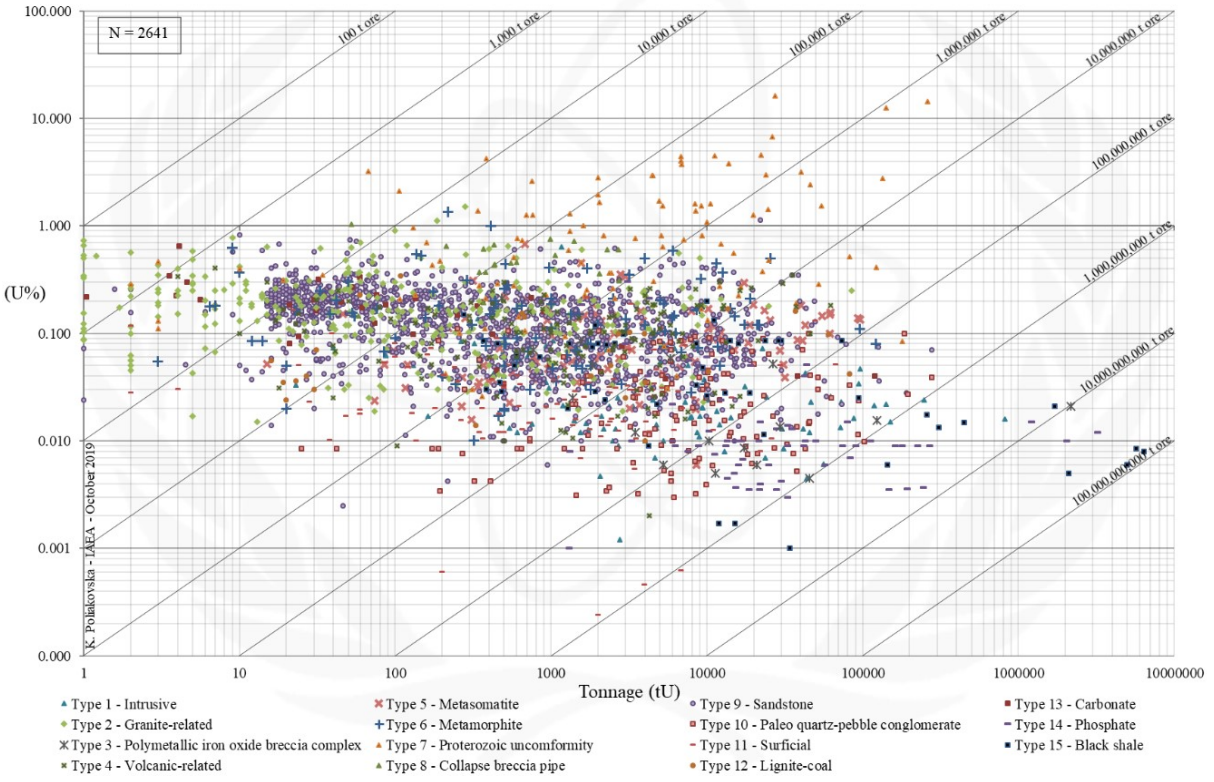

FIG. 3. Logarithmic grade and tonnage scatterplot of all deposits in the UDEPO database.

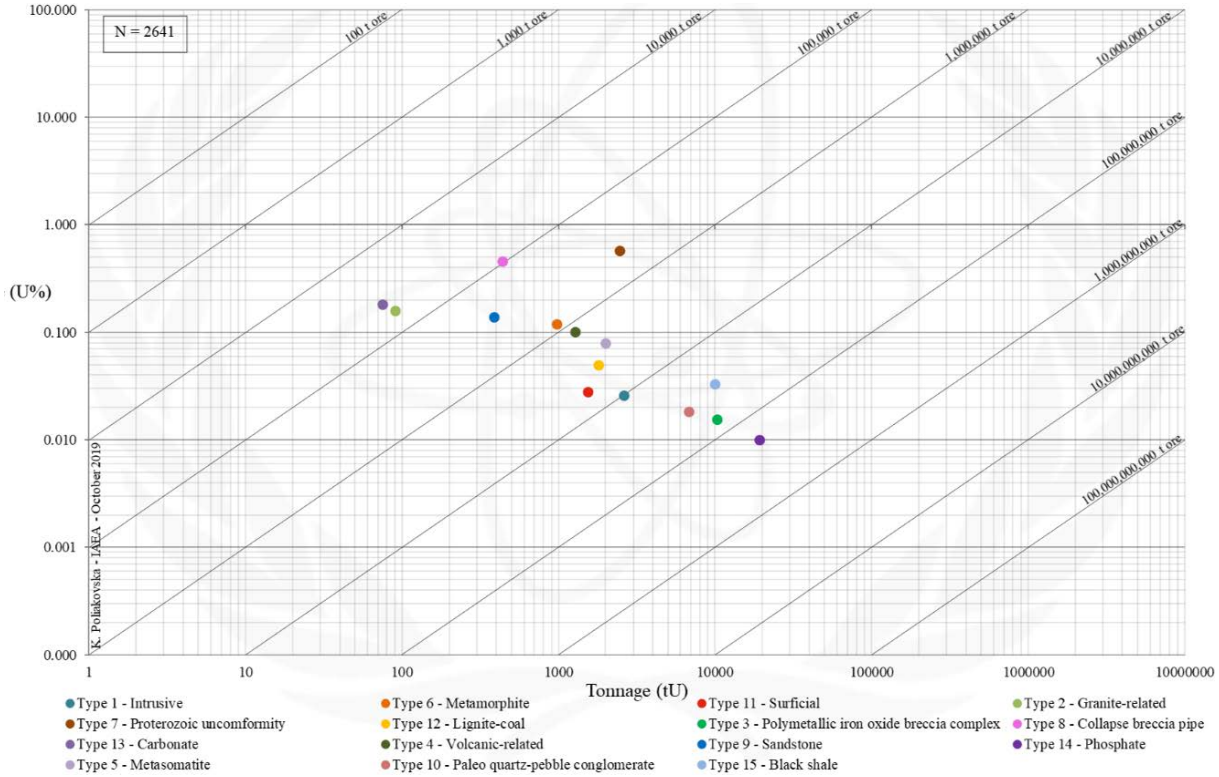

FIG. 4. Logarithmic medians of all deposit types in the UDEPO database.

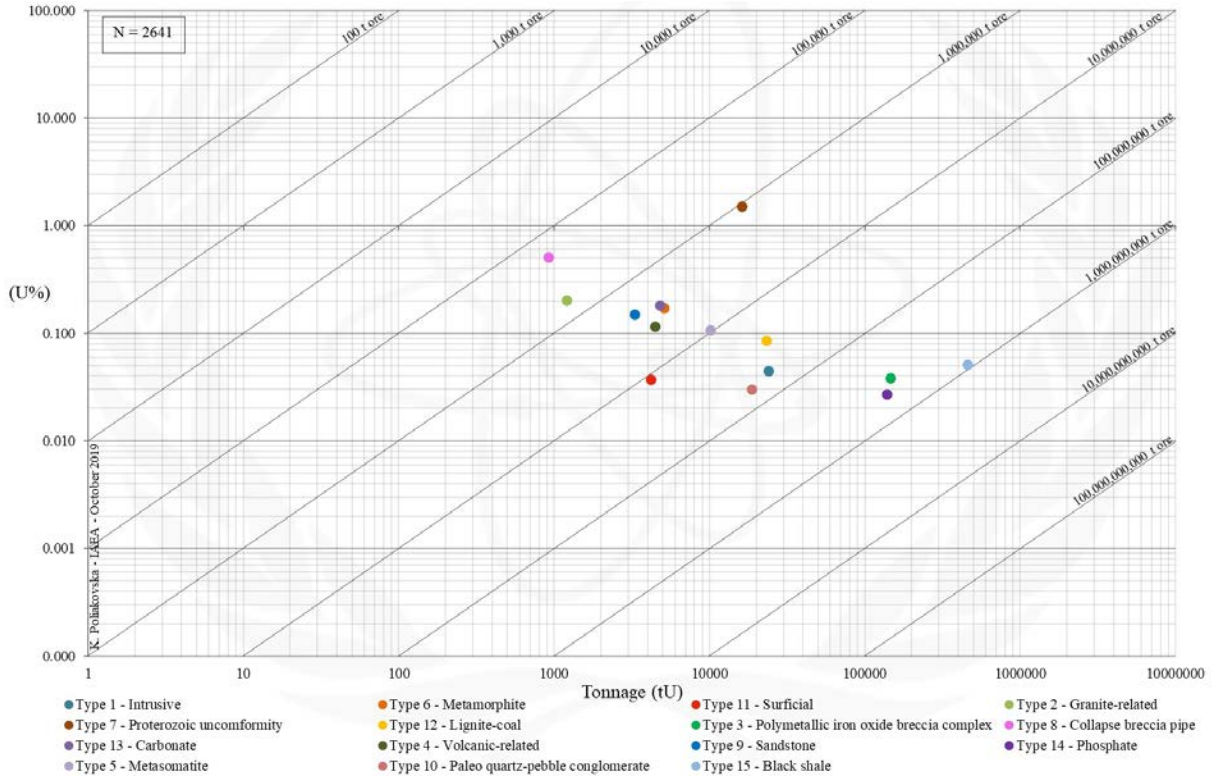

FIG. 5. Logarithmic means of all deposit types in the UDEPO database.

TABLE 1. IAEA URANIUM DEPOSIT CLASSIFICATION SCHEME

Deposit Type*		Deposit Subtype		Deposit Class		Examples
1	Intrusive	1.1	Anatectic (pegmatite–alaskite)			Rössing, Namibia; Bancroft district, Canada
		1.2	Plutonic	1.2.1	Quartz monzonite	Bingham Canyon, USA; Chuquicamata, Chile
				1.2.2	Peralkaline complex	Kvanefjeld, Greenland; Poços de Caldas, Brazil
				1.2.3	Carbonatite	Phalabora, South Africa; Catalão, Brazil
2	Granite-related	2.1	Endogranitic			La Crouzille district, France; Xiazhuang district, China
		2.2	Perigranitic			Příbram district, Czech Republic; Niederschlema, Germany
3	Polymetallic iron oxide breccia complex					Olympic Dam, Carrapateena, Australia
4	Volcanic-related	4.1	Stratabound			Dornod (No. 7 ore zone), Mongolia; Maureen, Australia
		4.2	Structure-bound			Streltsov-Antei, Russian Federation; Kurišková, Slovakia
		4.3	Volcano-sedimentary			Anderson Mine, USA; Sierra Pintada district, Argentina
5	Metasomatite	5.1	Sodium (Na)-metasomatite	5.1.1	Granite derived	Kirovograd district, Ukraine; Lagoa Real, Brazil
				5.1.2	Metasediment-metavolcanic derived	Krivoy Rog district, Ukraine
		5.2	Potassium (K)-metasomatite			Elkon district, Russian Federation
		5.3	Skarn			Mary Kathleen, Australia; Tranomaro, Madagascar
6	Metamorphite	6.1	Stratabound			Forstau, Austria; Nuottijarvi, Finland
		6.2	Structure-bound	6.2.1	Monometallic veins	Schwartzwalder, USA; Ace-Fay-Verna, Canada
				6.2.2	Polymetallic veins	Shinkolobwe, Democratic Republic of Congo
				6.2.3	Marble-hosted phosphate	Itataia, Brazil; Zaozernoye, Kazhakstan
7	Proterozoic unconformity	7.1	Unconformity-contact			Cigar Lake, Key Lake, McArthur River, Canada
		7.2	Basement-hosted			Jabiluka, Ranger, Australia; Eagle Point, Canada
		7.3	Stratiform fracture-controlled			Lambapur, Chitrial, India
8	Collapse breccia pipe					Arizona Strip, USA
9	Sandstone	9.1	Basal channel			Dalmatovskoye, Russian Federation; Beverley, Australia
		9.2	Tabular	9.2.1	Continental fluvial, uranium associated with intrinsic reductant	Arlit district, Niger
				9.2.2	Continental fluvial, uranium associated with extrinsic bitumen	Ambrosia Lake district (Grants region), USA
				9.2.3	Continental fluvial vanadium-uranium	Salt Wash member, USA
		9.3	Roll-front	9.3.1	Continental basin, uranium associated with intrinsic reductant	Wyoming basins, USA
				9.3.2	Continental to marginal marine, uranium associated with intrinsic reductant	Chu-Sarysu basin, Kazakhstan

Deposit Type*		Deposit Subtype		Deposit Class	Examples
			9.3.3	Marginal marine, uranium associated with extrinsic reductant	South Texas, USA
		9.4	Tectonic-lithologic		Lodève Basin, France; Franceville Basin, Gabon
		9.5	Mafic dykes/sills in sandstone		Westmoreland district, Australia; Matoush, Canada
10	Palaeo quartz-pebble conglomerate	10.1	Uranium-dominant		Elliot Lake district, Canada
		10.2	Gold-dominant		Witwatersrand Basin, South Africa
11	Surficial	11.1	Peat bog		Kamushanovskoye, Kyrgyzstan; Flodelle Creek, USA
		11.2	Fluvial valley		Yeelirrie, Australia; Langer Heinrich, Namibia
		11.3	Lacustrine-playa		Lake Maitland, Lake Way, Australia
		11.4	Pedogenic and fracture fill		Beslet, Bulgaria
		11.5	Placer		Kyzyl Ompul, Kyrgyzstan; Red River Valley, USA
12	Lignite-coal	12.1	Stratiform		Koldzhat, Kazakhstan; Williston Basin, USA
		12.2	Fracture-controlled		Freital, Germany; Turakavak, Kyrgyzstan
13	Carbonate	13.1	Stratabound		Tumalappalle, India
		13.2	Cataclastic		Mailuu-Suu, Kyrgyzstan; Todilto district, USA
		13.3	Palaeokarst		Sanbaqi, China; Tyuya-Muyun, Kyrgyzstan
14	Phosphate	14.1	Organic phosphorite		Mangyshlak Peninsula, Kazakhstan; Ergeninsky region, Russian Federation
		14.2	Minerochemical phosphorite		Phosphoria Formation, USA
		14.3	Continental phosphate		Bakouma district, Central African Republic
15	Black shale	15.1	Stratiform		Ranstad, Sweden; Chattanooga Shale Formation, USA
		15.2	Stockwork		Ronneburg district, Germany; Dzhantuar, Uzbekistan

Figure 7 provides a summary of the model structure and content fields. For of ease of use, the models are summarised with respect to detail provided. However, further information is available in the spreadsheets in Annex I, from which each model was derived. It should be noted that for Subtypes and Classes, only the provinces for the Deposit Type are shown because a more detailed subdivision has not been undertaken.

Item		Comments
Deposit type name and number		Identifying information as summarised in Table 1
Descriptive model	Brief description	Brief description of key characteristics of the described deposit type
	Subtypes and classes	Relevant deposit subtypes and classes as summarised in Table 1
	Type examples	Significant global examples representative of the described deposit type
	Genetically associated deposit types	List of uranium deposit types, subtypes and classes that are genetically associated with the described type
	Principal commodities	List of the principal commodities associated with the described deposit type
	Grades and tonnages	Grade and contained U tonnage data from log data where amount of data is sufficient
	Number of deposits	Number of deposits of this type/subtype/class in the UDEPO database
	Provinces	List of relevant IAEA uranium provinces (only for deposit types)
	Tectonic setting	List of tectonic setting(s) in which the described deposit type may form
	Typical geological age range	Information about the typical geological age range of the described deposit type
Mineral systems model	Source	– All critical geological processes required to mobilise the necessary ore components from their sources – Source processes are divided here into several constituent processes relating to provision/generation/mobilisation of: ▪ Energy to drive and sustain the mineral system ▪ An environment favourable for uranium deposition (ground preparation) ▪ Melts and/or fluids ▪ Ligands ▪ Metals ▪ Reductants, adsorbents and/or reactants
	Transport	– All critical geological processes required to transfer the ore components from source to trap ▪ Transport occurs exclusively via highly effective, permeable melt or fluid pathways that are available at the time the ore components are transportable
	Trap	– All critical geological processes required to form a suitable trap, or traps, along the transport pathway ▪ Traps are defined here as highly effective melt or fluid channels that can focus melt or fluid flow and accommodate significant amounts of metal ▪ Trap processes are divided here into two constituent processes related to the physical and chemical aspects of the trap
	Deposition	– All critical geological processes required to extract ore components from melts or fluids passing through the trap and depositing them
	Preservation	– All critical geological processes required to preserve the mineral system and associated mineral deposits through time
Key reference bibliography		List of references relevant to the type of mineral system

FIG 7: Schematic layout and content of uranium mineral systems summary tables.

4. URANIUM PROVINCES

The main use of deposits models in quantitative mineral resource assessments (QMRA), specifically the Three-Part method, of speculative or undiscovered resources also requires that the area to which this assessment is applied is accurately defined. Increasingly the approach to accurately defining this area is the same approach to that applied in Mineral Potential Modelling (MPM), where relevant input geoscience datasets are combined in a Geographic Information Systems computer environment to produce a spatial representation of ranked favourability of a region hosting a particular deposit type. The ranked favourable areas defined in this approach can then be used as defining the area — 'permissive tract' — outside of which there is negligible possibility that a deposit may occur.

The term 'permissive tract' explicitly implies that the area is defined with an approach towards QMRA in mind using specific methodologies appropriate to a relatively small area. For the purposes of a global delineation of such areas, the term uranium province is preferred due to the large scale, coarse, nature of the input and consequent output. Nevertheless, these provinces can serve as a first pass guide for Member States to develop more detailed tracts within provinces on which to utilise deposit models for QMRA. To this end, a preliminary portrayal of global uranium provinces has been generated [3].

Economic accumulations of uranium result from fractionation processes operating over a wide range of spatial and temporal scales. These processes commonly operate for limited periods of geologic time and within restricted volumes of the Earth's crust. The resulting mineralisation styles depend on which processes occur, the timescales over which they operate, and the nature of the materials affected. A two-dimensional area can be defined on the present-day Earth's surface within which all the critical components of a particular mineralising system are (or were once) present. The edges of these zones can be thought of as process boundaries, marking the geographical limits within which a particular ore-forming process operates, or operated at some time in the past.

The aim of this study is to define a global set of such favourable sub-provinces, each of which represents a distinct zone in which certain mineralising processes have had the potential to develop economic deposits of uranium. The sub-provinces are similar in concept to 'permissive tracts' commonly referred to in United States Geological Survey–related literature. Permissive tracts are defined as areas for which the probability of a particular type of deposit occurring outside the tract is negligible [18].

The study builds on and goes hand-in-hand with work by previous and current authors on the definition of uranium metallogenic provinces. Metallogenic provinces (or super-provinces) represent areas on the Earth with unusually elevated levels of metal endowment. The identification of uranium provinces reveals a fundamental characteristic of the nature of the underlying crust and represents an important first-order control on its propensity to generate and host uranium deposits. By contrast, this study is aimed at fractionation processes which occur relatively late in the ore formation process. Each uranium province may contain one or several uranium sub-provinces as defined in this study.

Most of the identified sub-provinces have demonstrable pedigree, hosting one or more known deposits; others are considered more speculative in that they are interpreted to possess all the critical components required for uranium deposit formation, but may not have seen any

significant historical discoveries. This study makes no attempt to differentiate between areas on this basis, or to rank areas according to their relative prospectivity. However, a summary of known deposits is presented within the attribute table of each sub-province allowing a coarse differentiation to be made between areas with demonstrated pedigree and those which can be considered to be more speculative in nature.

As should be expected, there is (sometimes significant) overlap between areas as each sub-province represents a different set of deposit styles and processes, and it is not unusual for the same area to be affected by several different combinations of mineralising processes over time. Only the provinces for the Deposit Type are shown because a more detailed subdivision has not been undertaken.

The work draws extensively on the work of Franz J. Dahlkamp, with many of the sub-province names being derived directly from the section titles in the three "Uranium Deposits of the World" volumes [19-21]. Additionally, the study relied on numerous journal articles, books, company reports and websites, etc. for background information on each area examined. Only publicly available spatial data were used in this study, with appropriate references given in the attribute table of each polygon. Obviously, the interpretation can only be as good as the data available for a particular area so an important early step in undertaking this study was to identify the best/most suitable spatial data to use for each area. High quality, robust data sets are routinely compiled and made available for only parts of the world, but fortunately, the volume and quality of data being generated and made public is constantly improving. The data must also be applicable to the problem and adequately describe the critical components of the mineralising system under consideration.

Analysis in many areas necessitates the use of lower fidelity, regional or even global data sets. Most continent-scale geological data and global compilations (e.g., 1:5 000 000 scale geology data) are extremely generalised in nature. They generally proved to be useable for this study, but in some cases, there are obvious omissions or over-simplifications in the underlying data. There are several instances where one or more UDEPO deposits apparently fall outside of their associated prospective area. For example, this may happen due to the available spatial dataset inadequately representing the subtle feature(s) with which the deposit is associated. In other cases, the interpreted subprovince over-estimates the size of the permissive area because prospective and non-prospective components have been generalised and mapped as the same feature in the source data. These are unavoidable consequences of using the current generation of publically available spatial data. It should be noted that there are also several cases where deposits plot outside their associated subprovince as a result of (commonly small) inaccuracy in co-ordinates in the UDEPO database. Buffers are used around favourable features in some cases to account for uncertainty in the spatial accuracy of certain data sets and for display purposes. The aggregated provinces for all 15 deposit types are shown in Fig. 8.

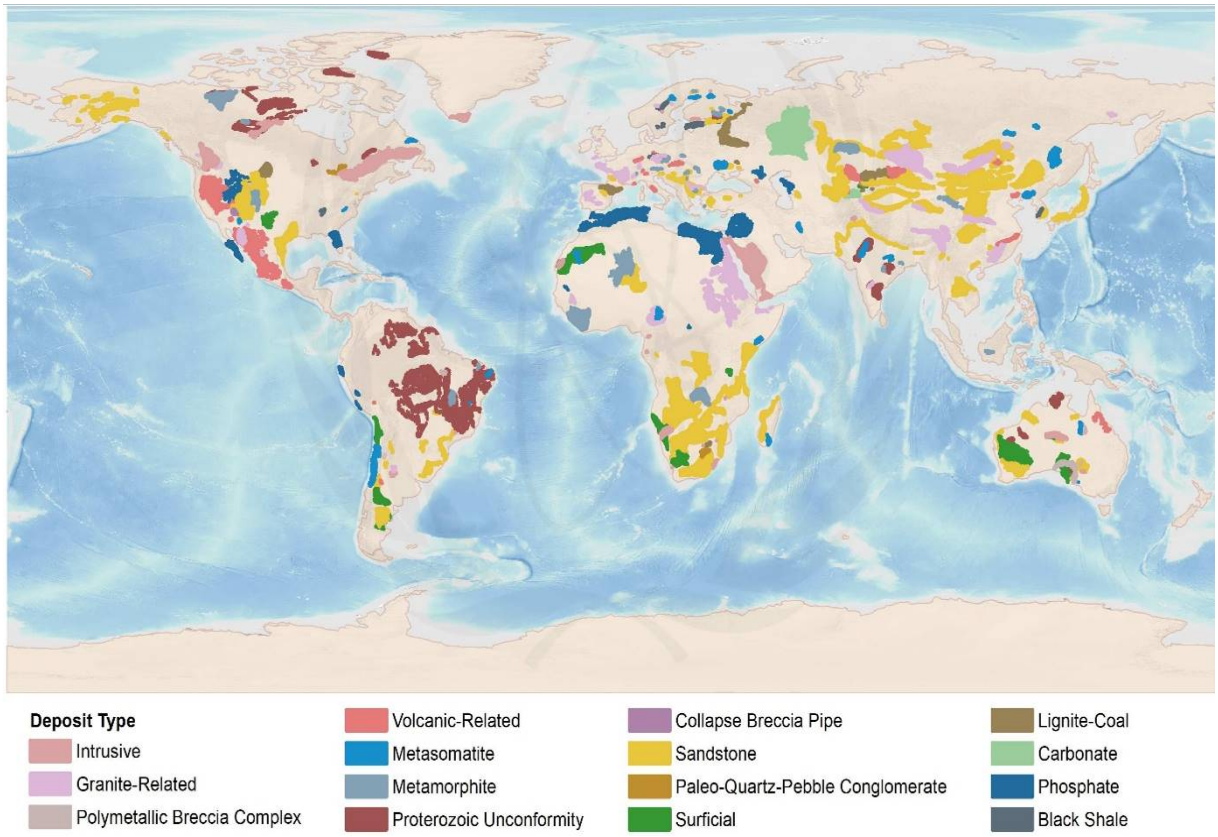

FIG. 8. Aggregated uranium provinces of the world. Many provinces have been exaggerated for clarity. Digital data courtesy M. Bruce.

5. SUMMARY AND CONCLUSIONS

The IAEA recognises 15 uranium deposit types, most comprising multiple subtypes, some of which are further subdivided into classes [5]. Essentially an empirical system, the IAEA classification scheme categorises uranium deposits chiefly by host rock and/or structure. Whilst invaluable for communication, reference and learning, this scheme comprises countless geological variables and, therefore, is not well suited to mineral potential modelling or quantitative resource assessments of undiscovered uranium resources.

The uranium deposit models presented here were generated in the framework of a mineral systems approach [11, 14-15] in which mineral deposits are regarded as products of a series of critical processes required to: (i) mobilise ore components from their sources, (ii) transport, (iii) accumulate them in more concentrated form and (iv) preserve them through time. These process-based models have greater predictive power and, thus, are better suited to mineral potential and quantitative resource assessment studies concerned with the number, size and location of speculative uranium resources.

The summary tables for each Deposit Type, Subtype and Class are presented in the following 15 Appendices correspondingto the 15 Deposit Types and their consitituent Subtypes and Classes. In the case of Classes, due to the low number of examples, the map or statistical graphics presented is of the overarching Subtype.

Appendix I

INTRUSIVE

TYPE 1. Intrusive

Brief Description

- Intrusive uranium deposits are a genetically diverse group of ores hosted by a wide variety of intrusive rocks with a broad range of petrochemical compositions.
- Deposits of this type are broadly divided into (1.1.) anatectic (pegmatite-alaskite) ores the genesis of which is linked to partial melting processes in high-temperature, low-pressure metamorphic environments and (1.2.) plutonic ores that represent products of primary magmatic differentiation processes.
- The plutonic subtype is further subdivided into three classes, namely (1.2.1.) quartz monzonite, (1.2.2.) peralkaline complex and (1.2.3.) carbonatite deposits. They constitute unconventional uranium resources, characterised by very low uranium concentrations that may be extractable as by-products only.

Subtypes and Classes

- 1.1. Anatectic (pegmatite-alaskite)
- 1.2. Plutonic
  - 1.2.1. Quartz monzonite
  - 1.2.2. Peralkaline complex
  - 1.2.3. Carbonatite

Type Examples

- Subtype 1.1. Rössing, Husab, Namibia
- Class 1.2.1. Bingham Canyon, Twin Buttes, Yerington, USA
- Class 1.2.2. Kvanefjeld, Greenland; Poços de Caldas, Brazil
- Class 1.2.3. Phalabora, South Africa; Catalão, Araxa, Brazil

Principal Commodities

- Subtype 1.1. U
- Class 1.2.1. Cu ± Au, Mo; U (by-product only)
- Subtype 1.2.2. REE, Nb ± Au, Be, Cu, Hf, Li, Sr, Ta, Th, Ti, Y, Zr, Zn; U (by-product only)

Grades (%) and Tonnages (tU)

- Average: 0.0441, 24 339.4
- Median: 0.0254, 2 640.0

Number of Deposits

- 138

Provinces

- Aileron Province, Ange, Arabian Shield, Bokan Mountain, Comechingones, Complexe dAdam Esseder, Damara Central Swakop, Grenville, Kanyika, Lolodorf Akongo, Mabounie, Mudjatik North, Mudjatik South, Oulad Dlim Massif, Phalaborwa, Pilanesberg Complex, Pocos de Caldas, Shuswap, Sillai Patti, Sokli, South Greenland, Wollaston.

Tectonic Setting

- Collisional orogens, magmatic arcs, intracontinental rifts

Typical Geological Age Range

- Precambrian to Neogene

Mineral Systems Model

Source

Ground preparation
- Collisional orogeny and post-orogenic collapse, or
- Formation of crustal magma staging chambers above a subduction zone, or
- Rifting, mafic underplating and lithospheric doming

Energy
- High heat flow, extreme geothermal gradient and partial melting of mantle and/or crustal sources, and
- Voluminous magmatism, and/or
- High temperature-low pressure metamorphism at upper amphibolite to granulite facies grade

Melts and fluids
- High-temperature, fluorite-rich melts of metaluminous to peraluminous composition, or
- Intermediate to felsic calc-alkaline arc-related melts, or
- Mantle-related peralkaline or carbonatite melts, and
- Associated magmatic-hydrothermal fluid circulation systems

Ligands
- F, CO_2, HCl, H_2S, SO_2, Cl, S, Ca, PO

Reductants and reactants
- Subtype 1.1. Marble, graphite, sulphides
- Classes 1.2.1 to 1.2.3. No information

Uranium
- Fractionated melts, or
- Crustal sources (crystalline basement rocks such as granitic gneisses or granitoids)

Transport

Fluid pathways
- Crustal-scale fault zones

Trap

Physical
- Transition from hot, weak ductile crust to cold, strong brittle crust, and/or
- Dilational deformation, permeability and suction focused on intrusions, and/or
- Focusing of the volatile phase into high strain zones, flanks and apexes of large basement or granitoid domes, fault-fracture networks, zones of brecciation or anticlinal fold axes, and/or
- Metasomatised magma chamber roof acting as a seal

Chemical
- Redox boundaries

Deposition

Fractional crystallisation and cooling
- Pressure and temperature decrease promoting magma cooling, fractional crystallisation and uranium enrichment in the ascending melt and volatile phase, or
- Gravitational settling at the base of a magma chamber

Exsolution, depressurisation and cooling of a magmatic-hydrothermal volatile phase
- Fracture and/or breccia controlled discharge of uraniferous volatile phase

Change in redox conditions
- Due to fluid/wallrock interaction
- Due to fluid mixing

Depositional processes affecting ore grades and tonnages
- Coalescence of uraniferous leucogranites promotes formation of larger orebodies
- Secondary remobilisation, redeposition and upgrading of uranium in the oxidised zone

Preservation
- Crustal extension and/or down-faulting or tilting of mineralised system soon after exhumation
- Relative tectonic stability post-mineralisation

Key Reference Bibliography

BERGER, V. I., SINGER, D. A., ORRIS, G. J., Carbonatites of the world, explored deposits of Nb and REE--database and grade and tonnage models. U.S. Geological Survey Open-File Report, 2009-1139, 17p (2009).

BASSON, I. J., GREENWAY, G., The Rössing uranium deposit: a product of late-kinematic localization of uraniferous granites in the Central Zone of the Damara Orogen, Namibia. Journal of African Earth Sciences, 38(5), 413-435 (2004).

FAN, H., CHEN, J., WANG, S., ZHAO, J., GU, D., MENG, Y., Genesis and uranium sources of leucogranite-hosted uranium deposits in the Gaudeanmus area, Central Damara Belt, Namibia: Study of element and Nd Isotope geochemistry. Acta Geologica Sinica, 91(6), 2126-2137 (2017).

INTERNATIONAL ATOMIC ENERGY AGENCY, Geological Classification of Uranium Deposits and Description of Selected Examples. IAEA-TECDOC Series, 1842, 415p (2018).

JOHN, D. A., AYUSO, R. A., BARTON, M. D., BLAKELY, R. J., BODNAR, R. J., DILLES, J. H., GRAY, F., GRAYBEAL, F. T., MARS, J. C., MCPHEE, D. K., SEAL, R. R., Porphyry copper deposit model, chapter B of mineral deposit models for resource assessment. U.S. Geological Survey Scientific Investigations Report, 2010–5070–B, 169p (2010).

KINNAIRD, J. A., NEX, P. A. M., A review of geological controls on uranium mineralisation in sheeted leucogranites within the Damara Orogen, Namibia. Applied Earth Science, 116(2), 68-85 (2007).

LANDTWING, M. R., FURRER, C., REDMOND, P. B., PETTKE, T., GUILLONG, M., HEINRICH, C. A., The Bingham Canyon porphyry Cu-Mo-Au deposit. III. Zoned copper-gold ore deposition by magmatic vapor expansion. Economic Geology, 105(1), 91-118 (2010).

PIRAJNO, F., Intracontinental anorogenic alkaline magmatism and carbonatites, associated mineral systems and the mantle plume connection. Gondwana Research, 27(3), 1181-1216 (2015).

RICHARDS, J. P., Tectono-magmatic precursors for porphyry Cu-(Mo-Au) deposit formation. Economic Geology, 98(8), 1515-1533 (2003).

SIMANDL, G. J., PARADIS, S., Carbonatites: related ore deposits, resources, footprint, and exploration methods. Applied Earth Science, 127(4), 123-152 (2018).

VERPLANCK, P. L., VAN GOSEN, B. S., SEAL, R. R, MCCAFFERTY, A. E., A deposit model for carbonatite and peralkaline intrusion-related rare earth element deposits. U.S. Geological Survey Scientific Investigations Report, 2010–5070-J, 58p (2014).

WILKINSON, J. J., Triggers for the formation of porphyry ore deposits in magmatic arcs. Nature Geoscience, 6(11), 917-925 (2013).

ZHANG, D., AUDÉTAT, A., What caused the formation of the giant Bingham Canyon porphyry Cu-Mo-Au deposit? Insights from melt inclusions and magmatic sulfides. Economic Geology, 112(2), 221-244 (2017).

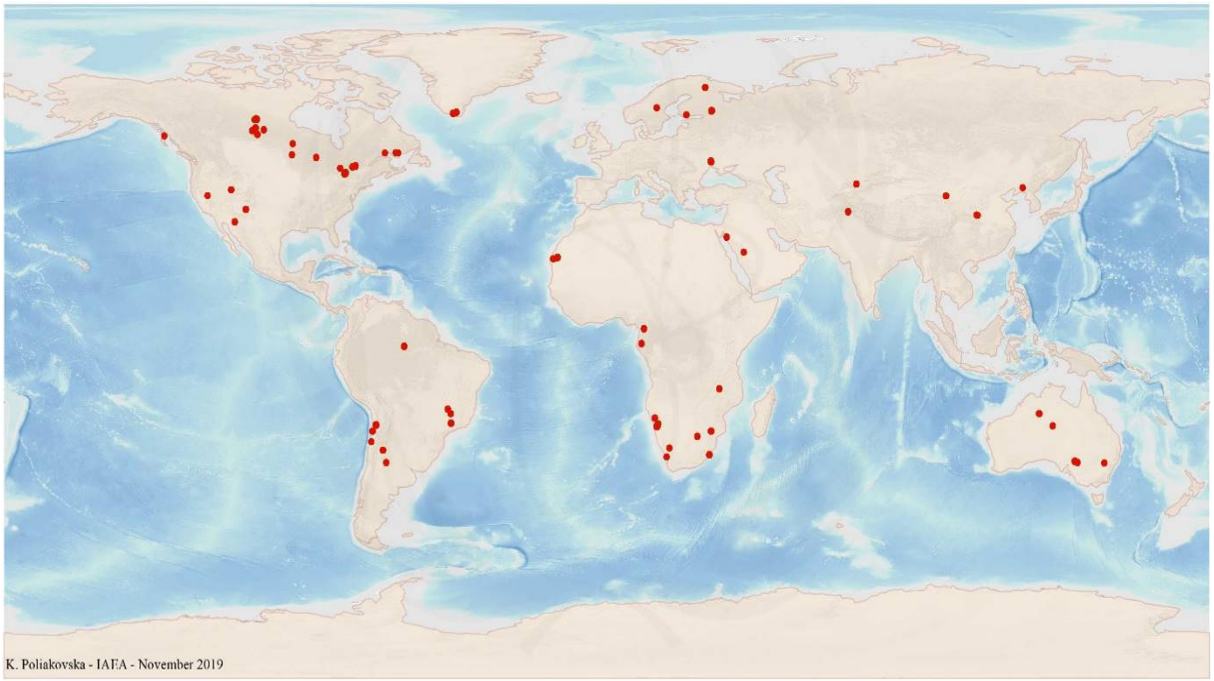

FIG. 1a. World distribution of selected Intrusive uranium deposits from the UDEPO database.

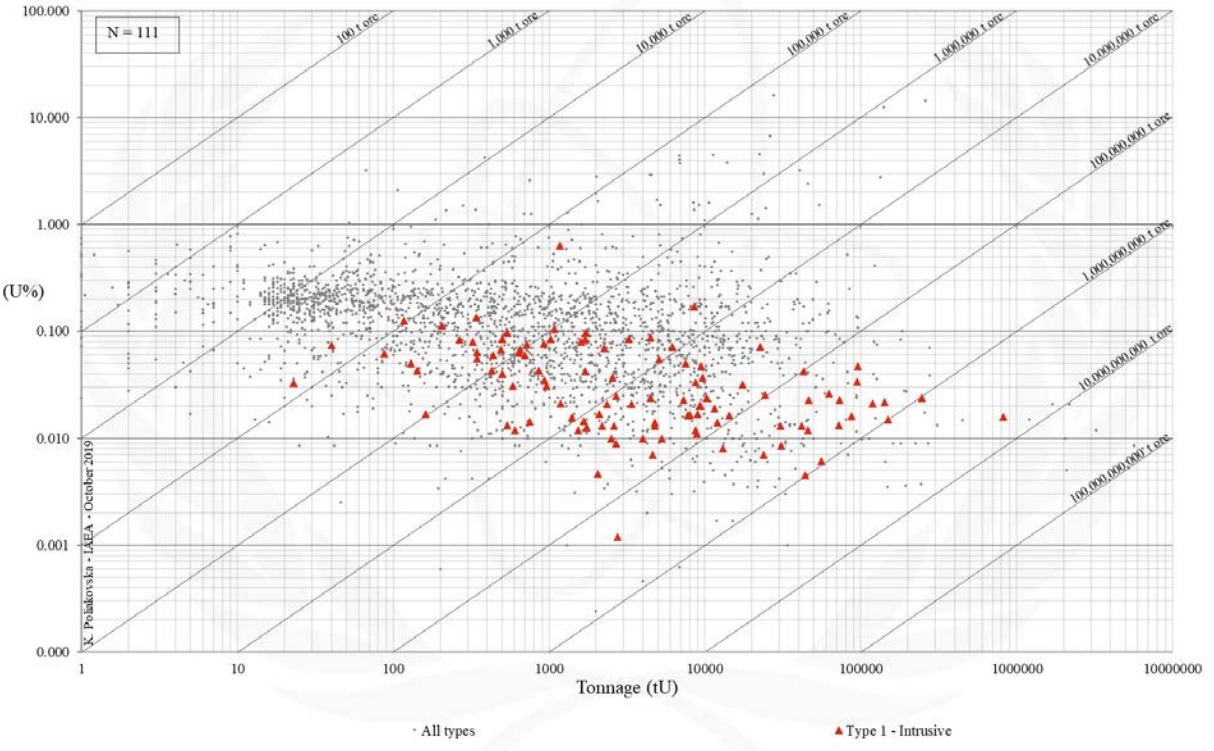

FIG. 1b. Grade and tonnage scatterplot highlighting Intrusive uranium deposits from the UDEPO database.

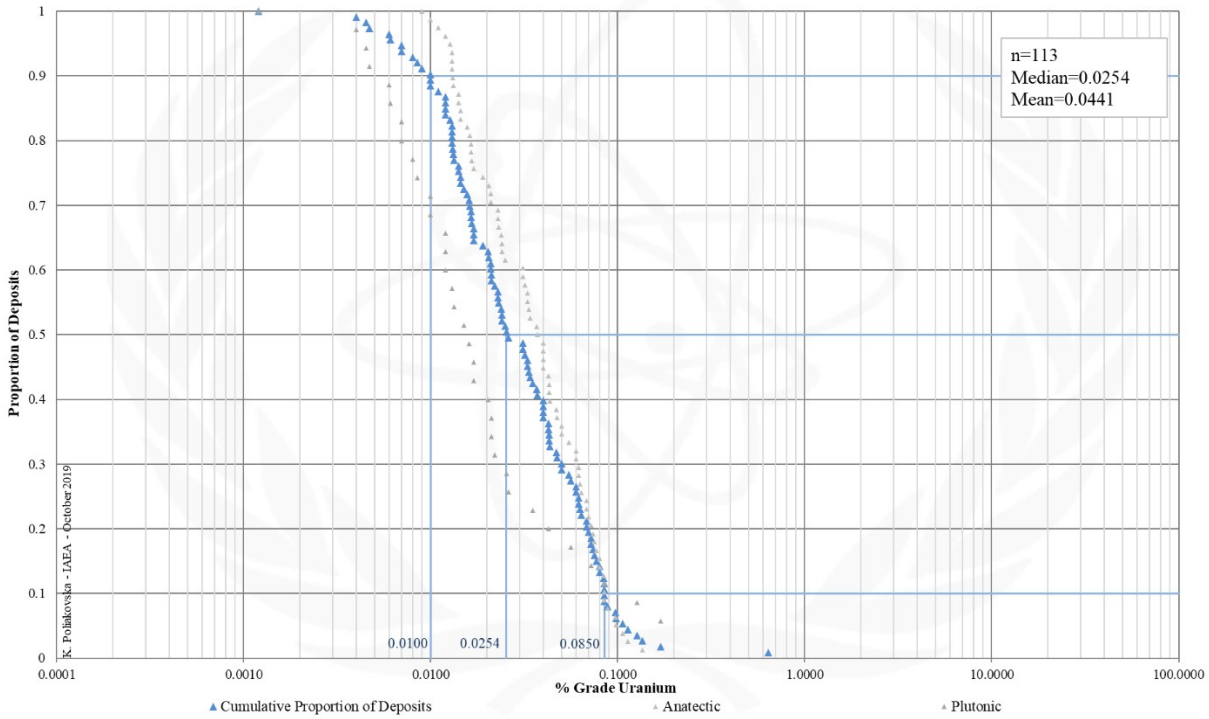

FIG. 1c. Grade Cumulative Probability Plot for 'Intrusive-type' uranium deposits from the UDEPO database.

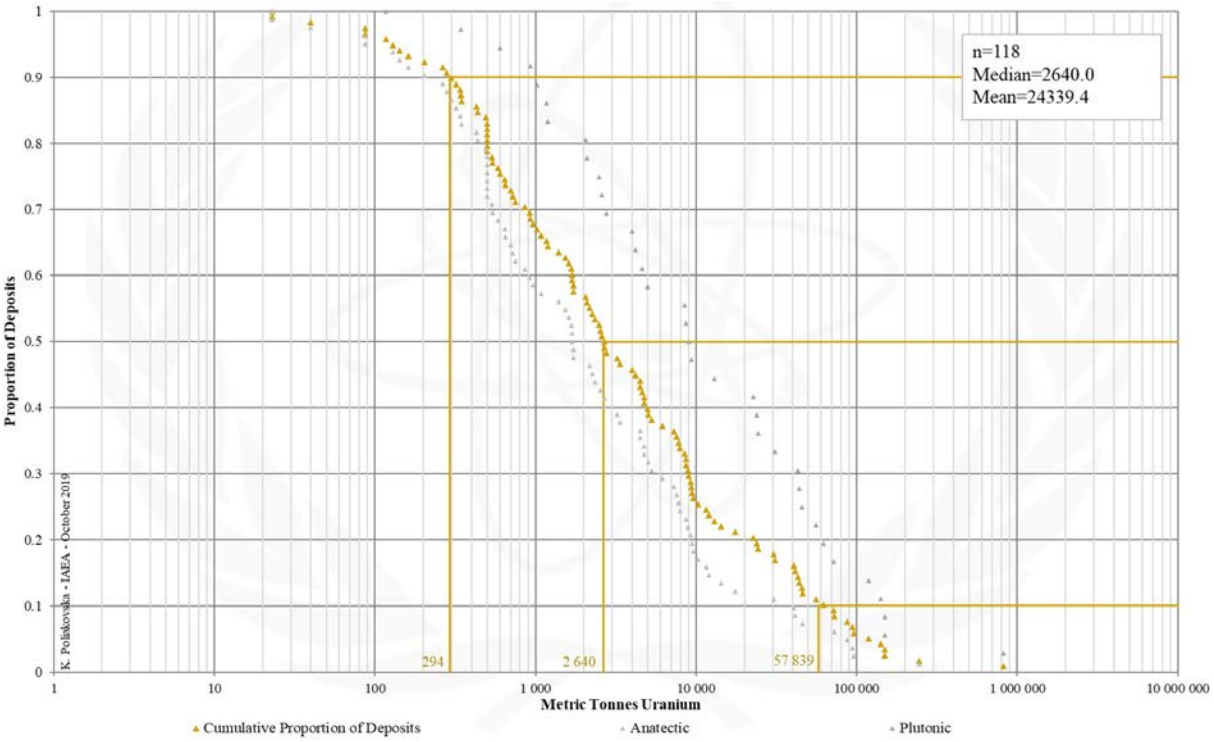

FIG. 1d. Tonnage Cumulative Probability Plot for Intrusive uranium deposits from the UDEPO database database.

SUBTYPE 1.1. Intrusive, Anatectic (Pegmatite-Alaskite)

Brief Description

- Anatectic deposits are typified by those in the Damara Orogen, Namibia, where uranium mineralisation was linked in space and time to partial melting processes in a high-temperature, low-pressure metamorphic environment.
- The uranium ores in this belt take the form of disseminations in pegmatite and alaskite (leucogranite) bodies that intruded strongly deformed, migmatised metasedimentary country rocks.
- Leucogranites range in size from small lenses and tabular sheets to large stocks and intrusions several hundreds of metres in diameter.
- No wallrock alteration is associated with the uranium ores.

Type Examples

- Rössing, Husab, Goanikontes, Z 20, Ongolo, Valencia, Garnet Valley, Namibia

Genetically Associated Deposit Types

- Subtype 5.3. Metasomatite, skarn

Principal Commodities

- U

Grades (%) and Tonnages (tU)

- Average: 0.0438, 11992.6
- Median: 0.0372, 1700.0

Number of Deposits

- 92

Provinces (undifferentiated from Intrusive Type)

- Aileron Province, Ange, Arabian Shield, Bokan Mountain, Comechingones, Complexe dAdam Esseder, Damara Central Swakop, Danfeng Shangnan, Grenville, Kanyika, Koegel Fontein, Lolodorf Akongo, Longshoushan, Mabounie, Mudjatik North, Mudjatik South, Oulad Dlim Massif, Palmottu, Phalaborwa, Pilanesberg Complex, Pocos de Caldas, Shuswap, Sillai Patti, Sokli, South Greenland, Wollaston.

Tectonic Setting

- Collisional orogens

Typical Geological Age Range

- Precambrian to Palaeozoic; Rössing: Cambrian (508 ± 2 Ma)

Mineral Systems Model

Source

Ground preparation
- Collisional orogeny
- Post-orogenic collapse

Energy
- High temperature-low pressure metamorphism at upper amphibolite to granulite facies grade
- High heat flow, extreme geothermal gradient and partial melting of crustal sources
- Voluminous magmatism, partial melting of basement rocks and widespread leucogranite emplacement

Melts and fluids
- High-temperature, metaluminous and peraluminous fluorite-rich melts
- Associated magmatic-hydrothermal fluid circulation systems

Ligands
- (?)F

Reductants and reactants
- Marble, graphite, sulphides

Uranium
- Crystalline basement rocks (e.g., migmatised metasedimentary rocks, granitic gneisses, granitoids)

Transport

Melt/fluid pathways
- Crustal-scale fault zones
- Leucogranite bodies represent local neosomatic melt pathways

Trap

Physical
- Transition from hot, weak, ductile crust to cold, strong, brittle crust
- Dilational deformation (possibly linked to dome rotation), permeability and suction focused on intrusions
- Focusing of the volatile phase into high strain zones, flanks and apexes of large basement or granitoid domes, fault-fracture networks or anticlinal fold axes

Chemical
- Redox boundaries

Deposition
Change in redox conditions – Interaction of oxidised, uranium-bearing magmatic-hydrothermal fluids with highly reduced carbonaceous or ferruginous rocks Fractional crystallisation and cooling – Pressure and temperature decrease promoting magma cooling, fractional crystallisation and uranium enrichment in the ascending melt and volatile phase, or Depositional processes affecting ore grades and tonnages – Coalescence of uraniferous leucogranites promotes formation of larger orebodies – Secondary remobilisation, redeposition and upgrading of uranium in the oxidised zone
Preservation
– Relative tectonic stability post-uranium mineralisation

Key Reference Bibliography

BASSON, I. J., GREENWAY, G., The Rössing uranium deposit: a product of late-kinematic localization of uraniferous granites in the Central Zone of the Damara Orogen, Namibia. Journal of African Earth Sciences, 38(5), 413-435 (2004).

FAN, H., CHEN, J., WANG, S., ZHAO, J., GU, D., MENG, Y., Genesis and uranium sources of leucogranite-hosted uranium deposits in the Gaudeanmus area, Central Damara Belt, Namibia: Study of element and Nd Isotope geochemistry. Acta Geologica Sinica, 91(6), 2126-2137 (2017).

INTERNATIONAL ATOMIC ENERGY AGENCY, Geological Classification of Uranium Deposits and Description of Selected Examples. IAEA-TECDOC Series, 1842, 415p (2018).

KINNAIRD, J. A., NEX, P. A. M., A review of geological controls on uranium mineralisation in sheeted leucogranites within the Damara Orogen, Namibia. Applied Earth Science, 116(2), 68-85 (2007).

SPIVEY, M., PENKETHMAN, A., CULPAN, N., Geology and mineralization of the recently discovered Rössing South uranium deposit, Namibia. Society of Economic Geologists, Special Publication, 15, 729-746 (2010).

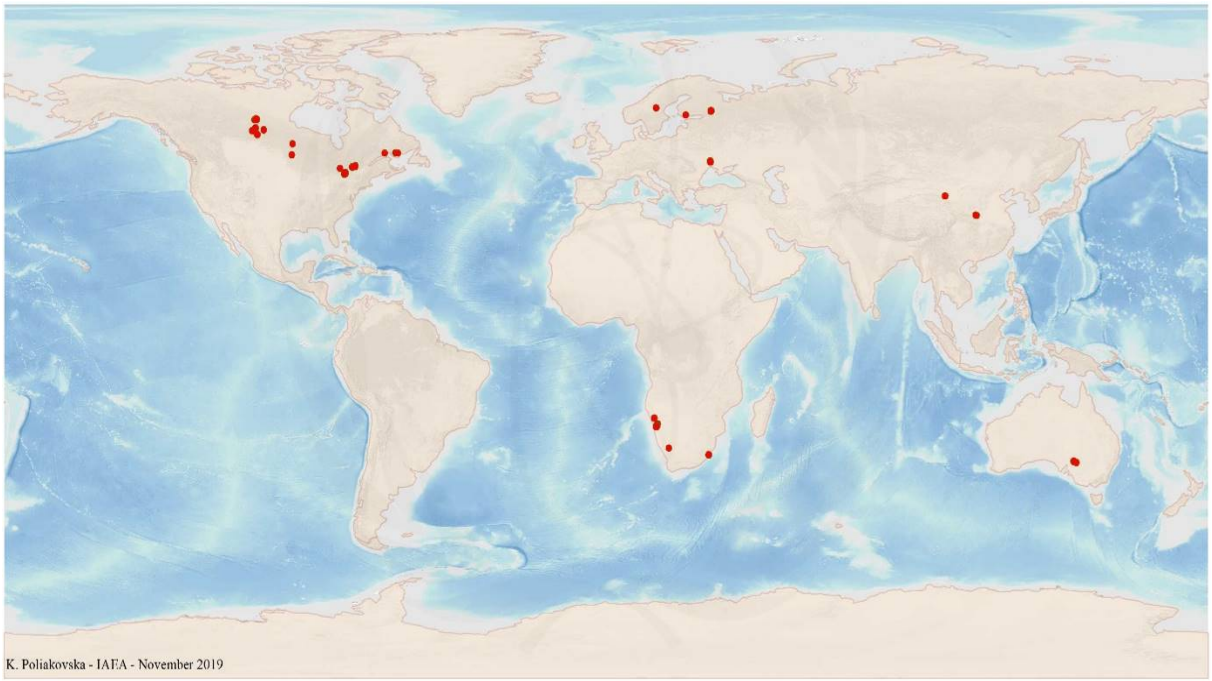

FIG. 1.1a. World distribution of selected Intrusive Anatectic uranium deposits from the UDEPO database.

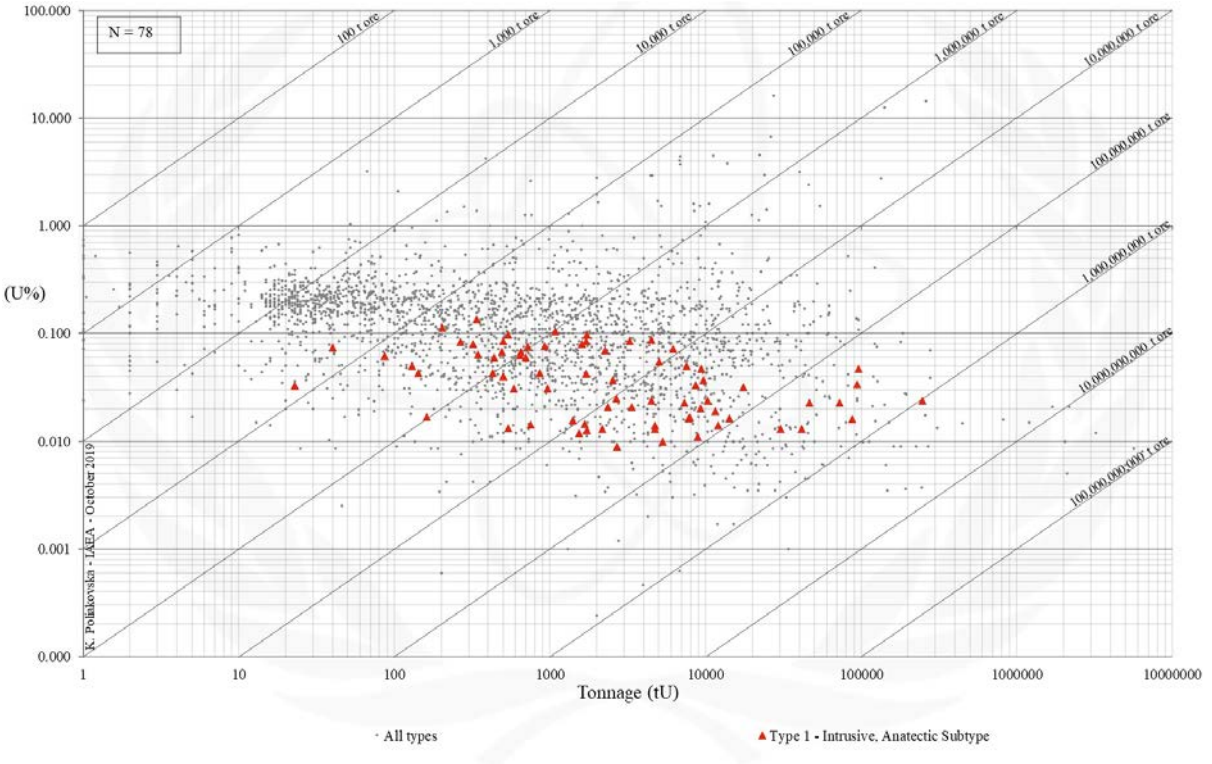

FIG. 1.1b. Grade and tonnage scatterplot highlighting Intrusive Anatectic uranium deposits from the UDEPO database.

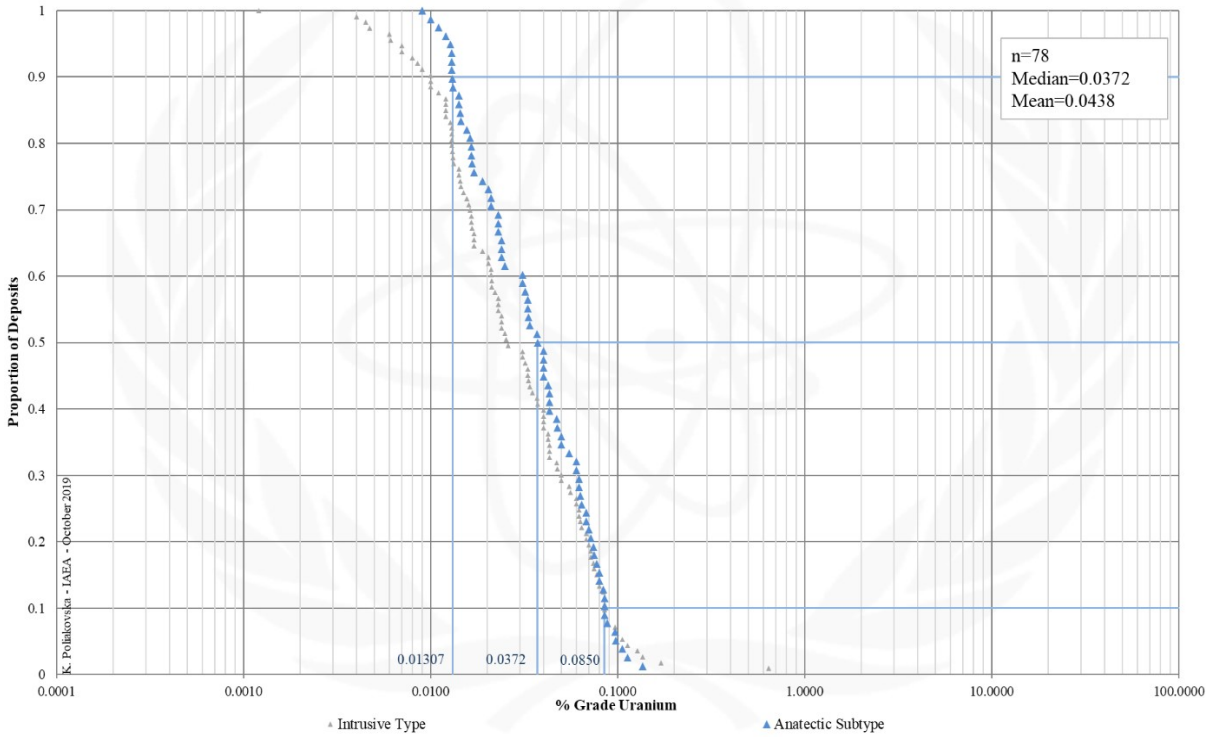

FIG. 1.1c. Grade Cumulative Probability Plot for Intrusive Anatectic uranium deposits from the UDEPO database.

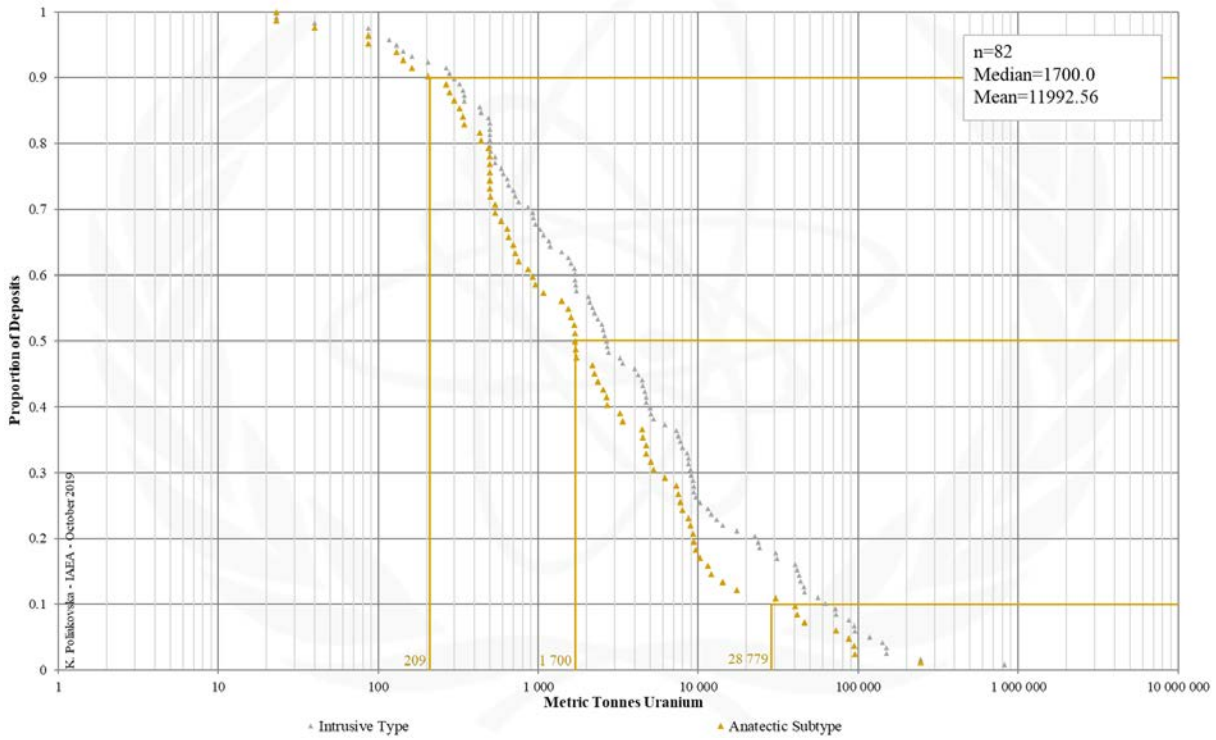

FIG. 1.1d. Tonnage Cumulative Probability Plot for Intrusive Anatectic uranium deposits from the UDEPO database.

SUBTYPE 1.2. Intrusive, Plutonic

Brief Description
- Subdivided into three classes: (1.2.1.) quartz monzonite, (1.2.2.) peralkaline complex, and (1.2.3.) carbonatite
- All classes are products of magmatic differentiation processes, albeit in different tectonic environments
- Quartz monzonite deposits are linked to highly differentiated granitic to quartz monzonitic porphyry complexes and porphyry-related copper ± molybdenum and/or gold ores in magmatic arc environments
- Peralkaline complex and carbonatite deposits are products of magmatic differentiation processes in intracontinental rift environments, which older to younger, typically grade in composition from ultramafic-mafic, to felsic, to carbonatite
- Plutonic deposits are characterised by very low and often refractory uranium concentrations (unconventional resources)
- In some cases, the uranium is recoverable as a by-product of copper or REE mining

Type Examples
- Class 1.2.1. Bingham Canyon, USA; Chuquicamata, Chile;
- Class 1.2.2. Kvanefjeld, Greenland; Poços de Caldas, Brazil
- Class 1.2.3. Phalabora, South Africa; Catalão, Brazil

Genetically Associated Deposit Types
- Subtype 2. Granite-related (applies to class 1.2.1. only)

Principal Commodities
- Class 1.2.1. Cu ± Au, Mo, Th, U (by-product only)
- Class 1.2.2. REE, Nb, Y ± Be, Cu, Hf, Li, Ta, Th, U (by-product only), Zn, Zr
- Class 1.2.3. REE, Nb, Sr, Th, Ti, Zr ± Au, Cu, U (by-product only)

Grades and Tonnages
- Average: : 0.0448, 52462.8
- Median: 0.0150, 8846.5

Number of Deposits
- Deposits: 46

Provinces
- Aileron Province, Ange, Arabian Shield, Bokan Mountain, Comechingones, Complexe dAdam Esseder, Damara

Tectonic Setting
- Class 1.2.1. Convergent plate margins
- Classes 1.2.2. and 1.2.3. Intracontinental rifts

Typical Geological Age Range
- Classes 1.2.1, 1.2.3, and 1.2.3. Archaean to Neogene; most large porphyry deposits are Mesozoic in age, or younger

Mineral Systems Model

Source – Class 1.2.1.

Ground preparation
- Development of long-lived crustal magma staging chambers in a magmatic arc above a (low-angle) subduction zone
- Melt generation in the mantle wedge and partial melting of the lower crust due to mafic underplating
- Crustal thickening/shortening, rapid uplift and exhumation triggered by collisional events

Energy
- Abnormally high geothermal gradient and high heat flow in a subduction zone environment

Melts and fluids
- Subduction-related magmatism and associated magmatic-hydrothermal fluid circulation systems

Ligands (no information for reductants and reactants)
- CO_2, HCl, H_2S, SO_2 and other volatile components

Metals
- Copper and gold may have mantle sources; molybdenum and uranium probably derived from crustal sources

Source – Classes 1.2.2. and 1.2.3.

Ground preparation
- Rifting accompanying mafic underplating and lithospheric doming
- Formation of (per-)alkaline igneous complexes associated with voluminous magmatism / large igneous provinces

Energy
- High heat flow, extreme geothermal gradient and partial melting of mantle sources

Melts and fluids
- Peralkaline or carbonatite magmas derived directly from mantle partial melts and/or indirectly by crystal fractionation of mantle-derived alkali-rich silicate melts
- Associated magmatic-hydrothermal fluid (Na-K-Cl-carbonate/bicarbonate ± F, SO_4 brine) circulation systems

Ligands (no information for reductants and reactants)
- F, Cl, S, Ca, PO

Metals
- REE may have mantle sources; uranium probably derived from crustal sources

Transport – Classes 1.2.1., 1.2.2 and 1.2.3

Melt/fluid pathways

- Regions having experienced (i) low-angle subduction of thicker than average oceanic crust (e.g., aseismic ridges, oceanic plateaus, or seamount chains), (ii) changes in dip of the subduction plate resulting in slab tearing or bending, (iii) changes from orthogonal to oblique subduction, (iv) changes in plate motion or subduction angle, promoting extension, dilational deformation and vertical permeability, or (v) reversals of arc polarity
- Dilational deformation, permeability, and fluid flux focused on subvolcanic complexes promoting vertical magma escape from crustal magma staging chambers during relaxation of regional compressional stress regime
- Crustal-scale fault zones or intracontinental rift zones

Trap – Class 1.2.1.

Physical

- Stalling of magma ascent within 1 to 4 km of the surface and emplacement into the crust of composite porphyry stocks with finger-, sill- or dyke-like porphyritic intrusions
- Exsolution of volatile phases from the cooling magma; consequential volume expansion and wallrock alteration
- Fracturing and/or brecciation of enclosing country rocks due to magmatic-hydrothermal and/or tectonic processes

Chemical

- Sulphide saturation of the magma and transfer of metals into the exsolved hydrothermal fluids

Trap – Classes 1.2.2. and 1.2.3.

Fenitisation

- Metasomatised (fenitised) magma chamber roof acts as a seal, preventing the escape of the volatile phase and promoting the accumulation of REE and associated ores within the magma chamber
- Alkali metasomatism results in (i) precipitation of fine-grained mineral phases, (ii) permeability destruction in the vent breccia, (iii) pressure build up, intense hydraulic fracturing/brecciation and explosive fluid/volatile release

Roof collapse

- Roof of the magma chamber collapses, promoting intense fracturing and/or brecciation of country rocks, channelling the ore-bearing residual melt and volatile phase outward into fault/shear zones, veins, and/or dykes

Deposition – Class 1.2.1.

Fluid cooling, depressurisation, and wallrock interaction

- Fracture- and breccia-controlled discharge of hydrothermal fluids up- and/or outwards from the magmatic source
- Metal deposition triggered by cooling and depressurisation of hydrothermal fluids and reaction with wallrocks
- Generation of extensive porphyry-related hydrothermal wallrock alteration envelopes, including overprinting (telescoping) of alteration zones linked to different magmatic-hydrothermal fluid phases

Deposition – Classes 1.2.2. and 1.2.3.

Fractional crystallisation

- Ascending melt depressurization and temperature decrease promotes metal enrichment in the residual water- and volatile-rich phases due to fractional crystallisation in the upper parts of magma chambers

Gravitational settling

- Gravitational settling of relatively dense REE and associated mineral phases at the base of the magma chamber

Fluid mixing

- Mixing of carbonatite-derived and Ca-rich formation waters causes (i) fluorite precipitation, (ii) decreased activity of F in the fluid, and (iii) destabilisation of the REE-fluoride complexes, and (iv) mineral deposition

Rapid decompression

- Hydraulic fracturing/brecciation induces rapid decompression that, in turn, triggers (i) boiling, (ii) separation of H_2O and CO_2, (iii) destabilisation of complexing ligands, and (iv) mineral deposition

Supergene enrichment

- Supergene enrichment due to weathering under tropical climatic conditions and conditions of high Eh and low pH

Preservation – Classes 1.2.1., 1.2.2 and 1.2.3

- Crustal extension and/or down-faulting or tilting of the system soon after exhumation, then relative tectonic stability

Key Reference Bibliography

ELLIOTT, H. A. L., WALL, F., CHAKHMOURADIAN, A. R., SIEGFRIED, P. R., DAHLGREN, S., WEATHERLEY, S., FINCH, A. A., MARKS, M. A. W., DOWMAN, E., DEADY, E., Fenites associated with carbonatite complexes: a review. Ore Geology Reviews, 93, 38-59 (2017).

INTERNATIONAL ATOMIC ENERGY AGENCY, Geological classification of uranium deposits and description of selected examples. IAEA TECDOC Series, 1842, 415p (2018).

PIRAJNO, F., Intracontinental anorogenic alkaline magmatism and carbonatites, associated mineral systems and the mantle plume connection. Gondwana Research, 27(3), 1181-1216 (2015).

RICHARDS, J. P., Tectono-magmatic precursors for porphyry Cu-(Mo-Au) deposit formation. Economic Geology, 98(8), 1515-1533 (2003).

SIMANDL, G. J., PARADIS, S., Carbonatites: related ore deposits, resources, footprint, and exploration methods. Applied Earth Science, 127(4), 123-152 (2018).

VERPLANCK, P. L., VAN GOSEN, B. S., SEAL, R. R, MCCAFFERTY, A. E., A deposit model for carbonatite and peralkaline intrusion-related rare earth element deposits. U.S. Geological Survey Scientific Investigations Report, 2010–5070-J, 58p (2014).

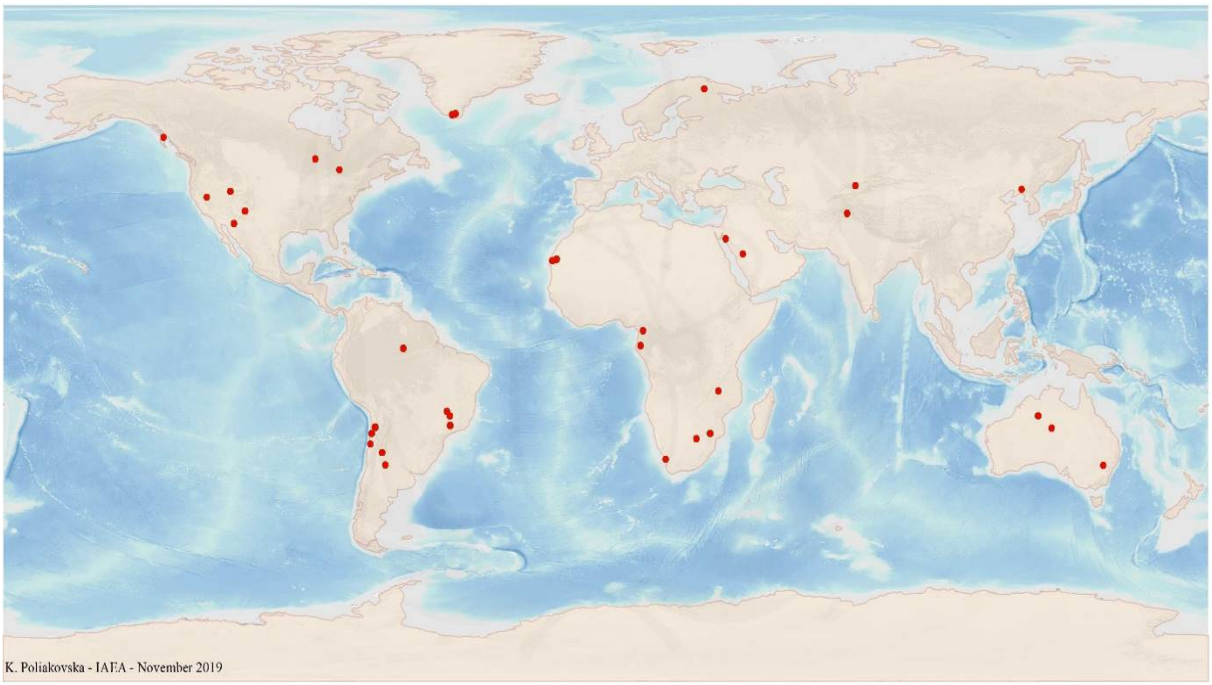

FIG. 1.2a. World distribution of selected Intrusive Plutonic uranium deposits from the UDEPO database.

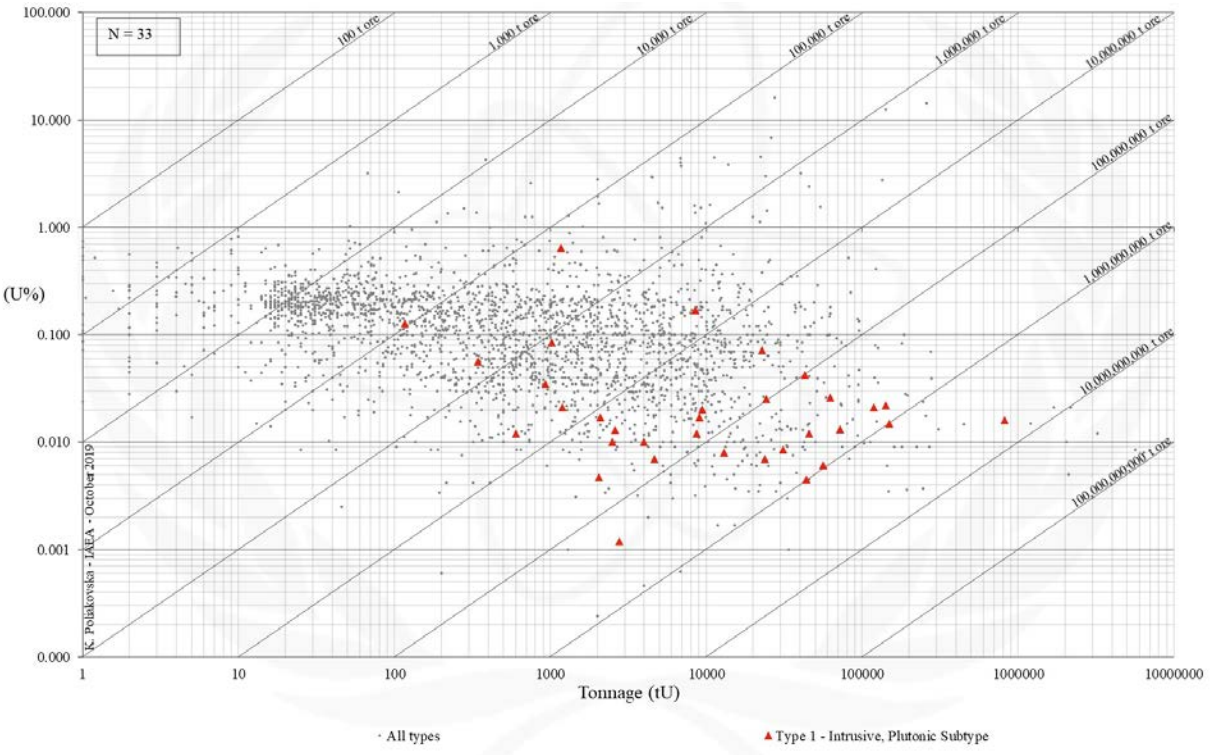

FIG. 1.2.1a. Grade and tonnage scatterplot highlighting Intrusive Plutonic uranium deposits from the UDEPO database.

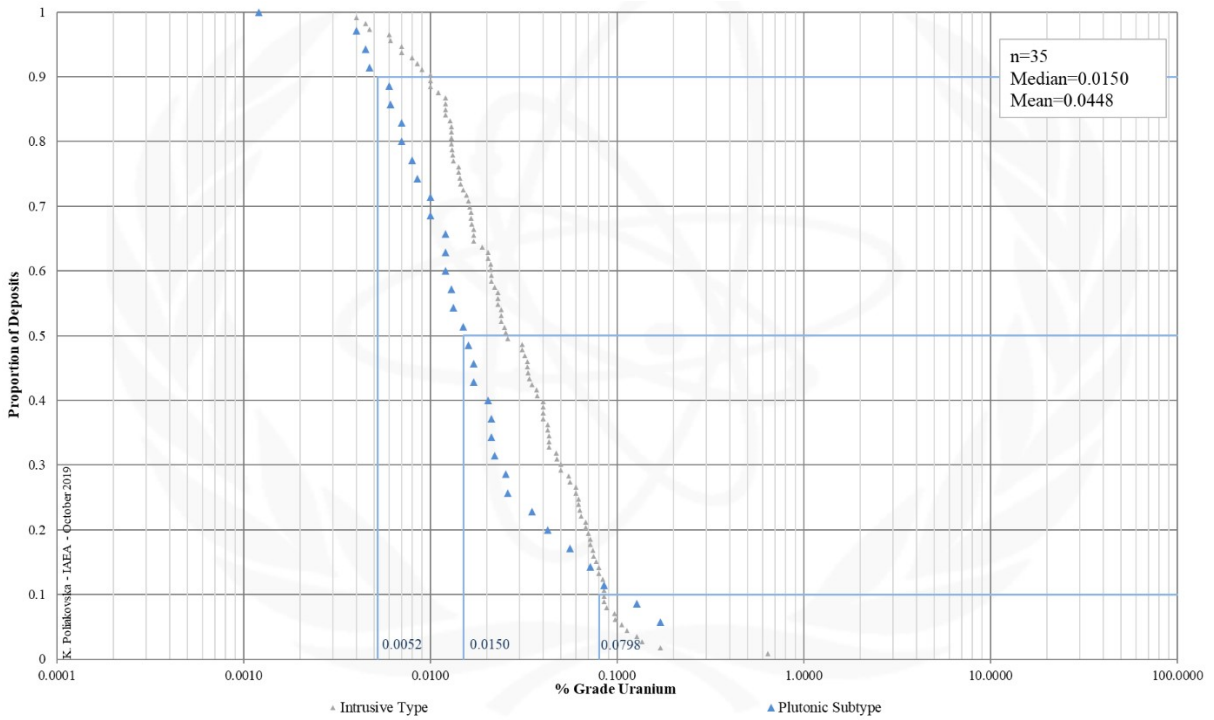

FIG. 1.2c. Grade Cumulative Probability Plot for Intrusive Plutonic uranium deposits from the UDEPO database.

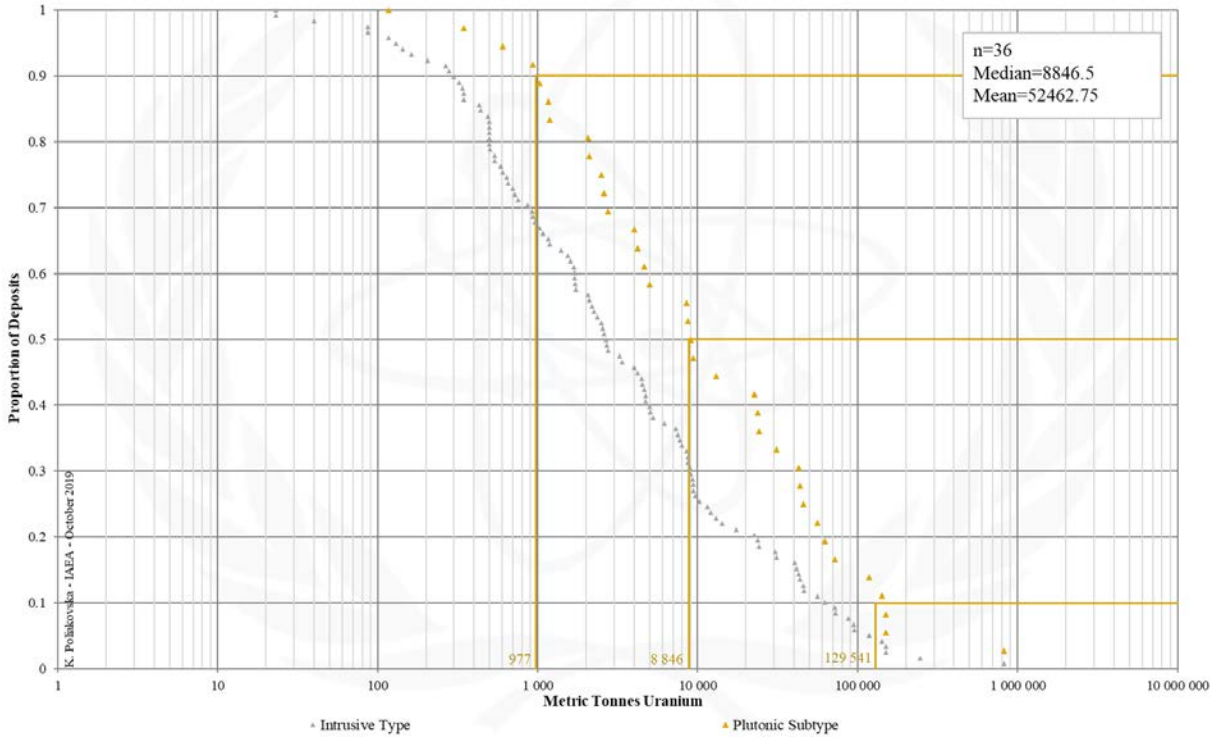

FIG. 1.2d. Tonnage Cumulative Probability Plot for Intrusive Plutonic uranium deposits from the UDEPO database.

CLASS 1.2.1. Intrusive, Plutonic, Quartz Monzonite

Brief Description

- Quartz monzonite deposits are products of magmatic differentiation processes linked to the formation of highly differentiated granitic to quartz monzonitic porphyry complexes and porphyry-related copper ± molybdenum and/or gold ores in magmatic arc environments.
- The ores have very low uranium concentrations that may be recoverable as a by-product of copper heap leaching as exemplified by the Bigham Canyon, Yerington and Twin Buttes mines.
- Quartz monzonite deposits constitute unconventional uranium resources.

Type Examples

- Bingham Canyon, Yerington, Twin Buttes, USA; Chuquicamata, Rodomiro Tomic, Chile

Genetically Associated Deposit Types

- Subtype 2. Granite-related

Principal Commodities

- Cu ± Au, Mo, Th, U (by-product only)

Grades (%) and Tonnages (tU)

- insufficent data

Number of Deposits

- 7

Provinces (undifferentiated from Intrusive Type)

- Aileron Province, Ange, Arabian Shield, Bokan Mountain, Comechingones, Complexe dAdam Esseder, Damara Central Swakop, Danfeng Shangnan, Grenville, Kanyika, Koegel Fontein, Lolodorf Akongo, Longshoushan, Mabounie, Mudjatik North, Mudjatik South, Oulad Dlim Massif, Palmottu, Phalaborwa, Pilanesberg Complex, Pocos de Caldas, Shuswap, Sillai Patti, Sokli, South Greenland, Wollaston.

Tectonic Setting

- Convergent plate margins

Typical Geological Age Range

- Broad age distribution from Archaean to Neogene; most large porphyry deposits are Mesozoic in age, or younger

Mineral Systems Model

Source

Ground preparation

- Development of a magmatic arc above a (low-angle) subduction zone;
- Melt generation in the mantle wedge below the arc and above the subduction zone;
- Partial melting of the lower crust due to mafic underplating of the crust above the mantle wedge;
- Formation of long-lived crustal magma staging chambers;
- Crustal thickening/shortening, rapid uplift and exhumation triggered by collisional events

Energy

- Abnormally high geothermal gradient and high heat flow in a subduction zone environment
- Partial melting of altered mantle wedge above a subducting plate

Melts and fluids

- Subduction-related magmatism
- Associated magmatic-hydrothermal fluid circulation systems

Ligands

- CO_2, HCl, H_2S, SO_2 and other volatile components

Reductants and reactants

- No information

Metals

- Copper and gold may have mantle sources
- Molybdenum and uranium are probably derived from crustal sources

Transport

Melt/fluid pathways

- Regions that recorded (i) low-angle subduction of thicker than average oceanic crust (e.g., aseismic ridges, oceanic plateaus, or seamount chains), (ii) changes in the dip of the subduction plate resulting in tearing or bending of the slab, (iii) changes from orthogonal to oblique subduction, (iv) changes in plate motion or angle of subduction, promoting extension, dilational deformation and vertical permeability, or (v) reversals of arc polarity
- Dilational deformation, permeability, and fluid flux focused on subvolcanic complexes promoting vertical magma escape from crustal magma staging chambers during relaxation of the regional compressional stress
- Crustal-scale fault zones

Trap

Physical

- Stalling of magma ascent within 1 to 4 km of the surface and emplacement into the crust of composite porphyry

stocks with finger-, sill- or dyke-like porphyritic intrusions
- Exsolution of volatile phases from the cooling magma and consequential volume expansion and wallrock alteration
- Recurring fracturing and/or brecciation of enclosing country rocks driven by multiple intrusive events and magmatic-hydrothermal and/or tectonic processes

Chemical
- Sulphide saturation of the magma
- Transfer of metals into hydrothermal fluids that exsolved from the magma

Deposition

Fluid cooling and depressurisation
- Fracture- and breccia-controlled discharge of hydrothermal fluids upwards and/or outwards from the magmatic source
- Metal deposition triggered by cooling and depressurisation of hydrothermal fluids

Fluid-wallrock interaction
- Metal deposition triggered by reaction of hydrothermal fluids with surrounding wall rocks
- Generation of extensive porphyry-related hydrothermal wallrock alteration envelopes, including overprinting (telescoping) of alteration zones linked to different magmatic-hydrothermal fluid phases

Preservation
- Crustal extension and/or down-faulting or tilting of the porphyry system soon after exhumation
- Relative tectonic stability post-mineralisation

Key Reference Bibliography

GRUEN, G., HEINRICH, C. A., SCHROEDER, K., The Bingham Canyon porphyry Cu-Mo-Au deposit. II. Vein geometry and ore shell formation by pressure-driven rock extension. Economic Geology, 105(1), 69-90 (2010).

INTERNATIONAL ATOMIC ENERGY AGENCY, Geological Classification of Uranium Deposits and Description of Selected Examples. IAEA-TECDOC Series, 1842, 415p (2018).

JOHN, D. A., AYUSO, R. A., BARTON, M. D., BLAKELY, R. J., BODNAR, R. J., DILLES, J. H., GRAY, F., GRAYBEAL, F. T., MARS, J. C., MCPHEE, D. K., SEAL, R. R., Porphyry copper deposit model, chapter B of mineral deposit models for resource assessment. U.S. Geological Survey Scientific Investigations Report, 2010–5070–B, 169p (2010).

LANDTWING, M. R., FURRER, C., REDMOND, P. B., PETTKE, T., GUILLONG, M., HEINRICH, C. A., The Bingham Canyon porphyry Cu-Mo-Au deposit. III. Zoned copper-gold ore deposition by magmatic vapor expansion. Economic Geology, 105(1), 91-118 (2010).

KREUZER, O. P., MILLER, A. V., PETERS, K. J., PAYNE, C., WILDMAN, C., PARTINGTON, G. A., PUCCIONI, E., MCMAHON, M. E., ETHERIDGE, M. A., Comparing prospectivity modelling results and past exploration data: a case study of porphyry Cu-Au mineral systems in the Macquarie Arc, Lachlan Fold Belt, New South Wales. Ore Geology Reviews, 71, 516-544 (2015).

REDMOND, P. B., EINAUDI, M. T., The Bingham Canyon porphyry Cu-Mo-Au deposit. I. Sequence of intrusions, vein formation, and sulfide deposition. Economic Geology, 105(1), 43-68 (2010).

RICHARDS, J. P., Tectono-magmatic precursors for porphyry Cu-(Mo-Au) deposit formation. Economic Geology, 98(8), 1515-1533 (2003).

WILKINSON, J. J., Triggers for the formation of porphyry ore deposits in magmatic arcs. Nature Geoscience, 6(11), 917-925 (2013).

ZHANG, D., AUDÉTAT, A., What caused the formation of the giant Bingham Canyon porphyry Cu-Mo-Au deposit? Insights from melt inclusions and magmatic sulfides. Economic Geology, 112(2), 221-244 (2017).

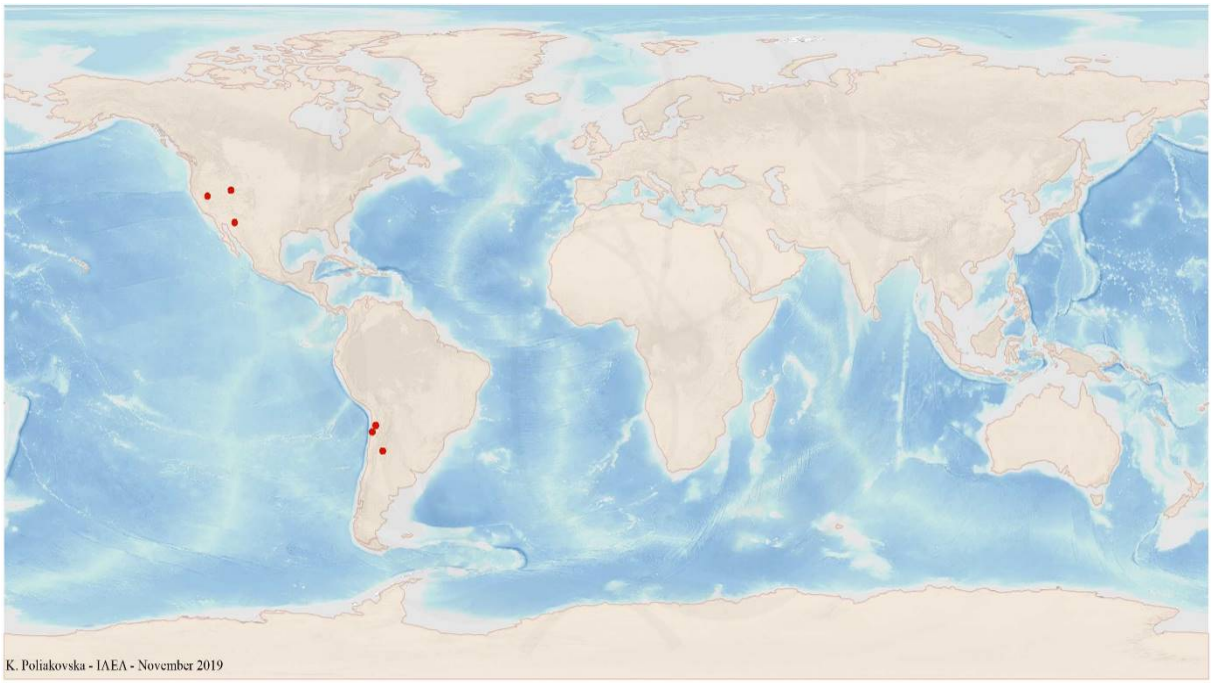

FIG. 1.2.1a. World distribution of selected Intrusive Plutonic Quartz Monzonite uranium deposits from the UDEPO database.

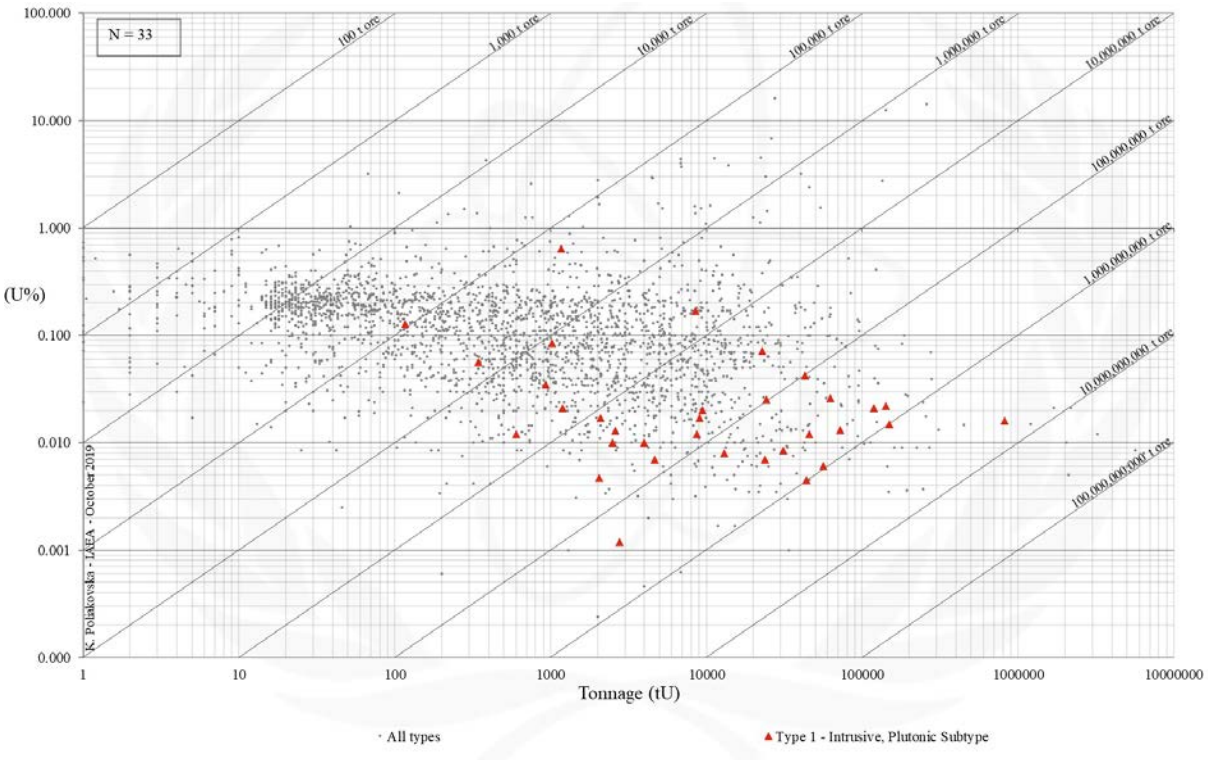

FIG. 1.2.1b. Grade and tonnage scatterplot highlighting Intrusive Plutonic data are shown due to lack of data for Quartz Monzonite Class of uranium deposits from the UDEPO database.

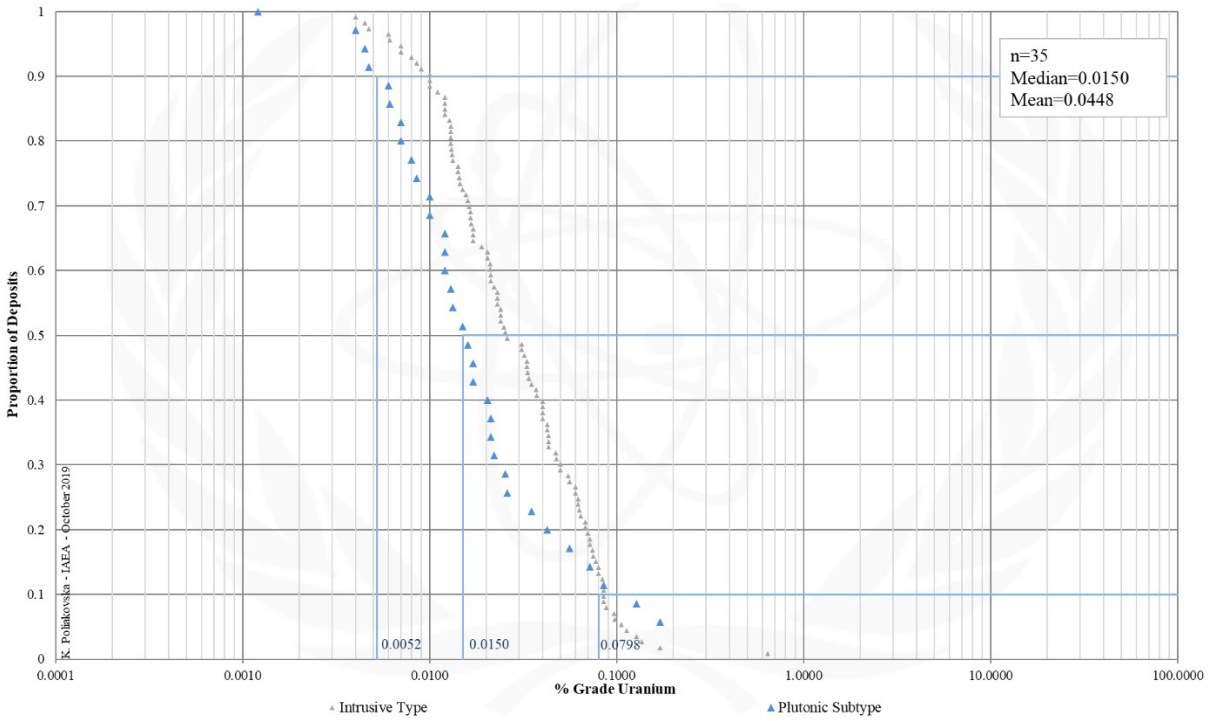

FIG. 1.2.1a. Grade Cumulative Probability Plot for Intrusive Plutonic data are shown due to lack of data for Quartz Monzonite Class of uranium deposits from the UDEPO database in comparison with Subtypes (grey).

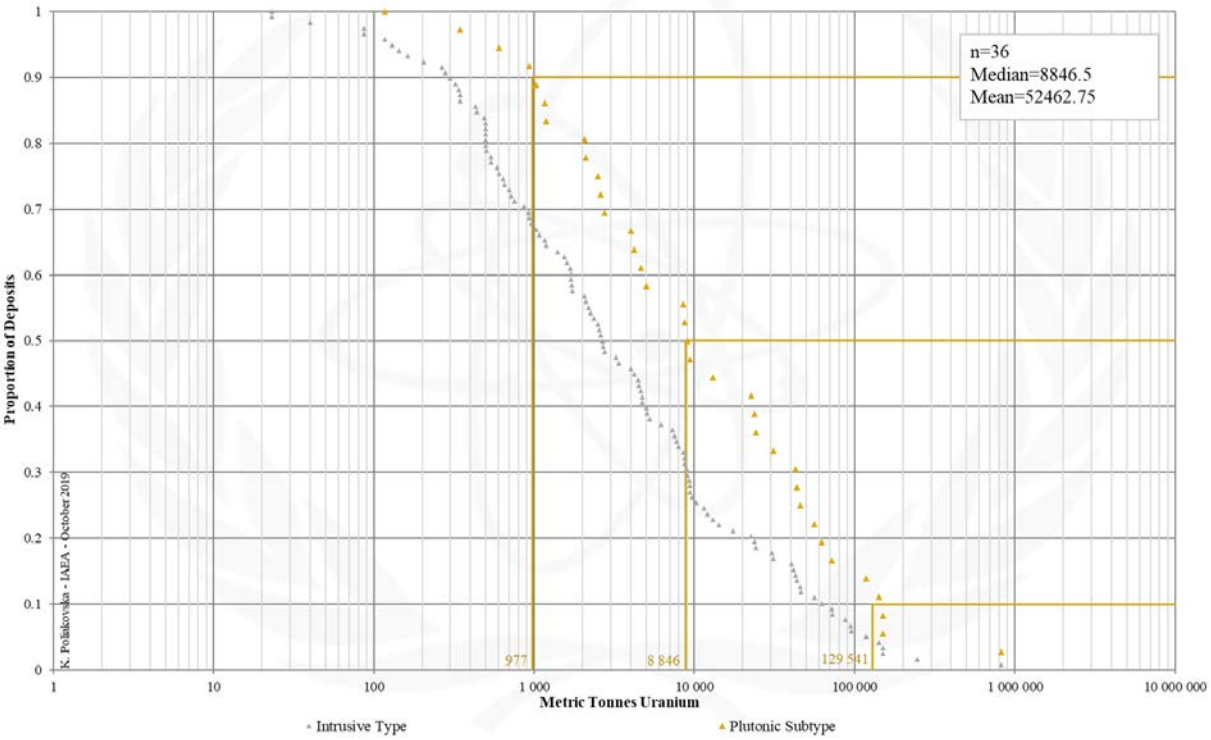

FIG. 1.2.1b. Tonnage Cumulative Probability Plot for Intrusive Plutonic data are shown due to lack of data for Quartz Monzonite Class uranium deposits.

CLASS 1.2.2. Intrusive, Plutonic, Peralkaline Complex

Brief Description

- Peralkaline complex deposits are products of magmatic differentiation processes in intracontinental rift environments linked to the formation of igneous complexes that typically illustrate a progression, from older to younger, of ultramafic-mafic to felsic to carbonatite compositions.
- REE deposits hosted in peralkaline igneous complexes may contain very low grade, often refractory uranium mineralisation taking the form of disseminations in the igneous hosts rocks. The uranium may be recoverable as a by-product of REE mining.
- Peralkaline complex deposits constitute unconventional uranium resources.

Type Examples

- Kvanefjeld, Greenland; Poços de Caldas, Brazil; Gurayah, Jabal Sayad, Saudi Arabia; Lolodorf, Cameroon; Twihinate, Morocco; Bokan Mountain, USA; Nolans Bore, Australia

Genetically Associated Deposit Types

- Class 1.2.3. Intrusive, plutonic, carbonatite

Principal Commodities

- REE, Nb, Y ± Be, Cu, Hf, Li, Ta, Th, U (by-product only), Zn, Zr

Grades (%) and Tonnages (tU)

- Average: 0.0675, 37391.2
- Median: 0.0212, 15851.5

Number of Deposits

- 18

Provinces (undifferentiated from Intrusive Type)

- Aileron Province, Ange, Arabian Shield, Bokan Mountain, Comechingones, Complexe dAdam Esseder, Damara Central Swakop, Danfeng Shangnan, Grenville, Kanyika, Koegel Fontein, Lolodorf Akongo, Longshoushan, Mabounie, Mudjatik North, Mudjatik South, Oulad Dlim Massif, Palmottu, Phalaborwa, Pilanesberg Complex, Pocos de Caldas, Shuswap, Sillai Patti, Sokli, South Greenland, Wollaston.

Tectonic Setting

- Intracontinental rifts

Typical Geological Age Range

- Broad age distribution from Archaean to Neogene

Mineral Systems Model

Source

Ground preparation
- Rifting
- Mafic underplating
- Lithospheric doming

Energy
- High heat flow, extreme geothermal gradient and partial melting of mantle sources
- Voluminous magmatism producing large igneous provinces composed of alkaline igneous rocks

Melts and fluids
- Peralkaline magmas derived from mantle partial melts and their differentiates
- Associated magmatic-hydrothermal fluid circulation systems

Ligands
- F, Cl, S, Ca, PO

Reductants and reactants
- No information

Metals
- REE may have mantle sources
- Uranium is probably derived from crustal sources

Transport

Melt/fluid pathways
- Intracontinental rift zones

Trap

Model (a)
- Metasomatised (fenitised) magma chamber roof acts as a seal, preventing the escape of the volatile phase and promoting the accumulation of REE and associated ores within the magma chamber

Model (b)
- Roof of the magma chamber is breached, promoting intense fracturing and/or brecciation of enclosing country rocks and accumulation of REE and associated ores in fault/shear zones, veins and/or dykes radiating outward

Model (c)

- Roof of the magma chamber collapses, channelling the residual melt and volatile phase into faults and fractures and leading to the formation of REE-rich vein systems

Deposition

Fractional crystallisation

- Pressure and temperature decrease promoting magma cooling and metal enrichment due to fractional crystallisation of the ascending melt
- Protracted magmatic differentiation and fractional crystallisation in crustal magma staging chambers leading to metal enrichment in water- and volatile-rich residual melts in the upper parts of magma chambers

Gravitational settling

- Gravitational settling to the base of the magma chamber of relatively dense REE and associated mineral phases and/or accumulation of REE and associated mineral phases in the magma chamber roof zone

Fluid/wallrock interaction

- Late magmatic-hydrothermal metal deposition triggered by fluid cooling and depressurisation, and by interaction of these fluids with the surrounding wall rocks

Supergene enrichment

- Supergene mineralisation in carbonatite weathering profiles under tropical climatic conditions and conditions of high Eh and low pH

Preservation

- Crustal extension and/or down-faulting or tilting of the igneous complex soon after exhumation
- Relative tectonic stability post-mineralisation

Key Reference Bibliography

BERGER, V. I., SINGER, D. A., ORRIS, G. J., Carbonatites of the world, explored deposits of Nb and REE--database and grade and tonnage models. U.S. Geological Survey Open-File Report, 2009-1139, 17p (2009).

INTERNATIONAL ATOMIC ENERGY AGENCY, Geological Classification of Uranium Deposits and Description of Selected Examples. IAEA-TECDOC Series, 1842, 415p (2018).

SIMANDL, G. J., PARADIS, S., Carbonatites: related ore deposits, resources, footprint, and exploration methods. Applied Earth Science, 127(4), 123-152 (2018).

VERPLANCK, P. L., VAN GOSEN, B. S., SEAL, R. R, MCCAFFERTY, A. E., A deposit model for carbonatite and peralkaline intrusion-related rare earth element deposits. U.S. Geological Survey Scientific Investigations Report, 2010–5070-J, 58p (2014).

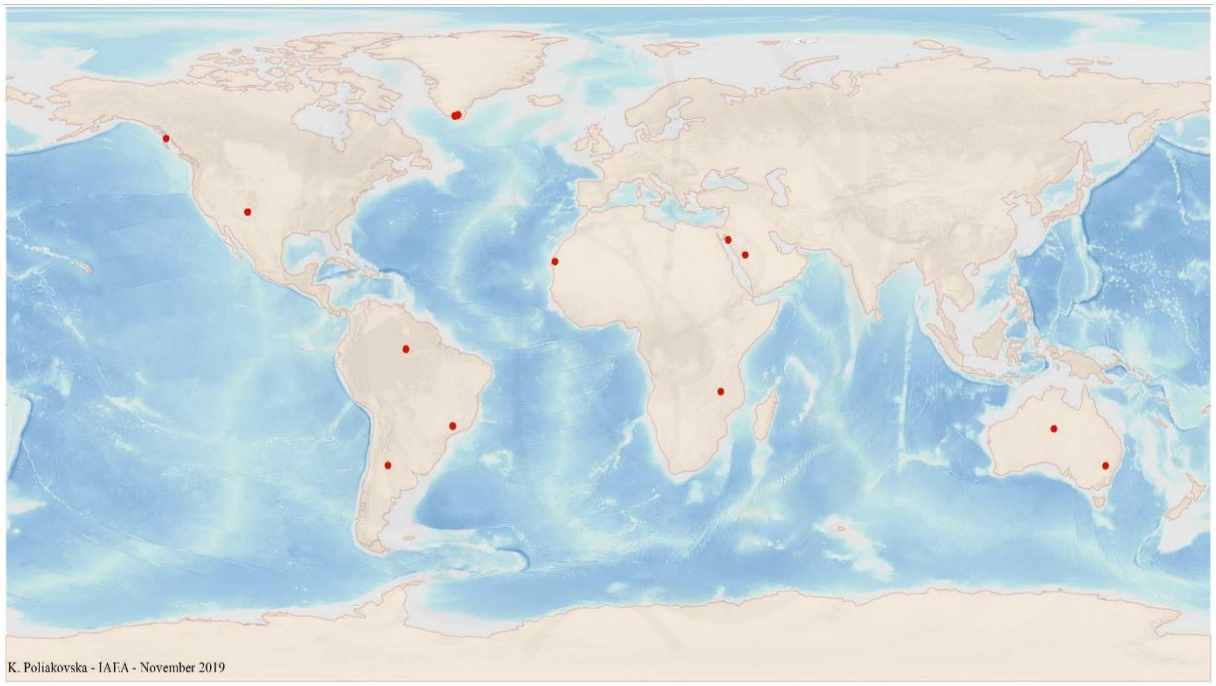

FIG. 1.2.2a. World distribution of selected Intrusive Plutonic Peralkaline Complex uranium deposits from the UDEPO database.

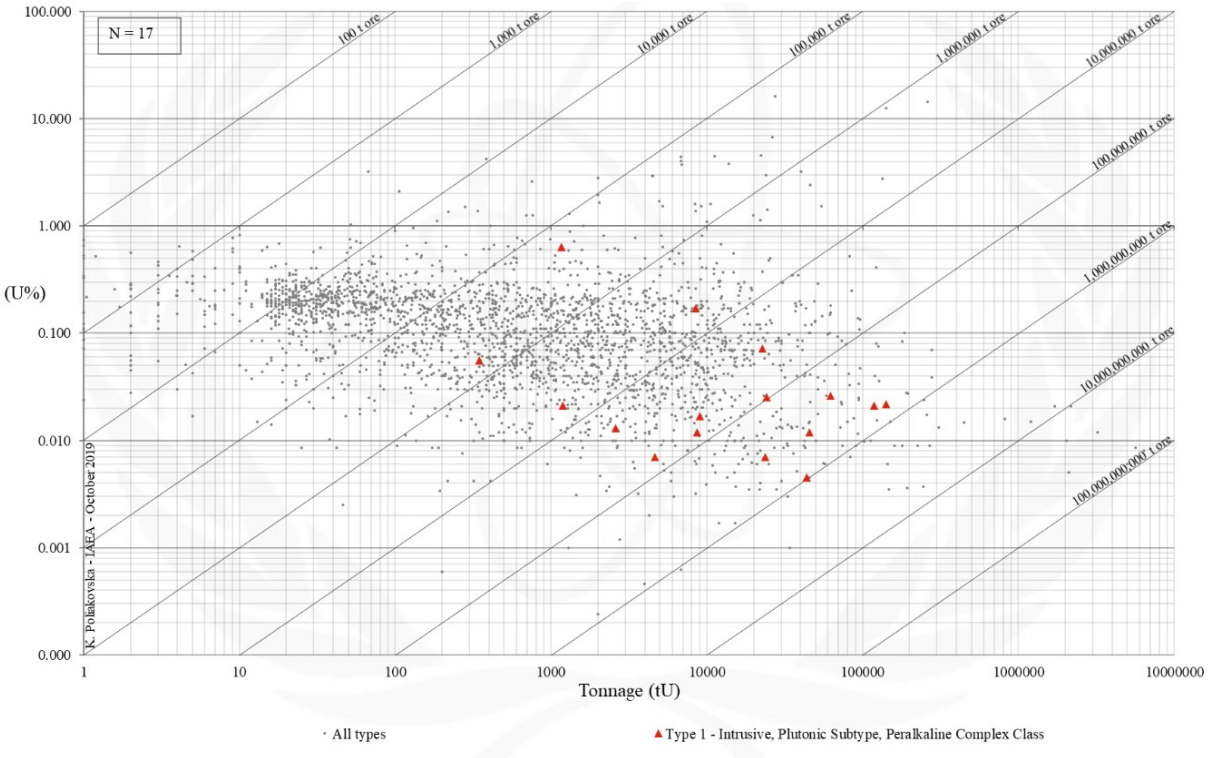

FIG. 1.2.2b. Grade and tonnage scatterplot highlighting Intrusive Plutonic Peralkaline Complex uranium deposits from the UDEPO database.

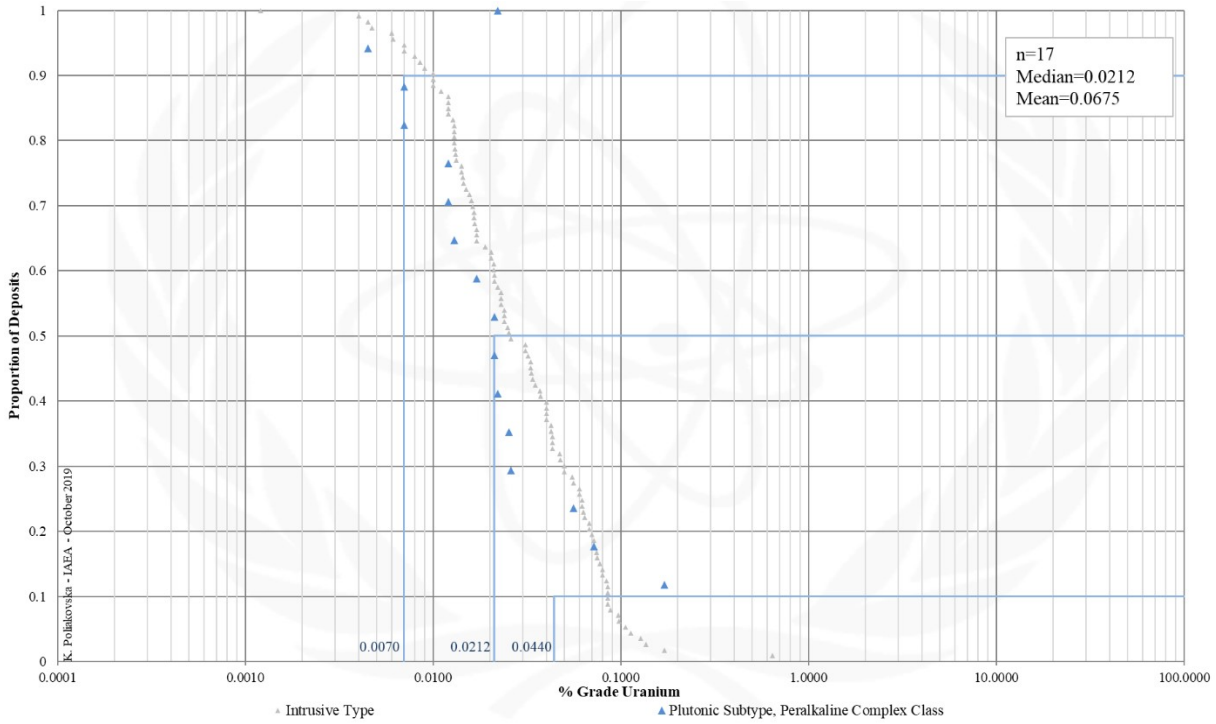

FIG. 1.2.2c. Grade Cumulative Probability Plot for Intrusive Plutonic Peralkaline Complex uranium deposits from the UDEPO database.

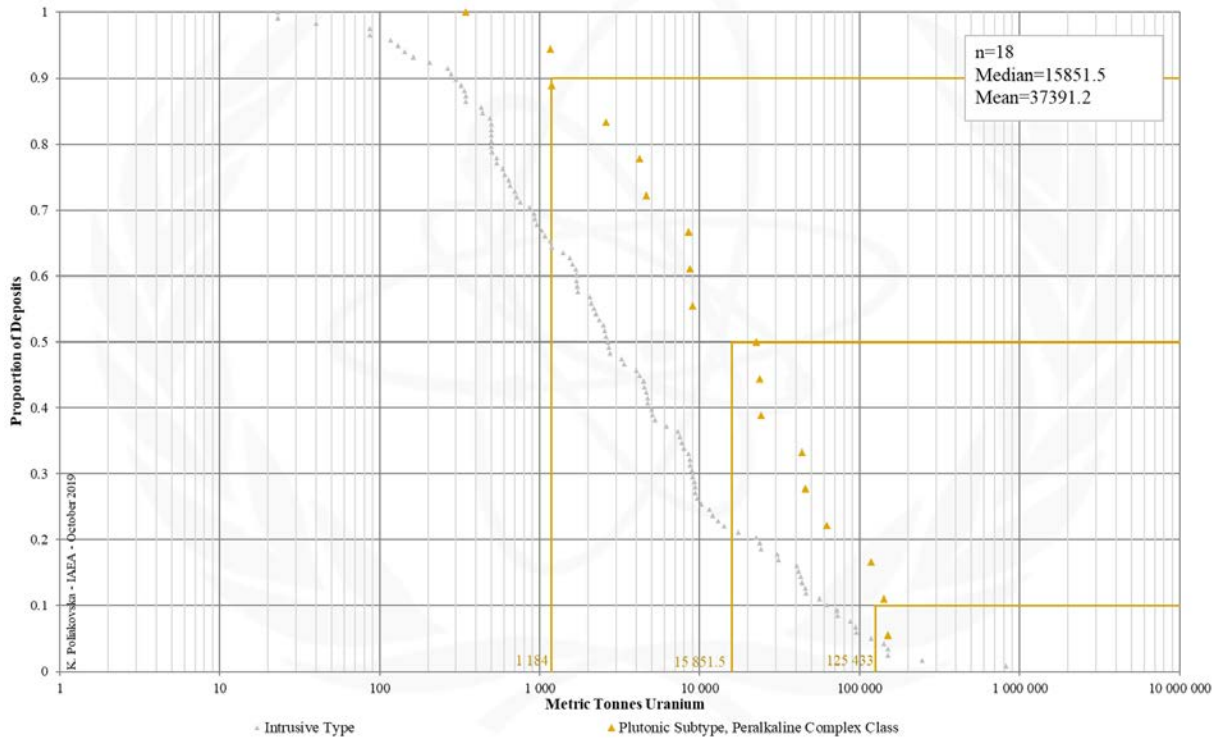

FIG. 1.2.2.d. Tonnage Cumulative Probability Plot for Intrusive Plutonic Peralkaline Complex uranium deposits from the UDEPO database.

CLASS 1.2.3. Intrusive, Plutonic, Carbonatite

Brief Description

- Similar to peralkaline complex deposits, carbonatite deposits are products of magmatic differentiation processes in intracontinental rift environments linked to the formation of igneous complexes that typically illustrate a progression, from older to younger, of ultramafic-mafic to felsic to carbonatite compositions.
- Carbonatites, commonly the final phase of peralkaline igneous complexes, are emplaced centrally and/or as dykes that may extend for kilometres into the surrounding country rocks. It is still uncertain whether the carbonatite magmas are generated as primary mantle melts or evolve from a parental alkaline-rich magma.
- REE deposits hosted in carbonatite deposits may contain very low grade, often refractory uranium mineralisation taking the form of disseminations in the igneous hosts rocks. The uranium may be recoverable as a by-product of copper mining as exemplified by the Phalabora mine.
- Carbonatite deposits constitute unconventional uranium resources.

Type Examples

- Phalabora, South Africa; Catalão, Araxa, Brazil; Sokli, Finland; Toongi, Australia

Genetically Associated Deposit Types

- Class 1.2.2. Intrusive, plutonic, peralkaline complex

Principal Commodities

- REE, Nb, Sr, Th, Ti, Zr ± Au, Cu, U (by-product only)

Grades (%) and Tonnages (tU)

- Average: 0.0183, 71500.0
- Median: 0.0120, 5000.0

Number of Deposits

- 20

Provinces (undifferentiated from Intrusive Type)

- Aileron Province, Ange, Arabian Shield, Bokan Mountain, Comechingones, Complexe dAdam Esseder, Damara Central Swakop, Danfeng Shangnan, Grenville, Kanyika, Koegel Fontein, Lolodorf Akongo, Longshoushan, Mabounie, Mudjatik North, Mudjatik South, Oulad Dlim Massif, Palmottu, Phalaborwa, Pilanesberg Complex, Pocos de Caldas, Shuswap, Sillai Patti, Sokli, South Greenland, Wollaston.

Tectonic Setting

- Intracontinental rifts

Typical Geological Age Range

- Broad age distribution from Palaeoproterozoic to Neogene

Mineral Systems Model

Source

Ground preparation
- Rifting
- Mafic underplating
- Lithospheric doming
- Formation of (per-)alkaline igneous complexes

Energy
- High heat flow, extreme geothermal gradient and partial melting of mantle sources
- Voluminous magmatism producing large igneous provinces composed of alkaline igneous rocks

Melts and fluids
- Carbonatite magmas derived directly from partial melting of mantle sources or indirectly by way of crystal fractionation of mantle-derived alkali-rich silicate melts
- Associated magmatic-hydrothermal fluid (Na-K-Cl-carbonate/bicarbonate ± F, SO_4 brine) circulation systems

Ligands
- F, Cl, S, Ca, PO

Reductants and reactants
- No information

Metals
- REE may have mantle sources
- Uranium is probably derived from crustal sources

Transport

Melt/fluid pathways
- Intracontinental rift zones

Trap

Stalling of magma ascent and cooling
- Exsolution of volatile phases from the cooling magma and consequential volume expansion (fracturing, brecciation) and wallrock alteration

Fenitisation

- Alkali metasomatism results in (i) precipitation of fine-grained mineral phases, (ii) permeability destruction in the vent breccia, (iii) pressure build up, intense hydraulic fracturing/brecciation and explosive release of fluids and volatiles from an evolving carbonatite magma below

Deposition

Fractional crystallisation

- Promotes enrichment of the residual carbonatite magma in H_2O

Rapid decompression

- Hydraulic fracturing/brecciation induces rapid decompression that, in turn, triggers (i) boiling, (ii) separation of H_2O and CO_2, (iii) destabilisation of complexing ligands, and (iv) mineral deposition

Fluid mixing

- Mixing of carbonatite-derived and Ca-rich formation waters causes (i) fluorite precipitation, (ii) decreased activity of F in the fluid, and (iii) destabilisation of the REE-fluoride complexes, and (iv) mineral deposition

Supergene processes

- Supergene mineralisation in carbonatite weathering profiles under tropical climatic conditions and conditions of high Eh and low pH

Preservation

- Crustal extension and/or down-faulting or tilting of the igneous complex soon after exhumation
- Relative tectonic stability post-mineralisation

Key Reference Bibliography

BERGER, V. I., SINGER, D. A., ORRIS, G. J., Carbonatites of the world, explored deposits of Nb and REE--database and grade and tonnage models. U.S. Geological Survey Open-File Report, 2009-1139, 17p (2009).

ELLIOTT, H. A. L., WALL, F., CHAKHMOURADIAN, A. R., SIEGFRIED, P. R., DAHLGREN, S., WEATHERLEY, S., FINCH, A. A., MARKS, M. A. W., DOWMAN, E., DEADY, E., Fenites associated with carbonatite complexes: a review. Ore Geology Reviews, 93, 38-59 (2017).

GIEBEL, R. J., GAUERT, C. D., MARKS, M. A., COSTIN, G., MARKL, G., Multi-stage formation of REE minerals in the Palabora Carbonatite Complex, South Africa. American Mineralogist, 102(6), 1218-1233 (2017).

INTERNATIONAL ATOMIC ENERGY AGENCY, Geological Classification of Uranium Deposits and Description of Selected Examples. IAEA-TECDOC Series, 1842, 415p (2018).

PIRAJNO, F., Intracontinental anorogenic alkaline magmatism and carbonatites, associated mineral systems and the mantle plume connection. Gondwana Research, 27(3), 1181-1216 (2015).

SIMANDL, G. J., PARADIS, S., Carbonatites: related ore deposits, resources, footprint, and exploration methods. Applied Earth Science, 127(4), 123-152 (2018).

VERPLANCK, P. L., VAN GOSEN, B. S., SEAL, R. R, MCCAFFERTY, A. E., A deposit model for carbonatite and peralkaline intrusion-related rare earth element deposits. U.S. Geological Survey Scientific Investigations Report, 2010–5070-J, 58p (2014).

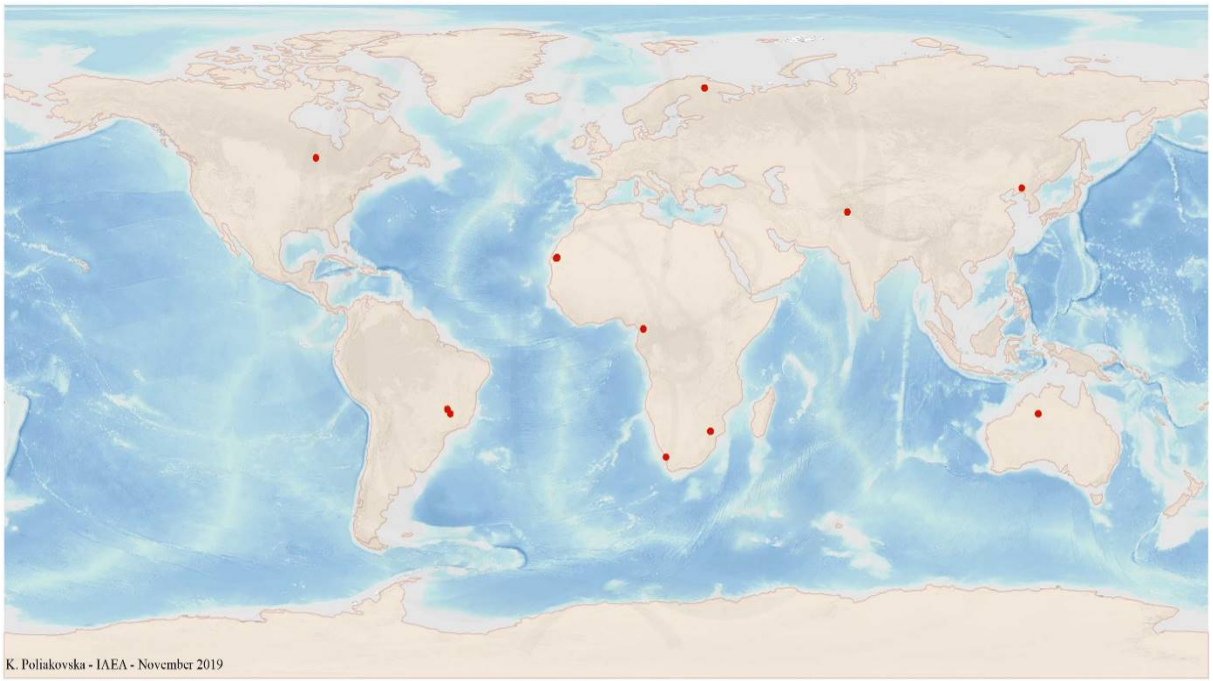

FIG. 1.2.3a. World distribution of selected Intrusive Plutonic Carbonatite uranium deposits from the UDEPO database.

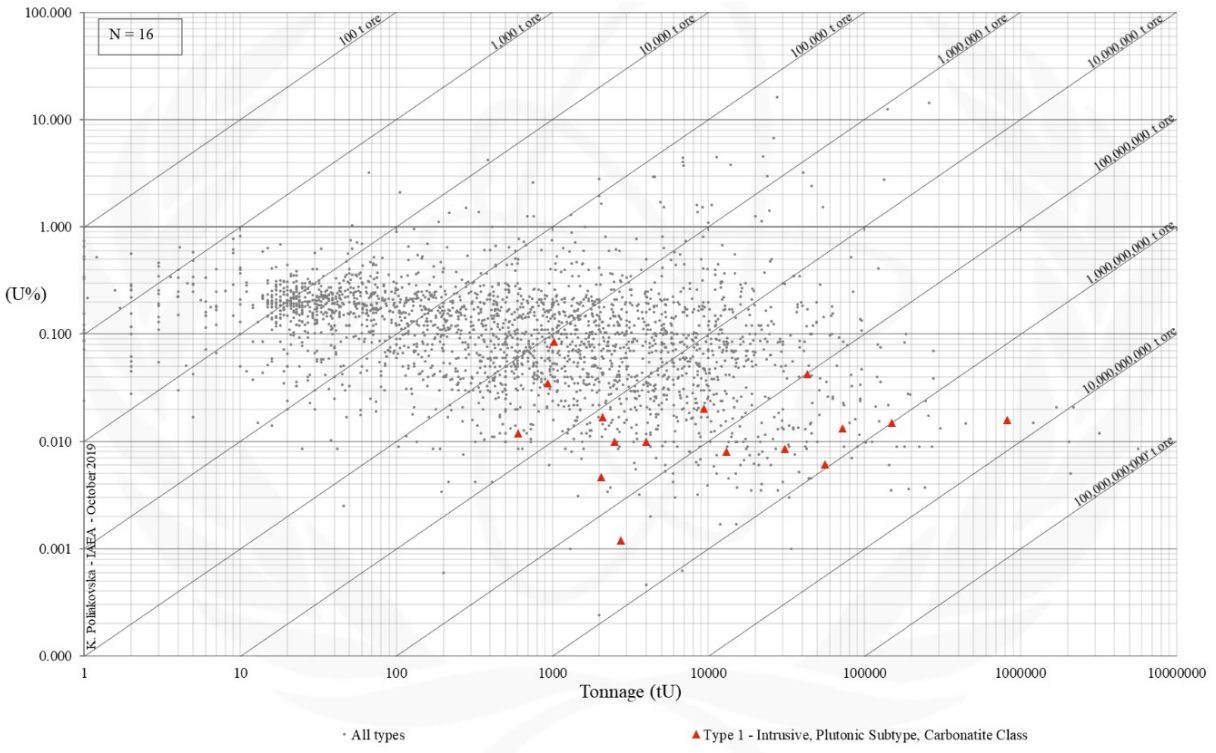

FIG. 1.2.3b. Grade and tonnage scatterplot highlighting Intrusive Plutonic Carbonatite uranium deposits from the UDEPO database.

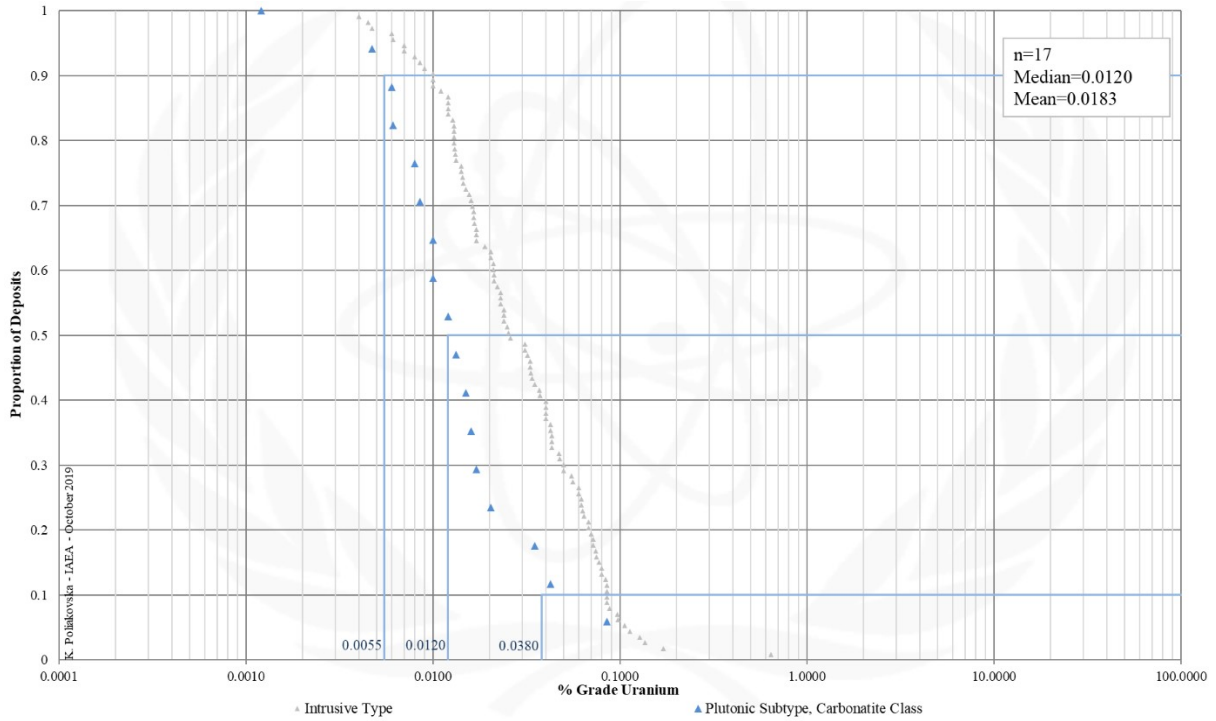

FIG. 1.2.3c. Grade Cumulative Probability Plot for Intrusive Plutonic Carbonatite uranium deposits from the UDEPO database.

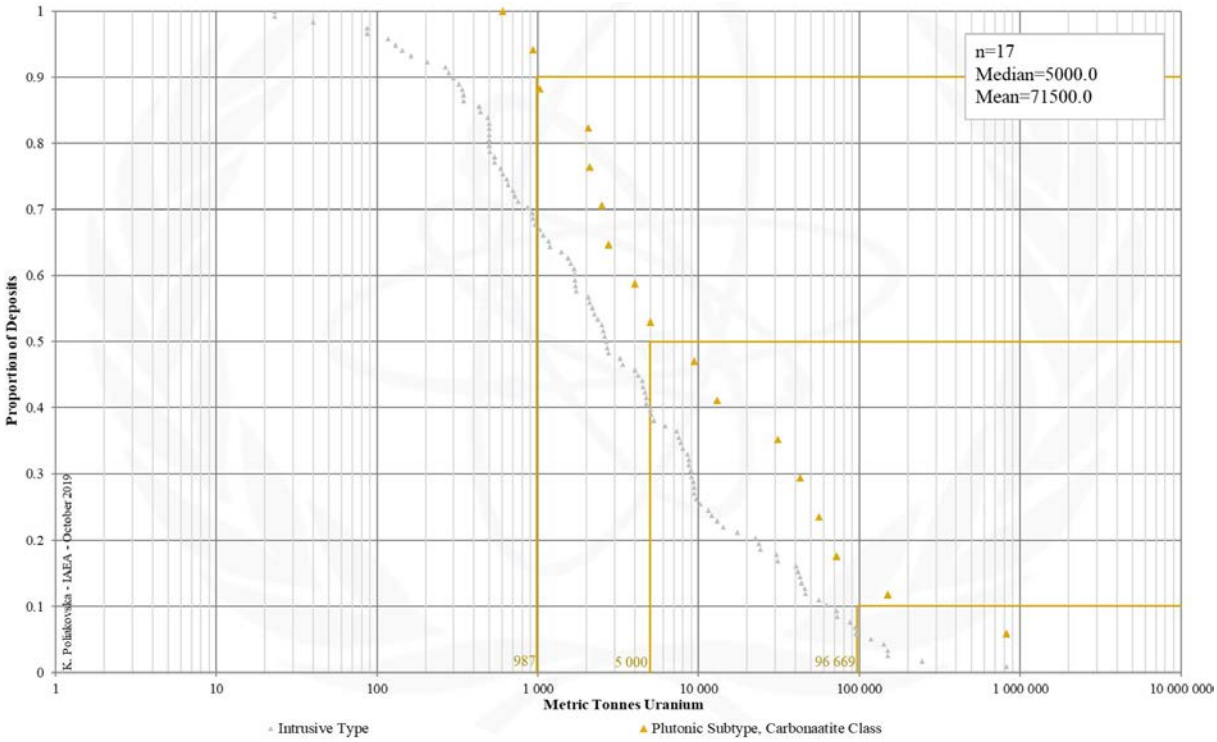

FIG. 1.2.3b. Tonnage Cumulative Probability Plot for Intrusive Plutonic Carbonatite uranium deposits from the UDEPO database.

Appendix II

GRANITE-RELATED

TYPE 2. Granite-Related

Brief Description

- Granite-related deposits occur in collisional orogen, well inboard of fossil convergent plate margins and often spatially associated with tin-tungsten and intrusion-related gold provinces.
- The uranium ores take the form of vein-, stockwork- or episyenite-hosted deposits enclosed by, at the contact with or in the periphery of granitic intrusions, in particular highly differentiated leucogranites.
- Two subtypes, endogranitic and perigranitic, can be distinguished based on their spatial relationships with granitic intrusions and the surrounding country rocks.
- Endogranitic deposits (subtype 2.1) are typically monometallic (U) and largely confined to granite.
- Perigranitic deposits (subtype 2.2), on the other hand, may be mono- (U) or polymetallic (U ± Ag, As, Bi, Co, Ni) and are typically confined to the country rocks at the contact with and/or surrounding granitic intrusions.

Subtypes

- 2.1. Granite-related, endogranitic
- 2.2. Granite-related, perigranitic

Type Examples

- Subtype 2.1. La Crouzille district, France; Xiazhuang district, China
- Subtype 2.2. Příbram district, Czech Republic; Niederschlema, Germany

Principal Commodities

- U ± Ag, As, Bi, Co, Ni

Grades (%) and Tonnages (tU)

- Average: 0.2030, 1280.8
- Median: 0.1600, 72.0

Number of Deposits

- 667

Provinces

- Alto Alentejo, Aguila, Altai Belt, Amorican Massif, Andujar, Asele, Bange Jiali, Beiras, Burgas, Burro Mountains, Cabeza de Araya, Central Bohemian, Chandu, Coast Plutonic Complex, Copper Mountain, Cornwall, Criffel Granodiorite, East Balkan, Erzgebirge Karlovy Vary Massif, Fichtelgebirge, Finhaut Salvan Aiguilles Rouges Massif, Gogi Kanchankayi, Horni Slavkov, Hotagen Olden Window, Janja Massif, Jiuyishan Jinjiling, Kedougou Kenieba, Kentai Daur, Korolevo Chasovo, La Haba Don Benito, La Jara Sierra De Altamira, La Preciosa, Los Gigantes, Massif Central, Mirandela, North Qinling, Northern Grauwackenzone West Balkan, Northern Rocky Mountains, Nubian Shield, Qimen Tagh, Rila Mountains, Savoy Alps, Schwarzwald, Sonora, Southern Kalyma River, Taoshan Zhuguang Belt, Tingogasta, Villar de Peralonso, West Sredna Gora, Western Cameroon Domain, Westsudetic Silesian.

Tectonic Setting

- Collisional orogens

Typical Geological Age Range

- Palaeozoic to Mesozoic

Mineral Systems Model

Source

Ground preparation

- Orogenesis
- Emplacement of uraniferous (leuco-)granitoids
- Hornfelsing of country rocks in contact metamorphic aureoles
- Development or reactivation of graben structures facilitating infiltration of meteoric and/or basinal brines
- Pervasive wallrock alteration prior to mineralisation

Energy

- High heat flow, extreme geothermal gradient and partial melting of mantle and/or crustal sources
- Voluminous magmatism and emplacement of felsic to intermediate, peraluminous intrusions

Fluids

- Magmatic-hydrothermal fluids
- Unknown, could be meteoric fluids, basinal brines, or metamorphic fluids

Ligands

- Ca, Na, CO_2

Reductants

- Reducing lithologies; sulphides; Fe^{2+} silicates; hydrocarbons; H_2S

Uranium

- Peraluminous U-enriched granitoids (in particular peraluminous two-mica leucogranites containing easily leachable uraninite); U-enriched high-K calc-alkaline granitoids; U-enriched basement rocks

Transport

Fluid pathways

- Crustal-scale fault zones

- Anticlinal hinge zones
- Stratigraphic aquifers (overlying basin successions)

Trap

Physical

- Transient breaching of physical barriers/seals, catastrophic rock failure and concomitant structurally controlled and highly focused fluid flow controlled by gradients in permeability and hydraulic head
- Gradients in permeability and hydraulic head are maximised at fault irregularities, fault tips and wings, fault intersections, fault damage zones characterised by high fracture density, competency contrasts, regional unconformities, apices of granitic cusps and ridges, strain shadows and contact aureoles around intrusive bodies, fold axes and fold axial cleavages, folds truncated by faults; lithological contacts or episyenites

Deposition

Phase separation

- Fluid unmixing due to depressurisation

Fluid/wallrock interaction

- Chance in redox conditions due to interaction of oxidised fluids and reduced wall rocks

Fluid mixing

- Chance in redox conditions due to interaction of oxidised fluids and reduced (H_2S-bearing) brines

Preservation

- Relative tectonic stability post-uranium mineralisation
- Subsidence and burial of the uranium mineralised rocks

Key Reference Bibliography

DAHLKAMP, F. J., Uranium Deposits of the World: Asia. Springer, Berlin, Heidelberg, 492p (2009).

DAHLKAMP, F. J., Uranium Deposits of the World: Europe. Springer, Berlin, Heidelberg, 792p (2016).

DOLNÍČEK, Z., RENÉ, M., HERMANNOVÁ, S., PROCHASKA, W., Origin of the Okrouhlá Radouň episyenite-hosted uranium deposit, Bohemian Massif, Czech Republic: fluid inclusion and stable isotope constraints. Mineralium Deposita, 49(4), 409-425 (2014).

INTERNATIONAL ATOMIC ENERGY AGENCY, Geological Classification of Uranium Deposits and Description of Selected Examples. IAEA-TECDOC Series, 1842, 415p (2018).

RUZICKA, V., Vein uranium deposits. Ore Geology Reviews, 8(3-4), 247-276 (1993).

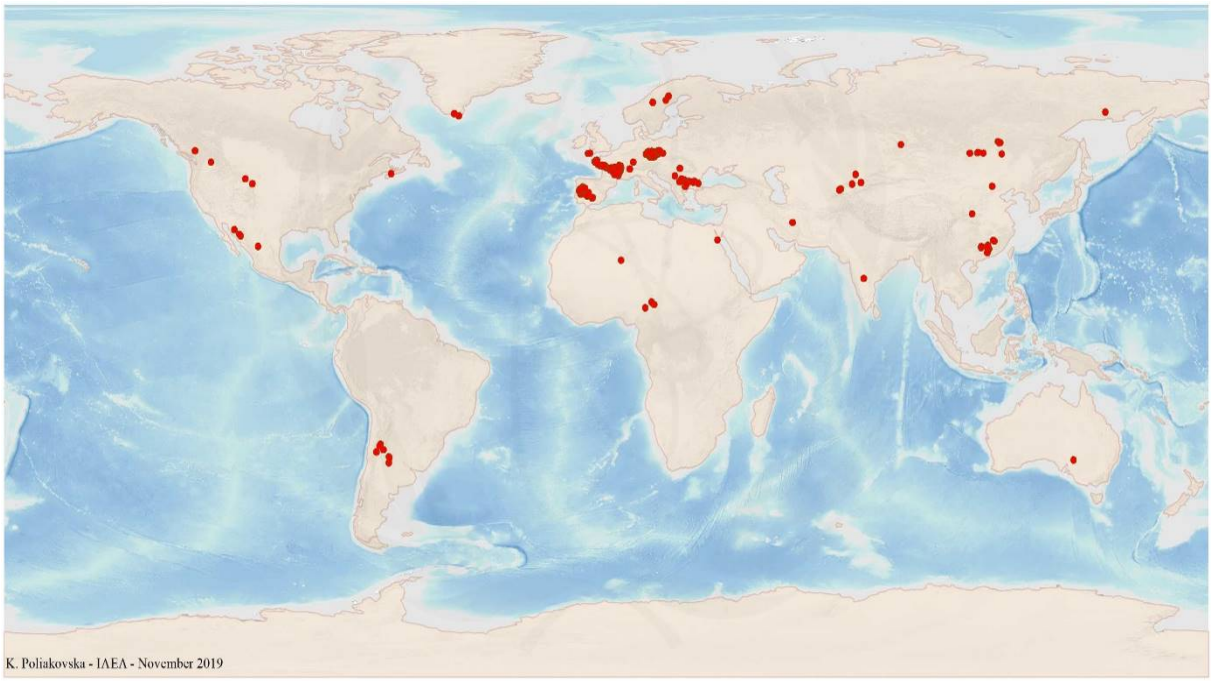

FIG. 2a. World distribution of selected Granite-Related uranium deposits from the UDEPO database.

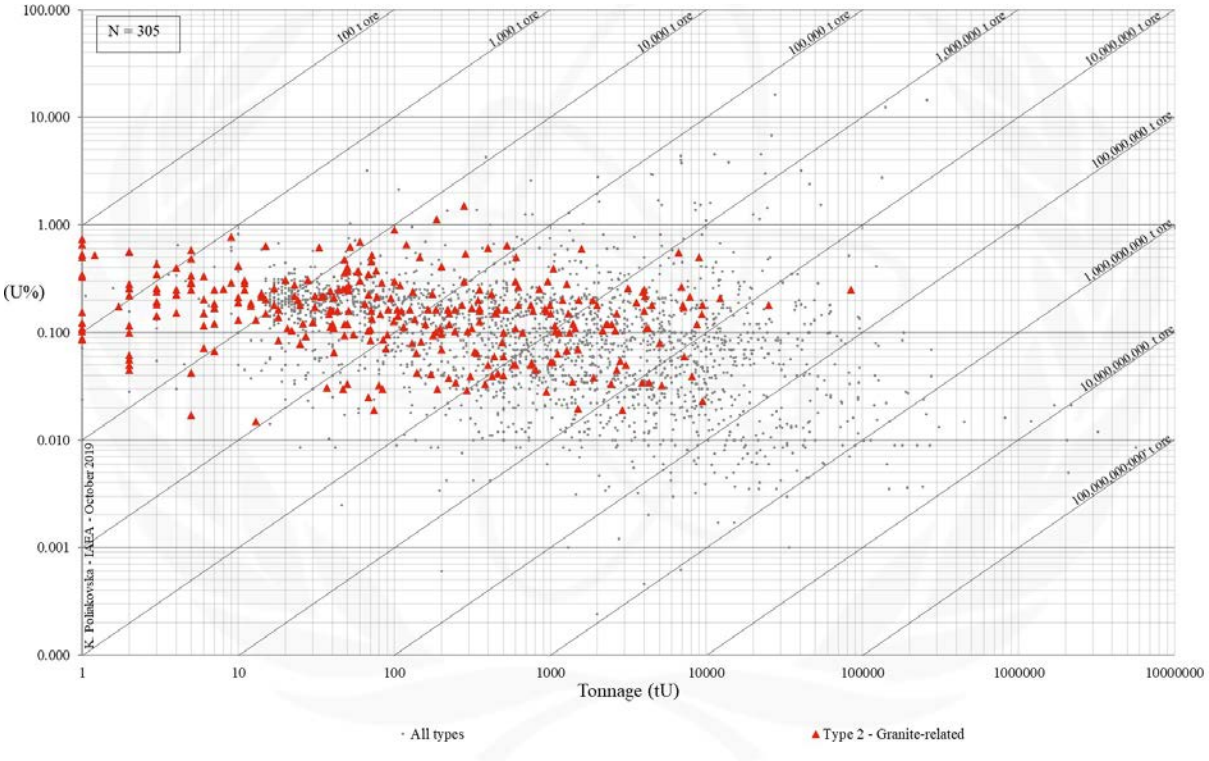

FIG. 2b. Grade and tonnage scatterplot highlighting Granite-Related uranium deposits from the UDEPO database.

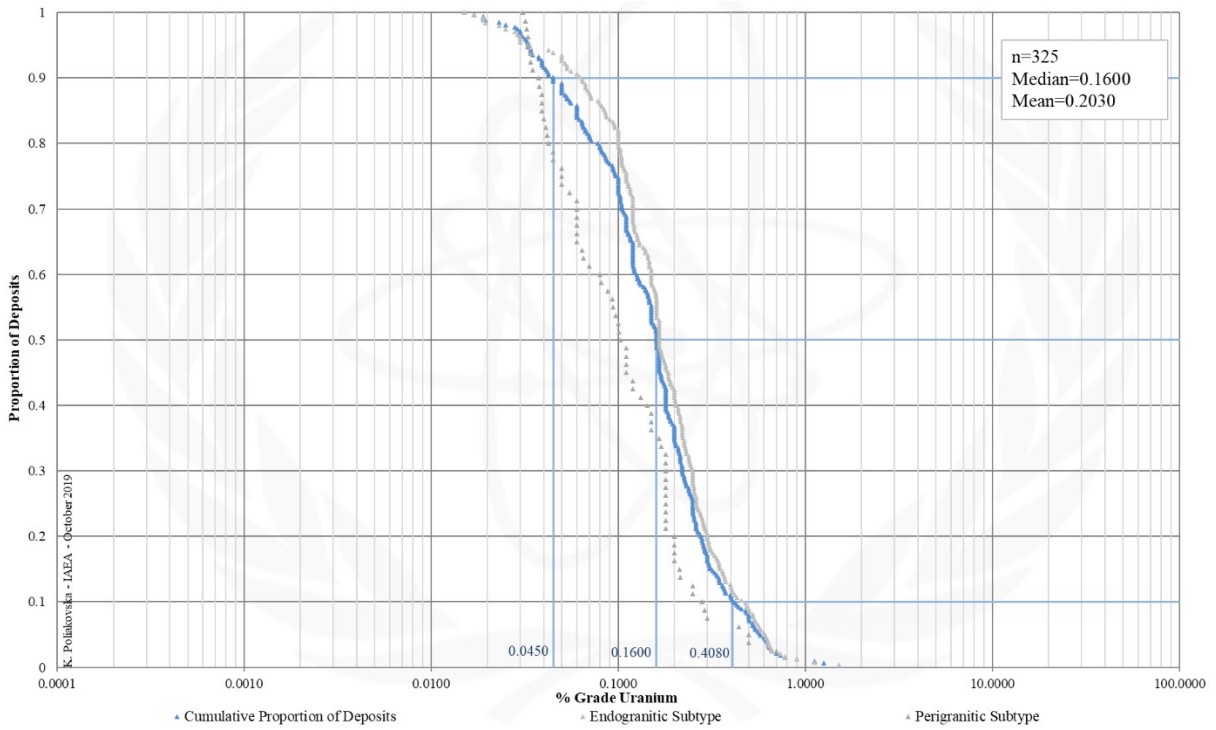

FIG. 2c. Grade Cumulative Probability Plot for Granite-Related uranium deposits from the UDEPO database.

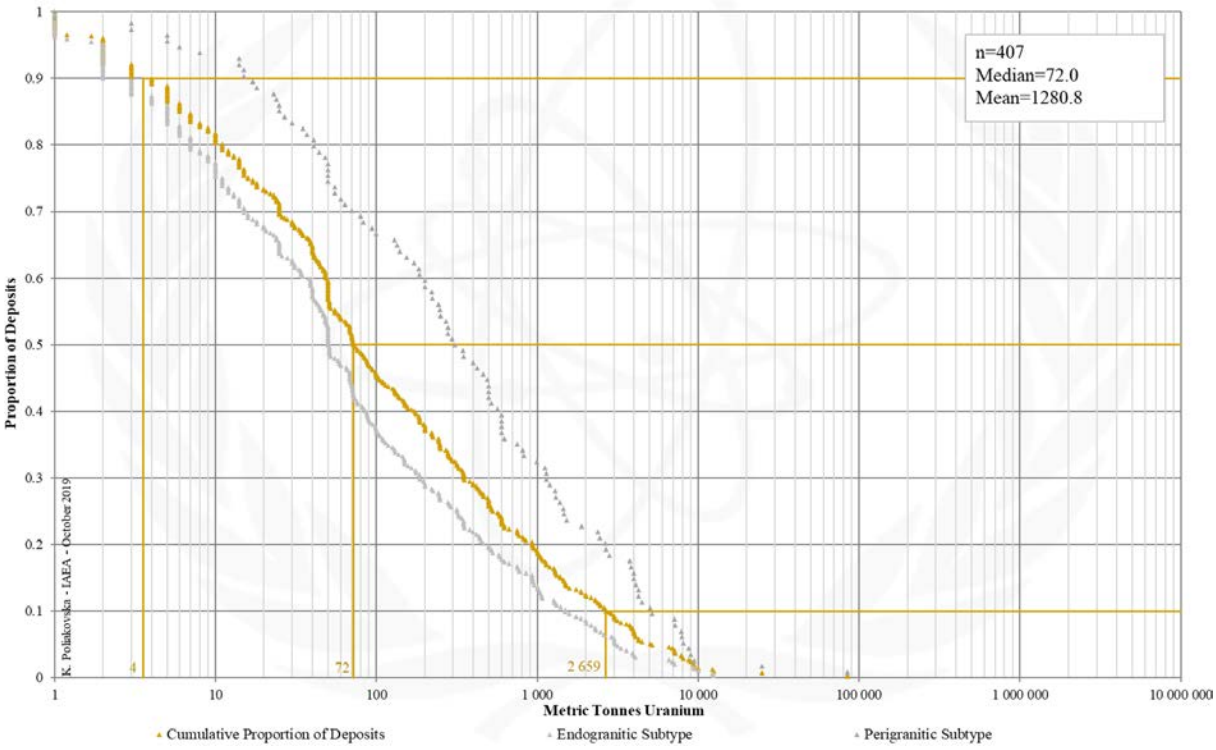

FIG. 2d. Tonnage Cumulative Probability Plot for Granite-Related uranium deposits from the UDEPO database.

SUBTYPE 2.1. Granite-Related, Endogranitic

Brief Description

- Granite-related deposits occur in collisional orogen, well inboard of fossil convergent plate margins and often spatially associated with tin-tungsten and intrusion-related gold provinces.
- The uranium ores take the form of vein-, stockwork- or episyenite-hosted deposits enclosed by, at the contact with or in the periphery of granitic intrusions, in particular highly differentiated leucogranites.
- Two subtypes, endogranitic and perigranitic, can be distinguished based on their spatial relationships with granitic intrusions and the surrounding country rocks.
- Endogranitic deposits (subtype 2.1) are typically monometallic (U) and largely confined to granite.

Type Examples

- La Crouzille, Bernardan and La Marche districts, France; Xiazhuang district, China; Gornoye, Russian Federation

Genetically Associated Deposit Types

- Subtype 1.1. Intrusive, anatectic (pegmatite-alaskite)
- Subtype 2.2. Granite-related, perigranitic
- Subtype 5.1.1. Metasomatite, Sodium (Na)-metasomatite, granite derived
- Subtype 5.3. Metasomatite, skarn

Principal Commodities

- U

Grades (%) and Tonnages (tU)

- Average: 0.2210, 595.5
- Median: 0.1650, 50

Number of Deposits

- 444

Provinces (undifferentiated from Granite-related Type)

- Alto Alentejo, Aguila, Altai Belt, Amorican Massif, Andujar, Asele, Bange Jiali, Beiras, Burgas, Burro Mountains, Cabeza de Araya, Central Bohemian, Chandu, Coast Plutonic Complex, Copper Mountain, Cornwall, Criffel Granodiorite, East Balkan, Erzgebirge Karlovy Vary Massif, Fichtelgebirge, Finhaut Salvan Aiguilles Rouges Massif, Gogi Kanchankayi, Horni Slavkov, Hotagen Olden Window, Janja Massif, Jiuyishan Jinjiling, Kedougou Kenieba, Kentai Daur, Korolevo Chasovo, La Haba Don Benito, La Jara Sierra De Altamira, La Preciosa, Los Gigantes, Massif Central, Mirandela, North Qinling, Northern Grauwackenzone West Balkan, Northern Rocky Mountains, Nubian Shield, Qimen Tagh, Rila Mountains, Savoy Alps, Schwarzwald, Sonora, Southern Kalyma River, Taoshan Zhuguang Belt, Tingogasta, Villar de Peralonso, West Bohemian, West Kunlanshan, West Sredna Gora

Tectonic Setting

- Collisional orogens

Typical Geological Age Range

- Palaeozoic to Mesozoic

Mineral Systems Model

Source

Ground preparation
- Orogenesis
- Emplacement of uraniferous (leuco-)granitoids
- Hornfelsing of country rocks in contact metamorphic aureoles
- Development or reactivation of graben structures facilitating infiltration of meteoric and/or basinal brines
- Pervasive wallrock alteration prior to mineralisation

Energy
- High heat flow, extreme geothermal gradient and partial melting of mantle and/or crustal sources
- Voluminous magmatism and emplacement of felsic to intermediate, peraluminous intrusions

Fluids
- Magmatic-hydrothermal fluids
- (?)Meteoric fluids, (?)basinal brines, (?)metamorphic fluids

Ligands
- Ca, Na, CO_2

Reductants
- Reducing lithologies; sulphides; Fe^{2+} silicates; hydrocarbons; H_2S

Uranium
- Peraluminous U-enriched granitoids (in particular peraluminous two-mica leucogranites containing easily leachable uraninite); U-enriched high-K calc-alkaline granitoids; U-enriched basement rocks

Transport

Fluid pathways
- Crustal-scale fault zones

- Anticlinal hinge zones
- Stratigraphic aquifers (overlying basin successions)

Trap

Physical

- Transient breaching of physical barriers/seals, catastrophic rock failure and concomitant structurally controlled and highly focused fluid flow controlled by gradients in permeability and hydraulic head
- Gradients in permeability and hydraulic head are maximised at fault irregularities, fault tips and wings, fault intersections, fault damage zones characterised by high fracture density, competency contrasts, regional unconformities, apices of granitic cusps and ridges, strain shadows and contact aureoles around intrusive bodies, fold axes and fold axial cleavages, folds truncated by faults; lithological contacts or episyenites

Deposition

Phase separation

- Fluid unmixing due to depressurisation

Fluid/wallrock interaction

- Chance in redox conditions due to interaction of oxidised fluids and reduced wall rocks

Fluid mixing

- Chance in redox conditions due to interaction of oxidised fluids and reduced (H_2S-bearing) brines

Preservation

- Relative tectonic stability post-uranium mineralisation
- Subsidence and burial of the uranium mineralised rocks

Key Reference Bibliography

DAHLKAMP, F. J., Uranium Deposits of the World: Asia. Springer, Berlin, Heidelberg, 492p (2009).
DAHLKAMP, F. J., Uranium Deposits of the World: Europe. Springer, Berlin, Heidelberg, 792p (2016).
DOLNÍČEK, Z., RENÉ, M., HERMANNOVÁ, S., PROCHASKA, W., Origin of the Okrouhlá Radouň episyenite-hosted uranium deposit, Bohemian Massif, Czech Republic: fluid inclusion and stable isotope constraints. Mineralium Deposita, 49(4), 409-425 (2014).
INTERNATIONAL ATOMIC ENERGY AGENCY, Geological Classification of Uranium Deposits and Description of Selected Examples. IAEA-TECDOC Series, 1842, 415p (2018).
RUZICKA, V., Vein uranium deposits. Ore Geology Reviews, 8(3-4), 247-276 (1993).

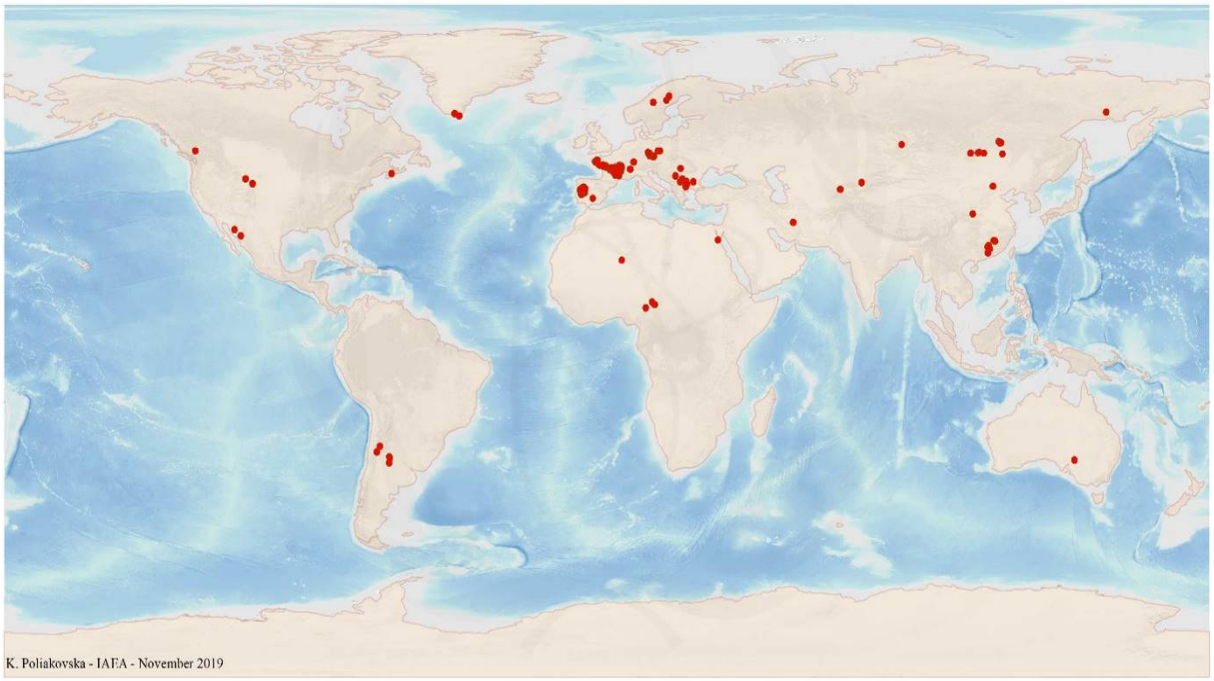

FIG. 2.1a. World distribution of selected Granite-Related Endogranitic uranium deposits from the UDEPO database.

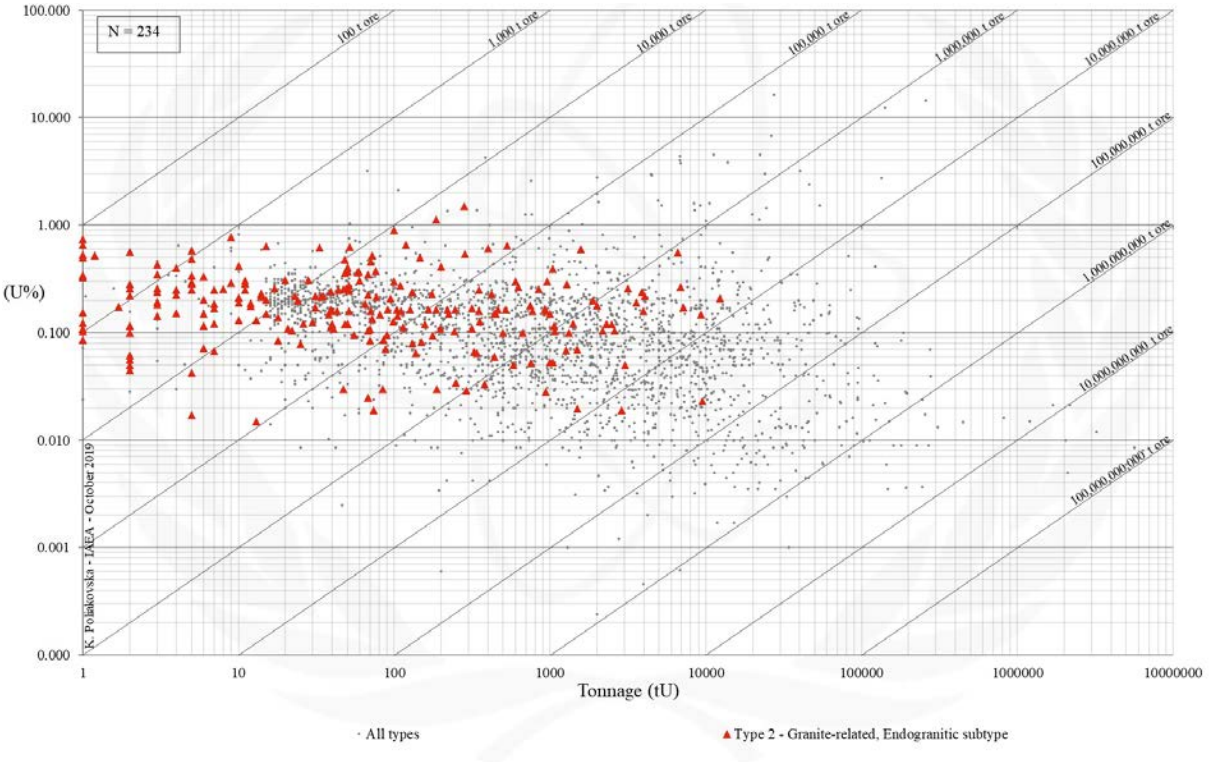

FIG. 2.1b. Grade and tonnage scatterplot highlighting Granite-Related Endogranitic uranium deposits from the UDEPO database.

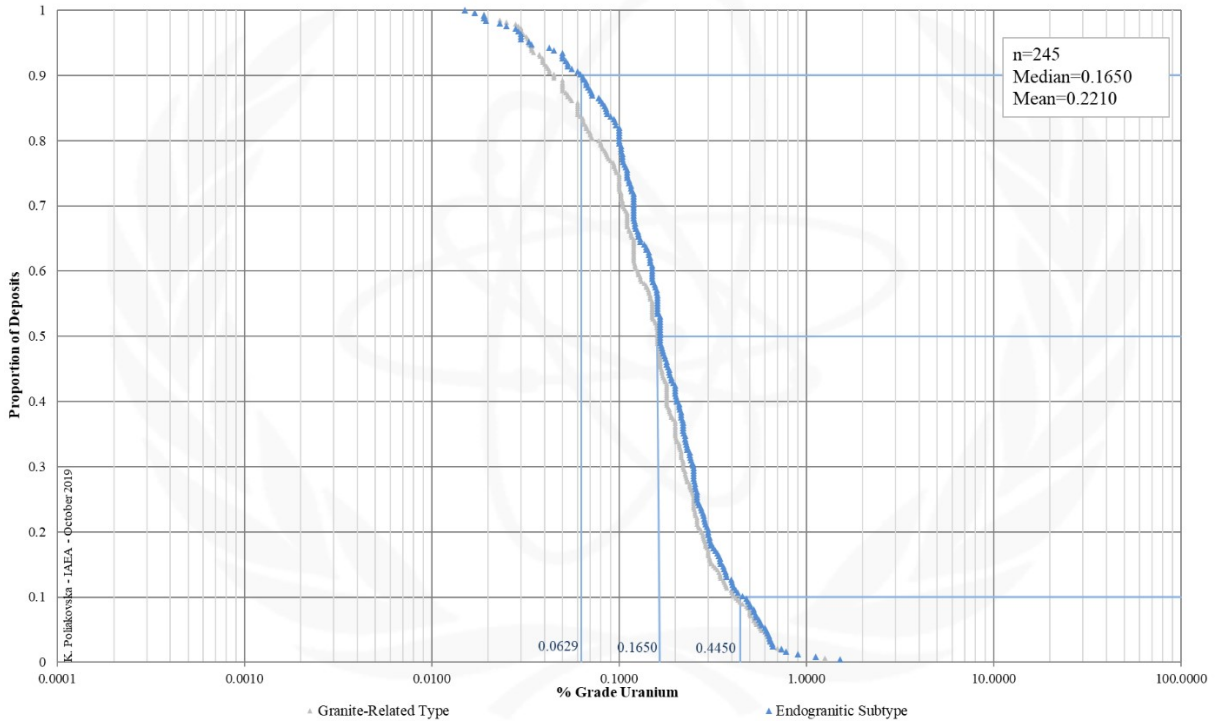

FIG. 2.1c. Grade Cumulative Probability Plot for Granite-Related Endogranitic uranium deposits from the UDEPO database.

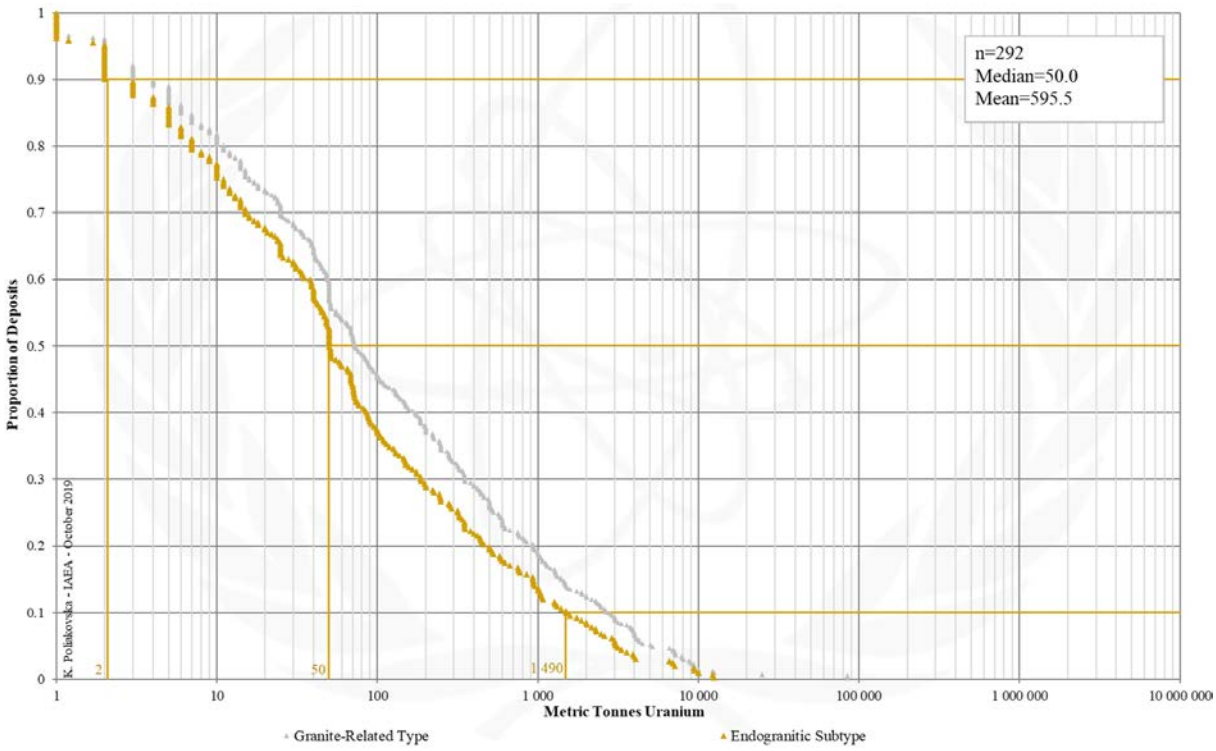

FIG. 2.1d. Tonnage Cumulative Probability Plot for Granite-Related Endogranitic uranium deposits from the UDEPO database.

SUBTYPE 2.2. Granite-Related, Perigranitic

Brief Description

- Granite-related deposits occur in collisional orogen, well inboard of fossil convergent plate margins and often spatially associated with tin-tungsten and intrusion-related gold provinces.
- The uranium ores take the form of vein-, stockwork- or episyenite-hosted deposits enclosed by, at the contact with or in the periphery of granitic intrusions, in particular highly differentiated leucogranites.
- Two subtypes, endogranitic and perigranitic, can be distinguished based on their spatial relationships with granitic intrusions and the surrounding country rocks.
- Perigranitic deposits (subtype 2.2), on the other hand, may be mono- (U) or polymetallic (U ± Ag, As, Bi, Co, Ni) and are typically confined to the country rocks at the contact with and/or surrounding granitic intrusions.

Type Examples

- Příbram district, Czech Republic; Niederschlema-Alberoda, Germany; Alto Alentejo district, Portugal

Genetically Associated Deposit Types

- Subtype 2.2. Granite-related, endogranitic

Principal Commodities

- U ± Ag, As, Bi, Co, Ni

Grades (%) and Tonnages (tU)

- Average: 0.1481, 2304.8
- Median: 0.1020, 301.5

Number of Deposits

- 222

Provinces (undifferentiated from Granite-related Type)

- Alto Alentejo, Aguila, Altai Belt, Amorican Massif, Andujar, Asele, Bange Jiali, Beiras, Burgas, Burro Mountains, Cabeza de Araya, Central Bohemian, Chandu, Coast Plutonic Complex, Copper Mountain, Cornwall, Criffel Granodiorite, East Balkan, Erzgebirge Karlovy Vary Massif, Fichtelgebirge, Finhaut Salvan Aiguilles Rouges Massif, Gogi Kanchankayi, Horni Slavkov, Hotagen Olden Window, Janja Massif, Jiuyishan Jinjiling, Kedougou Kenieba, Kentai Daur, Korolevo Chasovo, La Haba Don Benito, La Jara Sierra De Altamira, La Preciosa, Los Gigantes, Massif Central, Mirandela, North Qinling, Northern Grauwackenzone West Balkan, Northern Rocky Mountains, Nubian Shield, Qimen Tagh, Rila Mountains, Savoy Alps, Schwarzwald, Sonora, Southern Kalyma River, Taoshan Zhuguang Belt, Tingogasta, Villar de Peralonso, West Bohemian, West Kunlanshan, West Sredna Gora, Western Cameroon Domain, Westsudetic Silesian.

Tectonic Setting

- Collisional orogens

Typical Geological Age Range

- Palaeozoic to Mesozoic

Mineral Systems Model

Source

Ground preparation

- Orogenesis
- Emplacement of uraniferous (leuco-)granitoids
- Hornfelsing of country rocks in contact metamorphic aureoles
- Development or reactivation of graben structures facilitating infiltration of meteoric and/or basinal brines
- Pervasive wallrock alteration prior to mineralisation

Energy

- High heat flow, extreme geothermal gradient and partial melting of mantle and/or crustal sources
- Voluminous magmatism and emplacement of felsic to intermediate, peraluminous intrusions

Fluids

- Magmatic-hydrothermal fluids
- (?)Meteoric fluids, (?)basinal brines, (?)metamorphic fluids

Ligands

- Ca, Na, CO_2

Reductants

- Reducing lithologies; sulphides; Fe^{2+} silicates; hydrocarbons; H_2S

Uranium

- Peraluminous U-enriched granitoids (in particular peraluminous two-mica leucogranites containing easily leachable uraninite); U-enriched high-K calc-alkaline granitoids; U-enriched basement rocks

Transport

Fluid pathways

- Crustal-scale fault zones
- Anticlinal hinge zones
- Stratigraphic aquifers (overlying basin successions)

Trap

Physical

- Transient breaching of physical barriers/seals, catastrophic rock failure and concomitant structurally controlled and highly focused fluid flow controlled by gradients in permeability and hydraulic head
- Gradients in permeability and hydraulic head are maximised at fault irregularities, fault tips and wings, fault intersections, fault damage zones characterised by high fracture density, competency contrasts, regional unconformities, apices of granitic cusps and ridges, strain shadows and contact aureoles around intrusive bodies, fold axes and fold axial cleavages, folds truncated by faults; lithological contacts or episyenites

Deposition

Phase separation

- Fluid unmixing due to depressurisation

Fluid/wallrock interaction

- Chance in redox conditions due to interaction of oxidised fluids and reduced wall rocks

Fluid mixing

- Chance in redox conditions due to interaction of oxidised fluids and reduced (H_2S-bearing) brines

Preservation

- Relative tectonic stability post-uranium mineralisation
- Subsidence and burial of the uranium mineralised rocks

Key Reference Bibliography

DAHLKAMP, F. J., Uranium Deposits of the World: Asia. Springer, Berlin, Heidelberg, 492p (2009).
DAHLKAMP, F. J., Uranium Deposits of the World: Europe. Springer, Berlin, Heidelberg, 792p (2016).
DOLNÍČEK, Z., RENÉ, M., HERMANNOVÁ, S., PROCHASKA, W., Origin of the Okrouhlá Radouň episyenite-hosted uranium deposit, Bohemian Massif, Czech Republic: fluid inclusion and stable isotope constraints. Mineralium Deposita, 49(4), 409-425 (2014).
INTERNATIONAL ATOMIC ENERGY AGENCY, Geological Classification of Uranium Deposits and Description of Selected Examples. IAEA-TECDOC Series, 1842, 415p (2018).
RUZICKA, V., Vein uranium deposits. Ore Geology Reviews, 8(3-4), 247-276 (1993).

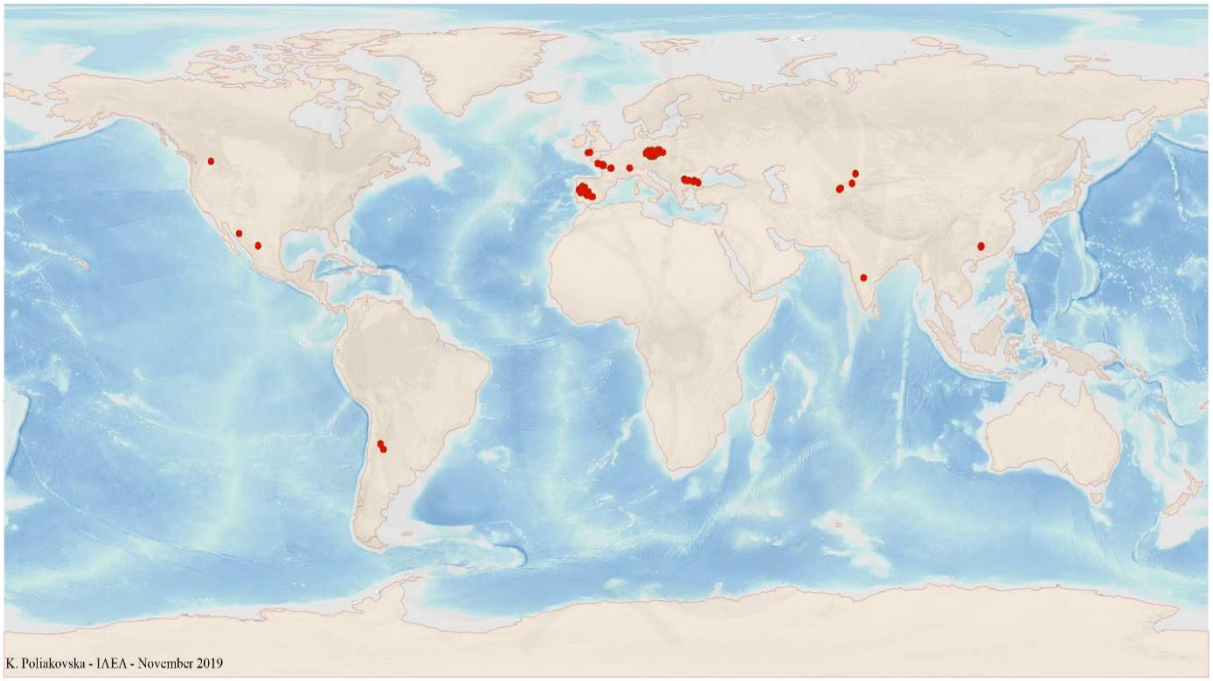

FIG. 2.2a. World distribution of selected Granite-Related Perigranitic uranium deposits from the UDEPO database.

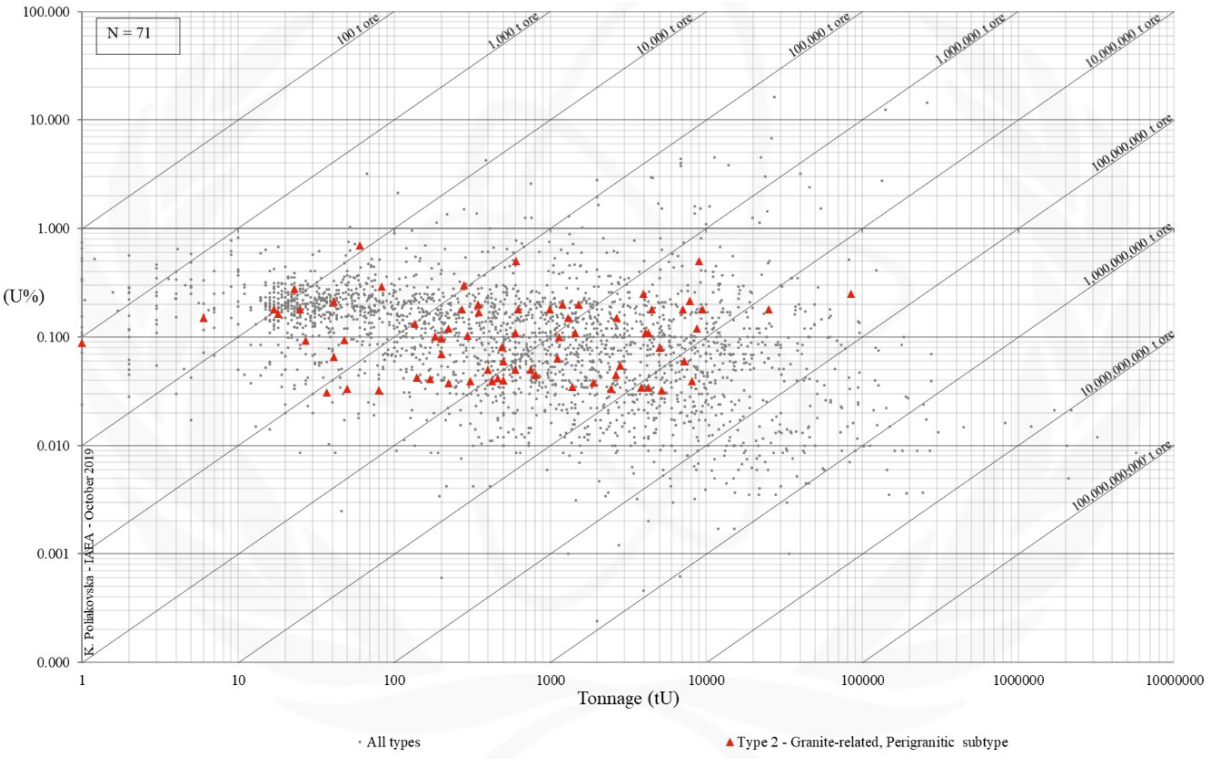

FIG. 2.2b. Grade and tonnage scatterplot highlighting Granite-Related Perigranitic uranium deposits from the UDEPO database.

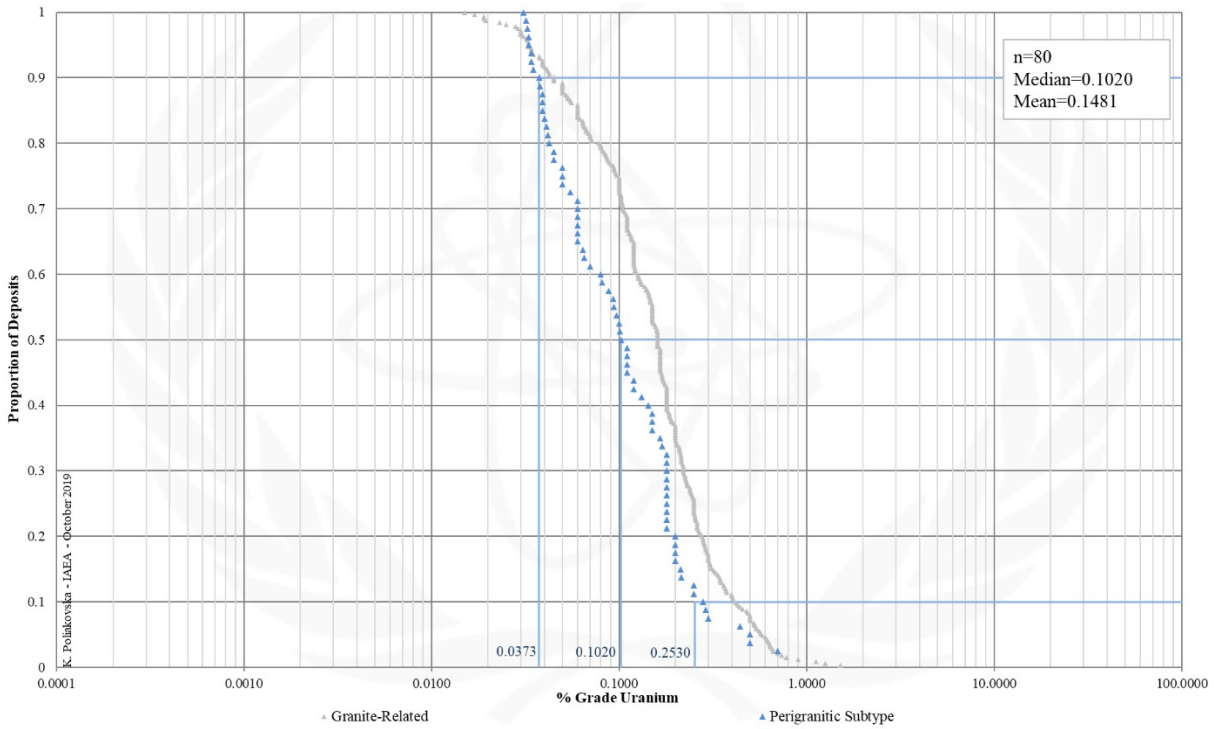

FIG. 2.2c. Grade Cumulative Probability Plot for Granite-Related Perigranitic uranium deposits from the UDEPO database.

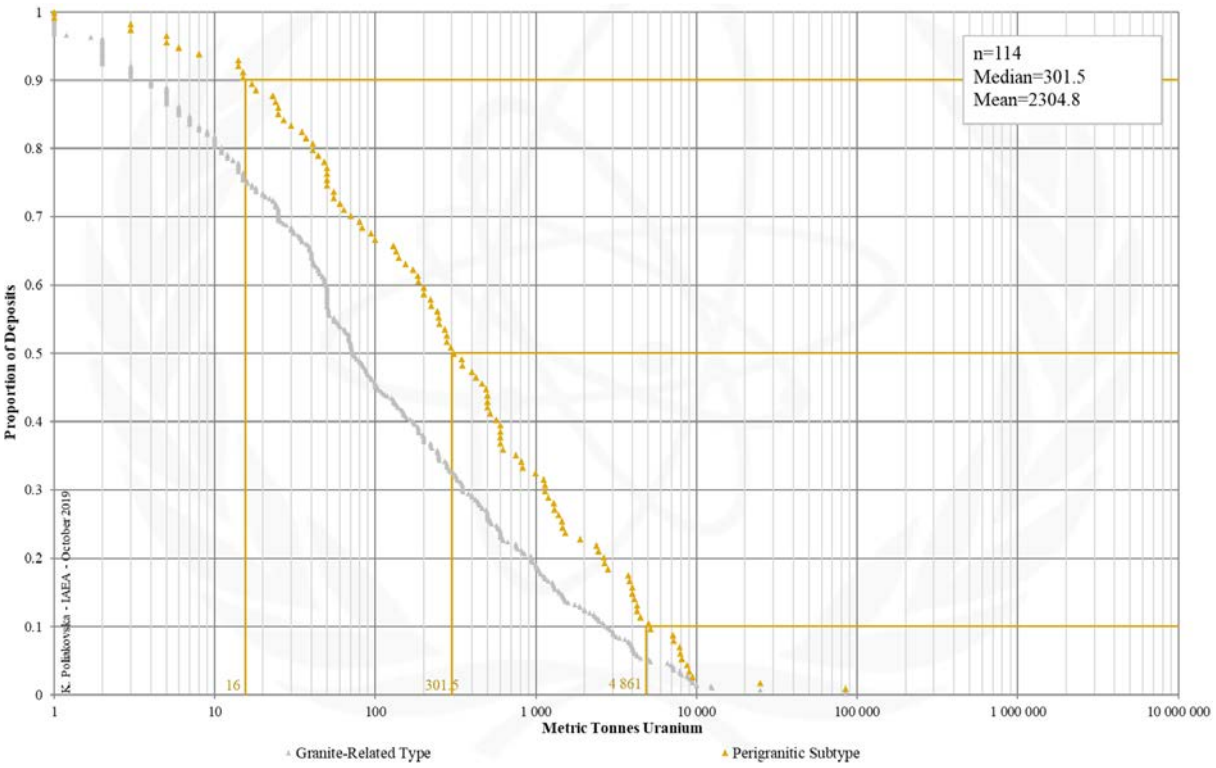

FIG. 2.2d. Tonnage Cumulative Probability Plot for Granite-Related Perigranitic uranium deposits from the UDEPO database.

Appendix III

POLYMETALLIC IRON OXIDE BRECCIA COMPLEX

TYPE 3. Polymetallic Iron Oxide Breccia Complex

Brief Description

- Polymetallic iron oxide breccia complex deposits are exemplified by the giant Mesoproterozoic Olympic Dam iron oxide copper-gold-uranium (IOCG-U) deposit.
- The polymetallic ores at Olympic Dam are contained entirely within a polyphase haematite-rich granite breccia, the outer boundary of which is gradational with the host granite.
- The breccia complex formed in a near-surface volcanic environment through progressive deformation and extensive hydrothermal alteration of the granite host and coeval with widespread emplacement of A- and I-type granitoid melts.
- The bulk of the uranium metal occurs in the copper ore domains, associated with copper-iron sulphides and potassic alteration assemblages.
- Olympic Dam is the only known polymetallic iron oxide breccia complex deposit that contains significant uranium resources, extracted as a co-product of copper mining.

Subtypes

- Not applicable

Type Examples

- Olympic Dam, Prominent Hill, Carrapateena, Mount Gee, Radium Ridge, Australia; Salobo, Brazil

Principal Commodities

- Cu, Au ± Ag, Fe, REE, U (co-product only), V

Grades (%) and Tonnages (tU)

- Average: 0.0385, 138014.6
- Median: 0.0155, 8064.0

Number of Deposits

- 20

Provinces

- Olympic IOCG Province, Mount Painter, Mount Isa East, Serra dos Carajas.

Tectonic Setting

- Intracratonic or continental margin rifts

Typical Geological Age Range

- Late Archaean to Pliocene; important deposits are late Archaean to Mesoproterozoic in age

Mineral Systems Model

Source

Ground preparation
- Development of a caldera or diatreme/maar volcanic complex
- Exhumation of an active magnetite-forming hydrothermal regime and its interaction with an oxidised groundwater or basinal hydrothermal regime

Energy
- High heat flow, extreme geothermal gradient and partial melting of mantle and crustal sources
- Voluminous anorogenic bimodal felsic and mafic volcanism and hypabyssal plutonism

Fluids
- Highly oxidised groundwaters
- High-temperature brines of magmatic-hydrothermal origin or in equilibrium with metamorphic basement rocks
- (?)Sulphur-bearing fluids

Ligands
- Cl, CO_2, F, S,

Reductants and reactants
- Evaporites; paragenetically older magnetite and/or hematite; reduced fluids

Metals
- High-temperature A- and I-type igneous rocks; mafic to ultramafic igneous rocks; basement or basinal rocks of continental back-arc or foreland affinity

Transport

Melt/fluid pathways
- Suture zones
- Crustal-scale fault zones (in particular long-lived basin growth faults)
- Stratigraphic aquifers
- Maar/diatreme-related vent zones

Trap

Physical
- Dilational deformation and fluid flow centred upon breccia complex and associated fault-fracture network
- Formation of hematite-rich breccias by repetitive hydrothermal brecciation, milling, and explosive venting

Chemical

- Development of a redox interface due to exhumation of an active magnetite-forming hydrothermal regime and its superposition over an oxidised groundwater regime

Deposition

Change in redox conditions

- Due to interaction between oxidised fluids and reduced iron accumulations, in particular where hematite has replaced earlier magnetite
- Due to mixing of oxidised groundwaters, or shallow basinal waters, with deep-sourced iron-rich brines of intermediate redox state

Preservation

- Relative tectonic stability post-mineralisation
- Subsidence and burial of the mineralised rocks

Key Reference Bibliography

CORRIVEAU, L., Iron oxide copper-gold (±Ag±Nb±P±REE±U) deposits: a Canadian perspective. In: GOODFELLOW, W. D. (Ed.), Mineral deposits of Canada: a synthesis of major deposit- types, district metallogeny, the evolution of geological provinces, and exploration methods. Geological Survey of Canada, Geological Association of Canada, Mineral Deposits Division Special Publication, 5, 307-328 (2007).

EHRIG, K., MCPHIE, J., KAMENETSKY, V. S., Geology and mineralogical zonation of the Olympic Dam iron oxide Cu-U-Au-Ag deposit, South Australia. Society of Economic Geologists Special Publication, 16, 237-267 (2012).

GEOSCIENCE AUSTRALIA, Iron oxide-copper-gold potential of the southern Arunta Region. Available for download from: https://data.gov.au/dataset/iron-oxide-copper-gold-potential-of-the-southern-arunta-region [last accessed on 22 November 2018] (2017).

HUSTON, D. L., VAN DER WIELEN, S. (Eds.), An assessment of the uranium and geothermal prospectivity of east-central South Australia. Geoscience Australia Record, 2011/34, 229p (2011).

INTERNATIONAL ATOMIC ENERGY AGENCY, Geological Classification of Uranium Deposits and Description of Selected Examples. IAEA-TECDOC Series, 1842, 415p (2018).

MCKAY, A. D., MIEZITIS, Y., Australia's uranium — resources, geology and development of deposits. AGSO-Geoscience Australia Mineral Resource Report, 1, 184p (2001).

SCHOFIELD, A. (Ed.), An assessment of the uranium and geothermal prospectivity of the southern Northern Territory. Geoscience Australia Record, 2012/51, 214p (2012).

SKIRROW, R. G., JAIRETH, S., HUSTON, D. L., BASTRAKOV, E. N., SCHOFIELD, A., VAN DER WIELEN, S. E., BARNICOAT, A. C., Uranium mineral systems: Processes, exploration criteria and a new deposit framework. Geoscience Australia Record, 2009/20, 44p (2009).

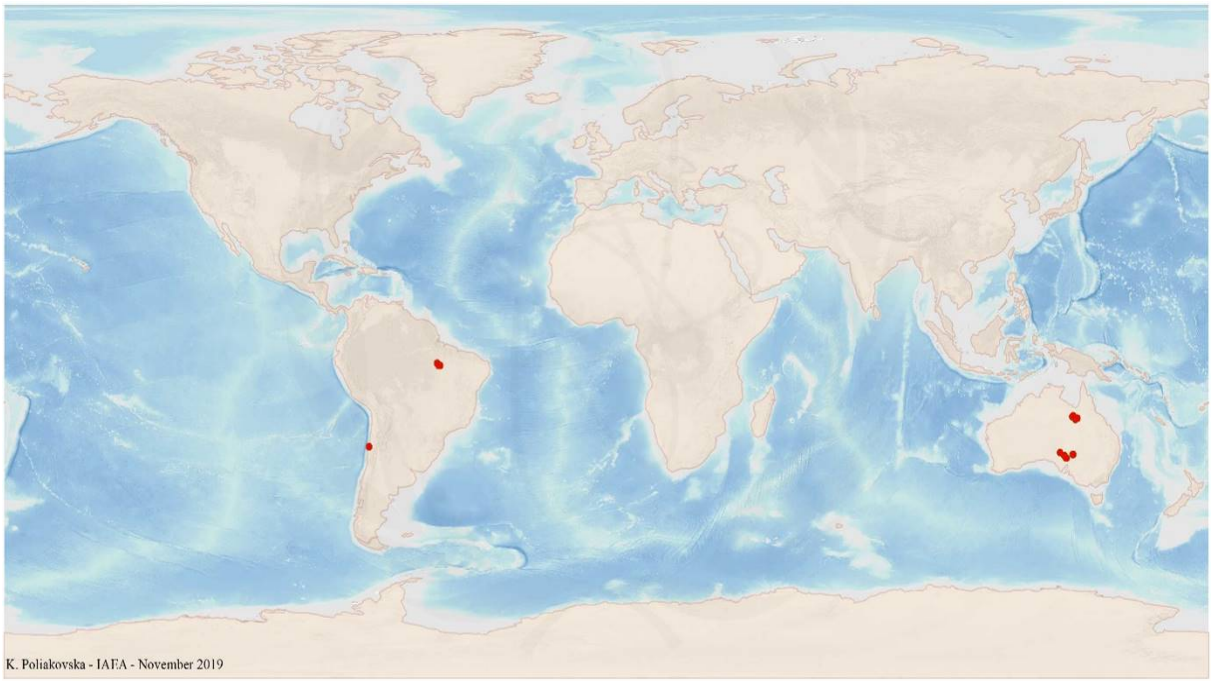

FIG. 3a. World distribution of selected Polymetallic Iron Oxide Breccia Complex uranium deposits from the UDEPO database.

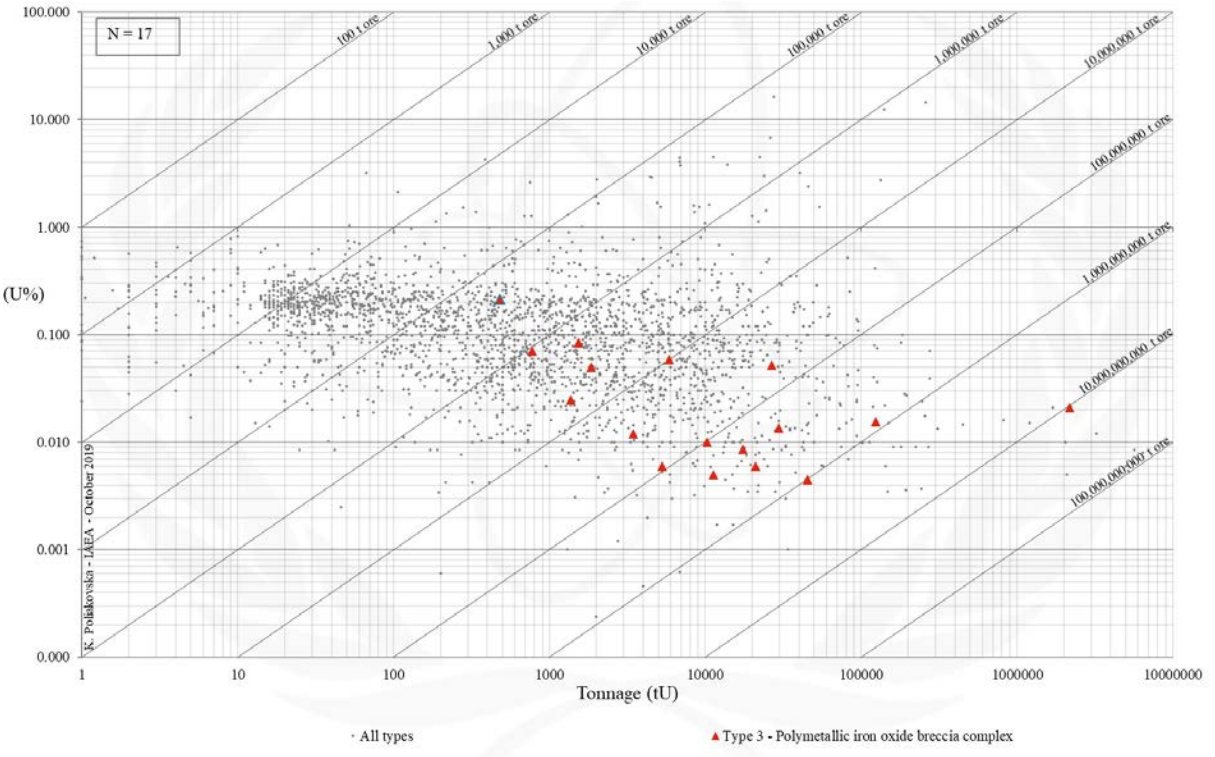

FIG. 3b. Grade and tonnage scatterplot highlighting Polymetallic Iron Oxide Breccia Complex uranium deposits from the UDEPO database.

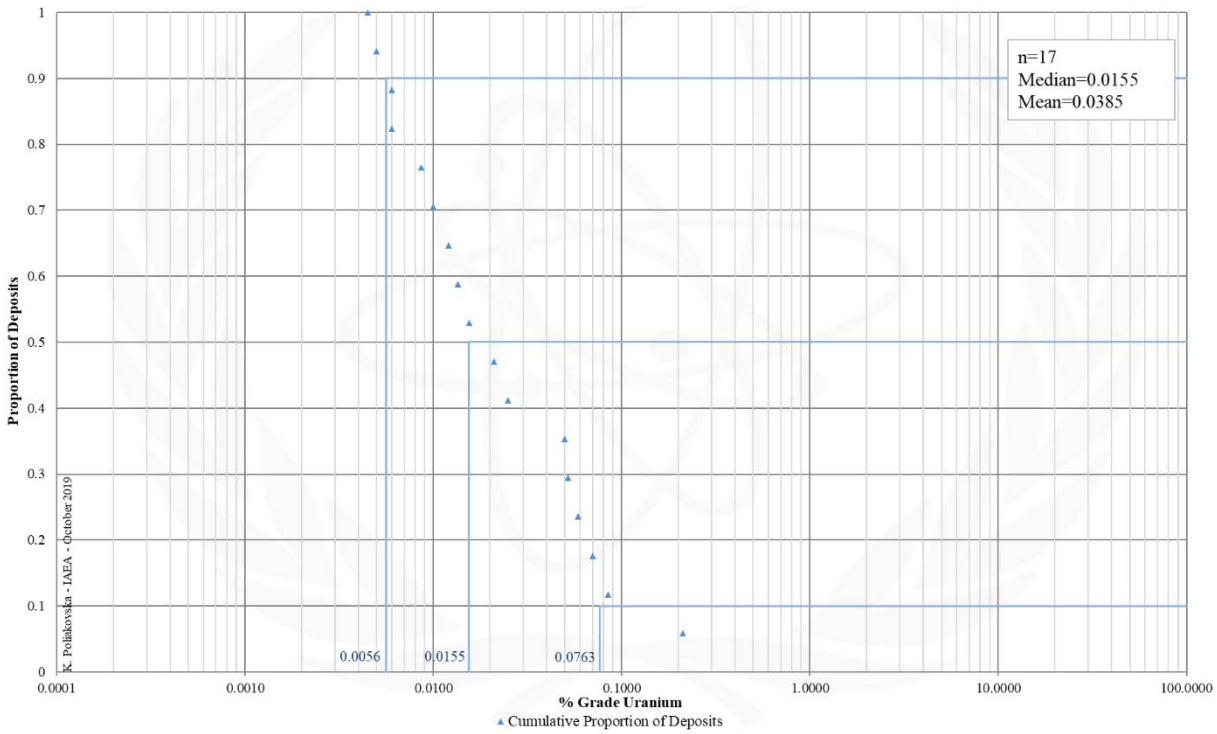

FIG. 3c. Grade Cumulative Probability Plot for Polymetallic Iron Oxide Breccia Complex uranium deposits from the UDEPO database.

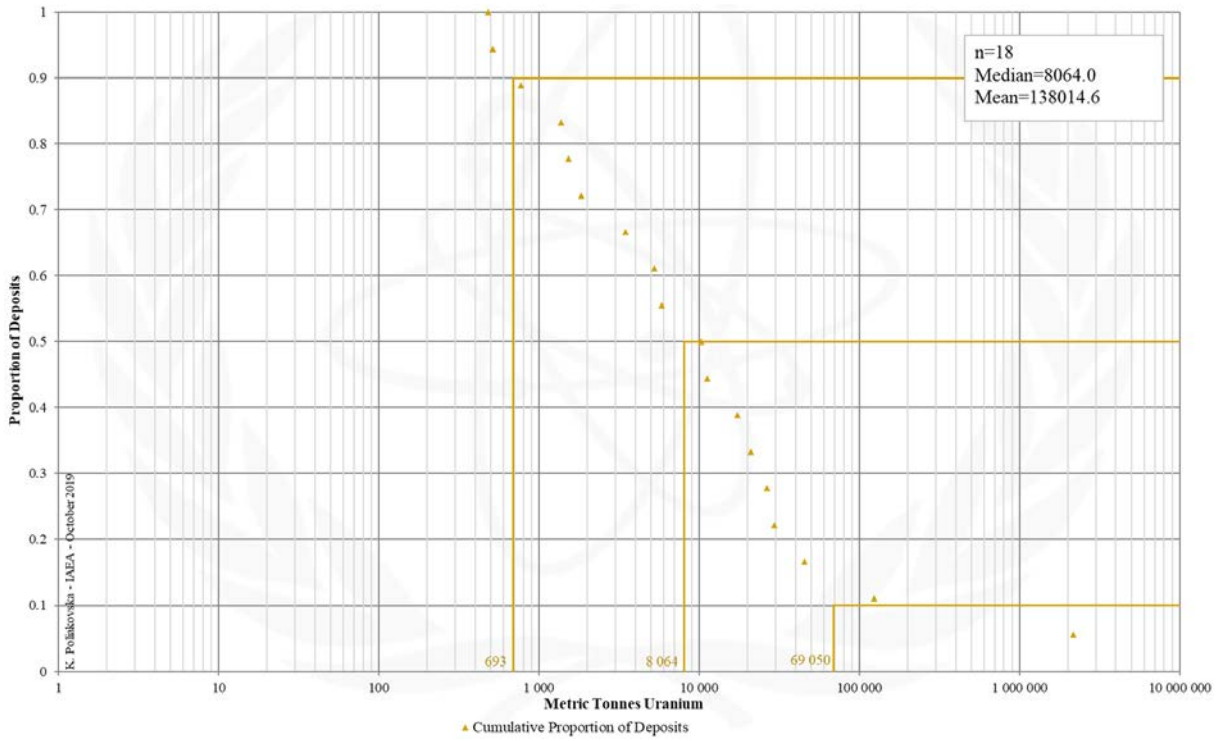

FIG. 3d. Tonnage Cumulative Probability Plot for Polymetallic Iron Oxide Breccia Complex uranium deposits from the UDEPO database.

Appendix IV

VOLCANIC-RELATED

TYPE 4. Volcanic-Related

Brief Description

- Volcanic-related deposits occur in caldera environments characterised by felsic to mafic volcanic lavas and subvolcanic intrusions, flow breccias, tuffs and intercalated pyroclastic and clastic sediments.
- Three subtypes can be distinguished: Stratabound, structure-bound, and volcano-sedimentary deposits. However, most volcanic-related deposits are of the structure-bound type.
- Stratabound deposits (subtype 4.1) take the form of uranium disseminations and impregnations in permeable and/or chemically reactive lava flows, flow breccias, tuffs and intercalated pyroclastic and clastic sedimentary units; structure-bound deposits (subtype 4.2) structurally-controlled veins and stockworks hosted by volcanic, subvolcanic and pyroclastic rocks; and volcano-sedimentary deposits (subtype 4.3) low-grade, peneconcordant uranium ores in carbonaceous, fluvio-lacustrine sediments deposited in the exocaldera environment.
-

Subtypes

- 4.1. Volcanic-related, stratabound
- 4.2. Volcanic-related, structure-bound
- 4.3. Volcanic-related, volcano-sedimentary

Type Examples

- Subtype 4.1. Dornod (No. 7 ore zone), Mongolia; Maureen, Australia
- Subtype 4.2. Streltsov-Antei, Russian Federation; Kurišková, Slovakia
- Subtype 4.3. Anderson Mine, USA; Sierra Pintada district, Argentina

Principal Commodities

- U ± Ag, As, B, Bi, Cu, F, Li, Mo, Ni, Pb, Sb, Sn, W

Grades (%) and Tonnages (tU)

- Average: 0.1151, 5034.2
- Median: 0.1000, 1725.0

Number of Deposits

- 237

Provinces

- Carpathians West, Choibalsan North, Date Creek Basin, Gang Hong Belt, Georgetown Charters Towers, Glarner St Galler Verrucano, Grand Basin, Karamazar, La Charbonnier, Latium, Macusani Plateau, Murphy, Northwest Saxony, Pacific Coast, Pribalkhash, Saar Nahe Trough, Sierra Madre Occidental, Sierra Pintada, Sorsele, Stravropol, Streltsovsk, Tlaxiaco Basin, Xincheng Qinglong Belt, Xuemisitan Potential Belt.

Tectonic Setting

- Intraplate 'hot spot' and intracontinental rift settings

Typical Geological Age Range

- Palaeoproterozoic to recent

Mineral Systems Model

Source

Ground preparation
- Uranium-enriched, pre-caldera basement
- Generation of peralkaline F-rich melts
- Formation of nested caldera complexes comprising strongly fractionated felsic volcanic rocks

Energy
- High heat flow, extreme geothermal gradient and partial melting of mantle and crustal sources
- Hypabyssal intrusions/sub-volcanic magma chambers
- Voluminous high-temperature magmatism and volcanism

Fluids
- Hydrothermal ± meteoric and geothermal fluids

Ligands
- F

Reductants
- Detrital vegetal matter in clastic sedimentary units, ferrous (Fe^{2+}) or ferric (Fe^{3+}) iron, H_2S

Uranium
- Highly fractionated volcanic rocks, in particular peralkaline, F-rich rhyolites
- Aphanitic volcanic rocks or volcanic glass
- Pre-caldera/basement granitoids

Transport

Fluid pathways
- Caldera-related fault-fracture systems
- Unconformity surfaces
- Stratigraphic aquifers

Trap

Physical
- Pipe-like feeder structures, caldera margin (ring) faults, intra-caldera/intra-formational fault-fracture systems, breccia pipes, fold structures
- Permeable sedimentary units, vesicular flow tops, volcanic breccias, rigid intrusive plugs, impermeable tuff or clay alteration caps
- Caldera moats

Chemical
- Sulphide accumulations
- Carbonaceous siliciclastic rocks containing detrital vegetal matter

Deposition

Phase separation
- Effervescence or boiling in conjunction with rapid cooling

Fluid/wallrock interaction
- Chance in redox conditions due to interaction of oxidised fluids and reduced wall rocks

Fluid mixing
- Change in redox conditions due to mixing of oxidising, alkaline fluids in which U^{6+} is stable as a bicarbonate complex with reducing, acidic fluids in which marcasite can form (i.e., uranium reduction by sulphur-based reductants)

Adsorption
- Uranium adsorption onto clay minerals, humic substances, colloidal silica or zeolites

Supergene processes
- Secondary uranium redistribution and enrichment

Preservation
- Relative tectonic stability post-uranium mineralisation
- Subsidence and burial of the uranium mineralised rocks
- Arid- to semiarid climatic conditions
- Thick vegetation cover

Key Reference Bibliography

DAHLKAMP, F. J., Uranium Deposits of the World: Asia. Springer, Berlin, Heidelberg, 492p (2009).
DAHLKAMP, F. J., Uranium Deposits of the World: USA and Latin America. Springer, Berlin, Heidelberg, 515p (2010).
INTERNATIONAL ATOMIC ENERGY AGENCY, Geological Classification of Uranium Deposits and Description of Selected Examples. IAEA-TECDOC Series, 1842, 415p (2018).
MUELLER, A., HALBACH, P., The Anderson Mine (Arizona); an early diagenetic uranium deposit in Miocene lake sediments. Economic Geology, 78(2), 275-292 (1983).
NASH, J. T., Volcanogenic uranium deposits — geology, geochemical processes, and criteria for resource assessment. U.S. Geological Survey Open-File Report, 2010-1001, 99p (2010).

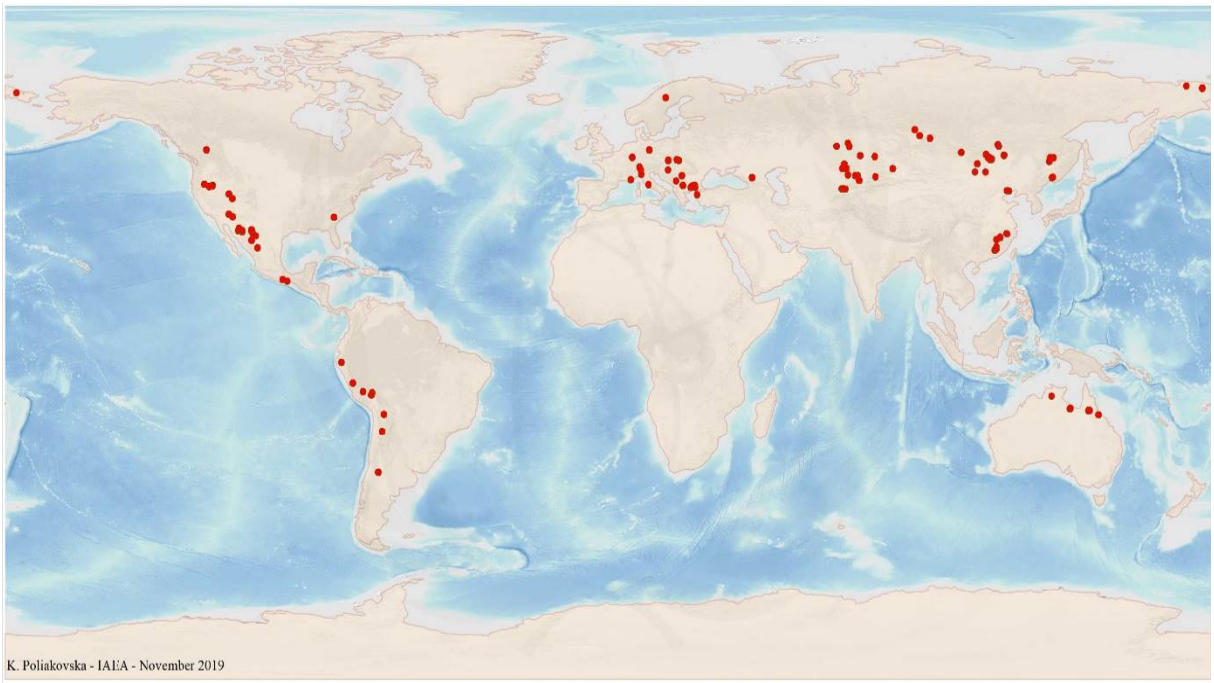

FIG. 4a. World distribution of selected Volcanic-Related uranium deposits from the UDEPO database.

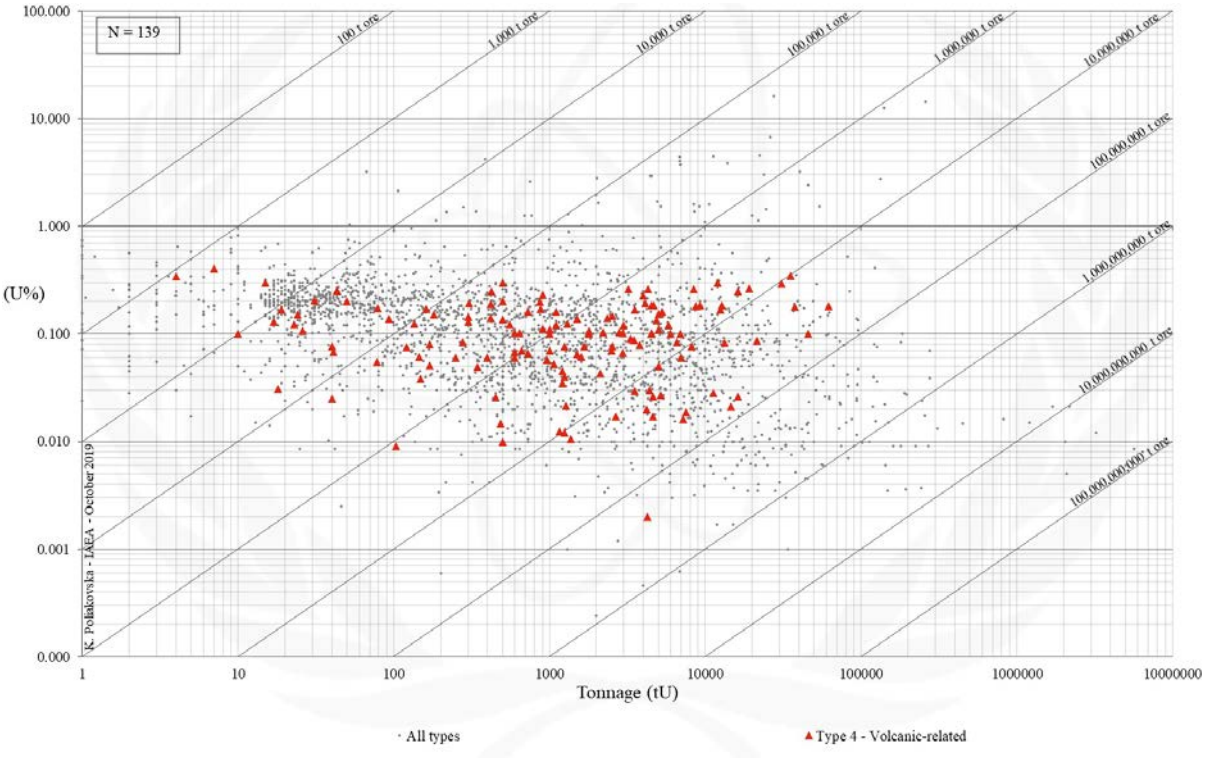

FIG. 4b. Grade and tonnage scatterplot highlighting Volcanic-Related uranium deposits from the UDEPO database.

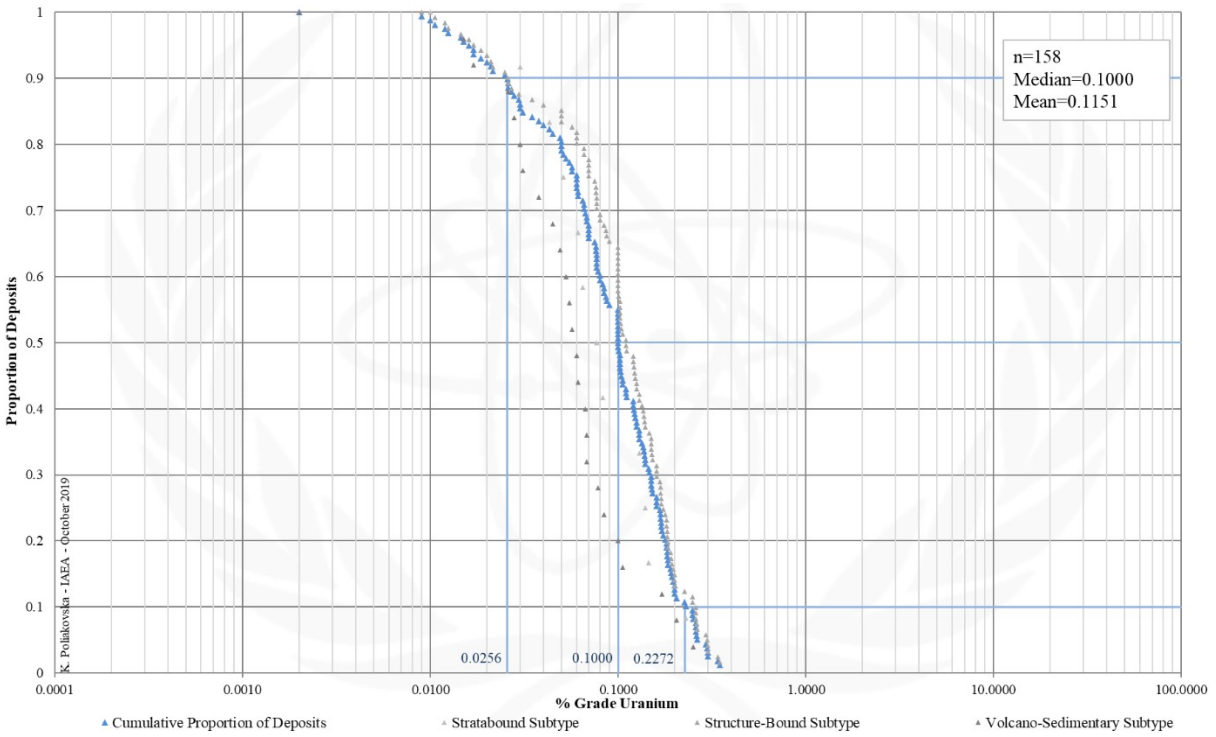

FIG. 4c. Grade Cumulative Probability Plot for Volcanic-Related uranium deposits from the UDEPO database.

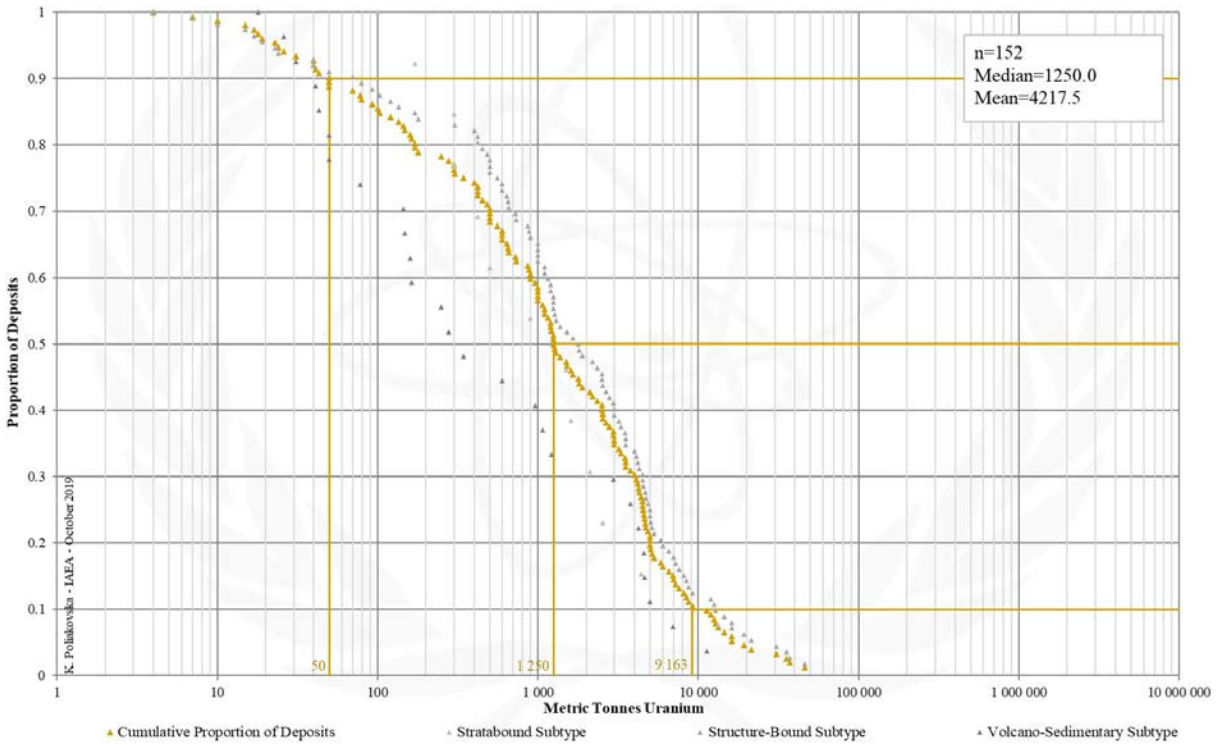

FIG. 4d. Tonnage Cumulative Probability Plot for Volcanic-Related uranium deposits from the UDEPO database.

SUBTYPE 4.1. Volcanic-Related, Stratabound

Brief Description
- Volcanic-related deposits occur in caldera environments characterised by felsic to mafic volcanic lavas and subvolcanic intrusions, flow breccias, tuffs and intercalated pyroclastic and clastic sediments.
- Stratabound deposits (subtype 4.1) take the form of uranium disseminations and impregnations in permeable and/or chemically reactive lava flows, flow breccias, tuffs and intercalated pyroclastic and clastic sedimentary units.

Genetically Associated Deposit Types
- Subtype 4.2. Volcanic-related, structure-bound
- Subtype 4.3. Volcanic-related, volcano-sedimentary

Type Examples
- Dornod Complex (No. 7 Ore Zone), Mongolia; Maureen, Australia; Aurora, USA; Yubilenoye, Russian Federation; Novazza, Italy; Margaritas, Mexico

Principal Commodities
- U, Mo, F ± Ag, As, Bi, Li, Pb, Sb, Sn, W

Grades (%) and Tonnages (tU)
- Average: 0.0888, 2164.4
- Median: 0.0710, 900.0

Number of Deposits
- 19

Provinces (undifferentiated from Volcanic-related Type)
- Carpathians West, Choibalsan North, Date Creek Basin, Gang Hong Belt, Georgetown Charters Towers, Glarner St Galler Verrucano, Grand Basin, Karamazar, La Charbonnier, Latium, Macusani Plateau, Murphy, Northwest Saxony, Pacific Coast, Pribalkhash, Saar Nahe Trough, Sierra Madre Occidental, Sierra Pintada, Sorsele, Stravropol, Streltsovsk, Tlaxiaco Basin, Xincheng Qinglong Belt, Xuemisitan Potential Belt.

Tectonic Setting
- Intraplate 'hot spot' and intracontinental rift settings

Typical Geological Age Range
- Palaeoproterozoic to recent

Mineral Systems Model

Source

Ground preparation
- Uranium-enriched, pre-caldera basement
- Generation of peralkaline F-rich melts
- Formation of nested caldera complexes comprising strongly fractionated felsic volcanic rocks

Energy
- High heat flow, extreme geothermal gradient and partial melting of mantle and crustal sources
- Hypabyssal intrusions/sub-volcanic magma chambers
- Voluminous high-temperature magmatism and volcanism

Fluids
- Hydrothermal ± meteoric and geothermal fluids

Ligands
- F

Reductants
- Detrital vegetal matter in clastic sedimentary units, ferrous (Fe^{2+}) or ferric (Fe^{3+}) iron, H_2S

Uranium
- Highly fractionated volcanic rocks, in particular peralkaline, F-rich rhyolites
- Aphanitic volcanic rocks or volcanic glass
- Pre-caldera/basement granitoids

Transport

Fluid pathways
- Caldera-related fault-fracture systems
- Unconformity surfaces
- Stratigraphic aquifers

Trap

Physical
- Permeable sedimentary units, vesicular flow tops, volcanic breccias, rigid intrusive plugs
- Impermeable tuff or clay alteration caps, caldera moat sediments

Chemical
- Sulphide accumulations
- Carbonaceous siliciclastic rocks containing detrital vegetal matter

Deposition

Phase separation
- Effervescence or boiling in conjunction with rapid cooling

Fluid/wallrock interaction
- Chance in redox conditions due to interaction of oxidised fluids and reduced wall rocks

Fluid mixing
- Change in redox conditions due to mixing of oxidising, alkaline fluids in which U^{6+} is stable as a bicarbonate complex with reducing, acidic fluids in which marcasite can form (i.e., uranium reduction by sulphur-based reductants)

Adsorption
- Uranium adsorption onto clay minerals, humic substances, colloidal silica or zeolites

Supergene processes
- Secondary uranium redistribution and enrichment

Preservation

- Relative tectonic stability post-uranium mineralisation
- Subsidence and burial of the uranium mineralised rocks
- Arid- to semiarid climatic conditions
- Thick vegetation cover

Key Reference Bibliography

DAHLKAMP, F. J., Uranium Deposits of the World: Asia. Springer, Berlin, Heidelberg, 492p (2009).
DAHLKAMP, F. J., Uranium Deposits of the World: USA and Latin America. Springer, Berlin, Heidelberg, 515p (2010).
INTERNATIONAL ATOMIC ENERGY AGENCY, Geological Classification of Uranium Deposits and Description of Selected Examples. IAEA-TECDOC Series, 1842, 415p (2018).
NASH, J. T., Volcanogenic uranium deposits — geology, geochemical processes, and criteria for resource assessment. U.S. Geological Survey Open-File Report, 2010-1001, 99p (2010).

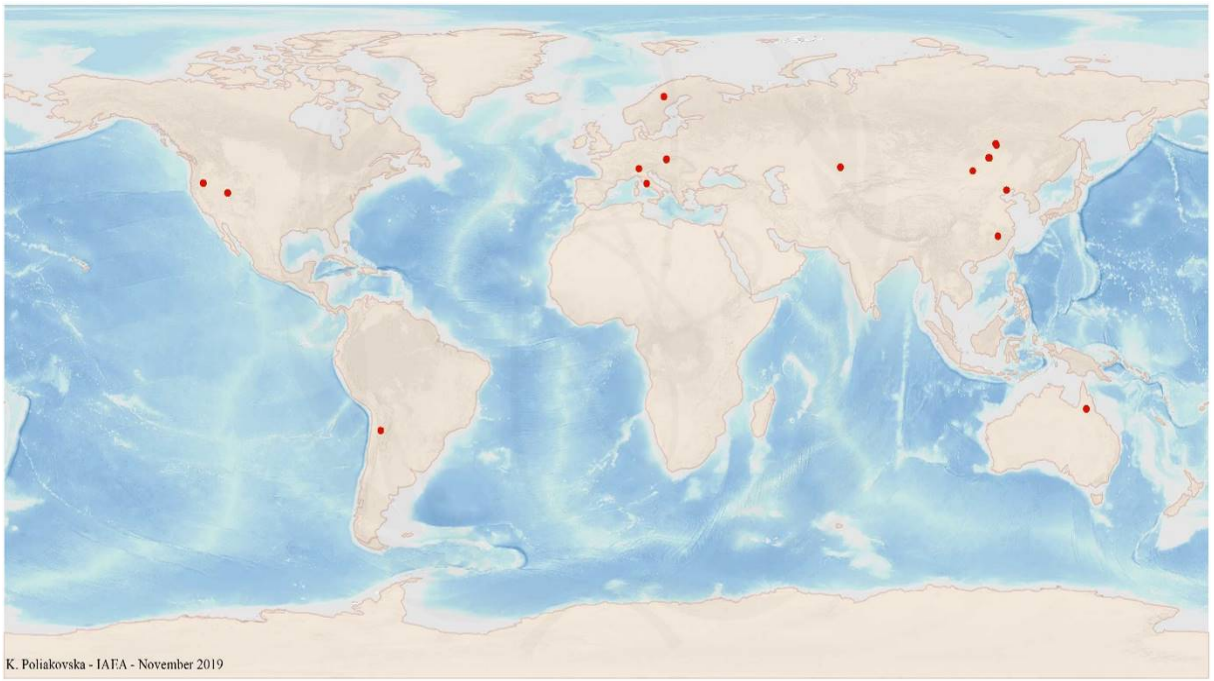

FIG. 4.1a. World distribution of selected Volcanic-Related Stratabound uranium deposits from the UDEPO database.

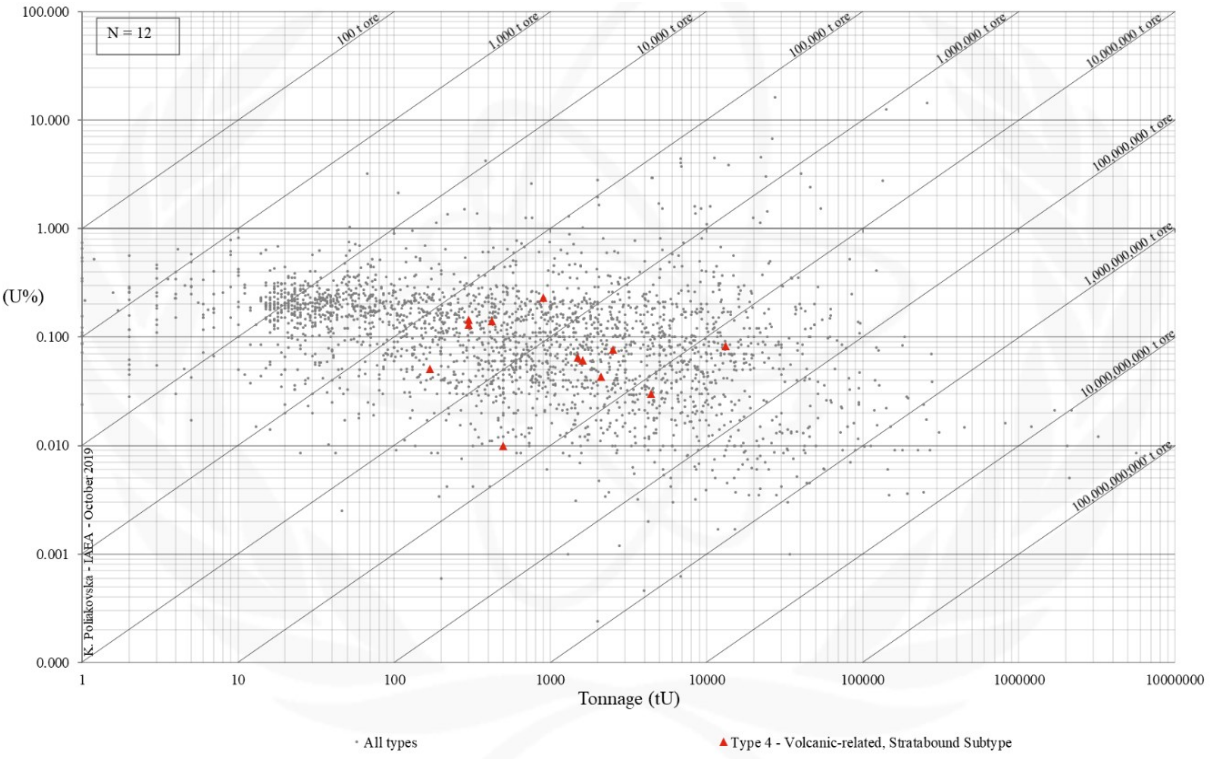

FIG. 4.1b. Grade and tonnage scatterplot highlighting Volcanic-Related Stratabound uranium deposits from the UDEPO database.

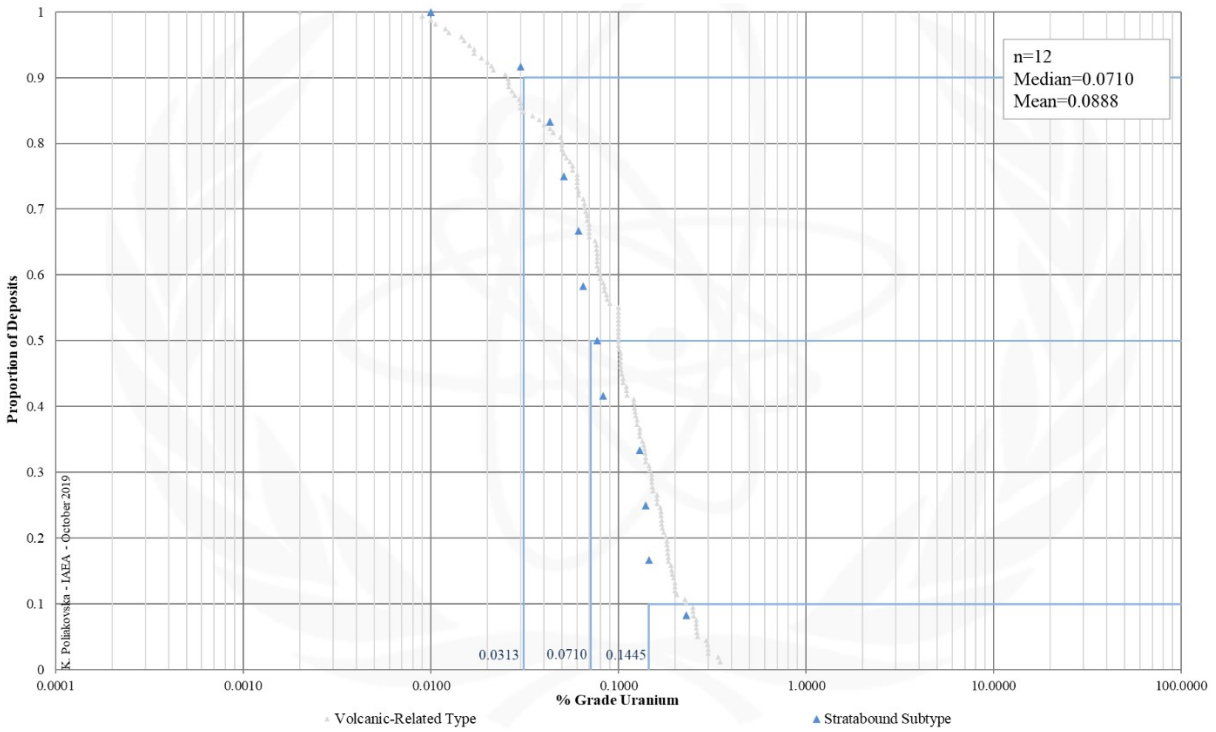

FIG. 4.1c. Grade Cumulative Probability Plot for Volcanic-Related Stratabound uranium deposits from the UDEPO database.

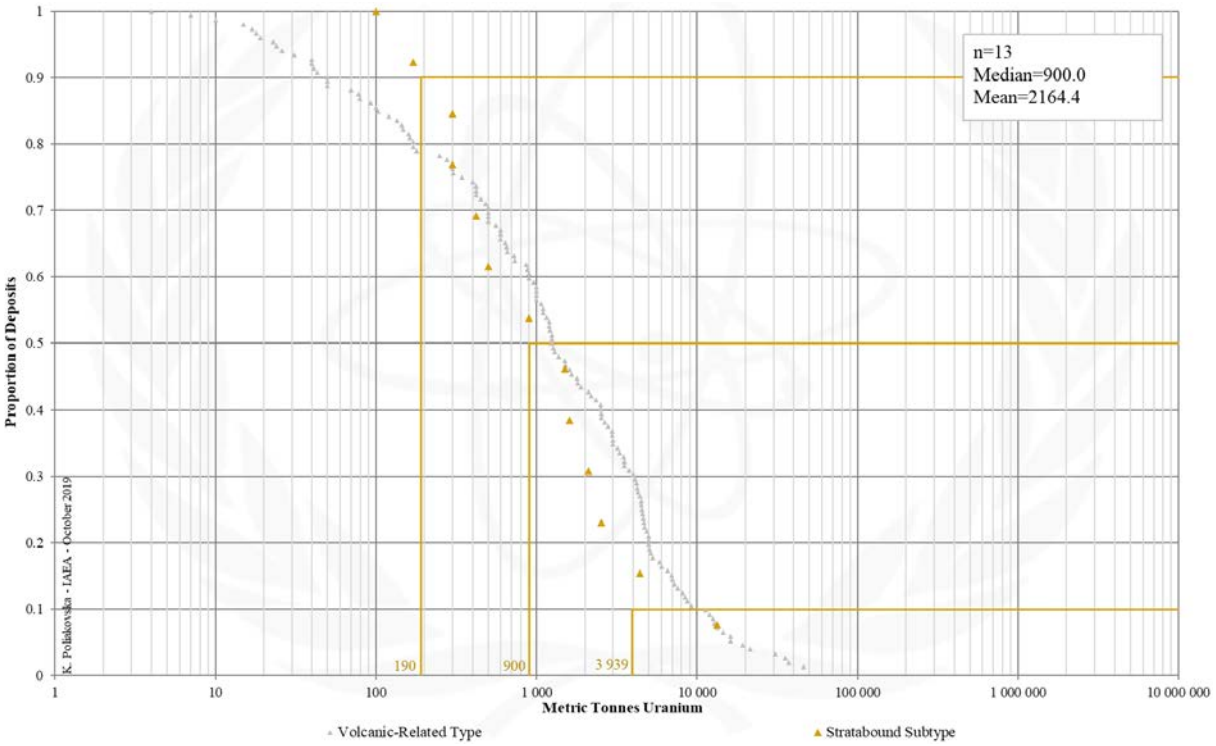

FIG. 4.1d. Tonnage Cumulative Probability Plot for Volcanic-Related Stratabound uranium deposits from the UDEPO database.

SUBTYPE 4.2. Volcanic-Related, Structure-Bound

Brief Description
- Volcanic-related deposits occur in caldera environments characterised by felsic to mafic volcanic lavas and subvolcanic intrusions, flow breccias, tuffs and intercalated pyroclastic and clastic sediments.
- Structure-bound deposits (subtype 4.2) take the form of structurally-controlled veins and stockworks hosted by volcanic, subvolcanic and pyroclastic rocks.

Genetically Associated Deposit Types
- Subtype 4.1. Volcanic-related, stratabound
- Subtype 4.3. Volcanic-related, volcano-sedimentary

Type Examples
- Streltsovskoye-Antei, Russian Federation; Dornod, Mongolia; Kurišková, Slovakia

Principal Commodities
- U, Mo, F ± Ag, As, Bi, Li, Pb, Sb, Sn, W

Grades (%) and Tonnages (tU)
- Average: 0.1269, 5034.2
- Median: 0.1100, 1725.0

Number of Deposits
- 186

Provinces (undifferentiated from Volcanic-related Type)
- Carpathians West, Choibalsan North, Date Creek Basin, Gang Hong Belt, Georgetown Charters Towers, Glarner St Galler Verrucano, Grand Basin, Karamazar, La Charbonnier, Latium, Macusani Plateau, Murphy, Northwest Saxony, Pacific Coast, Pribalkhash, Saar Nahe Trough, Sierra Madre Occidental, Sierra Pintada, Sorsele, Stravropol, Streltsovsk, Tlaxiaco Basin, Xincheng Qinglong Belt, Xuemisitan Potential Belt.

Tectonic Setting
- Intraplate 'hot spot' and intracontinental rift settings

Typical Geological Age Range
- Palaeoproterozoic to recent

Mineral Systems Model

Source

Ground preparation
- Uranium-enriched, pre-caldera basement
- Generation of peralkaline F-rich melts
- Formation of nested caldera complexes comprising strongly fractionated felsic volcanic rocks

Energy
- High heat flow, extreme geothermal gradient and partial melting of mantle and crustal sources
- Hypabyssal intrusions/sub-volcanic magma chambers
- Voluminous high-temperature magmatism and volcanism

Fluids
- Hydrothermal ± meteoric and geothermal fluids

Ligands
- F

Reductants
- Detrital vegetal matter in clastic sedimentary units, ferrous (Fe^{2+}) or ferric (Fe^{3+}) iron, H_2S

Uranium
- Highly fractionated volcanic rocks, in particular peralkaline, F-rich rhyolites
- Aphanitic volcanic rocks or volcanic glass
- Pre-caldera/basement granitoids

Transport

Fluid pathways
- Caldera-related fault-fracture systems
- Unconformity surfaces
- Stratigraphic aquifers

Trap

Physical
- Pipe-like feeder structures, caldera margin (ring) faults, intra-caldera/intra-formational fault-fracture systems, breccia pipes, fold structures
- Permeable sedimentary units, vesicular flow tops, volcanic breccias, rigid intrusive plugs
- Impermeable tuff or clay alteration caps, caldera moat sediments

Chemical
- Sulphide accumulations
- Carbonaceous siliciclastic rocks containing detrital vegetal matter

Deposition

Phase separation
- Effervescence or boiling in conjunction with rapid cooling

Fluid/wallrock interaction
- Chance in redox conditions due to interaction of oxidised fluids and reduced wall rocks

Fluid mixing
- Change in redox conditions due to mixing of oxidising, alkaline fluids in which U^{6+} is stable as a bicarbonate complex with reducing, acidic fluids in which marcasite can form (i.e., uranium reduction by sulphur-based reductants)

Adsorption
- Uranium adsorption onto clay minerals, humic substances, colloidal silica or zeolites

Supergene processes
- Secondary uranium redistribution and enrichment

Preservation

- Relative tectonic stability post-uranium mineralisation
- Subsidence and burial of the uranium mineralised rocks
- Arid- to semiarid climatic conditions
- Thick vegetation cover

Key Reference Bibliography

DAHLKAMP, F. J., Uranium Deposits of the World: Asia. Springer, Berlin, Heidelberg, 492p (2009).
DAHLKAMP, F. J., Uranium Deposits of the World: USA and Latin America. Springer, Berlin, Heidelberg, 515p (2010).
INTERNATIONAL ATOMIC ENERGY AGENCY, Geological Classification of Uranium Deposits and Description of Selected Examples. IAEA-TECDOC Series, 1842, 415p (2018).
NASH, J. T., Volcanogenic uranium deposits — geology, geochemical processes, and criteria for resource assessment. U.S. Geological Survey Open-File Report, 2010-1001, 99p (2010).

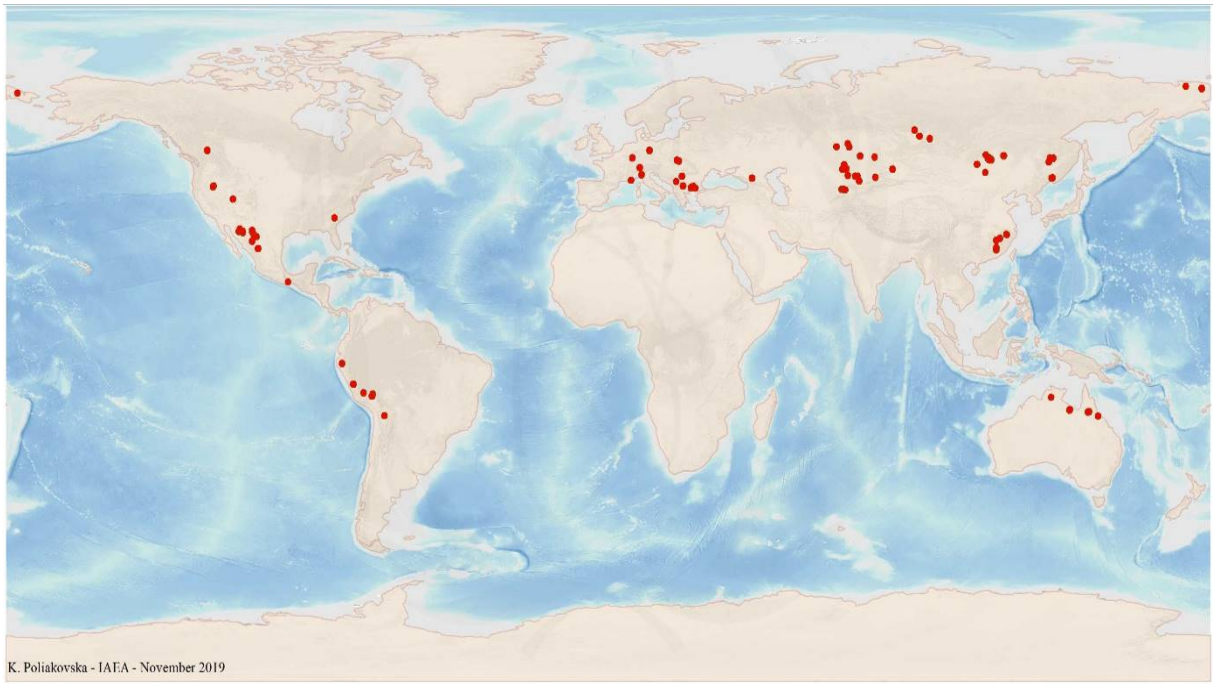

FIG. 4.2a. World distribution of selected Volcanic-Related Structure-Bound uranium deposits from the UDEPO database.

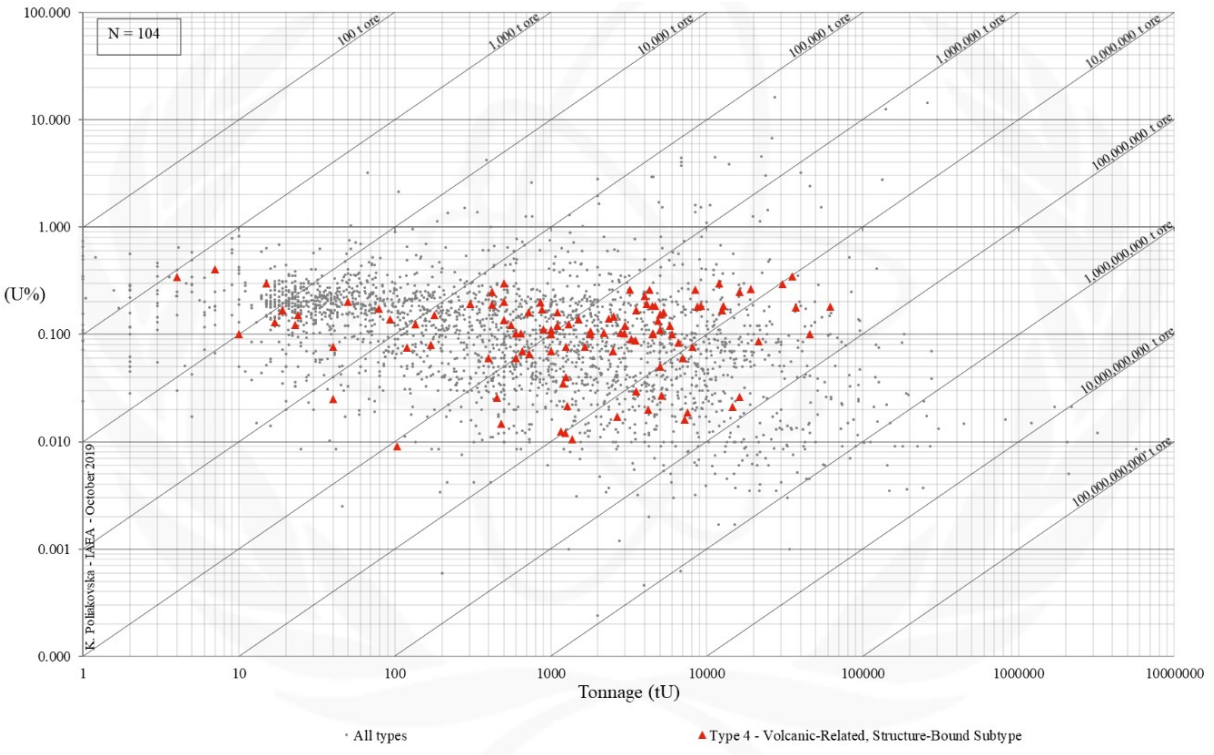

FIG. 4.2b. Grade and tonnage scatterplot highlighting Volcanic-Related Structure-Bound uranium deposits from the UDEPO database.

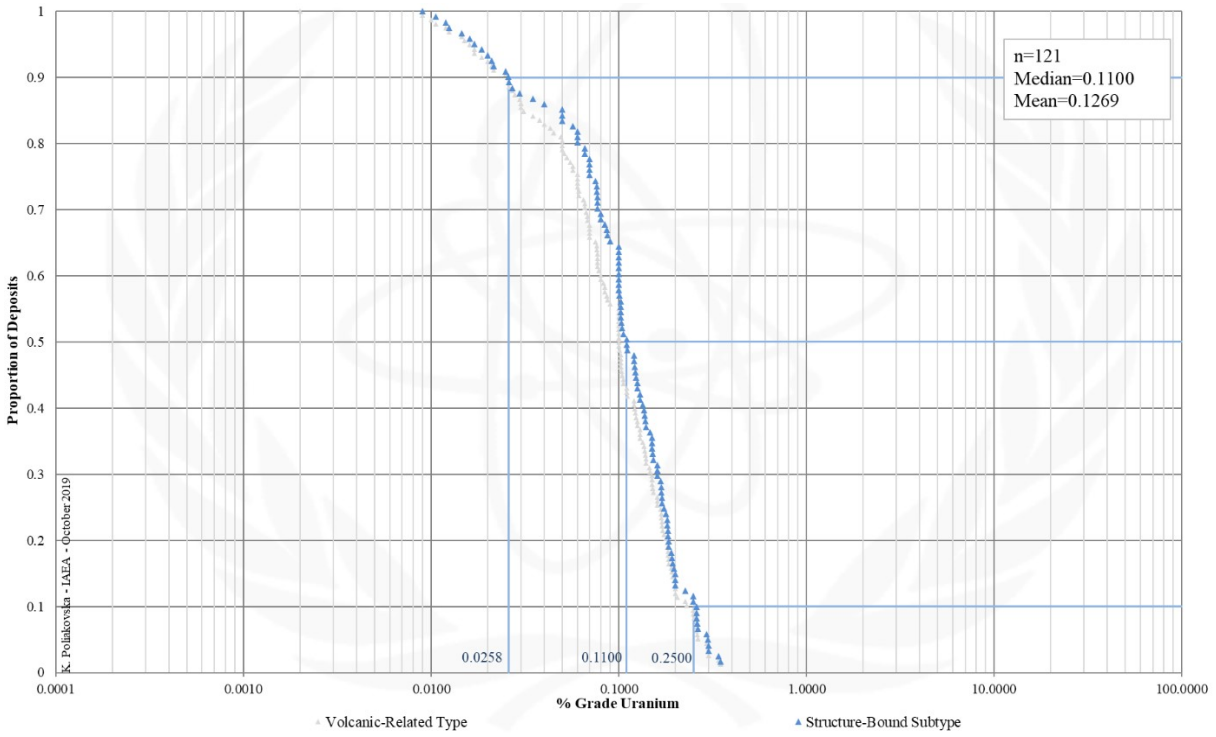

FIG. 4.2c. Grade Cumulative Probability Plot for Volcanic-Related Structure-Bound uranium deposits from the UDEPO database.

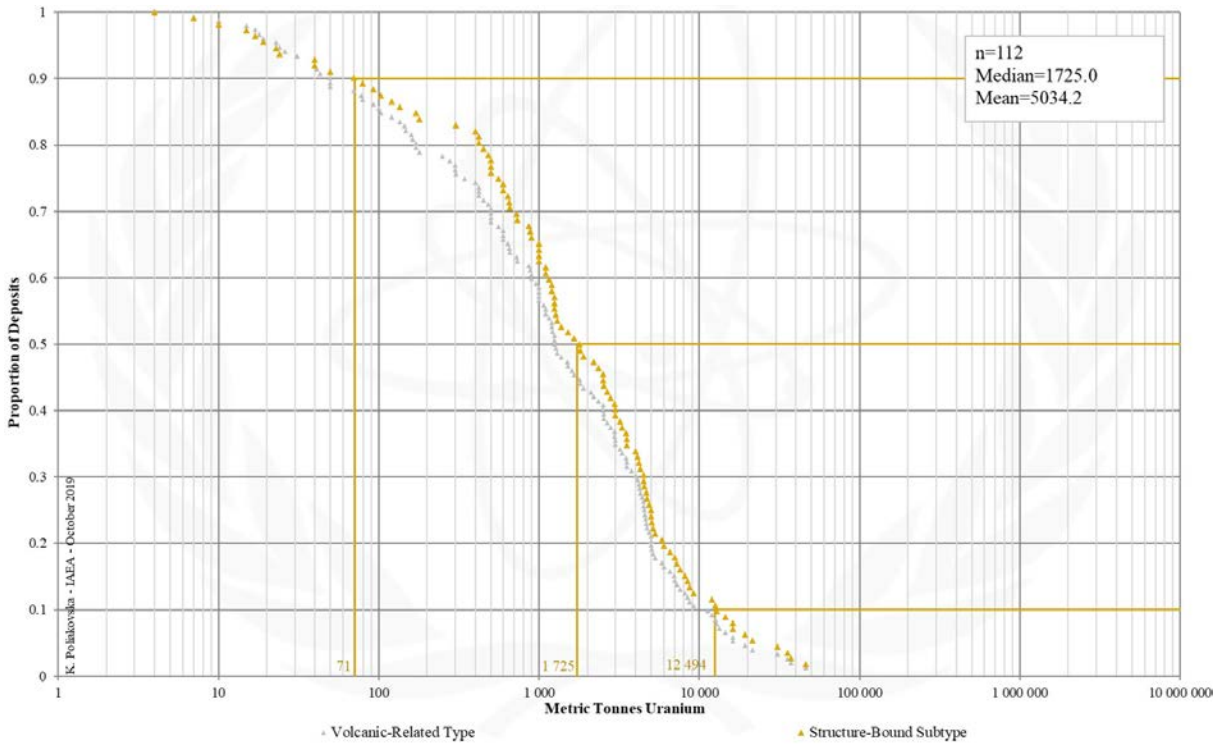

FIG. 4.2d. Tonnage Cumulative Probability Plot for Volcanic-Related Structure-Bound uranium deposits from the UDEPO database.

SUBTYPE 4.3. Volcanic-Related, Volcano-Sedimentary

Brief Description
- Volcanic-related deposits occur in caldera environments characterised by felsic to mafic volcanic lavas and subvolcanic intrusions, flow breccias, tuffs and intercalated pyroclastic and clastic sediments.
- Volcano-sedimentary deposits (subtype 4.3) take the form of low-grade, peneconcordant uranium ores in carbonaceous, fluvio-lacustrine sediments deposited in the exocaldera environment.

Genetically Associated Deposit Types
- Subtype 4.1. Volcanic-related, stratabound
- Subtype 4.2. Volcanic-related, structure-bound
- Subtype 12.1. Lignite-coal, stratiform

Type Examples
- Anderson Mine, USA; Sierra Pintada district, Argentina

Principal Commodities
- U ± B, Cu, F, Li, Mo, Ni, V

Grades (%) and Tonnages (tU)
- Average: 0.0706, 1818.2
- Median: 0.0570, 277.0

Number of Deposits
- 32

Provinces (undifferentiated from Volcanic-related Type)
- Carpathians West, Choibalsan North, Date Creek Basin, Gang Hong Belt, Georgetown Charters Towers, Glarner St Galler Verrucano, Grand Basin, Karamazar, La Charbonnier, Latium, Macusani Plateau, Murphy, Northwest Saxony, Pacific Coast, Pribalkhash, Saar Nahe Trough, Sierra Madre Occidental, Sierra Pintada, Sorsele, Stravropol, Streltsovsk, Tlaxiaco Basin, Xincheng Qinglong Belt, Xuemisitan Potential Belt.

Tectonic Setting
- Intraplate 'hot spot' and intracontinental rift settings

Typical Geological Age Range
- Palaeoproterozoic to recent

Mineral Systems Model

Source

Ground preparation
- Uranium-enriched, pre-caldera basement
- Generation of peralkaline F-rich melts
- Formation of nested caldera complexes comprising strongly fractionated felsic volcanic rocks

Energy
- High heat flow, extreme geothermal gradient and partial melting of mantle and crustal sources
- Hypabyssal intrusions/sub-volcanic magma chambers
- Voluminous high-temperature magmatism and volcanism

Fluids
- Hydrothermal ± meteoric and geothermal fluids

Ligands
- F

Reductants
- Detrital vegetal matter in clastic sedimentary units, ferrous (Fe^{2+}) or ferric (Fe^{3+}) iron, H_2S

Uranium
- Highly fractionated volcanic rocks, in particular peralkaline, F-rich rhyolites
- Aphanitic volcanic rocks or volcanic glass
- Pre-caldera/basement granitoids

Transport

Fluid pathways
- Caldera-related fault-fracture systems
- Unconformity surfaces
- Stratigraphic aquifers

Trap

Physical
- Permeable, tuffaceous lacustrine sandstone

Chemical
- Sulphide accumulations
- Detrital vegetal/carbonaceous matter

Deposition

Fluid/wallrock interaction

- Chance in redox conditions due to interaction of oxidised groundwaters and carbonaceous matter, sulphides and/or H_2S in

Adsorption

- Uranium adsorption onto clay minerals, humic substances, colloidal silica or zeolites

Supergene processes

- Secondary uranium redistribution and enrichment

Preservation

- Relative tectonic stability post-uranium mineralisation
- Subsidence and burial of the uranium mineralised rocks
- Arid- to semiarid climatic conditions
- Thick vegetation cover

Key Reference Bibliography

DAHLKAMP, F. J., Uranium Deposits of the World: Asia. Springer, Berlin, Heidelberg, 492p (2009).

DAHLKAMP, F. J., Uranium Deposits of the World: USA and Latin America. Springer, Berlin, Heidelberg, 515p (2010).

INTERNATIONAL ATOMIC ENERGY AGENCY, Geological Classification of Uranium Deposits and Description of Selected Examples. IAEA-TECDOC Series, 1842, 415p (2018).

MUELLER, A., HALBACH, P., The Anderson Mine (Arizona); an early diagenetic uranium deposit in Miocene lake sediments. Economic Geology, 78(2), 275-292 (1983).

NASH, J. T., Volcanogenic uranium deposits — geology, geochemical processes, and criteria for resource assessment. U.S. Geological Survey Open-File Report, 2010-1001, 99p (2010).

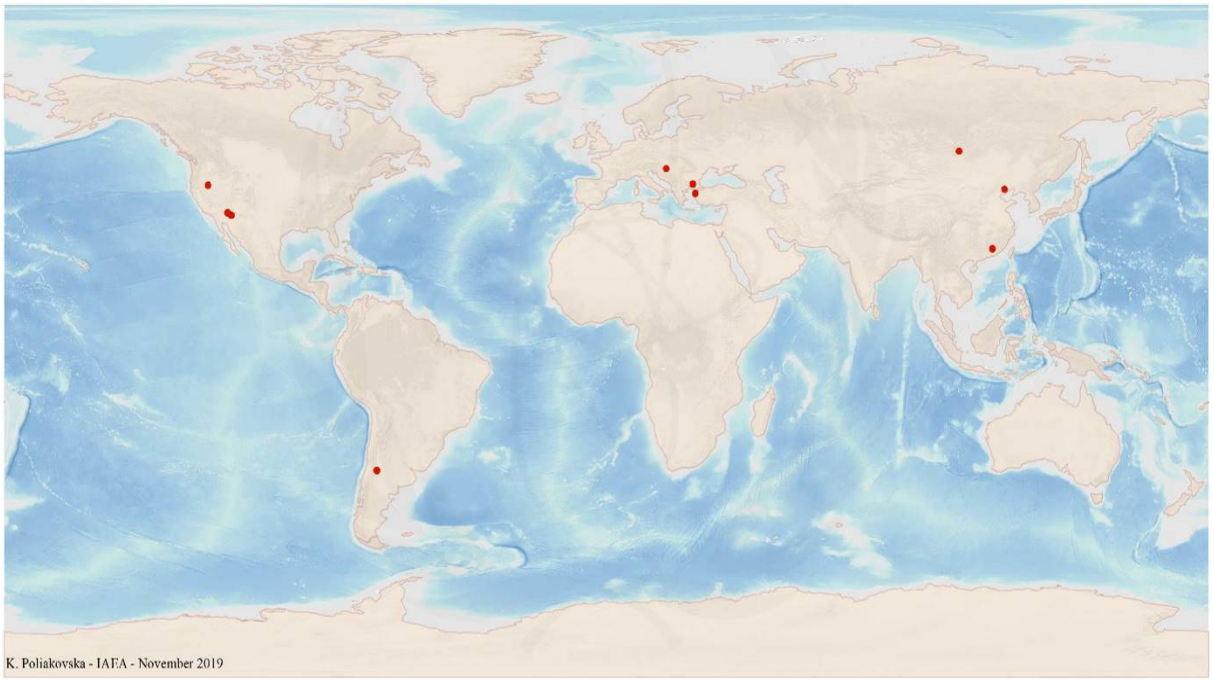

FIG. 4.3a. World distribution of selected Volcanic-Related Volcano-Sedimentary uranium deposits from the UDEPO database.

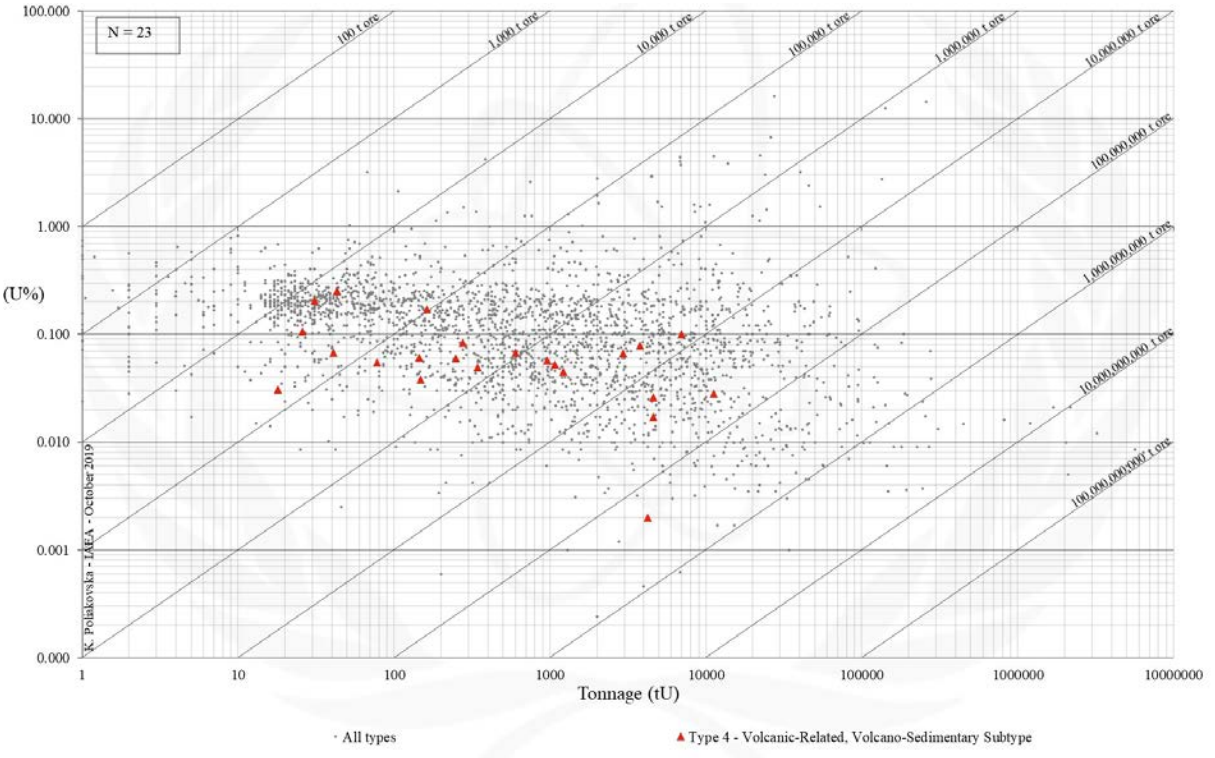

FIG. 4.3b. Grade and tonnage scatterplot highlighting Volcanic-Related Volcano-Sedimentary uranium deposits from the UDEPO database.

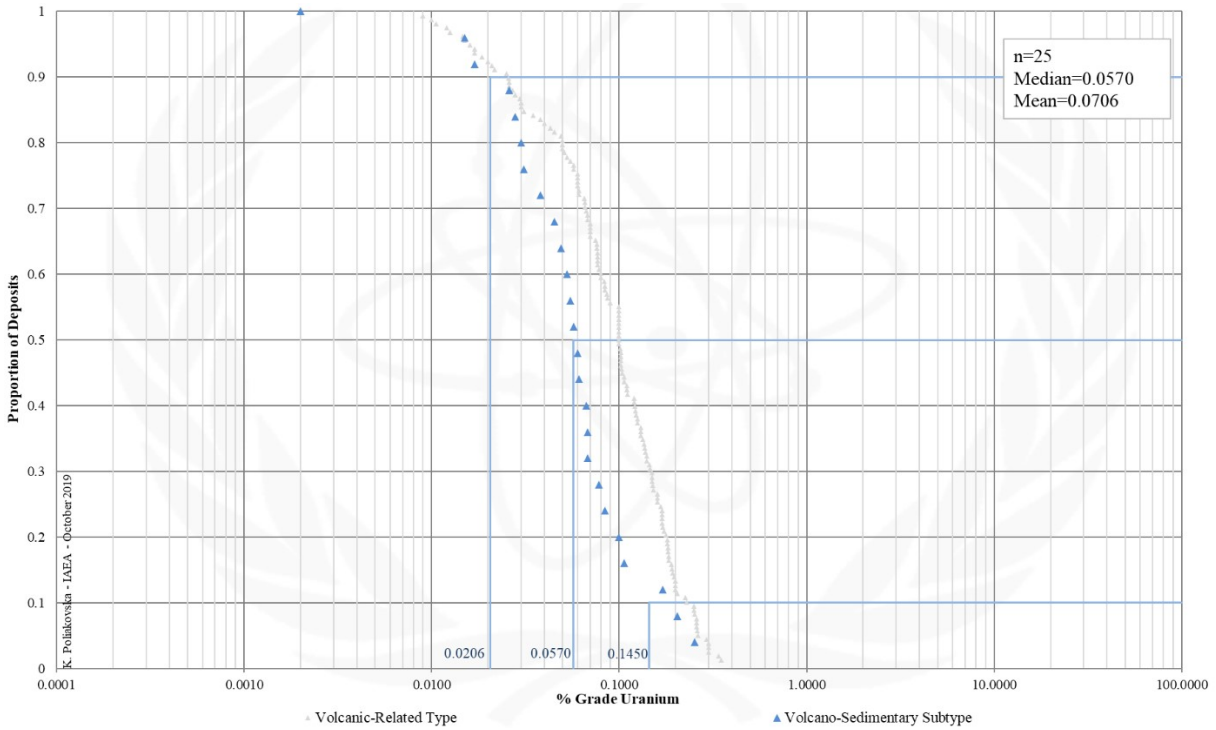

FIG. 4.3c. Grade Cumulative Probability Plot for Volcanic-Related Volcano-Sedimentary uranium deposits from the UDEPO database.

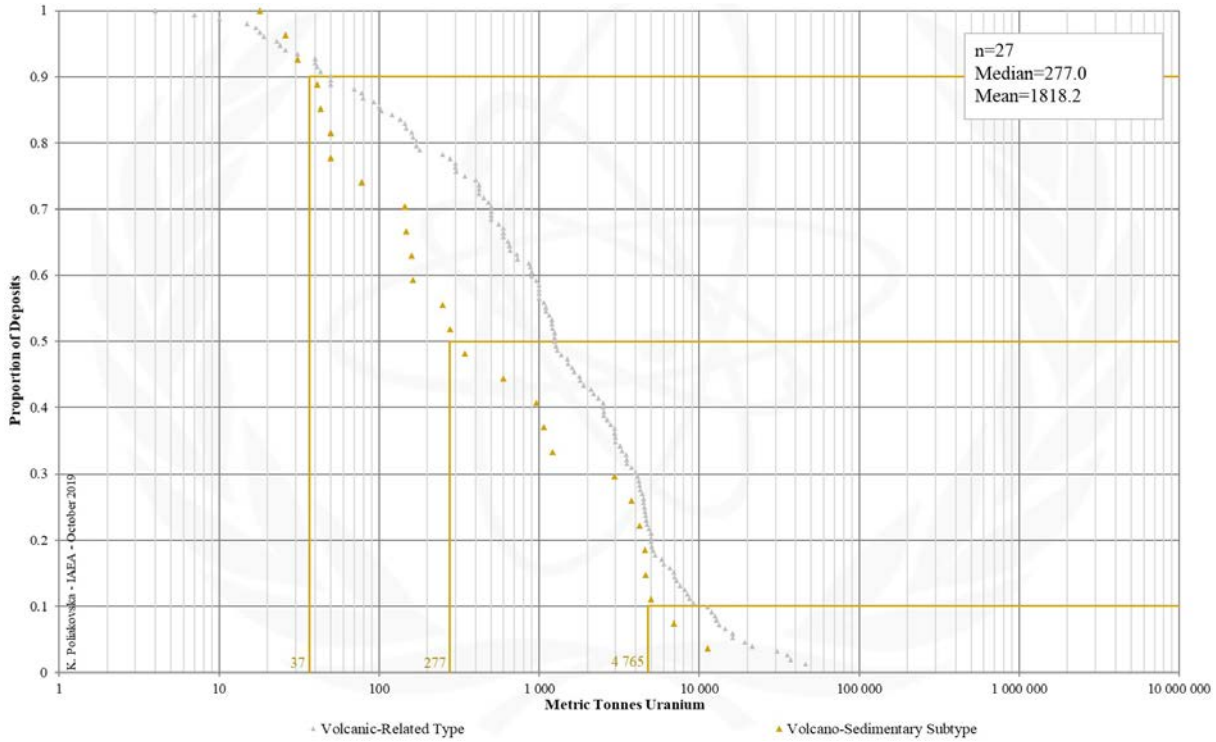

FIG. 4.3d. Tonnage Cumulative Probability Plot for Volcanic-Related Volcano-Sedimentary uranium deposits from the UDEPO database.

Appendix V

METASOMATITE

TYPE 5. Metasomatite

Brief Description

- Metasomatite deposits are products of intense sodium- or potassium-metasomatism along lithospheric fault systems giving rise to large volumes of albitised or illitised rock.
- The deposits take the form of structurally controlled, disseminated and vein-hosted ores of variable shape and size.
- Spatially and genetically associated metasomatic alteration zones are often substantial with strike lengths of up to several kilometres and vertical extents of up to two kilometres.
- Most metasomatite deposits are located in Precambrian cratons, in particular destabilised regions affected by prolonged or recurring episodes of tectono-magmatic activity.
- Three subtypes can be distinguished on the basis of their protoliths and type of metasomatism: Sodium (Na)-metasomatite, potassium (K)-metasomatite, and skarn.

Subtypes and Classes

- 5.1. Metasomatite, sodium (Na)-metasomatite
  - 5.1.1. Granite derived
  - 5.1.2. Metasediment-metavolcanic derived
- 5.2. Metasomatite, potassium (K)-metasomatite
- 5.3. Metasomatite, skarn

Type Examples

- Class 5.1.1. Kirovograd district, Ukraine; Lagoa Real, Brazil
- Class 5.1.2. Krivoy Rog district, Ukraine
- Subtype 5.2. Elkon district, Russian Federation
- Subtype 5.3. Mary Kathleen, Australia; Tranomaro, Madagascar

Principal Commodities

- U ± Ag, Au, Fe_3O_4, V, REE, Th

Grades (%) and Tonnages (tU)

- Average: 0.1060, 9297.1
- Median: 0.0763, 1747.0

Number of Deposits

- 161

Provinces

- Amur Ussuri, Aravalli, Arjeplog Arvidsjaur Sorsele, Bafq Posht e Badam, Bur Acaba, Central Mineral Belt, Chilenia, East Liaoning Belt, Elkon, Kalkadoon Leichhardt, Kirovograd Smolino, Kodar Udokan, Kuusamo, Lagoa Real, Lake Onega, Mary Kathleen, Mount Isa West, Olary Int Hermitage, Sierra Ancha Apache, Son Valley, Tranomaro

Tectonic Setting

- Collisional orogens; destabilised cratons

Typical Geological Age Range

- Palaeoproterozoic to Mesozoic

Mineral Systems Model

Source

Ground preparation
- Tectonic and thermal destabilisation of the host cratonic shield, or
- Collisional orogeny

Energy
- Regional metamorphism, or
- High heat flow, extreme geothermal gradient, partial melting of mantle and crustal sources and voluminous magmatism

Melts and fluids
- Subtype 5.1. Oxidised, low to moderately saline, alkaline fluids and reduced, mantle-derived fluids
- Subtype 5.2. Sulphur- and carbonate-bearing fluids
- Subtype 5.3. Highly saline brines (>30 wt% NaCl equivalent); high-temperature leucogranite melts and derivative magmatic-hydrothermal fluids

Ligands
- Ca, Cl, F, K, Na

Reductants and reactants
- Magnetiferous, hematitic, or garnetiferous skarns; carbonates; phosphates; Fe sulphides; Fe^{2+} silicates

Uranium
- Crystalline basement rocks; granitoids; felsic volcanic, volcaniclastic and siliciclastic rocks

Transport

Fluid pathways
- Crustal-scale fault zones
- Anticlinal hinge zones

Trap

Physical

- Transient breaching of physical barriers/seals, catastrophic rock failure and concomitant structurally controlled and highly focused fluid flow controlled by gradients in permeability and hydraulic head
- Gradients in permeability and hydraulic head are maximised at fault irregularities, fault tips and wings, fault intersections, fault damage zones characterised by high fracture density, rheological competency contrasts, regional unconformities, apices of granitic cusps and ridges, strain shadows and contact aureoles around intrusive bodies, boudinage and related strain shadows, fold noses and axial cleavages, truncated folds, strong penetrative fabric/schistosity, breccia zones, cataclasites, mylonites, episyenites and lithological contacts
- Albitisation resulting in a more brittle and permeable rock assemblage

Chemical

- Reactive lithological units such as marble or certain skarns
- Domains of intense metasomatism with abundant hematite, magnetite, sulphides and/or riebeckite
- Domains of authigenic dolomite or ankerite
- Zones of desilification

Deposition

Fluid cooling and depressurization

- Phase separation/CO_2 effervescence

Fluid/wallrock interaction

- Chance in redox conditions due to interaction of oxidised fluids and reduced wallrocks

Fluid mixing

- Change in redox conditions due to mixing of oxidising, uranium-bearing fluids with reducing, mantle-derived fluids

Supergene processes

- Secondary uranium redistribution and enrichment

Preservation

- Formation of steeply-dipping, vertically extensive uranium orebodies
- Relative tectonic stability post-uranium mineralisation
- Subsidence and burial of the uranium mineralised rocks

Key Reference Bibliography

DAHLKAMP, F. J., Uranium Deposits of the World: Asia. Springer, Berlin, Heidelberg, 492p (2009).

DAHLKAMP, F. J., Uranium Deposits of the World: Europe. Springer, Berlin, Heidelberg, 792p (2016).

INTERNATIONAL ATOMIC ENERGY AGENCY, Geological Classification of Uranium Deposits and Description of Selected Examples. IAEA-TECDOC Series 1842, 415p (2018).

KOUSKE, A. P., SUH, C. E., GHOGOMU, R. T., NGAKO, V., Na-metasomatism and uranium mineralization during a two-stage albitization at Kitongo, Northern Cameroon: structural and geochemical evidence. International Journal of Geosciences, 3(01), 258-279 (2012).

OLIVER, N. H. S., PEARSON, P. J., HOLCOMBE, R. J., ORD, A., Mary Kathleen metamorphic-hydrothermal uranium–rare–earth element deposit: ore genesis and numerical model of coupled deformation and fluid flow. Australian Journal of Earth Sciences, 46(3), 467-484 (1999).

SPARKES, G. W., Uranium mineralization within the Central Mineral Belt of Labrador: a summary of the diverse styles, settings and timing of mineralization. Government of Newfoundland and Labrador, Department of Natural Resources, Geological Survey, St. John's, Open File LAB/1684, 198p (2017).

WILDE, A., The Inca uraniferous skarn, Namibia: an unusual magmatic-hydrothermal deposit. Australian Institute of Geoscientists (AIG) Journal Paper, J2017-001, 1-11 (2017).

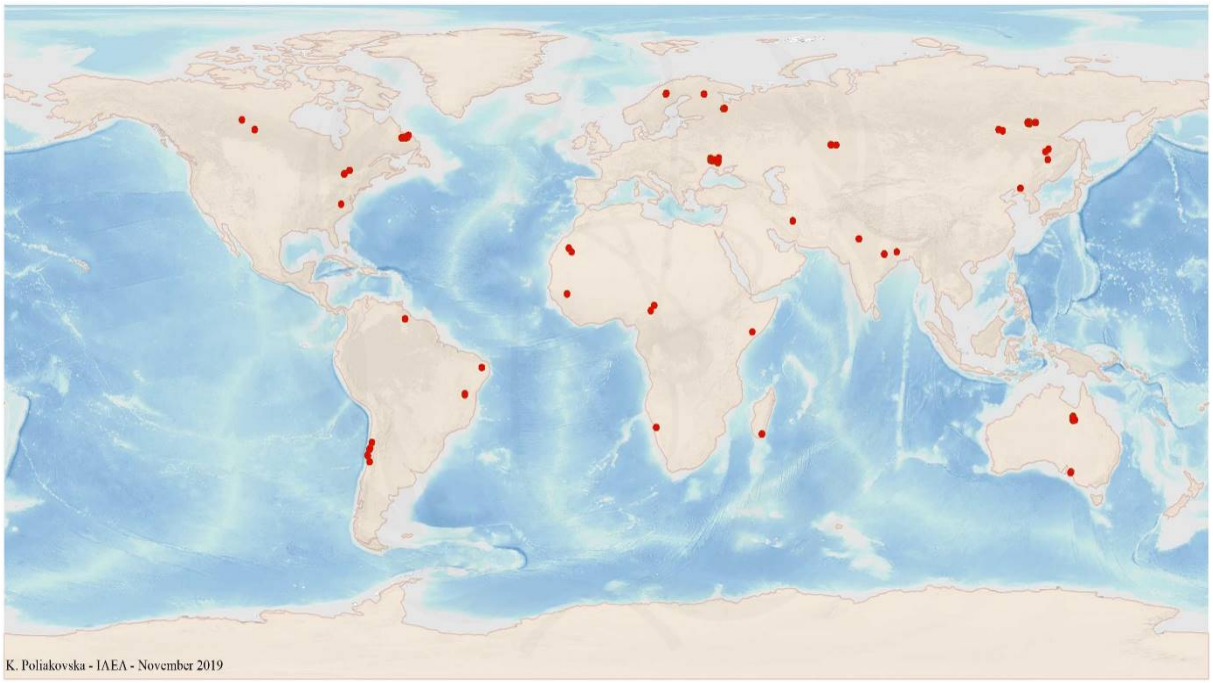

FIG. 5a. World distribution of selected Metasomatite uranium deposits from the UDEPO database.

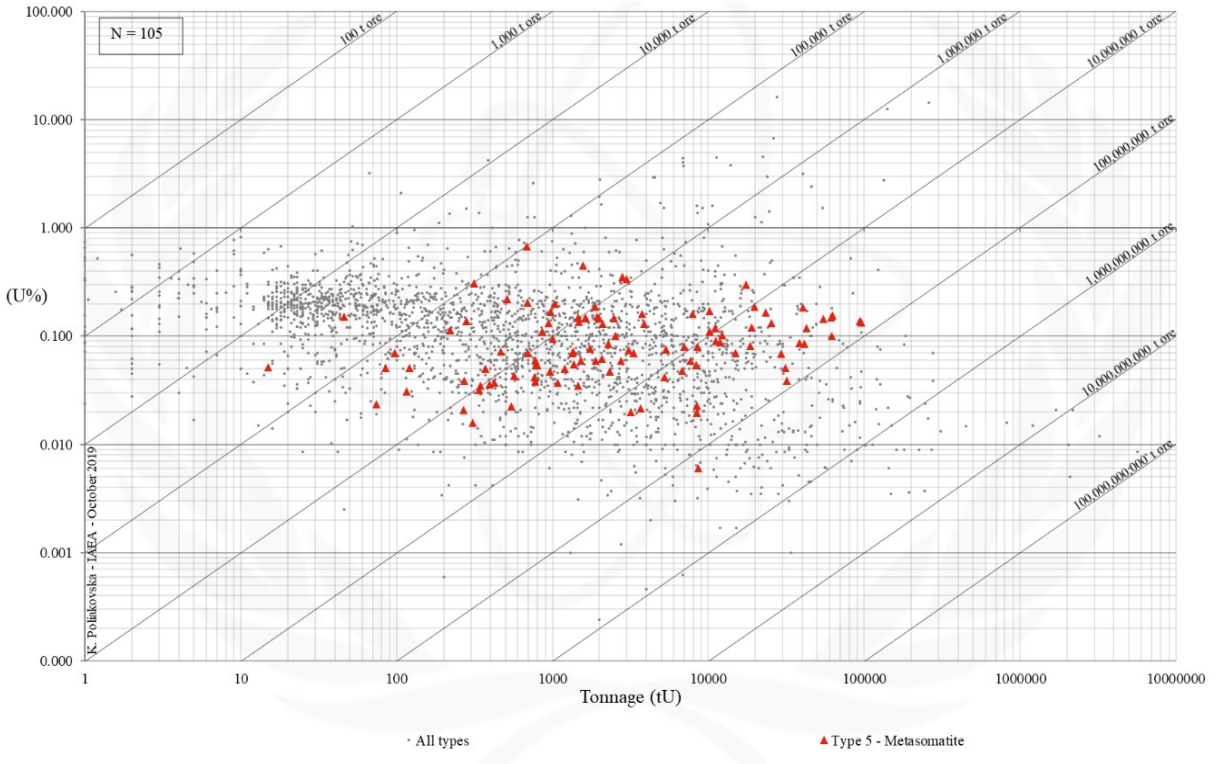

FIG. 5b. Grade and tonnage scatterplot highlighting Metasomatite uranium deposits from the UDEPO database.

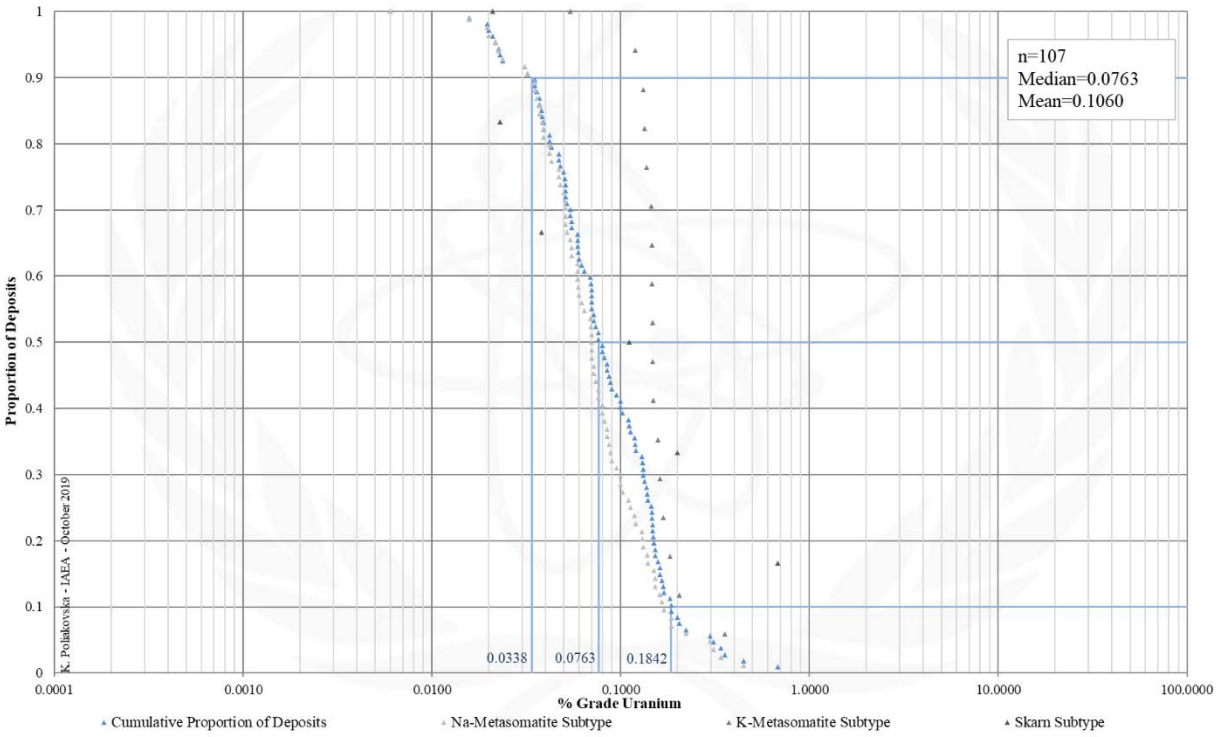

FIG. 5c. Grade Cumulative Probability Plot for Metasomatite uranium deposits from the UDEPO database.

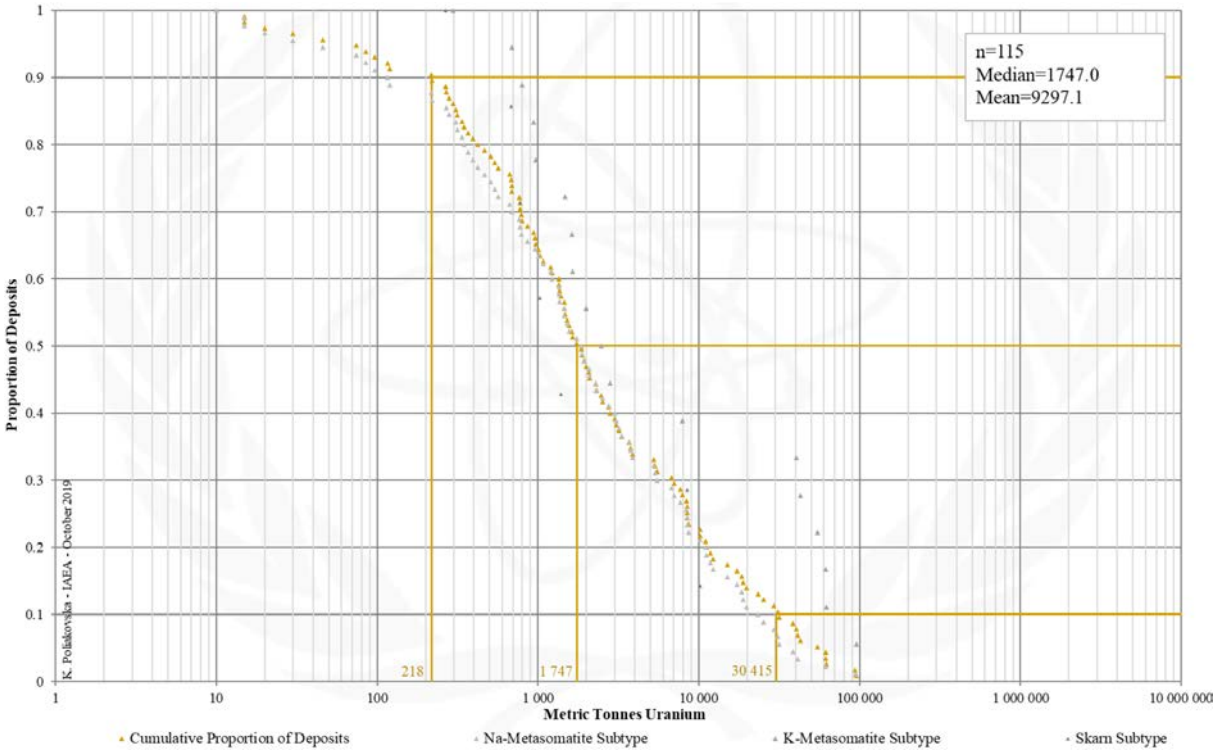

FIG. 5d. Tonnage Cumulative Probability Plot for Metasomatite uranium deposits from the UDEPO database.

SUBTYPE 5.1. Metasomatite, Sodium (Na)-Metasomatite

Brief Description
- Sodium (Na)-Metasomatite deposits are products of intense sodium-metasomatism along lithospheric fault systems giving rise to large volumes of albitised or illitised rock.
- The deposits take the form of structurally controlled, disseminated and vein-hosted ores of variable shape and size.
- Spatially and genetically associated metasomatic alteration zones are often substantial with strike lengths of up to several kilometres and vertical extents of up to two kilometres.
- Most sodium (Na)-metasomatite deposits are located in Precambrian cratons, in particular destabilised regions affected by prolonged or recurring episodes of tectono-magmatic activity.
- Sodium (Na)-metasomatite deposits are further divided into granite- and metasediment-metavolcanic-derived deposits.

Genetically Associated Deposit Types
- Subtype 5.2. Metasomatite, potassium (K)-metasomatite
- Subtype 5.3. Metasomatite, skarn

Type Examples
- Kirovograd district, Ukraine; Lagoa Real, Brazil; Aricheng, Guyana; Coles Hill, USA; Zheltorechenskoye, Krivoy Rog district, Ukraine; Michelin, Jacques Lake, Canada

Principal Commodities
- U ± V

Grades (%) and Tonnages (tU)
- Average: 0.0903, 7390.0
- Median: 0.0700, 1806.0

Number of Deposits
- 129

Provinces (undifferentiated from Metasomatite Type)
- Amur Ussuri, Aravalli, Arjeplog Arvidsjaur Sorsele, Bafq Posht e Badam, Bur Acaba, Central Mineral Belt, Chilenia, East Liaoning Belt, Elkon, Jajawal, Kalkadoon Leichhardt, Kirovograd Smolino, Kodar Udokan, Kuusamo, Lagoa Real, Lake Onega, Mary Kathleen, Mount Isa West, Olary Int Hermitage, Perapohja, Piedmont Province, Poli , Serido, Sierra Ancha Apache, Son Valley, Tranomaro

Tectonic Setting
- Destabilised cratons

Typical Geological Age Range
- Palaeo- to Mesoproterozoic

Mineral Systems Model

Source

Ground preparation
- Tectonic and thermal destabilisation of the host cratonic shield
- Protracted tectonic (polyphase deformation) and thermal history

Energy
- Regional metamorphism
- Voluminous post-orogenic magmatism
- (?)Deep-seated mantle plume

Fluids
- Oxidised, low to moderately saline, alkaline fluids
- Reduced, mantle-derived fluids

Ligands
- F

Reductants and reactants
- Hematite; magnetite; titanite; apatite; authigenic carbonates; Fe^{2+} silicates

Uranium
- Crystalline basement rocks; granitoids; felsic volcanic, volcaniclastic and siliciclastic rocks

Transport

Fluid pathways
- Crustal-scale fault zones
- Anticlinal hinge zones

Trap

Physical
- Transient breaching of physical barriers/seals, catastrophic rock failure and concomitant structurally controlled and highly focused fluid flow controlled by gradients in permeability and hydraulic head
- Gradients in permeability and hydraulic head are maximised at fault irregularities, fault tips and wings, fault intersections, fault damage zones characterised by high fracture density, rheological competency contrasts, regional unconformities, apices of granitic cusps and ridges, strain shadows and contact aureoles around intrusive

bodies, boudinage and related strain shadows, fold noses and axial cleavages, truncated folds, strong penetrative fabric/schistosity, breccia zones, cataclasites, mylonites, episyenites and lithological contacts
- Albitisation resulting in a more brittle and permeable rock assemblage

Chemical
- Domains of intense metasomatism with abundant hematite, magnetite, sulphides and/or riebeckite
- Domains of authigenic dolomite or ankerite

Deposition

Fluid cooling and depressurization
- Phase separation/CO_2 effervescence

Fluid/wallrock interaction
- Chance in redox conditions due to interaction of oxidised fluids and reduced wallrocks

Fluid mixing
- Change in redox conditions due to mixing of oxidising, uranium-bearing fluids with reducing, mantle-derived fluids

Supergene processes
- Secondary uranium redistribution and enrichment

Preservation

- Formation of steeply-dipping, vertically extensive uranium orebodies
- Relative tectonic stability post-uranium mineralisation
- Subsidence and burial of the uranium mineralised rocks

Key Reference Bibliography

DAHLKAMP, F. J., Uranium Deposits of the World: Europe. Springer, Berlin, Heidelberg, 792p (2016).

INTERNATIONAL ATOMIC ENERGY AGENCY, Geological Classification of Uranium Deposits and Description of Selected Examples. IAEA-TECDOC Series, 1842, 415p (2018).

KOUSKE, A. P., SUH, C. E., GHOGOMU, R. T., NGAKO, V., Na-metasomatism and uranium mineralization during a two-stage albitization at Kitongo, Northern Cameroon: structural and geochemical evidence. International Journal of Geosciences, 3(01), 258-279 (2012).

SPARKES, G. W., Uranium mineralization within the Central Mineral Belt of Labrador: a summary of the diverse styles, settings and timing of mineralization. Government of Newfoundland and Labrador, Department of Natural Resources, Geological Survey, St. John's, Open File LAB/1684, 198p (2017).

SPARKES, G. W., DUNNING, G. R., LANGILLE, A., The Michelin deposit: an example of albitite-hosted uranium mineralization within the Central Mineral Belt of Labrador. Newfoundland and Labrador Department of Natural Resources, Current Research Report 17-1, 219-238 (2017).

WILDE, A., The Inca 86arbonatiza skarn, Namibia: an unusual magmatic-hydrothermal deposit. Australian Institute of Geoscientists (AIG) Journal Paper, J2017-001, 1-11 (2017).

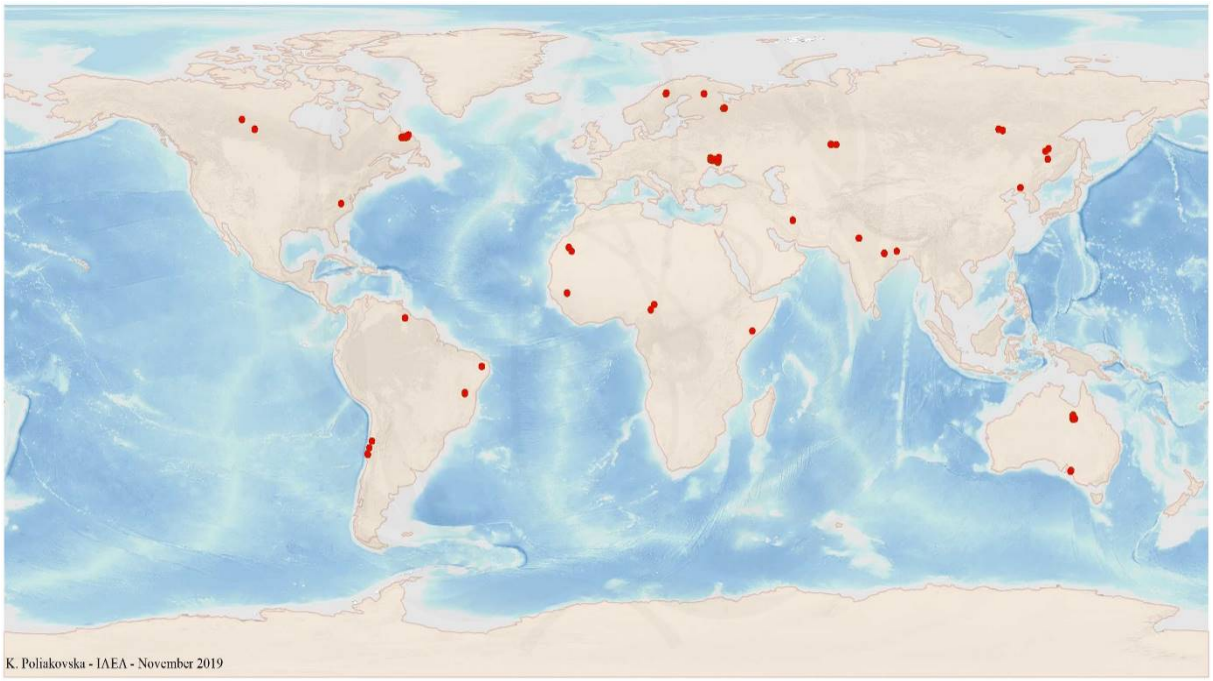

FIG. 5.1a. World distribution of selected Metasomatite Sodium (Na)-Metasomatite uranium deposits from the UDEPO database.

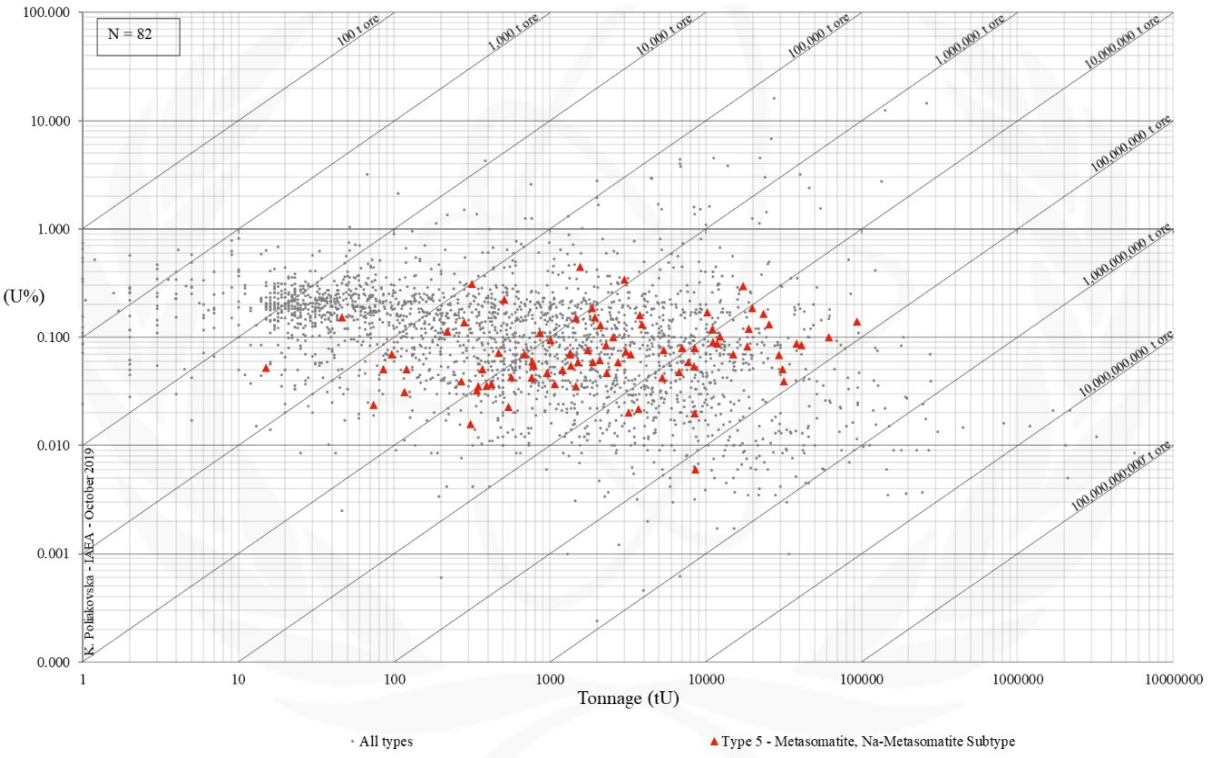

FIG. 5.1b. Grade and tonnage scatterplot highlighting Metasomatite Sodium (Na)-Metasomatite uranium deposits from the UDEPO database.

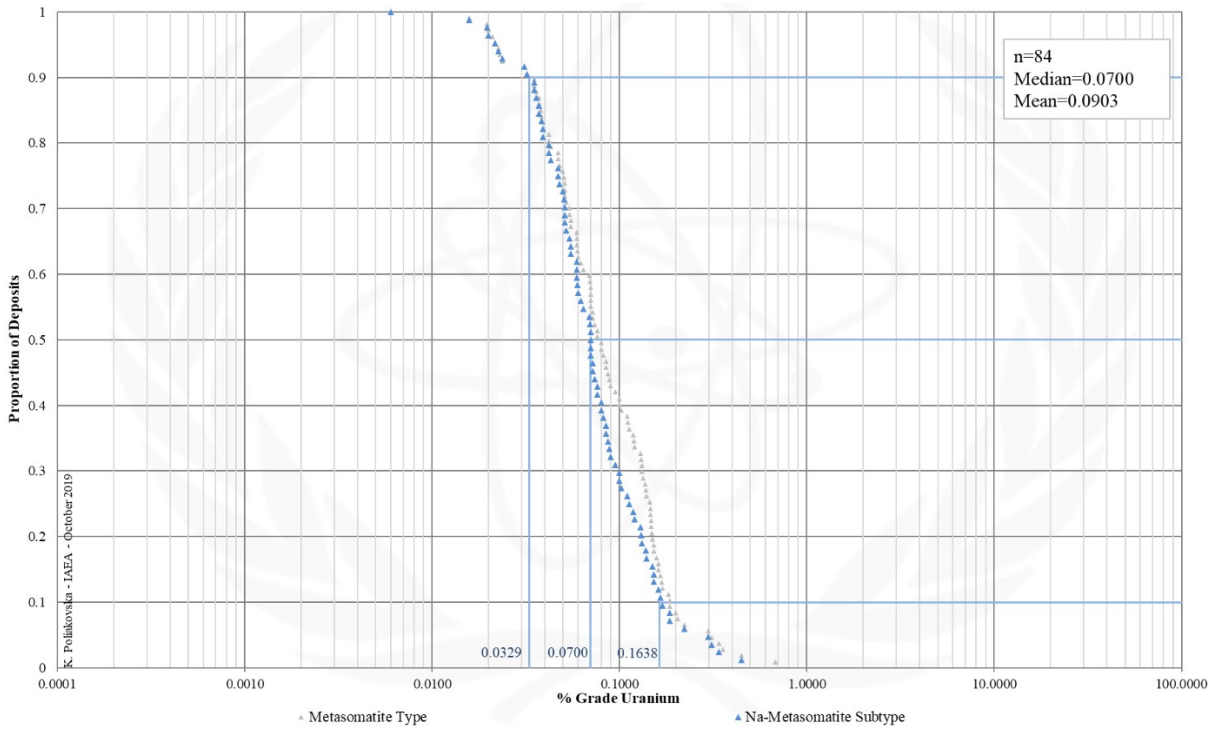

FIG. 5.1c. Grade Cumulative Probability Plot for Metasomatite Sodium (Na)-Metasomatite uranium deposits from the UDEPO database.

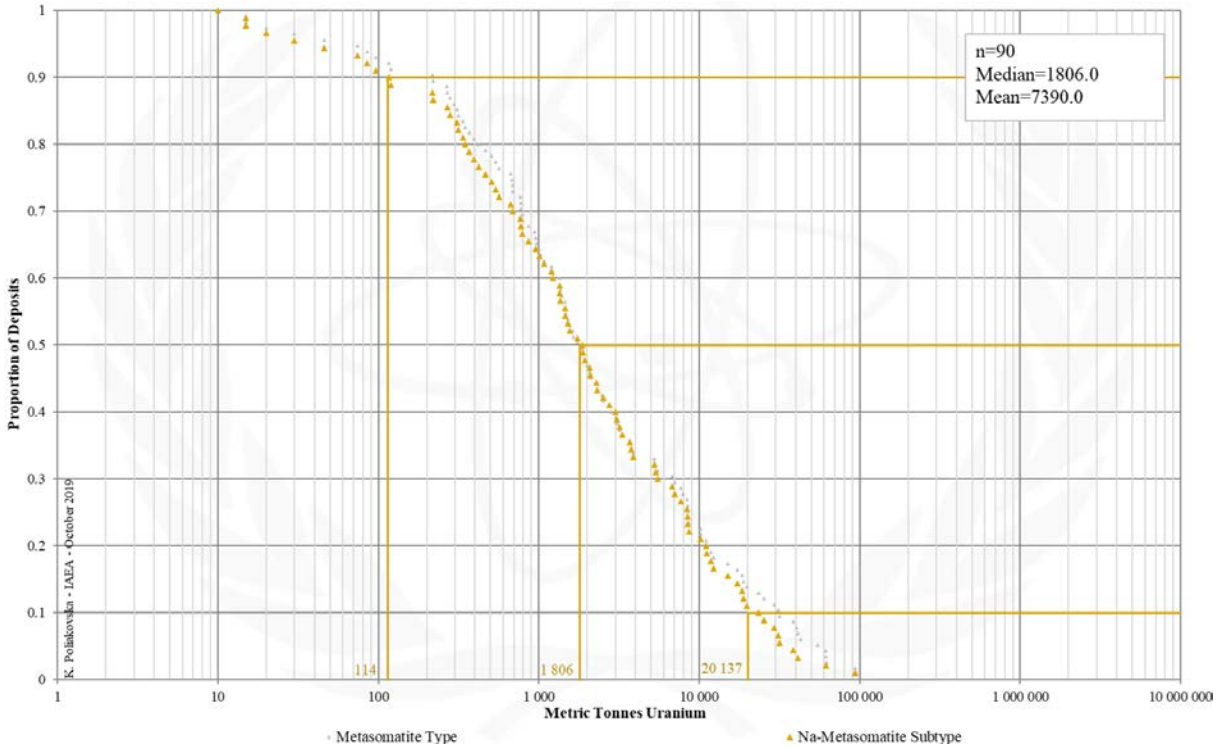

FIG. 5.1d. Tonnage Cumulative Probability Plot for Metasomatite Sodium (Na)-Metasomatite uranium deposits from the UDEPO database.

CLASS 5.1.1. Metasomatite, Sodium (Na)-Metasomatite, Granite Derived

Brief Description

- Granite derived sodium (Na)-metasomatite deposits are products of intense sodium-metasomatism along lithospheric fault systems giving rise to large volumes of albitised or illitised rock.
- The deposits take the form of structurally controlled, disseminated and vein-hosted ores of variable shape and size.
- Spatially and genetically associated metasomatic alteration zones are often substantial with strike lengths of up to several kilometres and vertical extents of up to two kilometres.
- Most granite derived sodium (Na)-metasomatite deposits are located in Precambrian cratons, in particular destabilised regions affected by prolonged or recurring episodes of tectono-magmatic activity.
-

Genetically Associated Deposit Types

- Subtype 5.2. Metasomatite, potassium (K)-metasomatite
- Subtype 5.3. Metasomatite, skarn

Type Examples

- Kirovograd district, Ukraine; Lagoa Real, Brazil; Aricheng, Guyana; Coles Hill, USA

Principal Commodities

- U ± V

Grades (%) and Tonnages (tU)

- Average: 0.0989, 3073.6
- Median: 0.0720, 1747.0

Number of Deposits

- 11

Provinces (undifferentiated from Metasomatite Type)

- Amur Ussuri, Aravalli, Arjeplog Arvidsjaur Sorsele, Bafq Posht e Badam, Bur Acaba, Central Mineral Belt, Chilenia, East Liaoning Belt, Elkon, Jajawal, Kalkadoon Leichhardt, Kirovograd Smolino, Kodar Udokan, Kuusamo, Lagoa Real, Lake Onega, Mary Kathleen, Mount Isa West, Olary Int Hermitage, Perapohja, Piedmont Province, Poli , Serido, Sierra Ancha Apache, Son Valley, Tranomaro

Tectonic Setting

- Destabilised cratons

Typical Geological Age Range

- Palaeo- to Mesoproterozoic

Mineral Systems Model

Source

Ground preparation
- Tectonic and thermal destabilisation of the host cratonic shield
- Protracted tectonic (polyphase deformation) and thermal history

Energy
- Regional metamorphism
- Voluminous post-orogenic magmatism
- (?)Deep-seated mantle plume

Fluids
- Oxidised, low to moderately saline, alkaline fluids
- Reduced, mantle-derived fluids

Ligands
- F

Reductants and reactants
- Hematite; magnetite; titanite; apatite; authigenic carbonates; Fe^{2+} silicates

Uranium
- Crystalline basement rocks; granitoids; felsic volcanic, volcaniclastic and siliciclastic rocks

Transport

Fluid pathways
- Crustal-scale fault zones
- Anticlinal hinge zones

Trap

Physical
- Transient breaching of physical barriers/seals, catastrophic rock failure and concomitant structurally controlled and highly focused fluid flow controlled by gradients in permeability and hydraulic head
- Gradients in permeability and hydraulic head are maximised at fault irregularities, fault tips and wings, fault intersections, fault damage zones characterised by high fracture density, rheological competency contrasts, regional unconformities, apices of granitic cusps and ridges, strain shadows and contact aureoles around intrusive bodies, boudinage and related strain shadows, fold noses and axial cleavages, truncated folds, strong penetrative

fabric/schistosity, breccia zones, cataclasites, mylonites, episyenites and lithological contacts
- Albitisation resulting in a more brittle and permeable rock assemblage

Chemical
- Domains of intense metasomatism with abundant hematite, magnetite, sulphides and/or riebeckite
- Domains of authigenic dolomite or ankerite

Deposition

Fluid cooling and depressurization
- Phase separation/CO_2 effervescence

Fluid/wallrock interaction
- Chance in redox conditions due to interaction of oxidised fluids and reduced wallrocks

Fluid mixing
- Change in redox conditions due to mixing of oxidising, uranium-bearing fluids with reducing, mantle-derived fluids

Supergene processes
- Secondary uranium redistribution and enrichment

Preservation

- Formation of steeply-dipping, vertically extensive uranium orebodies
- Relative tectonic stability post-uranium mineralisation
- Subsidence and burial of the uranium mineralised rocks

Key Reference Bibliography

DAHLKAMP, F. J., Uranium Deposits of the World: Europe. Springer, Berlin, Heidelberg, 792p (2016).

INTERNATIONAL ATOMIC ENERGY AGENCY, Geological Classification of Uranium Deposits and Description of Selected Examples. IAEA-TECDOC Series, 1842, 415p (2018).

KOUSKE, A. P., SUH, C. E., GHOGOMU, R. T., NGAKO, V., Na-metasomatism and uranium mineralization during a two-stage albitization at Kitongo, Northern Cameroon: structural and geochemical evidence. International Journal of Geosciences, 3(01), 258-279 (2012).

SPARKES, G. W., Uranium mineralization within the Central Mineral Belt of Labrador: a summary of the diverse styles, settings and timing of mineralization. Government of Newfoundland and Labrador, Department of Natural Resources, Geological Survey, St. John's, Open File LAB/1684, 198p (2017).

SPARKES, G. W., DUNNING, G. R., LANGILLE, A., The Michelin deposit: an example of albitite-hosted uranium mineralization within the Central Mineral Belt of Labrador. Newfoundland and Labrador Department of Natural Resources, Current Research Report 17-1, 219-238 (2017).

WILDE, A., The Inca 90arbonatiza skarn, Namibia: an unusual magmatic-hydrothermal deposit. Australian Institute of Geoscientists (AIG) Journal Paper, J2017-001, 1-11 (2017).

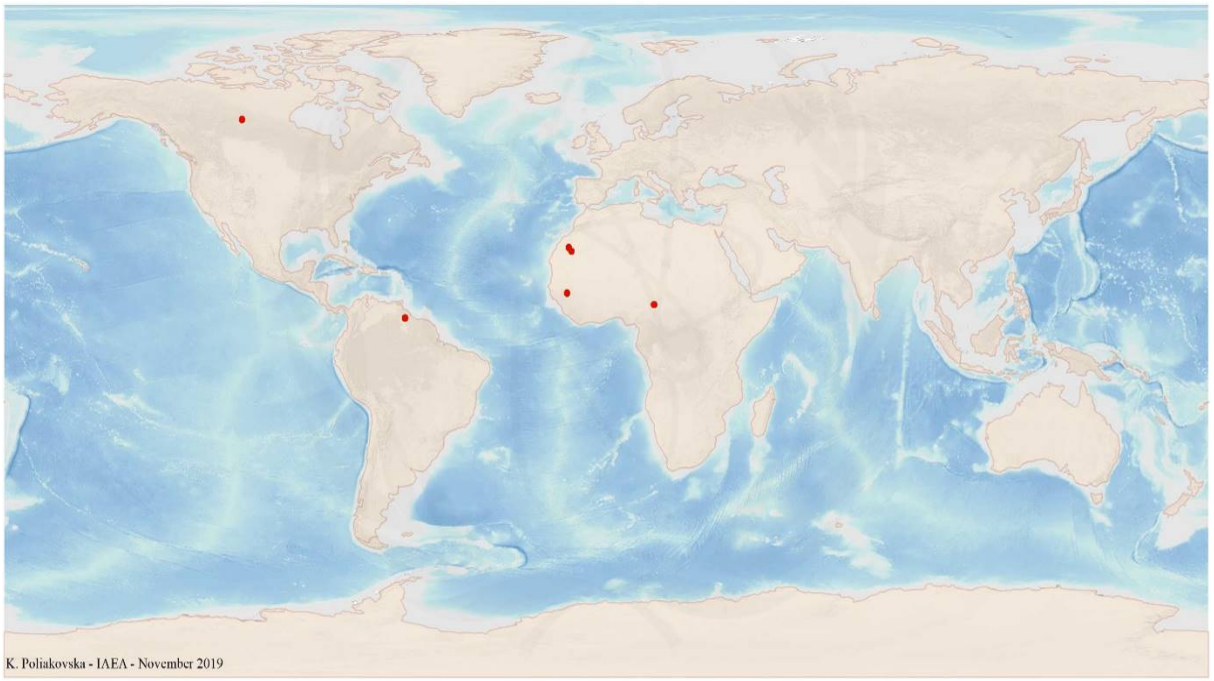

FIG. 5.1.1a. World distribution of selected Metasomatite Sodium (Na)-Metasomatite Granite Derived uranium deposits from the UDEPO database.

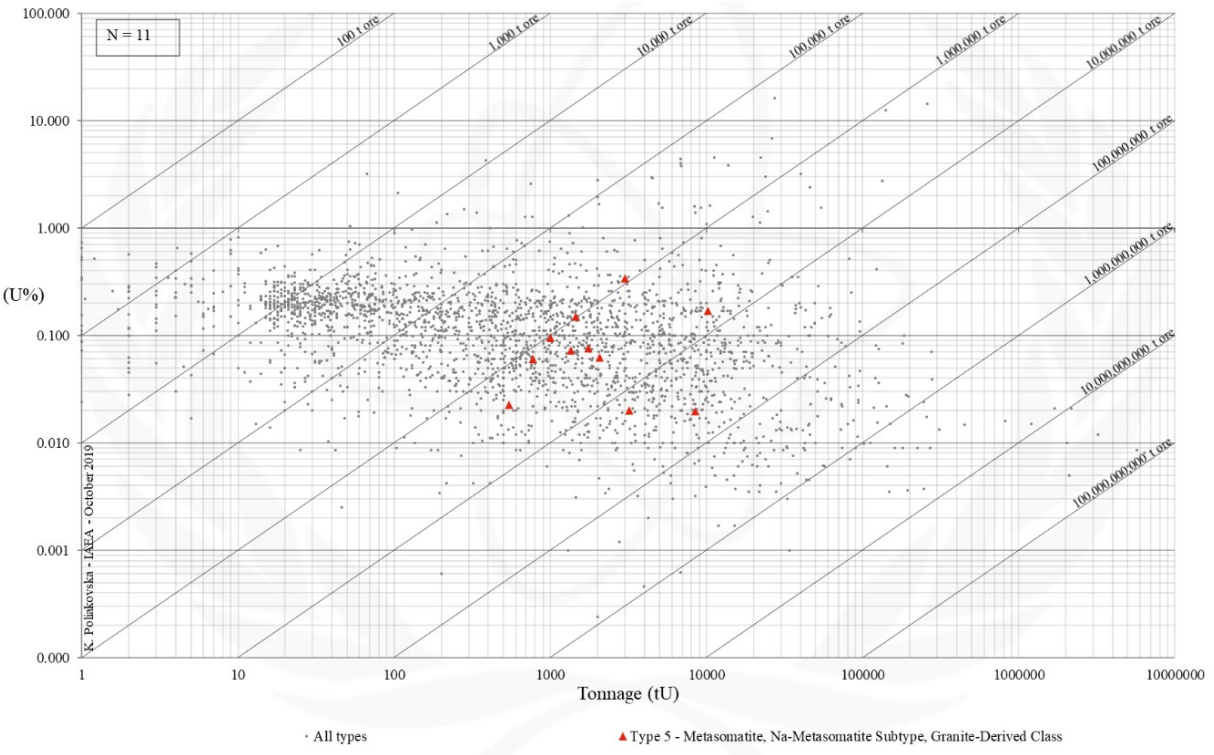

FIG. 5.1.1b. Grade and tonnage scatterplot highlighting Metasomatite Sodium (Na)-Metasomatite Granite Derived uranium deposits from the UDEPO database.

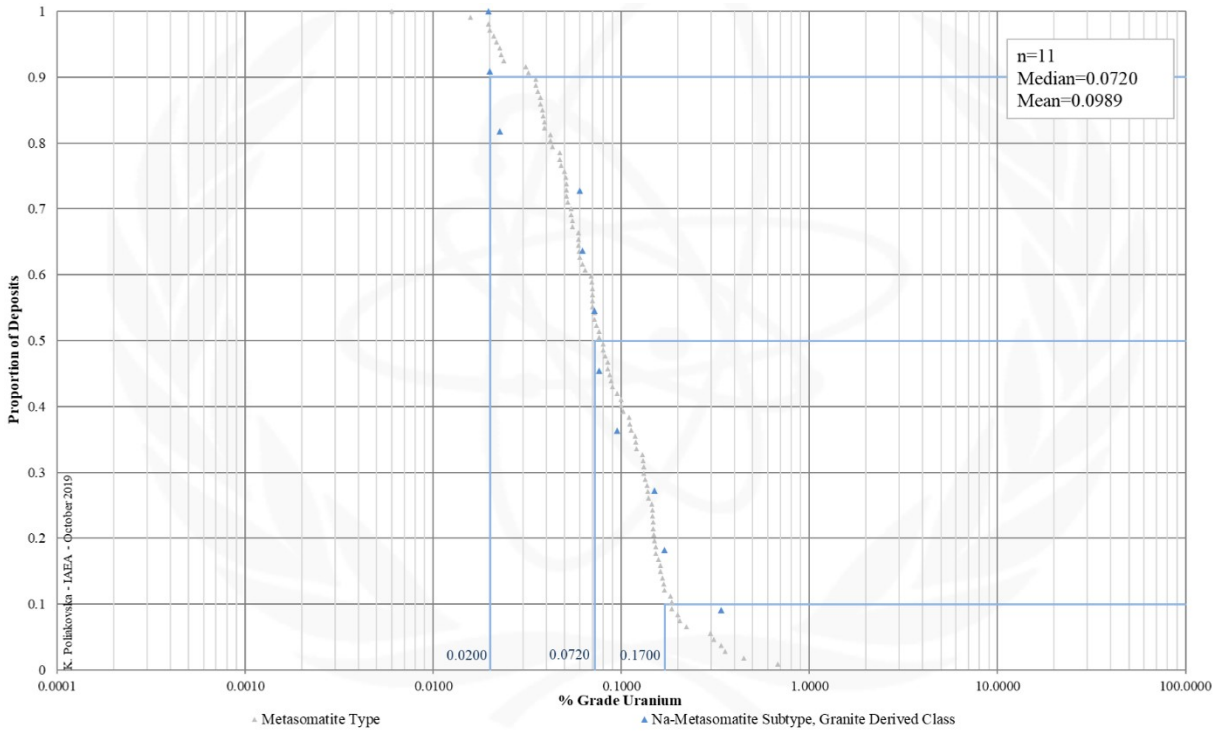

FIG. 5.1.1c. Grade Cumulative Probability Plot for Metasomatite Sodium (Na)-Metasomatite Granite Derived uranium deposits from the UDEPO database.

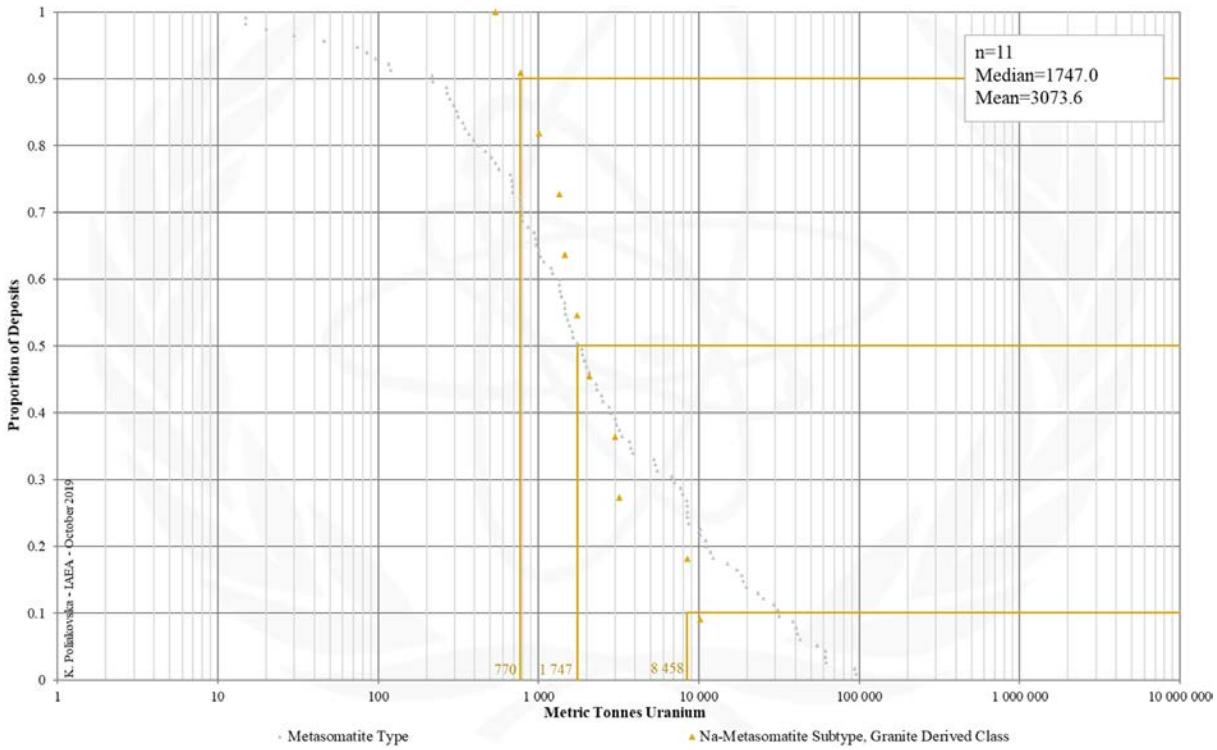

FIG. 5.1.1d. Tonnage Cumulative Probability Plot for Metasomatite Sodium (Na)-Metasomatite Granite Derived uranium deposits from the UDEPO database.

ClASS 5.1.2. Metasomatite, Sodium (Na)-Metasomatite, Metasediment-Metavolcanic Derived

Brief Description

- Metasomatite deposits are products of intense sodium- or potassium-metasomatism along lithospheric fault systems giving rise to large volumes of albitised or illitised rock.
- The deposits take the form of structurally controlled, disseminated and vein-hosted ores of variable shape and size.
- Spatially and genetically associated metasomatic alteration zones are often substantial with strike lengths of up to several kilometres and vertical extents of up to two kilometres.
- Most metasomatite deposits are located in Precambrian cratons, in particular destabilised regions affected by prolonged or recurring episodes of tectono-magmatic activity.
- Three subtypes can be distinguished on the basis of their protoliths and type of metasomatism: Sodium (Na)-metasomatite, potassium (K)-metasomatite, and skarn.
- Sodium (Na)-metasomatite deposits are further divided into granite- and metasediment-metavolcanic-derived deposits.

Genetically Associated Deposit Types

- Subtype 5.2. Metasomatite, potassium (K)-metasomatite
- Subtype 5.3. Metasomatite, skarn

Type Examples

- Krivoy Rog district, Ukraine; Michelin, Jacques Lake, Canada

Principal Commodities

- U ± V

Grades (%) and Tonnages (tU)

- Average: 0.0719, 7320.0
- Median: 0.0690, 1932.0

Number of Deposits

- 7

Provinces (undifferentiated from Metasomatite Type)

- Amur Ussuri, Aravalli, Arjeplog Arvidsjaur Sorsele, Bafq Posht e Badam, Bur Acaba, Central Mineral Belt, Chilenia, East Liaoning Belt, Elkon, Jajawal, Kalkadoon Leichhardt, Kirovograd Smolino, Kodar Udokan, Kuusamo, Lagoa Real, Lake Onega, Mary Kathleen, Mount Isa West, Olary Int Hermitage, Perapohja, Piedmont Province, Poli , Serido, Sierra Ancha Apache, Son Valley, Tranomaro

Tectonic Setting

- Destabilised cratons

Typical Geological Age Range

- Palaeo- to Mesoproterozoic

Mineral Systems Model

Source

Ground preparation

- Tectonic and thermal destabilisation of the host cratonic shield
- Protracted tectonic (polyphase deformation) and thermal history

Energy

- Regional metamorphism
- Voluminous post-orogenic magmatism
- (?)Deep-seated mantle plume

Fluids

- Oxidised, low to moderately saline, alkaline fluids
- Reduced, mantle-derived fluids

Ligands

- F

Reductants and reactants

- Hematite; magnetite; titanite; apatite; authigenic carbonates; Fe^{2+} silicates

Uranium

- Crystalline basement rocks; granitoids; felsic volcanic, volcaniclastic and siliciclastic rocks

Transport

Fluid pathways

- Crustal-scale fault zones
- Anticlinal hinge zones

Trap

Physical

- Transient breaching of physical barriers/seals, catastrophic rock failure and concomitant structurally controlled and highly focused fluid flow controlled by gradients in permeability and hydraulic head
- Gradients in permeability and hydraulic head are maximised at fault irregularities, fault tips and wings, fault intersections, fault damage zones characterised by high fracture density, rheological competency contrasts,

regional unconformities, apices of granitic cusps and ridges, strain shadows and contact aureoles around intrusive bodies, boudinage and related strain shadows, fold noses and axial cleavages, truncated folds, strong penetrative fabric/schistosity, breccia zones, cataclasites, mylonites, episyenites and lithological contacts
- Albitisation resulting in a more brittle and permeable rock assemblage

Chemical
- Domains of intense metasomatism with abundant hematite, magnetite, sulphides and/or riebeckite
- Domains of authigenic dolomite or ankerite

Deposition

Fluid cooling and depressurization
- Phase separation/CO_2 effervescence

Fluid/wallrock interaction
- Chance in redox conditions due to interaction of oxidised fluids and reduced wallrocks

Fluid mixing
- Change in redox conditions due to mixing of oxidising, uranium-bearing fluids with reducing, mantle-derived fluids

Supergene processes
- Secondary uranium redistribution and enrichment

Preservation

- Formation of steeply-dipping, vertically extensive uranium orebodies
- Relative tectonic stability post-uranium mineralisation
- Subsidence and burial of the uranium mineralised rocks

Key Reference Bibliography

DAHLKAMP, F. J., Uranium Deposits of the World: Europe. Springer, Berlin, Heidelberg, 792p (2016).

INTERNATIONAL ATOMIC ENERGY AGENCY, Geological Classification of Uranium Deposits and Description of Selected Examples. IAEA-TECDOC Series, 1842, 415p (2018).

KOUSKE, A. P., SUH, C. E., GHOGOMU, R. T., NGAKO, V., Na-metasomatism and uranium mineralization during a two-stage albitization at Kitongo, Northern Cameroon: structural and geochemical evidence. International Journal of Geosciences, 3(01), 258-279 (2012).

SPARKES, G. W., Uranium mineralization within the Central Mineral Belt of Labrador: a summary of the diverse styles, settings and timing of mineralization. Government of Newfoundland and Labrador, Department of Natural Resources, Geological Survey, St. John's, Open File LAB/1684, 198p (2017).

SPARKES, G. W., DUNNING, G. R., LANGILLE, A., The Michelin deposit: an example of albitite-hosted uranium mineralization within the Central Mineral Belt of Labrador. Newfoundland and Labrador Department of Natural Resources, Current Research Report 17-1, 219-238 (2017).

WILDE, A., The Inca uraniferous skarn, Namibia: an unusual magmatic-hydrothermal deposit. Australian Institute of Geoscientists (AIG) Journal Paper, J2017-001, 1-11 (2017).

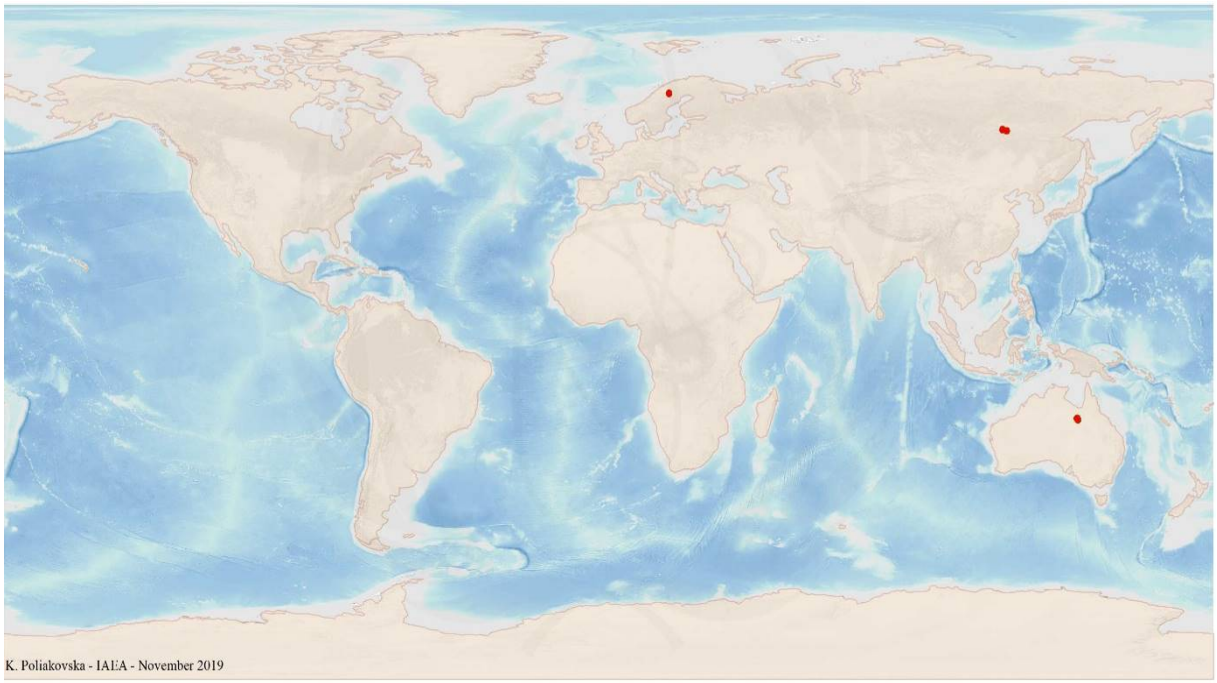

FIG. 5.1.2a. World distribution of selected Metasomatite Sodium (Na)-Metasomatite Metasediment-Metavolcanic Derived uranium deposits from the UDEPO database.

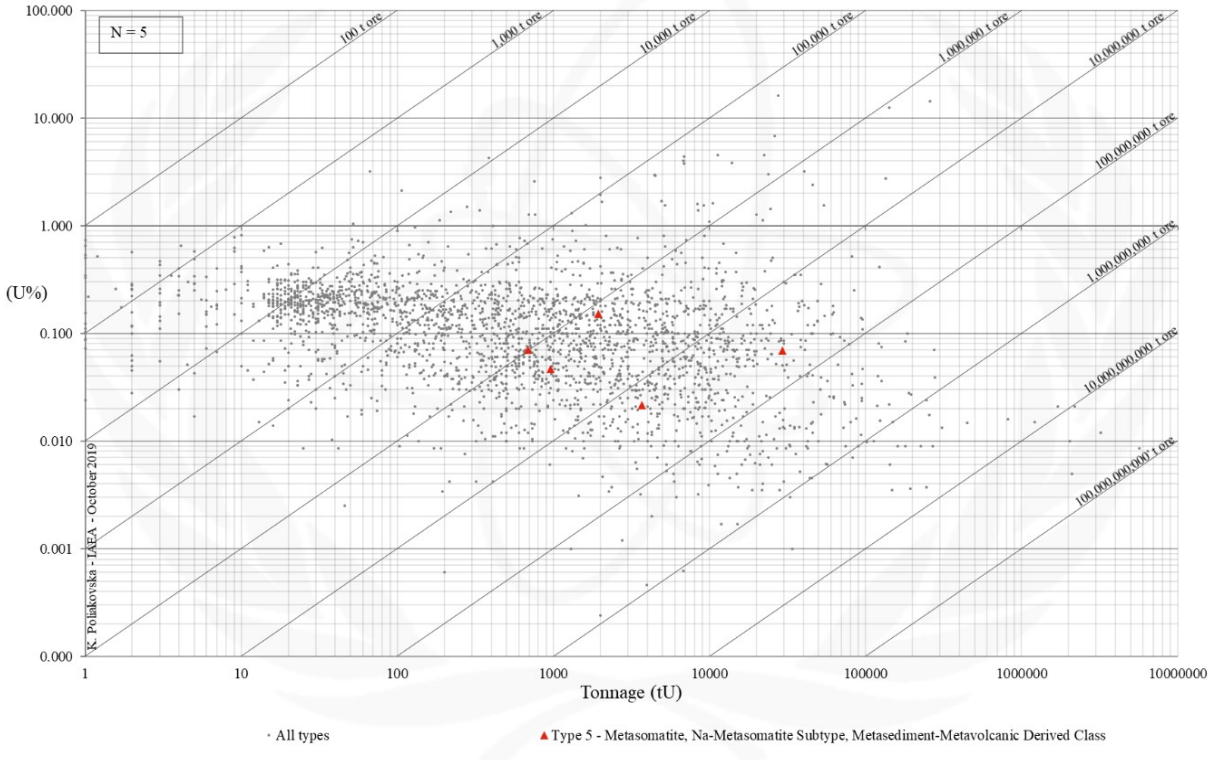

FIG. 5.1.2b. Grade and tonnage scatterplot highlighting Metasomatite Sodium (Na)-Metasomatite Metasediment-Metavolcanic Derived uranium deposits from the UDEPO database.

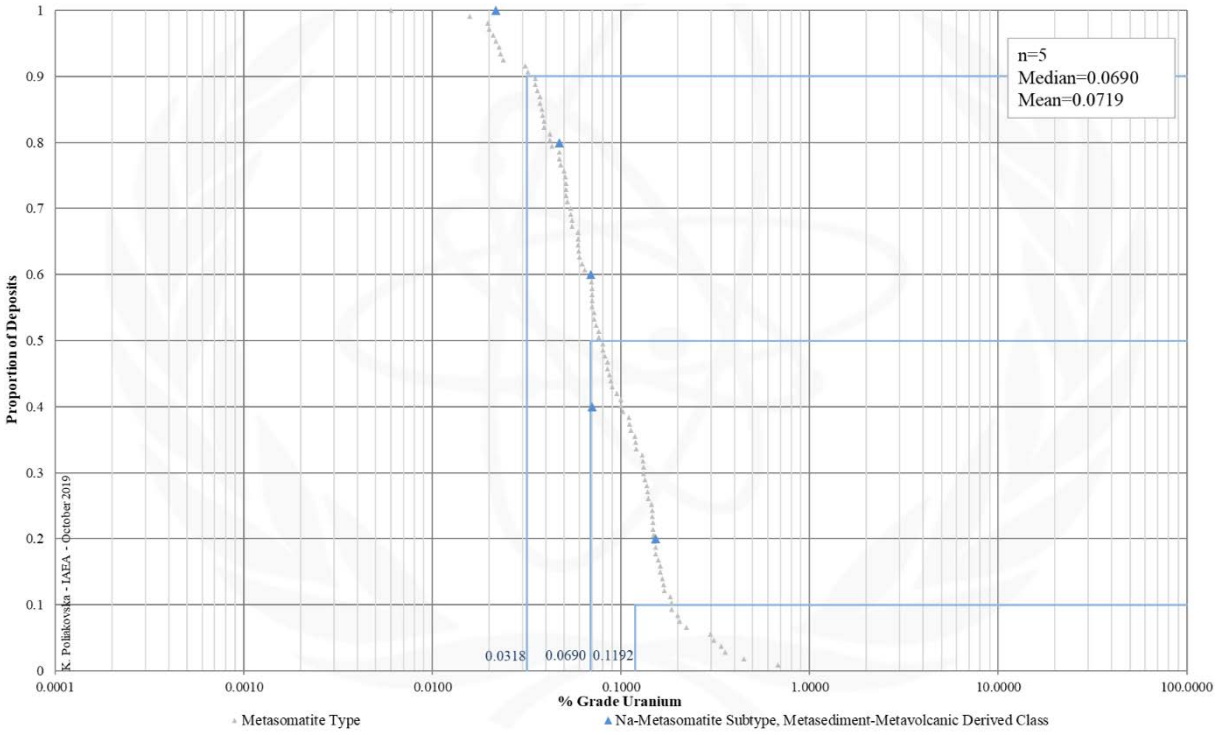

FIG. 5.1.2c. Grade Cumulative Probability Plot for Metasomatite Sodium (Na)-Metasomatite Metasediment-Metavolcanic Derived uranium deposits from the UDEPO database.

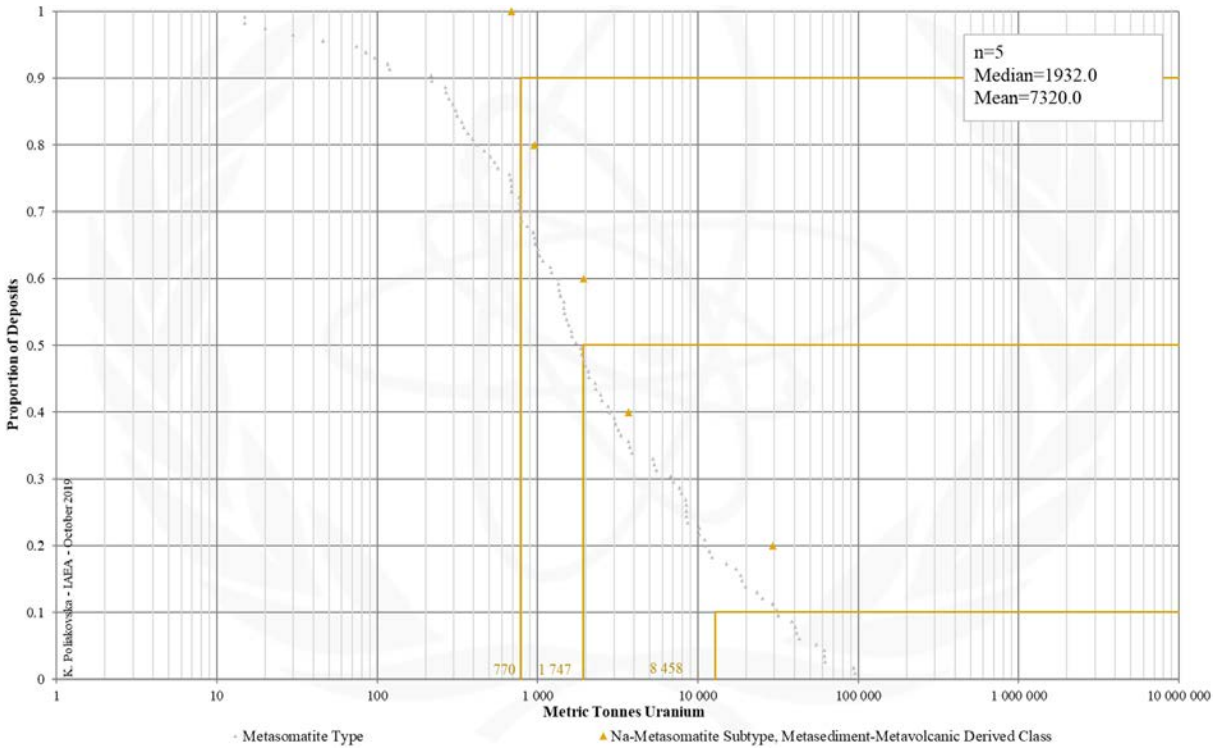

FIG. 5.1.2d. Tonnage distribution for Metasomatite Sodium (Na)-Metasomatite Metasediment-Metavolcanic Derived uranium deposits from the UDEPO database.

SUBTYPE 5.2. Metasomatite, Potassium (K)-Metasomatite

Brief Description
- Potassium (K)-metasomatite deposits are products of intense potassium-metasomatism along lithospheric fault systems giving rise to large volumes of albitised or illitised rock.
- The deposits take the form of structurally controlled, disseminated and vein-hosted ores of variable shape and size.
- Spatially and genetically associated metasomatic alteration zones are often substantial with strike lengths of up to several kilometres and vertical extents of up to two kilometres.
- Most potassium (K)-metasomatite deposits are located in Precambrian cratons, in particular destabilised regions affected by prolonged or recurring episodes of tectono-magmatic activity.
- Potassium (K)-metasomatite deposits are known exclusively from the Elkon district (Russian Federation).

Genetically Associated Deposit Types
- Subtype 5.1. Metasomatite, sodium (Na)-metasomatite
- Subtype 5.3. Metasomatite, skarn

Type Examples
- Elkon district, Russian Federation

Principal Commodities
- U, Au, Ag

Grades (%) and Tonnages (tU)
- Average: 0.1579, 21182.2
- Median: 0.1470, 2236.0

Number of Deposits
- 21

Provinces (undifferentiated from Metasomatite Type)
- Amur Ussuri, Aravalli, Arjeplog Arvidsjaur Sorsele, Bafq Posht e Badam, Bur Acaba, Central Mineral Belt, Chilenia, East Liaoning Belt, Elkon, Jajawal, Kalkadoon Leichhardt, Kirovograd Smolino, Kodar Udokan, Kuusamo, Lagoa Real, Lake Onega, Mary Kathleen, Mount Isa West, Olary Int Hermitage, Perapohja, Piedmont Province, Poli , Serido, Sierra Ancha Apache, Son Valley, Tranomaro

Tectonic Setting
- Destabilised cratons

Typical Geological Age Range
- Cretaceous

Mineral Systems Model

Source

Ground preparation
- Tectonic and thermal destabilisation of the host cratonic shield
- Protracted tectonic (polyphase deformation) and thermal history

Energy
- Voluminous post-orogenic magmatism
- (?)Deep-seated mantle plume

Fluids
- Sulphur- and carbonate-bearing fluids

Ligands
- (?)F

Reductants and reactants
- Fe-sulphides; Fe^{2+} silicates; authigenic carbonates

Uranium
- Crystalline basement rocks; granitoids

Transport

Fluid pathways
- Crustal-scale fault zones
- Horst and graben structures

Trap

Physical
- Transient breaching of physical barriers/seals, catastrophic rock failure and concomitant structurally controlled and highly focused fluid flow controlled by gradients in permeability and hydraulic head
- Gradients in permeability and hydraulic head are maximised at fault damage and breccia zones

Chemical
- Domains of intense metasomatism with abundant Fe-sulphides and carbonates
- Domains of desilicification

Deposition
Fluid cooling and depressurization – Phase separation/CO_2 effervescence Fluid/wallrock interaction – Chance in redox conditions due to interaction of oxidised fluids and reduced wallrocks
Preservation
– Formation of steeply-dipping, vertically extensive uranium orebodies – Relative tectonic stability post-uranium mineralisation – Subsidence and burial of the uranium mineralised rocks

Key Reference Bibliography

DAHLKAMP, F. J., Uranium Deposits of the World: Asia. Springer, Berlin, Heidelberg, 492p (2009).
GOLDFARB, R. J., HART, C., DAVIS, G., GROVES, D., East Asian gold: deciphering the anomaly of Phanerozoic gold in Precambrian cratons. Economic Geology, 102(3), 341-345 (2007).
INTERNATIONAL ATOMIC ENERGY AGENCY, Geological Classification of Uranium Deposits and Description of Selected Examples. IAEA-TECDOC Series, 1842, 415p (2018).

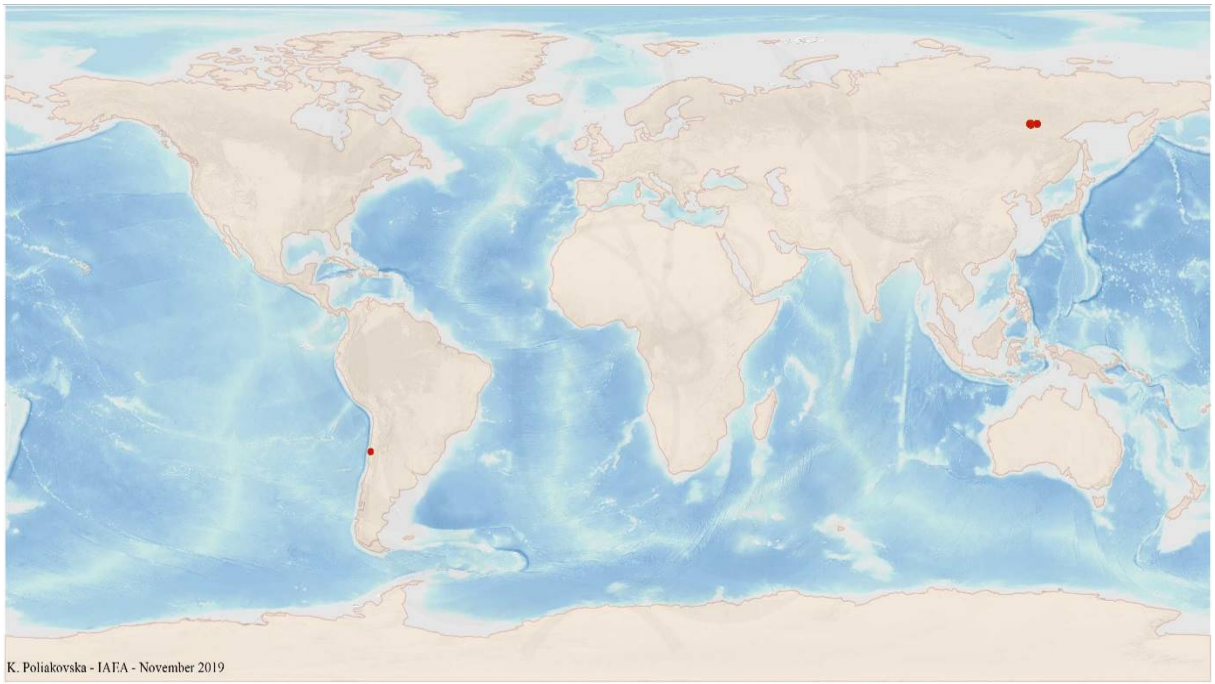

FIG. 5.2a. World distribution of selected Metasomatite Potassium (K)-Metasomatite uranium deposits from the UDEPO database.

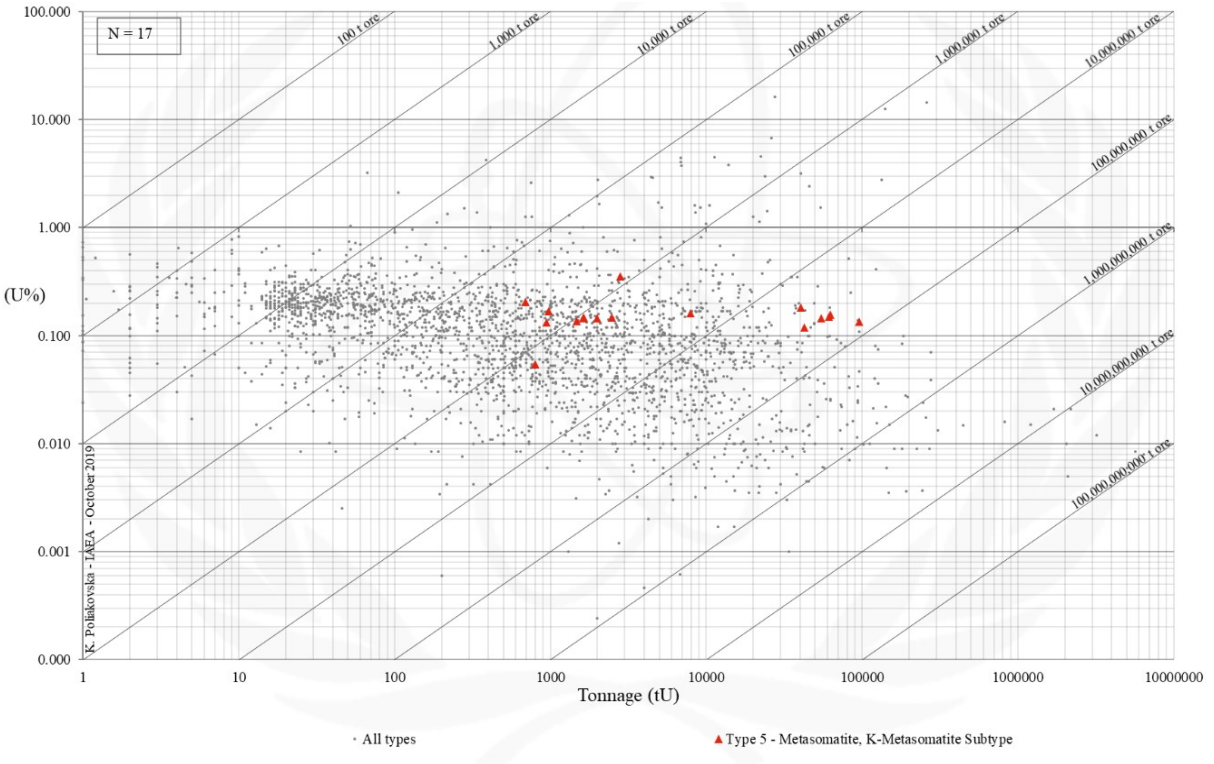

FIG. 5.2b. Grade and tonnage scatterplot highlighting Metasomatite Potassium (K)-Metasomatite uranium deposits from the UDEPO database.

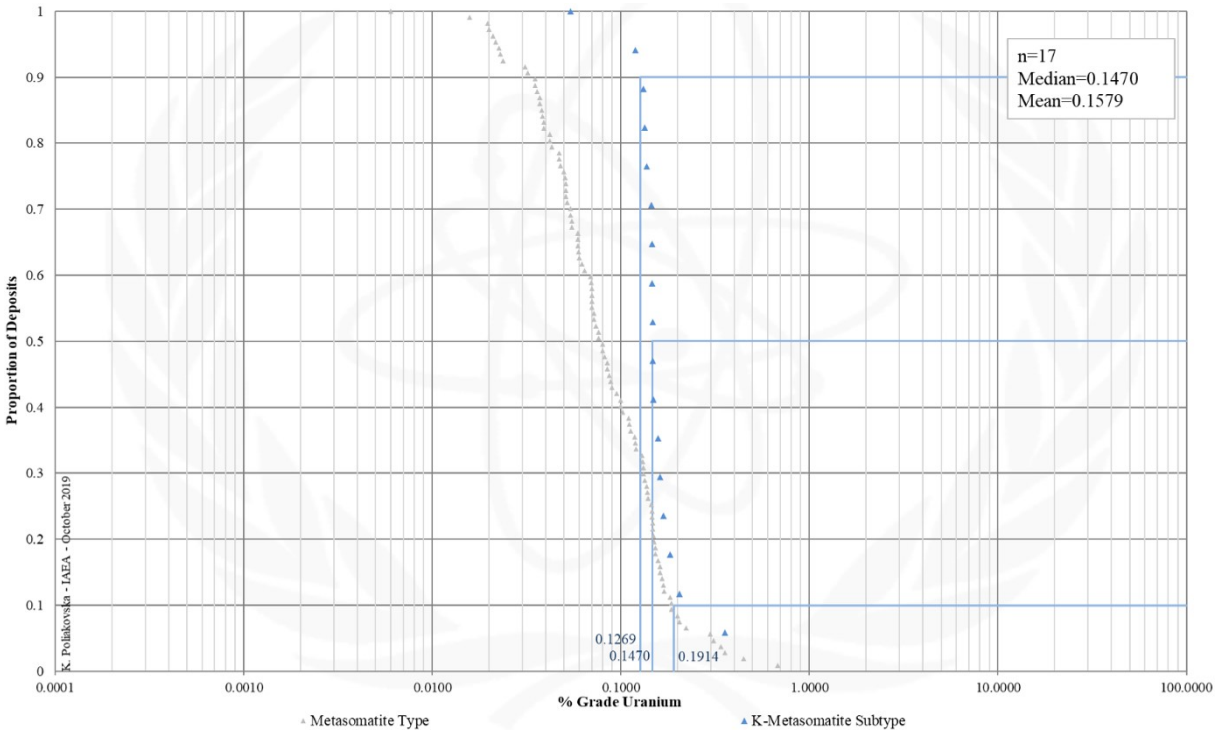

FIG. 5.2c. Grade Cumulative Probability Plot for Metasomatite Potassium (K)-Metasomatite uranium deposits from the UDEPO database.

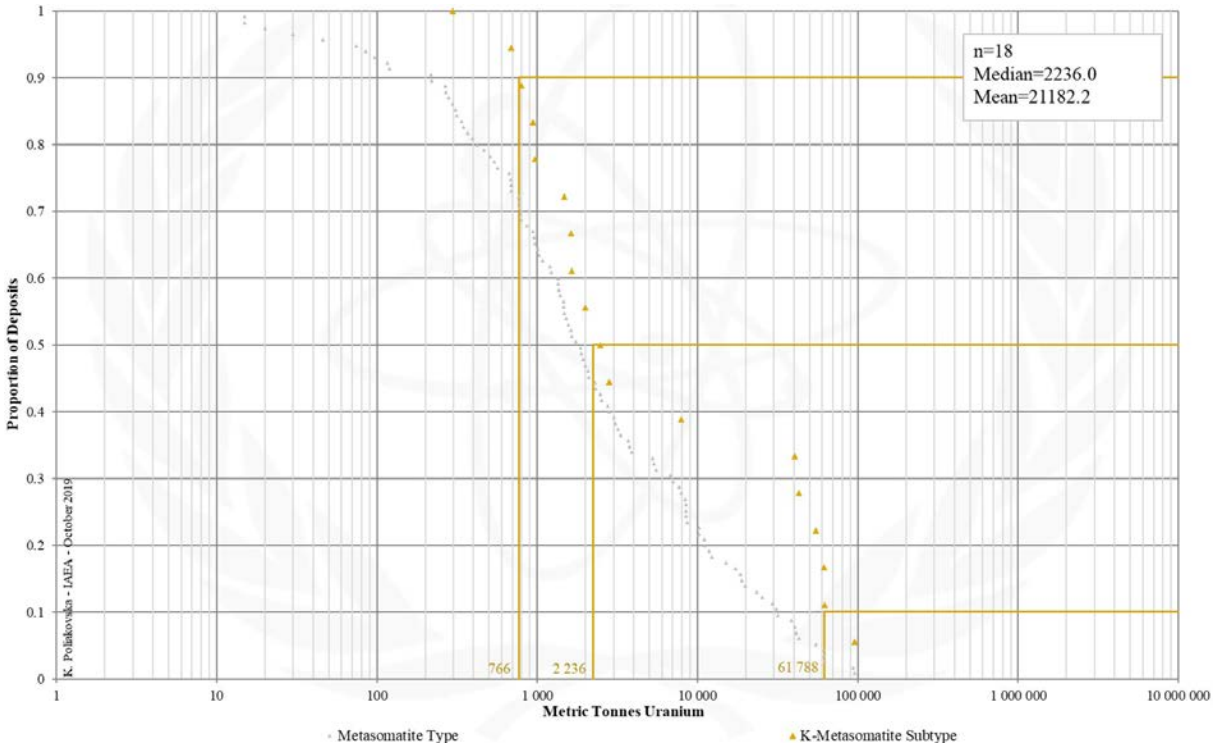

FIG. 5.2d. Tonnage Cumulative Probability Plot for Metasomatite Potassium (K)-Metasomatite uranium deposits from the UDEPO database.

SUBTYPE 5.3. Metasomatite, Skarn

Brief Description

- Skarn metasomatite deposits are products of intense sodium- or potassium-metasomatism along lithospheric fault systems giving rise to large volumes of albitised or illitised rock.
- The deposits take the form of structurally controlled, disseminated and vein-hosted ores of variable shape and size.
- Spatially and genetically associated metasomatic alteration zones are often substantial with strike lengths of up to several kilometres and vertical extents of up to two kilometres.
- Most skarn metasomatite deposits are located in Precambrian cratons, in particular destabilised regions affected by prolonged or recurring episodes of tectono-magmatic activity.
- Skarn metasomatite deposits are rare with only two significant examples recorded globally: Mary Kathleen (Australia) and Inca (Namibia).

Genetically Associated Deposit Types

- Subtype 1.1. Intrusive, anatectic (pegmatite-alaskite)
- Subtype 5.1. Metasomatite, sodium (Na)-metasomatite
- Subtype 5.2. Metasomatite, potassium (K)-metasomatite

Type Examples

- Mary Kathleen, Australia; Inca, Namibia; Tranomaro, Madagascar

Principal Commodities

- U, Th ± REE, Fe_3O_4

Grades (%) and Tonnages (tU)

- Average: 0.1788, 3255.0
- Median: 0.0745, 1030.0

Number of Deposits

- 7

Provinces (undifferentiated from Metasomatite Type)

- Amur Ussuri, Aravalli, Arjeplog Arvidsjaur Sorsele, Bafq Posht e Badam, Bur Acaba, Central Mineral Belt, Chilenia, East Liaoning Belt, Elkon, Jajawal, Kalkadoon Leichhardt, Kirovograd Smolino, Kodar Udokan, Kuusamo, Lagoa Real, Lake Onega, Mary Kathleen, Mount Isa West, Olary Int Hermitage, Perapohja, Piedmont Province, Poli , Serido, Sierra Ancha Apache, Son Valley, Tranomaro

Tectonic Setting

- Collisional orogens

Typical Geological Age Range

- Proterozoic to (?)Cambrian

Mineral Systems Model

Source

Ground preparation
- Collisional orogeny, and/or
- Contact metasomatism/skarnification

Energy
- Regional metamorphism, and/or
- High heat flow, extreme geothermal gradient, partial melting of mantle and crustal sources and voluminous magmatism

Melts and fluids
- Highly saline brines (>30 wt% NaCl equivalent), or
- High-temperature leucogranite melts and derivative magmatic-hydrothermal fluids

Ligands
- Ca, Cl, K, Na

Reductants and reactants
- Magnetiferous, hematitic, pyroxeniferous or garnetiferous skarns; carbonates

Uranium
- Crystalline basement rocks; granitoids; leucogranite melts

Transport

Fluid pathways
- Crustal-scale fault zones

Trap

Physical
- Transient breaching of physical barriers/seals, catastrophic rock failure and concomitant structurally controlled and highly focused fluid flow controlled by gradients in permeability and hydraulic head
- Gradients in permeability and hydraulic head are maximised at fault irregularities, fault tips and wings, fault intersections, fault damage zones characterised by high fracture density, rheological competency contrasts, strain shadows and contact aureoles around intrusive bodies, boudinage and related strain shadows, fold noses and axial

cleavages, truncated folds, breccia zones and lithological contacts
- Albitisation resulting in a more brittle and permeable rock assemblage

Chemical
- Reactive lithological units such as marble or certain skarns

Deposition

Fluid cooling and depressurization
- Phase separation/CO_2 effervescence

Fluid/wallrock interaction
- Chance in redox conditions due to interaction of oxidised fluids and reduced wallrocks

Fluid mixing
- Change in redox conditions due to mixing of oxidising, uranium-bearing fluids with reducing, mantle-derived fluids

Supergene processes
- Secondary uranium redistribution and enrichment

Preservation

- Relative tectonic stability post-uranium mineralisation

Key Reference Bibliography

DOS REIS SALLES, R., DE SOUZA FILHO, C. R., CUDAHY, T., VICENTE, L. E., MONTEIRO, L. V. S., Hyperspectral remote sensing applied to uranium exploration: a case study at the Mary Kathleen metamorphic-hydrothermal U-REE deposit, NW, Queensland, Australia. Journal of Geochemical Exploration, 179, 36-50 (2017).

HAMMERLI, J., SPANDLER, C., OLIVER, N. H. S., RUSK, B., Cl/Br of scapolite as a fluid tracer in the earth's crust: insights into fluid sources in the Mary Kathleen Fold Belt, Mt. Isa Inlier, Australia. Journal of Metamorphic Geology, 32(1), 93-112 (2014).

INTERNATIONAL ATOMIC ENERGY AGENCY, Geological Classification of Uranium Deposits and Description of Selected Examples. IAEA-TECDOC Series, 1842, 415p (2018).

OLIVER, N. H. S., PEARSON, P. J., HOLCOMBE, R. J., ORD, A., Mary Kathleen metamorphic-hydrothermal uranium–rare–earth element deposit: ore genesis and numerical model of coupled deformation and fluid flow. Australian Journal of Earth Sciences, 46(3), 467-484 (1999).

WILDE, A., The Inca 102arbonatiza skarn, Namibia: an unusual magmatic-hydrothermal deposit. Australian Institute of Geoscientists (AIG) Journal Paper, J2017-001, 1-11 (2017).

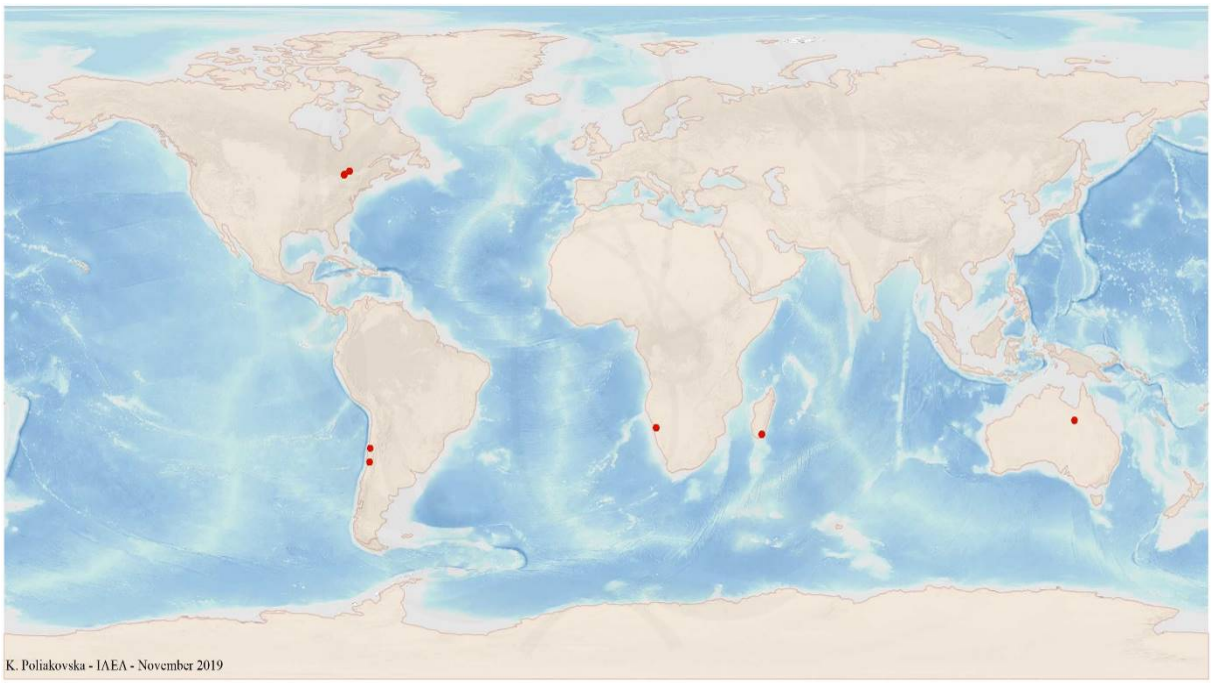

FIG. 5.3a. World distribution of selected Metasomatite Skarn uranium deposits from the UDEPO database.

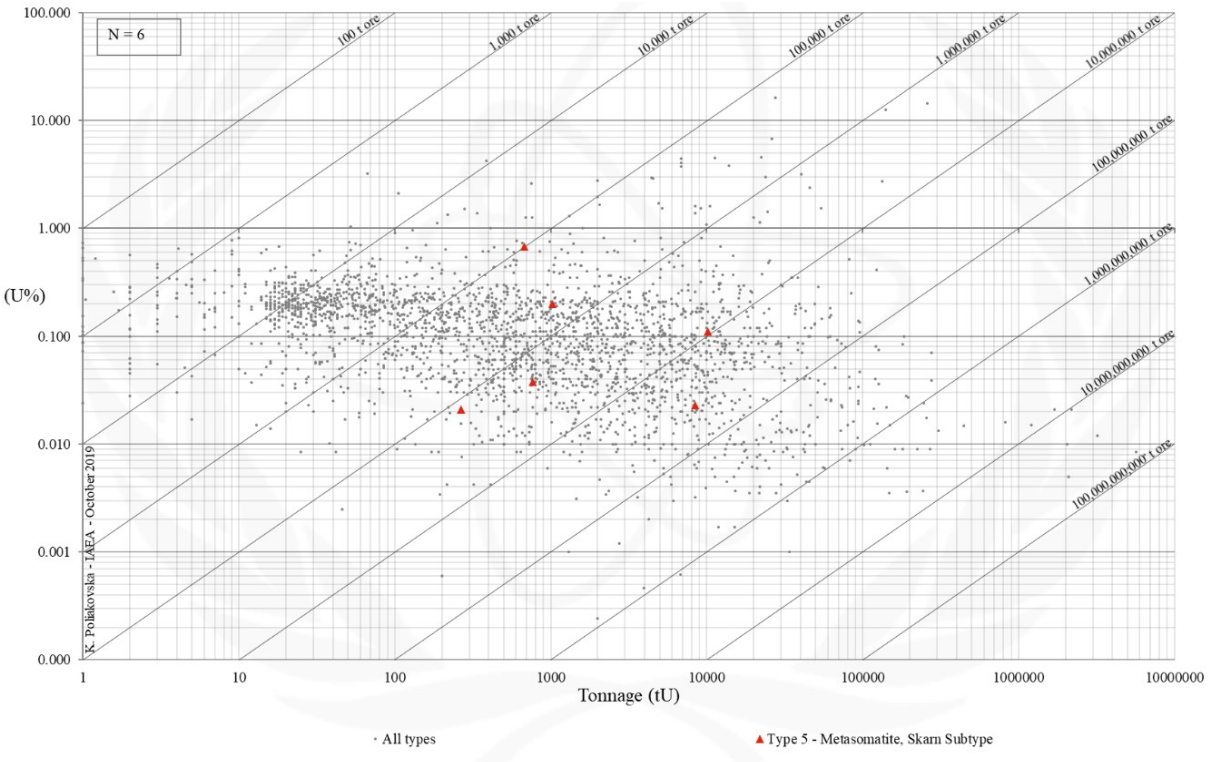

FIG. 5.3b. Grade and tonnage scatterplot highlighting Metasomatite Skarn uranium deposits from the UDEPO database.

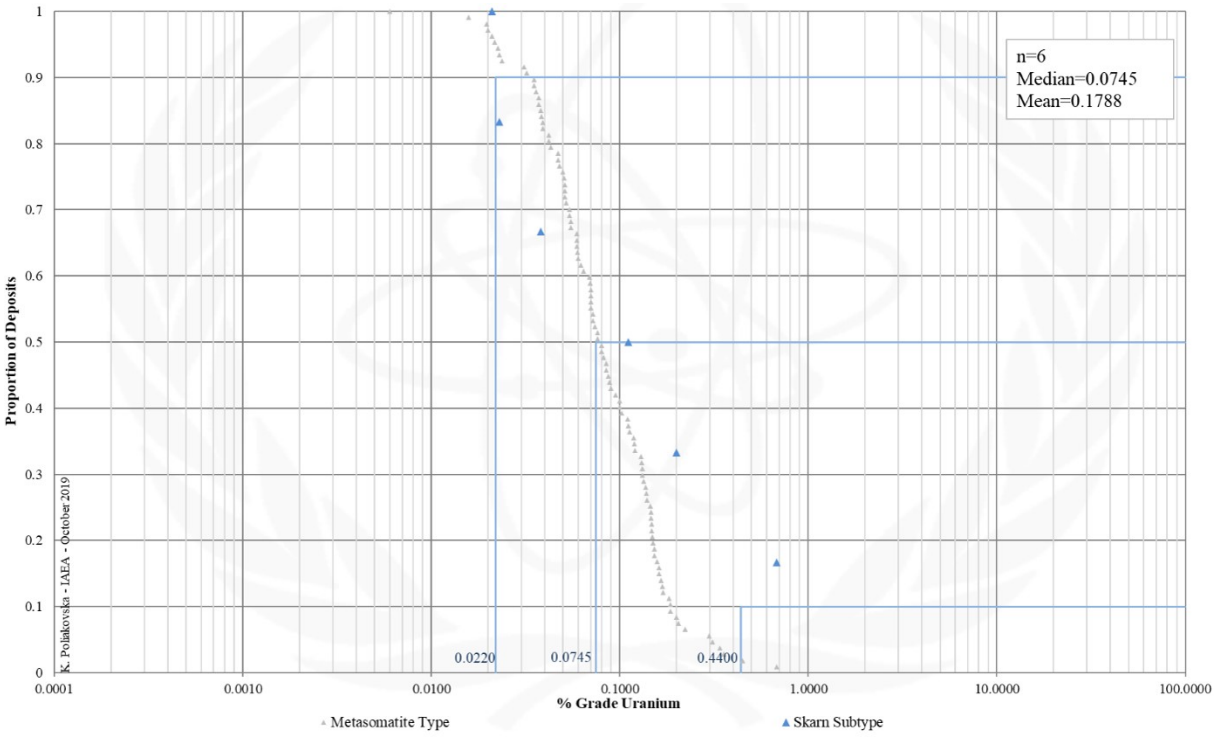

FIG. 5.3c. Grade Cumulative Probability Plot for Metasomatite Skarn uranium deposits from the UDEPO database.

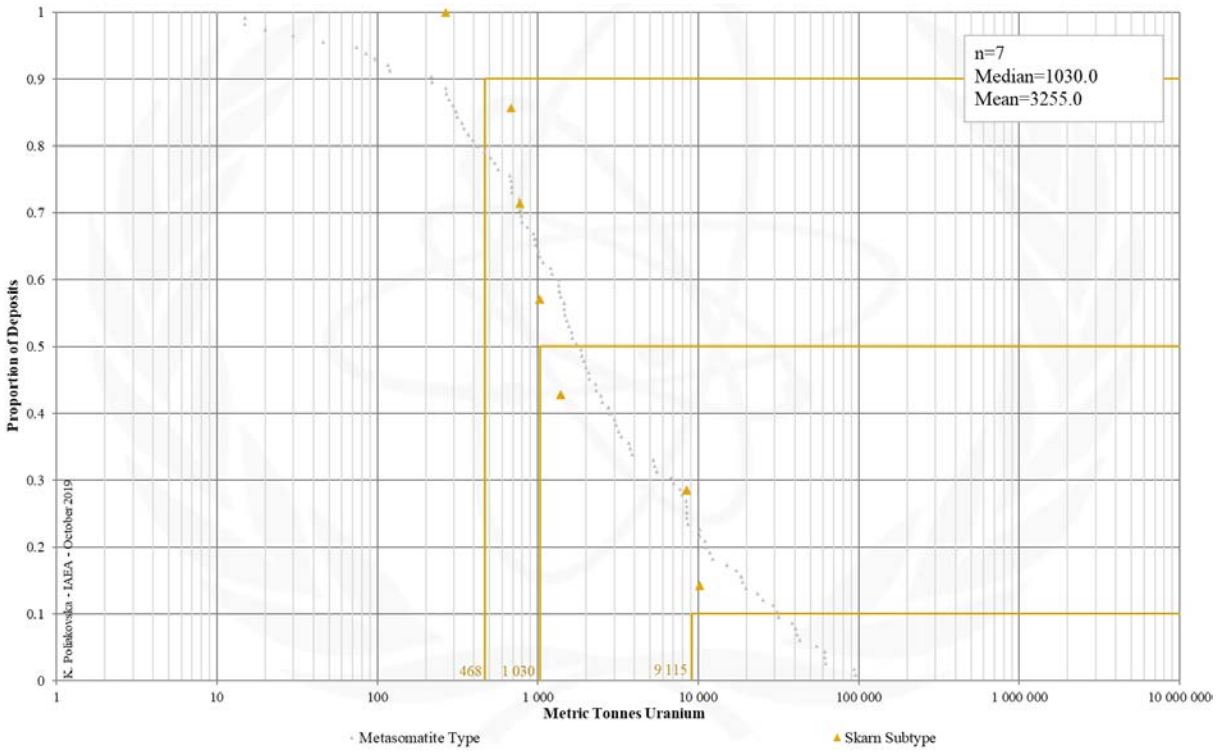

FIG. 5.3d. Tonnage distribution for Metasomatite Skarn uranium deposits from the UDEPO database.

Appendix VI

METAMORPHITE

TYPE 6. Metamorphite

Brief Description

- Metamorphite deposits are hosted by metamorphosed supracrustal rocks associated with collisional orogens of Precambrian to Cenozoic age.
- Two subtypes are recognised: (6.1.) Stratabound and (6.2.) structure-bound deposits.
- Stratabound ores take the form of irregularly distributed uranium impregnations and disseminations that are conformable to bedding. The formation of these ores is thought to be linked to chemical and physical changes of a uranium enriched sedimentary protolith during regional metamorphism, resulting in the redistribution and recrystallisation of primary synsedimentary uranium phases.
- Structure-bound deposits, on the other hand, take the form of structurally-controlled vein- and mylonite-hosted uranium ores precipitated from externally derived metamorphic fluids.

Subtypes and Classes

- 6.1. Stratabound
- 6.2. Structure-bound
  - 6.2.1. Monometallic veins
  - 6.2.2. Polymetallic veins
  - 6.2.3. Marble-hosted phosphate

Type Examples

- Subtype 6.1. Forstau, Austria; Nuottijarvi, Finland
- Subtype 6.2.
- Class 6.2.1. Schwartzwalder, USA; Ace-Fay-Verna, Canada
- Class 6.2.2. Shinkolobwe, Democratic Republic of Congo
- Class 6.2.3. Itataia, Brazil; Zaozernoye, Kazhakstan

Principal Commodities

- U ± Ag, As, Co, Cu, Fe, Mo, Ni, P, Pb, Zn

Grades (%) and Tonnages (tU)

- Average: 0.1625, 4331.4
- Median: 0.1095, 800.0

Number of Deposits

- Deposits: 245

Provinces

- Apuseni Mountains, Banat Mountains, Beaverlodge, Bodal Bhandaritola, Central African Copperbelt, Central Ceara, Eastern Carpathian, Gery Swietokrzyskie, Great Bear, Hoggar Shield West, Iserables, Kalan Basin, Kenema Man, Kokshetau, Kolari Kittilia, Lake Ladoga, Longshoushan, Lower Silesia, Radstadter Tauern, Rhodope Massif Central, Rio Preto Campos Belos, Singhbhum, South Bohemian, Southeast Bohemian, Southern Menderes Massif, Southern Rocky Mountains, West Moravian, Wolz Tauern.

Tectonic Setting

- Collisional orogens

Typical Geological Age Range

- Palaeoproterozoic to Cenozoic

Mineral Systems Model

Source

Ground preparation

- Subtype 6.1.: Intermontane basin formation and deposition of sedimentary successions with carbonaceous, uranium-enriched interbeds
- Class 6.2.1.: Protracted tectonothermal evolution
- Class 6.2.2.: Intracratonic basin formation and deposition and diagenesis of thick (>5 km) sedimentary piles
- Class 6.2.3.: Formation of a shallow marine/lagoonal environment and deposition of phosphatic ± uranium-enriched sediments and organic matter

Energy

- Orogenesis and postcollisional magmatism
- Greenschist to amphibolite facies grade metamorphism

Fluids

- Metamorphic fluids
- Possible contributions from deep-seated magmatic-hydrothermal fluids, oxidised, highly saline basinal brines and groundwaters

Ligands

- CO, Cl, F, OH

Reductants and reactants

- Graphite, Fe-sulphides, Fe^{2+} carbonates or silicates, S, SO_4, CH_4, carbonaceous matter, black shales, impure limestones/marbles,

Uranium
- Crystalline basement rocks, granitoids and syenites, intracratonic basin fill

Transport

Fluid pathways
- Crustal-scale fault zones
- Fold nappes and thrusts; domal structures
- Regional unconformity surfaces
- Permeable, oxidised sandstone and conglomerate aquifers; karst aquifers; diapiric breccia

Trap

Physical
- Fault-fracture systems; structural dilational zones (fault step-overs, splays, bends, fault intersections, en-échelon tension gashes); episyenites
- Karst voids and cavities; permeability barriers (marbles?); tectonic, dissolution or halokinetic breccias
- Lithological competency contrasts
- Schistosity planes; boudinage; mylonites; cataclasites
- Isoclinal folds; fold hinges and noses; truncated folds

Chemical
- Carbonaceous matter (carbonaceous karst dissolution breccia) and graphite
- Fe-sulphides and Fe-oxides
- Reduced strata (graphitic marble, black shale, chloritic breccia, amphibolite)
- Albitised rocks (quartz dissolution and 108arbonatization)

Deposition

Fluid cooling and depressurisation
- Phase separation/CO_2 effervescence

Change in redox conditions
- Due to mixing of oxidised, uranium-bearing fluids/brines and reduced metamorphic fluids
- Due to interaction of oxidised, uranium-bearing fluids and wallrock reductants
- Due to interaction of oxidised, uranium-bearing fluids and carbonate wallrocks

Metamorphic remobilisation and recrystallisation
- Pyrite-hematite buffered U remobilisation and reconcentration during metamorphism of the host sequence

Supergene processes
- Secondary uranium redistribution and enrichment

Preservation
- Relative tectonic stability post-uranium mineralisation
- Subsidence and burial of the uranium mineralised rocks

Key Reference Bibliography

ANGEIRAS, A. G., Geology and metallogeny of the northeastern Brazil uranium-phosphorus province emphasizing the Itataia deposit. Ore Geology Reviews, 3(1-3), 211-225 (1988).

DAHLKAMP, F., Uranium ore deposits. Springer, 460p (2013).

DAHLKAMP, F. J., Uranium Deposits of the World: Europe. Springer, Berlin, Heidelberg, 792p (2016).

DIENG, S., KYSER, K., GODIN, L., Tectonic history of the North American shield recorded in uranium deposits in the Beaverlodge area, northern Saskatchewan, Canada. Precambrian Research, 224, 316-340 (2013).

EGLINGER, A., ANDRÉ-MAYER, A. S., VANDERHAEGHE, O., MERCADIER, J., CUNEY, M., DECRÉE, S.,

ERKAN, E., Uran- und gipsführendes Permoskyth der östlichen Ostalpen. Jahrbuch der Geologischen Bundesanstalt (GBA), 120(2), 343-400 (1977).

FEYBESSE, J. L., MILESI, J. P., Geochemical signatures of uranium oxides in the Lufilian belt: from unconformity-related to syn-metamorphic uranium deposits during the Pan-African orogenic cycle. Ore Geology Reviews, 54, 197-213 (2013).

INTERNATIONAL ATOMIC ENERGY AGENCY, Geological Classification of Uranium Deposits and Description of Selected Examples. IAEA-TECDOC Series, 1842, 415p (2018).

LIANG, R., CHI, G., ASHTON, K., BLAMEY, N., FAYEK, M., Fluid compositions and PT conditions of vein-type uranium mineralization in the Beaverlodge uranium district, northern Saskatchewan, Canada. Ore Geology Reviews, 80, 460-483 (2017).

VERÍSSIMO, C. U. V., SANTOS, R. V., PARENTE, C. V., DE OLIVEIRA, C. G., CAVALCANTI, J. A. D., NETO, J. D. A. N., The Itataia phosphate-uranium deposit (Ceará, Brazil) new petrographic, geochemistry and isotope studies. Journal of South American Earth Sciences, 70, 115-144 (2016).

WALLACE, A. R., WHELAN, J. F., The Schwartzwalder uranium deposit, III: alteration, vein mineralization, light stable isotopes, and genesis of the deposit. Economic Geology, 81(4), 872-888 (1986).

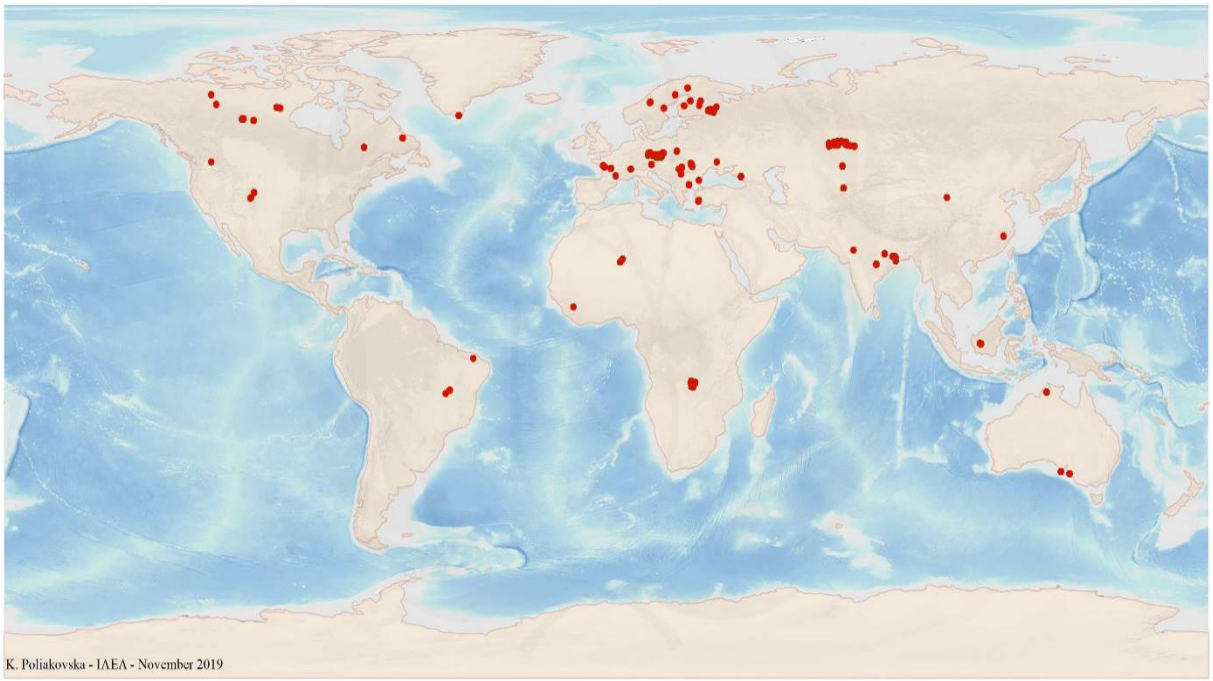

FIG. 6a. World distribution of selected Metamorphite uranium deposits from the UDEPO database.

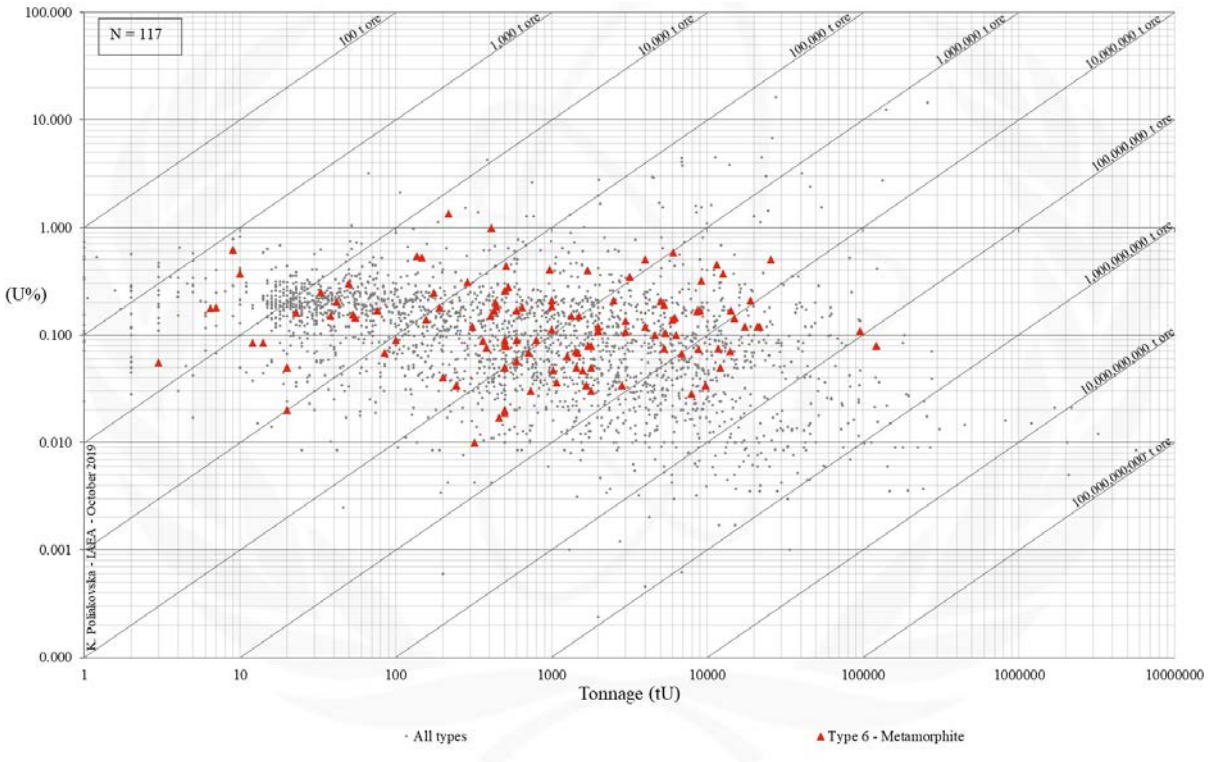

FIG. 6b. Grade and tonnage scatterplot highlighting Metamorphite uranium deposits from the UDEPO database.

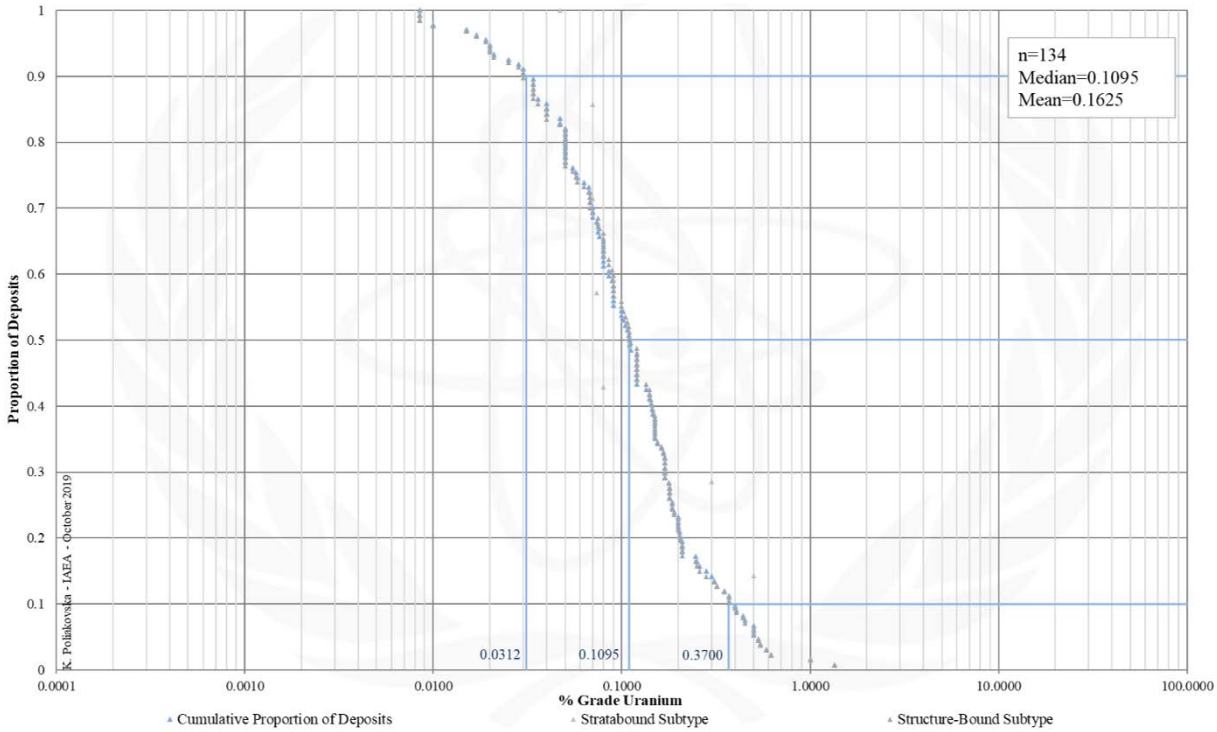

FIG. 6c. Grade Cumulative Probability Plot for Metamorphite uranium deposits from the UDEPO database.

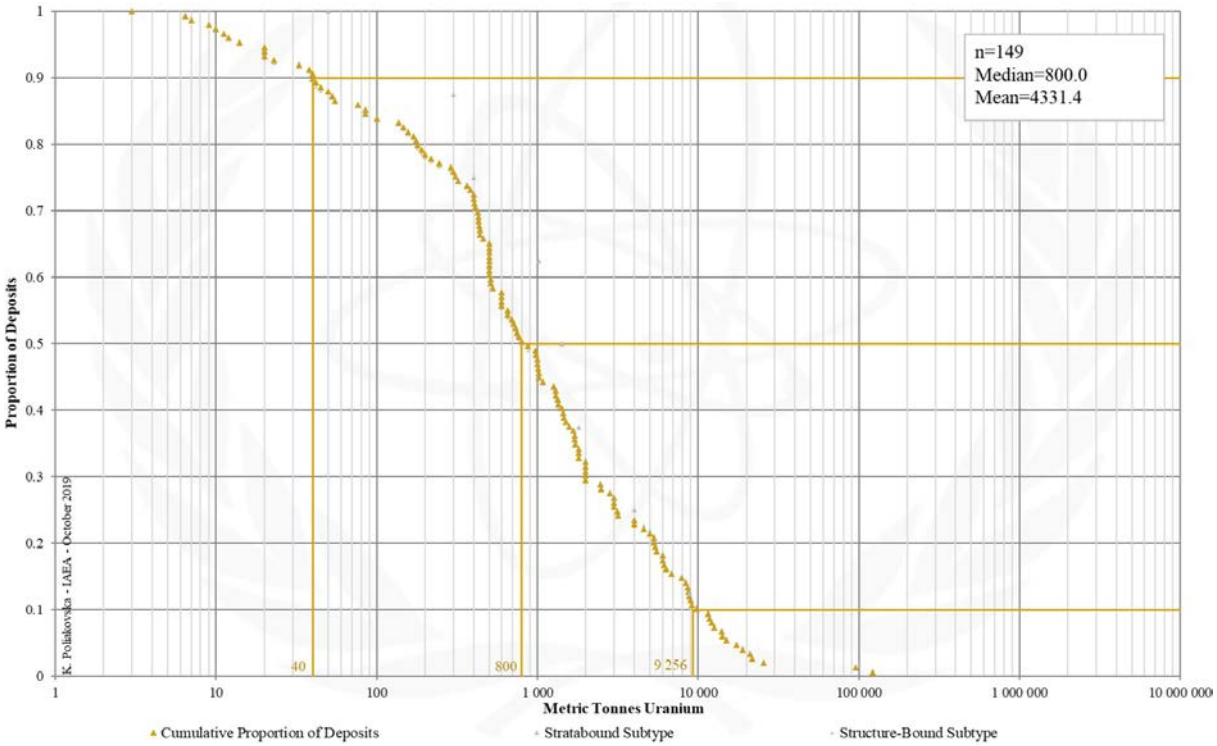

FIG. 6d. Tonnage Cumulative Probability Plot for Metamorphite uranium deposits from the UDEPO database.

SUBTYPE 6.1. Metamorphite, Stratabound

Brief Description

- Metamorphite deposits are hosted by metamorphosed supracrustal rocks associated with collisional orogens of Precambrian to Cenozoic age.
- Two subtypes are recognised: (6.1.) Stratabound and (6.2.) structure-bound deposits.
- Stratabound deposits take the form of irregularly distributed uranium impregnations and disseminations that are conformable to bedding.
- The formation of these ores is thought to be linked to chemical and physical changes of a uranium enriched sedimentary protolith during regional metamorphism, resulting in the redistribution and recrystallisation of primary synsedimentary uranium phases.

Type Examples

- Forstau (Austria)

Genetically Associated Deposit Types

- Subtype 6.2. Metamorphite, Structure-bound

Principal Commodities

- U ± Mo

Grades (%) and Tonnages (tU)

- Average: 0.1629, 2226.8
- Median: 0.0735, 1221.0

Number of Deposits

- Deposits: 10

Provinces (undifferentiated from Metamorphite Type)

- Apuseni Mountains, Banat Mountains, Beaverlodge, Bodal Bhandaritola, Central African Copperbelt, Central Ceara, Eastern Carpathian, Gery Swietokrzyskie, Great Bear, Hoggar Shield West, Iserables, Kalan Basin, Kenema Man, Kokshetau, Kolari Kittilia, Lake Ladoga, Longshoushan, Lower Silesia, Radstadter Tauern, Rhodope Massif Central, Rio Preto Campos Belos, Singhbhum, South Bohemian, Southeast Bohemian, Southern Menderes Massif, Southern Rocky Mountains, West Moravian, Wolz Tauern.

Tectonic Setting

- Collisional orogens

Typical Geological Age Range

- Palaeozoic (and possibly younger)

Mineral Systems Model

Source

Ground preparation
- Intermontane basin formation
- Deposition of sedimentary successions with carbonaceous, uranium-enriched interbeds

Energy
- Orogenesis
- Regional metamorphism

Fluids
- Metamorphic fluids

Ligands
- Cl, F, OH

Reductants
- Graphite, Fe-sulphides, Fe^{2+} carbonates or silicates

Uranium
- Granitoids and syenites

Transport

Fluid pathways
- Crustal-scale fault zones
- Fold nappes and thrusts; domal structures

Trap

Physical
- Lithological competency contrasts
- Schistosity planes (in particular deflections thereof)
- Fold hinges and noses

Chemical
- Graphite
- Fe-sulphides and Fe-oxides
- Fe^{2+} silicates

Deposition
Metamorphic remobilisation and recrystallisation – Pyrite-hematite buffered U remobilisation and reconcentration during metamorphism of the host sequence Fluid cooling and depressurisation – Phase separation/CO_2 effervescence Change in redox conditions – Due to interaction of oxidised, uranium-bearing fluids and wallrock reductants
Preservation
– Relative tectonic stability post-uranium mineralisation

Key Reference Bibliography

DAHLKAMP, F. J., Uranium Deposits of the World: Europe. Springer, Berlin, Heidelberg, 792p (2016).

ERKAN, E., Uran- und gipsführendes Permoskyth der östlichen Ostalpen. Jahrbuch der Geologischen Bundesanstalt (GBA), 120(2), 343-400 (1977).

INTERNATIONAL ATOMIC ENERGY AGENCY, Geological Classification of Uranium Deposits and Description of Selected Examples. IAEA-TECDOC Series, 1842, 415p (2018).

SCHERMANN, O., Erztypen und ihre Genese im Uranvorkommen von Forstau (vorlaeufiger Bericht). Verhandlungen der Geologischen Bundesanstalt (GBA), 3/79, 373-376 (1979).

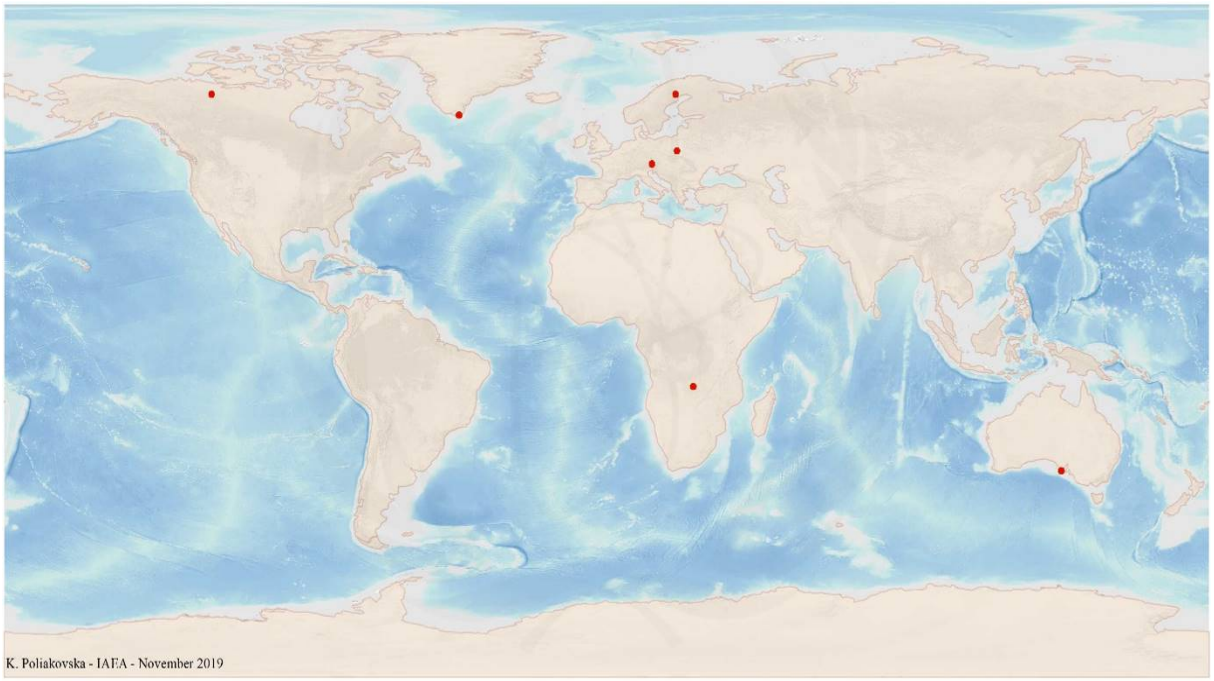

FIG. 6.1a. World distribution of selected Metamorphite Stratabound uranium deposits from the UDEPO database.

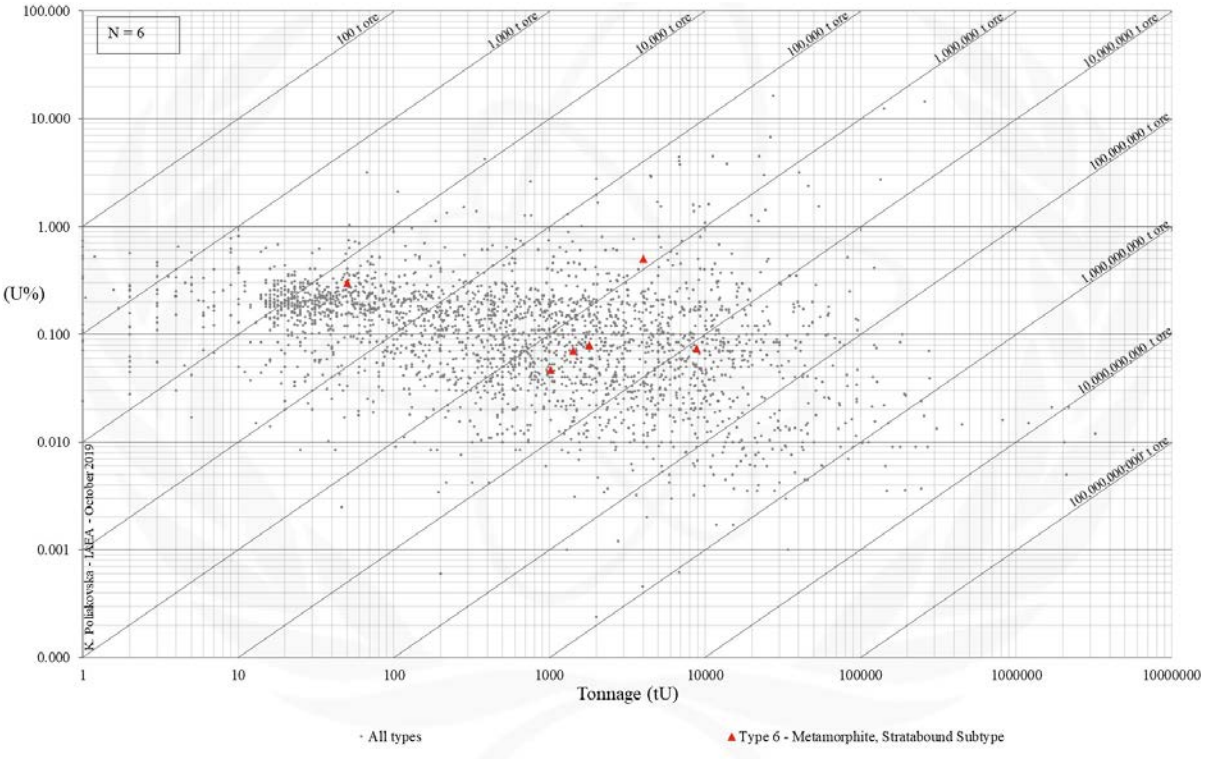

FIG. 6.1b. Grade and tonnage scatterplot highlighting Metamorphite Stratabound uranium deposits from the UDEPO database.

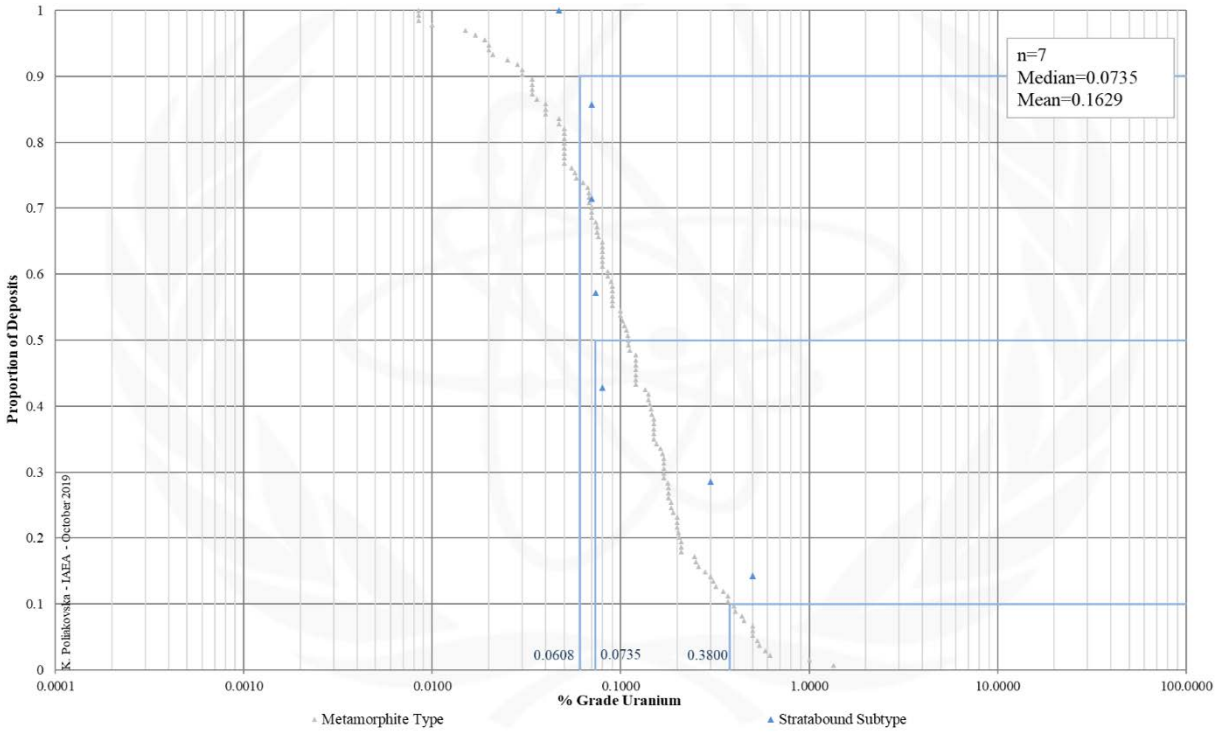

FIG. 6.1c. Grade Cumulative Probability Plot for Metamorphite Stratabound uranium deposits from the UDEPO database.

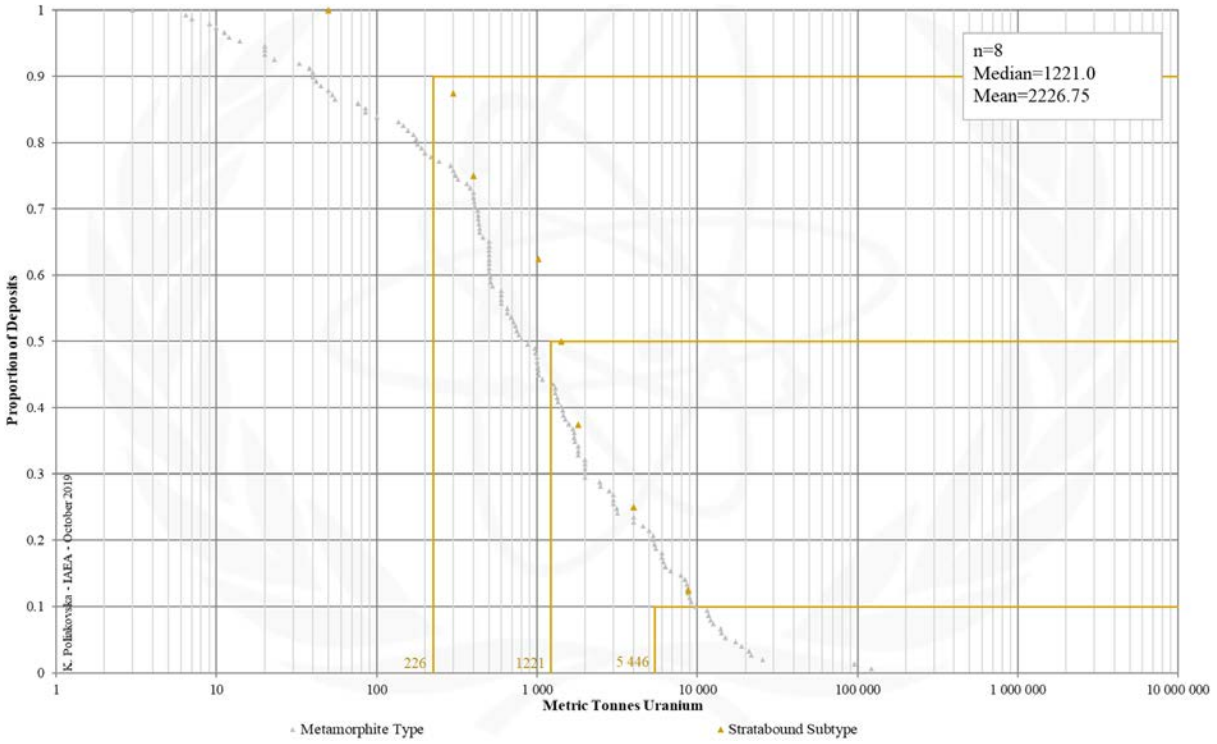

FIG. 6.1d. Tonnage Cumulative Probability Plot for Metamorphite Stratabound uranium deposits from the UDEPO database.

SUBTYPE 6.2. Metamorphite, Structure-Bound

Brief Description

- Metamorphite deposits are hosted by metamorphosed supracrustal rocks associated with collisional orogens of Precambrian to Cenozoic age.
- Two subtypes are recognised: (6.1.) Stratabound and (6.2.) structure-bound deposits.
- Structure-bound deposits take the form of structurally-controlled vein- and mylonite-hosted uranium ores precipitated from externally derived metamorphic fluids. The structure-bound subtype is further subdivided into three classes: (6.2.1.) Monometallic veins, (6.2.2.) polymetallic veins, and (6.2.3.) marble-hosted phosphate. Monometallic veins are characterised by simple uranium and gangue mineral assemblages deposited within dilational fault-fracture systems and fault-related breccia zones. The orebodies are typically accompanied by extensive and vertically continuous, multiphase wallrock alteration. Polymetallic veins are characterised by complex mineral assemblages of uranium, gangue and paragenetically younger nickel-cobalt arsenides, selenides and a variety of native metals. The ores take the form of vein, stockwork and breccia systems as well as disseminations. Marble-hosted phosphate deposits are exemplified by Itataia, Brazil, a complex, multiphase uraniferous phosphate deposit hosted by marbles and calc-silicate rocks.

Type Examples

- Class 6.2.1. Schwartzwalder, USA; Beaverlodge, Canada: Ace-Fay-Verna; Kamyshevoye, Kazakhstan. Class 6.2.2. Shinkolobwe, Democratic Republic of the Congo; Port Radium, Canada; Jaduguda, India. Class 6.2.3. Itataia/Santa Quitéria, Brazil; Zaozernoye, Kazhakstan

Genetically Associated Deposit Types

- Subtype 6.1. Metamorphite, Stratabound. Subtype 2.2. Granite-related, perigranitic. Type 5. Metasomatite. Type 7. Proterozoic unconformity

Principal Commodities

- Class 6.2.1. U. Class 6.2.2. U ± Ag, As, Co, Cu, Fe, Mo, Ni, Pb, Zn. Class 6.2.3. U, P

Grades (%) and Tonnages (tU)

- Average: 0.1625, 4450.8
- Median: 0.1100, 769.0

Number of Deposits

- 234

Provinces (undifferentiated from Metamorphite Type)

- Apuseni Mountains, Banat Mountains, Beaverlodge, Bodal Bhandaritola, Central African Copperbelt, Central Ceara, Eastern Carpathian, Gery Swietokrzyskie, Great Bear, Hoggar Shield West, Iserables, Kalan Basin, Kenema Man, , Rio Preto Campos Belos, Singhbhum, South Bohemian, Southeast Bohemian, Southern Menderes Massif.

Tectonic Setting

- Collisional orogens

Typical Geological Age Range

- Class 6.2.1. Precambrian to Cenozoic. Class 6.2.2. Proterozoic (and possibly younger). Class 6.2.2. Neoproterozoic to Mesozoic (and possibly younger)

Mineral Systems Model

Source

Ground preparation

- Protracted tectonothermal evolution
- Classes 6.2.1. and 6.2.2. Intracratonic basin formation and deposition and diagenesis of a thick (>5 km) sedimentary pile above a basal unconformity. Class 6.2.3. Formation of a shallow marine/lagoonal environment, deposition of phosphatic ± uranium-enriched sediments and organic matter

Energy

- Orogenesis and/or tectonic reactivation
- Postcollisional magmatism
- Regional (up to amphibolite facies grade) metamorphism
- Class 6.2.3. Uplift and topographic gradient (supergene mineralisation)

Fluids

- Classes 6.2.1. and 6.2.2. Metamorphic fluids, highly saline, oxidised basinal brines. Class 6.2.3. Magmatic-hydrothermal fluids, groundwaters (supergene mineralisation)

Ligands

- CO, Cl, F, OH

Reductants

- Black shales, carbonaceous matter, graphite, Fe-sulphides, Fe^{2+} carbonates or silicates, impure graphite-, diopside-, scapolite-, tremolite- and phlogopite-bearing limestones and marbles, S, SO_4, CH_4

Uranium

- Crystalline basement rocks, granitoids, intracratonic basin fill

Transport

Fluid pathways
- Crustal-scale fault zones
- Regional unconformity surfaces
- Permeable, oxidised sandstone and conglomerate aquifers above the unconformity
- Domal structures
- Karst aquifers

Trap — Classes 6.2.1. and 6.2.2.

Physical
- Fault-fracture systems and associated structural dilational (fault step-overs, splays, bends, fault intersections, en-échelon tension gashes) and associated tectonic breccia zones
- Halokinetic breccia
- Lithological competency contrasts
- Brittle overprints on earlier-formed ductile structures such as schistosity planes, iosoclinal folds, boudins, mylonites or cataclasites

Chemical
- Graphite
- Fe-sulphides and Fe-oxides
- Chloritic breccia
- Albitised rocks (quartz dissolution and carbonatisation)
- Carbonates
- Black shales

Trap — Class 6.2.3.

Physical
- Fault-fracture and breccia systems
- Episyenites
- Palaeokarst voids and cavities
- Fold hinge zones
- Structurally thickened marble succession
- Palaeo-watertable (supergene mineralisation)

Chemical
- Impure (± graphitic) marble
- Carbonaceous karst dissolution breccia
- Hematitisation, chloritisation and albitisation/episyenitisation (quartz dissolution)

Deposition — Classes 6.2.1. and 6.2.2.

Fluid cooling and depressurisation
- Phase separation/CO_2 effervescence

Change in redox conditions
- Due to mixing of oxidised, uranium-bearing fluids/brines and reduced metamorphic fluids
- Due to interaction of oxidised, uranium-bearing fluids and wallrock reductants

Supergene processes
- Secondary uranium redistribution and enrichment

Deposition — Class 6.2.3.

Metamorphic remobilisation and recrystallisation
- Remobilisation and recrystallisation of primary phosphate (and uranium?)

Change in redox conditions
- Due to sodium metasomatism (to date this mechanism is poorly characterised)
- Due to mixing of saline magmatic-hydrothermal fluids and heated groundwaters
- Due to interaction of uranium-bearing fluids and carbonate wallrocks

Supergene processes
- Secondary uranium redistribution and enrichment via heated groundwaters

Preservation
- Relative tectonic stability post-uranium mineralisation
- Subsidence and burial of the uranium mineralised rocks

Key Reference Bibliography

ANGEIRAS, A. G., Geology and metallogeny of the northeastern Brazil uranium-phosphorus province emphasizing the Itataia deposit. Ore Geology Reviews, 3(1-3), 211-225 (1988).
BALL, S., Hydrothermal nickel sulfide hosted in Neoproterozoic carbonate and evaporitic rocks of the Menda Central prospect, Democratic Republic of Congo. Unpublished MSc Thesis, Colorado School of Mines, 102p (2016).
DAHLKAMP, F., Uranium ore deposits. Springer, 460p (2013).
DECRÉE, S., DELOULE, E., DE PUTTER, T., DEWAELE, S., MEES, F., MARIGNAC, C., SIMS U-Pb ages for heterogenite from Katanga: implications for the genesis of Co-U deposits in Shinkolobwe. Goldschmidt Conference Abstracts 2011, Mineralogical Magazine, 75(3), 733 (2011).

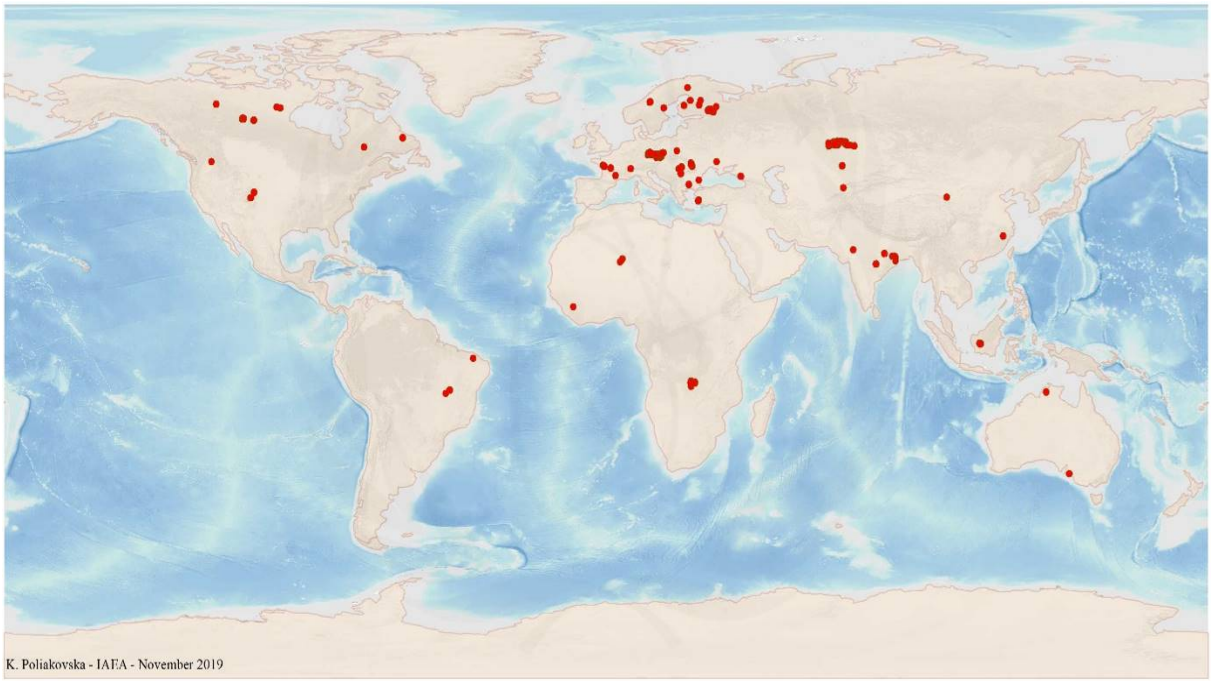

FIG. 6.2a. World distribution of selected Metamorphite Structure-Bound uranium deposits from the UDEPO database.

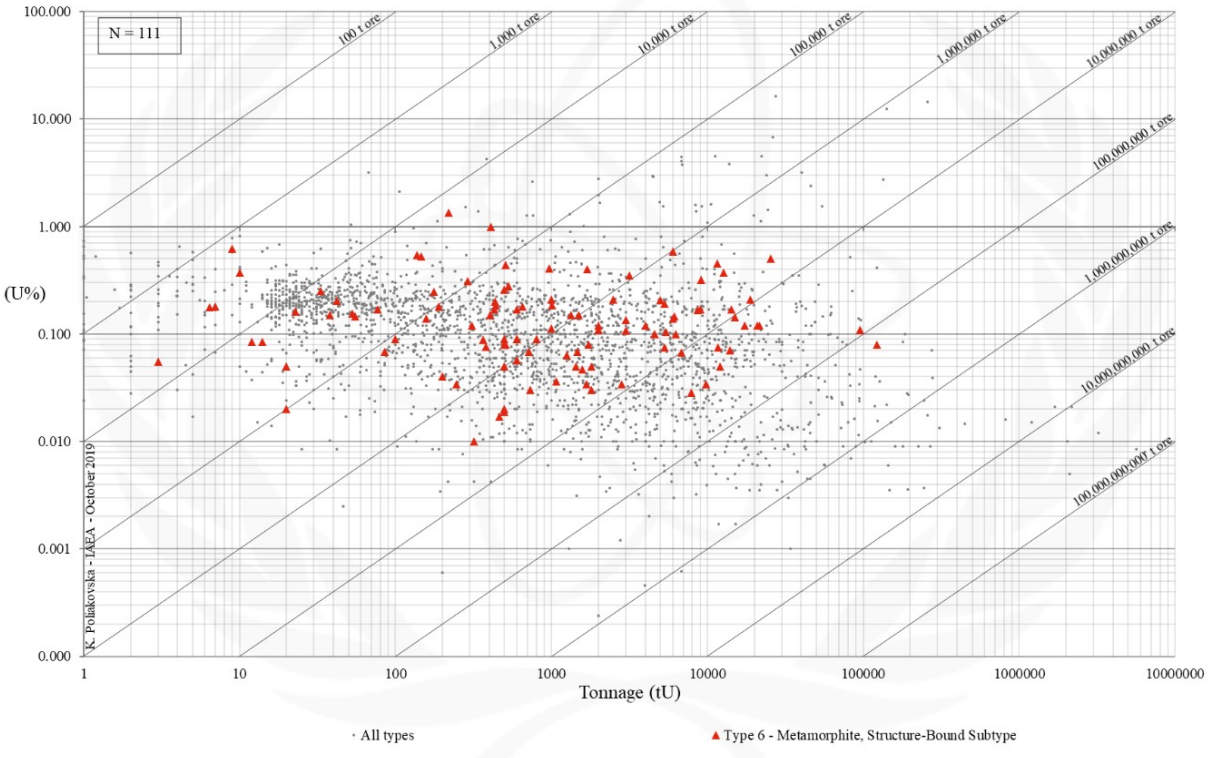

FIG. 6.2b. Grade and tonnage scatterplot highlighting Metamorphite Structure-Bound uranium deposits from the UDEPO database.

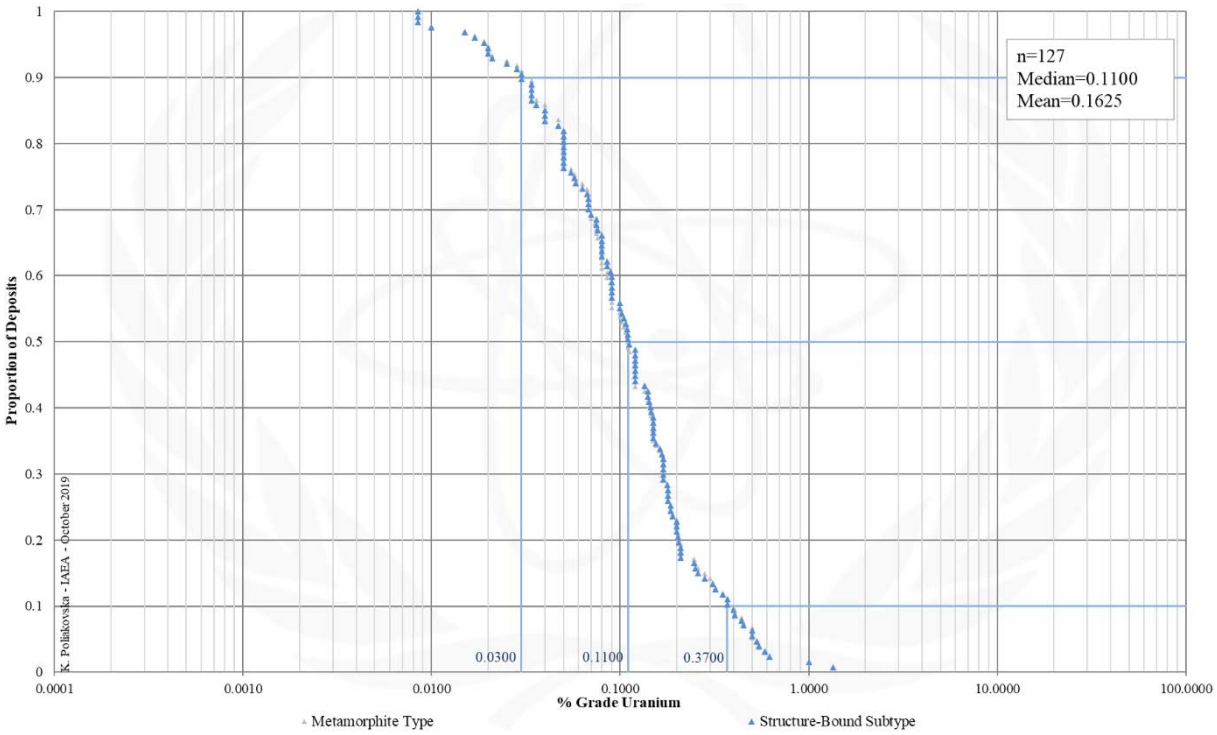

FIG. 6.2c. Grade Cumulative Probability Plot for Metamorphite Structure-Bound uranium deposits from the UDEPO database.

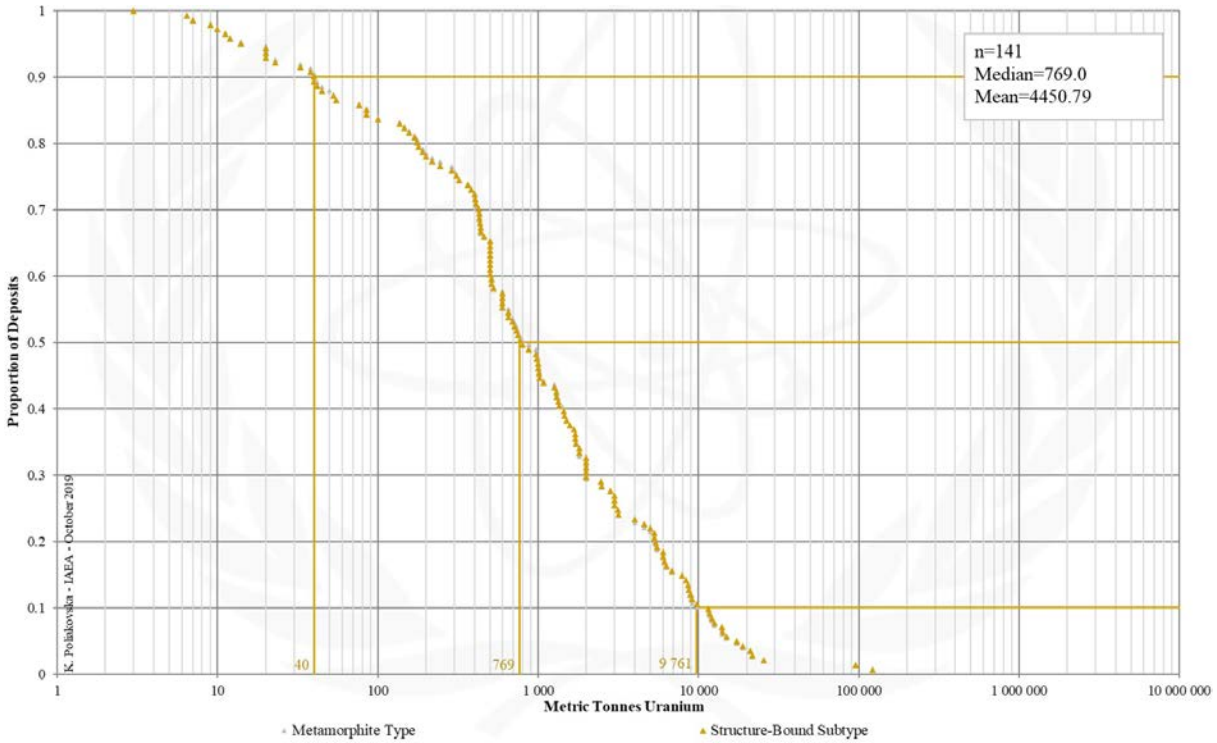

FIG. 6.2d. Tonnage Cumulative Probability Plot for Metamorphite Structure-Bound uranium deposits from the UDEPO database.

CLASS 6.2.1. Metamorphite, Structure-Bound, Monometallic Veins

Brief Description

- Metamorphite deposits are hosted by metamorphosed supracrustal rocks associated with collisional orogens of Precambrian to Cenozoic age.
- Two subtypes are recognised: (6.1.) Stratabound and (6.2.) structure-bound deposits.
- Structure-bound deposits take the form of structurally-controlled vein- and mylonite-hosted uranium ores precipitated from externally derived metamorphic fluids.
- The structure-bound subtype is further subdivided into three classes: (6.2.1.) Monometallic veins, (6.2.2.) polymetallic veins, and (6.2.3.) marble-hosted phosphate.
- Monometallic veins are characterised by simple uranium and gangue mineral assemblages deposited within dilational fault-fracture systems and fault-related breccia zones.
- The orebodies are typically accompanied by extensive and vertically continuous, multiphase wallrock alteration.

Type Examples

- Schwartzwalder, USA; Beaverlodge, Canada: Ace-Fay-Verna; Kamyshevoye, Kazakhstan

Genetically Associated Deposit Types

- Subtype 6.1. Metamorphite, Stratabound
- Class 6.2.2. Metamorphite, structure-bound, polymetallic veins
- Class 6.2.3. Metamorphite, structure-bound, marble-hosted phosphate
- Subtype 2.2. Granite-related, perigranitic
- Type 5. Metasomatite

Principal Commodities

- U

Grades (%) and Tonnages (tU)

- Average: 0.3187, 2265.8
- Median: 0.3187, 769.0

Number of Deposits

- Deposits: 5

Provinces (undifferentiated from Metamorphite Type)

- Apuseni Mountains, Banat Mountains, Beaverlodge, Bodal Bhandaritola, Central African Copperbelt, Central Ceara, Eastern Carpathian, Gery Swietokrzyskie, Great Bear, Hoggar Shield West, Iserables, Kalan Basin, Kenema Man, Kokshetau, Kolari Kittilia, Lake Ladoga, Longshoushan, Lower Silesia, Radstadter Tauern, Rhodope Massif Central, Rio Preto Campos Belos, Singhbhum, South Bohemian, Southeast Bohemian, Southern Menderes Massif, Southern Rocky Mountains, West Moravian, Wolz Tauern.

Tectonic Setting

- Collisional orogens

Typical Geological Age Range

- Precambrian to Cenozoic

Mineral Systems Model

Source

Ground preparation
- Protracted tectonothermal evolution

Energy
- Orogenesis and postcollisional magmatism
- Regional metamorphism

Fluids
- Metamorphic fluids
- Possible contribution from deep-seated magmatic-hydrothermal fluids and/or oxidised, highly saline basinal brines

Ligands
- CO, OH

Reductants
- Graphite, Fe-sulphides, Fe^{2+} carbonates or silicates, S, SO_4, CH_4

Uranium
- Crystalline basement rocks, intracratonic basin fill

Transport

Fluid pathways
- Crustal-scale fault zones

Trap

Physical
- Fault-fracture systems and associated structural dilational (fault step-overs, splays, bends, fault intersections, en-

échelon tension gashes) and breccia zones
- Lithological competency contrasts
- Brittle overprints on earlier-formed ductile structures such as schistosity planes, iosoclinal folds, boudins, mylonites or cataclasites
- Truncated folds

Chemical
- Graphite
- Fe-sulphides and Fe-oxides
- Chloritic breccia
- Albitised rocks (quartz dissolution and carbonatisation)

Deposition

Fluid cooling and depressurisation
- Phase separation/CO_2 effervescence

Change in redox conditions
- Due to mixing of oxidised, uranium-bearing fluids/brines and reduced metamorphic fluids
- Due to interaction of oxidised, uranium-bearing fluids and wallrock reductants

Preservation
- Relative tectonic stability post-uranium mineralisation
- Subsidence and burial of the uranium mineralised rocks

Key Reference Bibliography

DIENG, S., KYSER, K., GODIN, L., Tectonic history of the North American shield recorded in uranium deposits in the Beaverlodge area, northern Saskatchewan, Canada. Precambrian Research, 224, 316-340 (2013).
INTERNATIONAL ATOMIC ENERGY AGENCY, Geological Classification of Uranium Deposits and Description of Selected Examples. IAEA-TECDOC Series, 1842, 415p (2018).
LIANG, R., CHI, G., ASHTON, K., BLAMEY, N., FAYEK, M., Fluid compositions and PT conditions of vein-type uranium mineralization in the Beaverlodge uranium district, northern Saskatchewan, Canada. Ore Geology Reviews, 80, 460-483 (2017).
WALLACE, A. R., WHELAN, J. F., The Schwartzwalder uranium deposit, III: alteration, vein mineralization, light stable isotopes, and genesis of the deposit. Economic Geology, 81(4), 872-888 (1986).

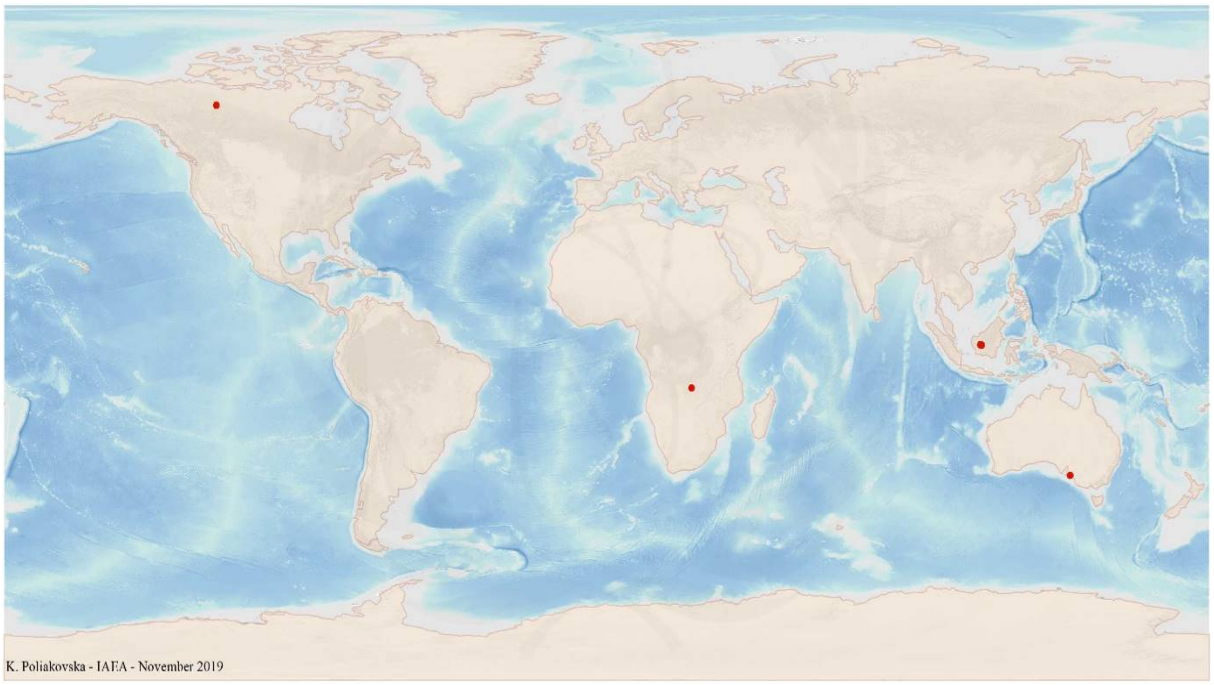

FIG. 6.2.1a. World distribution of selected Metamorphite Structure-Bound Monometallic Veins uranium deposits from the UDEPO database.

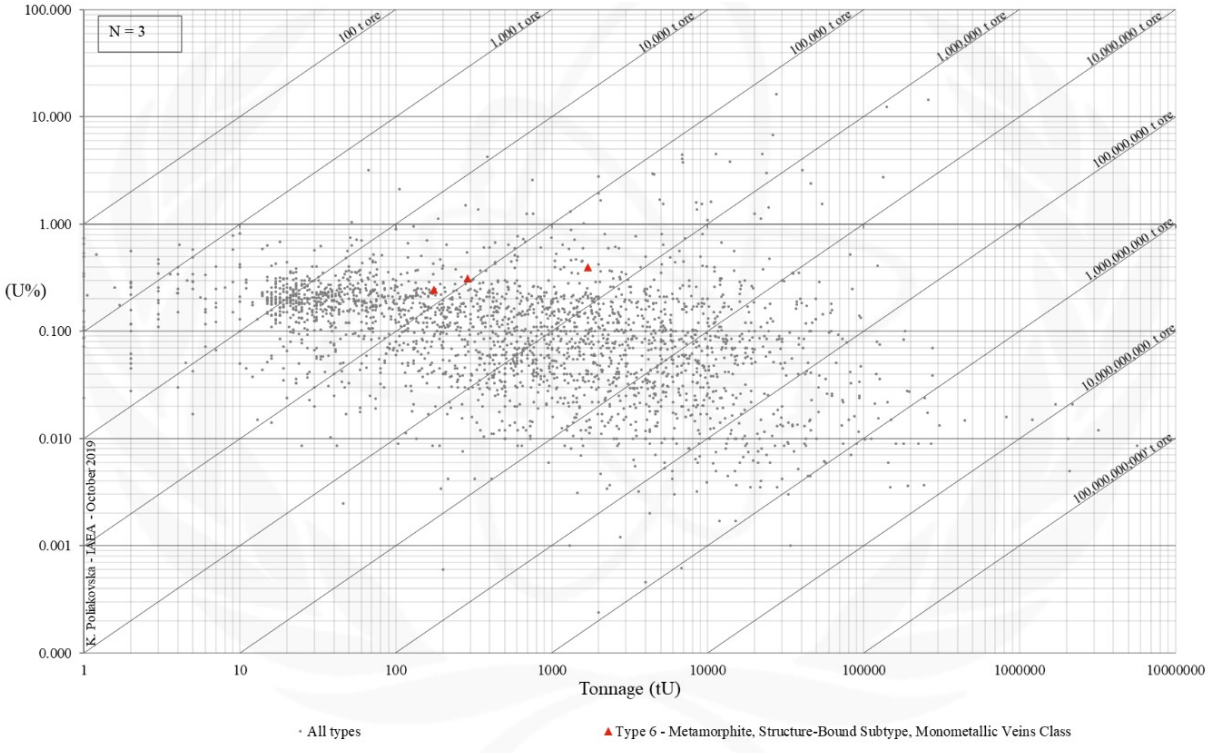

FIG. 6.2.1b. Grade and tonnage scatterplot highlighting Metamorphite Structure-Bound Monometallic Veins uranium deposits from the UDEPO database.

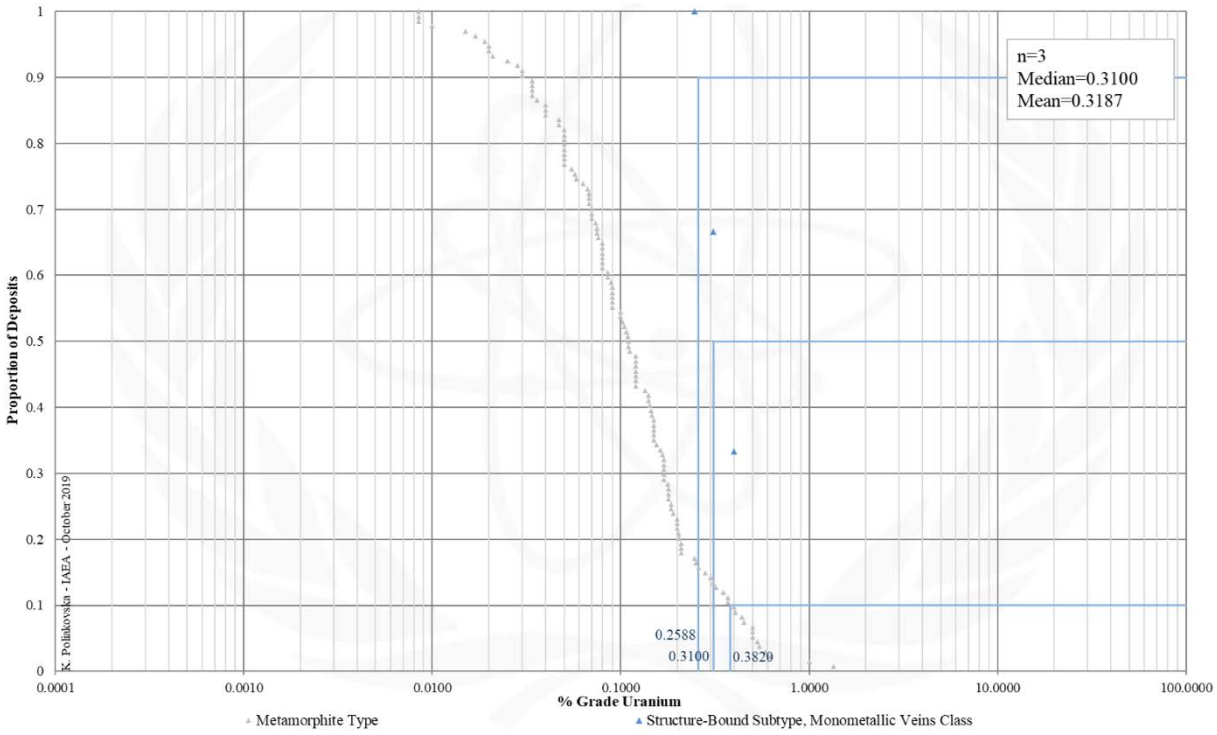

FIG. 6.2.1c. Grade Cumulative Probability Plot for Metamorphite Structure-Bound Monometallic Veins uranium deposits from the UDEPO database.

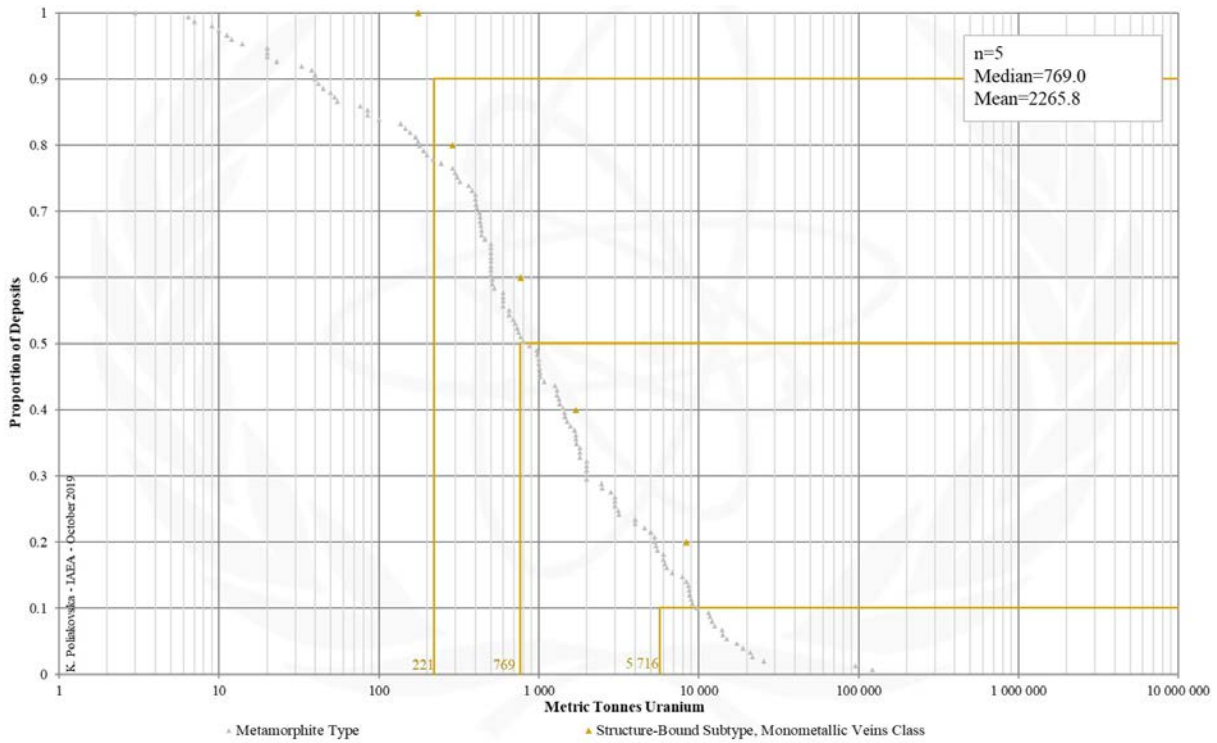

FIG. 6.2.1d. Tonnage Cumulative Probability Plot for Metamorphite Structure-Bound Monometallic Veins uranium deposits from the UDEPO database.

CLASS 6.2.2. Metamorphite, Structure-Bound, Polymetallic Veins

Brief Description

- Metamorphite deposits are hosted by metamorphosed supracrustal rocks associated with collisional orogens of Precambrian to Cenozoic age.
- Two subtypes are recognised: (6.1.) Stratabound and (6.2.) structure-bound deposits.
- Structure-bound deposits take the form of structurally-controlled vein- and mylonite-hosted uranium ores precipitated from externally derived metamorphic fluids.
- The structure-bound subtype is further subdivided into three classes: (6.2.1.) Monometallic veins, (6.2.2.) polymetallic veins, and (6.2.3.) marble-hosted phosphate.
- Polymetallic veins are characterised by complex mineral assemblages of uranium, gangue and paragenetically younger nickel-cobalt arsenides, selenides and a variety of native metals.
- The ores take the form of vein, stockwork and breccia systems as well as disseminations.

Type Examples

- Schwartzwalder, USA; Beaverlodge, Canada: Ace-Fay-Verna; Kamyshevoye, Kazakhstan

Genetically Associated Deposit Types

- Subtype 6.1. Metamorphite, Stratabound
- Class 6.2.1. Metamorphite, structure-bound, monometallic veins
- Class 6.2.3. Metamorphite, structure-bound, marble-hosted phosphate
- Subtype 2.2. Granite-related, perigranitic
- Type 5. Metasomatite
- Type 7. Proterozoic unconformity

Principal Commodities

- U ± Ag, As, Co, Cu, Fe, Mo, Ni, Pb, Zn

Grades (%) and Tonnages (tU)

- Average: 0,1505, 3572.3
- Median: 0.0485, 1399.5

Number of Deposits

- Deposits: 37

Provinces (undifferentiated from Metamorphite Type)

- Apuseni Mountains, Banat Mountains, Beaverlodge, Bodal Bhandaritola, Central African Copperbelt, Central Ceara, Eastern Carpathian, Gery Swietokrzyskie, Great Bear, Hoggar Shield West, Iserables, Kalan Basin, Kenema Man, Kokshetau, Kolari Kittilia, Lake Ladoga, Longshoushan, Lower Silesia, Radstadter Tauern, Rhodope Massif Central, Rio Preto Campos Belos, Singhbhum, South Bohemian, Southeast Bohemian, Southern Menderes Massif, Southern Rocky Mountains, West Moravian, Wolz Tauern.

Tectonic Setting

- Collisional orogens

Typical Geological Age Range

- Proterozoic (and possibly younger)

Mineral Systems Model

Source

Ground preparation
- Intracratonic basin formation
- Deposition and diagenesis of a thick (>5 km) sedimentary pile above a basal unconformity

Energy
- Orogenesis and/or tectonic reactivation
- Regional metamorphism

Fluids
- Highly saline, oxidised basinal brines

Ligands
- Cl, F, OH

Reductants and reactants
- Carbonates, black shales

Uranium
- Crystalline basement rocks, intracratonic basin fill

Transport

Fluid pathways
- Long-lived transcrustal fault zones in the basement
- Regional unconformity surfaces
- Permeable, oxidised sandstone and conglomerate aquifers above the unconformity
- Diapiric breccia

Trap
Physical – Fault-fracture systems and associated tectonic breccia zones – Halokinetic breccia Chemical – Carbonates, black shales
Deposition
Change in redox conditions – Due to mixing of oxidised, uranium-bearing brines and reduced metamorphic fluids – Due to interaction of oxidised, uranium-bearing fluids and wallrock reductants Supergene processes – Secondary uranium redistribution and enrichment
Preservation
– Relative tectonic stability post-uranium mineralisation – Subsidence and burial of the uranium mineralised rocks
Key Reference Bibliography
BALL, S., Hydrothermal nickel sulfide hosted in Neoproterozoic carbonate and evaporitic rocks of the Menda Central prospect, Democratic Republic of Congo. Unpublished MSc Thesis, Colorado School of Mines, 102p (2016). DAHLKAMP, F., Uranium ore deposits. Springer, 460p (2013). DECRÉE, S., DELOULE, E., DE PUTTER, T., DEWAELE, S., MEES, F., MARIGNAC, C., SIMS U-Pb ages for heterogenite from Katanga: implications for the genesis of Co-U deposits in Shinkolobwe. Goldschmidt Conference Abstracts 2011, Mineralogical Magazine, 75(3), 733 (2011). EGLINGER, A., ANDRÉ-MAYER, A. S., VANDERHAEGHE, O., MERCADIER, J., CUNEY, M., DECRÉE, S., INTERNATIONAL ATOMIC ENERGY AGENCY, Geological Classification of Uranium Deposits and Description of Selected Examples. IAEA-TECDOC Series, 1842, 415p (2018).

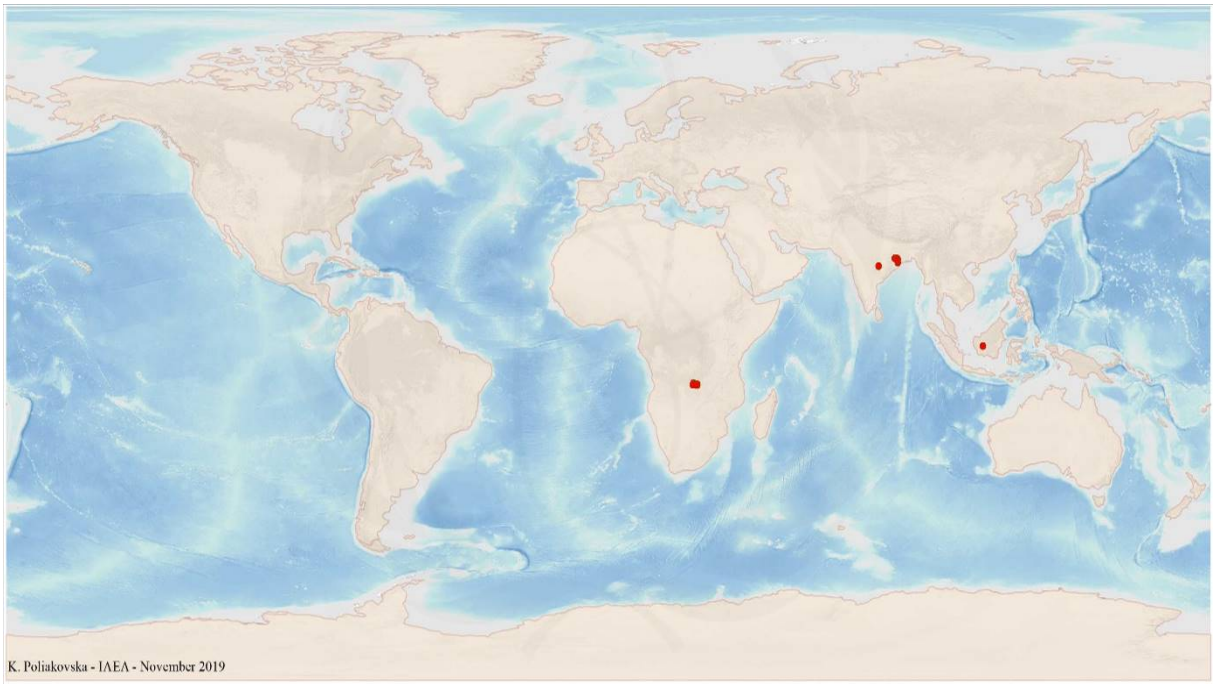

FIG. 6.2.2a. World distribution of selected Metamorphite Structure-Bound Polymetallic Veins uranium deposits from the UDEPO database.

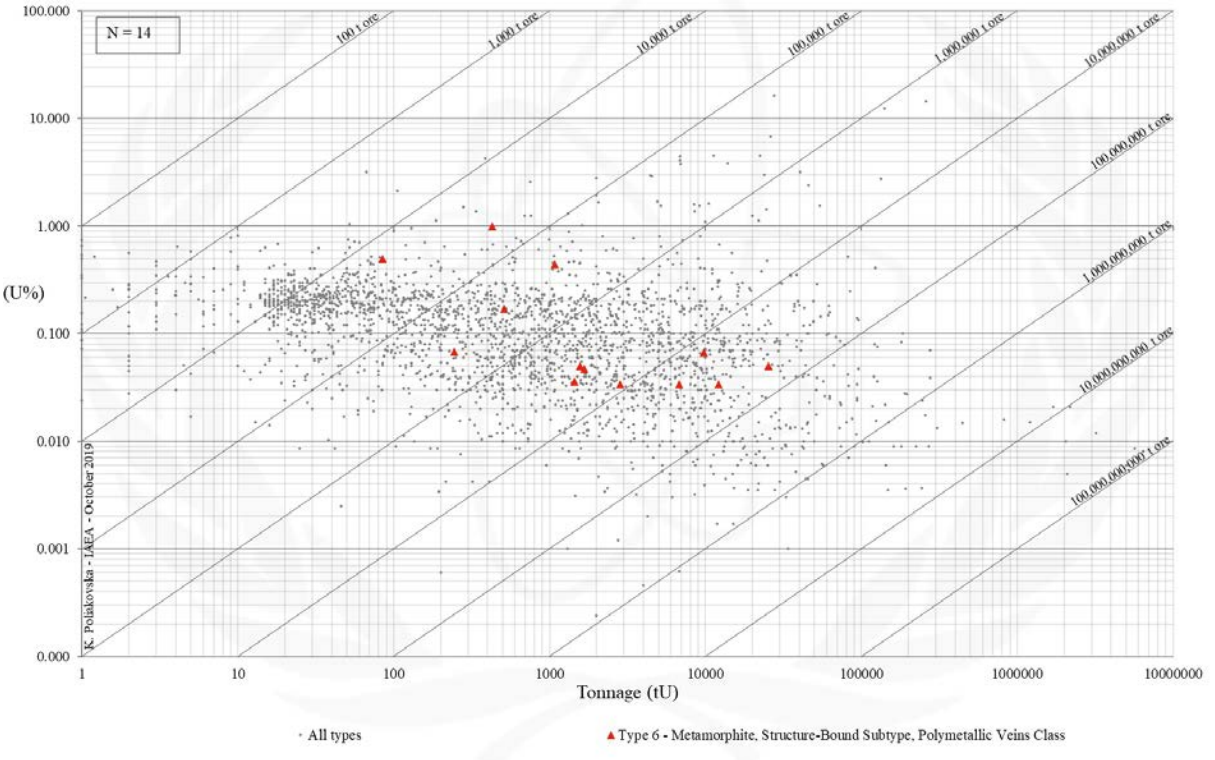

FIG. 6.2.2b. Grade and tonnage scatterplot highlighting Metamorphite Structure-Bound Polymetallic Veins uranium deposits from the UDEPO database.

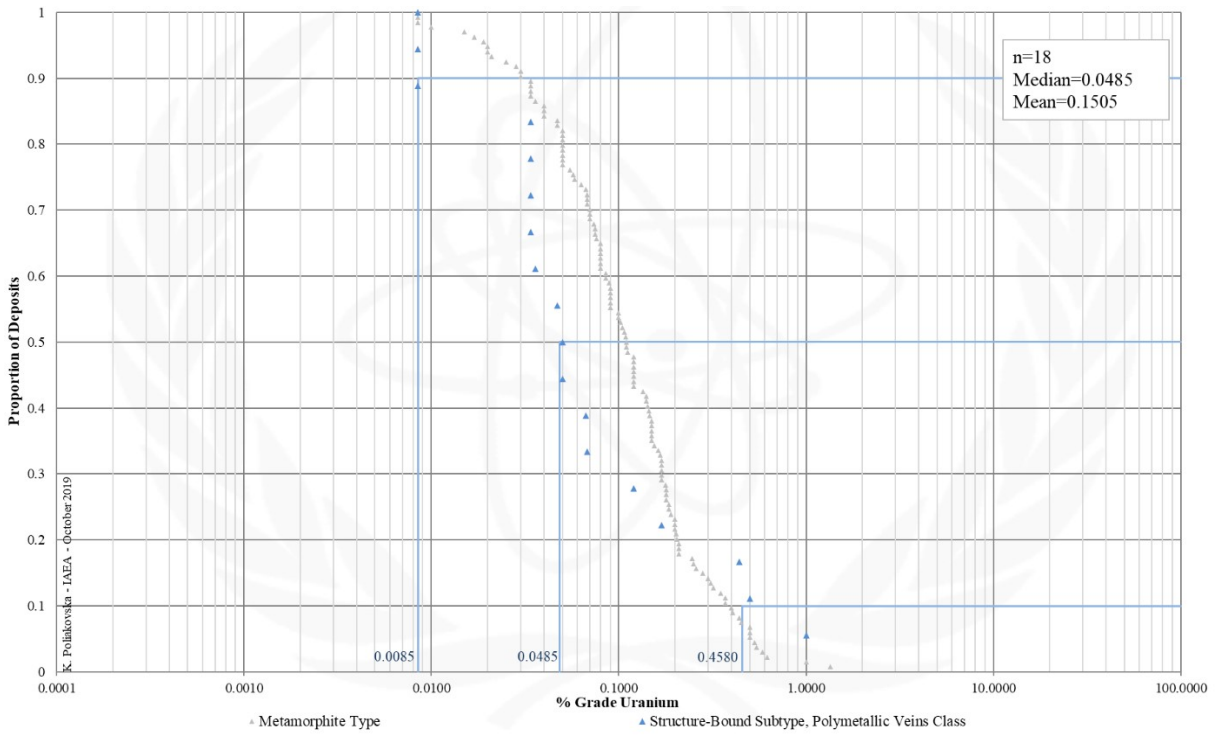

FIG. 6.2.2c. Grade Cumulative Probability Plot for Metamorphite Structure-Bound Polymetallic Veins uranium deposits from the UDEPO database.

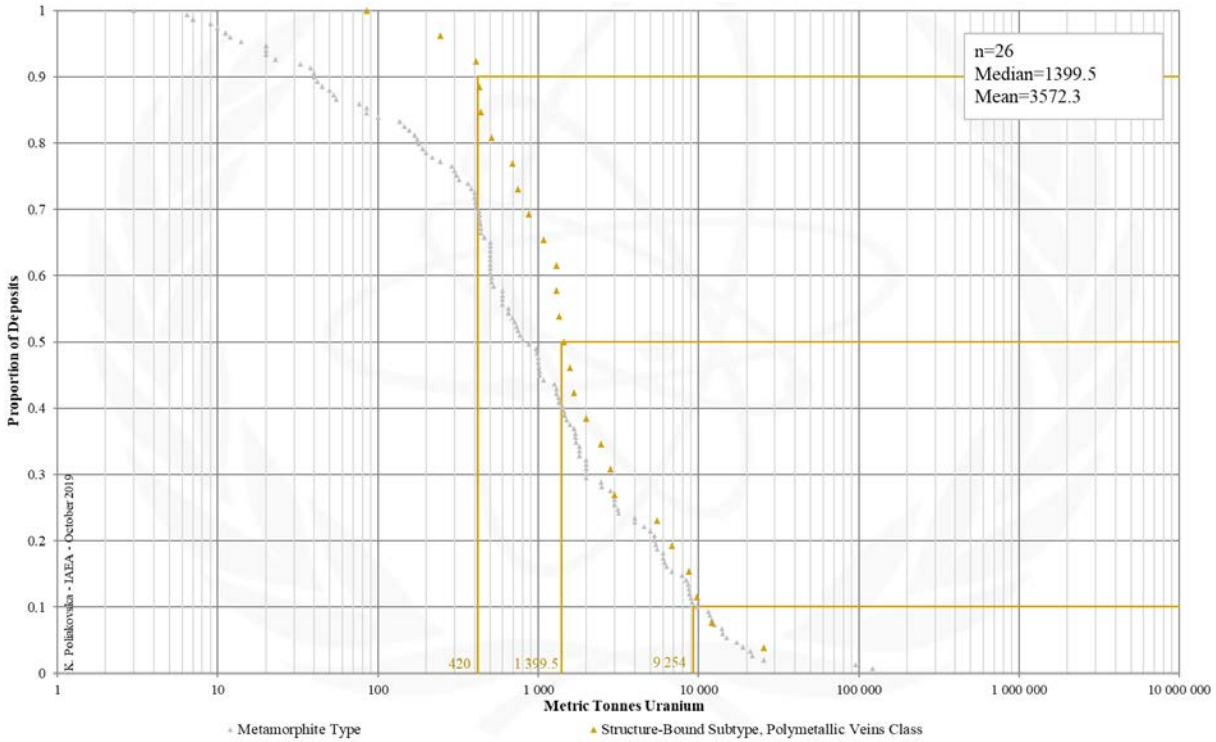

FIG. 6.2.2d. Tonnage Cumulative Probability Plot for Metamorphite Structure-Bound Polymetallic Veins uranium deposits from the UDEPO database.

CLASS 6.2.3. Metamorphite, Structure-Bound, Marble-Hosted Phosphate

Brief Description

- Metamorphite deposits are hosted by metamorphosed supracrustal rocks associated with collisional orogens of Precambrian to Cenozoic age.
- Two subtypes are recognised: (6.1.) Stratabound and (6.2.) structure-bound deposits.
- Structure-bound deposits take the form of structurally-controlled vein- and mylonite-hosted uranium ores precipitated from externally derived metamorphic fluids.
- The structure-bound subtype is further subdivided into three classes: (6.2.1.) Monometallic veins, (6.2.2.) polymetallic veins, and (6.2.3.) marble-hosted phosphate.
- Marble-hosted phosphate deposits are exemplified by Itataia, Brazil, a complex, multiphase uraniferous phosphate deposit hosted by marbles and calc-silicate rocks.
- The uranium-phosphate ores at Itataia can be subdivided into two groups: Black ore in episyenite and marble comprising coffinite, hydrothermal zircon and organic matter, and pink ore in marble, gneiss and episyenite comprising pink collophane.

Genetically Associated Deposit Types

- Subtype 6.1. Metamorphite, Stratabound
- Class 6.2.1. Metamorphite, structure-bound, monometallic veins
- Class 6.2.2. Metamorphite, structure-bound, polymetallic veins
- Subtype 5.1 Metasomatite, sodium (Na)-metasomatite

Type Examples

- Itataia/Santa Quitéria, Brazil; Zaozernoye, Kazhakstan

Principal Commodities

- U, P

Grades (%) and Tonnages (tU)

- Average: 0.0567, 14729.4
- Median: 0.0485, 1029.5

Number of Deposits

- Deposits: 13

Provinces (undifferentiated from Metamorphite Type)

- Apuseni Mountains, Banat Mountains, Beaverlodge, Bodal Bhandaritola, Central African Copperbelt, Central Ceara, Eastern Carpathian, Gery Swietokrzyskie, Great Bear, Hoggar Shield West, Iserables, Kalan Basin, Kenema Man, Kokshetau, Kolari Kittilia, Lake Ladoga, Longshoushan, Lower Silesia, Radstadter Tauern, Rhodope Massif Central, Rio Preto Campos Belos, Singhbhum, South Bohemian, Southeast Bohemian, Southern Menderes Massif, Southern Rocky Mountains, West Moravian, Wolz Tauern.

Tectonic Setting

- Collisional orogens

Typical Geological Age Range

- Neoproterozoic to Mesozoic (and possibly younger)

Mineral Systems Model

Source

Ground preparation

- Formation of a shallow marine/lagoonal environment
- Deposition of phosphatic ± uranium-enriched sediments and organic matter

Energy

- Orogenesis
- Amphibolite facies grade metamorphism
- Postcollisional magmatism
- Uplift and topographic gradient (supergene mineralisation)

Fluids

- Magmatic-hydrothermal fluids
- Groundwaters (supergene mineralisation)

Ligands

- Cl, F, OH

Reductants and reactants

- Carbonaceous matter, impure graphite-, diopside-, scapolite-, tremolite- and phlogopite-bearing limestones and marbles

Uranium

- Crystalline basement rocks, granitoids

Transport

Melt and fluid pathways

- Crustal-scale fault zones

- Domal structures
- Karst aquifers

Trap

Physical
- Fault-fracture and breccia systems
- Episyenites
- Palaeokarst voids and cavities
- Fold hinge zones
- Structurally thickened marble succession
- Palaeo-watertable (supergene mineralisation)

Chemical
- Impure (± graphitic) marble
- Carbonaceous karst dissolution breccia
- Hematitisation, chloritisation and albitisation/episyenitisation (quartz dissolution)

Deposition

Metamorphic remobilisation and recrystallisation
- Remobilisation and recrystallisation of primary phosphate (and uranium?)

Change in redox conditions
- Due to sodium metasomatism (to date this mechanism is poorly characterised)
- Due to mixing of saline magmatic-hydrothermal fluids and heated groundwaters
- Due to interaction of uranium-bearing fluids and carbonate wallrocks

Supergene processes
- Secondary uranium redistribution and enrichment via heated groundwaters

Preservation

- Relative tectonic stability post-uranium mineralisation
- Subsidence and burial of the uranium mineralised rocks

Key Reference Bibliography

ANGEIRAS, A. G., Geology and metallogeny of the northeastern Brazil uranium-phosphorus province emphasizing the Itataia deposit. Ore Geology Reviews, 3(1-3), 211-225 (1988).

INTERNATIONAL ATOMIC ENERGY AGENCY, Geological Classification of Uranium Deposits and Description of Selected Examples. IAEA-TECDOC Series, 1842, 415p (2018).

VERÍSSIMO, C. U. V., SANTOS, R. V., PARENTE, C. V., DE OLIVEIRA, C. G., CAVALCANTI, J. A. D., NETO, J. D. A. N., The Itataia phosphate-uranium deposit (Ceará, Brazil) new petrographic, geochemistry and isotope studies. Journal of South American Earth Sciences, 70, 115-144 (2016).

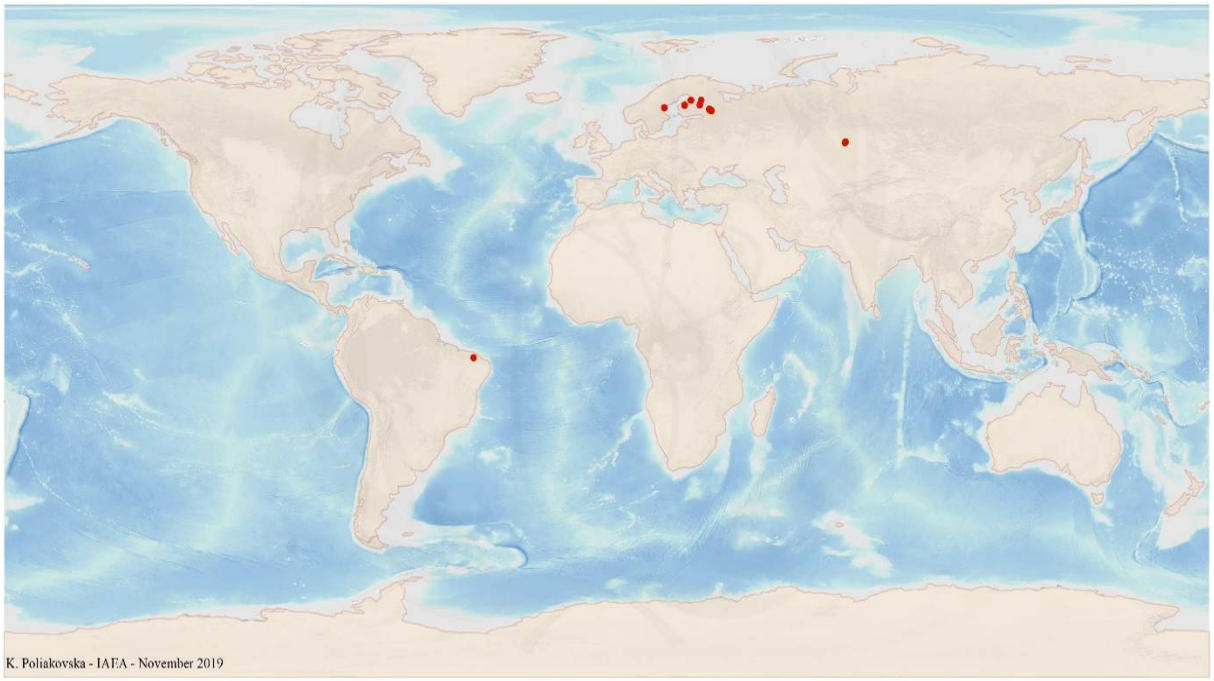

FIG. 6.2.3a. World distribution of selected Metamorphite Structure-Bound Marble-Hosted Phosphate uranium deposits from the UDEPO database.

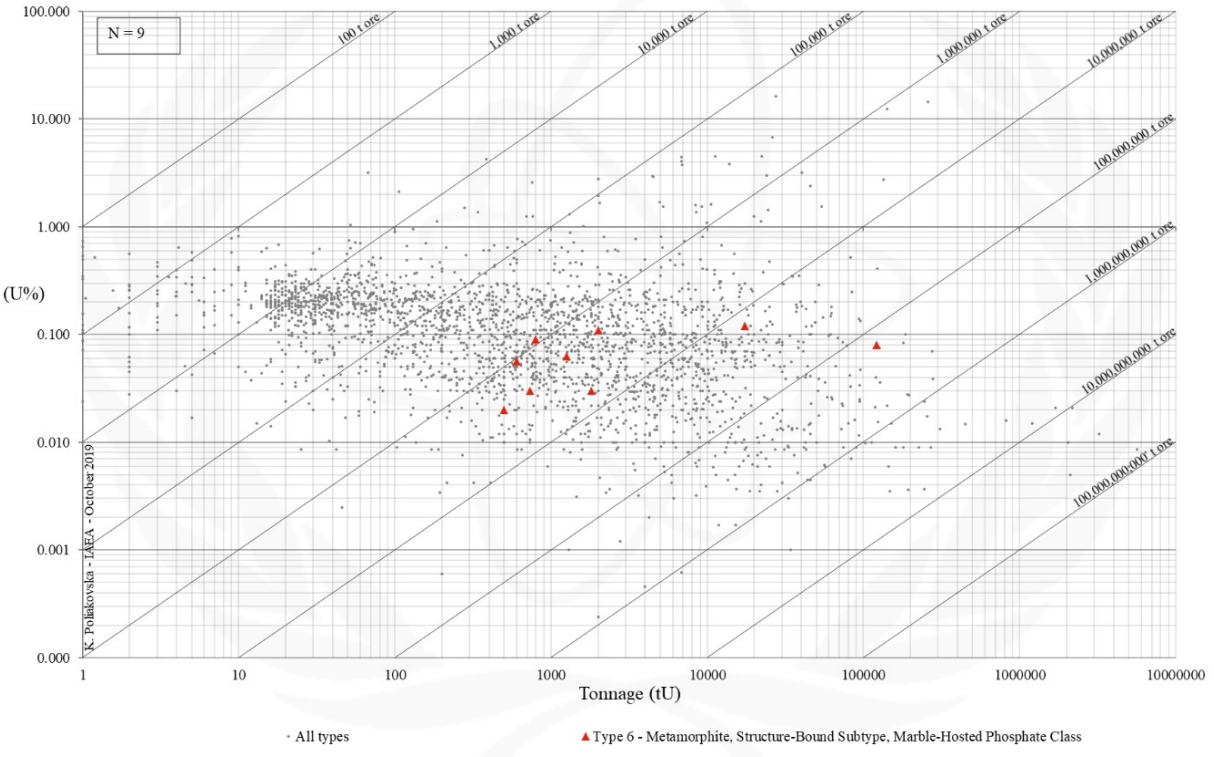

FIG. 6.2.3b. Grade and tonnage scatterplot highlighting Metamorphite Structure-Bound Marble-Hosted Phosphate uranium deposits from the UDEPO database.

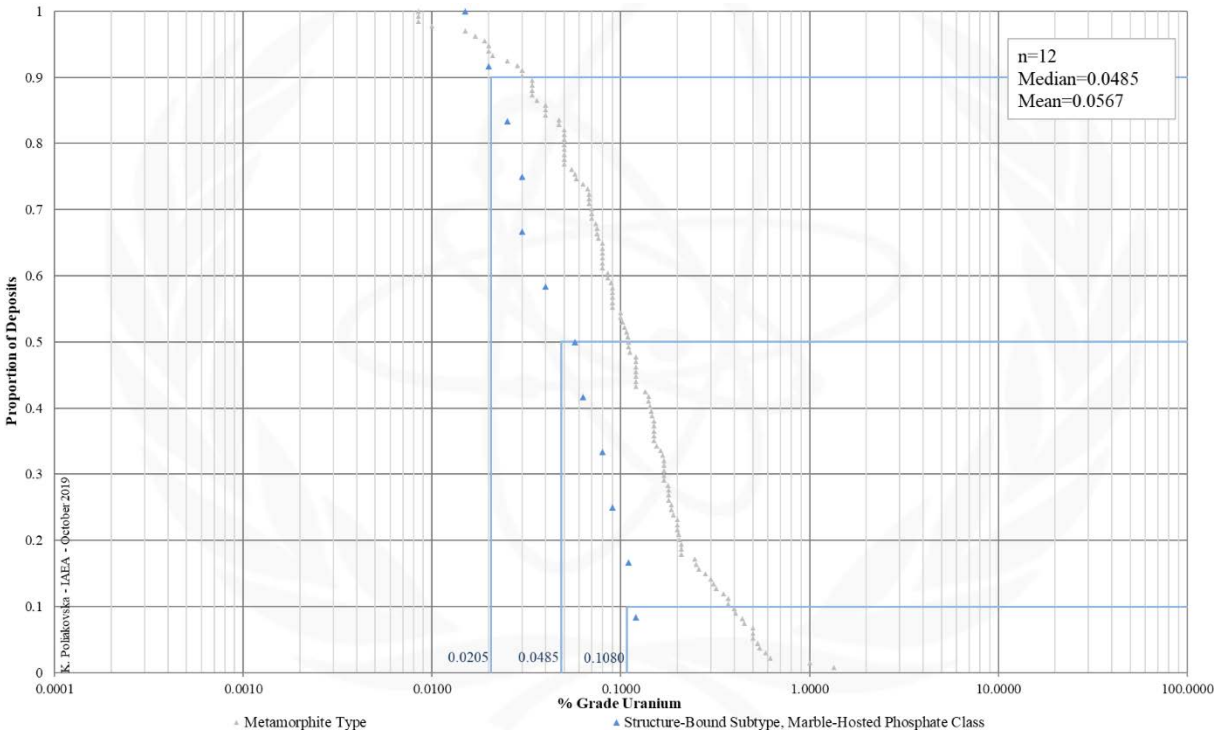

FIG. 6.2.3.c. Grade Cumulative Probability Plot for Metamorphite Structure-Bound Marble-Hosted Phosphate uranium deposits from the UDEPO database.

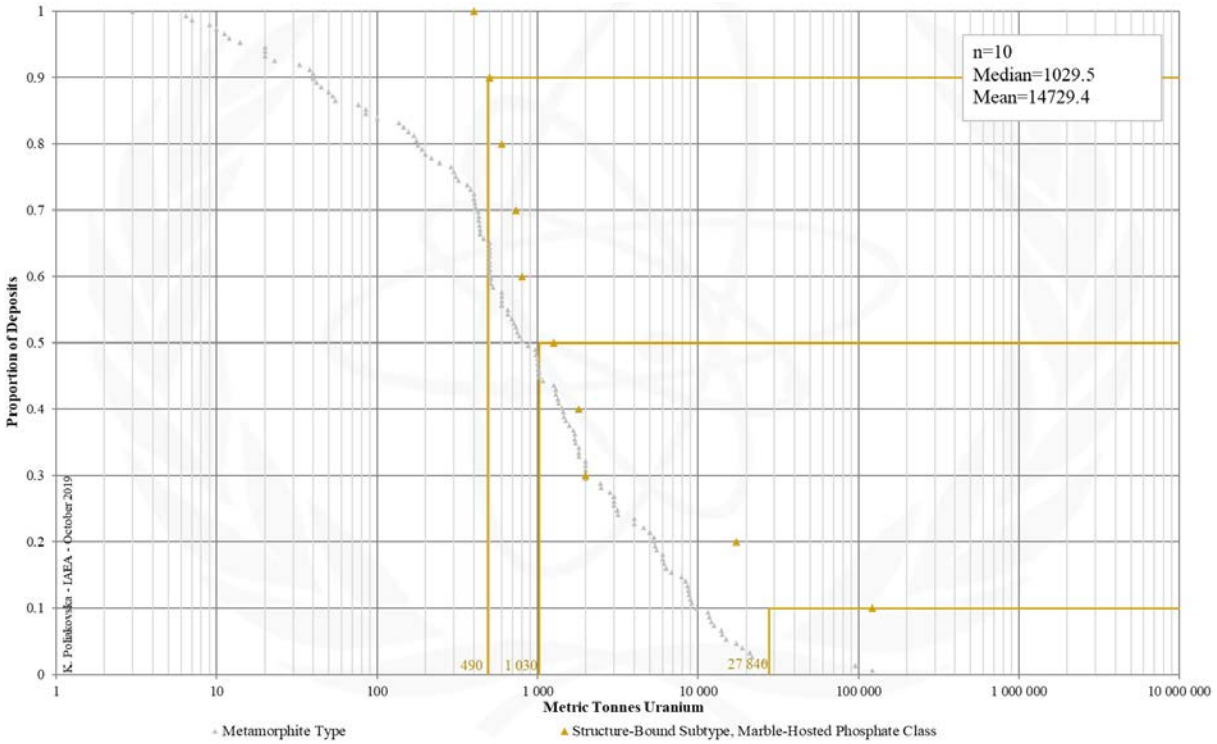

FIG. 6.2.3d. Tonnage Cumulative Probability Plot for Metamorphite Structure-Bound Marble-Hosted Phosphate uranium deposits from the UDEPO database.

Appendix VII

PROTEROZOIC UNCONFORMITY

TYPE 7. Proterozoic Unconformity

Brief Description

- Proterozoic unconformity deposits, predominantly found in the Athabasca Basin (Canada) and Pine Creek Orogen (Australia), are the economically most significant uranium producing systems globally.
- They occur at and immediately above or below unconformities separating relatively undeformed, intracratonic sandstone basins (typically Palaeo- to Mesoproterozoic) from underlying metamorphic basement rocks (typically Archaean to Palaeoproterozoic).
- Uranium ores take the form of structurally controlled pods, veins, breccias and replacements, mainly consisting of pitchblende although polymetallic ores also occur. Bitumen is a common component of the ores.
- Extensive domains of intense wallrock alteration (chlorite, white mica and clay and carbonate mineral assemblages) accompany the mineralisation.
- A typical feature of these deposits is that basement rocks immediately below the unconformity are often strongly haematite and clay altered, either as a result of palaeoweathering or diagenetic/hydrothermal alteration, or both.
- Three distinct subtypes are recognised: (7.1) unconformity-contact, (7.2) basement-hosted, and (7.3) stratiform structure-controlled uranium deposits.

Subtypes

- 7.1. Proterozoic unconformity, unconformity-contact
- 7.2. Proterozoic unconformity, basement hosted
- 7.3. Proterozoic unconformity, stratiform fracture-controlled

Type Examples

- Subtype 7.1. Cigar Lake, Key Lake, McArthur River, Canada; Angularli, Australia
- Subtype 7.2. Jabiluka, Ranger, Nabarlek, Australia; Eagle Point, Arrow, Triple R, Millenium, Kiggavik, Canada
- Subtype 7.3. Chitrial, Lambapur, Peddagattu, Koppunuru, India

Principal Commodities

- U ± Ni, Co, As, Mo, Pb, Cu, Au-Pt-Pd

Grades (%) and Tonnages (tU)

- Average: 1.5042, 15482.2
- Median: 0.5900, 2482.0

Number of Deposits

- Deposits: 121

Provinces

- Aravalli Delhi Basins, Ashburton, Athabasca Basin, Baxter Lake, Bhima Basin, Borborema Province, Borden Basin, Cariewerloo Basin, Central Amazon, Chhattisgarh Khariar Basin, Cuddapah Basin, Elu Basin, Hornby Bay Basin, Hurwitz Group, Maroni Itacaiunas, Mistassini Basin, Otish Basin, Pasha Ladoga Basin, Paterson, Pine Creek Orogen, Rio Negro Juruena, Rondonia San Ignacio, Roraima Basin, Sao Francisco Craton, Sibley Basin, Sucunduri Basin, Thelon Basin, Thule Basin, Tocantins.

Tectonic Setting

- Intracratonic basins

Typical Geological Age Range

- Late Palaeoproterozoic to Mesoproterozoic

Mineral Systems Model

Source

Ground preparation

- Intracratonic basin formation within basement rocks that are enriched in uranium ± graphite
- Deposition of a thick (>5-6 km) fluviatile sandstone succession
- Sandstone diagenesis above a basal unconformity between basin and basement rocks
- Aquifer evolution

Energy

- Changes in far-field plate boundary forces promoting reactivation of and tectonic activity along pre-existing structures
- Diagenetic compaction of basin sequences

Fluids

- Fluid 1: High NaCl, low Ca brines of diagenetic origin formed from dissolution of evaporites
- Fluid 2: High NaCl brines with higher Ca/Na ratios than Fluid 1 evolved from the latter after reacting with basement rocks below the unconformity
- Fluid 3: Low NaCl, hydrocarbon-rich fluids formed from hydrogenation of carbonaceous material in metasedimentary rocks below the unconformity

Ligands

- Ca and Cl, possibly sourced from intrabasinal evaporite sequences

Reductants

- Graphite, sulphides, hydrocarbons, bitumen, methane, H_2S, Fe^{2+} silicates, black shale

Uranium
- Uranium enriched granitic, metavolcanic and metasedimentary basement rocks, or pre-existing uranium ores below the unconformity
- Uranium-bearing detrital minerals in the sandstone-dominated basin fill such as monazite or zircon volcanic ash)
- Uranium-enriched palaeoregolith immediately below the unconformity

Transport

Fluid pathways
- Long-lived transcrustal fault zones in the basement
- Regional unconformity surface with or without palaeoregolith
- Permeable, oxidised sandstone and conglomerate aquifers above the unconformity

Trap

Physical
- Unconformity surface
- Dilational structural sites associated with faults and breccia zones at, below or above the unconformity
- Domains of sandstone dissolution at and above the unconformity

Chemical
- Rocks with Fe^{2+} silicates above the unconformity

Deposition

Change in redox conditions
- Due to mixing of highly oxidised brines (Fluid 1 and 2) travelling along the unconformity and down faults with upwelling reduced fluids (Fluid 3) travelling upwards along basement-rooted faults
- Due to interaction of oxidised, uranium-bearing fluids with highly reduced carbonaceous and ferruginous rocks

Preservation
- Relative tectonic stability post-uranium mineralisation
- Adequate conservation of the sandstone succession above the unconformity

Key Reference Bibliography

CHI, G., LI, Z., CHU, H., BETHUNE, K. M., QUIRT, D. H., LEDRU, P., NORMAND, C., CARD, C., BOSMAN, S., DAVIS, W. J., POTTER, E. G., A shallow-burial mineralization model for the unconformity-related uranium deposits in the Athabasca Basin. Economic Geology, 113(5), 1209-1217 (2018).

CHI, G., CHU, H., PETTS, D., POTTER, E., JACKSON, S., WILLIAMS-JONES, A., Uranium-rich diagenetic fluids provide the key to unconformity-related uranium mineralization in the Athabasca Basin. Scientific reports, 9:5530, https://doi.org/10.1038/s41598-019-42032-0 (2019).

CUNEY, M. L., World-class unconformity-related uranium deposits: Key factors for their genesis. In: Mao, J., Bierlein, F. P. (Eds.), Mineral Deposit Research: Meeting the Global Challenge. Proceedings of the Eighth Biennial SGA Meeting, Beijing, China, 18-21 August 2005, pp. 245-248 (2005).

HUSTON, D. L., VAN DER WIELEN, S. (Eds.), An assessment of the uranium and geothermal prospectivity of east-central South Australia. Geoscience Australia Record, 2011/34, 229p (2011).

INTERNATIONAL ATOMIC ENERGY AGENCY, Geological Classification of Uranium Deposits and Description of Selected Examples. IAEA-TECDOC Series, 1842, 415p (2018).

INTERNATIONAL ATOMIC ENERGY AGENCY, Unconformity-related Uranium Deposits. IAEA-TECDOC Series, 1857, 295p (2018).

JAIRETH, S., ROACH, I. C., BASTRAKOV, E., LIU, S., Basin-related uranium mineral systems in Australia: A review of critical features. Ore Geology Reviews, 76, 360-394 (2016).

KYSER, K., Uranium ore deposits. In: TUREKIAN, K., HOLLAND, H. (Eds.), Treatise on Geochemistry, 2nd Edition, Elsevier, 489-513 (2013).

MARTZ, P., MERCADIER, J., CATHELINEAU CATHELINEAU, M., BOIRON, M. C., QUIRT, D., DONEY, A., GERBEAUD, O., DE WALLY, E., LEDRU, P., Formation of U-rich mineralizing fluids through basinal brine migration within basement-hosted shear zones: A large-scale study of the fluid chemistry around the unconformity-related Cigar Lake U deposit (Saskatchewan, Canada). Chemical Geology, https://doi.org/10. 1016/j.chemgeo.2018.05.042 (2018).

SKIRROW, R. G., JAIRETH, S., HUSTON, D. L., BASTRAKOV, E. N., SCHOFIELD, A., VAN DER WIELEN, S. E., BARNICOAT, A. C., Uranium mineral systems: Processes, exploration criteria and a new deposit framework. Geoscience Australia Record, 2009/20, 44p (2009).

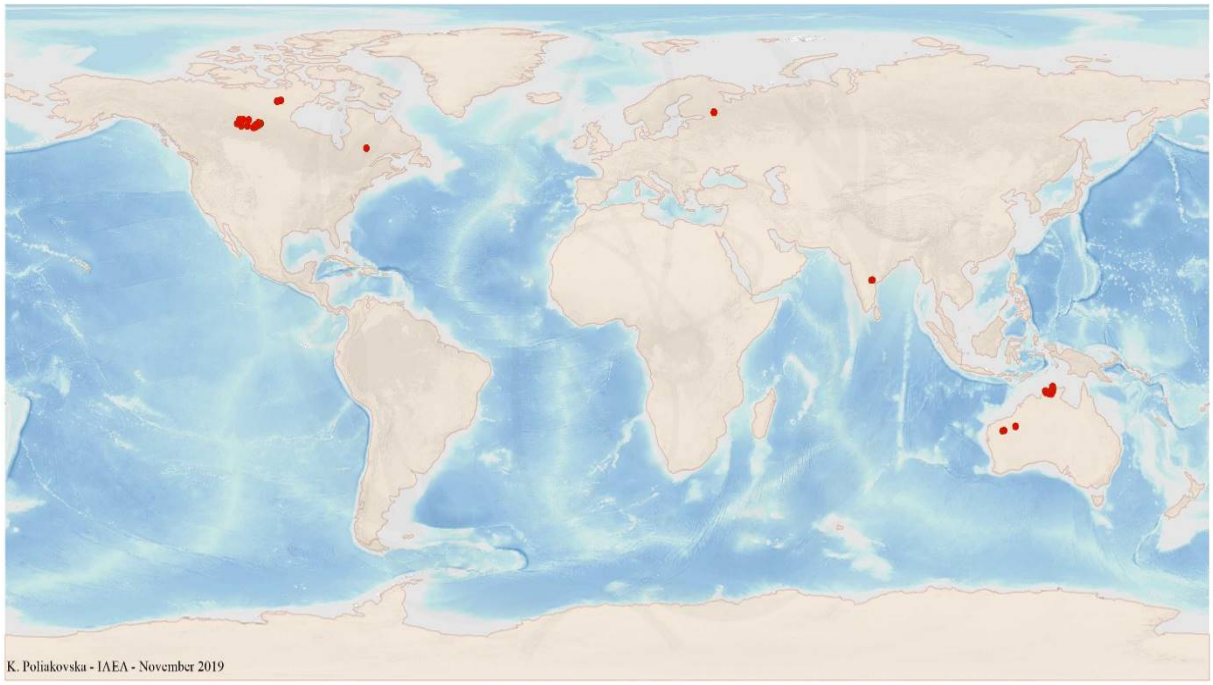

FIG. 7a. World distribution of selected Proterozoic Unconformity uranium deposits from the UDEPO database.

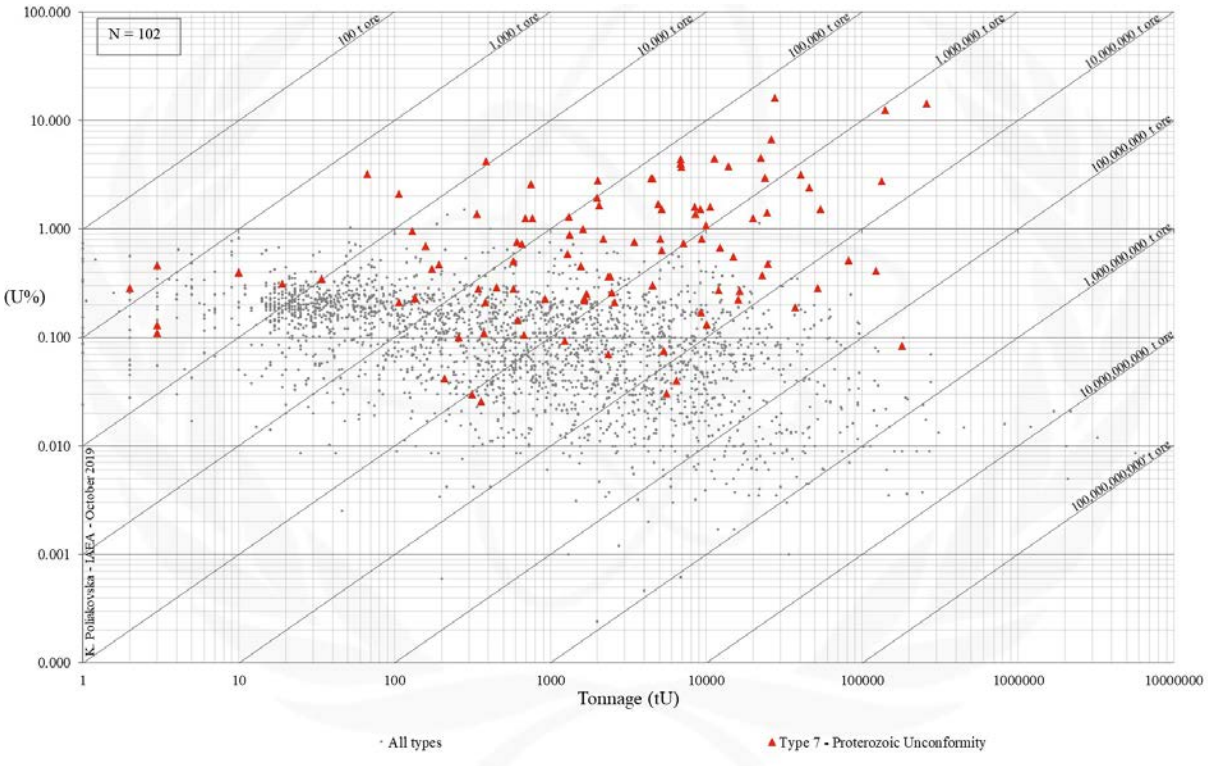

FIG. 7b. Grade and tonnage scatterplot highlighting Proterozoic Unconformity uranium deposits from the UDEPO database.

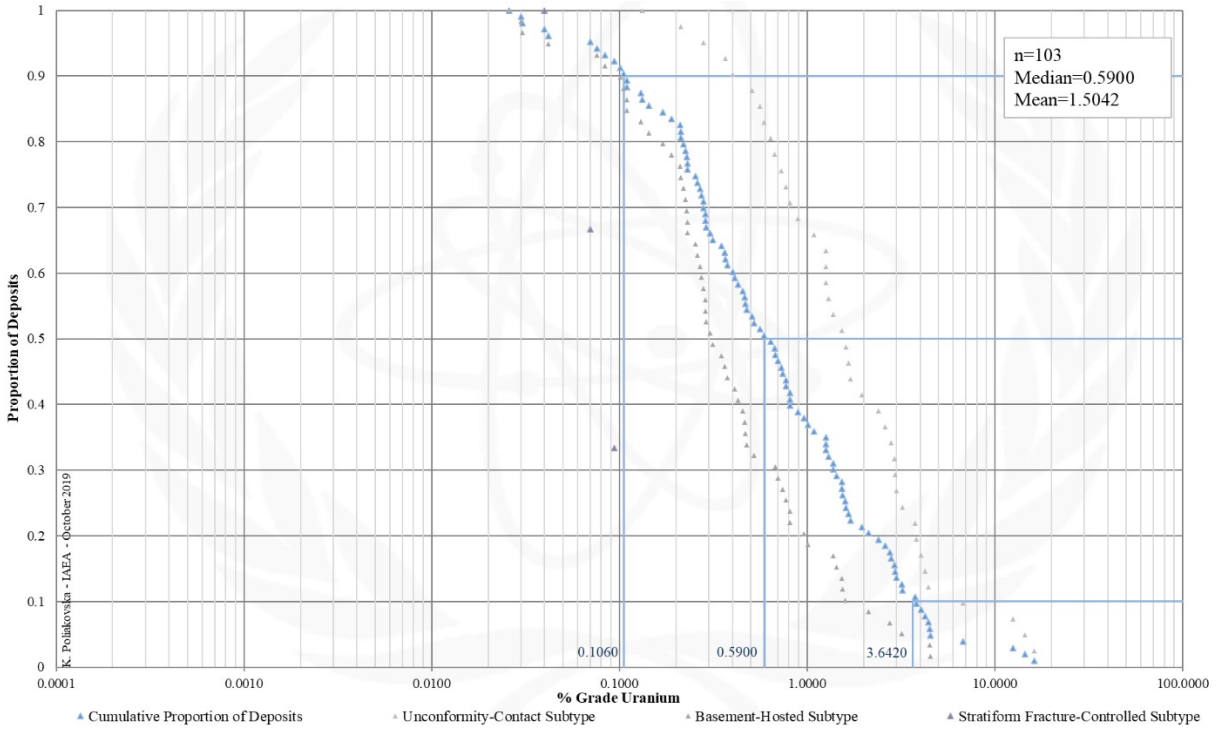

FIG. 7c. Grade Cumulative Probability Plot for Proterozoic Unconformity uranium deposits from the UDEPO database.

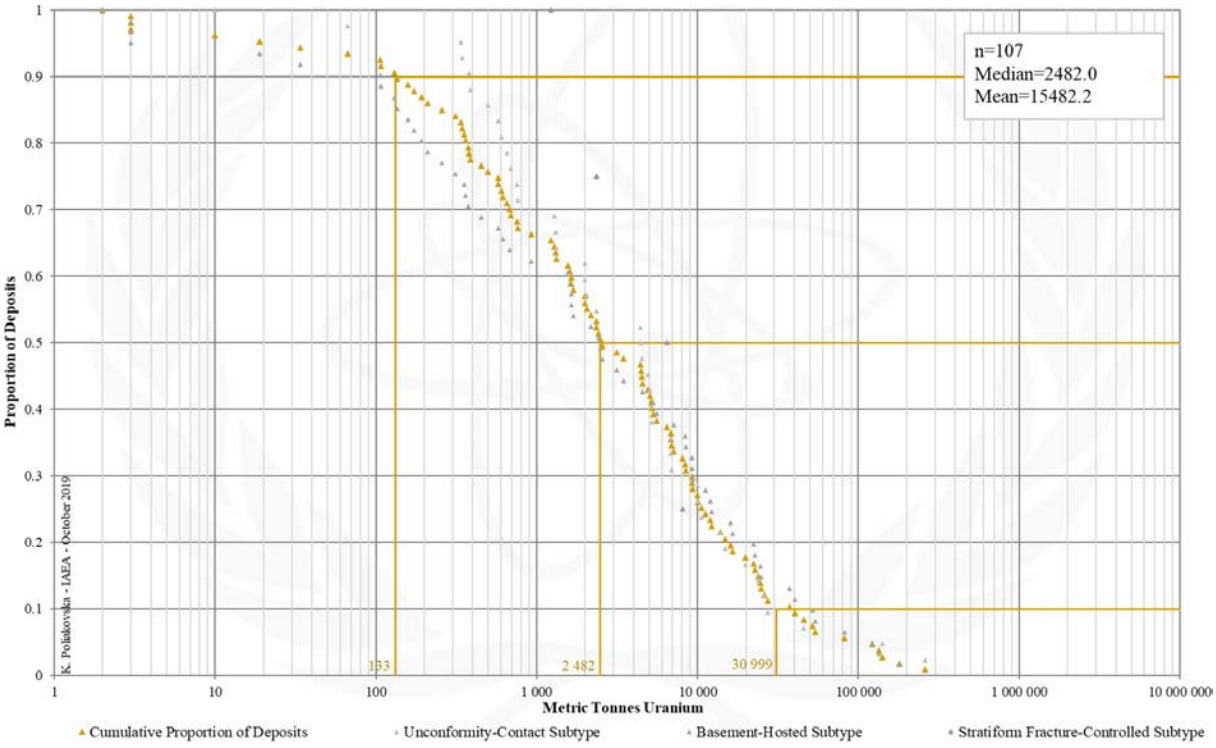

FIG. 7d. Tonnage Cumulative Probability Plot for Proterozoic Unconformity uranium deposits from the UDEPO database.

SUBTYPE 7.1. Proterozoic Unconformity, Unconformity-Contact

Brief Description

- Deposits of subtype 7.1. occur immediately above unconformity surfaces separating relatively undeformed, intracratonic sandstone basins (typically Palaeo- to Mesoproterozoic) from underlying metamorphic basement rocks (typically Archaean to Palaeoproterozoic).
- Uranium deposits of this subtype are commonly sandstone hosted. They often have high grade cores that are enveloped by lower grade halos. Root-like orebody extensions penetrating the underlying basement rocks are common, as are protrusions into overlying sedimentary successions where the mineralisation takes the form of 'perched' orebodies controlled by breccia and fault zones.
- Uranium ores take the form of structurally controlled pods, veins, breccias and replacements, mainly consisting of pitchblende although polymetallic ores also occur. Bitumen is a common component of the ores.
- Extensive domains of intense wallrock alteration (chlorite, white mica and clay and carbonate mineral assemblages) accompany the uranium mineralisation.
- A typical feature of Proterozoic unconformity uranium deposits is that basement rocks immediately below the unconformity are often strongly haematite and clay altered, either as a result of palaeoweathering or diagenetic/hydrothermal alteration, or both.

Type Examples

- Cigar Lake, Key Lake, McArthur River, Canada; Angularli, Australia; Karku, Russian Federation

Genetically Associated Deposit Types

- Subtype 7.2. Proterozoic unconformity, basement hosted
- Subtype 7.3. Proterozoic unconformity, stratiform fracture-controlled
- Subtype 9.5. Sandstone, mafic dykes/sills in Proterozoic sandstone

Principal Commodities

- U ± Ni, Co, As, Mo, Pb, Cu, Au-Pt-Pd

Grades (%) and Tonnages (tU)

- Average: 2.7711, 16097.6
- Median: 1.5350, 4423.0

Number of Deposits

- Deposits: 50

Provinces (undifferentiated from Proterozoic Unconformity Type)

- Aravalli Delhi Basins, Ashburton, Athabasca Basin, Baxter Lake, Bhima Basin, Borborema Province, Borden Basin, Cariewerloo Basin, Central Amazon, Chhattisgarh Khariar Basin, Cuddapah Basin, Elu Basin, Hornby Bay Basin, Hurwitz Group, Maroni Itacaiunas, Mistassini Basin, Otish Basin, Pasha Ladoga Basin, Paterson, Pine Creek Orogen, Rio Negro Juruena, Rondonia San Ignacio, Roraima Basin, Sao Francisco Craton, Sibley Basin, Sucunduri Basin, Thelon Basin, Thule Basin, Tocantins

Tectonic Setting

- Intracratonic basins

Typical Geological Age Range

- Late Palaeoproterozoic to Mesoproterozoic

Mineral Systems Model

Source

Ground preparation

- Intracratonic basin formation within basement rocks that are enriched in uranium ± graphite
- Deposition of a thick (>5-6 km) fluviatile sandstone succession
- Sandstone diagenesis above a basal unconformity between basin and basement rocks
- Aquifer evolution

Energy

- Changes in far-field plate boundary forces promoting reactivation of and tectonic activity along pre-existing structures
- Diagenetic compaction of basin sequences

Fluids

- Fluid 1: High NaCl, low Ca brines of diagenetic origin formed from dissolution of evaporites
- Fluid 2: High NaCl brines with higher Ca/Na ratios than Fluid 1 evolved from the latter after reacting with basement rocks below the unconformity
- Fluid 3: Low NaCl, hydrocarbon-rich fluids formed from hydrogenation of carbonaceous material in metasedimentary rocks below the unconformity

Ligands

- Ca and Cl, possibly sourced from intrabasinal evaporite sequences

Reductants

- Graphite, sulphides, hydrocarbons, bitumen, methane, Fe^{2+} silicates

Uranium
- Uranium enriched granitic, metavolcanic and metasedimentary basement rocks, or pre-existing uranium ores, below the unconformity
- Uranium-bearing detrital minerals in the sandstone-dominated basin fill such as monazite or zircon volcanic ash)
- Uranium-enriched palaeoregolith immediately below the unconformity

Transport

Fluid pathways
- Long-lived transcrustal fault zones in the basement
- Regional unconformity surface with or without palaeoregolith
- Permeable, oxidised sandstone and conglomerate aquifers above the unconformity

Trap

Physical
- Unconformity surface
- Dilational structural sites associated with faults and breccia zones at, below or above the unconformity
- Domains of sandstone dissolution at and above the unconformity

Chemical
- Rocks with Fe^{2+} silicates above the unconformity

Deposition

Change in redox conditions
- Due to mixing of highly oxidised brines (Fluid 1 and 2) travelling along the unconformity and down faults with upwelling reduced fluids (Fluid 3) travelling upwards along basement-rooted faults
- Due to interaction of oxidised, uranium-bearing fluids with highly reduced carbonaceous and ferruginous rocks

Preservation
- Relative tectonic stability post-uranium mineralisation
- Adequate conservation of the sandstone succession above the unconformity

Key Reference Bibliography

BABU, P. R., BANERJEE, R., ACHAR, K. K., Srisailam and Palnad sub-basins: Potential geological domains for unconformity-related uranium mineralisation in India. Exploration and Research for Atomic Minerals, 22, 21-42 (2012).

BASU, H., PRAKASH, K., KUMAR, K. M., THIRUPATHI, P. V., PAUL, A., PANDIT, S. A., CHAKI, A., Chloritization and its bearing on uranium mineralization in Madyalabodu area, Cuddapah district, Andhra Pradesh. Journal of the Geological Society of India, 84(3), 281-291 (2014).

CHI, G., LI, Z., CHU, H., BETHUNE, K. M., QUIRT, D. H., LEDRU, P., NORMAND, C., CARD, C., BOSMAN, S., DAVIS, W. J., POTTER, E. G., A shallow-burial mineralization model for the unconformity-related uranium deposits in the Athabasca Basin. Economic Geology, 113(5), 1209-1217 (2018).

CHI, G., CHU, H., PETTS, D., POTTER, E., JACKSON, S., WILLIAMS-JONES, A., Uranium-rich diagenetic fluids provide the key to unconformity-related uranium mineralization in the Athabasca Basin. Scientific reports, 9:5530, https://doi.org/10.1038/s41598-019-42032-0 (2019).

CUNEY, M. L., World-class unconformity-related uranium deposits: Key factors for their genesis. In: Mao, J., Bierlein, F. P. (Eds.), Mineral Deposit Research: Meeting the Global Challenge. Proceedings of the Eighth Biennial SGA Meeting, Beijing, China, 18-21 August 2005, pp. 245-248 (2005).

DAHLKAMP, F. J., Uranium Deposits of the World: Asia. Springer, Berlin, Heidelberg, 492p (2009).

HUSTON, D. L., VAN DER WIELEN, S. (Eds.), An assessment of the uranium and geothermal prospectivity of east-central South Australia. Geoscience Australia Record, 2011/34, 229p (2011).

INTERNATIONAL ATOMIC ENERGY AGENCY, Geological Classification of Uranium Deposits and Description of Selected Examples. IAEA-TECDOC Series, 1842, 415p (2018).

INTERNATIONAL ATOMIC ENERGY AGENCY, Unconformity-Related Uranium Deposits. IAEA-TECDOC Series, 1857, 295p (2018).

JAIRETH, S., ROACH, I. C., BASTRAKOV, E., LIU, S., Basin-related uranium mineral systems in Australia: A review of critical features. Ore Geology Reviews, 76, 360-394 (2016).

KYSER, K., Uranium ore deposits. In: TUREKIAN, K., HOLLAND, H. (Eds.), Treatise on Geochemistry, 2nd Edition, Elsevier, 489-513 (2013).

MARTZ, P., MERCADIER, J., CATHELINEAU CATHELINEAU, M., BOIRON, M. C., QUIRT, D., DONEY, A., GERBEAUD, O., DE WALLY, E., LEDRU, P., Formation of U-rich mineralizing fluids through basinal brine migration within basement-hosted shear zones: A large-scale study of the fluid chemistry around the unconformity-related Cigar Lake U deposit (Saskatchewan, Canada). Chemical Geology, https://doi.org/10. 1016/j.chemgeo.2018.05.042 (2018).

SKIRROW, R. G., JAIRETH, S., HUSTON, D. L., BASTRAKOV, E. N., SCHOFIELD, A., VAN DER WIELEN, S. E., BARNICOAT, A. C., Uranium mineral systems: Processes, exploration criteria and a new deposit framework. Geoscience Australia Record, 2009/20, 44p (2009).

SINGH, R. V., SINHA, R. M., BISHT, B. S., BANERJEE, D. C. , Hydrogeochemical exploration for unconformity-related uranium mineralization: example from Palnadu sub-basin, Cuddapah Basin, Andhra Pradesh, India. Journal of Geochemical Exploration, 76(2), 71-92 (2002).

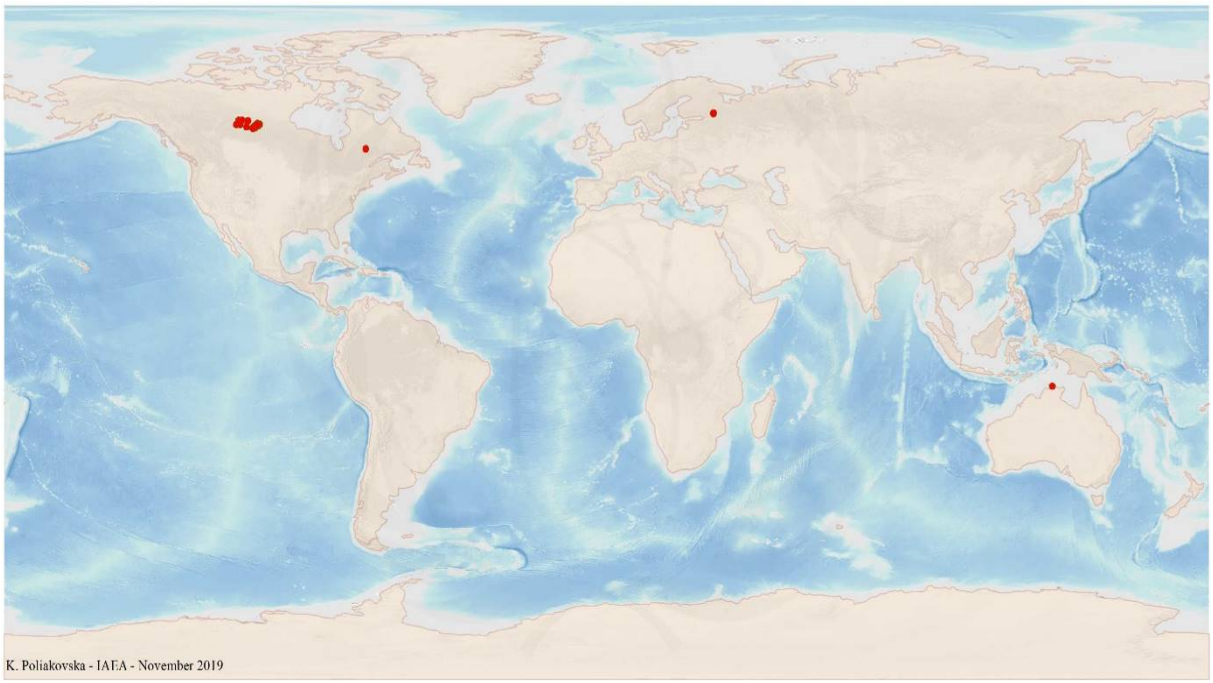

FIG. 7.1a. World distribution of selected Proterozoic Unconformity Unconformity-Contact uranium deposits from the UDEPO database.

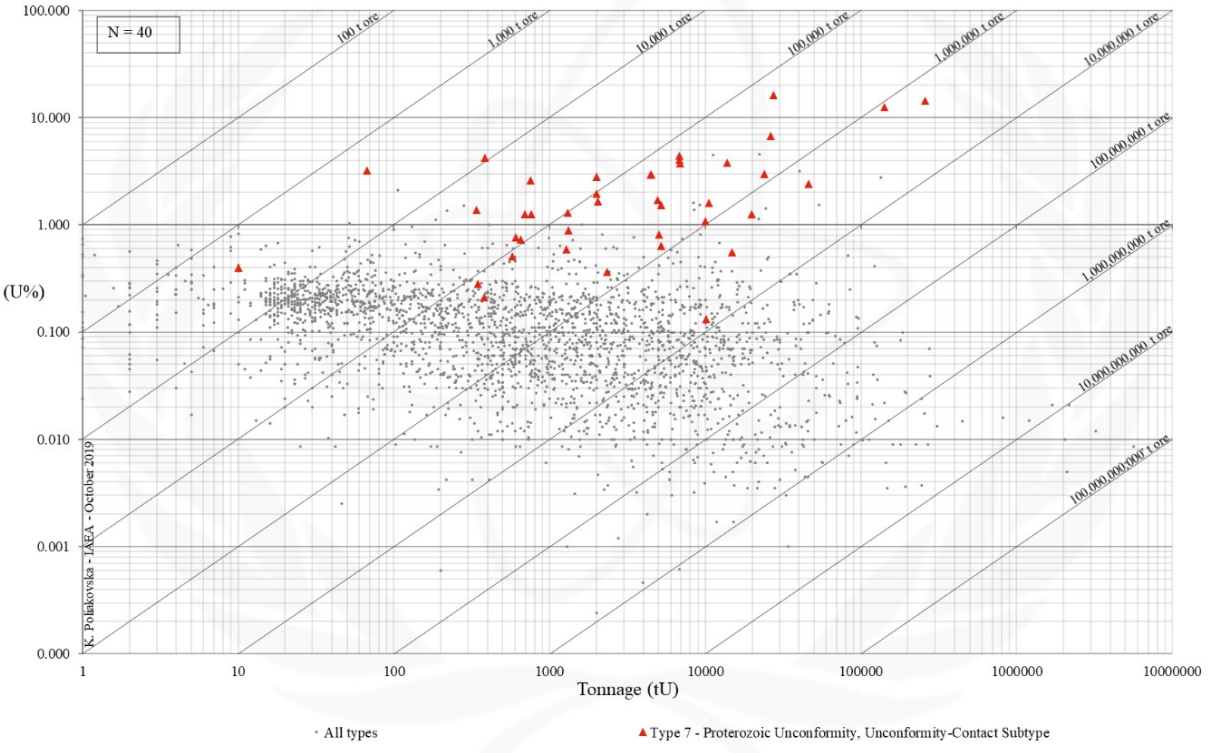

FIG. 7.1b. Grade and tonnage scatterplot highlighting Proterozoic Unconformity Unconformity-Contact uranium deposits from the UDEPO database.

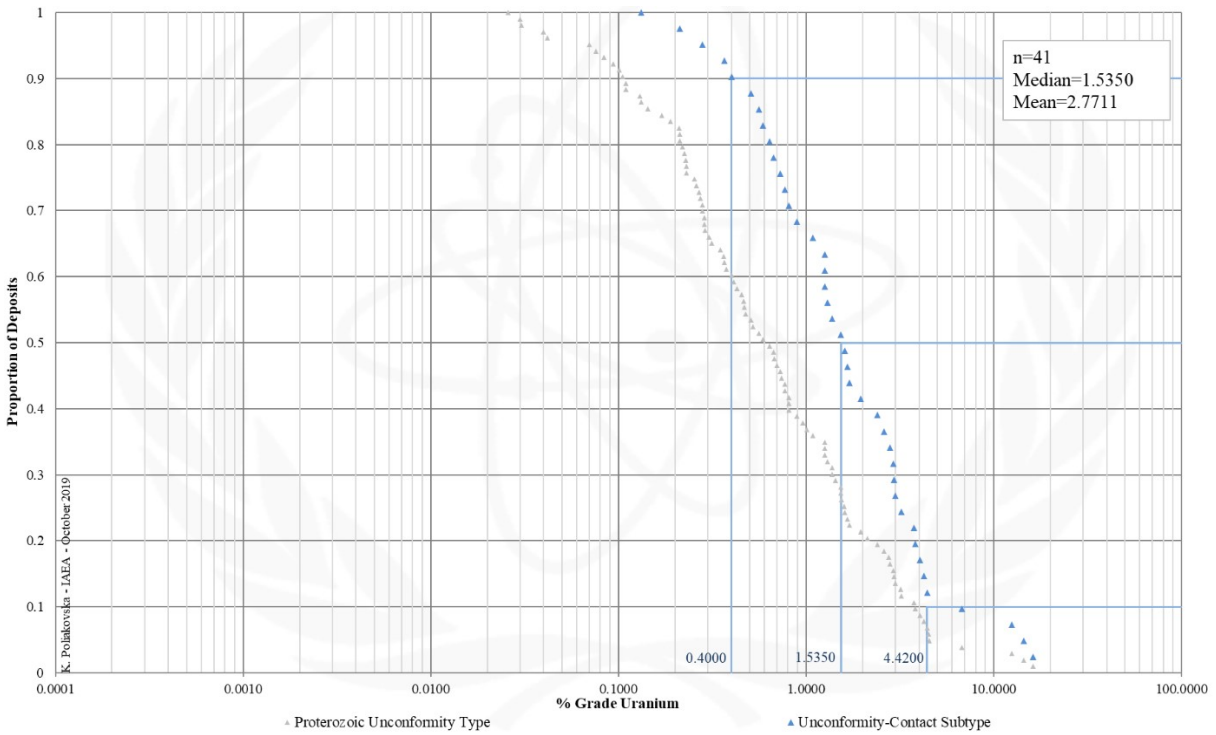

FIG. 7.1c. Grade Cumulative Probability Plot for Proterozoic Unconformity Unconformity-Contact uranium deposits from the UDEPO database.

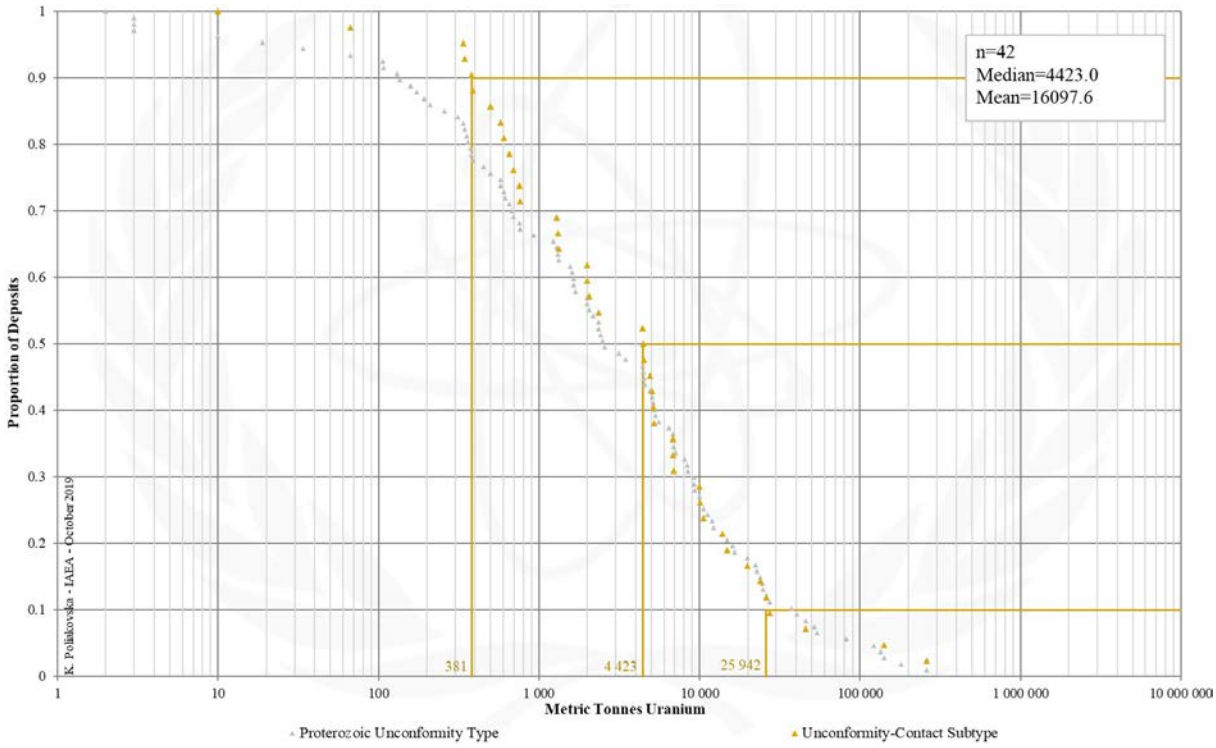

FIG. 7.1d. Tonnage distribution for Proterozoic Unconformity Unconformity-Contact uranium deposits from the UDEPO database.

SUBTYPE 7.2. Proterozoic Unconformity, Basement-Hosted

Brief Description

- Deposits of subtype 7.2. occur at or immediately below unconformity surfaces separating relatively undeformed, intracratonic sandstone basins (typically Palaeo- to Mesoproterozoic) from underlying metamorphic basement rocks (typically Archaean to Palaeoproterozoic).
- Uranium deposits of this subtype are commonly hosted by metasedimentary basement rocks with high grade ores typically associated with brecciated graphitic schist or gneiss.
- The uranium ores take the form of veins, disseminations and wallrock replacements, typically occupying moderately- to steeply-dipping fault-fracture and breccia zones that may have vertical extents of greater 1,000 m. The orebodies are predominantly monometallic although some deposits contain gold and minor platinum-palladium mineralisation or, less commonly, copper, lead, cobalt and nickel.
- Domains of intense wallrock alteration (chlorite, white mica and clay and carbonate mineral assemblages) accompany the mineralisation.
- A typical feature of Proterozoic unconformity uranium deposits is that basement rocks immediately below the unconformity are often strongly haematite and clay altered, either as a result of palaeoweathering or diagenetic/hydrothermal alteration, or both.

Type Examples

- Jabiluka, Ranger, Nabarlek, Australia; Eagle Point, Arrow, Triple R, Millenium, Kiggavik, Andrew Lake, Canada

Genetically Associated Deposit Types

- Subtype 7.1. Proterozoic unconformity, unconformity-contact
- Subtype 7.3. Proterozoic unconformity, stratiform fracture-controlled
- Subtype 9.5. Sandstone, mafic dykes/sills in Proterozoic sandstone

Principal Commodities

- U ± Ni, Co, As, Mo, Pb, Cu, Au-Pt-Pd

Grades (%) and Tonnages (tU)

- Average: 0.6968, 15777.4
- Median: 0.3030, 2425.0

Number of Deposits

- Deposits: 65

Provinces (undifferentiated from Proterozoic Unconformity Type)

- Aravalli Delhi Basins, Ashburton, Athabasca Basin, Baxter Lake, Bhima Basin, Borborema Province, Borden Basin, Cariewerloo Basin, Central Amazon, Chhattisgarh Khariar Basin, Cuddapah Basin, Elu Basin, Hornby Bay Basin, Hurwitz Group, Maroni Itacaiunas, Mistassini Basin, Otish Basin, Pasha Ladoga Basin, Paterson, Pine Creek Orogen, Rio Negro Juruena, Rondonia San Ignacio, Roraima Basin, Sao Francisco Craton, Sibley Basin, Sucunduri Basin, Thelon Basin, Thule Basin, Tocantins

Tectonic Setting

- Intracratonic basins

Typical Geological Age Range

- Late Palaeoproterozoic to Mesoproterozoic

Mineral Systems Model

Source

Ground preparation

- Intracratonic basin formation within basement rocks that are enriched in uranium ± graphite
- Deposition of a thick (>5-6 km) fluviatile sandstone succession
- Sandstone diagenesis above a basal unconformity between basin and basement rocks
- Aquifer evolution

Energy

- Changes in far-field plate boundary forces promoting reactivation of and tectonic activity along pre-existing structures
- Diagenetic compaction of basin sequences

Fluids

- Fluid 1: High NaCl, low Ca brines of diagenetic origin formed from dissolution of evaporites
- Fluid 2: High NaCl brines with higher Ca/Na ratios than Fluid 1 evolved from the latter after reacting with basement rocks below the unconformity
- Fluid 3: Low NaCl, hydrocarbon-rich fluids formed from hydrogenation of carbonaceous material in metasedimentary rocks below the unconformity

Ligands

- Ca and Cl, possibly sourced from intrabasinal evaporite sequences

Reductants

- Graphite, sulphides, hydrocarbons, bitumen, methane

Uranium

- Uranium enriched granitic, felsic volcanic and metasedimentary basement rocks or pre-existing ores below the unconformity
- Uranium-bearing detrital minerals in the sandstone-dominated basin fill such as monazite or zircon volcanic ash)
- Uranium-enriched palaeoregolith immediately below the unconformity

Transport

Fluid pathways
- Long-lived transcrustal fault zones in the basement
- Regional unconformity surface with or without palaeoregolith
- Permeable, oxidised sandstone and conglomerate aquifers above the unconformity

Trap

Physical
- Unconformity surface
- Dilational structural sites associated with faults and breccia zones at or below the unconformity

Chemical
- Graphitic/carbonaceous basement rocks

Deposition

Change in redox conditions
- Due to mixing of highly oxidised brines (Fluid 1 and 2) travelling along the unconformity and down faults with upwelling reduced fluids (Fluid 3) travelling upwards along basement-rooted faults
- Due to interaction of oxidised, uranium-bearing fluids with highly reduced carbonaceous rocks

Preservation
- Relative tectonic stability post-uranium mineralisation
- Adequate conservation of the sandstone succession above the unconformity

Key Reference Bibliography

CHI, G., LI, Z., CHU, H., BETHUNE, K. M., QUIRT, D. H., LEDRU, P., NORMAND, C., CARD, C., BOSMAN, S., DAVIS, W. J., POTTER, E. G., A shallow-burial mineralization model for the unconformity-related uranium deposits in the Athabasca Basin. Economic Geology, 113(5), 1209-1217 (2018).

CHI, G., CHU, H., PETTS, D., POTTER, E., JACKSON, S., WILLIAMS-JONES, A., Uranium-rich diagenetic fluids provide the key to unconformity-related uranium mineralization in the Athabasca Basin. Scientific reports, 9:5530, https://doi.org/10.1038/s41598-019-42032-0 (2019).

CUNEY, M. L., World-class unconformity-related uranium deposits: Key factors for their genesis. In: Mao, J., Bierlein, F. P. (Eds.), Mineral Deposit Research: Meeting the Global Challenge. Proceedings of the Eighth Biennial SGA Meeting, Beijing, China, 18-21 August 2005, pp. 245-248 (2005).

HUSTON, D. L., VAN DER WIELEN, S. (Eds.), An assessment of the uranium and geothermal prospectivity of east-central South Australia. Geoscience Australia Record, 2011/34, 229p (2011).

INTERNATIONAL ATOMIC ENERGY AGENCY, Geological Classification of Uranium Deposits and Description of Selected Examples. IAEA-TECDOC Series, 1842, 415p (2018).

INTERNATIONAL ATOMIC ENERGY AGENCY, Unconformity-related Uranium Deposits. IAEA-TECDOC Series, 1857, 295p (2018).

JAIRETH, S., ROACH, I. C., BASTRAKOV, E., LIU, S., Basin-related uranium mineral systems in Australia: A review of critical features. Ore Geology Reviews, 76, 360-394 (2016).

KYSER, K., Uranium ore deposits. In: TUREKIAN, K., HOLLAND, H. (Eds.), Treatise on Geochemistry, 2nd Edition, Elsevier, 489-513 (2013).

MARTZ, P., MERCADIER, J., CATHELINEAU CATHELINEAU, M., BOIRON, M. C., QUIRT, D., DONEY, A., GERBEAUD, O., DE WALLY, E., LEDRU, P., Formation of U-rich mineralizing fluids through basinal brine migration within basement-hosted shear zones: A large-scale study of the fluid chemistry around the unconformity-related Cigar Lake U deposit (Saskatchewan, Canada). Chemical Geology, https://doi.org/10. 1016/j.chemgeo.2018.05.042 (2018).

SKIRROW, R. G., JAIRETH, S., HUSTON, D. L., BASTRAKOV, E. N., SCHOFIELD, A., VAN DER WIELEN, S. E., BARNICOAT, A. C., Uranium mineral systems: Processes, exploration criteria and a new deposit framework. Geoscience Australia Record, 2009/20, 44p (2009).

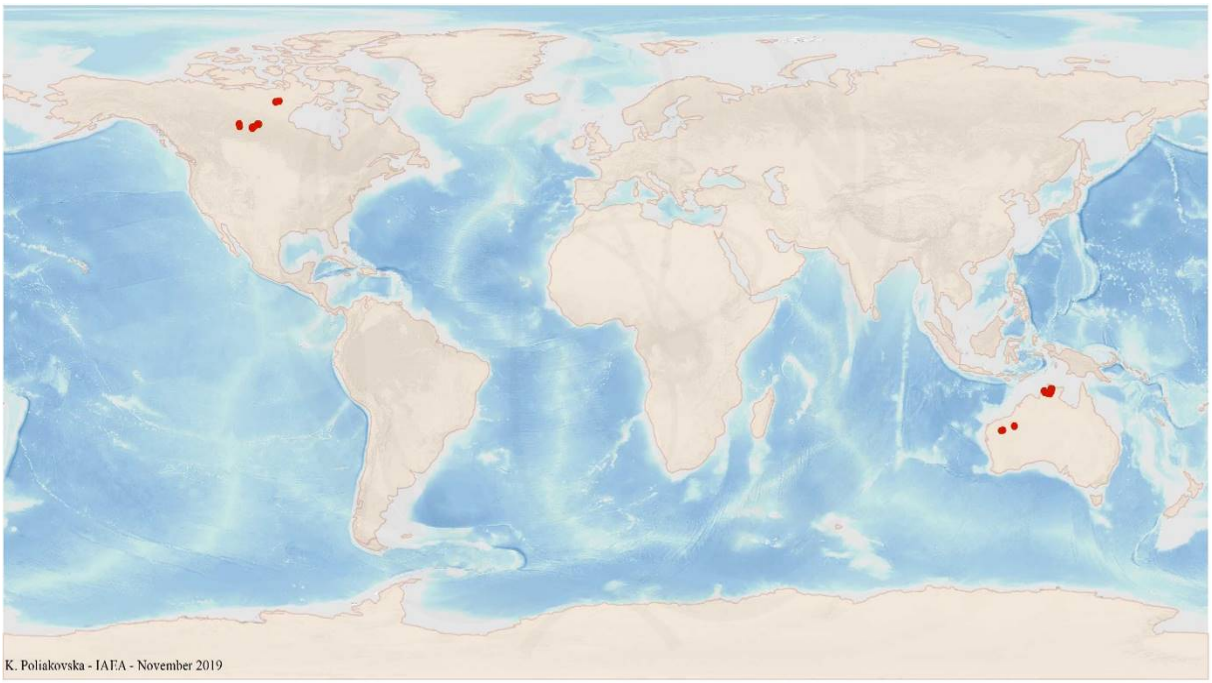

FIG. 7.2a. World distribution of selected Proterozoic Unconformity Basement-Hosted uranium deposits from the UDEPO database.

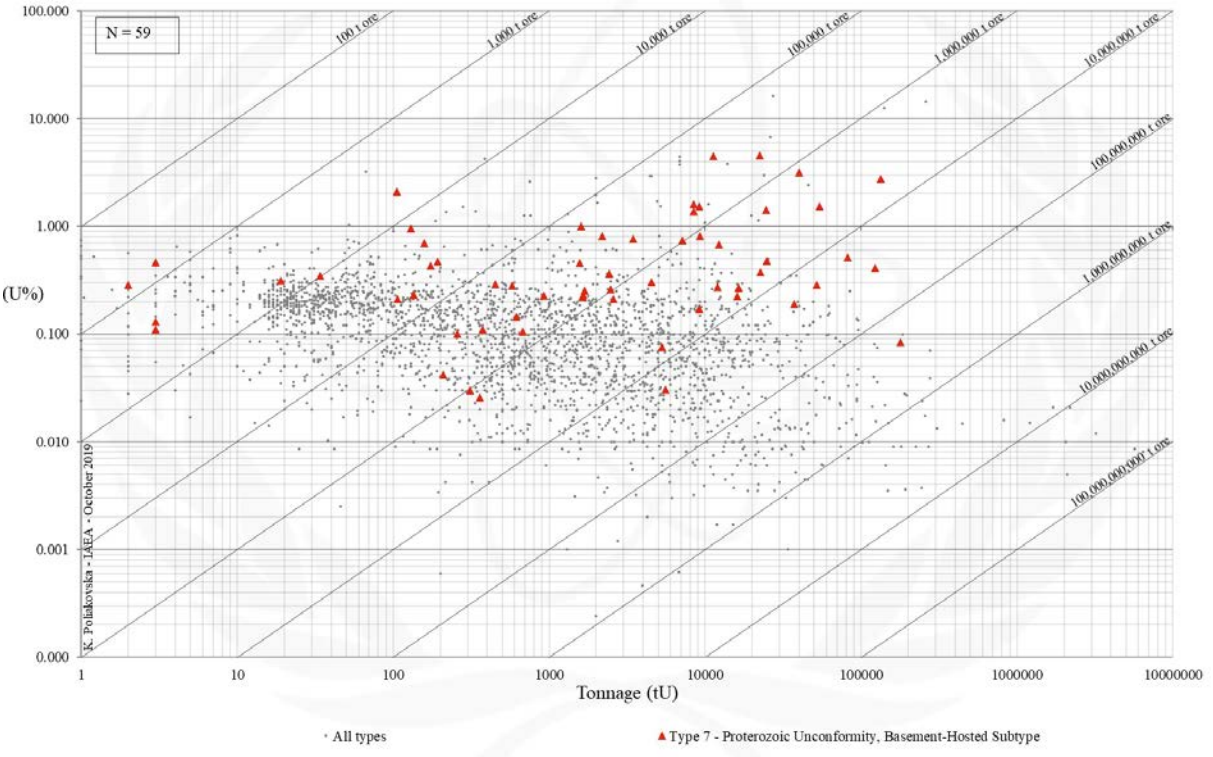

FIG. 7.2b. Grade and tonnage scatterplot highlighting Proterozoic Unconformity Basement-Hosted uranium deposits from the UDEPO database.

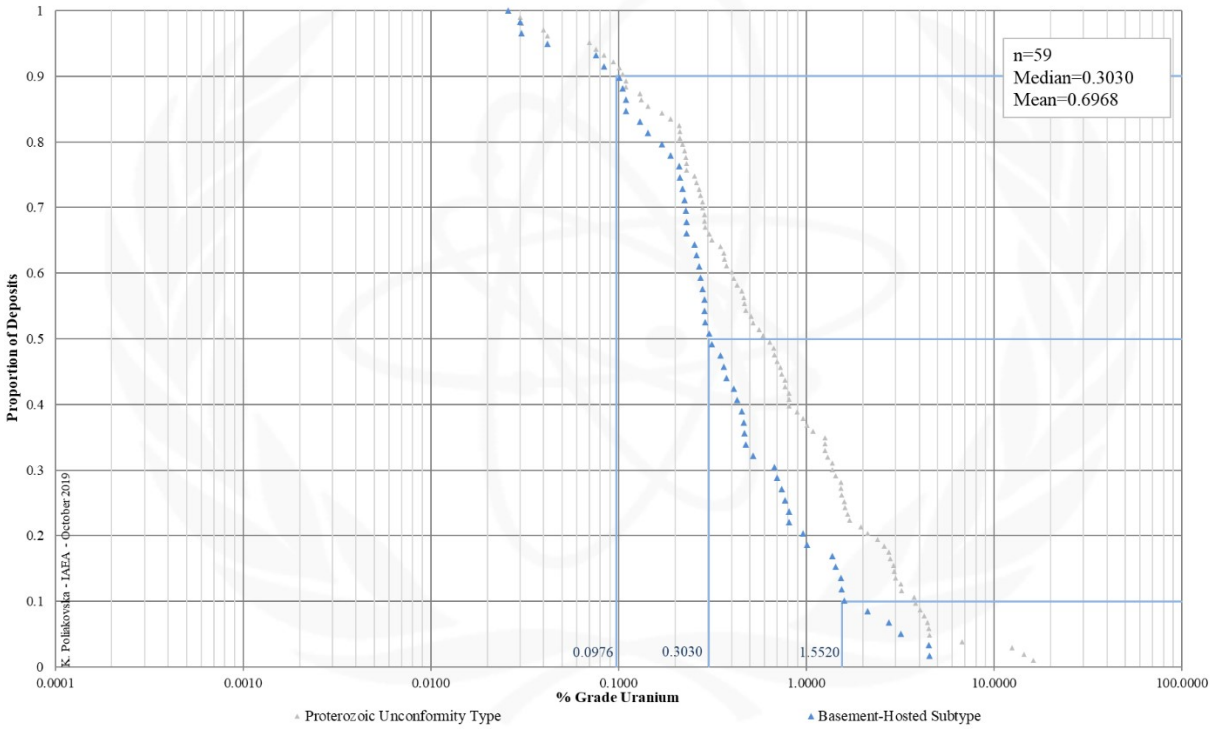

FIG. 7.2c. Grade Cumulative Probability Plot for Proterozoic Unconformity Basement-Hosted uranium deposits from the UDEPO database.

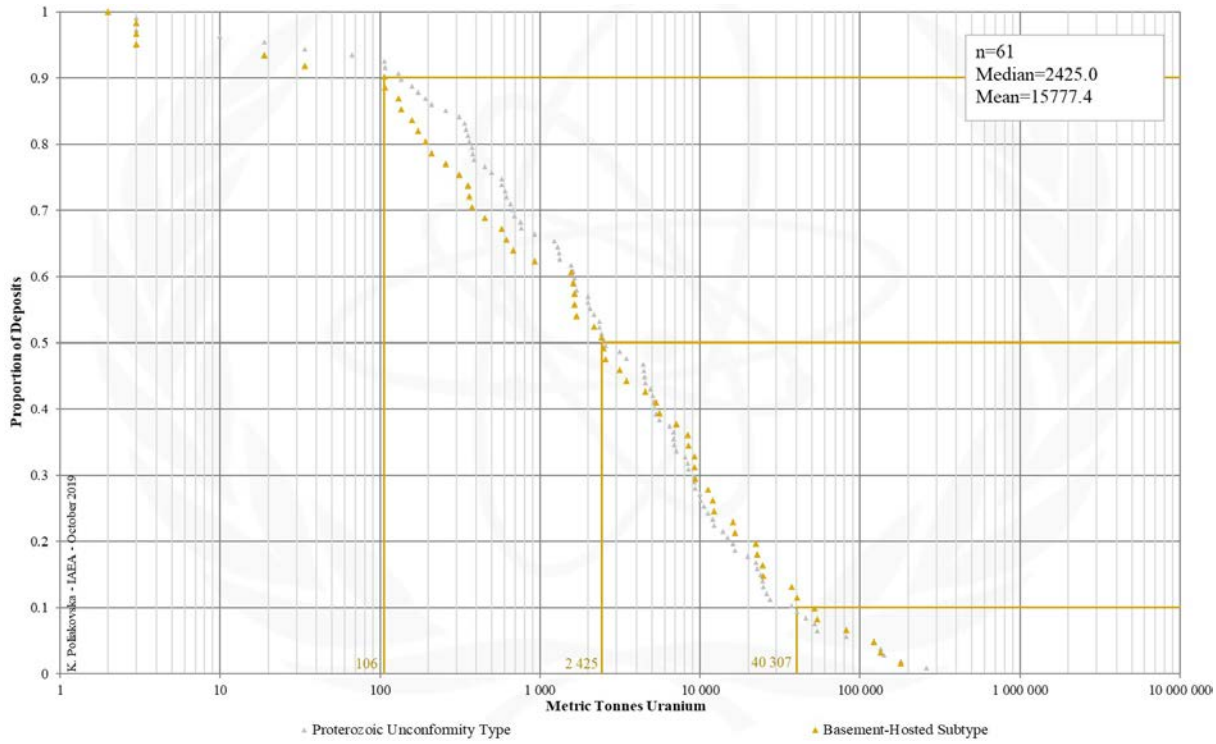

FIG. 7.2d. Tonnage distribution for Proterozoic Unconformity Basement-Hosted uranium deposits from the UDEPO database.

SUBTYPE 7.3. Proterozoic Unconformity, Stratiform Fracture-Controlled

Brief Description

- Deposits of subtype 7.3. occur at, immediately above and below unconformity surfaces separating relatively undeformed, intracratonic sandstone basins (typically Palaeo- to Mesoproterozoic) from underlying uranium-thorium granites (typically Archaean). They are known exclusively from the Cuddapah Basin (India).
- Uranium deposits of this subtype take the form of lenticular and sheet-like bodies confined to narrow (up to 5 m-thick) stratabound zones developed along the unconformity. In some deposits, the uranium mineralisation is mostly contained within the granitic basement below the unconformity whilst elsewhere the uranium ores are primarily contained within a basal conglomerate unit immediately above the unconformity.
- The richest stratiform ores are spatially coincident with prominent basement-hosted fracture systems, in particular where the fractures are closely spaced and intersect the unconformity surface. At such localities, the fracture systems are often filled with quartz veins, minor uranium ± lead and copper mineralisation and, locally, blebs of organic matter.
- The uranium ores are accompanied by pervasive wallrock alteration characterised by silification, chloritisation, epidotisation and illitisation.

Type Examples

- Chitrial, Lambapur, Peddagattu, Koppunuru, India

Genetically Associated Deposit Types

- Subtype 7.1. Proterozoic unconformity, unconformity-contact
- Subtype 7.2. Proterozoic unconformity, basement hosted
- Subtype 9.5. Sandstone, mafic dykes/sills in Proterozoic sandstone

Principal Commodities

- U ± Pb, Cu

Grades (%) and Tonnages (tU)

- Average: 0.0680, 4518.0
- Median: 0.0700, 4387.0

Number of Deposits

- Deposits: 4

Provinces (undifferentiated from Proterozoic Unconformity Type)

- Aravalli Delhi Basins, Ashburton, Athabasca Basin, Baxter Lake, Bhima Basin, Borborema Province, Borden Basin, Cariewerloo Basin, Central Amazon, Chhattisgarh Khariar Basin, Cuddapah Basin, Elu Basin, Hornby Bay Basin, Hurwitz Group, Maroni Itacaiunas, Mistassini Basin, Otish Basin, Pasha Ladoga Basin, Paterson, Pine Creek Orogen, Rio Negro Juruena, Rondonia San Ignacio, Roraima Basin, Sao Francisco Craton, Sibley Basin, Sucunduri Basin, Thelon Basin, Thule Basin, Tocantins

Tectonic Setting

- Intracratonic basins

Typical Geological Age Range

- Mesoproterozoic

Mineral Systems Model

Source

Ground preparation

- Intracratonic basin formation
- Deposition of a thick (>5-6 km) fluviatile sandstone succession
- Sandstone diagenesis above a basal unconformity between basin and basement rocks
- Aquifer evolution
- Chloritization of basement granitoids below the unconformity

Energy

- Changes in far-field plate boundary forces promoting reactivation of and tectonic activity along pre-existing structures
- Diagenetic compaction of basin sequences

Fluids

- High NaCl brines of diagenetic origin

Ligands

- No information

Reductants

- Nascent hydrogen, H_2S, pyrite, organic matter, carbonaceous black shale

Uranium

- Uranium enriched granitic basement rocks

Transport

Fluid pathways

- Long-lived transcrustal fault zones in the basement
- Regional unconformity surface with or without palaeoregolith

- Permeable, oxidised sandstone and conglomerate aquifers above the unconformity

Trap

Physical
- Unconformity surface
- Dilational structural sites associated with faults and breccia zones at or below the unconformity

Chemical
- Chloritised (Fe^{2+}-bearing) basement rocks

Deposition

Adsorption
- Of uranyl complexes by chlorite and subsequent formation of uranium mineral phases

Change in redox conditions
- Due to interaction of oxidised, uranium-bearing fluids and reduced basement rocks below the unconformity
- Due to interaction of oxidised, uranium-bearing fluids and nascent hydrogen/H_2S generated or introduced during chloritisation of the basement rocks below the unconformity
- Due to interaction of oxidised, uranium-bearing fluids and reductants in sandstone and black shale above the unconformity

Preservation

- Relative tectonic stability post-uranium mineralisation
- Adequate conservation of the sandstone succession above the unconformity

Key Reference Bibliography

BABU, P. R., BANERJEE, R., ACHAR, K. K., Srisailam and Palnad sub-basins: Potential geological domains for unconformity-related uranium mineralisation in India. Exploration and Research for Atomic Minerals, 22, 21-42 (2012).

BASU, H., PRAKASH, K., KUMAR, K. M., THIRUPATHI, P. V., PAUL, A., PANDIT, S. A., CHAKI, A., Chloritization and its bearing on uranium mineralization in Madyalabodu area, Cuddapah district, Andhra Pradesh. Journal of the Geological Society of India, 84(3), 281-291 (2014).

DAHLKAMP, F. J., Uranium Deposits of the World: Asia. Springer, Berlin, Heidelberg, 492p (2009).

CHI, G., CHU, H., PETTS, D., POTTER, E., JACKSON, S., WILLIAMS-JONES, A., Uranium-rich diagenetic fluids provide the key to unconformity-related uranium mineralization in the Athabasca Basin. Scientific Reports, 9:5530, https://doi.org/10.1038/s41598-019-42032-0 (2019).

INTERNATIONAL ATOMIC ENERGY AGENCY, Geological Classification of Uranium Deposits and Description of Selected Examples. IAEA-TECDOC Series 1842, 415p (2018).

INTERNATIONAL ATOMIC ENERGY AGENCY, Unconformity-related uranium deposits. IAEA TECDOC Series, 1857, 295p (2018).

SINGH, R. V., SINHA, R. M., BISHT, B. S., BANERJEE, D. C. , Hydrogeochemical exploration for unconformity-related uranium mineralization: example from Palnadu sub-basin, Cuddapah Basin, Andhra Pradesh, India. Journal of Geochemical Exploration, 76(2), 71-92 (2002).

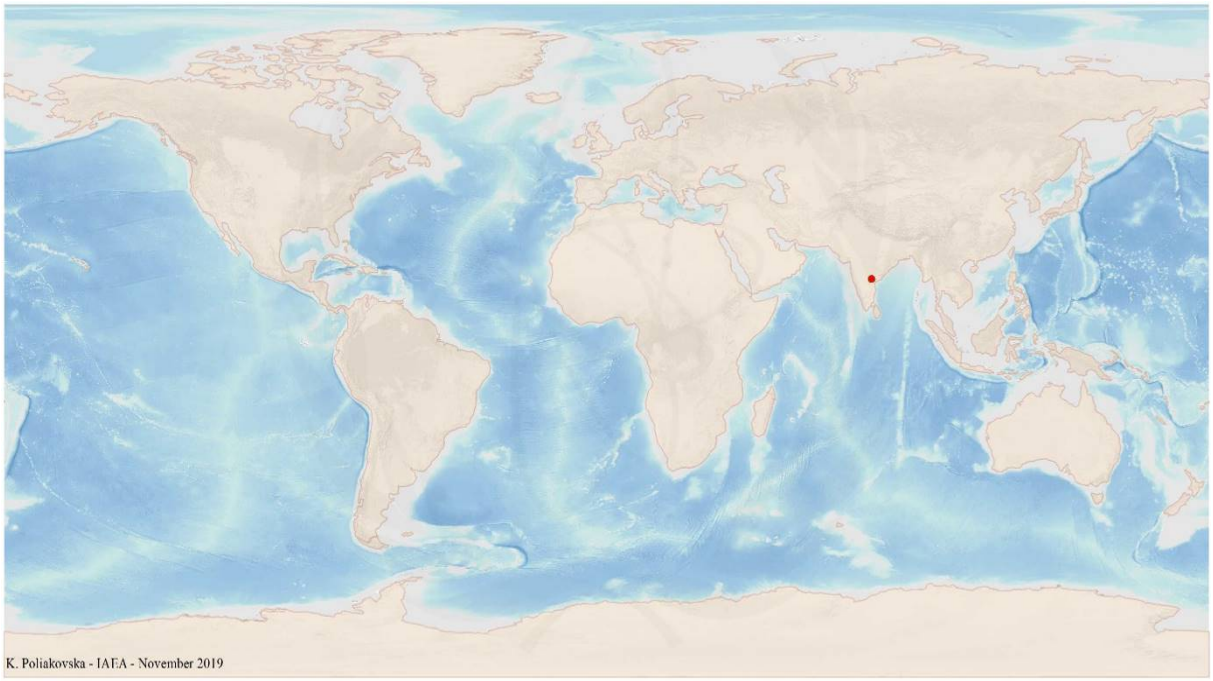

FIG. 7.3a. World distribution of selected Proterozoic Unconformity Stratiform Fracture-Controlled uranium deposits from the UDEPO database.

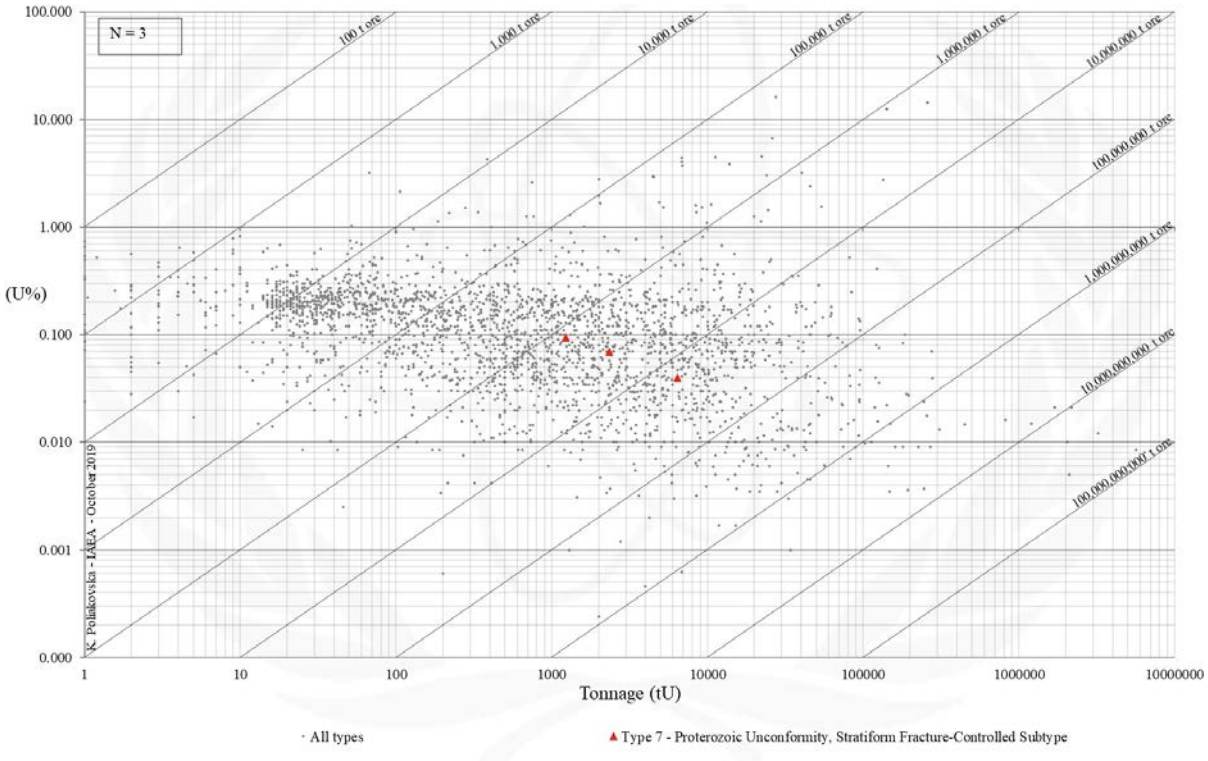

FIG. 7.3b. Grade and tonnage scatterplot highlighting Proterozoic Unconformity Stratiform Fracture-Controlled uranium deposits from the UDEPO database.

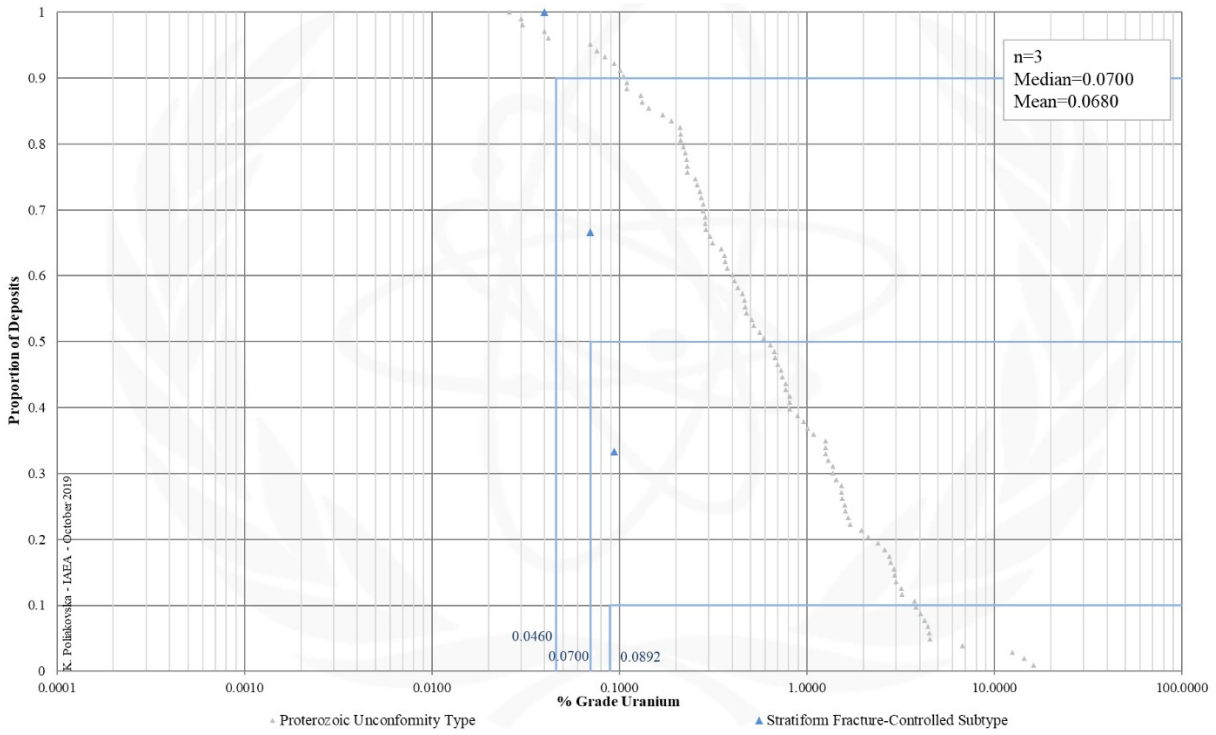

FIG. 7.3c. Grade Cumulative Probability Plot for Proterozoic Unconformity Stratiform Fracture-Controlled uranium deposits from the UDEPO database.

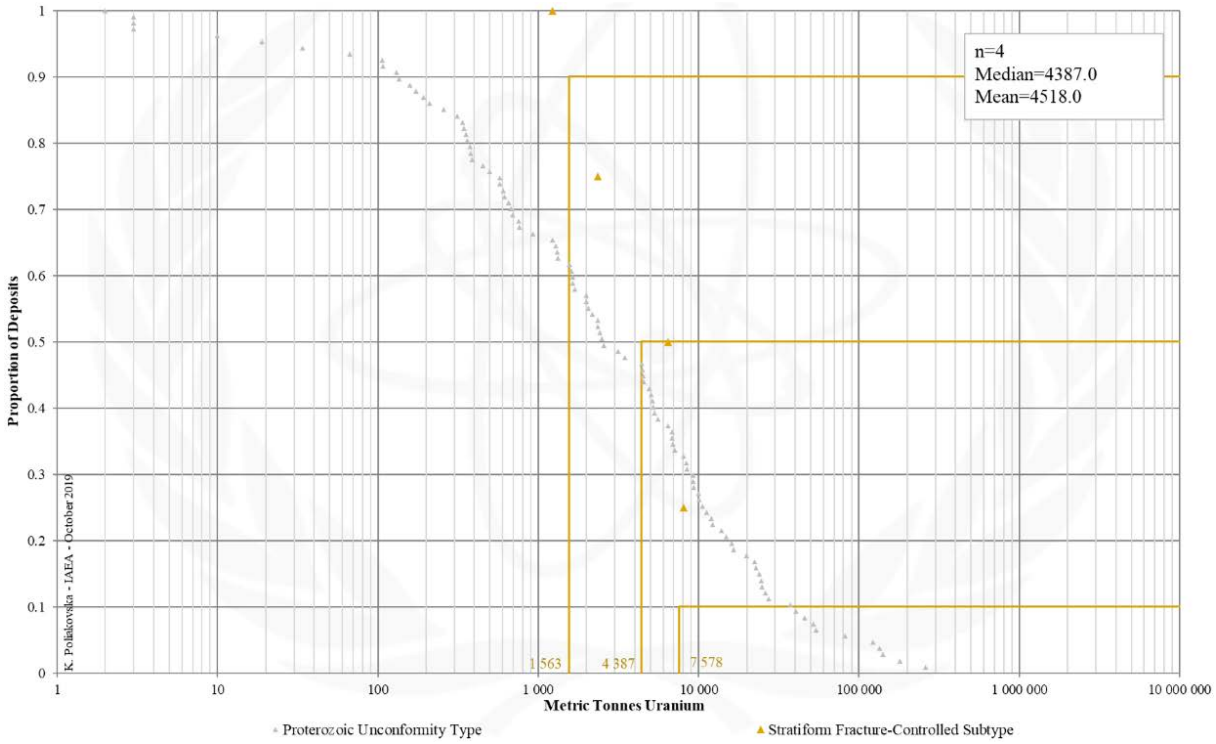

FIG. 7.3d. Tonnage Cumulative Probability Plot for Proterozoic Unconformity Stratiform Fracture-Controlled uranium deposits from the UDEPO database.

Appendix VIII

COLLAPSE BRECCIA PIPE

TYPE 8. Collapse Breccia Pipe

Brief Description
- Collapse breccia pipe deposits are known exclusively from northwestern Arizona (USA).
- Deposits of this type are centred upon vertical collapse breccia pipes that developed in marine platform carbonates deposited in a tectonically stable cratonic environment.
- The uranium ores take the form of disseminations, replacements and fracture fill hosted by solution collapse breccias within and arcuate ring fractures surrounding the pipes.
- Uranium mineralisation is thought to be linked to upward directed artesian flow of basinal brines through the permeable breccia column and mixing of these brines with uranium-bearing, oxidising waters that flowed laterally through oxidised sandstone aquifers.

Subtypes
- Not applicable

Genetically Associated Deposit Types
- Mississippi Valley-type (MVT) lead-zinc deposits

Type Examples
- Hacks, Pigeon, Orphan Lode, Kanab North, Sage, Hermit: Arizona Strip, USA

Principal Commodities
- U, Cu ± Ag, Co, Nd, Ni, Pb, V, REE, Zn

Grades (%) and Tonnages (tU)
- Average: 0.5099, 919.7
- Median: 0.4600, 435.0

Number of Deposits
- Deposits: 19

Provinces
- Arizona Strip.

Tectonic Setting
- Tectonically stable cratonic environments

Typical Geological Age Range
- Late Permian to early Cretaceous

Mineral Systems Model

Source

Ground preparation
- Stable tectonic block with long-lived low hydrologic gradient
- Development of a passive margin carbonate platform
- Diagenesis of the carbonate host rocks
- Long period of karsting and repeated upward stoping

Energy
- Uplift and steepening of hydrological gradient linked to distal orogeny

Fluids
- Saline basinal brines
- Groundwaters

Ligands
- Cl

Reductants and reactants
- Sulphate evaporites; sulphides; reduced sulphur; pyrobitumen

Metals
- Crystalline basement rocks; volcanic rocks; redbed sandstones

Transport

Fluid pathways
- Crustal-scale fault zones and connected lower-order fault systems
- Stratigraphic aquifers

Trap

Physical
- Repeated upward stoping, fracturing and permeability creation centred upon collapse breccia pipes
- Upward directed artesian flow of basinal brines through the permeable breccia column and surrounding ring fracture systems
- Fault intersections

Chemical
- Redox gradients

Deposition

Change in redox conditions

- Due to mixing of laterally flowing, oxidised, uranium-bearing groundwaters from overlying sandstone aquifers with upward flowing reducing brines that entering the pipes from below
- Due to interaction between oxidised fluids and reductants in the wallrocks, sulphidic breccia fill, and/or hydrocarbons or pyrobitumen

Preservation

- Relative tectonic stability post-mineralisation
- Subsidence and burial of the mineralised rocks with deeper-seated, surface blind breccia pipes less likely to be subjected to deep oxidation
- Massive sulphide caps above the uranium ores prevent or delay deep oxidation

Key Reference Bibliography

FINCH, W., Descriptive model of solution-collapse breccia pipe uranium deposits. Developments in Mineral Deposit Modeling, U.S. Geological Survey Bulletin, 2004, 33-35 (2004).

INTERNATIONAL ATOMIC ENERGY AGENCY, World Distribution of Uranium Deposits (UDEPO). IAEA-TECDOC Series, 1843, 247p (2016).

INTERNATIONAL ATOMIC ENERGY AGENCY, Geological Classification of Uranium Deposits and Description of Selected Examples. IAEA-TECDOC Series, 1842, 415p (2018).

LEACH, D. L., TAYLOR, R. D., FEY, D. L., DIEHL, S. F., SALTUS, R. W., A deposit model for Mississippi Valley-type lead-zinc ores. Chapter A of Mineral Deposit Models for Resource Assessment, U.S. Geological Survey Scientific Investigations Report 2010–5070–A, 52p (2010).

THOMAS, D., ZALUSKI, G., BRISBIN, D., DREVER, G., Uranium deposit models with an emphasis on sedimentary–associated types. Unpublished Presentation, Cameco Corporation, 91p (2006).

WENRICH, K. J., TITLEY, S. R., Uranium exploration for northern Arizona (USA) breccia pipes in the 21st century and consideration of genetic models. Ores and Orogenesis: Circum-Pacific Tectonics, Geologic Evolution, and Ore Deposits, Arizona Geological Society Digest, 22(620), 295-309 (2008).

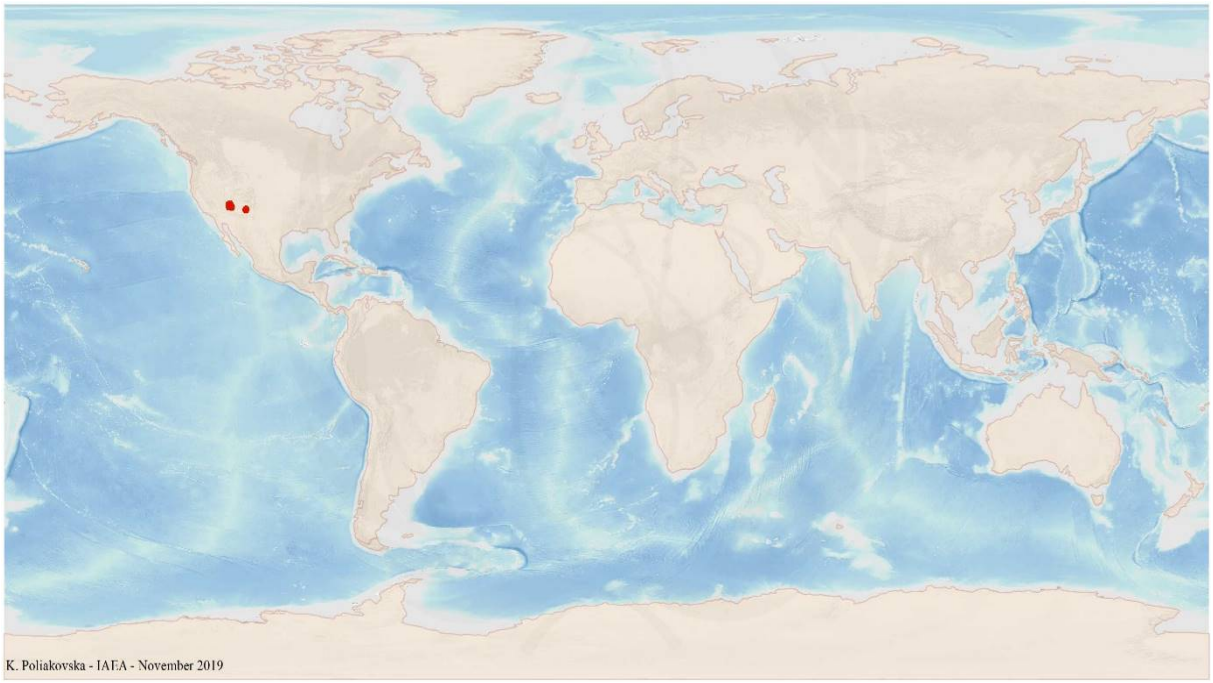

FIG. 8a. World distribution of selected Collapse Breccia Pipe uranium deposits from the UDEPO database.

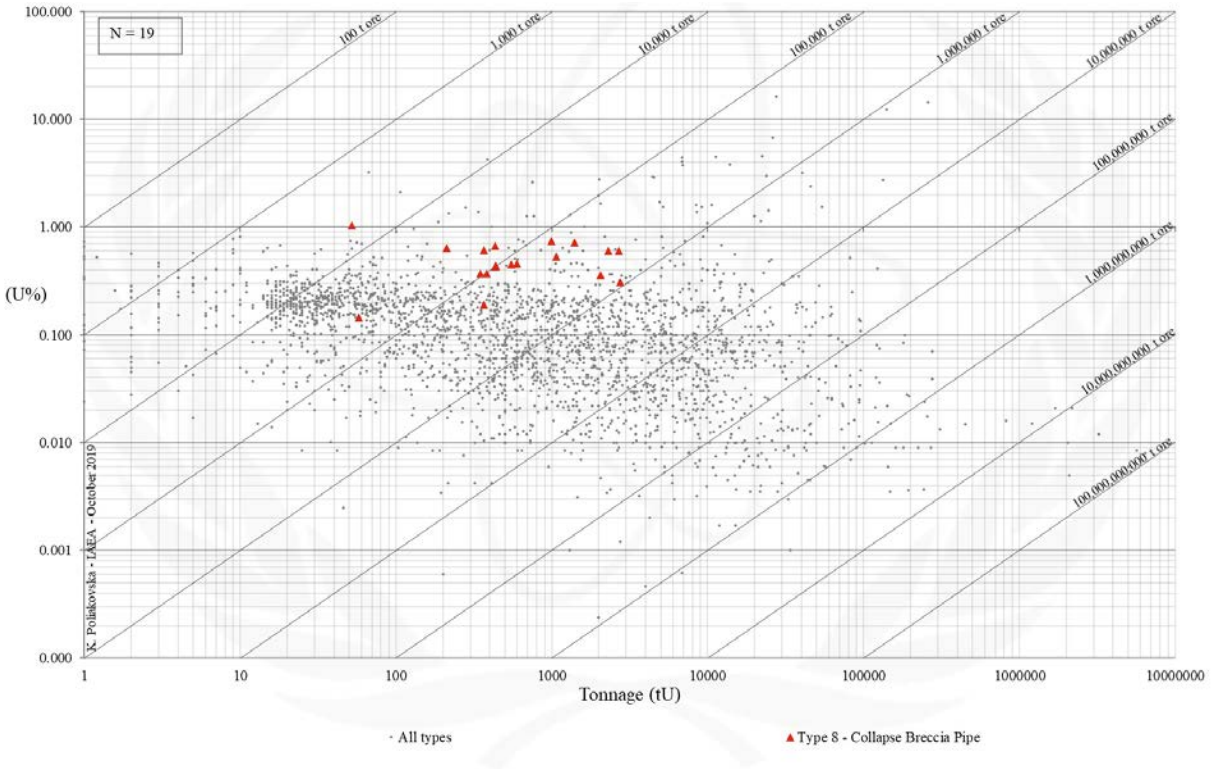

FIG. 8b. Grade and tonnage scatterplot highlighting Collapse Breccia Pipe uranium deposits from the UDEPO database.

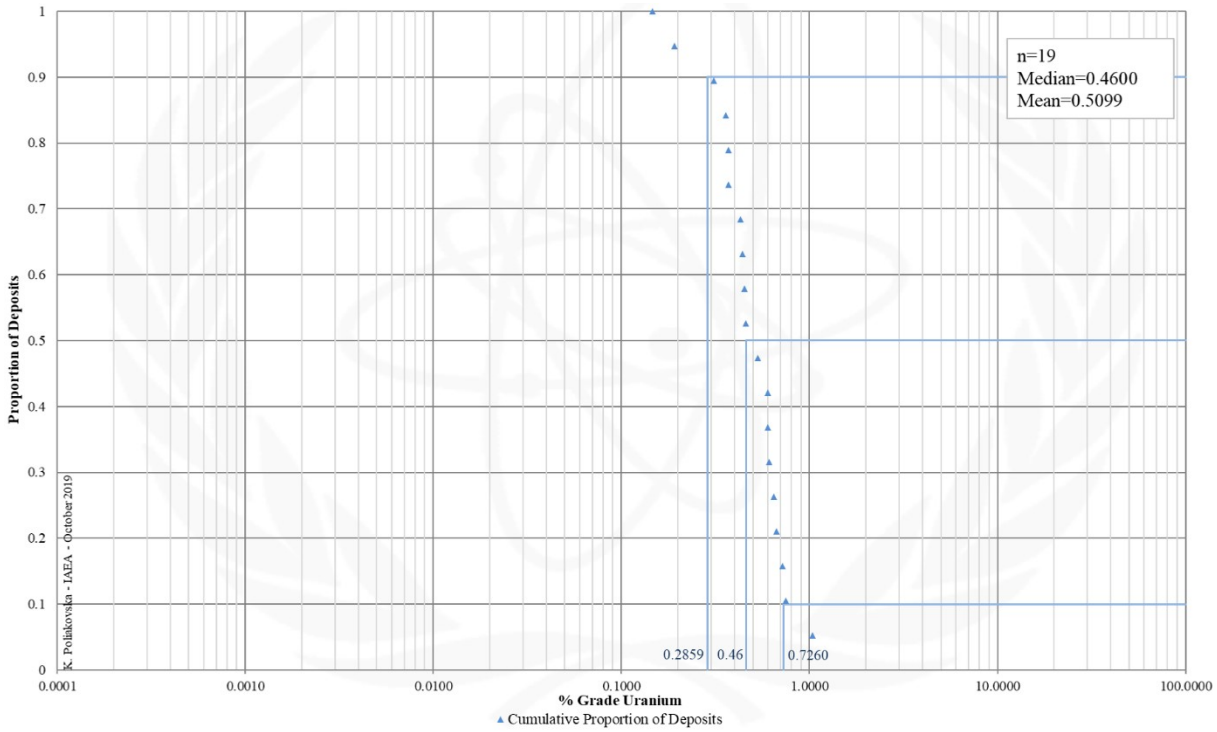

FIG. 8c. Grade Cumulative Probability Plot for Collapse Breccia Pipe uranium deposits from the UDEPO database.

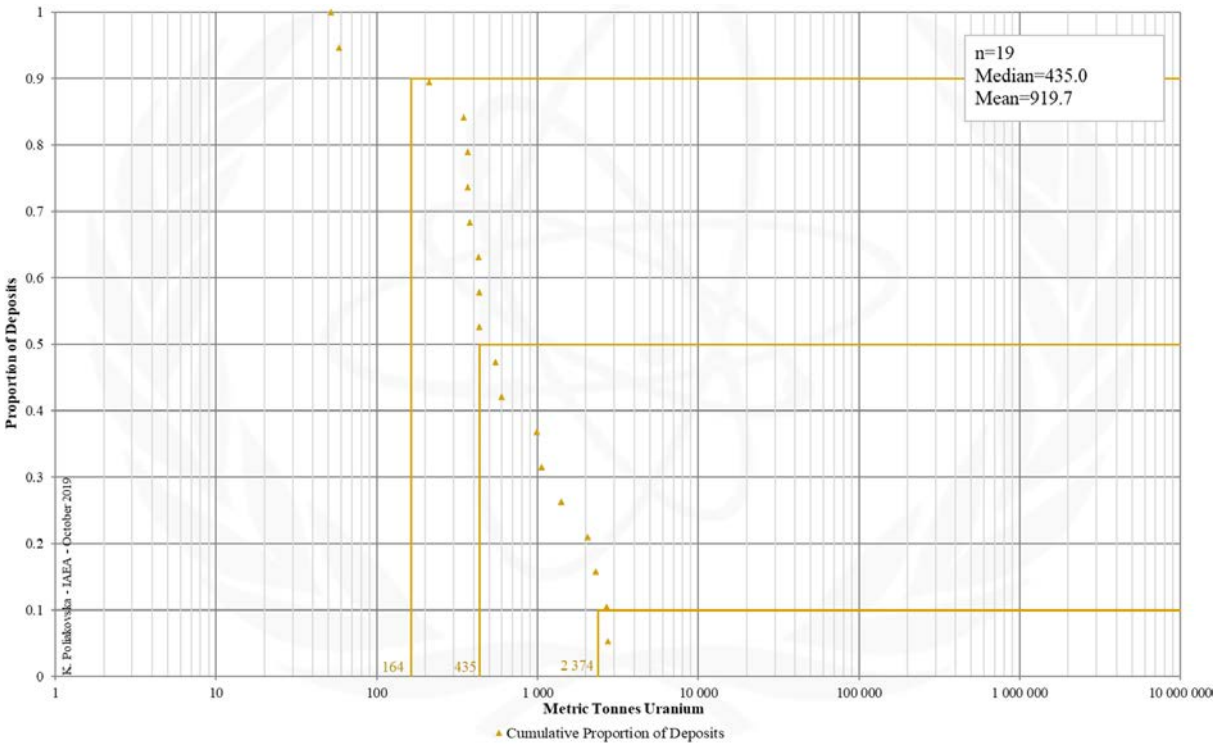

FIG. 8d. Tonnage Cumulative Probability Plot for Collapse Breccia Pipe uranium deposits from the UDEPO database.

Appendix IX

SANDSTONE

TYPE 9. Sandstone

Brief Description

- Sandstone deposits refer to uranium accumulations in medium- to coarse-grained siliciclastic sedimentary rocks deposited in continental fluvial, lacustrine or shallow-marine sedimentary environments.
- Uranium is precipitated by reduction processes caused by the presence of a variety of possible reducing agents within the host sandstone such as intrinsic detrital plant debris, sulphides, ferro-magnesian minerals, anaerobic sulphate-reducing bacteria, or extrinsic migrated fluids from underlying hydrocarbon reservoirs.
- Sandstone deposits are divided into five subtypes with many gradual transitions between them: (9.1) Basal channel, (9.2) tabular, (9.3) roll-front, (9.4) tectonic-lithologic, and (9.5) mafic dyke/sills in Proterozoic sandstones.

Subtypes and Classes

- 9.1. Basal channel. 9.2. Tabular. 9.2.1. Continental fluvial, uranium associated with intrinsic reductant. 9.2.2. Continental fluvial, uranium associated with extrinsic bitumen. 9.2.3. Continental fluvial vanadium-uranium. 9.3. Roll-front. 9.3.1. Continental basin, uranium associated with intrinsic reductant. 9.3.2. Continental to marginal marine, uranium associated with intrinsic reductant. 9.3.3. Marginal marine, uranium associated with extrinsic reductant. 9.4. Tectonic-lithologic. 9.5. Mafic dykes/sills in Proterozoic sandstone

Type Examples

- Subtype 9.1. Dalmatovskoye, Russian Federation; Beverley, Australia. Class 9.2.1. Arlit district, Niger. Class 9.2.2. Ambrosia Lake district (Grants region), USA. Class 9.2.3. Salt Wash member, USA. Class 9.3.1. Wyoming basins, USA. Class 9.3.2. Chu-Sarysu basin, Kazakhstan. Class 9.3.3. South Texas, USA. Subtype 9.4. Lodève Basin, France; Franceville Basin, Gabon. Subtype 9.5. Westmoreland district, Australia; Matoush, Canada

Principal Commodities

- U ± Au, Cr, Mo, Re, Sc, Se, Te, V

Grades (%) and Tonnages (tU)

- Average: 0.1494, 3473.7
- Median: 0.1380, 426.0

Number of Deposits

- Deposits: 1561

Provinces

- Alaska Alexander, Alaska Darby Hogatza, Alaska Kokrines Hodzana, Alaska Kuskokwim White Mountains, Alaska Northern Alaska Range, Alaska Porcupine, Alaska Prince William Sound, Alaska Western Alaska Range, Alaska Yukon Tanana, Amadeus Basin, Apuseni Mountains, Aquitaine Basin, Bayingebi Basin Bandan Jilin , BC Okanagan, Bighorn Basin, Black Hills, Black Mesa Basin, Bohemian Basin North, Carnarvon Basin, Carpathians South, Casper Arch, Cerilly Bourbon, Choibalsan Basin, Choir Nyalga Basin, Chu Sarysu Basin, Colio Basin Vol Koli, Congo Basin, Rhodope Massif, Ruhuhu Selous Basins, Saint Pierre du Cantal, San Jorge Gulf Basin, San Juan Basin, Sarysu Basin North, Sebinkarahisar, Shirley Basin, Shiwan Dashan Basin, Sichuan Basin, Siwalik, Slovenia Permian.

Tectonic Setting

- Continental platforms or intracratonic, intermontane, volcanigenic or sag basins in tectonically stable cratonic environments

Typical Geological Age Range

- Subtypes 9.1 to 9.4. Palaeozoic to Cenozoic. Subtype 9.5. Palaeo- to Mesoproterozoic

Mineral Systems Model

Source

Ground preparation

- Basin formation ± salt tectonism ± thermal maturation/diagenesis ± emplacement of mafic dykes and sills

Energy

- Subtypes 9.1 to 9.3 and 9.5. Steepening of hydrological gradient linked to diagenetic compaction, salt tectonics, basin subsidence, eustatic sea level drops, basement uplift due to tectonic reactivation, doming, orogenesis, crustal thinning or far-field tectonic events
- Subtype 9.4. Addition of heat into the crust linked to orogenesis, crustal thinning and magmatism

Fluids and gases

- Shallow, oxidised, neutral to alkaline groundwaters
- Deeper, reduced groundwaters
- Oxidised basinal brines
- Reduced hydrocarbon-bearing brines
- CO, H_2S, CH_4, N_2 gases

Ligands

- Ca, Cl, CO_3, P, S

Reductants and reactants

- Organic matter, humic substances, biogenic and non-biogenic H_2S, hydrocarbons, methane, Fe^{2+} sulphides, Fe^{2+} silicates, iron oxides, carbonates

Uranium

- Crystalline basement rocks, granitoids, basin fill (interbedded volcanic ash units), pre-existing uranium deposits

Transport

Fluid pathways

- Regional sandstone aquifers
- Karst aquifers
- Palaeovalleys
- Fault-fracture systems (in particular basin growth structures tapping deeper basin sequences, underlying basins or basement)

Trap

Physical

- Palaeovalley bends, confluences, basal scours and/or areas of channel-widening
- Point bar, braid bar, bar-head, coastal barrier-bar sequences
- Hanging- and footwall aquicludes, lithological permeability barriers
- Fault-fracture systems, fault intersections, tension gashes, stylolites, soft sediment deformational structures, intraformational breccia
- Salt domes, shale diapirs, brachyanticlines, monoclines
- Lithological competency contrasts

Chemical

- In-situ reductants within the host aquifers or wallrocks
- Mobile reductants related to oil and gas systems
- Regional redox fronts

Deposition

Change in redox conditions

- Due to interaction of oxidised, uranium-bearing groundwaters or brines with in-situ or mobile reductants
- Due to mixing of oxidised, uranium-bearing groundwaters or brines and reduced fluids
- Linked to acid neutralisation due to interaction between uranium-bearing fluids and carbonates

Adsorption

- Adsorption of organically complexed uranium onto clays or Fe^{2+} silicate surfaces

Phase separation (subtype 9.4. only)

- Fluid unmixing due to depressurisation

Preservation

- Physical isolation of uranium mineralisation from the flow of oxidised groundwaters
- Re-reduction of uranium mineralised sequences
- (Diagenetic) alteration or very low grade metamorphism of host sequences post-uranium mineralisation
- Capping of uranium-mineralised sequences by younger lavas
- Basin subsidence
- Relative tectonic stability post-uranium mineralisation

Key Reference Bibliography

ALEXANDRE, P., KYSER, K., LAYTON-MATTHEWS, D., BEYER, S. R., HIATT, E. E., LAFONTAINE, J., Formation of the enigmatic Matoush uranium deposit in the Paleoprotozoic Otish Basin, Quebec, Canada. Mineralium Deposita, 50(7), 825-845 (2015).

BOBERG, W. W., The nature and development of the Wyoming uranium province. In: SIRON, C. R., HITZMAN, M. W., MCLEOD, R. (Eds.), The challenge of finding new mineral resources: Global metallogeny, innovative exploration, and new discoveries. Society of Economic Geologists Special Publication, 15, 317-338 (2010).

DAHLKAMP, F. J., Uranium Deposits of the World: USA and Latin America. Springer, Berlin, Heidelberg, 515p (2010).

DAHLKAMP, F. J., Uranium Deposits of the World: Europe. Springer, Berlin, Heidelberg, 792p (2016).

GAUTHIER-LAFAYE, F., WEBER, F., The Francevillian (lower Proterozoic) uranium ore deposits of Gabon. Economic Geology, 84(8), 2267-2285 (1989).

GAUTHIER-LAFAYE, F., HOLLIGER, P., BLANC, P. L., Natural fission reactors in the Franceville basin, Gabon: A review of the conditions and results of a "critical event" in a geologic system. Geochimica et Cosmochimica Acta, 60(23), 4831-4852 (1996).

HALL, S. M., MIHALASKY, M. J., TURECK, K. R., HAMMARSTROM, J. M., HANNON, M. T., Genetic and grade and tonnage models for sandstone-hosted roll-type uranium deposits, Texas Coastal Plain, USA. Ore Geology Reviews, 80, 716-753 (2017).

HUSTON, D. L., VAN DER WIELEN, S. (Eds.), An assessment of the uranium and geothermal prospectivity of east-central South Australia. Geoscience Australia Record, 2011/34, 229p (2011).

INTERNATIONAL ATOMIC ENERGY AGENCY, Geological Classification of Uranium Deposits and Description of Selected Examples. IAEA-TECDOC Series, 1842, 415p (2018).

JAIRETH, S., MCKAY, A., LAMBERT, I., Association of large sandstone uranium deposits with hydrocarbons. AusGeo News, 89, 8-12 (2008).

JAIRETH, S., ROACH, I. C., BASTRAKOV, E., LIU, S., Basin-related uranium mineral systems in Australia: A review of critical features. Ore Geology Reviews, 76, 360-394 (2016).

KYSER, K., Uranium ore deposits. In: TUREKIAN, K., HOLLAND, H. (Eds.), Treatise on Geochemistry, 2nd Edition, Elsevier, 489-513 (2013).

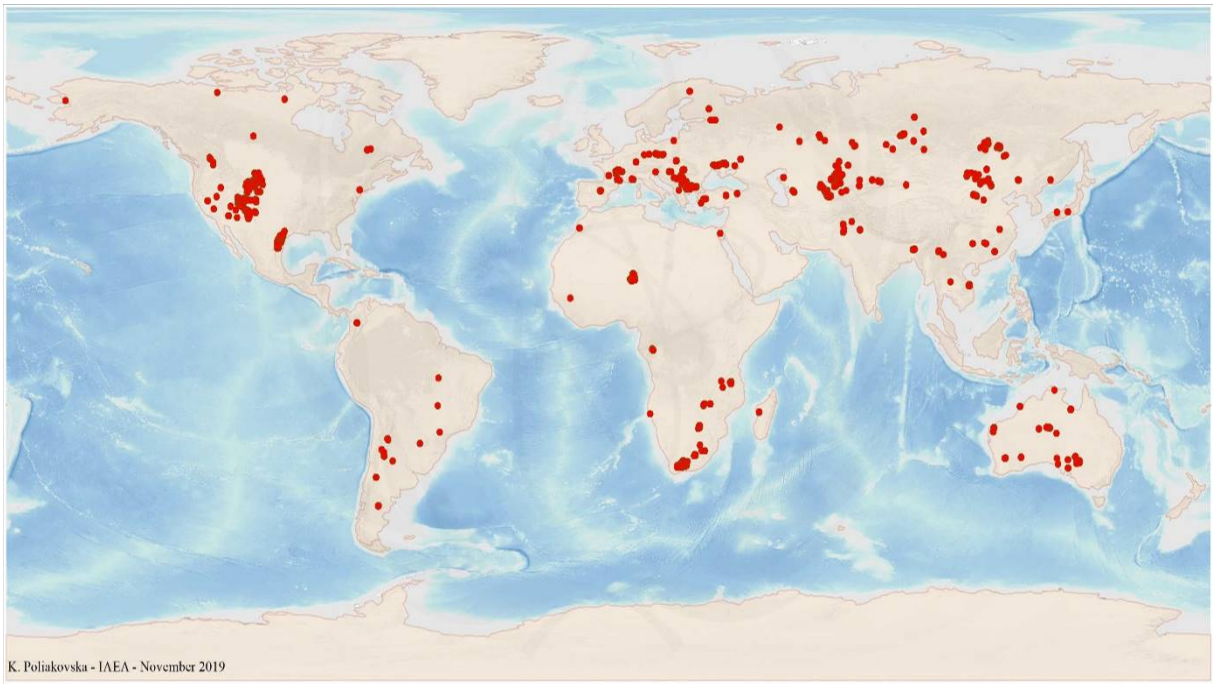

FIG. 9a. World distribution of selected Sandstone uranium deposits from the UDEPO database.

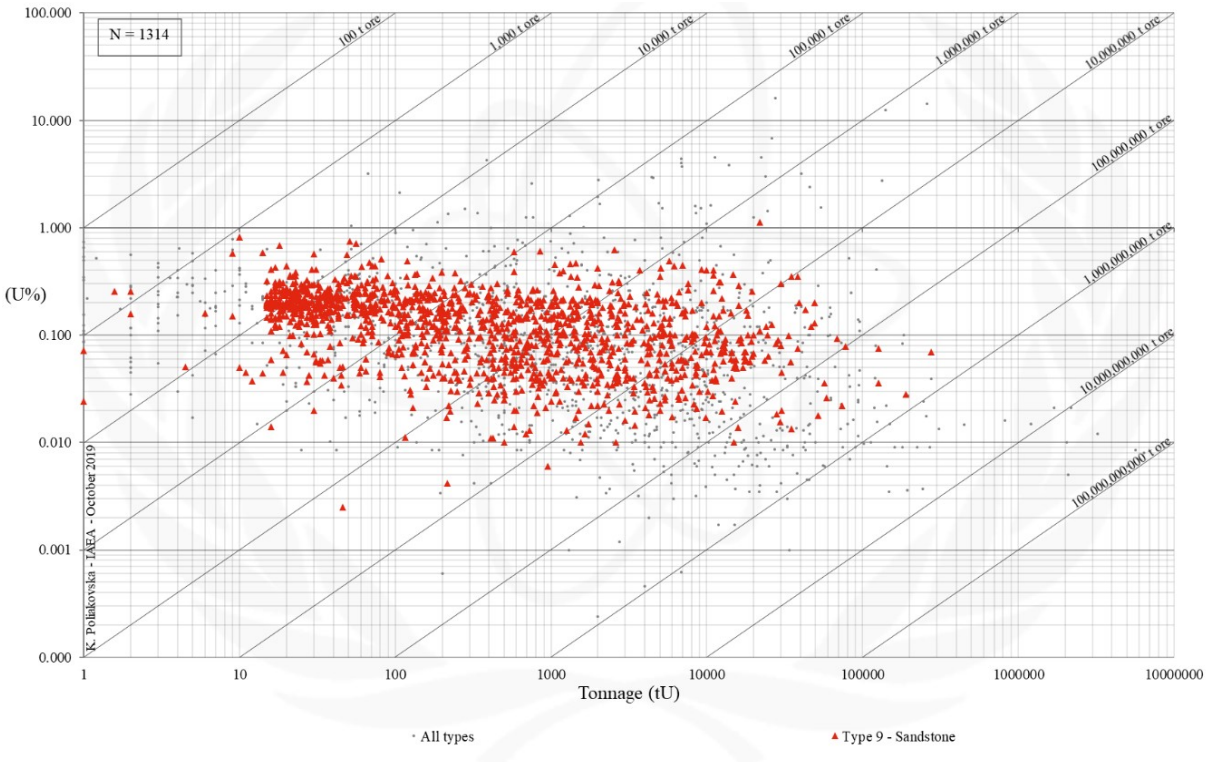

FIG. 9b. Grade and tonnage scatterplot highlighting Sandstone uranium deposits from the UDEPO database.

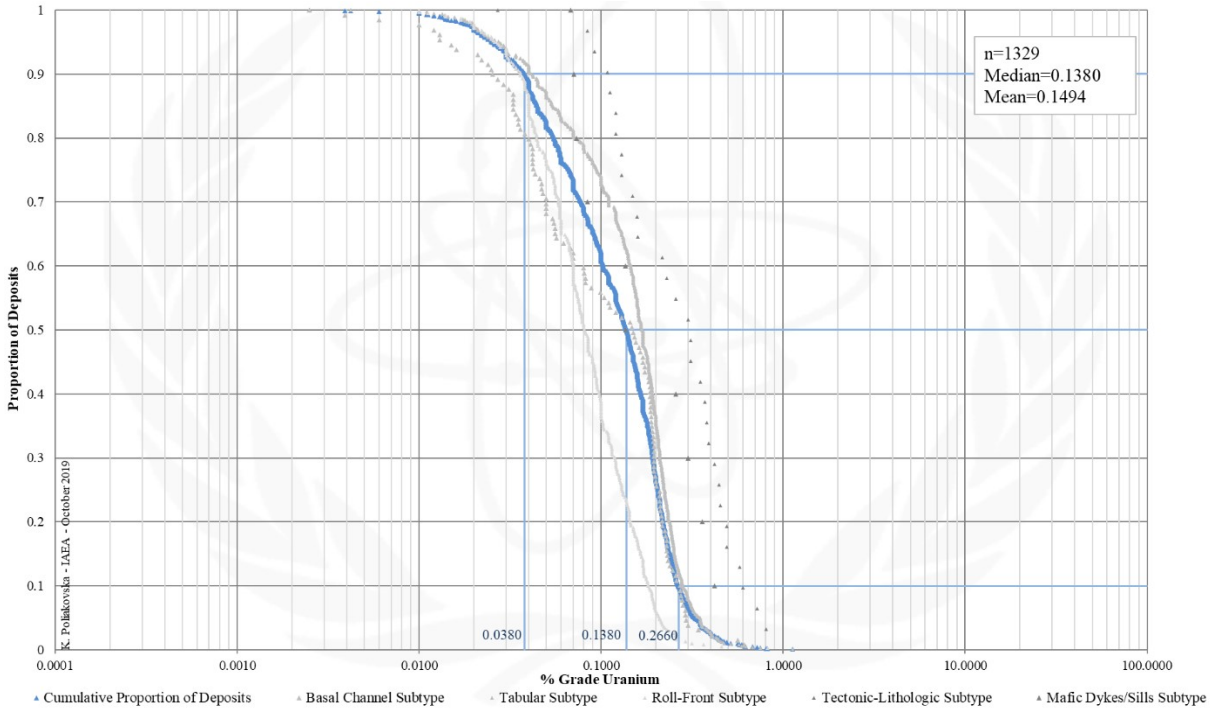

FIG. 9c. Grade Cumulative Probability Plot for Sandstone uranium deposits from the UDEPO database.

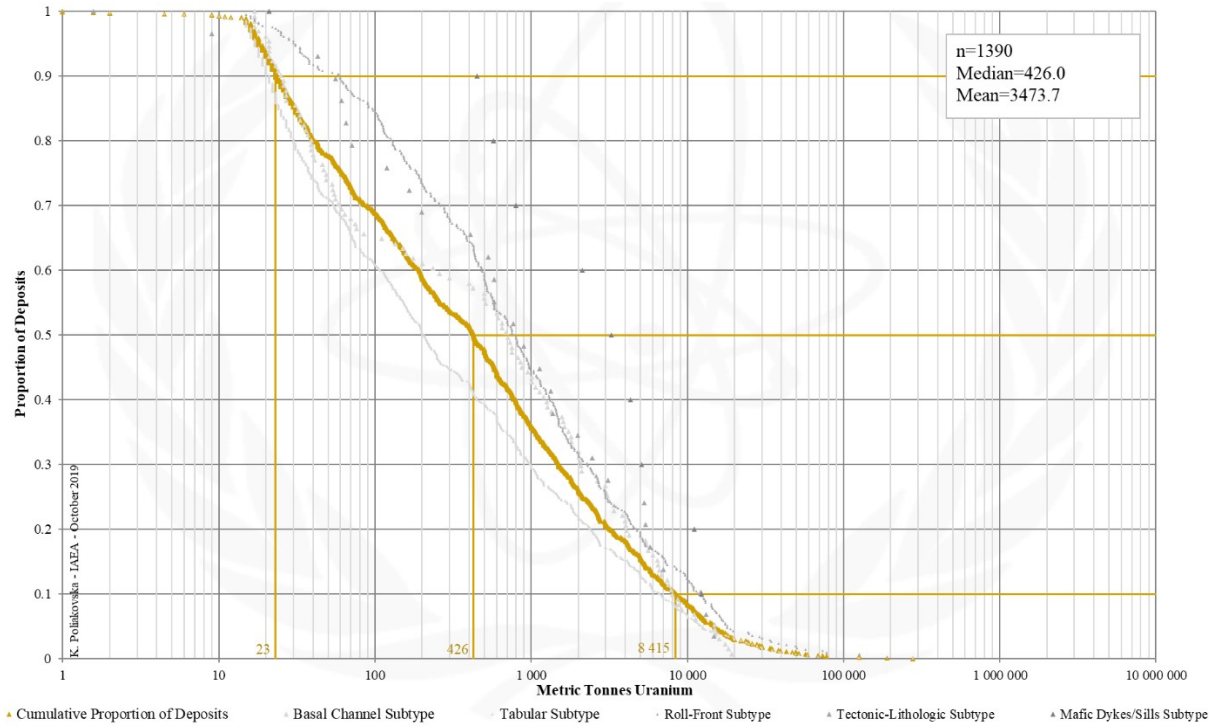

FIG. 9d. Tonnage Cumulative Probability Plot for Sandstone uranium deposits from the UDEPO database.

SUBTYPE 9.1. Sandstone, Basal Channel

Brief Description

- Sandstone deposits refer to uranium accumulations in medium- to coarse-grained siliciclastic sedimentary rocks deposited in continental fluvial, lacustrine or shallow-marine sedimentary environments.
- Uranium is precipitated by reduction processes caused by the presence of a variety of possible reducing agents within the host sandstone such as intrinsic detrital plant debris, sulphides, ferro-magnesian minerals, anaerobic sulphate-reducing bacteria, or extrinsic migrated fluids from underlying hydrocarbon reservoirs.
- Basal channel deposits occur in palaeovalley systems filled with highly permeable, poorly consolidated fluvial sediments.
- The uranium ores are typically associated with detrital plant debris forming ribbon-like, stratiform orebodies.

Type Examples

- Ryst Kuil, South Africa; Semizbai, Kazakhstan; Beverley, Four Mile, Australia; Dalmatovskoye, Malinovskoye, Khiagdinskoye, Khiagda, Russian Federation; Tono district, Japan; Blizzard, Canada

Genetically Associated Deposit Types

- Subtype 9.2. Sandstone, tabular
- Subtype 9.3. Sandstone, roll-front
- Subtype 12.1. Lignite-coal, stratiform

Principal Commodities

- U

Grades (%) and Tonnages (tU)

- Average: 0.1393, 2573.0
- Median: 0.1470, 687.0

Number of Deposits

- Deposits: 173

Provinces (undifferentiated from Sandstone Type)

- Alaska Alexander, Alaska Darby Hogatza, Alaska Kokrines Hodzana, Alaska Kuskokwim White Mountains, Alaska Northern Alaska Range, Alaska Porcupine, Alaska Prince William Sound, Alaska Western Alaska Range, Alaska Yukon Tanana, Amadeus Basin, Apuseni Mountains, Aquitaine Basin, Bayingebi Basin Bandan Jilin , BC Okanagan, Bighorn Basin, Black Hills, Black Mesa Basin, Bohemian Basin North, Carnarvon Basin, Carpathians South, Casper Arch, Cerilly Bourbon, Choibalsan Basin, Choir Nyalga Basin, Chu Sarysu Basin, Colio Basin Vol Koli, Congo Basin, Cosquin, Denver Basin, Dnieper Basin, Duruma Tanga Basin, Erlian Basin, Etosha Basin, Fergana Basin, Forez, Franceville Basin, Frome Embayment, Geosinclinal Andino, Gobi Basin Central, Gobi Basin East, Gobi Basin South, Green River Basin, Guandacol, Gyeongsang Basin, Hengyang Basin, Iberian Cordillera, Iullemmeden Basin, Japan Basal Channel, Junggar Basin, Kaiparowits Basin, Kalahari Basin East, Kalahari Basin West, Karasburg Basin, Karoo Basin Mesozoic, Karoo Basin Permian, Khorat Plateau, Kokshetau East, Kokshetau West, Kolari Kittila, Kyzylkum, Lake Ladoga, Laramine Hanna Shirley Basins, Lebombo Nuanetsi Basin, Lodeve Basin, Luangwa Lukusashi Basins, Massif Central South West, Mecsek Mountains, Meghalaya Plateau, Menderes Massif, Morondava Basin, Mount Pisgah, Murphy, Nebraska Plains White River Group, Ngalia Basin Sandstone, Nong Son Basin, Norte Subandino, North Canning Basin, Ordos Basin, Pannonian Basin South, Paradox Basin, Parana Basin Amorinopolis Ipora, Parana Basin Durazno, Parana Basin Figueira, Parana Basin Melo Fraile Muerto, Parana Basin Oviedo Yuti, Parana Basin Rio Grandense Shield, Piceance Basin, Pirie Basin, Powder River Basin, Qaidam Basin, Rhodope Massif, Ruhuhu Selous Basins, Saint Pierre du Cantal, San Jorge Gulf Basin, San Juan Basin, Sarysu Basin North, Sebinkarahisar, Shirley Basin, Shiwan Dashan Basin, Sichuan Basin, Siwalik, Slovenia Permian, Songliao Basin, Southwestern Donets Basin, Spokane Mountain Sherwood, Sukhbaatar Basin, Syr Darya Basin, Tallahassee Creek, Tamsag Basin, Tarim Basin North, Tarim Basin South, Taurkyr Dome, Temrezli Basin, Texas Coastal Plain - Catahoula-Oakville, Texas Coastal Plain - Clairborne-Jackson, Texas Coastal Plain - Goliad-Willis-Lissie, Thrace Basin, Tinogasta, Transbaykal Central, Transural, Tuha Basin, Tuli Basin, Uinta Basin, Washakie Cenozoic, Washakie SandWash GreatDivide Mesozoic, West Balkan, West Siberia, West Yunnan, Wind River Basin, Yenisey, Yilgarn South, Yili Ily Basins.

Tectonic Setting

- Continental platforms or intracratonic, intermontane, volcanigenic or sag basins in tectonically stable cratonic environments

Typical Geological Age Range

- Palaeozoic to Cenozoic

Mineral Systems Model

Source

Ground preparation
- Basin formation

Energy
- Steepening of hydrological gradient linked to basement uplift due to tectonic reactivation or far-field tectonic events

Fluids
- Shallow, oxidised, neutral to alkaline groundwaters

- Reduced hydrocarbon-bearing brines

Ligands
- Ca, S

Reductants
- Organic matter, biogenic and non-biogenic H_2S, hydrocarbons, sulphides

Uranium
- Crystalline basement rocks, granitoids, basin fill (in particular interbedded volcanic ash units), pre-existing uranium deposits

Transport

Fluid pathways
- Regional sandstone aquifers
- Palaeovalleys
- Fault-fracture systems (in particular basin growth structures tapping deeper basin sequences, underlying basins or basement)

Trap

Physical
- Palaeovalley bends, confluences, basal scours and/or areas of channel-widening
- Bar-head sequences
- Fault-fracture systems

Chemical
- In-situ reductants within the host aquifers or wallrocks
- Mobile reductants related to oil and gas systems

Deposition

Change in redox conditions
- Due to interaction of oxidised, uranium-bearing groundwaters or brines with in-situ or mobile reductants
- Due to mixing of oxidised, uranium-bearing groundwaters or brines and reduced fluids

Preservation
- Physical isolation of uranium mineralisation from the flow of oxidised groundwaters
- Capping of uranium-mineralised sequences by younger lavas
- Relative tectonic stability post-uranium mineralisation

Key Reference Bibliography

HUSTON, D. L., VAN DER WIELEN, S. (Eds.), An assessment of the uranium and geothermal prospectivity of east-central South Australia. Geoscience Australia Record, 2011/34, 229p (2011).
INTERNATIONAL ATOMIC ENERGY AGENCY, Geological Classification of Uranium Deposits and Description of Selected Examples. IAEA-TECDOC Series, 1842, 415p (2018).
JAIRETH, S., ROACH, I. C., BASTRAKOV, E., LIU, S., Basin-related uranium mineral systems in Australia: A review of critical features. Ore Geology Reviews, 76, 360-394 (2016).
KYSER, K., Uranium ore deposits. In: TUREKIAN, K., HOLLAND, H. (Eds.), Treatise on Geochemistry, 2nd Edition, Elsevier, 489-513 (2013).

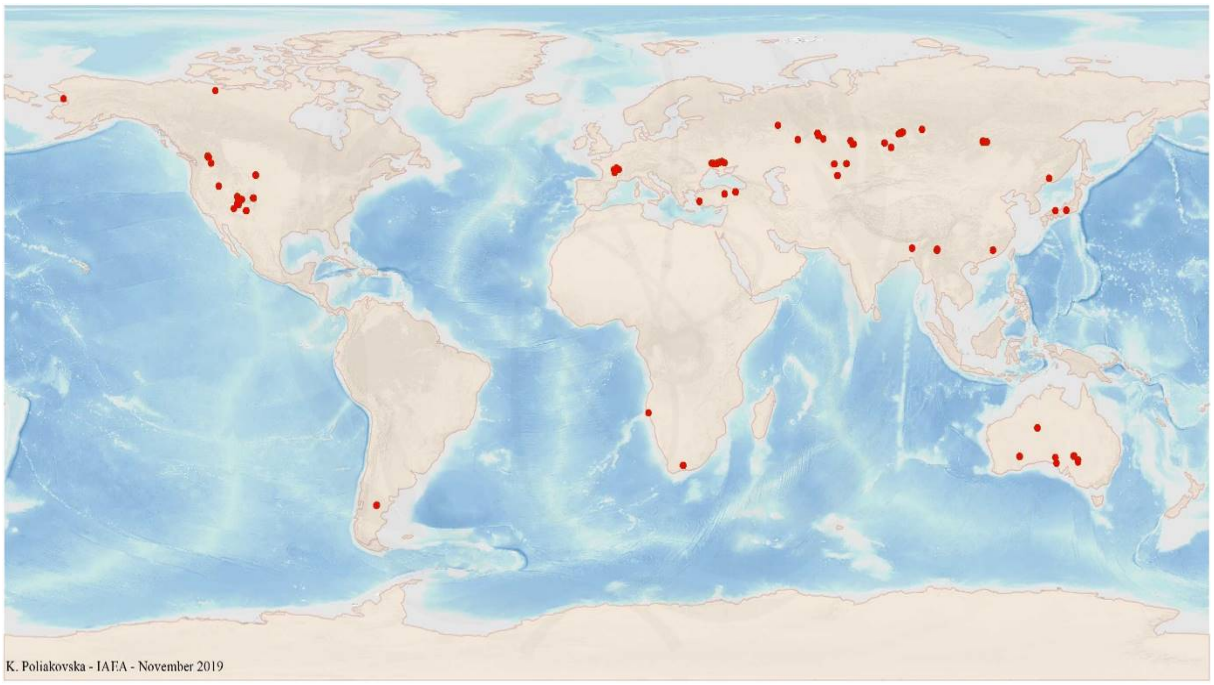

FIG. 9.1a. World distribution of selected Sandstone Basal Channel uranium deposits from the UDEPO database.

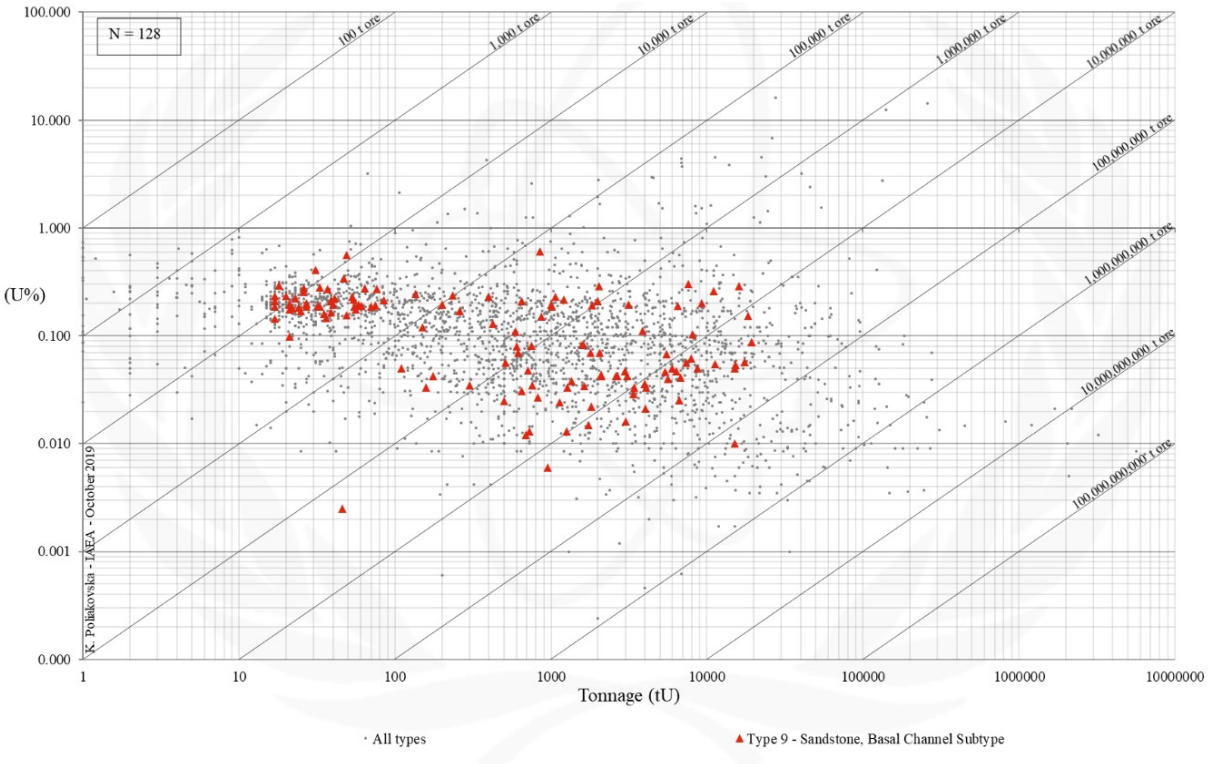

FIG. 9.1b. Grade and tonnage scatterplot highlighting Sandstone Basal Channel uranium deposits from the UDEPO database.

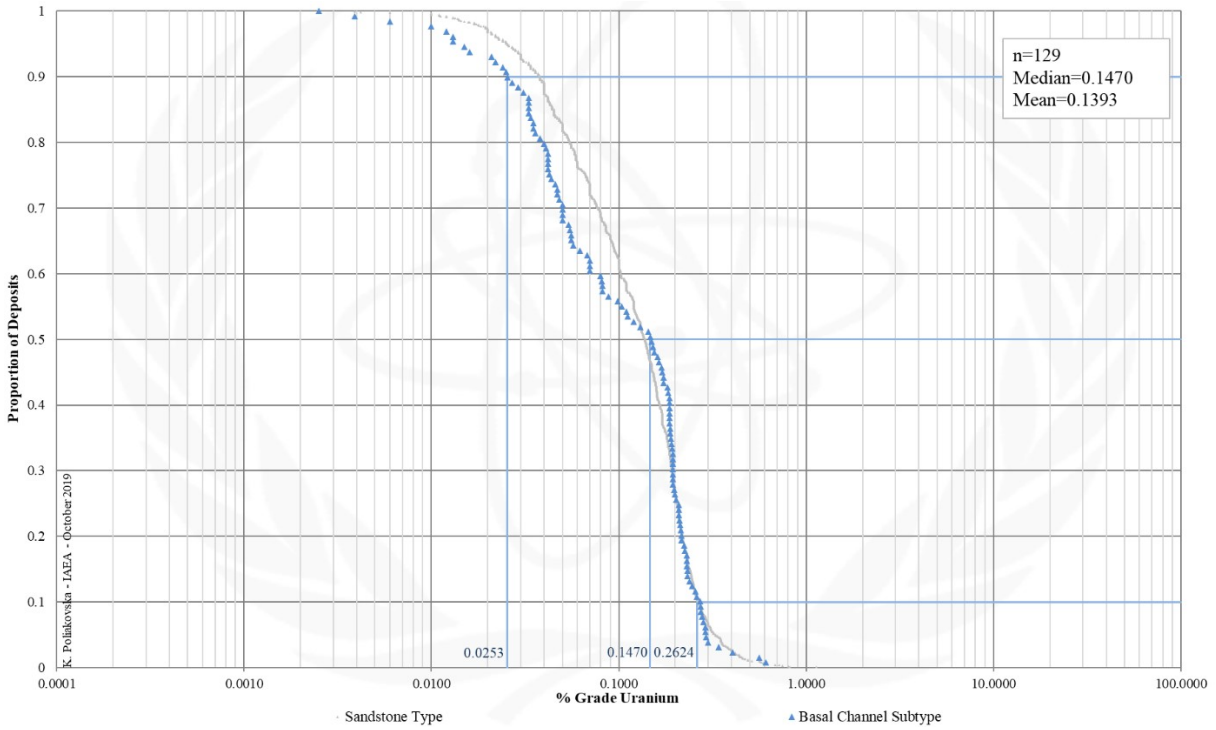

FIG. 9.1c. Grade Cumulative Probability Plot for Sandstone Basal Channel uranium deposits from the UDEPO database.

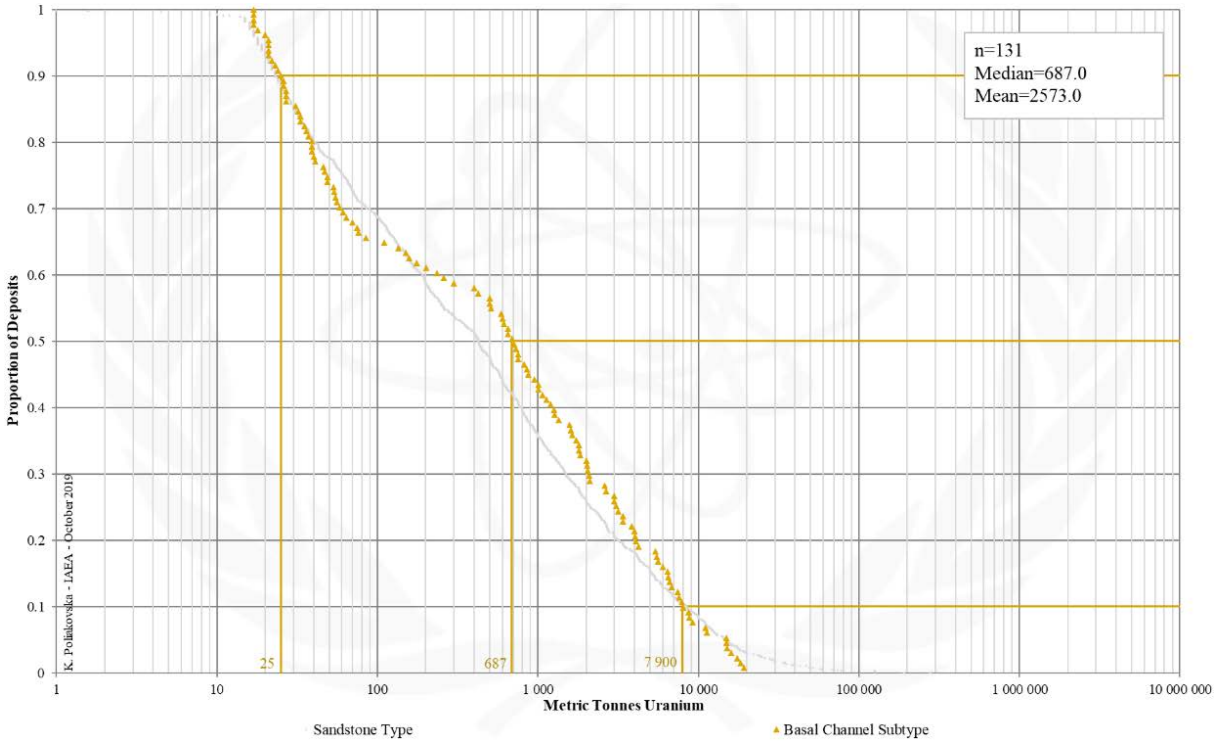

FIG. 9.1d. Tonnage Cumulative Probability Plot for Sandstone Basal Channel uranium deposits from the UDEPO database.

SUBTYPE 9.2. Sandstone, Tabular

Brief Description

- Sandstone deposits refer to uranium accumulations in medium- to coarse-grained siliciclastic sedimentary rocks deposited in continental fluvial, lacustrine or shallow-marine sedimentary environments.
- Uranium is precipitated by reduction processes caused by the presence of a variety of possible reducing agents within the host sandstone such as intrinsic detrital plant debris, sulphides, ferro-magnesian minerals, anaerobic sulphate-reducing bacteria, or extrinsic migrated fluids from underlying hydrocarbon reservoirs.
- Tabular deposits are further subdivided into several classes based on the type and nature of the respective reducing agent or their metal association: (9.2.1.) Continental fluvial, uranium associated with an intrinsic reductant, (9.2.2.) continental fluvial, uranium associated with extrinsic bitumen, and (9.2.3.) continental fluvial vanadium-uranium.
- Continental fluvial deposits in which uranium is associated with an intrinsic reductant form in palaeovalley systems dominated by reduced fluviatile sandstone with abundant detrital plant debris. The uranium ores take the form of matrix impregnations and disseminations within the channel fill, forming irregularly-shaped broadly tabular orebodies.
- Continental fluvial deposits in which uranium is associated with an extrinsic reductant form in alluvial fan environments, typically comprised of braided, straight and sinuous channel facies sands. The uranium ores are spatially associated with humates that were introduced into the originally organic-poor host sands by laterally migrating groundwaters. The orebodies are typically undulating, tabular, strongly elongate lenses peneconcordant with bedding.
- Continental fluvial vanadium-uranium deposits occur in reduced fluvial sandstone often deposited as part of a thick sequence of continental red bed sediments. The host sands contain carbonaceous plant debris similar to continental fluvial deposits in which uranium is associated with intrinsic reductants. The orebodies are commonly tabular, elongate and peneconcordant with bedding.

Type Examples

- Class 9.2.1. Arlit, Imouraren, Akouta, Niger; Coutras, France
- Class 9.2.2. Ambrosia Lake/Grants district, USA
- Class 9.2.3. Salt Wash member: Henry Basin, Uravan Mineral Belt, USA

Genetically Associated Deposit Types

- Subtype 9.1. Basal channel
- Subtype 9.3. Roll-front
- Subtype 12.1. Lignite-coal, stratiform

Principal Commodities

- U ± V

Grades (%) and Tonnages (tU)

- Average: 0.1696, 2919.0
- Median: 0.1675, 205.0

Number of Deposits

- 880

Provinces (undifferentiated from Sandstone Type)

- Alaska Alexander, Alaska Darby Hogatza, Alaska Kokrines Hodzana, Alaska Kuskokwim White Mountains, Alaska Northern Alaska Range, Alaska Porcupine, Alaska Prince William Sound, Alaska Western Alaska Range, Alaska Yukon Tanana, Amadeus Basin, Apuseni Mountains, Aquitaine Basin, Bayingebi Basin Bandan Jilin , BC Okanagan, Bighorn Basin, Black Hills, Black Mesa Basin, Bohemian Basin North, Carnarvon Basin, Carpathians South, Casper Arch, Cerilly Bourbon, Choibalsan Basin, Choir Nyalga Basin, Chu Sarysu Basin, Colio Basin Vol Koli, Congo Basin, Cosquin, Denver Basin, Dnieper Basin, Duruma Tanga Basin, Erlian Basin, Etosha Basin, Fergana Basin, Forez, Franceville Basin, Frome Embayment, Geosinclinal Andino, Gobi Basin South, Green River Basin, Guandacol, Kaiparowits Basin, Parana Basin Melo Fraile Muerto, Parana Basin Oviedo Yuti, Parana Basin Rio Grandense Shield, Piceance Basin, Pirie Basin, Powder River Basin, San Jorge Gulf Basin, San Juan Basin, Sarysu Basin North, Sebinkarahisar, Shirley Basin, Shiwan Dashan Basin, Sichuan Basin, Songliao Basin, Southwestern Donets Basin, Spokane Mountain Sherwood, Sukhbaatar Basin, Syr Darya Basin, Tallahassee Creek, Tamsag Basin, Tarim Basin North, Tarim Basin South, Taurkyr Dome, Temrezli Basin, Texas Coastal Plain - Catahoula-Oakville, Texas Coastal Plain - Clairborne-Jackson, Texas Coastal Plain - Goliad-Willis-Lissie, Thrace Basin, Tinogasta, Transbaykal Central, Transural, Tuha Basin, Tuli Basin, Uinta Basin, Washakie Cenozoic, Washakie SandWash GreatDivide Mesozoic, West Balkan, West Siberia, West Yunnan, Wind River Basin, Yenisey, Yilgarn South, Yili Ily Basins.

Tectonic Setting

- Continental platforms or intracratonic, intermontane, volcanigenic or sag basins in tectonically stable cratonic environments

Typical Geological Age Range

- Palaeozoic to Cenozoic

Mineral Systems Model

Source

Ground preparation

- Basin formation ± salt tectonism

Energy
- Steepening of hydrological gradient linked to basement uplift due to tectonic reactivation or far-field tectonic events
- Possible contribution from diagenetic compaction and/or salt tectonics

Fluids
- Shallow, oxidised, neutral to alkaline groundwaters
- Reduced hydrocarbon-bearing brines
- Possible involvement of oxidised basinal brines and deeper-seated, reduced groundwaters

Ligands
- Ca, CO_3, S

Reductants
- Organic matter, humic substances, biogenic and non-biogenic H_2S, hydrocarbons, sulphides

Uranium
- Crystalline basement rocks, granitoids, basin fill (in particular interbedded volcanic ash units), pre-existing uranium deposits

Vanadium
- Detrital magnetite and ilmenite contained within the basin fill

Transport

Fluid pathways
- Regional sandstone aquifers
- Palaeovalleys
- Fault-fracture systems (in particular basin growth structures tapping deeper basin sequences, underlying basins or basement)

Trap

Physical
- Palaeovalley bends, confluences, basal scours and/or areas of channel-widening
- Point bar, braid bar, bar-head sequences
- Fault-fracture systems
- Folds
- Salt domes

Chemical
- In-situ, intrinsic reductants within the host aquifers or wallrocks
- Mobile, extrinsic reductants related to oil and gas systems
- Regional redox fronts

Deposition

Change in redox conditions
- Due to interaction of oxidised, uranium-bearing groundwaters or brines with in-situ, intrinsic or mobile, extrinsic reductants
- Due to mixing of oxidised, uranium-bearing groundwaters or brines and (± strongly) reduced (± vanadium-bearing) fluids (deeper groundwater system or basinal brines?) in reducing palaeovalley environments
- Linked to acid neutralisation due to interaction between uranium-bearing fluids and carbonates

Adsorption
- Adsorption of organically complexed uranium onto clays or Fe^{2+} silicate surfaces

Preservation
- Physical isolation of uranium mineralisation from the flow of oxidised groundwaters
- Capping of uranium-mineralised sequences by younger lavas
- Relative tectonic stability post-uranium mineralisation

Key Reference Bibliography

DAHLKAMP, F. J., Uranium Deposits of the World: USA and Latin America. Springer, Berlin, Heidelberg, 515p (2010).
DAHLKAMP, F. J., Uranium Deposits of the World: Europe. Springer, Berlin, Heidelberg, 792p (2016).
HUSTON, D. L., VAN DER WIELEN, S. (Eds.), An assessment of the uranium and geothermal prospectivity of east-central South Australia. Geoscience Australia Record, 2011/34, 229p (2011).
INTERNATIONAL ATOMIC ENERGY AGENCY, Geological Classification of Uranium Deposits and Description of Selected Examples. IAEA-TECDOC Series, 1842, 415p (2018).
JAIRETH, S., ROACH, I. C., BASTRAKOV, E., LIU, S., Basin-related uranium mineral systems in Australia: A review of critical features. Ore Geology Reviews, 76, 360-394 (2016).
KYSER, K., Uranium ore deposits. In: TUREKIAN, K., HOLLAND, H. (Eds.), Treatise on Geochemistry, 2nd Edition, Elsevier, 489-513 (2013).
SALZE, D., BELCOURT, O., HAROUNA, M., The first stage in the formation of the uranium deposit of Arlit, Niger: Role of a new non-continental organic matter. Ore Geology Reviews, 102, 604-617 (2018).
SHAWE, D. R., Uranium-vanadium deposits of the Slick Rock district, Colorado. U.S. Geological Survey Professional Paper 576-F, 80p., 20 plates (2011).

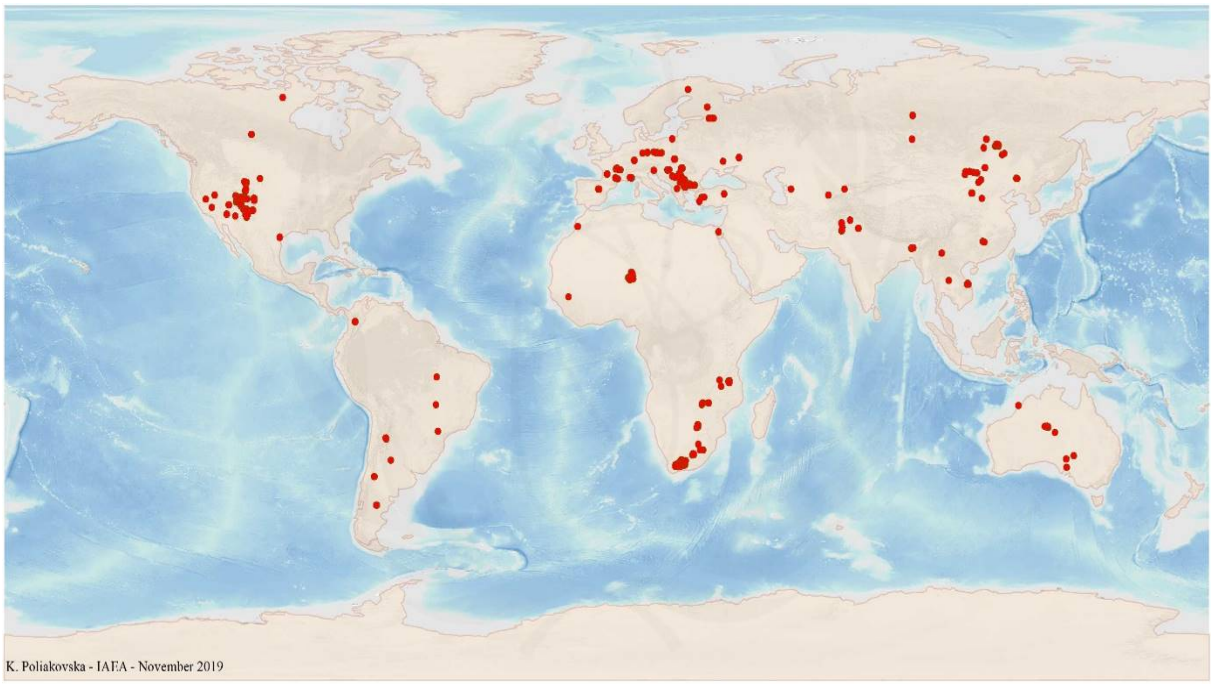

FIG. 9.2a. World distribution of selected Sandstone Tabular uranium deposits from the UDEPO database.

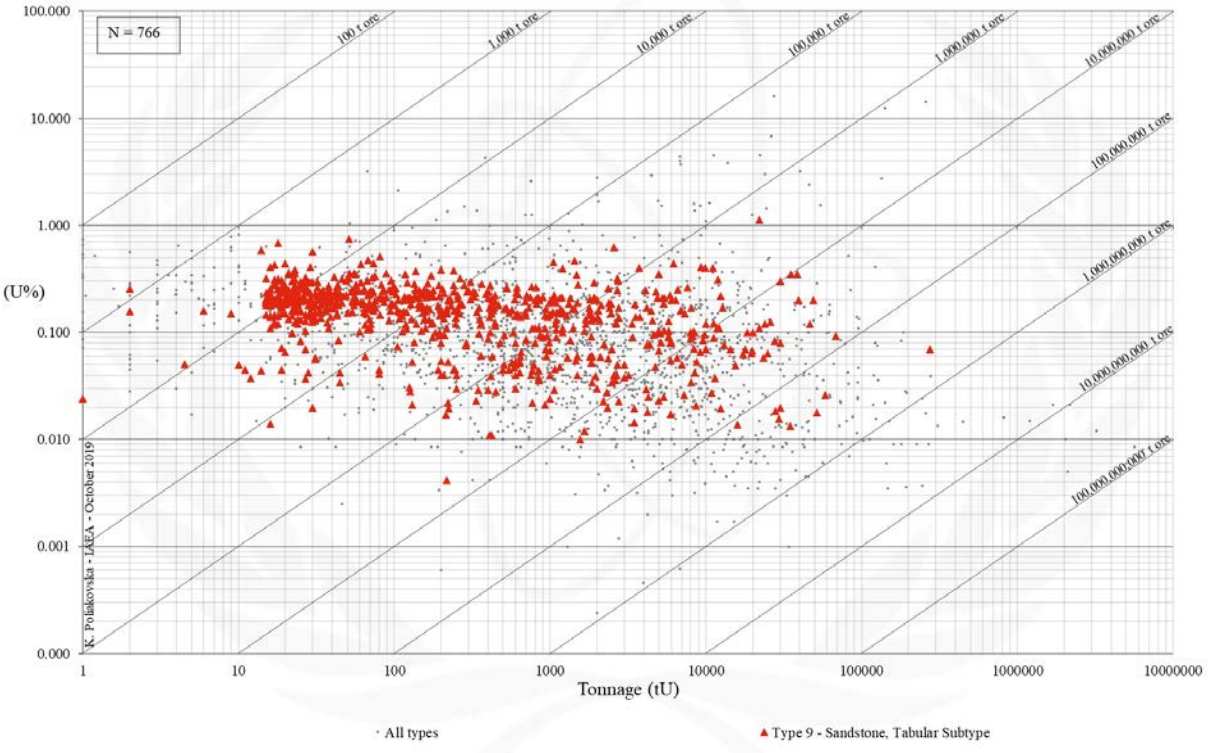

FIG. 9.2b. Grade and tonnage scatterplot highlighting Sandstone Tabular uranium deposits from the UDEPO database.

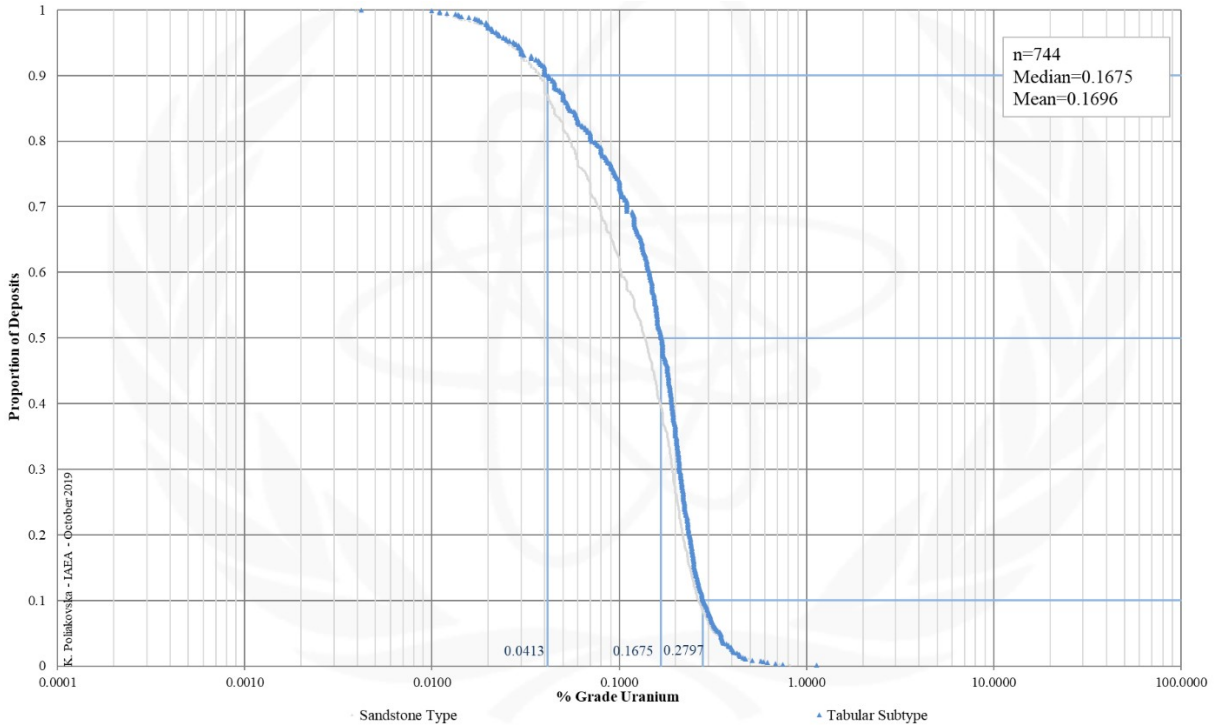

FIG. 9.2c. Grade Cumulative Probability Plot for Sandstone Tabular uranium deposits from the UDEPO database.

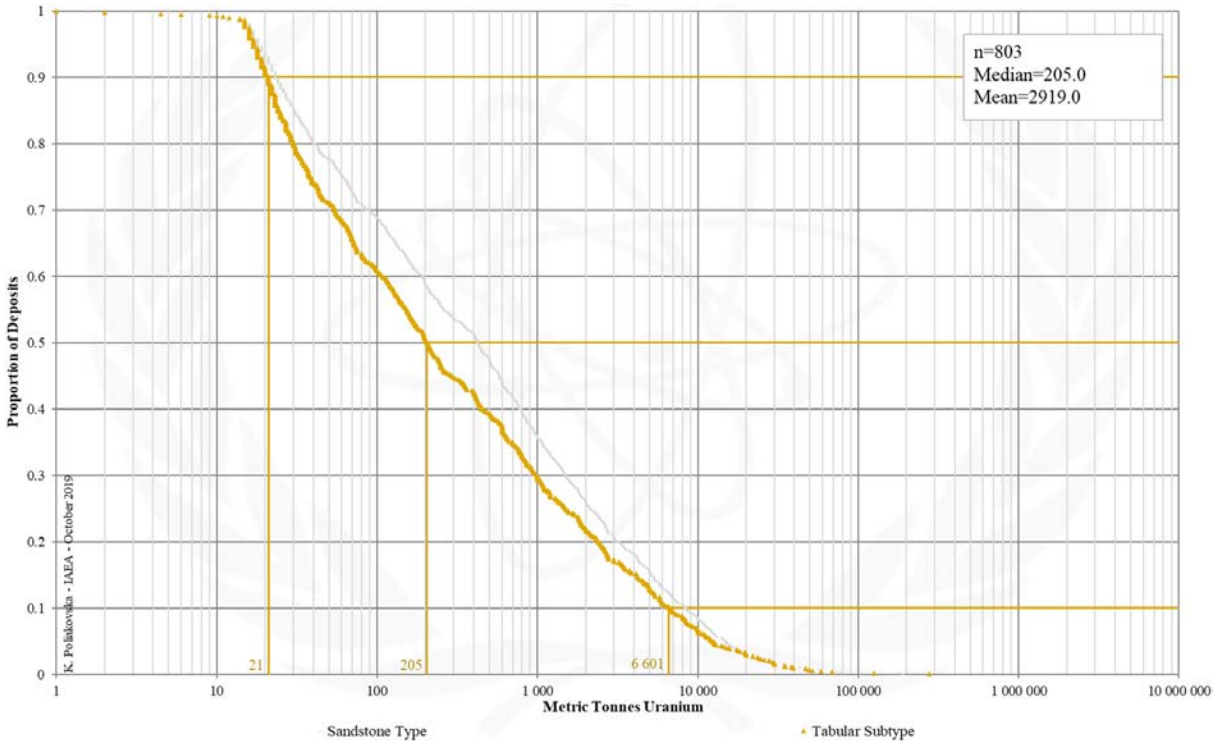

FIG. 9.2d. Tonnage Cumulative Probability Plot for Sandstone Tabular uranium deposits from the UDEPO database.

CLASS 9.2.1. Sandstone, Tabular, Continental Fluvial, Intrinsic Reductant

Brief Description

- Sandstone deposits refer to uranium accumulations in medium- to coarse-grained siliciclastic sedimentary rocks deposited in continental fluvial, lacustrine or shallow-marine sedimentary environments.
- Uranium is precipitated by reduction processes caused by the presence of a variety of possible reducing agents within the host sandstone such as detrital plant debris, sulphides, ferro-magnesian minerals, anaerobic sulphate-reducing bacteria or migrated fluids from underlying hydrocarbon reservoirs.
- Sandstone deposits are divided into five subtypes with many gradual transitions between them: (9.1) Basal channel, (9.2) tabular, (9.3) roll-front, (9.4) tectonic-lithologic, and (9.5) mafic dyke/sills in Proterozoic sandstones.
- Tabular deposits are further subdivided into several classes based on the type and nature of the respective reducing agent or their metal association: (9.2.1.) Continental fluvial, uranium associated with an intrinsic reductant, (9.2.2.) continental fluvial, uranium associated with extrinsic bitumen, and (9.2.3.) continental fluvial vanadium-uranium.
- Continental fluvial deposits in which uranium is associated with an intrinsic reductant form in palaeovalley systems dominated by reduced fluviatile sandstone with abundant detrital plant debris
- The uranium ores take the form of matrix impregnations and disseminations within the channel fill, forming irregularly-shaped yet broadly tabular orebodies.

Type Examples

- Arlit, Imouraren, Akouta, Niger; Coutras, France

Genetically Associated Deposit Types

- Subtype 9.1. Basal channel
- Subtype 9.3. Roll-front
- Subtype 12.1. Lignite-coal, stratiform

Principal Commodities

- U

Grades (%) and Tonnages (tU)

- Average: insufficent data
- Median: insufficent data

Number of Deposits

- Deposits: insufficent data

Provinces (undifferentiated from Sandstone Type)

- Alaska Alexander, Alaska Darby Hogatza, Alaska Kokrines Hodzana, Alaska Kuskokwim White Mountains, Alaska Northern Alaska Range, Alaska Porcupine, Alaska Prince William Sound, Alaska Western Alaska Range, Alaska Yukon Tanana, Amadeus Basin, Apuseni Mountains, Aquitaine Basin, Bayingebi Basin Bandan Jilin , BC Okanagan, Bighorn Basin, Black Hills, Black Mesa Basin, Bohemian Basin North, Carnarvon Basin, Carpathians South, Casper Arch, Cerilly Bourbon, Choibalsan Basin, Choir Nyalga Basin, Chu Sarysu Basin, Colio Basin Vol Koli, Congo Basin, Cosquin, Denver Basin, Dnieper Basin, Duruma Tanga Basin, Erlian Basin, Etosha Basin, Fergana Basin, Forez, Franceville Basin, Frome Embayment, Geosinclinal Andino, Gobi Basin Central, Gobi Basin East, Gobi Basin South, Green River Basin, Guandacol, Gyeongsang Basin, Hengyang Basin, Iberian Cordillera, Iullemmeden Basin, Japan Basal Channel, Junggar Basin, Kaiparowits Basin, Kalahari Basin East, Kalahari Basin West, Karasburg Basin, Karoo Basin Mesozoic, Karoo Basin Permian, Khorat Plateau, Kokshetau East, Kokshetau West, Kolari Kittila, Kyzylkum, Lake Ladoga, Laramine Hanna Shirley Basins, Lebombo Nuanetsi Basin, Lodeve Basin, Luangwa Lukusashi Basins, Massif Central South West, Mecsek Mountains, Meghalaya Plateau, Menderes Massif, Morondava Basin, Mount Pisgah, Murphy, Nebraska Plains White River Group, Ngalia Basin Sandstone, Nong Son Basin, Norte Subandino, North Canning Basin, Ordos Basin, Pannonian Basin South, Paradox Basin, Parana Basin Amorinopolis Ipora, Parana Basin Durazno, Parana Basin Figueira, Parana Basin Melo Fraile Muerto, Parana Basin Oviedo Yuti, Parana Basin Rio Grandense Shield, Piceance Basin, Pirie Basin, Powder River Basin, Qaidam Basin, Rhodope Massif, Ruhuhu Selous Basins, Saint Pierre du Cantal, San Jorge Gulf Basin, San Juan Basin, Sarysu Basin North, Sebinkarahisar, Shirley Basin, Shiwan Dashan Basin, Sichuan Basin, Siwalik, Slovenia Permian, Songliao Basin, Southwestern Donets Basin, Spokane Mountain Sherwood, Sukhbaatar Basin, Syr Darya Basin, Tallahassee Creek, Tamsag Basin, Tarim Basin North, Tarim Basin South, Taurkyr Dome, Temrezli Basin, Texas Coastal Plain - Catahoula-Oakville, Texas Coastal Plain - Clairborne-Jackson, Texas Coastal Plain - Goliad-Willis-Lissie, Thrace Basin, Tinogasta, Transbaykal Central, Transural, Tuha Basin, Tuli Basin, Uinta Basin, Washakie Cenozoic, Washakie SandWash GreatDivide Mesozoic, West Balkan, West Siberia, West Yunnan, Wind River Basin, Yenisey, Yilgarn South, Yili Ily Basins.

Tectonic Setting

- Continental platforms or intracratonic, intermontane, volcanigenic or sag basins in tectonically stable cratonic environments

Typical Geological Age Range

- Palaeozoic to Cenozoic

Mineral Systems Model

Source

Ground preparation

- Basin formation ± salt tectonism

Energy
- Steepening of hydrological gradient linked to basement uplift due to tectonic reactivation or far-field tectonic events
- Possible contribution from diagenetic compaction and/or salt tectonics

Fluids
- Shallow, oxidised, neutral to alkaline groundwaters
- Reduced hydrocarbon-bearing brines
- Possible involvement of oxidised basinal brines and deeper-seated, reduced groundwaters

Ligands
- Ca, CO_3, S

Reductants
- Organic matter, humic substances, biogenic and non-biogenic H_2S, hydrocarbons, sulphides

Uranium
- Crystalline basement rocks, granitoids, basin fill (in particular interbedded volcanic ash units), pre-existing uranium deposits

Transport

Fluid pathways
- Regional sandstone aquifers
- Palaeovalleys
- Fault-fracture systems (in particular basin growth structures tapping deeper basin sequences, underlying basins or basement)

Trap

Physical
- Palaeovalley bends, confluences, basal scours and/or areas of channel-widening
- Point bar, braid bar, bar-head sequences
- Fault-fracture systems

Chemical
- In-situ, intrinsic reductants within the host aquifers or wallrocks
- Regional redox fronts

Deposition

Change in redox conditions
- Due to interaction of oxidised, uranium-bearing groundwaters or brines with in-situ, intrinsic reductants
- Due to mixing of oxidised, uranium-bearing groundwaters or brines and reduced fluids
- Linked to acid neutralisation due to interaction between uranium-bearing fluids and carbonates

Adsorption
- Adsorption of organically complexed uranium onto clays or Fe^{2+} silicate surfaces

Preservation
- Physical isolation of uranium mineralisation from the flow of oxidised groundwaters
- Capping of uranium-mineralised sequences by younger lavas
- Relative tectonic stability post-uranium mineralisation

Key Reference Bibliography

DAHLKAMP, F. J., Uranium Deposits of the World: USA and Latin America. Springer, Berlin, Heidelberg, 515p (2010).
DAHLKAMP, F. J., Uranium Deposits of the World: Europe. Springer, Berlin, Heidelberg, 792p (2016).
HUSTON, D. L., VAN DER WIELEN, S. (Eds.), An assessment of the uranium and geothermal prospectivity of east-central South Australia. Geoscience Australia Record, 2011/34, 229p (2011).
INTERNATIONAL ATOMIC ENERGY AGENCY, Geological classification of uranium deposits and description of selected examples. IAEA TECDOC Series, 1842, 415p (2018).
JAIRETH, S., ROACH, I. C., BASTRAKOV, E., LIU, S., Basin-related uranium mineral systems in Australia: A review of critical features. Ore Geology Reviews, 76, 360-394 (2016).
KYSER, K., Uranium ore deposits. In: TUREKIAN, K., HOLLAND, H. (Eds.), Treatise on Geochemistry, 2nd Edition, Elsevier, 489-513 (2013).
SALZE, D., BELCOURT, O., HAROUNA, M., The first stage in the formation of the uranium deposit of Arlit, Niger: Role of a new non-continental organic matter. Ore Geology Reviews, 102, 604-617 (2018).

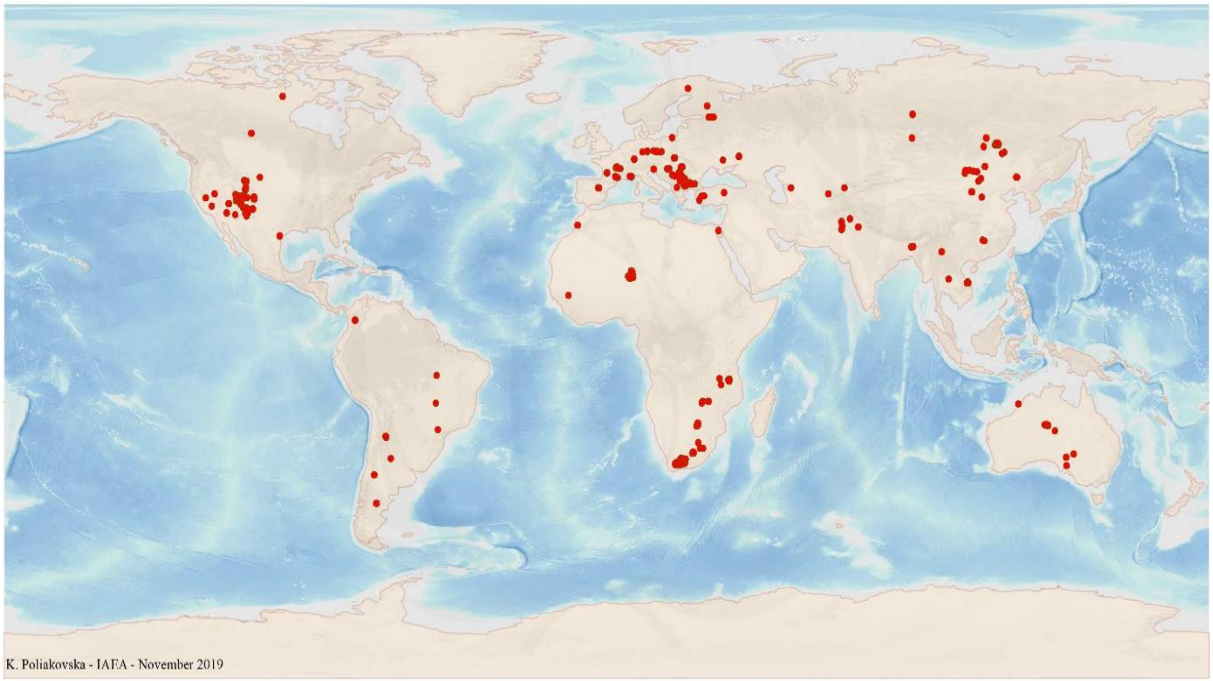

FIG. 9.2.1a. World distribution of selected Sandstone Tabular data are shown due to lack of data for Continental Fluvial Intrinsic Reductant uranium deposits from the UDEPO database.

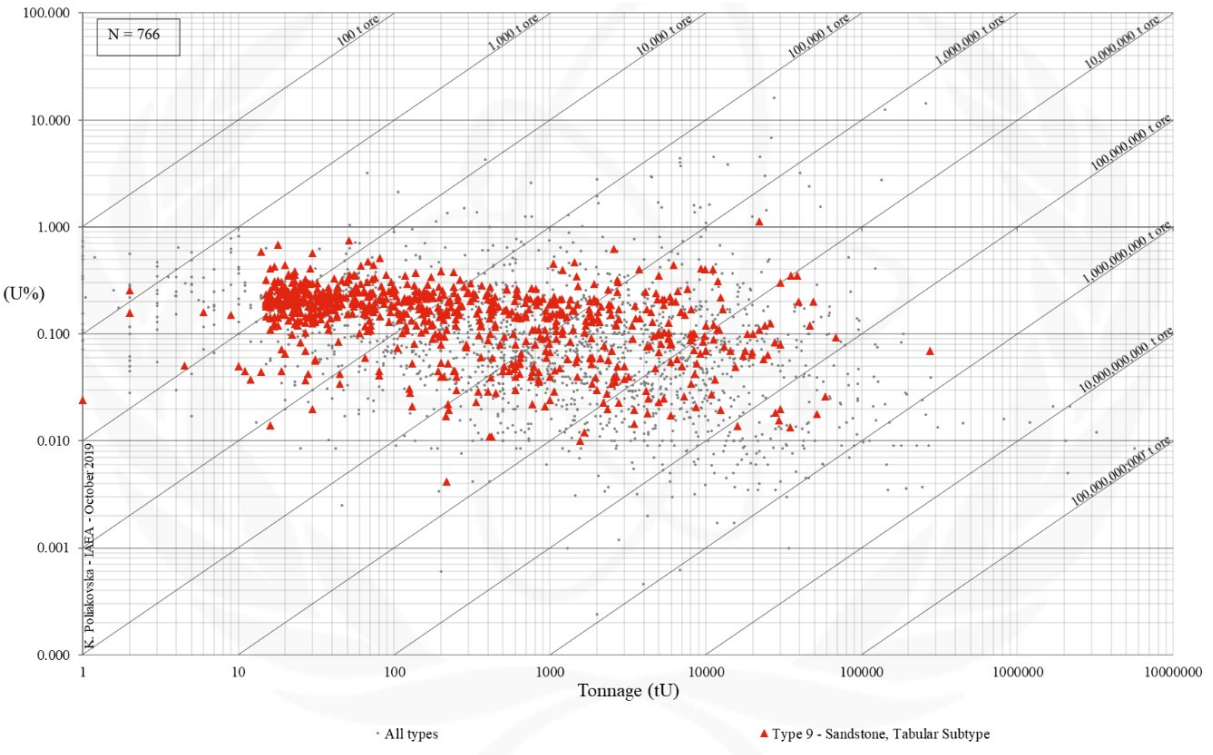

FIG. 9.2.1b. Grade and tonnage scatterplot highlighting Sandstone Tabular data are shown due to lack of data for Continental Fluvial Intrinsic Reductant uranium deposits from the UDEPO database.

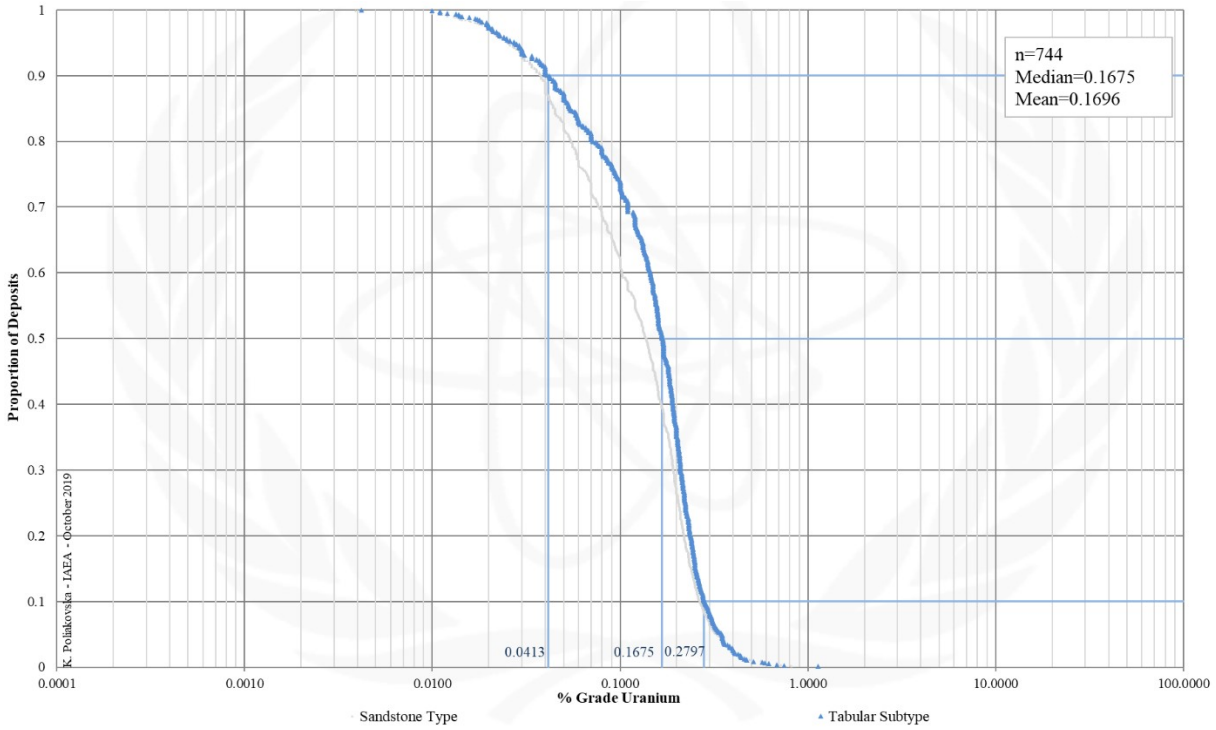

FIG. 9.2.1c. Grade Cumulative Probability Plot for Sandstone Tabular data are shown due to lack of data for Continental Fluvial Intrinsic Reductant uranium deposits from the UDEPO database.

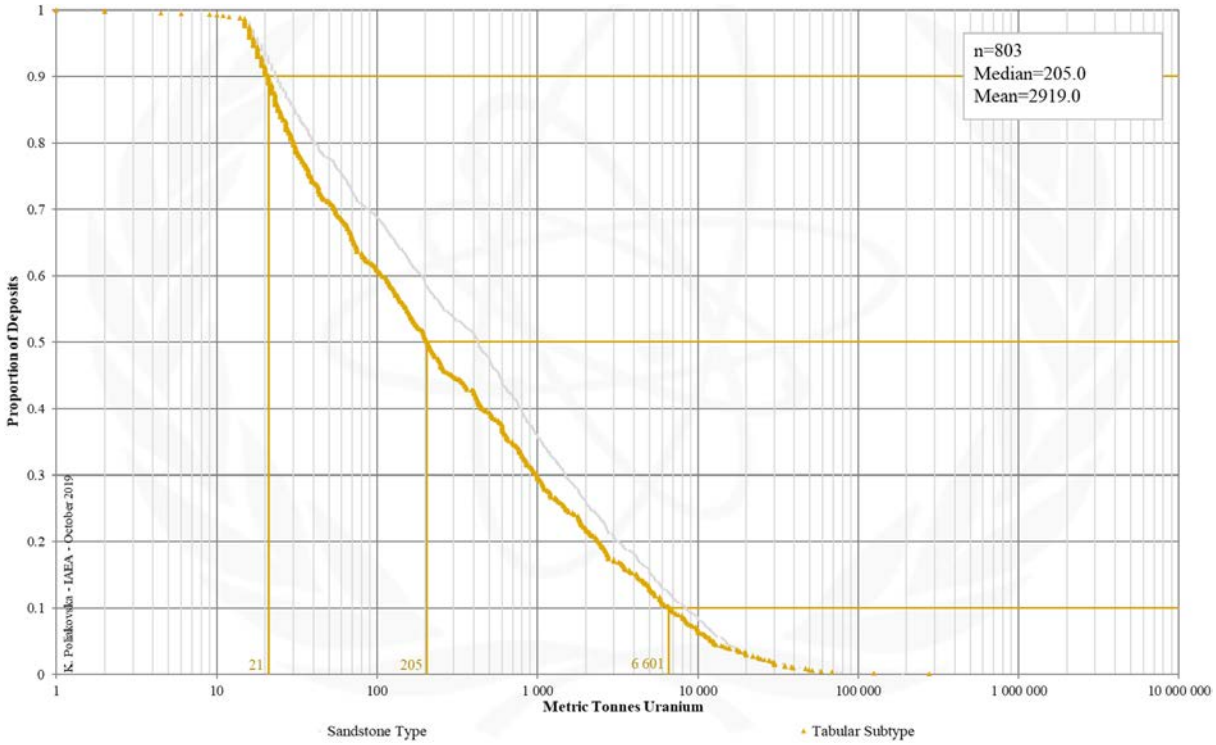

FIG. 9.2.1d. Tonnage Cumulative Probability Plot for Sandstone Tabular data are shown due to lack of data for Continental Fluvial Intrinsic Reductant uranium deposits from the UDEPO database.

CLASS 9.2.2. Sandstone, Tabular, Continental Fluvial, Extrinsic Bitumen

Brief Description

- Sandstone deposits refer to uranium accumulations in medium- to coarse-grained siliciclastic sedimentary rocks deposited in continental fluvial, lacustrine or shallow-marine sedimentary environments.
- Uranium is precipitated by reduction processes caused by the presence of a variety of possible reducing agents within the host sandstone such as detrital plant debris, sulphides, ferro-magnesian minerals, anaerobic sulphate-reducing bacteria or migrated fluids from underlying hydrocarbon reservoirs.
- Sandstone deposits are divided into five subtypes with many gradual transitions between them: (9.1) Basal channel, (9.2) tabular, (9.3) roll-front, (9.4) tectonic-lithologic, and (9.5) mafic dyke/sills in Proterozoic sandstones.
- Tabular deposits are further subdivided into several classes based on the type and nature of the respective reducing agent or their metal association: (9.2.1.) Continental fluvial, uranium associated with an intrinsic reductant, (9.2.2.) continental fluvial, uranium associated with extrinsic bitumen, and (9.2.3.) continental fluvial vanadium-uranium.
- Continental fluvial deposits in which uranium is associated with an extrinsic reductant form in alluvial fan environments, typically comprised of braided, straight and sinuous channel facies sands.
- The uranium ores are spatially associated with humates that were introduced into the originally organic-poor host sands by laterally migrating groundwaters.
- The orebodies are typically undulating, tabular, strongly elongate lenses peneconcordant with bedding.

Type Examples

- Ambrosia Lake/Grants district, USA

Genetically Associated Deposit Types

- Subtype 9.1. Basal channel
- Subtype 9.3. Roll-front

Principal Commodities

- U

Grades (%) and Tonnages (tU)

- Average: insufficent data
- Median: insufficent data

Number of Deposits

- Deposits: insufficent data

Provinces (undifferentiated from Sandstone Type)

- Alaska Alexander, Alaska Darby Hogatza, Alaska Kokrines Hodzana, Alaska Kuskokwim White Mountains, Alaska Northern Alaska Range, Alaska Porcupine, Alaska Prince William Sound, Alaska Western Alaska Range, Alaska Yukon Tanana, Amadeus Basin, Apuseni Mountains, Aquitaine Basin, Bayingebi Basin Bandan Jilin , BC Okanagan, Bighorn Basin, Black Hills, Black Mesa Basin, Bohemian Basin North, Carnarvon Basin, Carpathians South, Casper Arch, Cerilly Bourbon, Choibalsan Basin, Choir Nyalga Basin, Chu Sarysu Basin, Colio Basin Vol Koli, Congo Basin, Cosquin, Denver Basin, Dnieper Basin, Duruma Tanga Basin, Erlian Basin, Etosha Basin, Fergana Basin, Forez, Franceville Basin, Frome Embayment, Geosinclinal Andino, Gobi Basin Central, Gobi Basin East, Gobi Basin South, Green River Basin, Guandacol, Gyeongsang Basin, Hengyang Basin, Iberian Cordillera, Iullemmeden Basin, Japan Basal Channel, Junggar Basin, Kaiparowits Basin, Kalahari Basin East, Kalahari Basin West, Karasburg Basin, Karoo Basin Mesozoic, Karoo Basin Permian, Khorat Plateau, Kokshetau East, Kokshetau West, Kolari Kittila, Kyzylkum, Lake Ladoga, Laramine Hanna Shirley Basins, Lebombo Nuanetsi Basin, Lodeve Basin, Luangwa Lukusashi Basins, Massif Central South West, Mecsek Mountains, Meghalaya Plateau, Menderes Massif, Morondava Basin, Mount Pisgah, Murphy, Nebraska Plains White River Group, Ngalia Basin Sandstone, Nong Son Basin, Norte Subandino, North Canning Basin, Ordos Basin, Pannonian Basin South, Paradox Basin, Parana Basin Amorinopolis Ipora, Parana Basin Durazno, Parana Basin Figueira, Parana Basin Melo Fraile Muerto, Parana Basin Oviedo Yuti, Parana Basin Rio Grandense Shield, Piceance Basin, Pirie Basin, Powder River Basin, Qaidam Basin, Rhodope Massif, Ruhuhu Selous Basins, Saint Pierre du Cantal, San Jorge Gulf Basin, San Juan Basin, Sarysu Basin North, Sebinkarahisar, Shirley Basin, Shiwan Dashan Basin, Sichuan Basin, Siwalik, Slovenia Permian, Songliao Basin, Southwestern Donets Basin, Spokane Mountain Sherwood, Sukhbaatar Basin, Syr Darya Basin, Tallahassee Creek, Tamsag Basin, Tarim Basin North, Tarim Basin South, Taurkyr Dome, Temrezli Basin, Texas Coastal Plain - Catahoula-Oakville, Texas Coastal Plain - Clairborne-Jackson, Texas Coastal Plain - Goliad-Willis-Lissie, Thrace Basin, Tinogasta, Transbaykal Central, Transural, Tuha Basin, Tuli Basin, Uinta Basin, Washakie Cenozoic, Washakie SandWash GreatDivide Mesozoic, West Balkan, West Siberia, West Yunnan, Wind River Basin, Yenisey, Yilgarn South, Yili Ily Basins.

Tectonic Setting

- Continental platforms or intracratonic, intermontane, volcanigenic or sag basins in tectonically stable cratonic environments

Typical Geological Age Range

- Palaeozoic to Cenozoic

Mineral Systems Model

Source

Ground preparation

- Basin formation ± salt tectonism

Energy
- Steepening of hydrological gradient linked to basement uplift due to tectonic reactivation or far-field tectonic events
- Possible contribution from diagenetic compaction and/or salt tectonics

Fluids
- Shallow, oxidised, neutral to alkaline groundwaters
- Reduced hydrocarbon-bearing brines
- Possible involvement of oxidised basinal brines and deeper-seated, reduced groundwaters

Ligands
- Ca, CO_3, S

Reductants
- Organic matter, humic substances, biogenic and non-biogenic H_2S, hydrocarbons, sulphides

Uranium
- Crystalline basement rocks, granitoids, basin fill (in particular interbedded volcanic ash units), pre-existing uranium deposits

Transport

Fluid pathways
- Regional sandstone aquifers
- Palaeovalleys
- Fault-fracture systems (in particular basin growth structures tapping deeper basin sequences, underlying basins or basement)

Trap

Physical
- Palaeovalley bends, confluences, basal scours and/or areas of channel-widening
- Point bar, braid bar, bar-head sequences
- Fault-fracture systems

Chemical
- Mobile, extrinsic reductants related to oil and gas systems
- Regional redox fronts

Deposition

Change in redox conditions
- Due to interaction of oxidised, uranium-bearing groundwaters or brines with mobile, extrinsic reductants
- Due to mixing of oxidised, uranium-bearing groundwaters or brines and reduced fluids

Adsorption
- Adsorption of organically complexed uranium onto clays or Fe^{2+} silicate surfaces

Preservation
- Physical isolation of uranium mineralisation from the flow of oxidised groundwaters
- Capping of uranium-mineralised sequences by younger lavas
- Relative tectonic stability post-uranium mineralisation

Key Reference Bibliography

DAHLKAMP, F. J., Uranium Deposits of the World: USA and Latin America. Springer, Berlin, Heidelberg, 515p (2010).

DAHLKAMP, F. J., Uranium Deposits of the World: Europe. Springer, Berlin, Heidelberg, 792p (2016).

HUSTON, D. L., VAN DER WIELEN, S. (Eds.), An assessment of the uranium and geothermal prospectivity of east-central South Australia. Geoscience Australia Record, 2011/34, 229p (2011).

INTERNATIONAL ATOMIC ENERGY AGENCY, Geological Classification of Uranium Deposits and Description of Selected Examples. IAEA-TECDOC Series, 1842, 415p (2018).

JAIRETH, S., ROACH, I. C., BASTRAKOV, E., LIU, S., Basin-related uranium mineral systems in Australia: A review of critical features. Ore Geology Reviews, 76, 360-394 (2016).

KYSER, K., Uranium ore deposits. In: TUREKIAN, K., HOLLAND, H. (Eds.), Treatise on Geochemistry, 2nd Edition, Elsevier, 489-513 (2013).

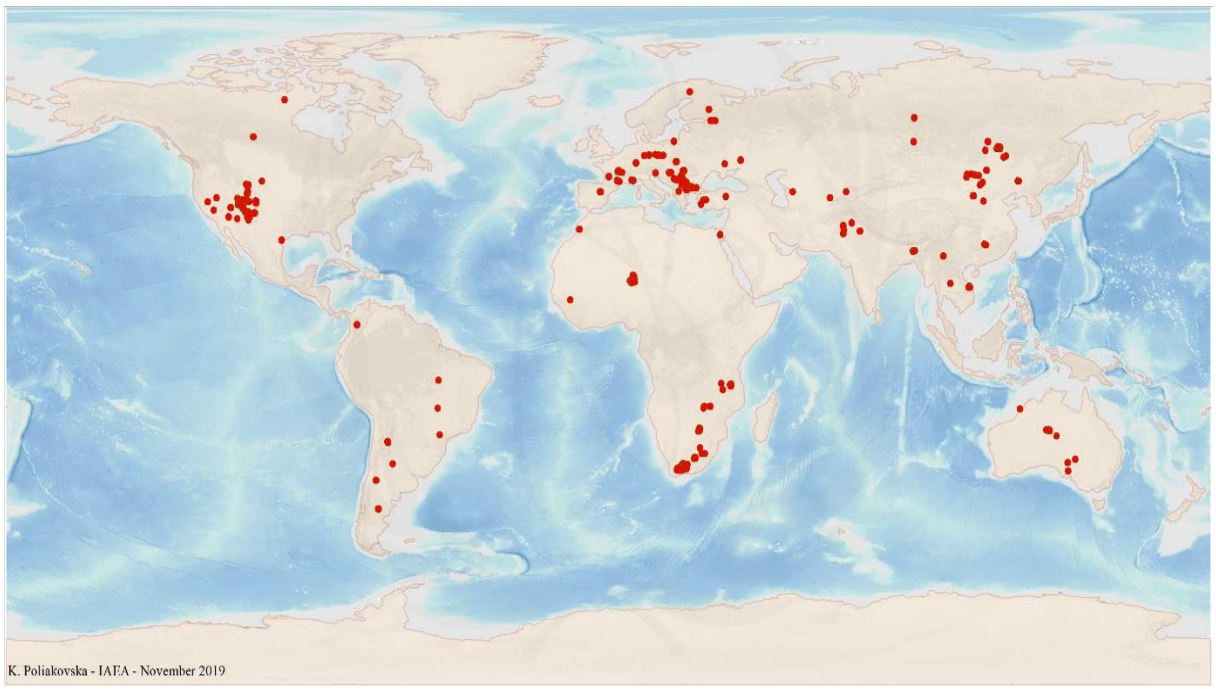

FIG. 9.2.2a. World distribution of selected Sandstone Tabular data are shown due to lack of data for Continental Fluvial Extrinsic Bitumen uranium deposits from the UDEPO database.

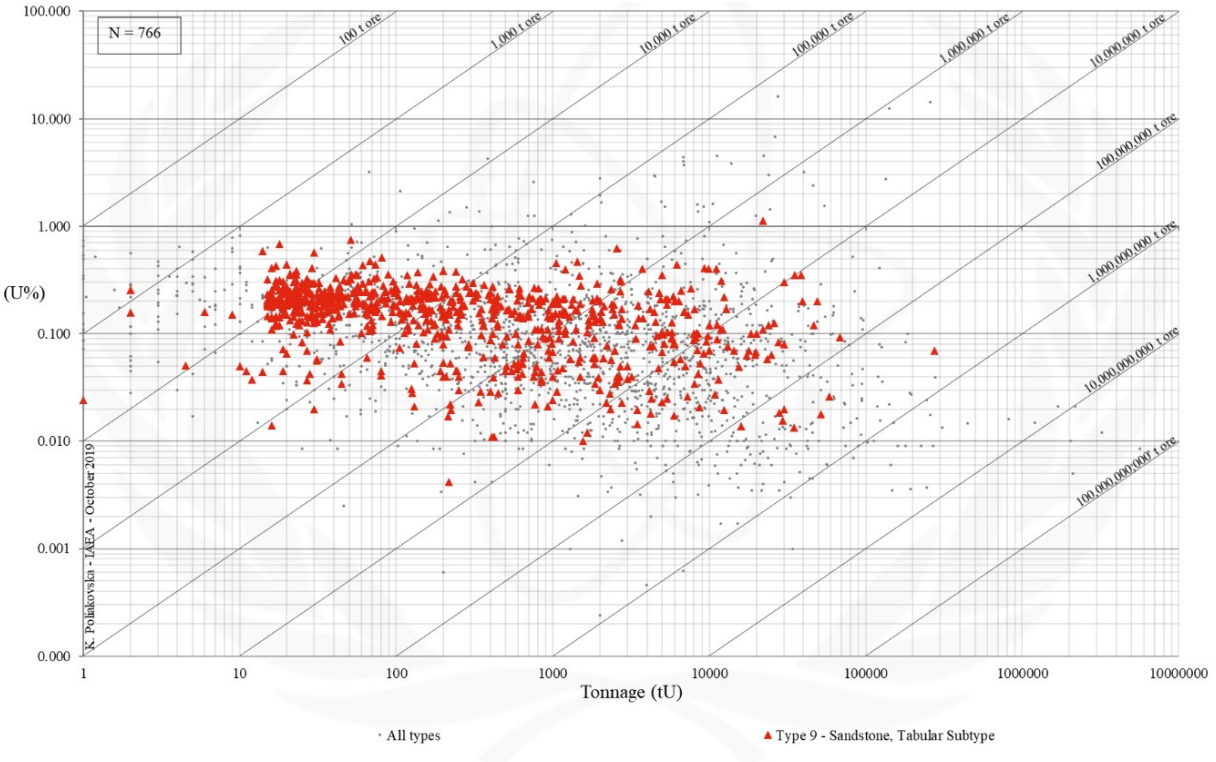

FIG. 9.2.2b. Grade and tonnage scatterplot highlighting Sandstone Tabular data are shown due to lack of data for Continental Fluvial Extrinsic Bitumen uranium deposits from the UDEPO database.

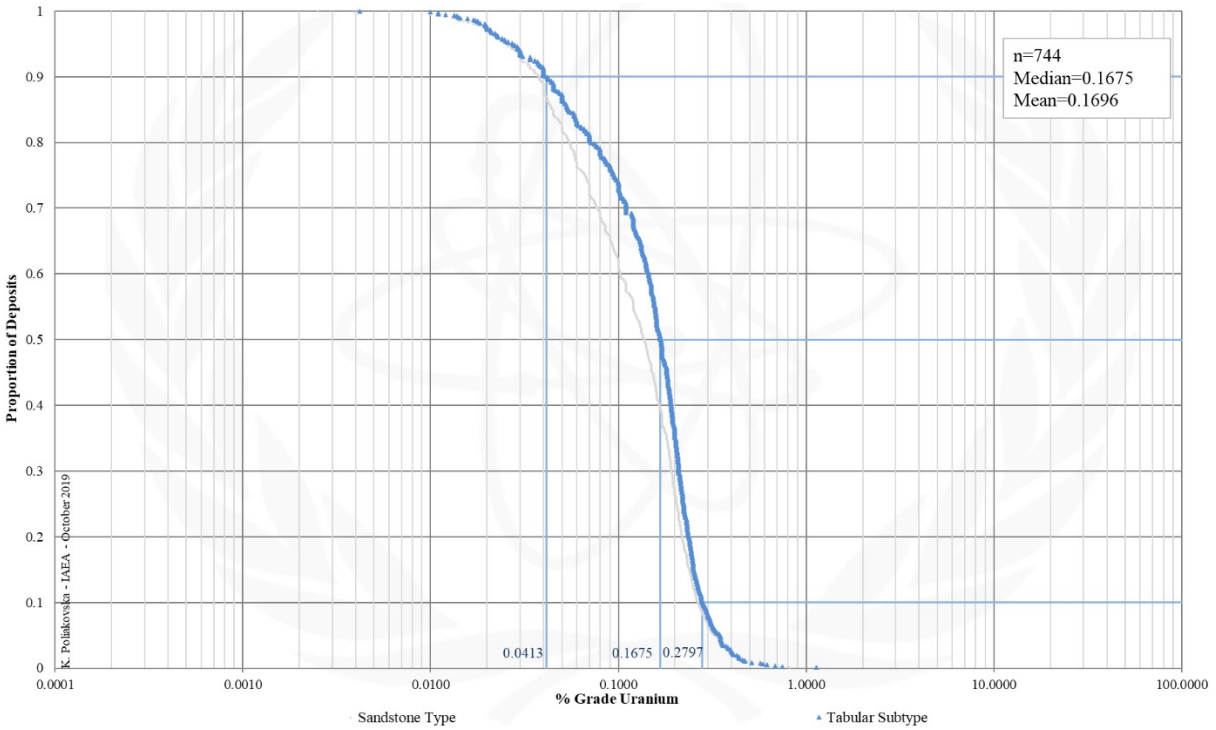

FIG. 9.2.2c. Grade Cumulative Probability Plot for Sandstone Tabular data are shown due to lack of data for Continental Fluvial Extrinsic Bitumen uranium deposits from the UDEPO database.

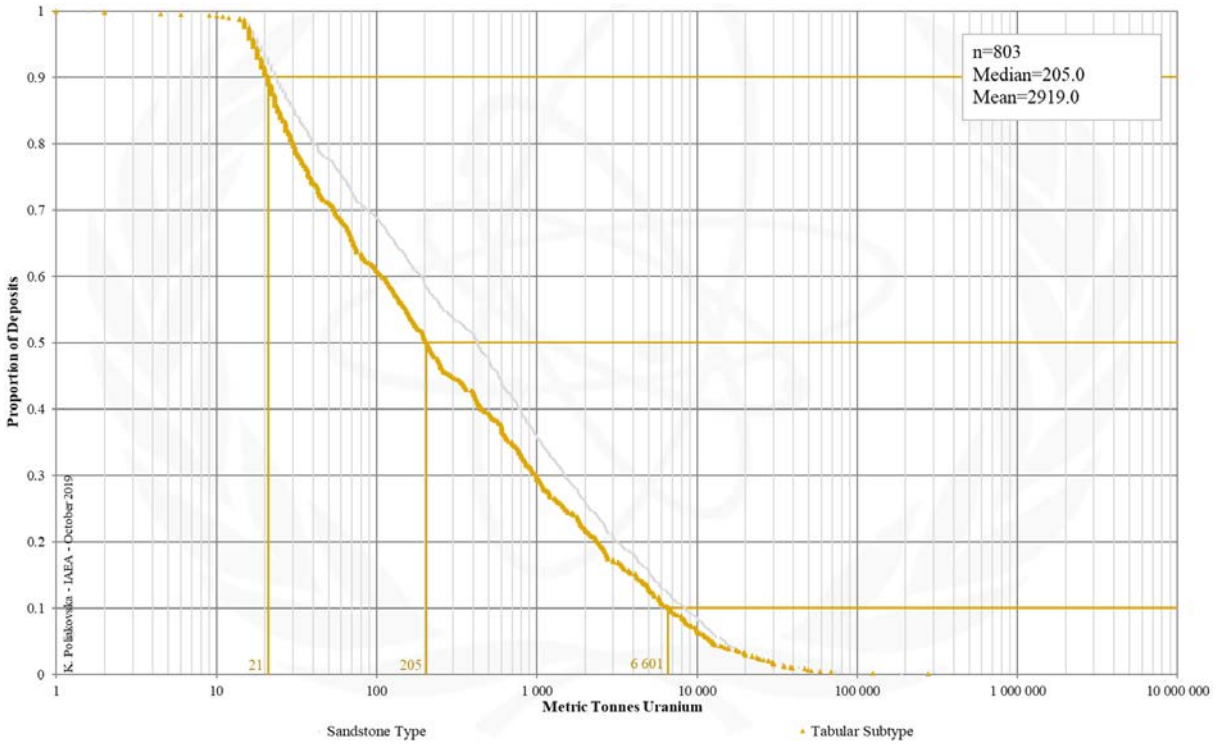

FIG. 9.2.2d. Tonnage Cumulative Probability Plot for Sandstone Tabular data are shown due to lack of data for Continental Fluvial Extrinsic Bitumen uranium deposits from the UDEPO database.

CLASS 9.2.3. Sandstone, Tabular, Continental Fluvial Vanadium-Uranium

Brief Description

- Sandstone deposits refer to uranium accumulations in medium- to coarse-grained siliciclastic sedimentary rocks deposited in continental fluvial, lacustrine or shallow-marine sedimentary environments.
- Uranium is precipitated by reduction processes caused by the presence of a variety of possible reducing agents within the host sandstone such as detrital plant debris, sulphides, ferro-magnesian minerals, anaerobic sulphate-reducing bacteria or migrated fluids from underlying hydrocarbon reservoirs.
- Sandstone deposits are divided into five subtypes with many gradual transitions between them: (9.1) Basal channel, (9.2) tabular, (9.3) roll-front, (9.4) tectonic-lithologic, and (9.5) mafic dyke/sills in Proterozoic sandstones.
- Tabular deposits are further subdivided into several classes based on the type and nature of the respective reducing agent or their metal association: (9.2.1.) Continental fluvial, uranium associated with an intrinsic reductant, (9.2.2.) continental fluvial, uranium associated with extrinsic bitumen, and (9.2.3.) continental fluvial vanadium-uranium.
- Continental fluvial vanadium-uranium deposits occur in reduced fluvial sandstone often deposited as part of a thick sequence of continental red bed sediments.
- The host sands contain carbonaceous plant debris similar to continental fluvial deposits in which uranium is associated with intrinsic reductants.
- The orebodies are commonly tabular, elongate and peneconcordant with bedding.

Type Examples

- Salt Wash member: Henry Basin, Uravan Mineral Belt, USA

Genetically Associated Deposit Types

- Subtype 9.1. Basal channel
- Subtype 9.3. Roll-front
- Subtype 12.1. Lignite-coal, stratiform

Principal Commodities

- U, V

Grades (%) and Tonnages (tU)

- Average: insufficent data
- Median: insufficent data

Number of Deposits

- Deposits: insufficent data

Provinces (undifferentiated from Sandstone Type)

- Alaska Alexander, Alaska Darby Hogatza, Alaska Kokrines Hodzana, Alaska Kuskokwim White Mountains, Alaska Northern Alaska Range, Alaska Porcupine, Alaska Prince William Sound, Alaska Western Alaska Range, Alaska Yukon Tanana, Amadeus Basin, Apuseni Mountains, Aquitaine Basin, Bayingebi Basin Bandan Jilin , BC Okanagan, Bighorn Basin, Black Hills, Black Mesa Basin, Bohemian Basin North, Carnarvon Basin, Carpathians South, Casper Arch, Cerilly Bourbon, Choibalsan Basin, Choir Nyalga Basin, Chu Sarysu Basin, Colio Basin Vol Koli, Congo Basin, Cosquin, Denver Basin, Dnieper Basin, Duruma Tanga Basin, Erlian Basin, Etosha Basin, Fergana Basin, Forez, Franceville Basin, Frome Embayment, Geosinclinal Andino, Gobi Basin Central, Gobi Basin East, Gobi Basin South, Green River Basin, Guandacol, Gyeongsang Basin, Hengyang Basin, Iberian Cordillera, Iullemmeden Basin, Japan Basal Channel, Junggar Basin, Kaiparowits Basin, Kalahari Basin East, Kalahari Basin West, Karasburg Basin, Karoo Basin Mesozoic, Karoo Basin Permian, Khorat Plateau, Kokshetau East, Kokshetau West, Kolari Kittila, Kyzylkum, Lake Ladoga, Laramine Hanna Shirley Basins, Lebombo Nuanetsi Basin, Lodeve Basin, Luangwa Lukusashi Basins, Massif Central South West, Mecsek Mountains, Meghalaya Plateau, Menderes Massif, Morondava Basin, Mount Pisgah, Murphy, Ngalia Basin Sandstone, Nong Son Basin, Norte Subandino, North Canning Basin, Ordos Basin, Pannonian Basin South, Paradox Basin, Parana Basin, Parana Basin Durazno, Parana Basin Figueira, Parana Basin Melo Fraile Muerto, Parana Basin Oviedo Yuti, Parana Basin Rio Grandense Shield, Piceance Basin, Pirie Basin, Powder River Basin, Qaidam Basin, Rhodope Massif, Ruhuhu Selous Basins, Saint Pierre du Cantal, San Jorge Gulf Basin, San Juan Basin, Sarysu Basin North, Sebinkarahisar, Shirley Basin, Shiwan Dashan Basin, Sichuan Basin, Siwalik, Slovenia Permian, Songliao Basin, Southwestern Donets Basin, Spokane Mountain Sherwood, Sukhbaatar Basin, Syr Darya Basin, Tallahassee Creek, Temrezli Basin, Texas Coastal Plain - Catahoula-Oakville, Texas Coastal Plain - Clairborne-Jackson, Texas Coastal Plain - Goliad-Willis-Lissie, Thrace Basin, Tinogasta, Transbaykal Central, Transural, Tuha Basin, Tuli Basin, Uinta Basin, Washakie Cenozoic, Washakie SandWash GreatDivide Mesozoic, West Balkan, West Siberia, West Yunnan, Wind River Basin, Yenisey, Yilgarn South, Yili Ily Basins.

Tectonic Setting

- Continental platforms or intracratonic, intermontane, volcanigenic or sag basins in tectonically stable cratonic environments

Typical Geological Age Range

- Palaeozoic to Cenozoic

Mineral Systems Model

Source

Ground preparation

- Basin formation ± salt tectonism

Energy
- Steepening of hydrological gradient linked to basement uplift due to tectonic reactivation or far-field tectonic events
- Possible contribution from diagenetic compaction and/or salt tectonics

Fluids
- Shallow, oxidised, neutral to alkaline groundwaters
- Deeper, reduced groundwaters and/or basinal brines

Ligands
- No information

Reductants
- Organic matter, humic substances, biogenic and non-biogenic H_2S, hydrocarbons, sulphides

Uranium
- Crystalline basement rocks, granitoids, basin fill (in particular interbedded volcanic ash units), pre-existing uranium deposits

Vanadium
- Detrital magnetite and ilmenite contained within the basin fill

Transport

Fluid pathways
- Regional sandstone aquifers
- Palaeovalleys
- Fault-fracture systems (in particular basin growth structures tapping deeper basin sequences, underlying basins or basement)

Trap

Physical
- Palaeovalley bends, confluences, basal scours and/or areas of channel-widening
- Point bar, braid bar, bar-head sequences
- Fault-fracture systems
- Folds
- Salt domes

Chemical
- In-situ, intrinsic reductants within the host aquifers or wallrocks
- Mobile, extrinsic reductants related to oil and gas systems
- Regional redox fronts

Deposition

Change in redox conditions
- Due to mixing of oxidised, uranium-bearing groundwaters and strongly reduced vanadium-bearing fluids (deeper groundwater system or basinal brines?) in reducing palaeovalley environments

Preservation
- Physical isolation of uranium mineralisation from the flow of oxidised groundwaters
- Capping of uranium-mineralised sequences by younger lavas
- Relative tectonic stability post-uranium mineralisation

Key Reference Bibliography

DAHLKAMP, F. J., Uranium Deposits of the World: USA and Latin America. Springer, Berlin, Heidelberg, 515p (2010).
HUSTON, D. L., VAN DER WIELEN, S. (Eds.), An assessment of the uranium and geothermal prospectivity of east-central South Australia. Geoscience Australia Record, 2011/34, 229p (2011).
INTERNATIONAL ATOMIC ENERGY AGENCY, Geological Classification of Uranium Deposits and Description of Selected Examples. IAEA-TECDOC Series, 1842, 415p (2018).
JAIRETH, S., ROACH, I. C., BASTRAKOV, E., LIU, S., Basin-related uranium mineral systems in Australia: A review of critical features. Ore Geology Reviews, 76, 360-394 (2016).
KYSER, K., Uranium ore deposits. In: TUREKIAN, K., HOLLAND, H. (Eds.), Treatise on Geochemistry, 2nd Edition, Elsevier, 489-513 (2013).
SHAWE, D. R., Uranium-vanadium deposits of the Slick Rock district, Colorado. U.S. Geological Survey Professional Paper 576-F, 80p., 20 plates (2011).

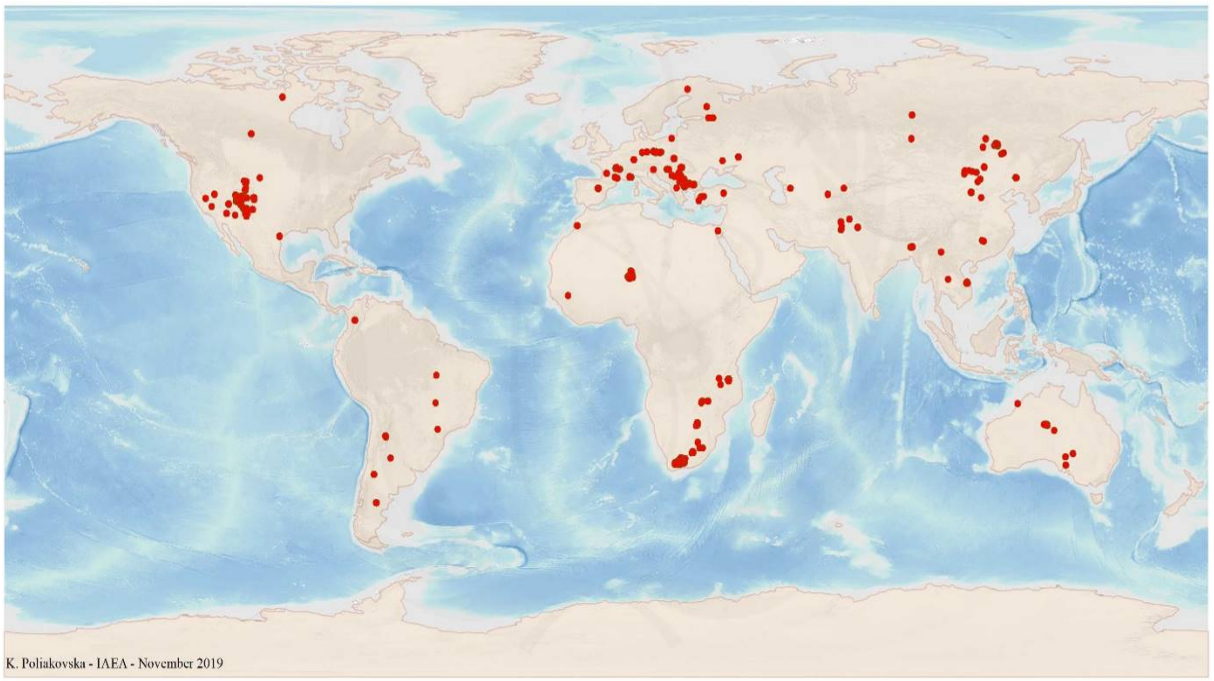

FIG. 9.2.3a. World distribution of selected Sandstone Tabular data are shown due to lack of data for Continental Fluvial Vanadium-Uranium uranium deposits from the UDEPO database.

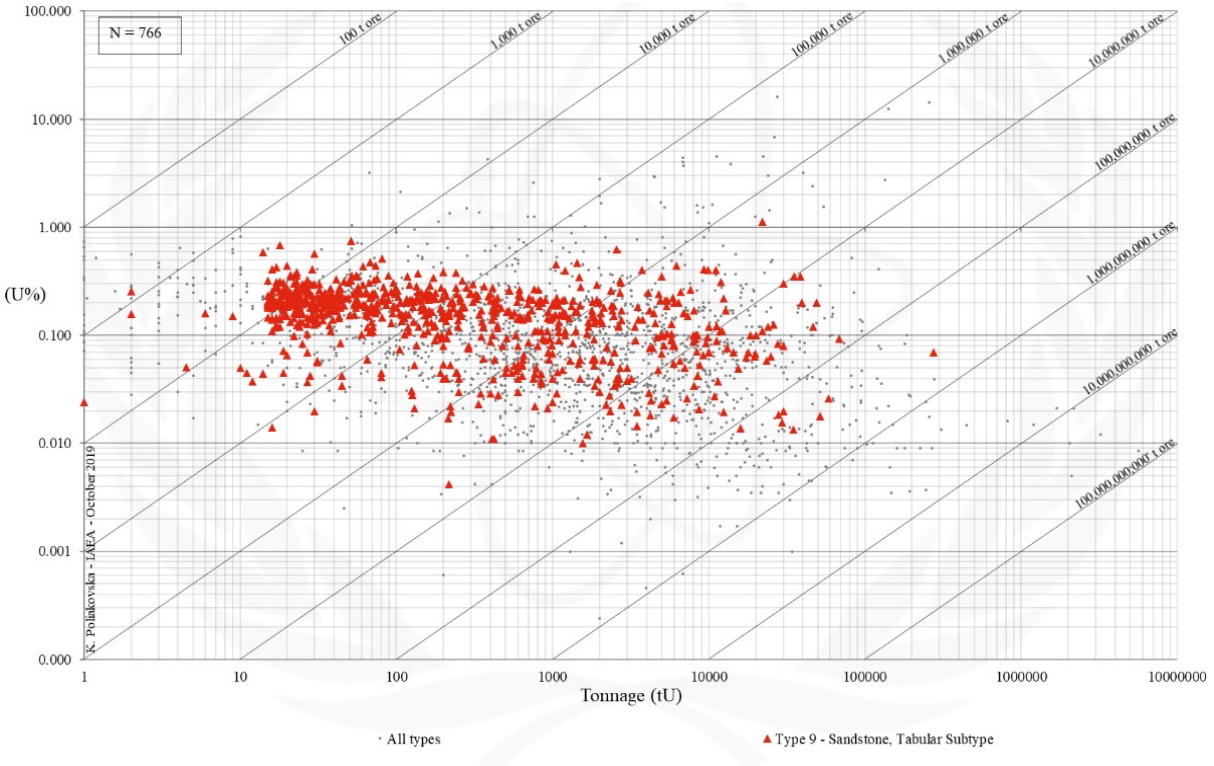

FIG. 9.2.3b. Grade and tonnage scatterplot highlighting Sandstone Tabular data are shown due to lack of data for Continental Fluvial Vanadium-Uranium uranium deposits from the UDEPO database.

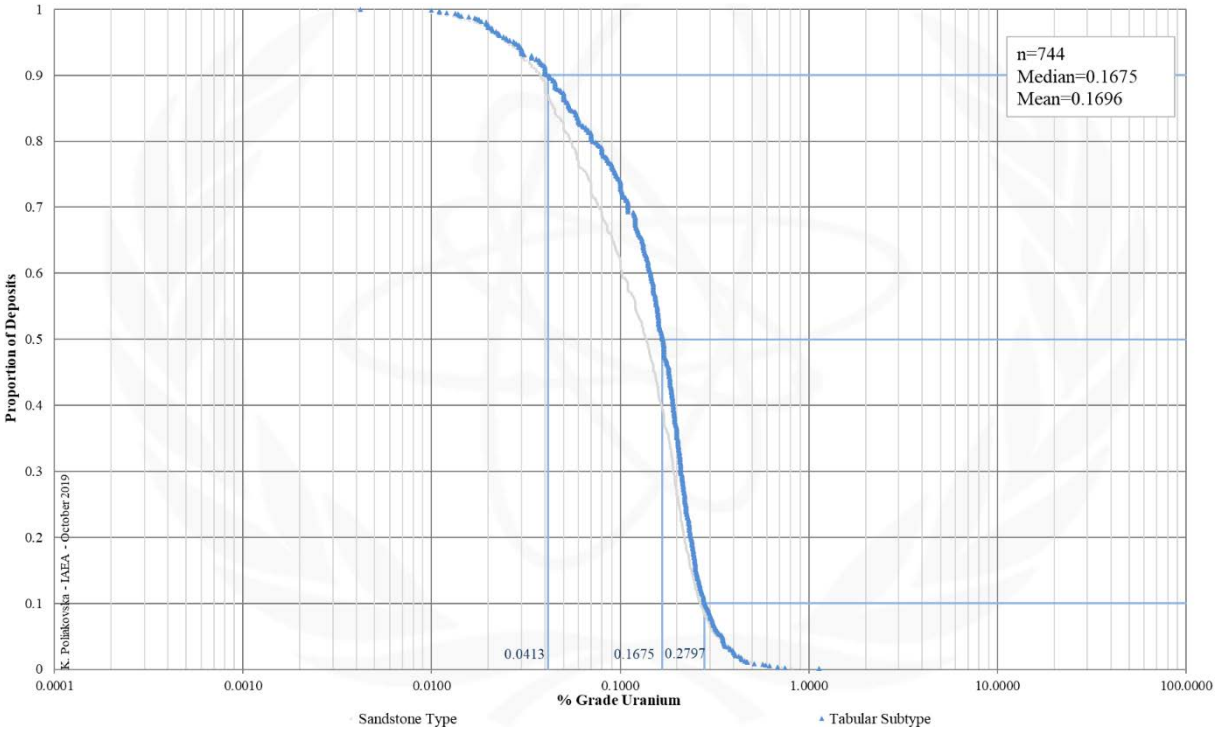

FIG. 9.2.3c. Grade Cumulative Probability Plot for Sandstone Tabular data are shown due to lack of data for Continental Fluvial Vanadium-Uranium uranium deposits from the UDEPO database.

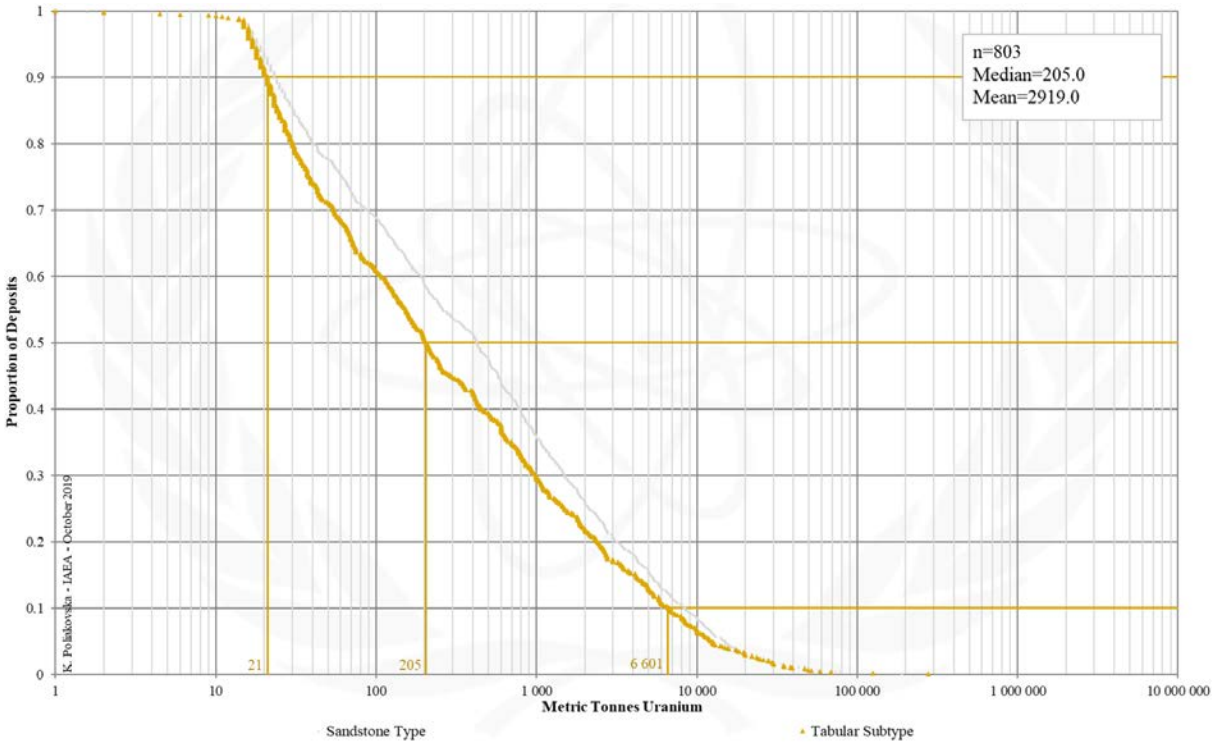

FIG. 9.2.3d. Tonnage Cumulative Probability Plot for Sandstone Tabular data are shown due to lack of data for Continental Fluvial Vanadium-Uranium uranium deposits from the UDEPO database.

SUBTYPE 9.3. Sandstone, Roll-Front

Brief Description

- Sandstone deposits refer to uranium accumulations in medium- to coarse-grained siliciclastic sedimentary rocks deposited in continental fluvial, lacustrine or shallow-marine sedimentary environments.
- Uranium is precipitated by reduction processes caused by the presence of a variety of possible reducing agents within the host sandstone such as intrinsic detrital plant debris, sulphides, ferro-magnesian minerals, anaerobic sulphate-reducing bacteria, extrinsic or migrated fluids from underlying hydrocarbon reservoirs.
- Roll-front deposits are further subdivided into classes based on the type and nature of the respective reducing agent and sedimentary environment: (9.3.1.) Continental basin, uranium associated with intrinsic reductant, (9.3.2.) continental to marginal marine, uranium associated with intrinsic reductant, and (9.3.3.) marginal marine, uranium associated with extrinsic reductant.
- Continental basin and continental to marginal marine deposits in which uranium is associated with an intrinsic reductant are localised along redox fronts between oxidised and reduced sandstone. The roll-shaped orebodies occur in highly permeable sandstones confined between hanging- and footwall aquicludes. The uranium ores take the form of disseminations on the down-gradient side of the redox front.
- Marginal marine deposits in which uranium is associated with extrinsic reductants are localised along faults and in contact with iron sulphide-bearing sandstone. Typical ore host environments include point bar, lateral bar and crevasse splay sediments in fluvial sequences, and barrier and offshore bar sediments in shallow marine sequences.

Genetically Associated Deposit Types

- Subtype 9.1. Basal channel
- Subtype 9.2. Tabular

Type Examples

- Class 9.3.1. Wyoming basins, USA
- Class 9.3.2. Inkai, Moinkum, Karamurun, Zarechnoye: Chu-Sarysu basin, Kazakhstan
- Class 9.3.3. South Texas region, USA

Principal Commodities

- U ± Mo, Re, Sc, Se, Te, V

Grades (%) and Tonnages (tU)

- Average: 0.0985, 4903.3
- Median: 0.0810, 757.0

Number of Deposits

- 457

Provinces (undifferentiated from Sandstone Type)

- Alaska Alexander, Alaska Darby Hogatza, Alaska Kokrines Hodzana, Alaska Kuskokwim White Mountains, Alaska Northern Alaska Range, Alaska Porcupine, Alaska Prince William Sound, Alaska Western Alaska Range, Alaska Yukon Tanana, Amadeus Basin, Apuseni Mountains, Aquitaine Basin, Bayingebi Basin Bandan Jilin , BC Okanagan, Bighorn Basin, Black Hills, Black Mesa Basin, Bohemian Basin North, Carnarvon Basin, Carpathians South, Casper Arch, Cerilly Bourbon, Choibalsan Basin, Choir Nyalga Basin, Chu Sarysu Basin, Colio Basin Vol Koli, Congo Basin, Cosquin, Denver Basin, Dnieper Basin, Duruma Tanga Basin, Erlian Basin, Etosha Basin, Fergana Basin, Forez, Franceville Basin, Frome Embayment, Geosinclinal Andino, Gobi Basin Central, Gobi Basin East, Gobi Basin South, Green River Basin, Guandacol, Gyeongsang Basin, Hengyang Basin, Iberian Cordillera, Iullemmeden Basin, Japan Basal Channel, Junggar Basin, Kaiparowits Basin, Lodeve Basin, Luangwa Lukusashi Basins, Massif Central South West, Mecsek Mountains, Ngalia Basin Sandstone, Norte Subandino, North Canning Basin, Ordos Basin, Parana Basin Amorinopolis Ipora, Parana Basin Durazno, Parana Basin Figueira, Parana Basin Melo Fraile Muerto, Parana Basin Oviedo Yuti, Parana Basin, Powder River Basin, Qaidam Basin, Rhodope Massif, Ruhuhu Selous Basins, Saint Pierre du Cantal, San Jorge Gulf Basin, San Juan Basin, Sarysu Basin North, Sebinkarahisar, Shirley Basin, Shiwan Dashan Basin, Sichuan Basin, Siwalik, Slovenia Permian, Songliao Basin, Southwestern Donets Basin, Spokane Mountain Sherwood, Syr Darya Basin, Tallahassee Creek, Tamsag Basin, Tarim Basin North, Texas Coastal Plain - Catahoula-Oakville, Texas Coastal Plain - Clairborne-Jackson, Texas Coastal Plain - Goliad-Willis-Lissie, Transbaykal Central, Transural, Tuli Basin, West Balkan, West Siberia, Wind River Basin, Yenisey, Yilgarn South, Yili Ily Basins.

Tectonic Setting

- Continental platforms or intracratonic, intermontane, volcanigenic or sag basins in tectonically stable cratonic environments

Typical Geological Age Range

- Palaeozoic to Cenozoic

Mineral Systems Model

Source

Ground preparation

- Orogeny, basin formation, salt tectonism, basement uplift

Energy

- Steepening of hydrological gradient linked to tectonic reactivation/orogenesis, significant sea level drops or salt tectonics

Fluids and gases
- Shallow, oxidised, neutral to alkaline groundwaters
- Reduced hydrocarbon-bearing brines
- CO, H_2S, CH_4, N_2 gases

Ligands
- Ca, Cl, CO_3, P, S

Reductants and reactants
- Organic matter, humic substances, biogenic and non-biogenic H_2S, hydrocarbons, sulphides

Uranium
- Crystalline basement rocks, granitoids (in the sediment source regions), basin fill (in particular interbedded volcanic ash units)

Transport

Fluid pathways
- Regional sandstone aquifers
- Palaeovalleys
- Fault-fracture systems (in particular basin growth structures tapping deeper basin sequences, underlying basins or basement)

Trap

Physical
- Highly permeable fluvial channel sand and gravel facies sediments in palaeovalleys
- Palaeovalleys intercepting interconnected, highly permeable coastal barrier-bar sands
- Hanging- and footwall aquicludes, lithological permeability barriers
- Fault-fracture systems
- Salt domes, shale diapirs, brachyanticlines, monoclines

Chemical
- Intrinsic reductants within the host aquifers or wallrocks
- Extrinsic reductants related to oil and gas systems
- Regional redox fronts

Deposition

Change in redox conditions
- Due to interaction of oxidised, uranium-bearing groundwaters with in-situ, intrinsic reductants
- Due to mixing of oxidised, uranium-bearing groundwaters with reduced hydrocarbon-bearing brines or gases
- Linked to acid neutralisation due to interaction between uranium-bearing fluids and carbonates

Adsorption
- Adsorption of organically complexed uranium onto clays

Preservation

- Physical isolation of uranium mineralisation from the flow of oxidised groundwaters
- Re-reduction of uranium mineralised sequences
- (Diagenetic) alteration of host sequences post-uranium mineralisation
- Basin subsidence
- Relative tectonic stability post-uranium mineralisation

Key Reference Bibliography

BOBERG, W. W., The nature and development of the Wyoming uranium province. In: SIRON, C. R., HITZMAN, M. W., MCLEOD, R. (Eds.), The challenge of finding new mineral resources: Global metallogeny, innovative exploration, and new discoveries. Society of Economic Geologists Special Publication, 15, 317-338 (2010).

DAHLKAMP, F. J., Uranium Deposits of the World: USA and Latin America. Springer, Berlin, Heidelberg, 515p (2010).

HALL, S. M., MIHALASKY, M. J., TURECK, K. R., HAMMARSTROM, J. M., HANNON, M. T., Genetic and grade and tonnage models for sandstone-hosted roll-type uranium deposits, Texas Coastal Plain, USA. Ore Geology Reviews, 80, 716-753 (2017).

HUSTON, D. L., VAN DER WIELEN, S. (Eds.), An assessment of the uranium and geothermal prospectivity of east-central South Australia. Geoscience Australia Record, 2011/34, 229p (2011).

INTERNATIONAL ATOMIC ENERGY AGENCY, Geological Classification of Uranium Deposits and Description of Selected Examples. IAEA-TECDOC Series, 1842, 415p (2018).

JAIRETH, S., MCKAY, A., LAMBERT, I., Association of large sandstone uranium deposits with hydrocarbons. AusGeo News, 89, 8-12 (2008).

JAIRETH, S., ROACH, I. C., BASTRAKOV, E., LIU, S., Basin-related uranium mineral systems in Australia: A review of critical features. Ore Geology Reviews, 76, 360-394 (2016).

KYSER, K., Uranium ore deposits. In: TUREKIAN, K., HOLLAND, H. (Eds.), Treatise on Geochemistry, 2nd Edition, Elsevier, 489-513 (2013).

MIHALASKY, M. J., HALL, S. M., HAMMARSTROM, J. M., TURECK, K. R., HANNON, M. T., BREIT, G. N., ZIELINSKI, R. A., Assessment of undiscovered sandstone-hosted uranium resources in the Texas Coastal Plain, 2015. USGS Fact Sheet 2015-3069, 4p (2015).

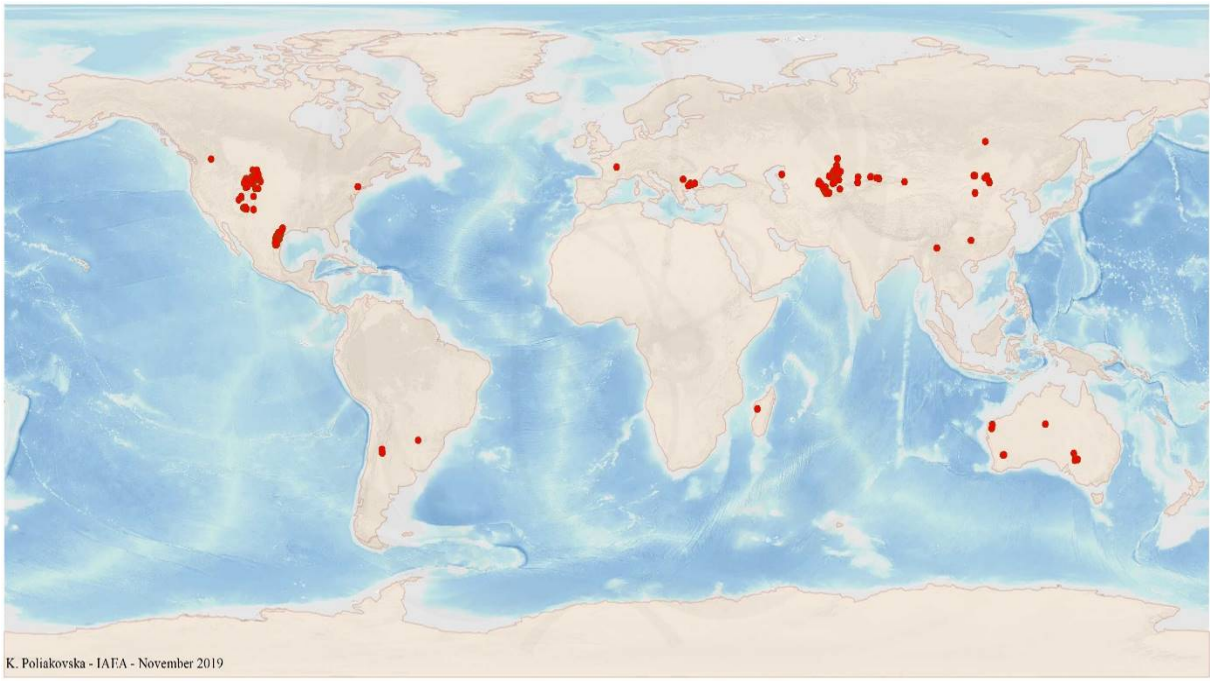

FIG. 9.3a. World distribution of selected Sandstone Roll-Front uranium deposits from the UDEPO database.

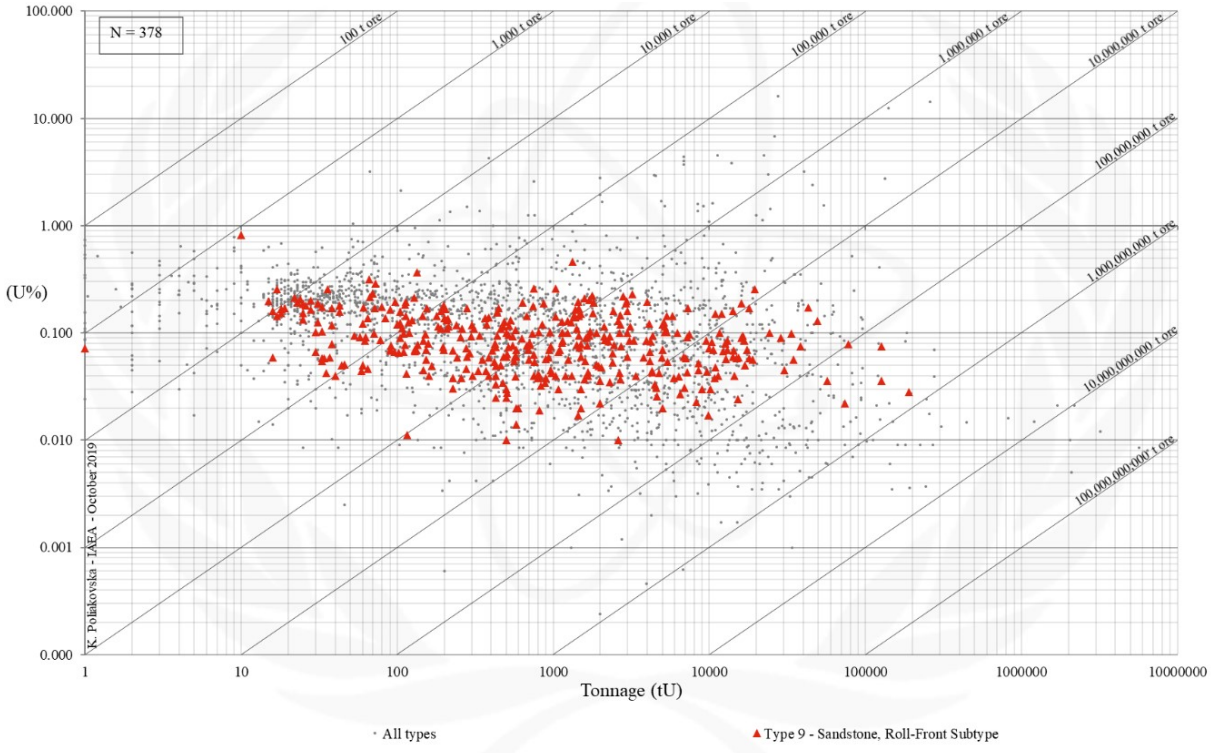

FIG. 9.3b. Grade and tonnage scatterplot highlighting Sandstone Roll-Front uranium deposits from the UDEPO database.

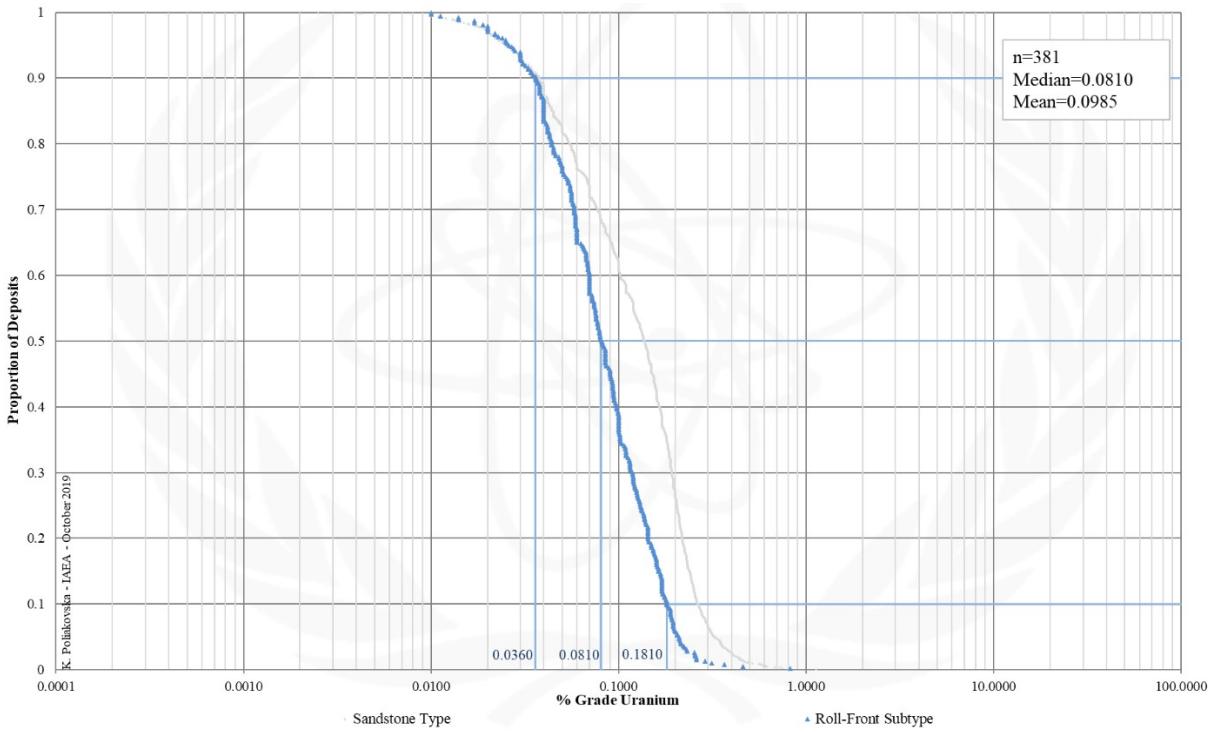

FIG. 9.3c. Grade Cumulative Probability Plot for Sandstone Roll-Front uranium deposits from the UDEPO database.

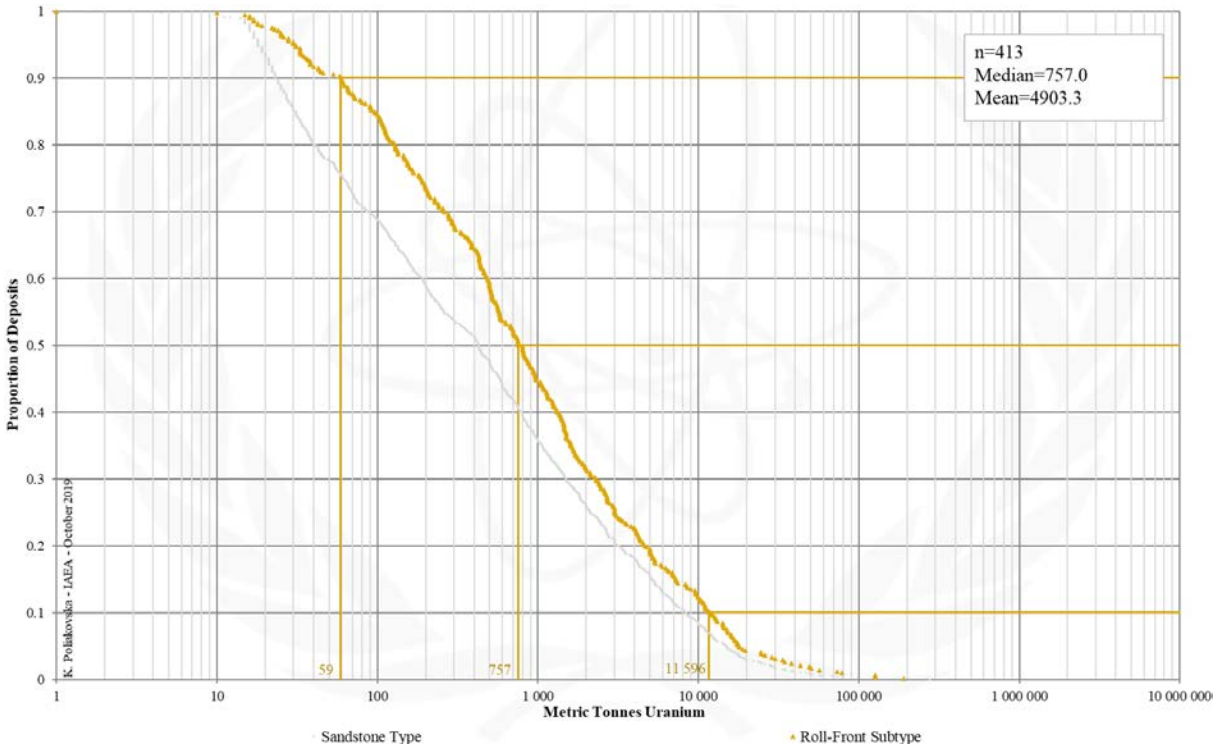

FIG. 9.3d. Tonnage Cumulative Probability Plot for Sandstone Roll-Front uranium deposits from the UDEPO database.

CLASS 9.3.1. Sandstone, Roll-Front, Continental Basin, Intrinsic Reductant

Brief Description

- Sandstone deposits refer to uranium accumulations in medium- to coarse-grained siliciclastic sedimentary rocks deposited in continental fluvial, lacustrine or shallow-marine sedimentary environments.
- Uranium is precipitated by reduction processes caused by the presence of a variety of possible reducing agents within the host sandstone such as detrital plant debris, sulphides, ferro-magnesian minerals, anaerobic sulphate-reducing bacteria or migrated fluids from underlying hydrocarbon reservoirs.
- Sandstone deposits are divided into five subtypes with many gradual transitions between them: (9.1) Basal channel, (9.2) tabular, (9.3) roll-front, (9.4) tectonic-lithologic, and (9.5) mafic dyke/sills in Proterozoic sandstones.
- Roll-front deposits are further subdivided into classes based on the type and nature of the respective reducing agent and sedimentary environment: (9.3.1.) Continental basin, uranium associated with intrinsic reductant, (9.3.2.) continental to marginal marine, uranium associated with intrinsic reductant, and (9.3.3.) marginal marine, uranium associated with extrinsic reductant.
- Continental basin deposits in which uranium is associated with an intrinsic reductant are localised along redox fronts between oxidised and reduced sandstone.
- The roll-shaped orebodies occur in highly permeable sandstones confined between impermeable layers.
- The uranium ores take the form of disseminations on the down-gradient side of the redox front.

Genetically Associated Deposit Types

- Subtype 9.1. Basal channel
- Subtype 9.2. Tabular
- Class 9.3.2. Continental to marginal marine, uranium associated with intrinsic reductant
- Class 9.3.3. Marginal marine, uranium associated with extrinsic reductant

Type Examples

- Wyoming basins, USA

Principal Commodities

- U ± Mo, Se, Te, V

Grades (%) and Tonnages (tU)

- Average: insufficent data
- Median: insufficent data

Number of Deposits

- Deposits: insufficent data

Provinces (undifferentiated from Sandstone Type)

- Alaska Alexander, Alaska Darby Hogatza, Alaska Kokrines Hodzana, Alaska Kuskokwim White Mountains, Alaska Northern Alaska Range, Alaska Porcupine, Alaska Prince William Sound, Alaska Western Alaska Range, Alaska Yukon Tanana, Amadeus Basin, Apuseni Mountains, Aquitaine Basin, Bayingebi Basin Bandan Jilin , BC Okanagan, Bighorn Basin, Black Hills, Black Mesa Basin, Bohemian Basin North, Carnarvon Basin, Carpathians South, Casper Arch, Cerilly Bourbon, Choibalsan Basin, Choir Nyalga Basin, Chu Sarysu Basin, Colio Basin Vol Koli, Congo Basin, Cosquin, Denver Basin, Dnieper Basin, Duruma Tanga Basin, Erlian Basin, Etosha Basin, Fergana Basin, Forez, Franceville Basin, Frome Embayment, Geosinclinal Andino, Gobi Basin Central, Gobi Basin East, Gobi Basin South, Green River Basin, Guandacol, Gyeongsang Basin, Hengyang Basin, Iberian Cordillera, Iullemmeden Basin, Japan Basal Channel, Junggar Basin, Kaiparowits Basin, Kalahari Basin East, Kalahari Basin West, Karasburg Basin, Karoo Basin Mesozoic, Karoo Basin Permian, Khorat Plateau, Kokshetau East, Kokshetau West, Kolari Kittila, Kyzylkum, Lake Ladoga, Laramine Hanna Shirley Basins, Lebombo Nuanetsi Basin, Lodeve Basin, Luangwa Lukusashi Basins, Massif Central South West, Mecsek Mountains, Meghalaya Plateau, Menderes Massif, Morondava Basin, Mount Pisgah, Murphy, Nebraska Plains White River Group, Ngalia Basin Sandstone, Nong Son Basin, Norte Subandino, North Canning Basin, Ordos Basin, Pannonian Basin South, Paradox Basin, Parana Basin Amorinopolis Ipora, Parana Basin Durazno, Parana Basin Figueira, Parana Basin Oviedo Yuti, Parana Basin Rio Grandense Shield, Pirie Basin, Powder River Basin, Qaidam Basin, Rhodope Massif, Ruhuhu Selous Basins, Saint Pierre du Cantal, San Jorge Gulf Basin, San Juan Basin, Sarysu Basin North, Sebinkarahisar, Shirley Basin, Shiwan Dashan Basin, Sichuan Basin, Siwalik, Songliao Basin, Southwestern Donets Basin, Spokane Mountain Sherwood, Sukhbaatar Basin, Syr Darya Basin, Tallahassee Creek, Tamsag Basin, Tarim Basin North, Tarim Basin South, Taurkyr Dome, Temrezli Basin, Texas Coastal Plain - Catahoula-Oakville, Texas Coastal Plain - Clairborne-Jackson, Texas Coastal Plain - Goliad-Willis-Lissie, Thrace Basin, Tinogasta, Transbaykal Central, Tuli Basin, Washakie Cenozoic, Washakie SandWash GreatDivide Mesozoic, West Siberia, West Yunnan, Wind River Basin, Yenisey, Yilgarn South, Yili Ily Basins.

Tectonic Setting

- Intracratonic or intermontane basins in tectonically stable cratonic environments

Typical Geological Age Range

- Palaeozoic to Cenozoic

Mineral Systems Model

Source

Ground preparation

- Orogeny, basin formation, basement uplift

Energy
- Steepening of hydrological gradient linked to tectonic reactivation/orogenesis

Fluids and gases
- Shallow, oxidised, neutral to alkaline groundwaters
- Reduced hydrocarbon-bearing brines
- CO, H_2S, CH_4, N_2 gases

Ligands
- Ca, Cl, CO_3, P, S

Reductants and reactants
- Organic matter, biogenic and non-biogenic H_2S, hydrocarbons, sulphides

Uranium
- Crystalline basement rocks, granitoids, basin fill (in particular interbedded volcanic ash units)

Transport

Fluid pathways
- Regional sandstone aquifers
- Palaeovalleys
- Fault-fracture systems (in particular basin growth structures tapping deeper basin sequences, underlying basins or basement)

Trap

Physical
- Highly permeable fluvial channel sand and gravel facies sediments in palaeovalleys
- Hanging- and footwall aquicludes, lithological permeability barriers
- Fault-fracture systems
- Salt domes, brachyanticlines, monoclines

Chemical
- In-situ reductants within the host aquifers or wallrocks
- Mobile reductants related to oil and gas systems
- Regional redox fronts

Deposition

Change in redox conditions
- Due to interaction of oxidised, uranium-bearing groundwaters with in-situ, intrinsic reductants
- Due to mixing of oxidised, uranium-bearing groundwaters with reduced hydrocarbon-bearing brines
- Linked to acid neutralisation due to interaction between uranium-bearing fluids and carbonates

Preservation

- Physical isolation of uranium mineralisation from the flow of oxidised groundwaters
- Re-reduction of uranium mineralised sequences
- (Diagenetic) alteration of host sequences post-uranium mineralisation
- Basin subsidence
- Relative tectonic stability post-uranium mineralisation

Key Reference Bibliography

BOBERG, W. W., The nature and development of the Wyoming uranium province. In: SIRON, C. R., HITZMAN, M. W., MCLEOD, R. (Eds.), The challenge of finding new mineral resources: Global metallogeny, innovative exploration, and new discoveries. Society of Economic Geologists Special Publication, 15, 317-338 (2010).

DAHLKAMP, F. J., Uranium Deposits of the World: USA and Latin America. Springer, Berlin, Heidelberg, 515p (2010).

HUSTON, D. L., VAN DER WIELEN, S. (Eds.), An assessment of the uranium and geothermal prospectivity of east-central South Australia. Geoscience Australia Record, 2011/34, 229p (2011).

INTERNATIONAL ATOMIC ENERGY AGENCY, Geological Classification of Uranium Deposits and Description of Selected Examples. IAEA-TECDOC Series, 1842, 415p (2018).

JAIRETH, S., ROACH, I. C., BASTRAKOV, E., LIU, S., Basin-related uranium mineral systems in Australia: A review of critical features. Ore Geology Reviews, 76, 360-394 (2016).

KYSER, K., Uranium ore deposits. In: TUREKIAN, K., HOLLAND, H. (Eds.), Treatise on Geochemistry, 2nd Edition, Elsevier, 489-513 (2013).

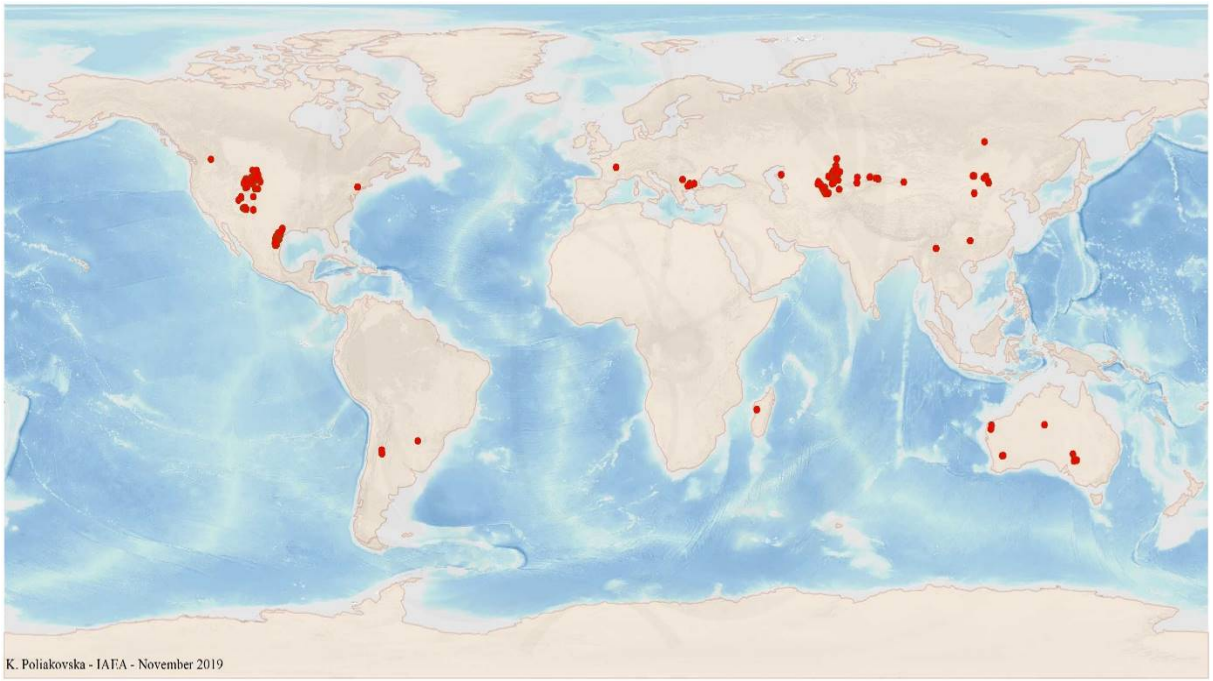

FIG. 9.3.1a. World distribution of selected Sandstone Roll-Front data are shown due to lack of data for Continental Basin Intrinsic Reductant uranium deposits from the UDEPO database.

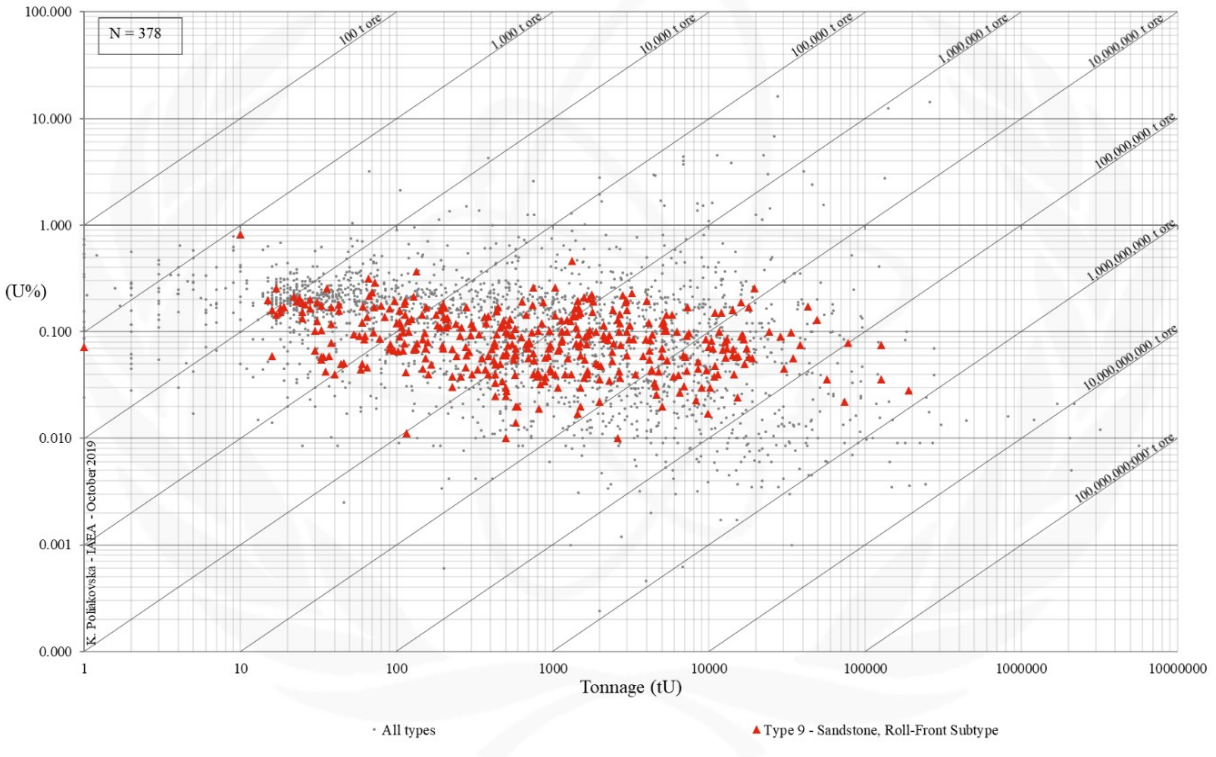

FIG. 9.3.1b. Grade and tonnage scatterplot highlighting Sandstone Roll-Front data are shown due to lack of data for Continental Basin Intrinsic Reductant uranium deposits from the UDEPO database.

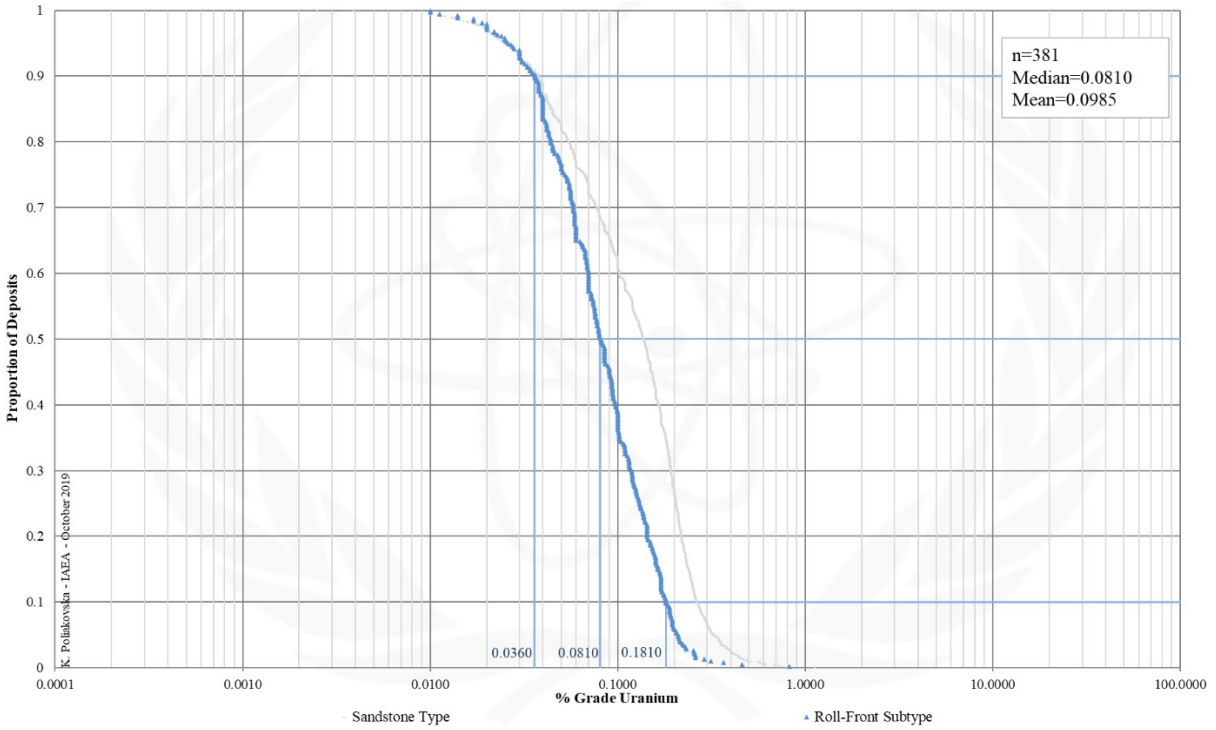

FIG. 9.3.1c. Grade Cumulative Probability Plot for Sandstone Roll-Front data are shown due to lack of data for Continental Basin Intrinsic Reductant uranium deposits from the UDEPO database.

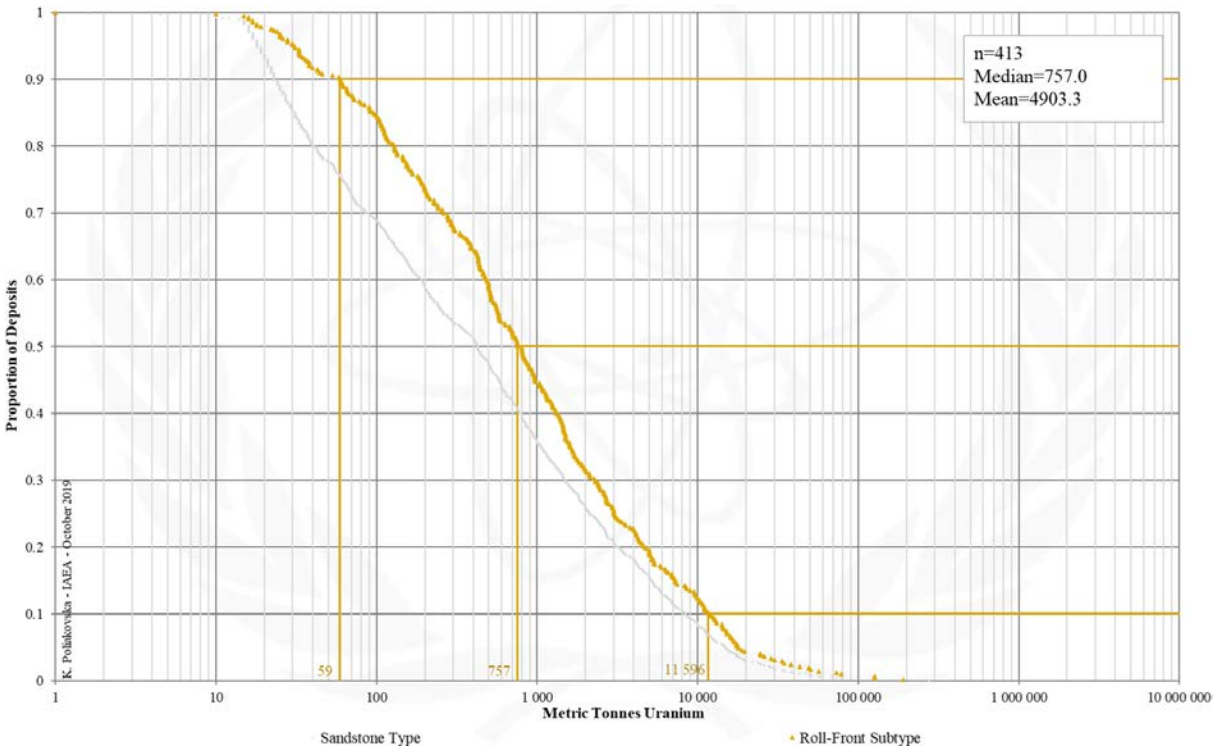

FIG. 9.3.1d. Tonnage Cumulative Probability Plot for Sandstone Roll-Front data are shown due to lack of data for Continental Basin Intrinsic Reductant uranium deposits from the UDEPO database.

CLASS 9.3.2. Sandstone, Roll-Front, Continental to Marginal Marine, Intrinsic Reductant

Brief Description

- Sandstone deposits refer to uranium accumulations in medium- to coarse-grained siliciclastic sedimentary rocks deposited in continental fluvial, lacustrine or shallow-marine sedimentary environments.
- Uranium is precipitated by reduction processes caused by the presence of a variety of possible reducing agents within the host sandstone such as detrital plant debris, sulphides, ferro-magnesian minerals, anaerobic sulphate-reducing bacteria or migrated fluids from underlying hydrocarbon reservoirs.
- Sandstone deposits are divided into five subtypes with many gradual transitions between them: (9.1) Basal channel, (9.2) tabular, (9.3) roll-front, (9.4) tectonic-lithologic, and (9.5) mafic dyke/sills in Proterozoic sandstones.
- Roll-front deposits are further subdivided into classes based on the type and nature of the respective reducing agent and sedimentary environment: (9.3.1.) Continental basin, uranium associated with intrinsic reductant, (9.3.2.) continental to marginal marine, uranium associated with intrinsic reductant, and (9.3.3.) marginal marine, uranium associated with extrinsic reductant.
- Continental to marginal marine deposits in which uranium is associated with an intrinsic reductant are localised along redox fronts between oxidised and reduced sandstone.
- The roll-shaped orebodies occur in highly permeable sandstones confined between hanging- and footwall aquicludes.
- The uranium ores take the form of disseminations on the down-gradient side of the redox front.

Genetically Associated Deposit Types

- Subtype 9.1. Basal channel
- Subtype 9.2. Tabular
- Class 9.3.1. Continental basin, uranium associated with intrinsic reductant
- Class 9.3.3. Marginal marine, uranium associated with extrinsic reductant

Type Examples

- Inkai, Moinkum, Karamurun, Zarechnoye: Chu-Sarysu basin, Kazakhstan

Principal Commodities

- U ± Re, Se, Sc

Grades (%) and Tonnages (tU)

- Average: insufficent data
- Median: insufficent data

Number of Deposits

- Deposits: insufficent data

Provinces (undifferentiated from Sandstone Type)

- Alaska Alexander, Alaska Darby Hogatza, Alaska Kokrines Hodzana, Alaska Kuskokwim White Mountains, Alaska Northern Alaska Range, Alaska Porcupine, Alaska Prince William Sound, Alaska Western Alaska Range, Alaska Yukon Tanana, Amadeus Basin, Apuseni Mountains, Aquitaine Basin, Bayingebi Basin Bandan Jilin , BC Okanagan, Bighorn Basin, Black Hills, Black Mesa Basin, Bohemian Basin North, Carnarvon Basin, Carpathians South, Casper Arch, Cerilly Bourbon, Choibalsan Basin, Choir Nyalga Basin, Chu Sarysu Basin, Colio Basin Vol Koli, Congo Basin, Cosquin, Denver Basin, Dnieper Basin, Duruma Tanga Basin, Erlian Basin, Etosha Basin, Fergana Basin, Forez, Franceville Basin, Frome Embayment, Geosinclinal Andino, Gobi Basin Central, Gobi Basin East, Gobi Basin South, Green River Basin, Guandacol, Gyeongsang Basin, Hengyang Basin, Iberian Cordillera, Iullemmeden Basin, Japan Basal Channel, Junggar Basin, Kaiparowits Basin, Kalahari Basin East, Kalahari Basin West, Karasburg Basin, Karoo Basin Mesozoic, Karoo Basin Permian, Khorat Plateau, Kokshetau East, Kokshetau West, Kolari Kittila, Kyzylkum, Nebraska Plains White River Group, Ngalia Basin Sandstone, Nong Son Basin, Norte Subandino, North Canning Basin, Ordos Basin, Pannonian Basin South, Paradox Basin, Parana Basin Amorinopolis Ipora, Parana Basin Durazno, Parana Basin Figueira, Parana Basin Melo Fraile Muerto, Parana Basin Oviedo Yuti, Parana Basin Rio Grandense Shield, Piceance Basin, Pirie Basin, Powder River Basin, Qaidam Basin, Rhodope Massif, Ruhuhu Selous Basins, Saint Pierre du Cantal, San Jorge Gulf Basin, San Juan Basin, Sarysu Basin North, Sebinkarahisar, Shirley Basin, Shiwan Dashan Basin, Sichuan Basin, Siwalik, Slovenia Permian, Songliao Basin, Southwestern Donets Basin, Spokane Mountain Sherwood, Sukhbaatar Basin, Syr Darya Basin, Tallahassee Creek, Tamsag Basin, Tarim Basin North, Tarim Basin South, Taurkyr Dome, Texas Coastal Plain - Clairborne-Jackson, Texas Coastal Plain - Goliad-Willis-Lissie, Thrace Basin, Tinogasta, Transbaykal Central, Transural, Tuha Basin, Tuli Basin, Uinta Basin, Washakie Cenozoic, Washakie SandWash GreatDivide Mesozoic, West Yunnan, Wind River Basin, Yenisey, Yilgarn South, Yili Ily Basins.

Tectonic Setting

- Continental platforms or intracratonic, intermontane, volcanigenic or sag basins in tectonically stable cratonic environments

Typical Geological Age Range

- Palaeozoic to Cenozoic

Mineral Systems Model

Source

Ground preparation

- Orogeny, basin formation, basement uplift

Energy
- Steepening of hydrological gradient linked to tectonic reactivation/orogenesis

Fluids and gases
- Shallow, oxidised, neutral to alkaline groundwaters
- Reduced hydrocarbon-bearing brines
- CO, H_2S, CH_4, N_2 gases

Ligands
- Ca, Cl, CO_3, P, S

Reductants and reactants
- Organic matter, biogenic and non-biogenic H_2S, hydrocarbons, sulphides

Uranium
- Crystalline basement rocks, granitoids, basin fill (in particular interbedded volcanic ash units)

Transport

Fluid pathways
- Regional sandstone aquifers
- Palaeovalleys
- Fault-fracture systems (in particular basin growth structures tapping deeper basin sequences, underlying basins or basement)

Trap

Physical
- Highly permeable fluvial channel sand and gravel facies sediments in palaeovalleys
- Hanging- and footwall aquicludes, lithological permeability barriers
- Fault-fracture systems
- Salt domes, brachyanticlines, monoclines

Chemical
- In-situ reductants within the host aquifers or wallrocks
- Mobile reductants related to oil and gas systems
- Regional redox fronts

Deposition

Change in redox conditions
- Due to interaction of oxidised, uranium-bearing groundwaters with in-situ, intrinsic reductants
- Due to mixing of oxidised, uranium-bearing groundwaters with reduced hydrocarbon-bearing brines

Preservation

- Physical isolation of uranium mineralisation from the flow of oxidised groundwaters
- Re-reduction of uranium mineralised sequences
- (Diagenetic) alteration of host sequences post-uranium mineralisation
- Basin subsidence
- Relative tectonic stability post-uranium mineralisation

Key Reference Bibliography

DAHLKAMP, F. J., Uranium Deposits of the World: USA and Latin America. Springer, Berlin, Heidelberg, 515p (2010).

HUSTON, D. L., VAN DER WIELEN, S. (Eds.), An assessment of the uranium and geothermal prospectivity of east-central South Australia. Geoscience Australia Record, 2011/34, 229p (2011).

INTERNATIONAL ATOMIC ENERGY AGENCY, Geological Classification of Uranium Deposits and Description of Selected Examples. IAEA-TECDOC Series, 1842, 415p (2018).

JAIRETH, S., MCKAY, A., LAMBERT, I., Association of large sandstone uranium deposits with hydrocarbons. AusGeo News, 89, 8-12 (2008).

JAIRETH, S., ROACH, I. C., BASTRAKOV, E., LIU, S., Basin-related uranium mineral systems in Australia: A review of critical features. Ore Geology Reviews, 76, 360-394 (2016).

KYSER, K., Uranium ore deposits. In: TUREKIAN, K., HOLLAND, H. (Eds.), Treatise on Geochemistry, 2nd Edition, Elsevier, 489-513 (2013).

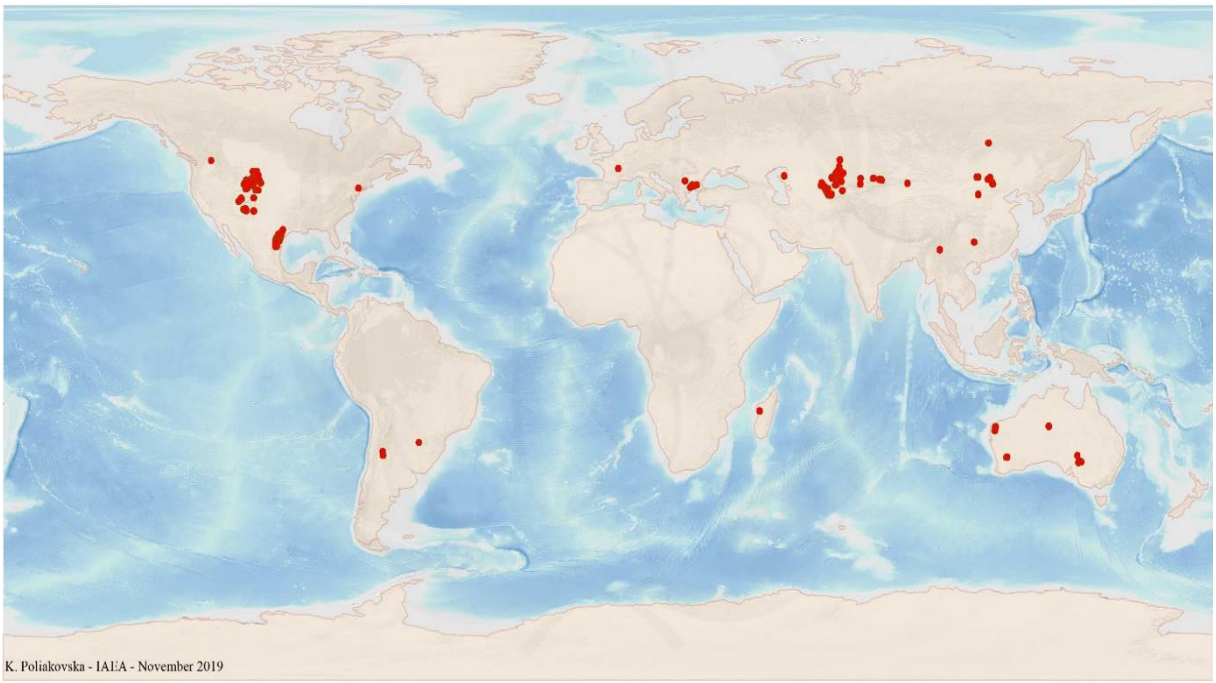

FIG. 9.3.2a. World distribution of selected Sandstone Roll-Front data are shown due to lack of data for Continental to Marginal Marine Intrinsic Reductant uranium deposits from the UDEPO database.

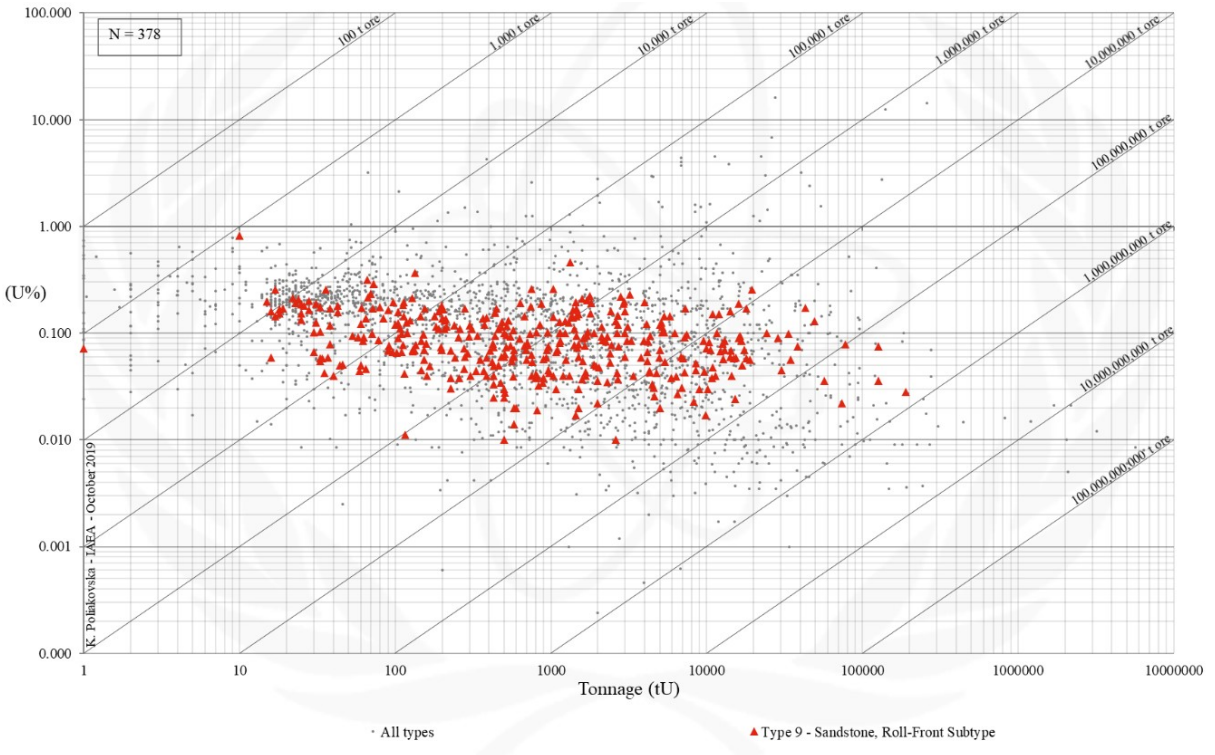

FIG. 9.3.2b. Grade and tonnage scatterplot highlighting Sandstone Roll-Front data are shown due to lack of data for Continental to Marginal Marine Intrinsic Reductant uranium deposits from the UDEPO database.

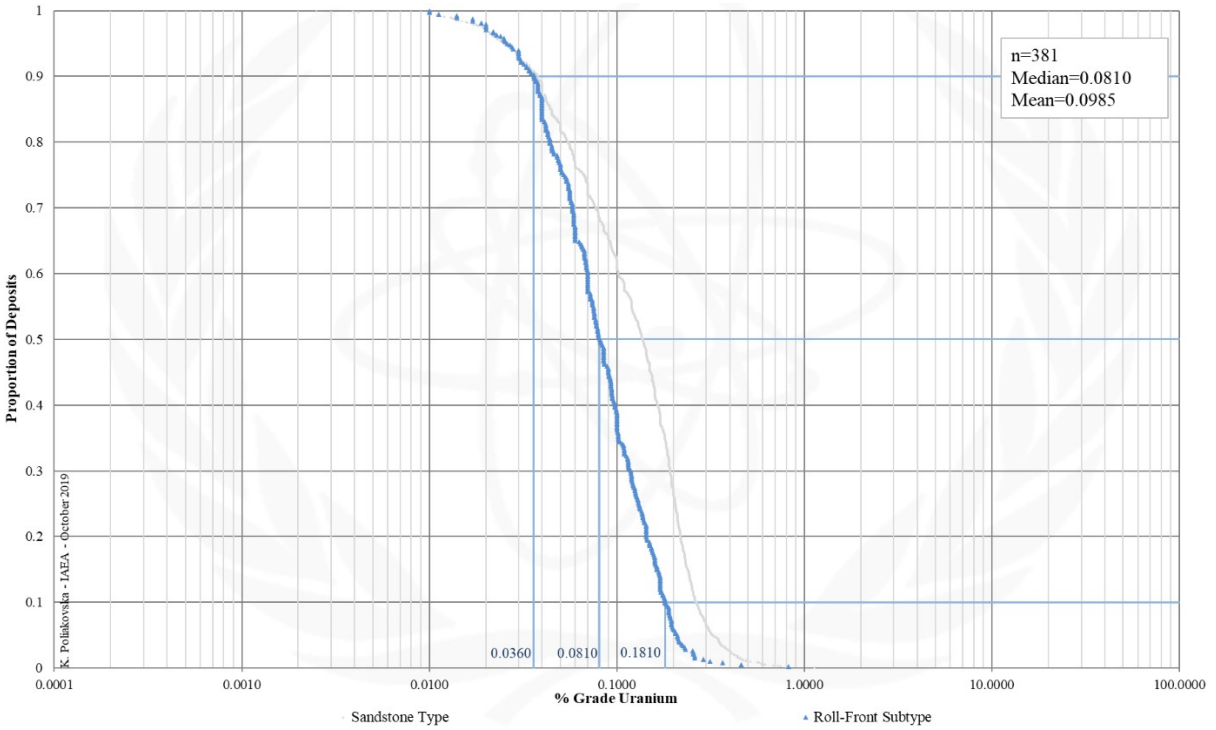

FIG. 9.3.2c. Grade Cumulative Probability Plot for Sandstone Roll-Front data are shown due to lack of data for Continental to Marginal Marine Intrinsic Reductant uranium deposits from the UDEPO database.

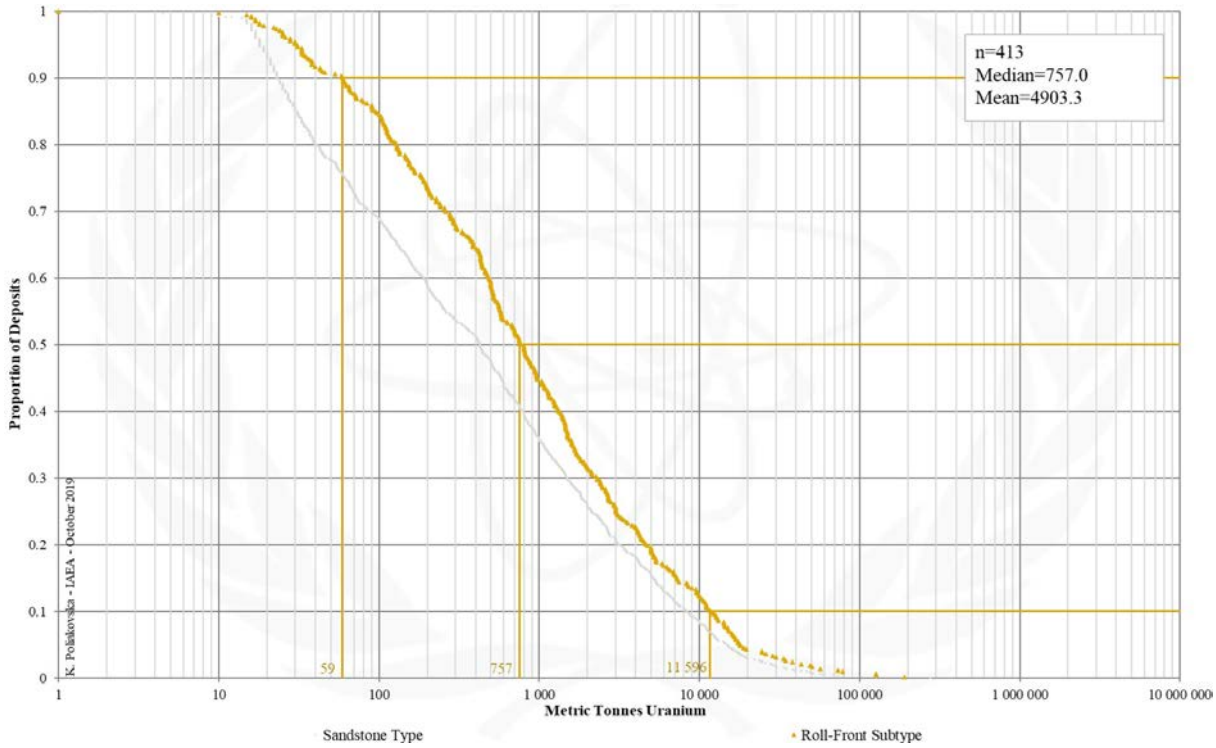

FIG. 9.3.2d. Tonnage Cumulative Probability Plot for Sandstone Roll-Front data are shown due to lack of data for Continental to Marginal Marine Intrinsic Reductant uranium deposits from the UDEPO database.

CLASS 9.3.3. Sandstone, Roll-Front, Marginal Marine, Extrinsic Reductant

Brief Description

- Sandstone deposits refer to uranium accumulations in medium- to coarse-grained siliciclastic sedimentary rocks deposited in continental fluvial, lacustrine or shallow-marine sedimentary environments.
- Uranium is precipitated by reduction processes caused by the presence of a variety of possible reducing agents within the host sandstone such as detrital plant debris, sulphides, ferro-magnesian minerals, anaerobic sulphate-reducing bacteria or migrated fluids from underlying hydrocarbon reservoirs.
- Sandstone deposits are divided into five subtypes with many gradual transitions between them: (9.1) Basal channel, (9.2) tabular, (9.3) roll-front, (9.4) tectonic-lithologic, and (9.5) mafic dyke/sills in Proterozoic sandstones.
- Roll-front deposits are further subdivided into classes based on the type and nature of the respective reducing agent and sedimentary environment: (9.3.1.) Continental basin, uranium associated with intrinsic reductant, (9.3.2.) continental to marginal marine, uranium associated with intrinsic reductant, and (9.3.3.) marginal marine, uranium associated with extrinsic reductant.
- Marginal marine deposits in which uranium is associated with extrinsic reductants are localised along faults and in contact with iron sulphide-bearing sandstone.
- Typical ore host environments include point bar, lateral bar and crevasse splay sediments in fluvial sequences, and barrier and offshore bar sediments in shallow marine sequences.

Genetically Associated Deposit Types

- Subtype 9.1. Basal channel
- Subtype 9.2. Tabular
- Class 9.3.1. Continental basin, uranium associated with intrinsic reductant
- Class 9.3.2. Continental to marginal marine, uranium associated with intrinsic reductant

Type Examples

- South Texas region, USA

Principal Commodities

- U

Grades (%) and Tonnages (tU)

- Average: insufficent data
- Median: insufficent data

Number of Deposits

- Deposits: insufficent data

Provinces (undifferentiated from Sandstone Type)

- Alaska Alexander, Alaska Darby Hogatza, Alaska Kokrines Hodzana, Alaska Kuskokwim White Mountains, Alaska Northern Alaska Range, Alaska Porcupine, Alaska Prince William Sound, Alaska Western Alaska Range, Alaska Yukon Tanana, Amadeus Basin, Apuseni Mountains, Aquitaine Basin, Bayingebi Basin Bandan Jilin , BC Okanagan, Bighorn Basin, Black Hills, Black Mesa Basin, Bohemian Basin North, Carnarvon Basin, Carpathians South, Casper Arch, Cerilly Bourbon, Choibalsan Basin, Choir Nyalga Basin, Chu Sarysu Basin, Colio Basin Vol Koli, Congo Basin, Cosquin, Denver Basin, Dnieper Basin, Duruma Tanga Basin, Erlian Basin, Etosha Basin, Fergana Basin, Forez, Franceville Basin, Frome Embayment, Geosinclinal Andino, Gobi Basin Central, Gobi Basin East, Gobi Basin South, Green River Basin, Guandacol, Gyeongsang Basin, Hengyang Basin, Iberian Cordillera, Iullemmeden Basin, Japan Basal Channel, Junggar Basin, Kaiparowits Basin, Kalahari Basin East, Kalahari Basin West, Karasburg Basin, Karoo Basin Mesozoic, Karoo Basin Permian, Khorat Plateau, Kokshetau East, Kokshetau West, Kolari Kittila, Kyzylkum, Lake Ladoga, Nebraska Plains White River Group, Ngalia Basin Sandstone, Nong Son Basin, Norte Subandino, North Canning Basin, Ordos Basin, Pannonian Basin South, Paradox Basin, Parana Basin Amorinopolis Ipora, Parana Basin Durazno, Parana Basin Figueira, Parana Basin Melo Fraile Muerto, Parana Basin Oviedo Yuti, Parana Basin Rio Grandense Shield, Piceance Basin, Pirie Basin, Powder River Basin, Qaidam Basin, Rhodope Massif, Ruhuhu Selous Basins, Saint Pierre du Cantal, San Jorge Gulf Basin, San Juan Basin, Sarysu Basin North, Sebinkarahisar, Shirley Basin, Shiwan Dashan Basin, Sichuan Basin, Siwalik, Slovenia Permian, Songliao Basin, Southwestern Donets Basin, Spokane Mountain Sherwood, Sukhbaatar Basin, Syr Darya Basin, Tallahassee Creek, Tamsag Basin, Tarim Basin North, Tarim Basin South, Taurkyr Dome, Temrezli Basin, Texas Coastal Plain - Catahoula-Oakville, Texas Coastal Plain - Clairborne-Jackson, Texas Coastal Plain - Goliad-Willis-Lissie, Thrace Basin, Tinogasta, Transbaykal Central, Transural, Tuha Basin, Tuli Basin, Uinta Basin, Washakie Cenozoic, Washakie SandWash GreatDivide Mesozoic, West Balkan, West Siberia, West Yunnan, Wind River Basin, Yenisey, Yilgarn South, Yili Ily Basins.

Tectonic Setting

- Continental platform basins in tectonically stable cratonic environments

Typical Geological Age Range

- Palaeozoic to Cenozoic

Mineral Systems Model

Source

Ground preparation

- Basin formation
- Salt tectonism

Energy
- Steepening of hydrological gradient linked to significant sea level drops and salt tectonics

Fluids
- Shallow, oxidised, neutral to alkaline groundwaters
- Reduced hydrocarbon-bearing brines

Ligands
- Ca, Cl, CO_3, P, S

Reductants and reactants
- Organic matter, humic substances, biogenic and non-biogenic H_2S, hydrocarbons, sulphides

Uranium
- Crystalline basement rocks and granitoids (in the sediment source regions)
- Basin fill (in particular interbedded volcanic ash units)

Transport

Fluid pathways
- Regional sandstone aquifers
- Palaeovalleys
- Fault-fracture systems (in particular basin growth structures tapping deeper basin sequences, underlying basins or basement)

Trap

Physical
- Palaeovalleys intercepting interconnected, highly permeable coastal barrier-bar sands
- Salt domes, shale diapirs
- Fault-fracture systems

Chemical
- Intrinsic reductants within the host aquifers or wallrocks
- Extrinsic reductants related to oil and gas systems
- Regional redox fronts

Deposition

Change in redox conditions
- Due to interaction of oxidised, uranium-bearing groundwaters with intrinsic reductants
- Due to mixing of oxidised, uranium-bearing groundwaters with reduced hydrocarbon-bearing brines or gases

Adsorption
- Adsorption of organically complexed uranium onto clays

Preservation
- Physical isolation of uranium mineralisation from the flow of oxidised groundwaters
- Re-reduction of uranium mineralised sequences
- (Diagenetic) alteration of host sequences post-uranium mineralisation
- Basin subsidence
- Relative tectonic stability post-uranium mineralisation

Key Reference Bibliography

DAHLKAMP, F. J., Uranium Deposits of the World: USA and Latin America. Springer, Berlin, Heidelberg, 515p (2010).

HALL, S. M., MIHALASKY, M. J., TURECK, K. R., HAMMARSTROM, J. M., HANNON, M. T., Genetic and grade and tonnage models for sandstone-hosted roll-type uranium deposits, Texas Coastal Plain, USA. Ore Geology Reviews, 80, 716-753 (2017).

HUSTON, D. L., VAN DER WIELEN, S. (Eds.), An assessment of the uranium and geothermal prospectivity of east-central South Australia. Geoscience Australia Record, 2011/34, 229p (2011).

INTERNATIONAL ATOMIC ENERGY AGENCY, Geological Classification of Uranium Deposits and Description of Selected Examples. IAEA-TECDOC Series, 1842, 415p (2018).

JAIRETH, S., ROACH, I. C., BASTRAKOV, E., LIU, S., Basin-related uranium mineral systems in Australia: A review of critical features. Ore Geology Reviews, 76, 360-394 (2016).

KYSER, K., Uranium ore deposits. In: TUREKIAN, K., HOLLAND, H. (Eds.), Treatise on Geochemistry, 2nd Edition, Elsevier, 489-513 (2013).

MIHALASKY, M. J., HALL, S. M., HAMMARSTROM, J. M., TURECK, K. R., HANNON, M. T., BREIT, G. N., ZIELINSKI, R. A., Assessment of undiscovered sandstone-hosted uranium resources in the Texas Coastal Plain, 2015. USGS Fact Sheet 2015-3069, 4p (2015).

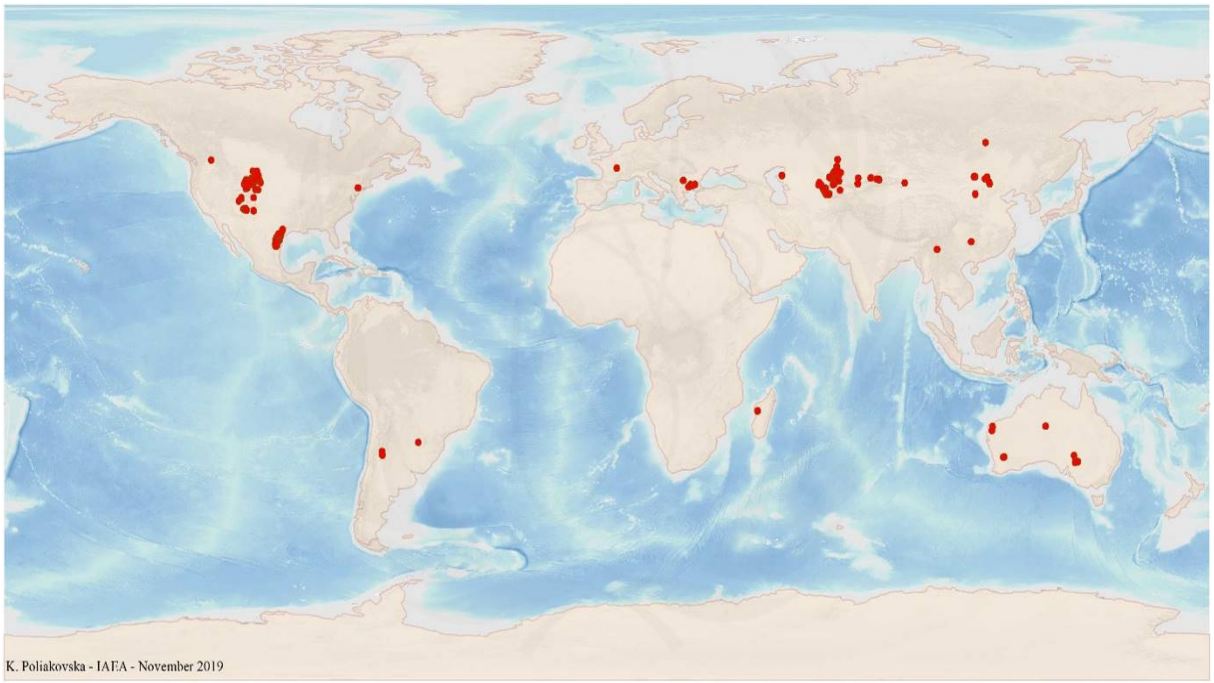

FIG. 9.3.3a. World distribution of selected Sandstone Roll-Front data are shown due to lack of data for Marginal Marine Extrinsic Reductant uranium deposits from the UDEPO database.

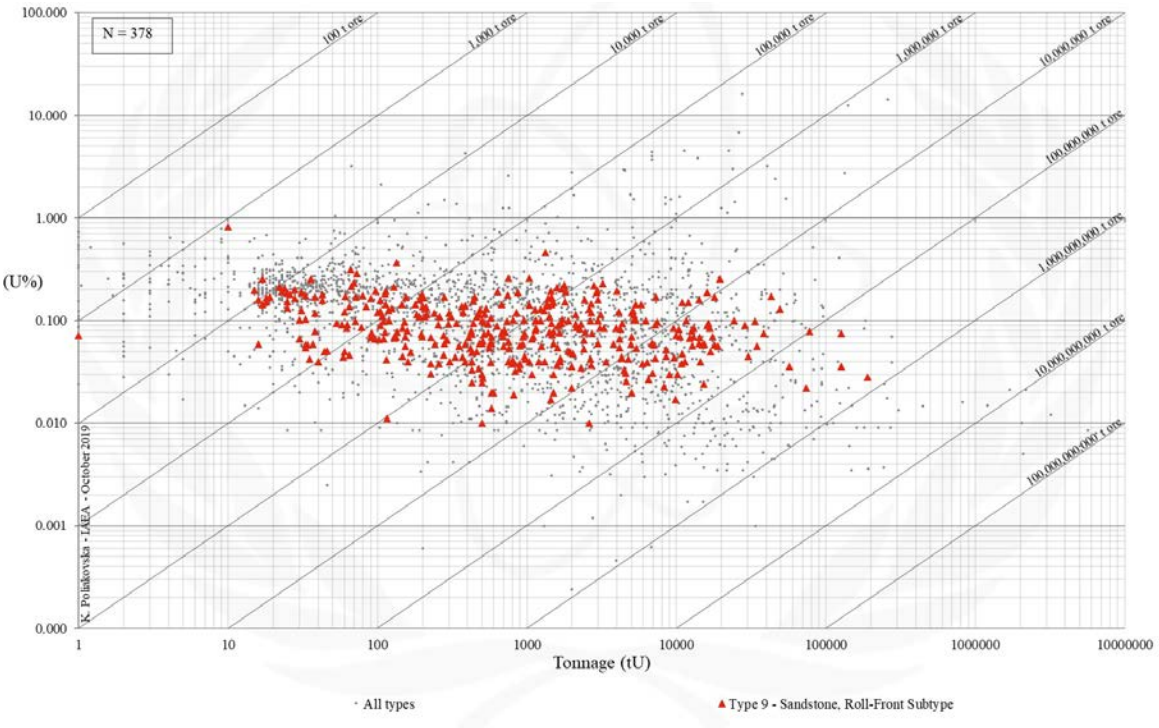

FIG. 9.3.3b. Grade and tonnage scatterplot highlighting Sandstone Roll-Front data are shown due to lack of data for Marginal Marine Extrinsic Reductant uranium deposits from the UDEPO database.

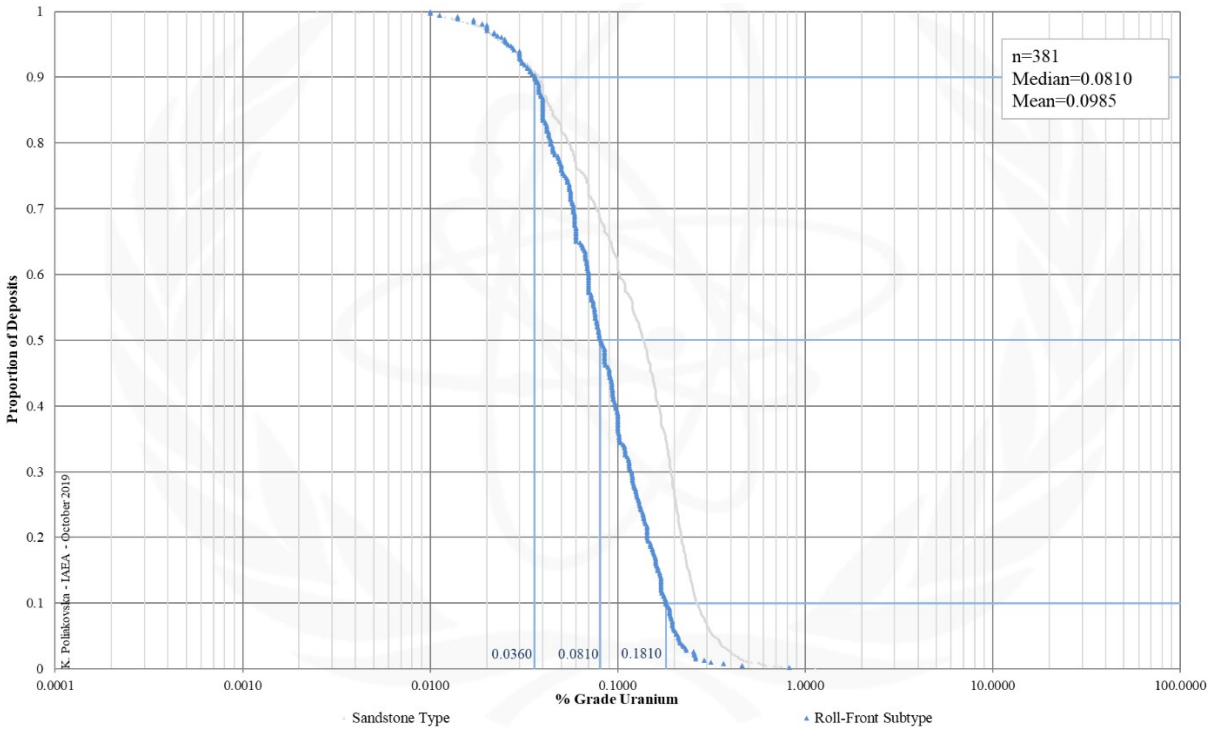

FIG. 9.3.3c. Grade Cumulative Probability Plot for Sandstone Roll-Front data are shown due to lack of data for Marginal Marine Extrinsic Reductant uranium deposits from the UDEPO database.

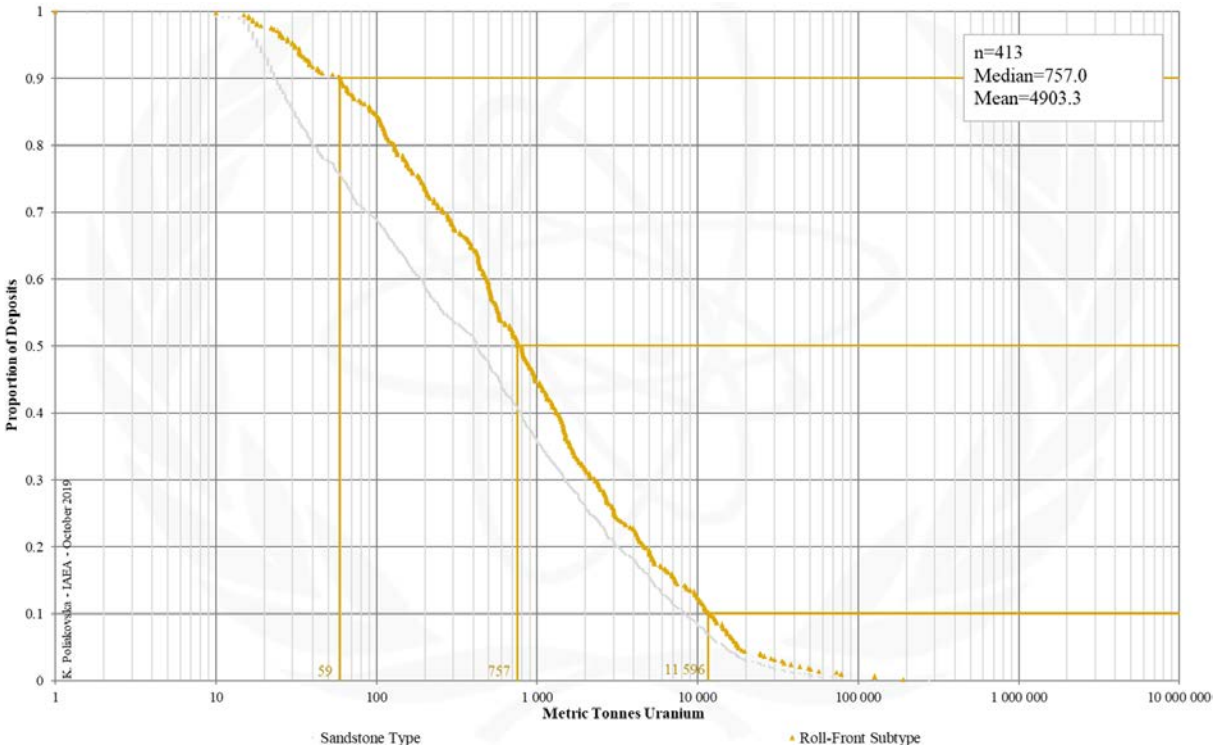

FIG. 9.3.3d. Tonnage Cumulative Probability Plot for Sandstone Roll-Front data are shown due to lack of data for Marginal Marine Extrinsic Reductant uranium deposits from the UDEPO database.

CLASS 9.4. Sandstone, Tectonic-Lithologic

Brief Description

- Sandstone deposits refer to uranium accumulations in medium- to coarse-grained siliciclastic sedimentary rocks deposited in continental fluvial, lacustrine or shallow-marine sedimentary environments.
- Uranium is precipitated by reduction processes caused by the presence of a variety of possible reducing agents within the host sandstone such as intrinsic detrital plant debris, sulphides, ferro-magnesian minerals, anaerobic sulphate-reducing bacteria, or extrinsic migrated fluids from underlying hydrocarbon reservoirs.
- Tectonic-lithologic deposits exhibit strong structural and lithological permeability controls on uranium mineralisation.
- Hydrocarbon traps play an important role in the localisation and generation of these deposits.

Genetically Associated Deposit Types

- Subtype 9.1. Basal channel
- Subtype 9.2. Tabular
- Subtype 9.3. Roll-front
- Subtype 9.5. Mafic dykes/sills in Proterozoic sandstone

Type Examples

- Lodève Basin, France; Franceville Basin, Gabon

Principal Commodities

- U ± Mo

Grades (%) and Tonnages (tU)

- Average: 0.3063, 2746.9
- Median: 0.3000, 770.0

Number of Deposits

- Deposits: 32

Provinces (undifferentiated from Sandstone Type)

- Alaska Alexander, Alaska Darby Hogatza, Alaska Kokrines Hodzana, Alaska Kuskokwim White Mountains, Alaska Northern Alaska Range, Alaska Porcupine, Alaska Prince William Sound, Alaska Western Alaska Range, Alaska Yukon Tanana, Amadeus Basin, Apuseni Mountains, Aquitaine Basin, Bayingebi Basin Bandan Jilin , BC Okanagan, Bighorn Basin, Black Hills, Black Mesa Basin, Bohemian Basin North, Carnarvon Basin, Carpathians South, Casper Arch, Cerilly Bourbon, Choibalsan Basin, Choir Nyalga Basin, Chu Sarysu Basin, Colio Basin Vol Koli, Congo Basin, Cosquin, Denver Basin, Dnieper Basin, Duruma Tanga Basin, Erlian Basin, Etosha Basin, Fergana Basin, Forez, Franceville Basin, Frome Embayment, Geosinclinal Andino, Gobi Basin Central, Gobi Basin East, Gobi Basin South, Green River Basin, Guandacol, Gyeongsang Basin, Hengyang Basin, Iberian Cordillera, Iullemmeden Basin, Japan Basal Channel, Junggar Basin, Kaiparowits Basin, Kalahari Basin East, Kalahari Basin West, Karasburg Basin, Karoo Basin Mesozoic, Karoo Basin Permian, Khorat Plateau, Kokshetau East, Kokshetau West, Kolari Kittila, Kyzylkum, Lake Ladoga, Laramine Hanna Shirley Basins, Lebombo Nuanetsi Basin, Lodeve Basin, Luangwa Lukusashi Basins, Massif Central South West, Mecsek Mountains, Meghalaya Plateau, Menderes Massif, Morondava Basin, Mount Pisgah, Murphy, Nebraska Plains White River Group, Ngalia Basin Sandstone, Nong Son Basin, Norte Subandino, North Canning Basin, Ordos Basin, Pannonian Basin South, Paradox Basin, Parana Basin Amorinopolis Ipora, Parana Basin Durazno, Parana Basin Figueira, Parana Basin Melo Fraile Muerto, Parana Basin Oviedo Yuti, Parana Basin Rio Grandense Shield, Piceance Basin, Pirie Basin, Powder River Basin, Qaidam Basin, Rhodope Massif, Ruhuhu Selous Basins, Saint Pierre du Cantal, San Jorge Gulf Basin, San Juan Basin, Sarysu Basin North, Sebinkarahisar, Shirley Basin, Shiwan Dashan Basin, Sichuan Basin, Siwalik, Slovenia Permian, Songliao Basin, Southwestern Donets Basin, Spokane Mountain Sherwood, Sukhbaatar Basin, Syr Darya Basin, Tallahassee Creek, Tamsag Basin, Tarim Basin North, Tarim Basin South, Taurkyr Dome, Temrezli Basin, Texas Coastal Plain - Catahoula-Oakville, Texas Coastal Plain - Clairborne-Jackson, Texas Coastal Plain - Goliad-Willis-Lissie, Thrace Basin, Tinogasta, Transbaykal Central, Transural, Tuha Basin, Tuli Basin, Uinta Basin, Washakie Cenozoic, Washakie SandWash GreatDivide Mesozoic, West Balkan, West Siberia, West Yunnan, Wind River Basin, Yenisey, Yilgarn South, Yili Ily Basins.

Tectonic Setting

- Intracratonic basins in tectonically stable cratonic environments

Typical Geological Age Range

- Palaeozoic to Cenozoic

Mineral Systems Model

Source

Ground preparation

- Intracratonic basin formation, deposition of a thick sedimentary pile, thermal maturation/diagenesis of the basin fill, formation, migration and trapping of hydrocarbons

Energy

- Addition of heat into the crust linked to (far-field) orogenesis, crustal thinning and/or magmatism

Fluids

- Oxidised basinal brines

Ligands

- CO_3

Reductants and reactants
- Organic matter, biogenic and non-biogenic H_2S, hydrocarbons

Uranium
- Crystalline basement rocks, granitoids, basin fill (in particular interbedded volcanic ash units and coarse fluvial sandstones and conglomerates)

Transport

Fluid pathways
- Regional sandstone aquifers
- Karst aquifers
- Fault-fracture systems (in particular basin growth structures tapping deeper basin sequences, underlying basins or basement)

Trap

Physical
- Palaeovalleys comprising coarser, more permeable sandstones and conglomerates
- Fault-fracture systems, fault intersections, tension gashes, stylolites
- Monoclines, drag folds
- Soft sediment deformational structures, intraformational breccia
- Petroleum-style structural traps
- Lithological permeability barriers

Chemical
- Reductants within the host aquifers and/or wallrocks
- Reductants related to oil and gas systems

Deposition

Change in redox conditions
- Due to interaction of oxidised, uranium-bearing fluids with carbonaceous wallrocks or hydrocarbons

Phase separation
- Fluid unmixing due to hydraulic fracturing and depressurisation

Preservation
- Very low grade metamorphism of host sequences post-uranium mineralisation
- Relative tectonic stability post-uranium mineralisation

Key Reference Bibliography

DAHLKAMP, F. J., Uranium Deposits of the World: Europe. Springer, Berlin, Heidelberg, 792p (2016).

GAUTHIER-LAFAYE, F., WEBER, F., The Francevillian (lower Proterozoic) uranium ore deposits of Gabon. Economic Geology, 84(8), 2267-2285 (1989).

GAUTHIER-LAFAYE, F., HOLLIGER, P., BLANC, P. L., Natural fission reactors in the Franceville basin, Gabon: A review of the conditions and results of a "critical event" in a geologic system. Geochimica et Cosmochimica Acta, 60(23), 4831-4852 (1996).

INTERNATIONAL ATOMIC ENERGY AGENCY, Geological Classification of Uranium Deposits and Description of Selected Examples. IAEA-TECDOC Series, 1842, 415p (2018).

MOSSMAN, D. J., GAUTHIER-LAFAYE, F., JACKSON, S. E., Black shales, organic matter, ore genesis and hydrocarbon generation in the Paleoproterozoic Franceville Series, Gabon. Precambrian Research, 137(3-4), 253-272 (2005).

NDONGO, A., GUIRAUD, M., VENNIN, E., MBINA, M., BUONCRISTIANI, J. F., THOMAZO, C., FLOTTÉ, N., Control of fluid-pressure on early deformation structures in the Paleoproterozoic extensional Franceville Basin (SE Gabon). Precambrian Research, 277, 1-25 (2016).

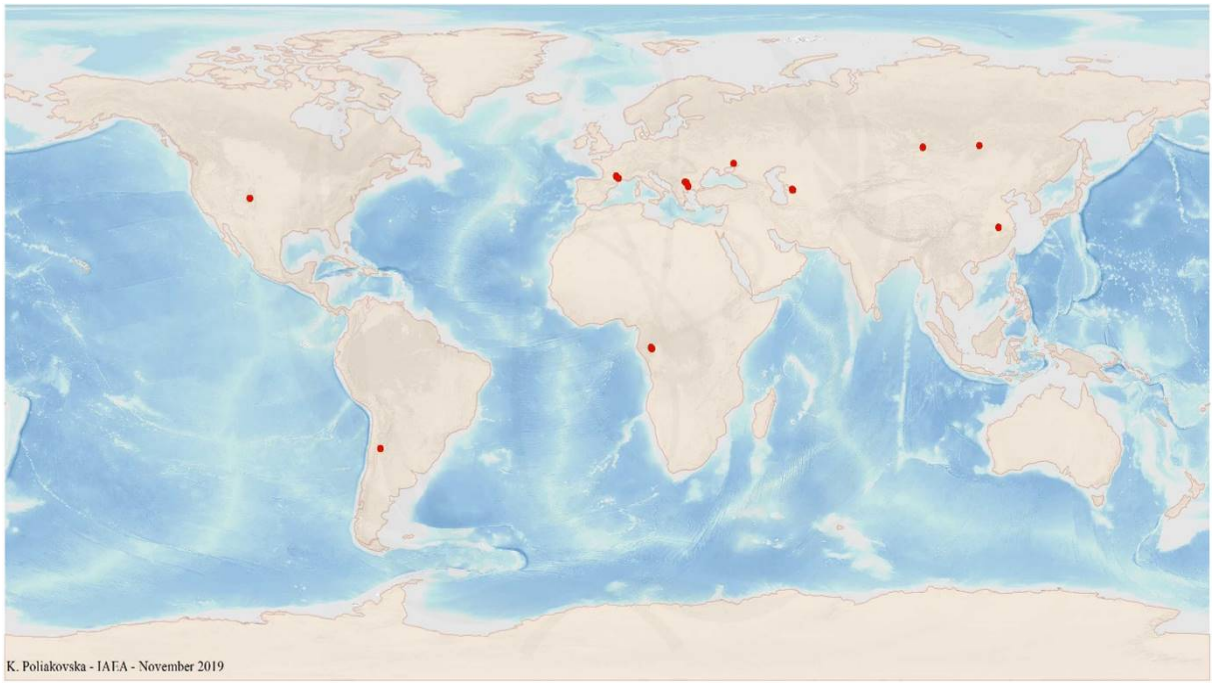

FIG. 9.4a. World distribution of selected Sandstone Tectonic-Lithologic uranium deposits from the UDEPO database.

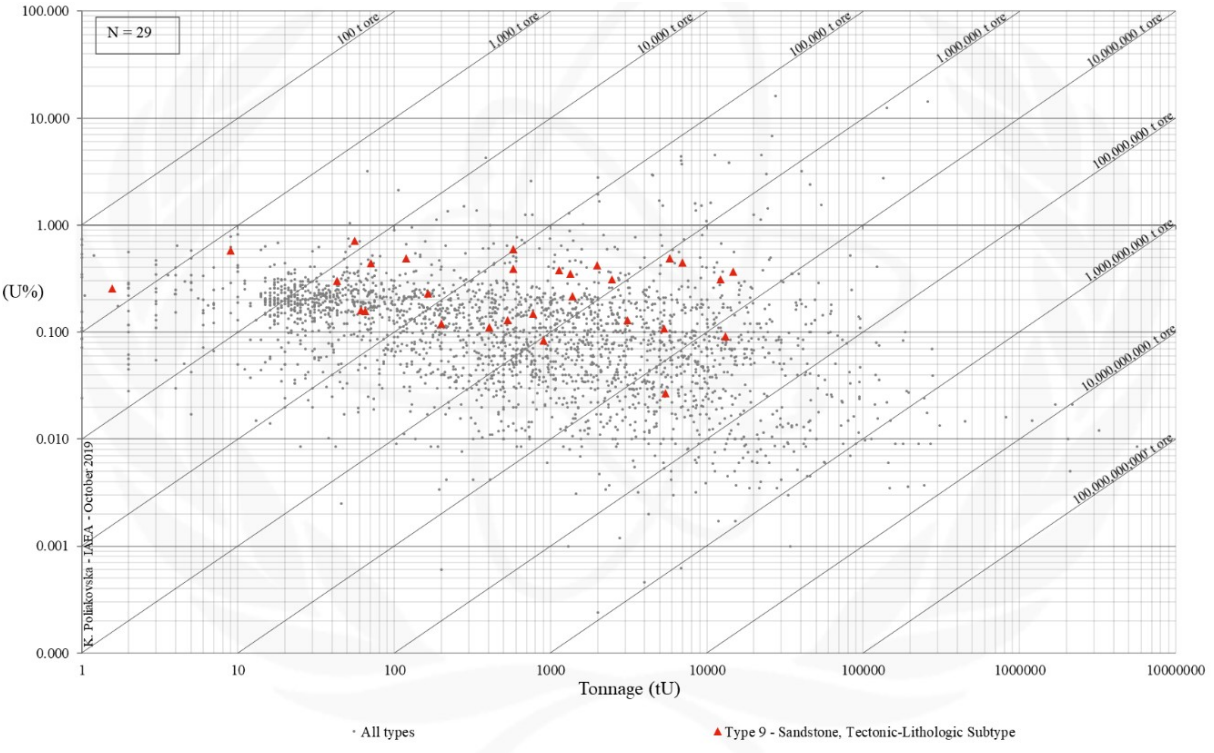

FIG. 9.4b. Grade and tonnage scatterplot highlighting Sandstone Tectonic-Lithologic uranium deposits from the UDEPO database.

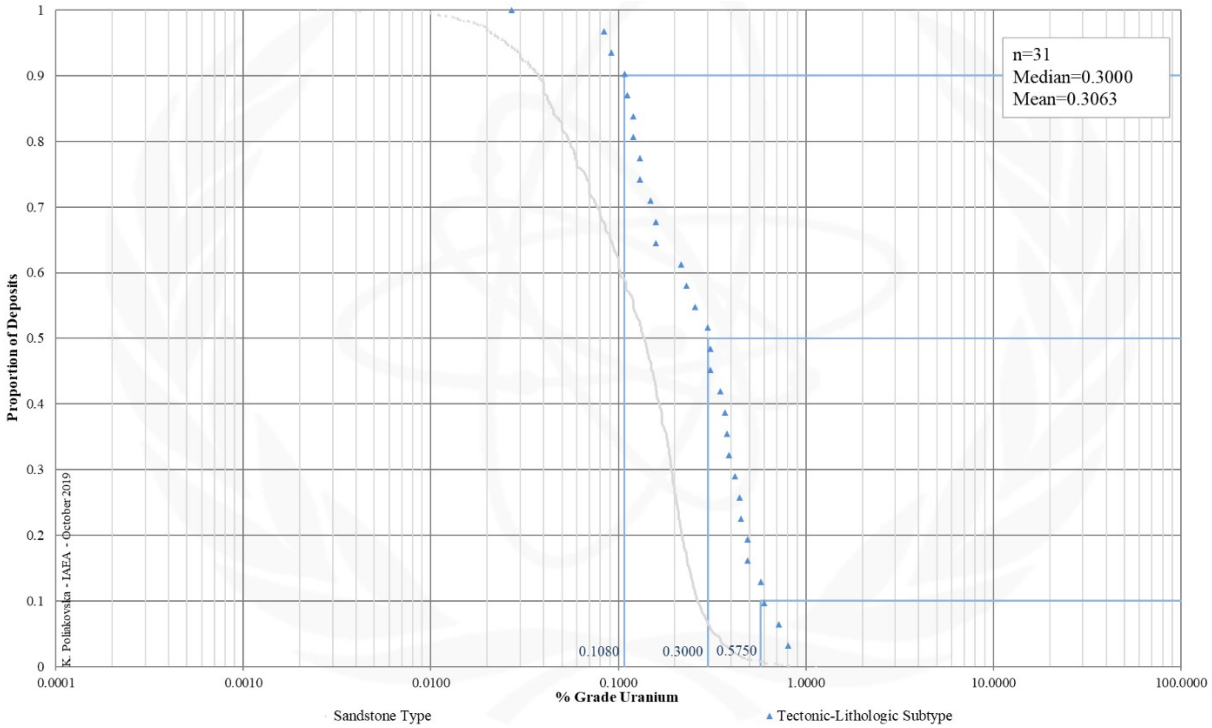

FIG. 9.4c. Grade Cumulative Probability Plot for Sandstone Tectonic-Lithologic uranium deposits from the UDEPO database.

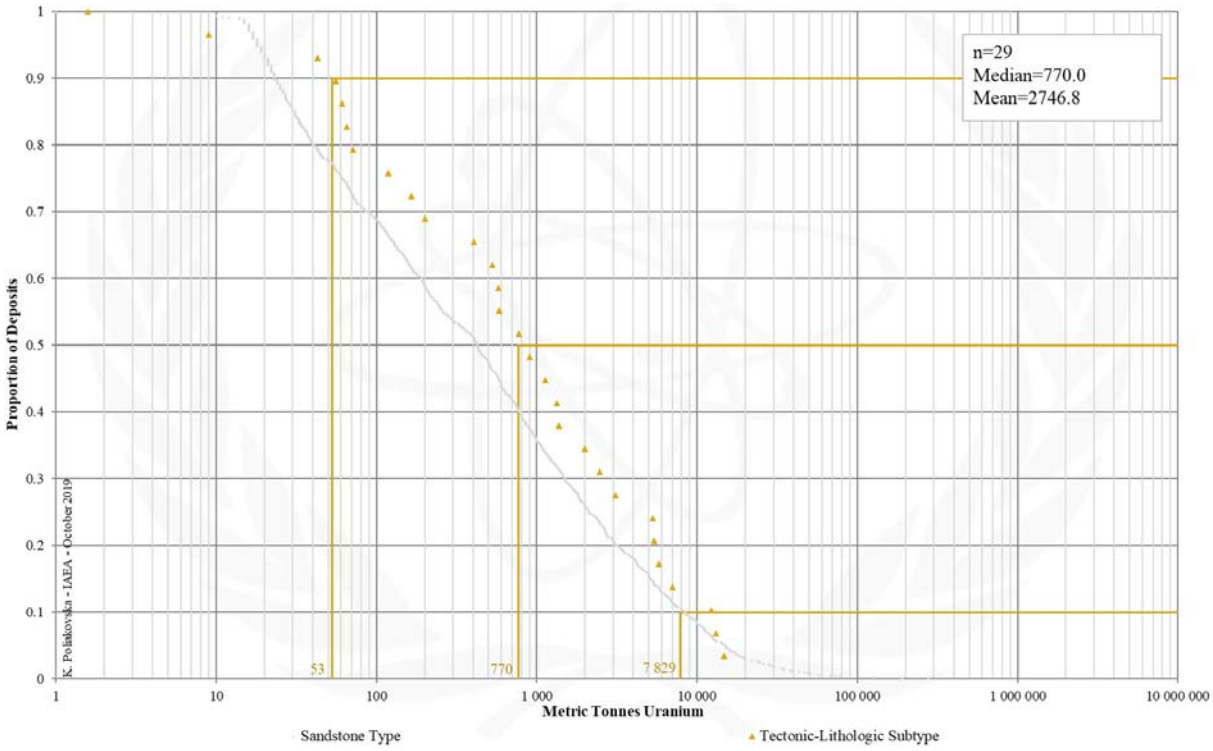

FIG. 9.4d. Tonnage Cumulative Probability Plot for Sandstone Tectonic-Lithologic uranium deposits from the UDEPO database.

SUBTYPE 9.5. Sandstone, Mafic Dykes/Sills in Proterozoic Sandstone

Brief Description

- Sandstone deposits refer to uranium accumulations in medium- to coarse-grained siliciclastic sedimentary rocks deposited in continental fluvial, lacustrine or shallow-marine sedimentary environments.
- Uranium is precipitated by reduction processes caused by the presence of a variety of possible reducing agents within the host sandstone such as intrinsic detrital plant debris, sulphides, ferro-magnesian minerals, anaerobic sulphate-reducing bacteria, or extrinsic migrated fluids from underlying hydrocarbon reservoirs.
- Deposits associated with mafic dyke/sills in Proterozoic sandstones take the form of vein-like, semi-massive and disseminated uranium ores that are hosted by poorly sorted, coarse-grained fluvial sandstones and conglomerates, mafic dykes and sills and the contact zones between these lithologies.
- The rigid, ferrous iron-rich dykes/sills act to focus deformation and fluid flow and as reductants.

Genetically Associated Deposit Types

- Subtype 9.1. Basal channel
- Subtype 9.2. Tabular
- Subtype 9.3. Roll-front
- Subtype 9.4. Tectonic-lithologic
- Subtype 7.1. Unconformity-contact

Type Examples

- Redtree, Junnagunna, and Huarabagoo: Westmoreland district, Australia; Matoush, Canada

Principal Commodities

- U ± Au, Cr

Grades (%) and Tonnages (tU)

- Average: 0.1906, 4005.0
- Median: 0.1360, 2692.5

Number of Deposits

- Deposits: 10

Provinces (undifferentiated from Sandstone Type)

- Alaska Alexander, Alaska Darby Hogatza, Alaska Kokrines Hodzana, Alaska Kuskokwim White Mountains, Alaska Northern Alaska Range, Alaska Porcupine, Alaska Prince William Sound, Alaska Western Alaska Range, Alaska Yukon Tanana, Amadeus Basin, Apuseni Mountains, Aquitaine Basin, Bayingebi Basin Bandan Jilin , BC Okanagan, Bighorn Basin, Black Hills, Black Mesa Basin, Bohemian Basin North, Carnarvon Basin, Carpathians South, Casper Arch, Cerilly Bourbon, Choibalsan Basin, Choir Nyalga Basin, Chu Sarysu Basin, Colio Basin Vol Koli, Congo Basin, Cosquin, Denver Basin, Dnieper Basin, Duruma Tanga Basin, Erlian Basin, Etosha Basin, Fergana Basin, Forez, Franceville Basin, Frome Embayment, Geosinclinal Andino, Gobi Basin Central, Gobi Basin East, Gobi Basin South, Green River Basin, Guandacol, Gyeongsang Basin, Hengyang Basin, Iberian Cordillera, Iullemmeden Basin, Japan Basal Channel, Junggar Basin, Kaiparowits Basin, Kalahari Basin East, Kalahari Basin West, Karasburg Basin, Karoo Basin Mesozoic, Karoo Basin Permian, Khorat Plateau, Kokshetau East, Kokshetau West, Kolari Kittila, Kyzylkum, Lake Ladoga, Laramine Hanna Shirley Basins, Lebombo Nuanetsi Basin, Lodeve Basin, Luangwa Lukusashi Basins, Massif Central South West, Mecsek Mountains, Meghalaya Plateau, Menderes Massif, Morondava Basin, Mount Pisgah, Murphy, Nebraska Plains White River Group, Ngalia Basin Sandstone, Nong Son Basin, Norte Subandino, North Canning Basin, Ordos Basin, Pannonian Basin South, Paradox Basin, Parana Basin Amorinopolis Ipora, Parana Basin Durazno, Parana Basin Figueira, Parana Basin Melo Fraile Muerto, Parana Basin Oviedo Yuti, Parana Basin Rio Grandense Shield, Piceance Basin, Pirie Basin, Powder River Basin, Qaidam Basin, Rhodope Massif, Ruhuhu Selous Basins, Saint Pierre du Cantal, San Jorge Gulf Basin, San Juan Basin, Sarysu Basin North, Sebinkarahisar, Shirley Basin, Shiwan Dashan Basin, Sichuan Basin, Siwalik, Slovenia Permian, Songliao Basin, Southwestern Donets Basin, Spokane Mountain Sherwood, Sukhbaatar Basin, Syr Darya Basin, Tallahassee Creek, Tamsag Basin, Tarim Basin North, Tarim Basin South, Taurkyr Dome, Temrezli Basin, Texas Coastal Plain - Catahoula-Oakville, Texas Coastal Plain - Clairborne-Jackson, Texas Coastal Plain - Goliad-Willis-Lissie, Thrace Basin, Tinogasta, Transbaykal Central, Transural, Tuha Basin, Tuli Basin, Uinta Basin, Washakie Cenozoic, Washakie SandWash GreatDivide Mesozoic, West Balkan, West Siberia, West Yunnan, Wind River Basin, Yenisey, Yilgarn South, Yili Ily Basins.

Tectonic Setting

- Intracratonic basins

Typical Geological Age Range

- Palaeo- to Mesoproterozoic

Mineral Systems Model

Source

Ground preparation
- Basin formation, diagenesis, emplacement of mafic dykes/sills

Energy
- Far-field tectonic events

Fluids
- Oxidised basinal brines

Ligands
- No information

Reductants
- Iron oxides, Fe^{2+} and Cr-V silicates

Uranium
- Crystalline basement rocks, pegmatites, granitoids, basin fill (in particular interbedded volcanic ash units and refractory mineral phases in sandstone such as zircon, monazite, and apatite)

Transport

Fluid pathways
- Regional sandstone aquifers
- Fault-fracture systems (in particular basin growth structures tapping deeper basin sequences, underlying basins or basement)

Trap

Physical
- Fault-fracture systems, fault intersections
- Permeable sandstone units tapped by Fault-fracture systems
- Lithological competency contrasts

Chemical
- Strongly reduced dykes/sills and associated zones of metasomatism

Deposition

Change in redox conditions
- Due to interaction of oxidised, uranium-bearing brines with strongly reduced wallrocks

Preservation

- Physical isolation of uranium mineralisation from the flow of oxidised groundwaters
- Capping of uranium-mineralised sequences by younger lavas
- Relative tectonic stability post-uranium mineralisation

Key Reference Bibliography

ALEXANDRE, P., KYSER, K., LAYTON-MATTHEWS, D., BEYER, S. R., HIATT, E. E., LAFONTAINE, J., Formation of the enigmatic Matoush uranium deposit in the Paleoprotozoic Otish Basin, Quebec, Canada. Mineralium Deposita, 50(7), 825-845 (2015).

INTERNATIONAL ATOMIC ENERGY AGENCY, Geological Classification of Uranium Deposits and Description of Selected Examples. IAEA-TECDOC Series, 1842, 415p (2018).

MCKAY, A. D., MIEZITIS, Y., Australia's uranium resources, geology and development of deposits. AGSO–Geoscience Australia, Mineral Resource Report, 1, 184p (2001).

POLITO, P. A., KYSER, T. K., RHEINBERGER, G., SOUTHGATE, P. N., A paragenetic and isotopic study of the Proterozoic Westmoreland uranium deposits, Southern McArthur Basin, Northern Territory, Australia. Economic Geology, 100(6), 1243-1260 (2005).

POLITO, P. A., KYSER, T. K., JACKSON, M. J., The role of sandstone diagenesis and aquifer evolution in the formation of uranium and zinc-lead deposits, southern McArthur Basin, Northern Territory, Australia. Economic Geology, 101(6), 1189-1209 (2006).

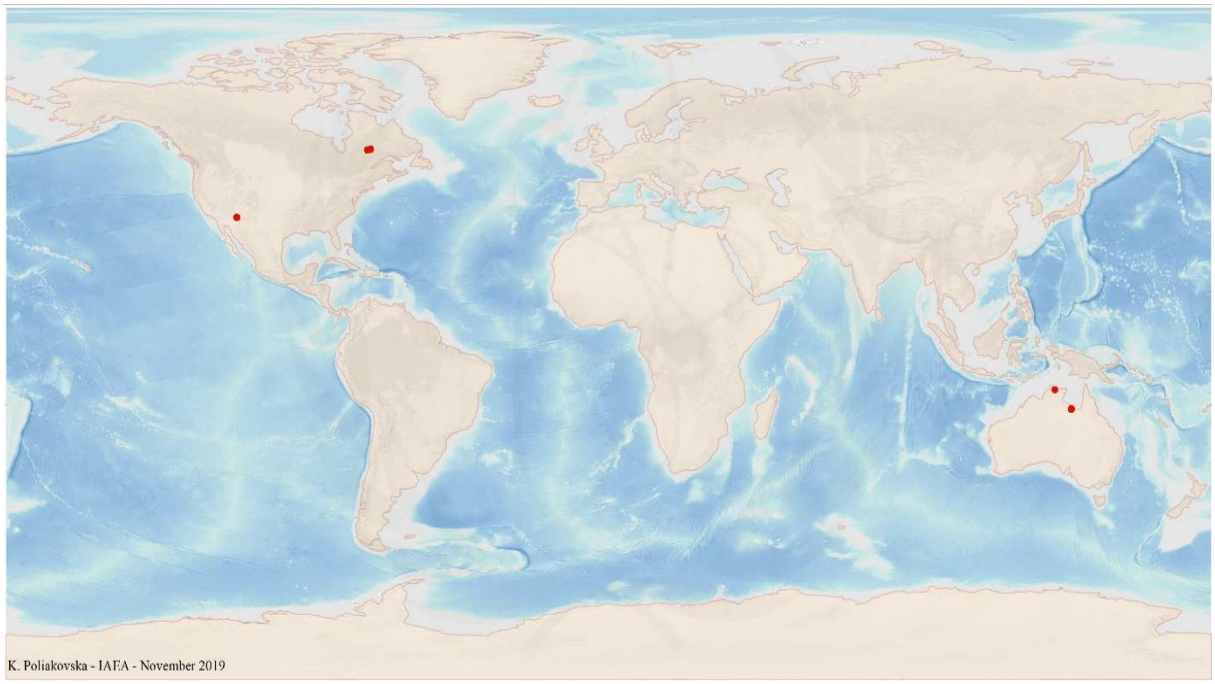

FIG. 9.5a. World distribution of selected Sandstone Mafic Dykes/Sills in Proterozoic Sandstone uranium deposits from the UDEPO database.

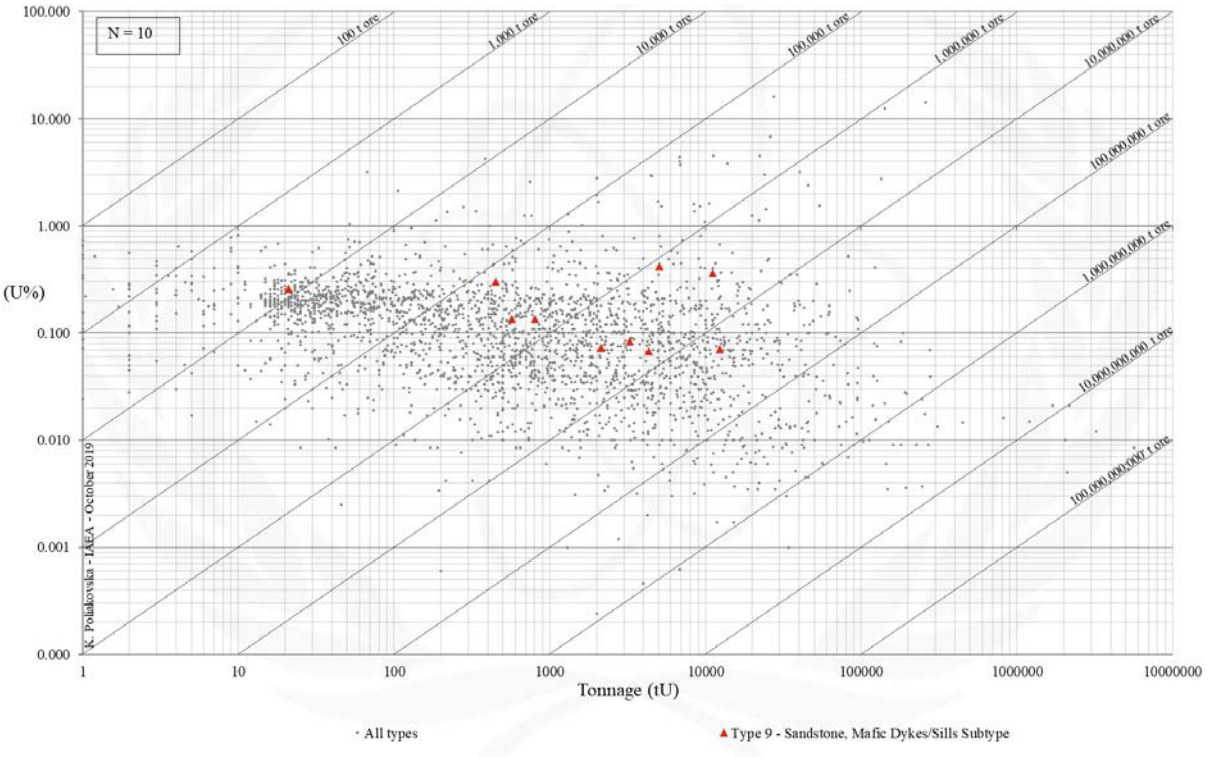

FIG. 9.5b. Grade and tonnage scatterplot highlighting Sandstone Mafic Dykes/Sills in Proterozoic Sandstone uranium deposits from the UDEPO database.

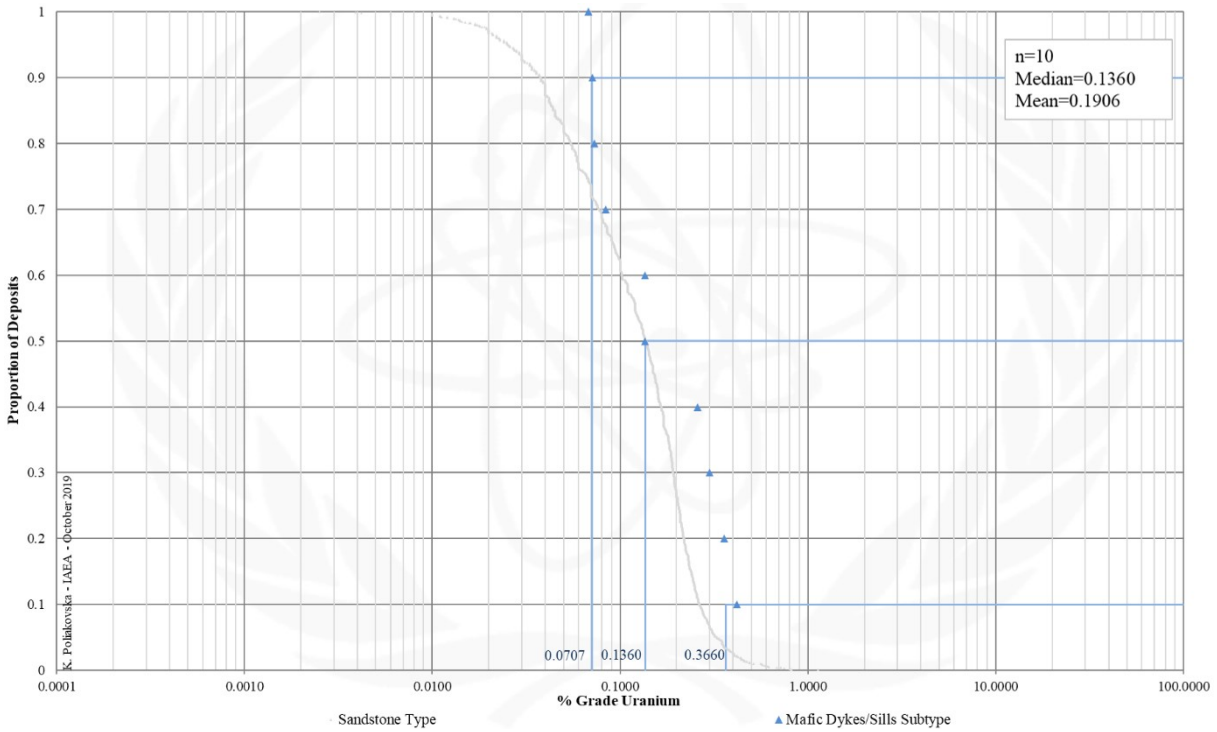

FIG. 9.5c. Grade Cumulative Probability Plot for Sandstone Mafic Dykes/Sills in Proterozoic Sandstone uranium deposits from the UDEPO database.

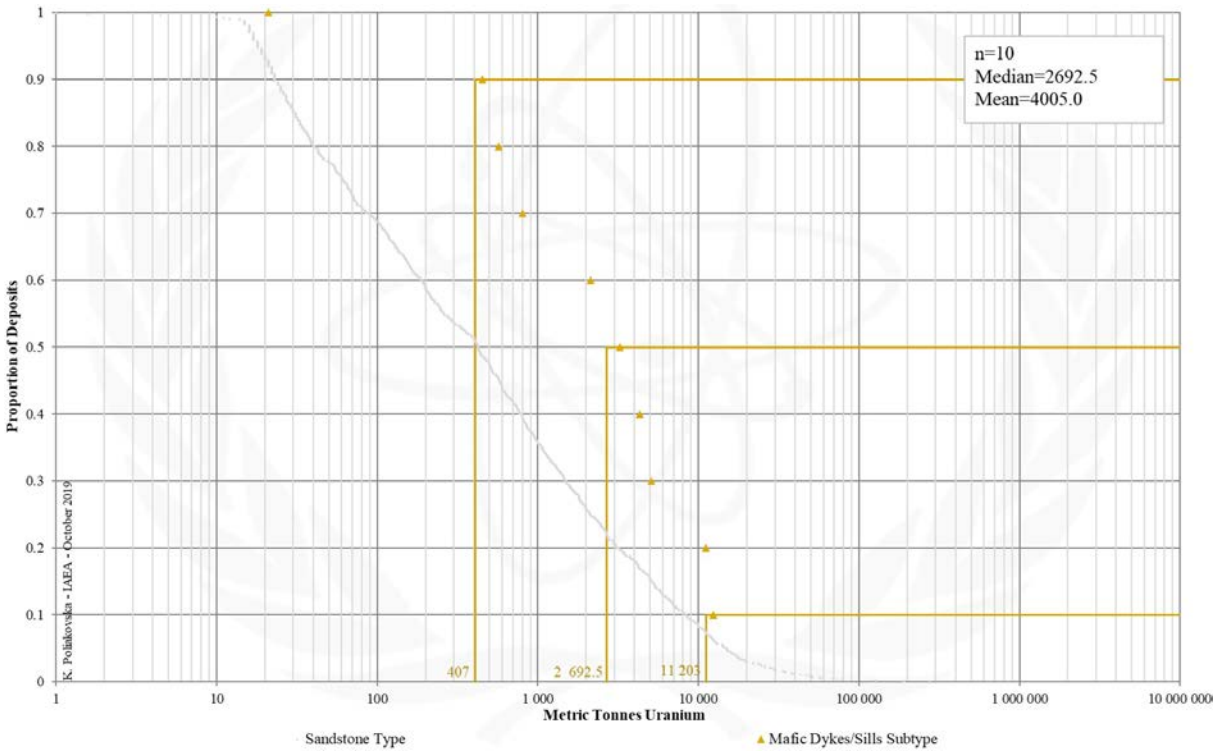

FIG. 9.5d. Tonnage Cumulative Probability Plot for Sandstone Mafic Dykes/Sills in Proterozoic Sandstone uranium deposits from the UDEPO database.

Appendix X

PALAEO QUARTZ-PEBBLE CONGLOMERATE

Type 10. Palaeo Quartz-Pebble Conglomerate

Brief Description
- Detrital uranium ores occur in palaeo quartz-pebble conglomerates of Archaean to early Palaeoproterozoic age.
- The host conglomerates were deposited at the base of and within fluviatile braided river and shallow marine transgressive sedimentary complexes that formed in intracratonic or foreland basins.
- The genesis of palaeo quartz-pebble conglomerate deposits is one of the most controversial topics in economic geology, with the current debate focused on modified placer versus hydrothermal origins.
- Two subtypes are distinguished: (10.1.) Uranium dominant, and (10.2.) gold dominant deposits.

Subtypes
- 10.1. Palaeo quartz-pebble conglomerate, uranium-dominant
- 10.2. Palaeo quartz-pebble conglomerate, gold-dominant

Type Examples
- Subtype 10.1. Elliot Lake district, Canada
- Subtype 10.2. Witwatersrand Basin, South Africa

Principal Commodities
- Subtype 10.1. U, Th, REE ± Au
- Subtype 10.2. Au, U (by-product only) ± Th, REE, Cr, PGM

Grades (%) and Tonnages (tU)
- Average: 0.0296, 18563.5
- Median: 0.0192, 6785.0

Number of Deposits
- Deposits: 147

Provinces
- Huronian Basin, Quadrilatero Ferrifero, Serra de Jacobina, Witwatersrand.

Tectonic Setting
- Intracratonic and (?)foreland basins

Typical Geological Age Range
- Archaean to early Palaeoproterozoic

Mineral Systems Model *(considering both modified placer and hydrothermal origins)*

Source

Ground preparation
- Reduced atmosphere and absence of any plant life
- Onset of plate tectonics and emplacement of peraluminous granites with accessory uraninite
- Intracratonic basin formation
- Intense chemical weathering and erosion of uranium/gold source rocks
- Deposition of fluviatile braided river and shallow marine transgressive sedimentary complexes

Energy
- Ocean currents, or
- Far-field tectonic activity resulting in local uplift and rejuvenation or modification of drainage systems, or
- Orogenesis

Fluids
- Surface waters feeding and sustaining fluvial systems, or
- Seawaters, or
- Meteoric waters, or
- Metamorphic fluids

Ligands
- No information

Reductants
- Cyanobacterial mats, liquid hydrocarbons

Uranium/gold
- Meteoric and shallow seawaters, or
- Peraluminous granites with accessory uraninite, and/or
- Mafic rocks

Transport

Fluid pathways
- Fast flowing, high-energy, braided fluvial systems, or
- Shallow marine currents, or
- Crustal-scale shear zones and interconnected fault-fracture systems

Trap

Physical
- Abrupt changes in fluvial channel morphology promoting changes in stream energy conditions, and

- Lenticular conglomerate beds and gravel bars, or
- Unconformity surfaces

Chemical

- Cyanobacterial/microbial mats thriving in low-energy shallow lake or near-coastal environments
- Liquid hydrocarbons released from intrabasinal shale units

Deposition

Decrease in current velocity

- Decrease in fluvial/shallow marine current velocity below the level required for further transport of heavy detrital minerals, promoting placer deposition
- Repeated sediment reworking, selective sorting of mineral grains by mass and volume and further placer concentration

Change in redox conditions

- Due to oxidative precipitation on the surface of O_2-producing microbial mats in a reduced atmosphere
- Due to interaction of gold- and/or uranium-bearing hydrothermal fluids with reduced wallrocks
- Due to interaction of gold- and/or uranium bearing hydrothermal fluids with pyrobitumen/kerogen seams

Remobilisation and redeposition

- Dissolution of detrital uraninite by liquid hydrocarbons and redeposition in pyrobitumen/kerogen seams
- Hydrothermal recycling of gold by hydrothermal fluids
- Dissolution and reprecipitation of primary ores during post-depositional tectonothermal/metamorphic events

Preservation

- Capping of uranium-mineralised sequences by younger flood basalts
- Deep burial and/or downfaulting of uranium mineralised sequences
- Presence of reductants associated with uranium mineralised sequences

Key Reference Bibliography

BERGEN, L., FAYEK, M., Petrography and geochronology of the Pele Mountain quartz-pebble conglomerate uranium deposit, Elliot Lake District, Canada. American Mineralogist, 97(8-9), 1274-1283 (2012).

BURRON, I., DA COSTA, G., SHARPE, R., FAYEK, M., GAUERT, C., HOFMANN, A., 3.2 Ga detrital uraninite in the Witwatersrand Basin, South Africa: Evidence of a reducing Archean atmosphere. Geology, 46(4), 295-298 (2018).

FRIMMEL, H. E., MINTER, W. E. L., Recent developments concerning the geological history and genesis of the Witwatersrand gold deposits, South Africa. Society of Economic Geologists Special Publication, 9, 17-46 (2002).

FRIMMEL, H. E., GROVES, D. I., KIRK, J., RUIZ, J., CHESLEY, J., MINTER, W. E. L., The formation and preservation of the Witwatersrand goldfields, the world's largest gold province. Economic Geology 100th Anniversary Volume, 769-797 (2005).

FRIMMEL, H. E., HENNIGH, Q., First whiffs of atmospheric oxygen triggered onset of crustal gold cycle. Mineralium Deposita, 50(1), 5-23 (2015).

FUCHS, S., WILLIAMS-JONES, A. E., PRZYBYLOWICZ, W. J., The origin of the gold and uranium ores of the Black Reef Formation, Transvaal Supergroup, South Africa. Ore Geology Reviews, 72, 149-164 (2016a).

FUCHS, S., WILLIAMS-JONES, A. E., JACKSON, S. E., PRZYBYLOWICZ, W. J., Metal distribution in pyrobitumen of the Carbon Leader Reef, Witwatersrand Supergroup, South Africa: Evidence for liquid hydrocarbon ore fluids. Chemical Geology, 426, 45-59 (2016b).

HEINRICH, C. A., Witwatersrand gold deposits formed by volcanic rain, anoxic rivers and Archaean life. Nature Geoscience, 8(3), 206 (2015).

INTERNATIONAL ATOMIC ENERGY AGENCY, Geological Classification of Uranium Deposits and Description of Selected Examples. IAEA-TECDOC Series, 1842, 415p (2018).

LAW, J. D. M., PHILLIPS, G. N., Hydrothermal replacement model for Witwatersrand gold. Economic Geology 100th Anniversary Volume, 799-811 (2005).

ONO, S., FAYEK, M., Decoupling of O and Pb isotope systems of uraninite in the early Proterozoic conglomerates in the Elliot Lake district. Chemical Geology, 288(1-2), 1-13 (2011).

PHILLIPS, G. N., POWELL, R., Hydrothermal alteration in the Witwatersrand goldfields. Ore Geology Reviews, 65, 245-273 (2015).

WHYMARK, W. E., FRIMMEL, H. E., Regional gold-enrichment of conglomerates in Paleoproterozoic supergroups formed during the 2.45 Ga rifting of Kenorland. Ore Geology Reviews, 101, 985-996 (2018).

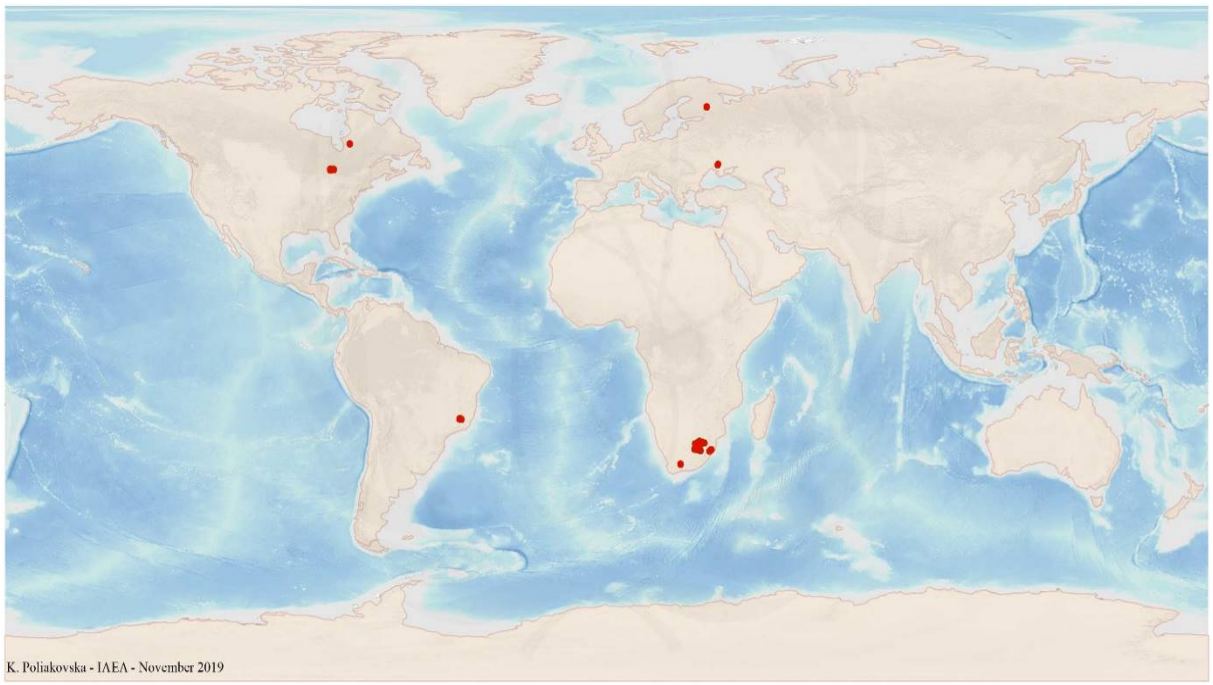

FIG. 10a. World distribution of selected Palaeo Quartz-Pebble Conglomerate uranium deposits from the UDEPO database.

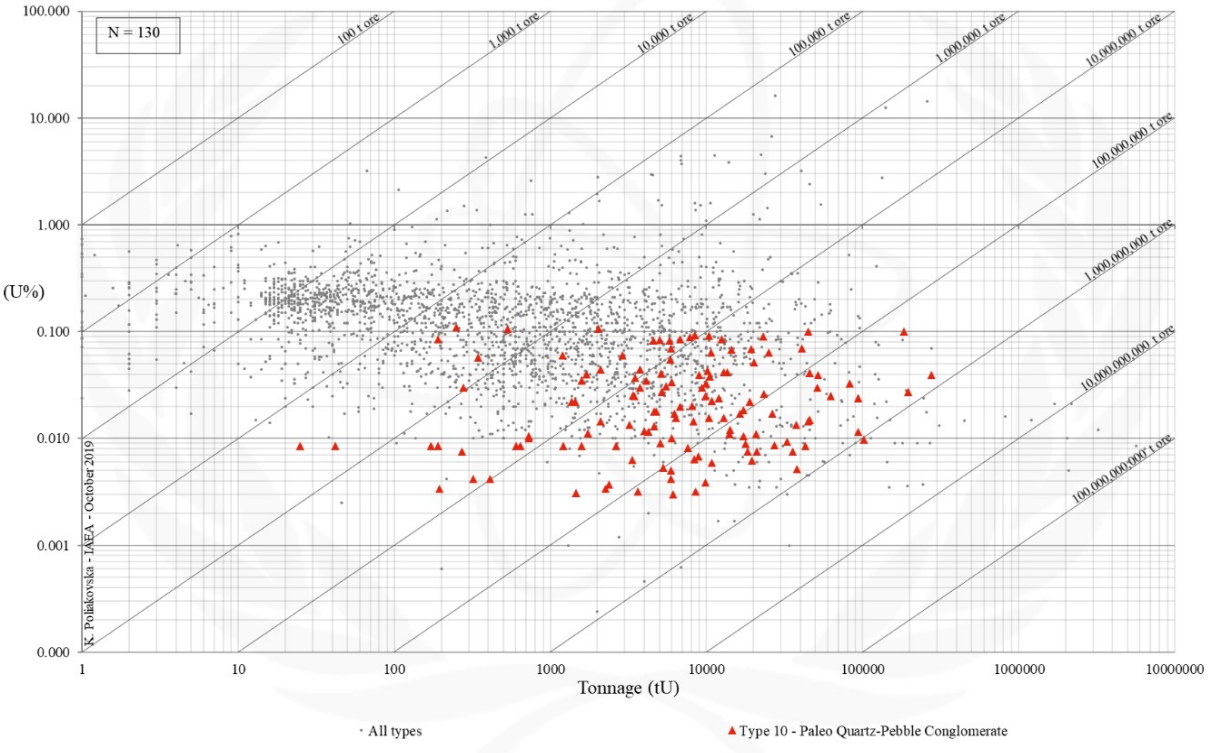

FIG. 10b. Grade and tonnage scatterplot highlighting Palaeo Quartz-Pebble Conglomerate uranium deposits from the UDEPO database.

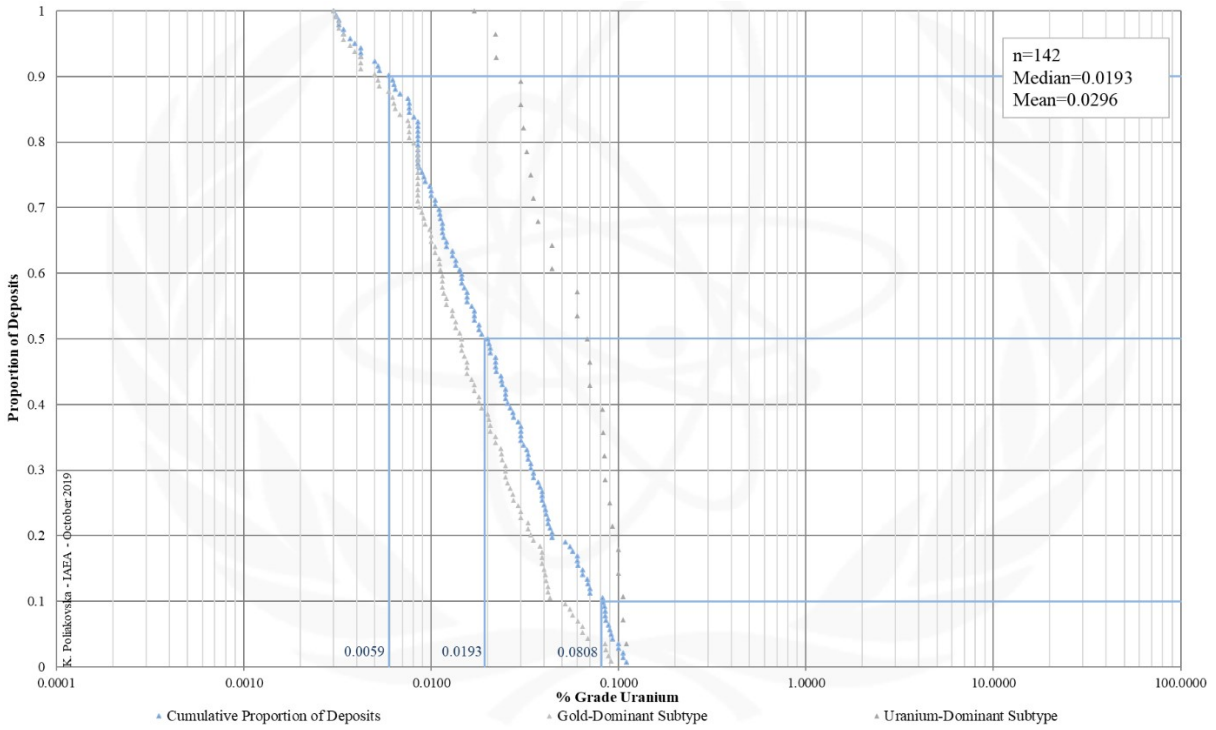

FIG. 10c. Grade Cumulative Probability Plot for Palaeo Quartz-Pebble Conglomerate uranium deposits from the UDEPO database.

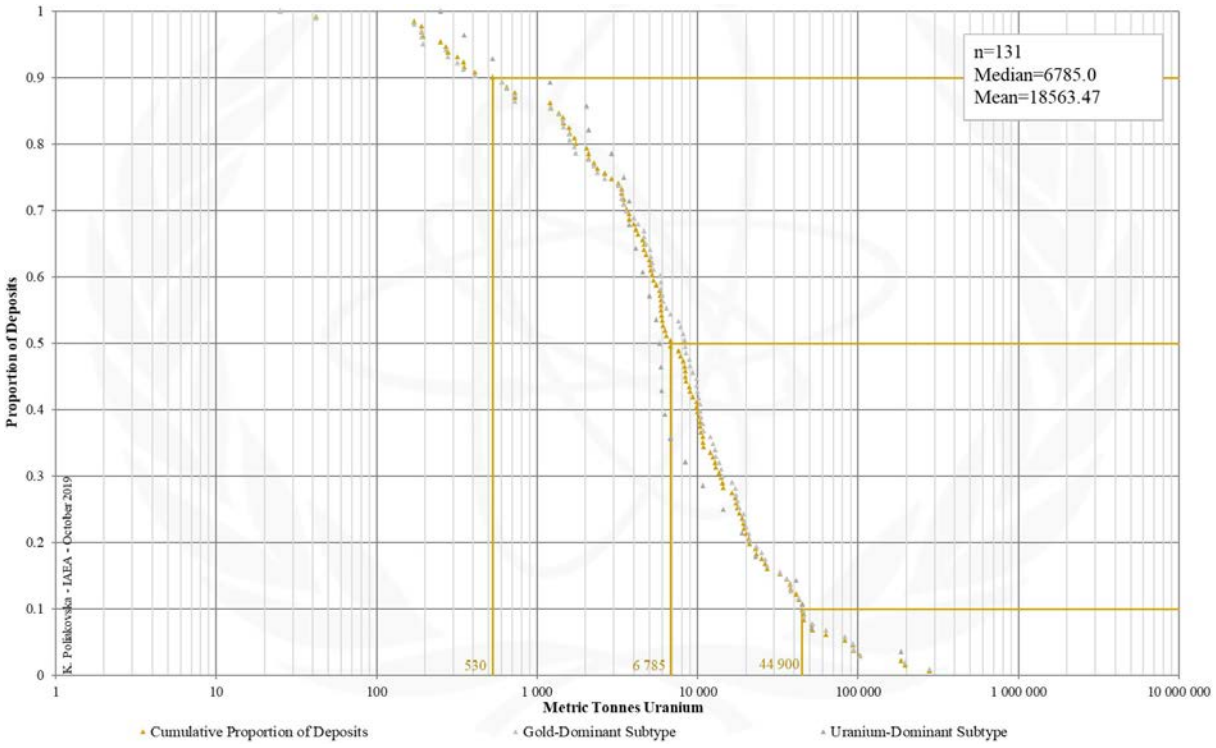

FIG. 10d. Tonnage Cumulative Probability Plot for Palaeo Quartz-Pebble Conglomerate uranium deposits from the UDEPO database.

SUBTYPE 10.1. Palaeo Quartz-Pebble Conglomerate, Uranium-Dominant

Brief Description
- Detrital uranium ores occur in palaeo quartz-pebble conglomerates of Archaean to early Palaeoproterozoic age.
- The host conglomerates were deposited at the base of and within fluviatile braided river and shallow marine transgressive sedimentary complexes that formed in intracratonic or foreland basins.
- The genesis of palaeo quartz-pebble conglomerate deposits is one of the most controversial topics in economic geology, with the current debate focused on modified placer versus hydrothermal origins.
- Uranium dominant deposits occur as stratiform and stratabound ores hosted by cross-bedded, oligomictic quartz-pebble conglomerate beds that also contain abundant pyrite, the main detrital and authigenic heavy mineral, and kerogen.

Type Examples
- Blind River-Elliot Lake district, Canada

Genetically Associated Deposit Types
- Subtype 10.2. Gold-dominant

Principal Commodities
- U, Th, REE ± Au

Grades (%) and Tonnages (tU)
- Average: 0.0623, 16731.2
- Median: 0.0640, 5667.0

Number of Deposits
- Deposits: 30

Provinces (undifferentiated from Palaeo Quartz-Pebble Conglomerate Type)
- Huronian Basin, Quadrilatero Ferrifero, Serra de Jacobina, Witwatersrand.

Tectonic Setting
- Intracratonic basins

Typical Geological Age Range
- Early Palaeoproterozoic

Mineral Systems Model

Source

Ground preparation
- Reduced atmosphere and absence of any plant life
- Onset of plate tectonics and emplacement of peraluminous granites with accessory uraninite
- Intracratonic basin formation
- Intense chemical weathering and erosion of uranium/gold source rocks
- Deposition of fluviatile braided river complexes

Energy
- Far-field tectonic activity resulting in local uplift and rejuvenation or modification of drainage systems

Fluids
- Surface waters feeding and sustaining fluvial systems

Ligands
- No information

Reductants
- Cyanobacterial mats, liquid hydrocarbons

Uranium
- Peraluminous granitoids and pegmatites with accessory uraninite

Transport

Fluid pathways
- Fast flowing, high-energy, braided fluvial systems

Trap

Physical
- Abrupt changes in fluvial channel morphology promoting changes in stream energy conditions

Chemical
- Cyanobacterial/microbial mats
- Liquid hydrocarbons

Deposition

Decrease in current velocity
- Decrease in fluvial/shallow marine current velocity below the level required for further transport of heavy detrital minerals, promoting placer deposition
- Repeated sediment reworking, selective sorting of mineral grains by mass and volume and further placer concentration

Remobilisation and redeposition
- Dissolution and reprecipitation of primary ores during post-depositional tectonothermal/metamorphic events

Preservation
– Capping of uranium-mineralised sequences by younger flood basalts – Deep burial and/or downfaulting of uranium mineralised sequences – Presence of reductants associated with uranium mineralised sequences

Key Reference Bibliography

BERGEN, L., FAYEK, M., Petrography and geochronology of the Pele Mountain quartz-pebble conglomerate uranium deposit, Elliot Lake District, Canada. American Mineralogist, 97(8-9), 1274-1283 (2012).
INTERNATIONAL ATOMIC ENERGY AGENCY, Geological Classification of Uranium Deposits and Description of Selected Examples. IAEA-TECDOC Series, 1842, 415p (2018).
ONO, S., FAYEK, M., Decoupling of O and Pb isotope systems of uraninite in the early Proterozoic conglomerates in the Elliot Lake district. Chemical Geology, 288(1-2), 1-13 (2011).
WHYMARK, W. E., FRIMMEL, H. E., Regional gold-enrichment of conglomerates in Paleoproterozoic supergroups formed during the 2.45 Ga rifting of Kenorland. Ore Geology Reviews, 101, 985-996 (2018).

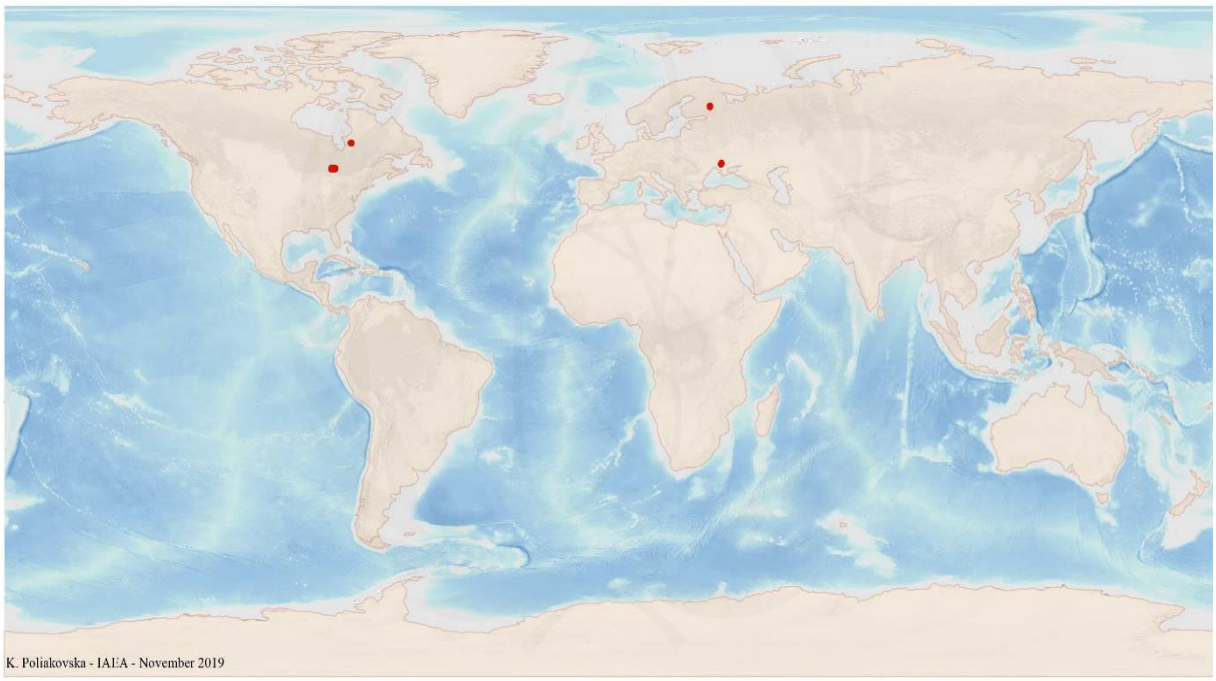

FIG. 10.1a. World distribution of selected Palaeo Quartz-Pebble Conglomerate Uranium-Dominant uranium deposits from the UDEPO database.

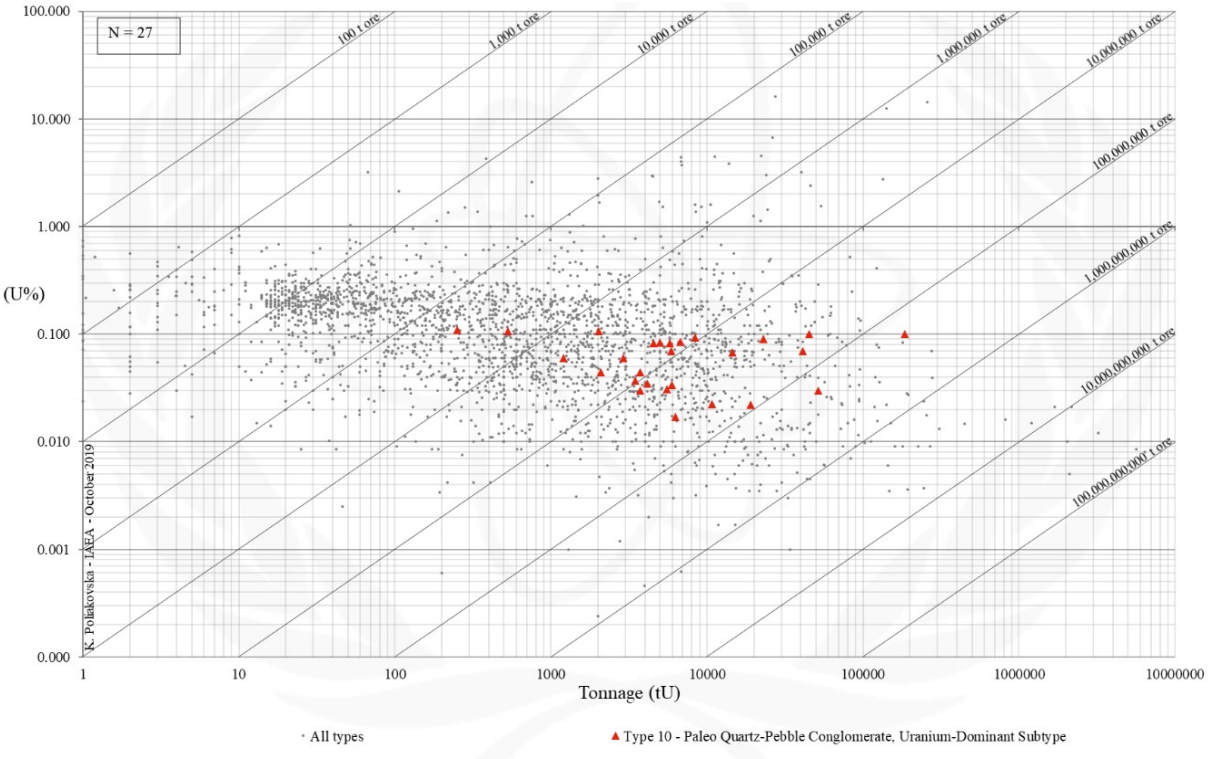

FIG. 10.1b. Grade and tonnage scatterplot highlighting Palaeo Quartz-Pebble Conglomerate Uranium-Dominant uranium deposits from the UDEPO database.

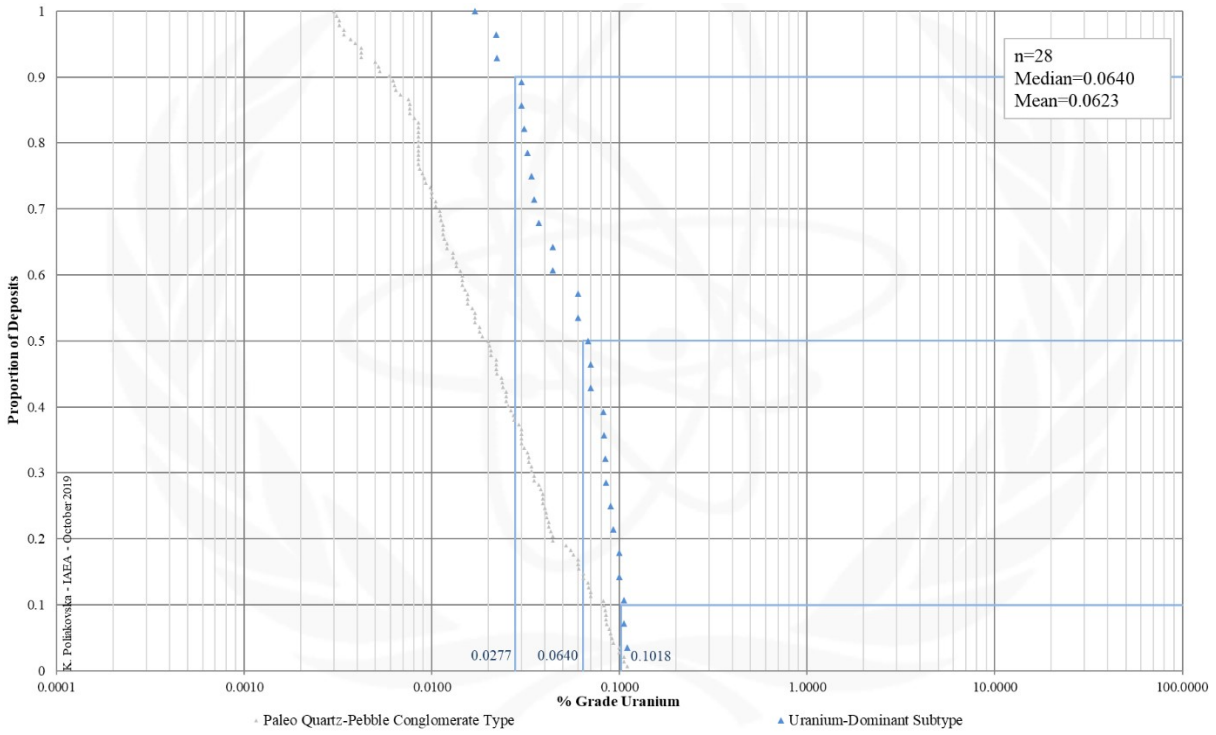

FIG. 10.1c. Grade Cumulative Probability Plot for Palaeo Quartz-Pebble Conglomerate Uranium-Dominant uranium deposits from the UDEPO database.

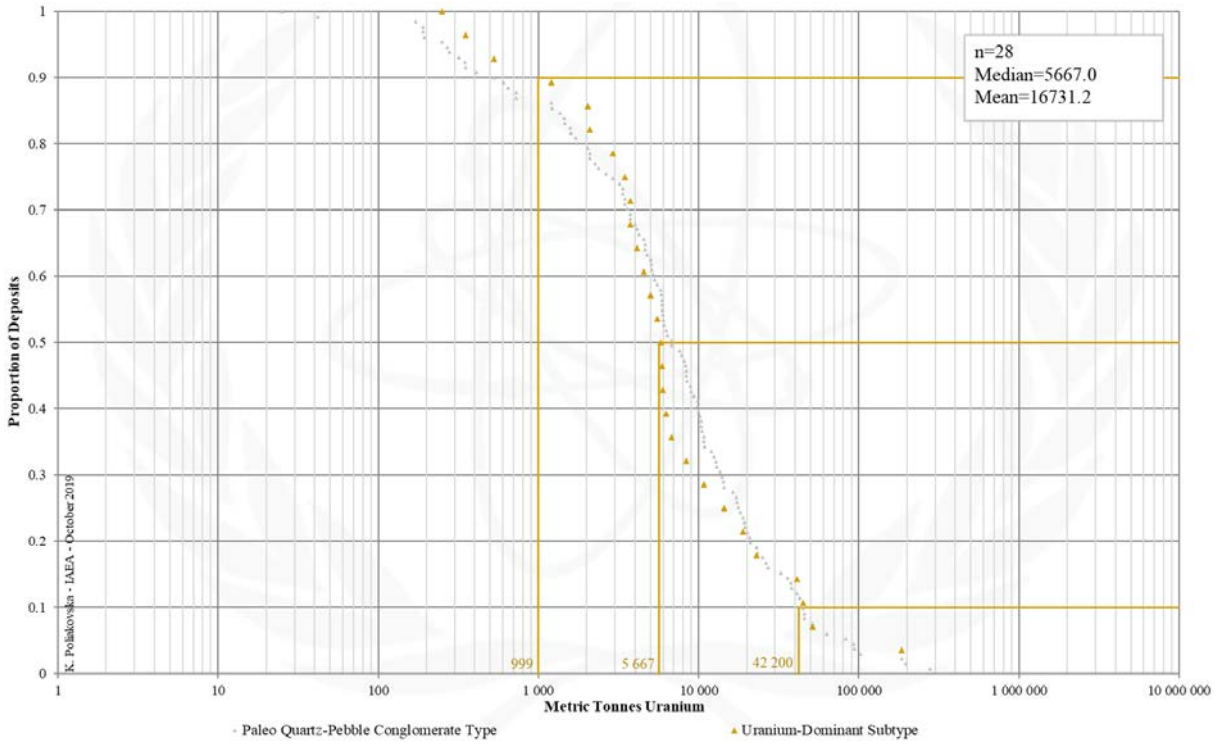

FIG. 10.1d. Tonnage Cumulative Probability Plot for Palaeo Quartz-Pebble Conglomerate Uranium-Dominant uranium deposits from the UDEPO database.

SUBTYPE 10.2. Palaeo Quartz-Pebble Conglomerate, Gold-Dominant

Brief Description
- Detrital uranium ores occur in palaeo quartz-pebble conglomerates of Archaean to early Palaeoproterozoic age.
- The host conglomerates were deposited at the base of and within fluviatile braided river and shallow marine transgressive sedimentary complexes that formed in intracratonic or foreland basins.
- The genesis of palaeo quartz-pebble conglomerate deposits is one of the most controversial topics in economic geology, with the current debate focused on modified placer versus hydrothermal origins.
- Gold-dominant deposits are exemplified by the Mesoarchaean quartz-pebble conglomerate deposits of the Witwatersrand Basin where uranium is extracted as a by-product of gold mining.
- Recent in-situ U-Pb dates of uraninite grains from the Witwatersrand support their detrital origin, lending significant weight to a modified palaeoplacer model for the uranium (and gold?) mineralisation.

Type Examples
- Witwatersrand Basin, South Africa

Genetically Associated Deposit Types
- Subtype 10.1. Uranium-dominant

Principal Commodities
- Au, U (by-product only) ± Th, REE, Cr, PGM

Grades (%) and Tonnages (tU)
- Average: 0.0215, 19061.6
- Median: 0.0144, 8265.0

Number of Deposits
- Deposits: 117

Provinces (undifferentiated from Palaeo Quartz-Pebble Conglomerate Type)
- Huronian Basin, Quadrilatero Ferrifero, Serra de Jacobina, Witwatersrand.

Tectonic Setting
- Intracratonic and possibly foreland basins

Typical Geological Age Range
- Archaean

Mineral Systems Model *(considering both modified placer and hydrothermal origins)*

Source

Ground preparation
- Reduced atmosphere and absence of any plant life
- Onset of plate tectonics and emplacement of peraluminous granites with accessory uraninite
- Intracratonic basin formation
- Intense chemical weathering and erosion of uranium/gold source rocks
- Deposition of fluviatile braided river and shallow marine transgressive sedimentary complexes

Energy
- Ocean currents, or
- Far-field tectonic activity resulting in local uplift and rejuvenation or modification of drainage systems, or
- Orogenesis

Fluids
- Surface waters feeding and sustaining fluvial systems, or
- Seawaters, or
- Meteoric waters, or
- Metamorphic fluids

Ligands
- No information

Reductants
- Cyanobacterial mats, liquid hydrocarbons

Uranium/gold
- Meteoric and shallow seawaters, or
- Peraluminous granites with accessory uraninite, and/or
- Mafic rocks

Transport

Fluid pathways
- Fast flowing, high-energy, braided fluvial systems, or
- Shallow marine currents, or
- Crustal-scale shear zones and interconnected fault-fracture systems

Trap

Physical
- Abrupt changes in fluvial channel morphology promoting changes in stream energy conditions, and

- Lenticular conglomerate beds and gravel bars, or
- Unconformity surfaces

Chemical

- Cyanobacterial/microbial mats thriving in low-energy shallow lake or near-coastal environments
- Liquid hydrocarbons released from intrabasinal shale units

Deposition

Decrease in current velocity

- Decrease in fluvial/shallow marine current velocity below the level required for further transport of heavy detrital minerals, promoting placer deposition
- Repeated sediment reworking, selective sorting of mineral grains by mass and volume and further placer concentration

Change in redox conditions

- Due to oxidative precipitation on the surface of O_2-producing microbial mats in a reduced atmosphere
- Due to interaction of gold- and/or uranium-bearing hydrothermal fluids with reduced wallrocks
- Due to interaction of gold- and/or uranium bearing hydrothermal fluids with pyrobitumen/kerogen seams

Remobilisation and redeposition

- Dissolution of detrital uraninite by liquid hydrocarbons and redeposition in pyrobitumen/kerogen seams
- Hydrothermal recycling of gold by hydrothermal fluids
- Dissolution and reprecipitation of primary ores during post-depositional tectonothermal/metamorphic events

Preservation

- Capping of uranium-mineralised sequences by younger flood basalts
- Deep burial and/or downfaulting of uranium mineralised sequences
- Presence of reductants associated with uranium mineralised sequences

Key Reference Bibliography

BURRON, I., DA COSTA, G., SHARPE, R., FAYEK, M., GAUERT, C., HOFMANN, A., 3.2 Ga detrital uraninite in the Witwatersrand Basin, South Africa: Evidence of a reducing Archean atmosphere. Geology, 46(4), 295-298 (2018).

FRIMMEL, H. E., MINTER, W. E. L., Recent developments concerning the geological history and genesis of the Witwatersrand gold deposits, South Africa. Society of Economic Geologists Special Publication, 9, 17-46 (2002).

FRIMMEL, H. E., GROVES, D. I., KIRK, J., RUIZ, J., CHESLEY, J., MINTER, W. E. L., The formation and preservation of the Witwatersrand goldfields, the world's largest gold province. Economic Geology 100th Anniversary Volume, 769-797 (2005).

FRIMMEL, H. E., HENNIGH, Q., First whiffs of atmospheric oxygen triggered onset of crustal gold cycle. Mineralium Deposita, 50(1), 5-23 (2015).

FUCHS, S., WILLIAMS-JONES, A. E., PRZYBYLOWICZ, W. J., The origin of the gold and uranium ores of the Black Reef Formation, Transvaal Supergroup, South Africa. Ore Geology Reviews, 72, 149-164 (2016a).

FUCHS, S., WILLIAMS-JONES, A. E., JACKSON, S. E., PRZYBYLOWICZ, W. J., Metal distribution in pyrobitumen of the Carbon Leader Reef, Witwatersrand Supergroup, South Africa: Evidence for liquid hydrocarbon ore fluids. Chemical Geology, 426, 45-59 (2016b).

HEINRICH, C. A., Witwatersrand gold deposits formed by volcanic rain, anoxic rivers and Archaean life. Nature Geoscience, 8(3), 206 (2015).

INTERNATIONAL ATOMIC ENERGY AGENCY, Geological Classification of Uranium Deposits and Description of Selected Examples. IAEA-TECDOC Series, 1842, 415p (2018).

LAW, J. D. M., PHILLIPS, G. N., Hydrothermal replacement model for Witwatersrand gold. Economic Geology 100th Anniversary Volume, 799-811 (2005).

PHILLIPS, G. N., POWELL, R., Hydrothermal alteration in the Witwatersrand goldfields. Ore Geology Reviews, 65, 245-273 (2015).

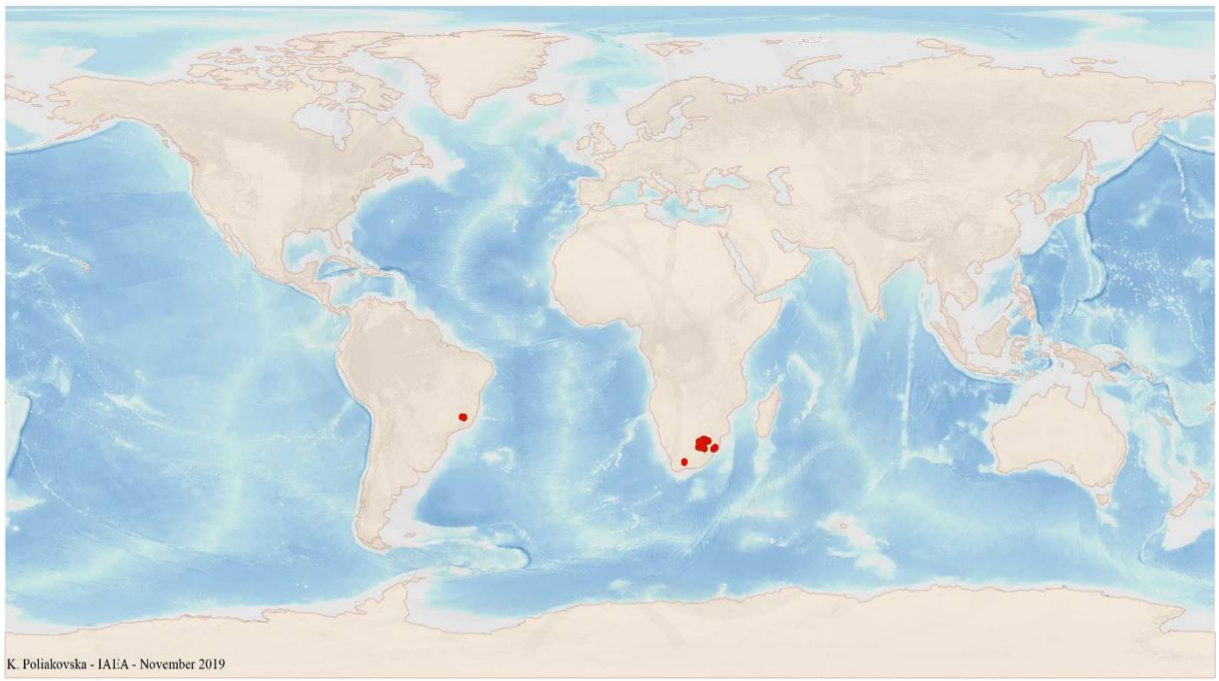

FIG. 10.2a. World distribution of selected Palaeo Quartz-Pebble Conglomerate Gold-Dominant uranium deposits from the UDEPO database.

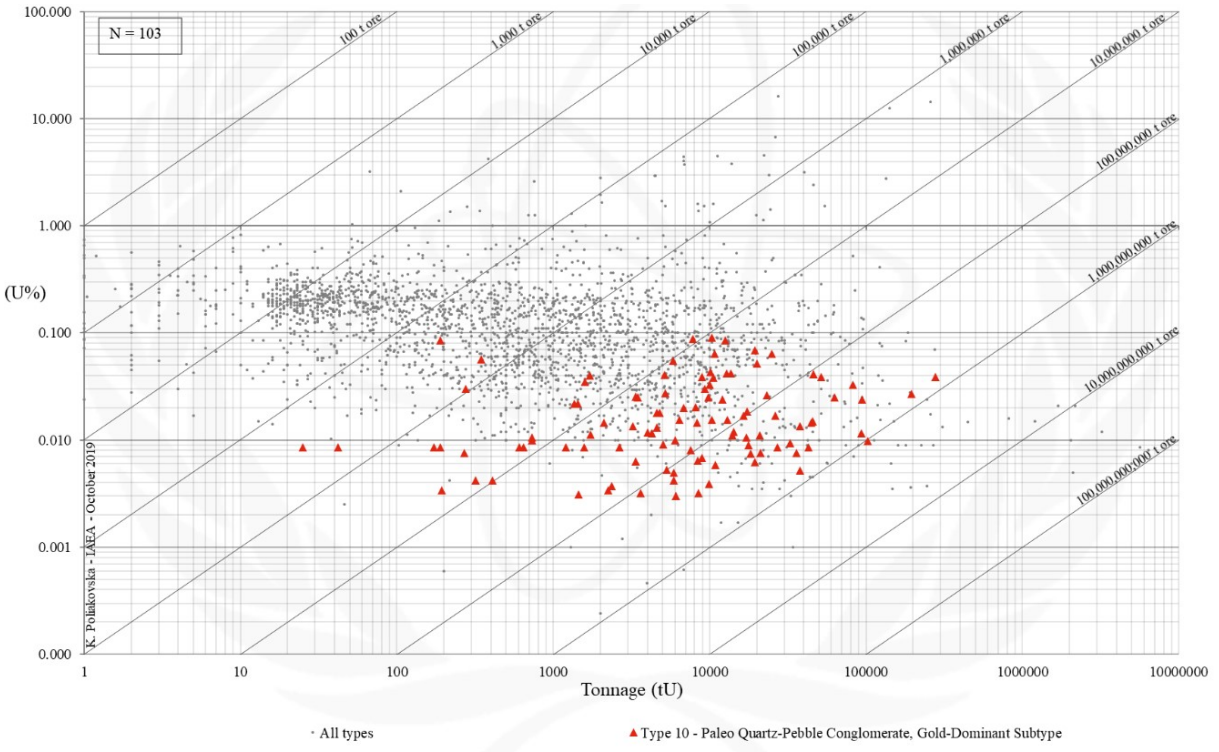

FIG. 10.2b. Grade and tonnage scatterplot highlighting Palaeo Quartz-Pebble Conglomerate Gold-Dominant uranium deposits from the UDEPO database.

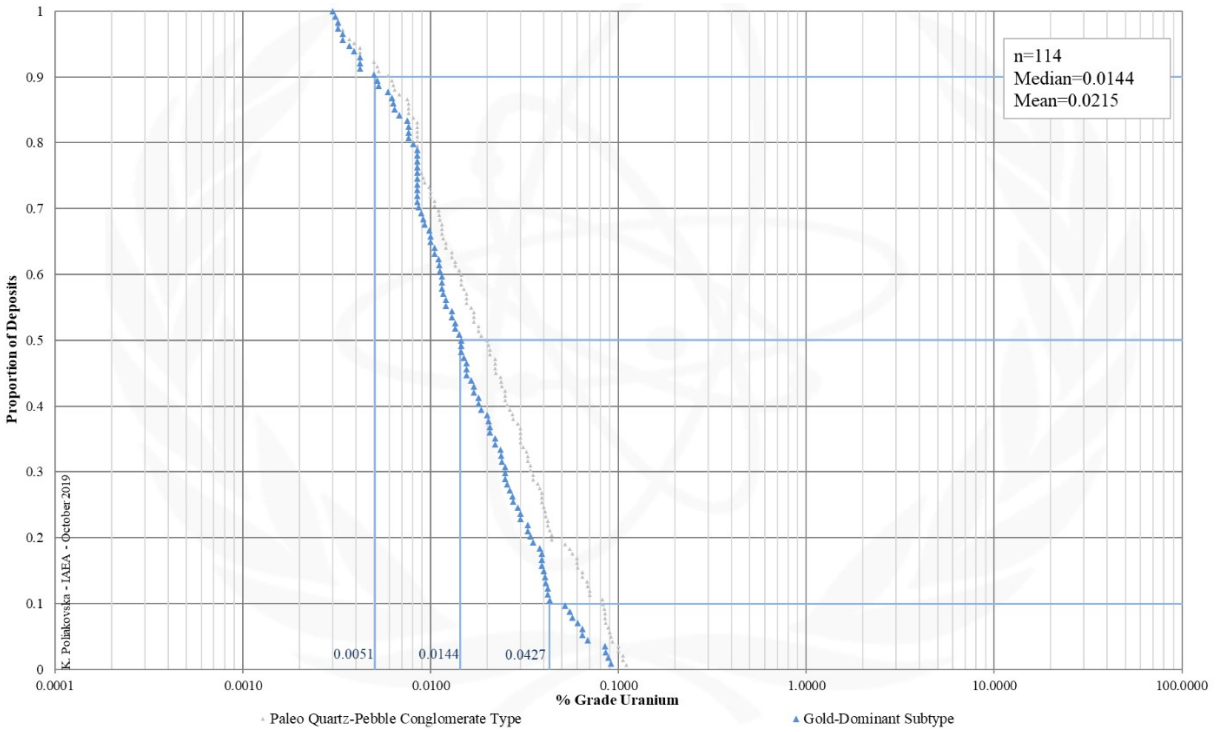

FIG. 10.2c. Grade Cumulative Probability Plot for Palaeo Quartz-Pebble Conglomerate Gold-Dominant uranium deposits from the UDEPO database.

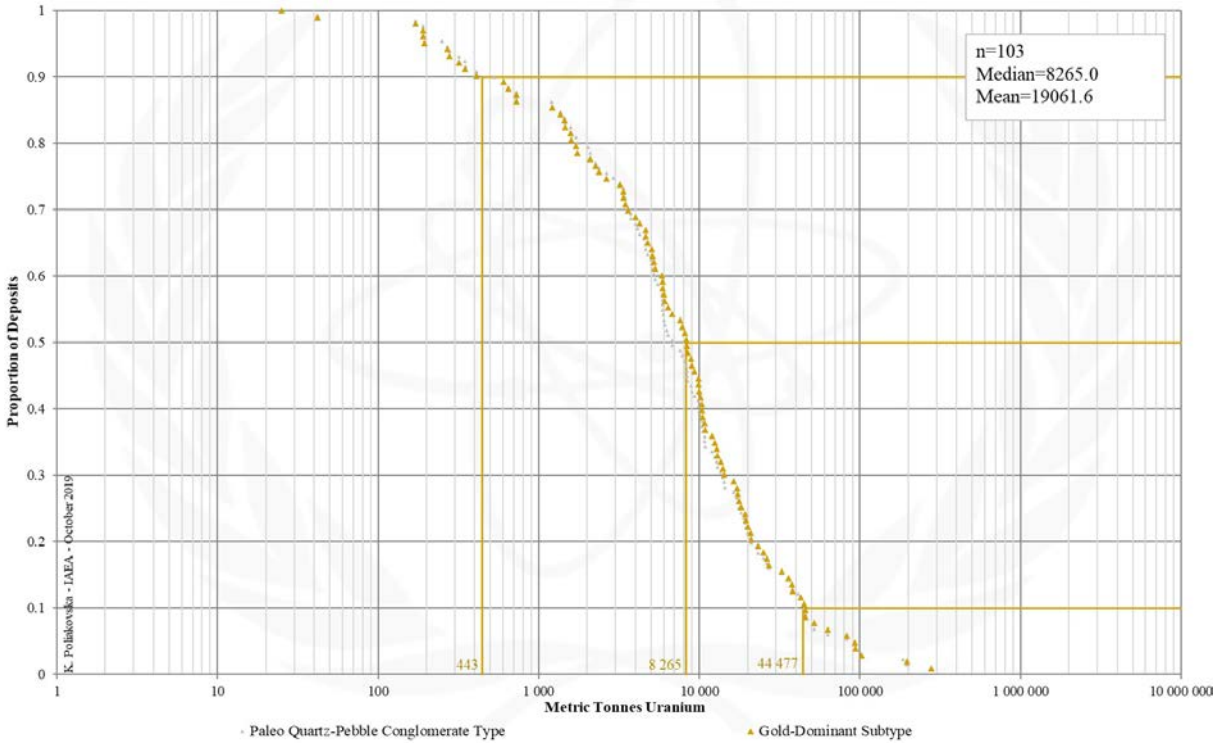

FIG. 10.2d. Tonnage Cumulative Probability Plot for Palaeo Quartz-Pebble Conglomerate Gold-Dominant uranium deposits from the UDEPO database.

Appendix XI

SURFICIAL

TYPE 11. Surficial

Brief Description

- Surficial deposits cover a diverse group of young (Tertiary to recent), near-surface uranium concentrations in un- or poorly consolidated sediments or soils.
- Five subtypes are distinguished based on their sedimentary host environments, the causative fluid systems and respective uranium precipitation mechanisms: (11.1.) Peat bog, (11.2.) fluvial valley, (11.3.) lacustrine-playa, (11.4.) pedogenic and fracture fill, and (11.5.) placer.
- Only the genetically related fluvial valley and lacustrine-playa deposits are known to form uranium accumulations of economic significance.

Subtypes

- 11.1. Peat bog. 11.2. Fluvial valley. 11.3. Lacustrine-playa. 11.4. Pedogenic and fracture fill. 11.5. Placer

Type Examples

- Subtype 11.1. Kamushanovskoye, Kyrgyzstan; Flodelle Creek, USA. Subtype 11.2. Yeelirrie, Australia; Langer Heinrich, Namibia. Subtype 11.3. Lake Maitland, Lake Way, Australia. Subtype 11.4. Beslet, Bulgaria. Subtype 11.5. Kyzyl Ompul, Kyrgyzstan; Red River Valley, USA

Principal Commodities

- Subtypes 11.1.to 11.4. U ± V. Subtype 11.5. Th, Zr, Ti, P, Fe, REE, U (by- or coproduct only)

Grades (%) and Tonnages (tU)

- Average: 0.0371, 4190.0
- Median: 0.0280, 1397.5

Number of Deposits

- Deposits: 133

Provinces

- BC Okanagan Valley, Chile Nth, Chu Basin East, Gascoyne, Gawler Craton, Mayoni Bahi, Namib Desert, Neuquen Basin South, Ngalia Basin, San Jorge Chunut, Texas Southern High Plains, Upington, Volga Ural, Yilgarn North.

Tectonic Setting

- Subtypes 11.1. and 11.4. Intermontane basins, intracratonic basins. Subtypes 11.2. to 11.3. Tectonically stable, peneplained cratonic environments. Subtype 11.5. Tectonically stable cratonic/platform environments, stable passive plate margins, intermontane plateaus, accretionary orogenic belts, volcanic arcs and back-arcs

Typical Geological Age Range

- Subtypes 11.1.to 11.4. Tertiary to Recent. Subtype 11.5. Mesozoic to Recent

Mineral Systems Model

Source

Ground preparation

- Subtype 11.1. Orogenesis; structural preparation (in particular fracturing) of source rocks; actively eroding mountainous terrain; glaciation and deposition of highly permeable till aquifers. Subtypes 11.2. to 11.3. Structural preparation (in particular fracturing) of source rocks; development of tectonically stable peneplain environments; formation and burial of long-lived fluvial river systems; climate change from humid to (semi-)arid; deep weathering/oxidation. Subtype 11.4. Juxtaposition of uraniferous granitoids against young, highly porous sedimentary successions; structural preparation (in particular fracturing) of source rocks; deep weathering/oxidation. Subtype 11.5. Deposition or emplacement of suitable source rocks; exposure of source rocks to deep weathering/oxidation; formation (± burial) of long-lived fluvial river systems

Energy

- Subtypes 11.1. and 11.4. Steep topographic and hydrological gradients, hydrostatic pressure. Subtypes 11.2. to 11.3. Evaporation, low topographic and hydrological gradients, hydrostatic pressure. Subtype 11.5. Steep topographic and hydrological gradients, hydrostatic pressure, fluvial and ocean currents, far-field tectonic activity resulting in local uplift and rejuvenation or modification of drainage systems

Fluids

- Subtypes 11.1. to 11.4. Groundwaters ± surface waters. Subtype 11.5. Surface waters

Ligands

- Subtype 11.1. Ca. Subtypes 11.2. to 11.3. Ca, S. Subtypes 11.4. to 11.5. No information

Reductants, oxidants and adsorbents

- Subtypes 11.1. and 11.4. Organic matter, sulphate reducing bacteria, iron sulphides, ± H_2S, CH_4, clays, reduced groundwaters. Subtypes 11.2. to 11.3. Calcrete, clays, organic matter, oxygenated waters ± playa lake chemical deltas. Subtype 11.5. Not required

Uranium

- Crystalline basement rocks, granitoids, felsic volcanic rocks, pre-existing uranium accumulations, palaeovalley fill, glacial till

Transport

Fluid pathways

- Subtypes 11.1. to 11.3. Groundwater aquifers. Subtype 11.4. Groundwater aquifers; faults. Subtype 11.5. Fluvial

channels; ocean currents

Trap

Physical

- Subtype 11.1. Low-gradient stream sections; stream blockages (e.g., landslides, beaver dams); groundwater mounds; artesian wells; fault-fracture zones. Subtypes 11.2. to 11.3. Low-gradient palaeovalley sections; palaeovalley bends; palaeovalley confluences; aquifer blockages; playa lake entries; valley calcretes. Subtype 11.4. Artesian wells; groundwater mounds; deeply oxidised fault-fracture zones. Subtype 11.5. Abrupt changes in fluvial channel morphology promoting changes in stream energy conditions, including channel constrictions, enlargements or convergences, migrating channel meanders, bedrock gradient changes, irregular bedrock morphologies and depressions and/or cobbles and boulders; morphological barriers affecting ocean wave and wind energy; interplay between longshore drift and onshore-offshore currents; high energy swell/surf/storm wave action driving large sand fluxes onshore and alongshore; marine transgressions; downwarping of sedimentary basins

Chemical

- Subtype 11.1. Organic ± clay-rich wetland environments (e.g., marshes, bogs, swamps). Subtypes 11.2. to 11.3. Zones of groundwater pooling/upwelling; valley calcretes; chemical playa lake deltas. Subtype 11.4. Redox interfaces. Subtype 11.5. Not required

Deposition

Change in redox conditions

- Subtype 11.1. Due to (i) interaction between oxidised uranium-bearing groundwaters and reductants; and/or (ii) evapotranspiration promoting changes in groundwater chemistry. Subtypes 11.2. to 11.3. Due to (i) interaction between oxidised uranium-bearing groundwaters and reductants; (ii) interaction between oxidised uranium-bearing groundwaters and $CaCO_3$ accumulations; (iii) mixing of oxidised uranium-bearing groundwaters and groundwaters from deeper reservoirs; (iv) mixing of oxidised uranium-bearing groundwaters and highly saline playa lake waters; (v) changes in pH, Eh and partial pressure of CO_2; (vi) evaporation/evapotranspiration promoting changes in water chemistry; and/or (vii) colloidal precipitation. Subtype 11.4. Due to (i) reduction/oxidation processes controlled by bacterial/microbial activity; (ii) mixing of oxidised uranium-bearing groundwaters and deeper, reduced groundwaters; (iii) interaction of oxidised uranium-bearing with reductants; and/or (iv) evapotranspiration promoting changes in groundwater chemistry

Adsorption

- Subtype 11.1. Adsorption of uranium onto organic matter. Subtypes 11.2. to 11.3. Adsorption of uranium onto clays and organic matter. Subtype 11.4. Adsorption of uranium onto clays

Decrease in current velocity

- Subtype 11.5. (i) Decrease in fluvial/shallow marine current velocity below the level required for further transport of heavy detrital minerals, promoting placer deposition; and (ii) repeated sediment reworking, selective sorting of mineral grains by mass and volume and further placer concentration

Preservation

- Tectonic stability
- Climatic stability
- Remobilisation and redeposition
- Subtype 11.1. only: Location in remote, undeveloped regions (human activity may result in wetland destruction and/or reduction of water availability)

Key Reference Bibliography

CHUDASAMA, B., PORWAL, A. K., GONZÁLEZ-ÁLVAREZ, I., THAKUR, S., WILDE, A., KREUZER, O. P., Calcrete-hosted surficial uranium systems in Western Australia: Prospectivity modeling and quantitative estimates of resources. 1. Origin of calcrete uranium deposits in surficial environments: Ore Geology Reviews, 102, 906-936 (2018).

CHUDASAMA, B., KREUZER, O. P., THAKUR, S., PORWAL, A. K., BUCKINGHAM, A. J., Surficial uranium mineral systems in Western Australia: Geologically permissive tracts and undiscovered endowment. In: Quantitative and spatial evaluations of undiscovered uranium resources. IAEA TECDOC Series, 1861, 446-614 (2018).

DAHLKAMP, F. J., Uranium Deposits of the World: Asia. Springer, Berlin, Heidelberg, 492p (2009).

DAHLKAMP, F. J., Uranium Deposits of the World: Europe. Springer, Berlin, Heidelberg, 792p (2016).

ELS, G., ERIKSSON, P., Placer formation and placer minerals. Ore Geology Reviews, 4, 373-375 (2006).

GARNETT, R. H. T., BASSETT, N. C., Placer deposits. In: HEDENQUIST, J. W., THOMPSON, J. F. H, GOLDFARB, R. J., RICHARDS, J. P. (eds.), Economic Geology 100th Anniversary Volume, 813-843 (2005).

HOATSON, D. M., JAIRETH, S., MIEZITIS, Y., The major rare-earth-element deposits of Australia: geological setting, exploration, and resources. Geoscience Australia, 204p (2017).

INTERNATIONAL ATOMIC ENERGY AGENCY, Geological Classification of Uranium Deposits and Description of Selected Examples. IAEA-TECDOC Series, 1842, 415p (2018).

JAIRETH, S., ROACH, I. C., BASTRAKOV, E., LIU, S., Basin-related uranium mineral systems in Australia: A reviewof critical features. Ore Geology Reviews, 76, 360-394 (2015).

LEVSON, V. M., Surficial placers. In: LEFEBURE, D. V., RAY, G. E. (eds.), Selected British Columbia Mineral Deposit Profiles, Volume 1 - Metallics and Coal. British Columbia Ministry of Employment and Investment, Open File Report 1995-20, 21-23 (1995).

NOBLE, R. R. P., GRAY, D. J., REID, N., Regional exploration for channel and playa uranium deposits in Western Australia using groundwater. Applied Geochemistry, 26, 1956-1974 (2011).

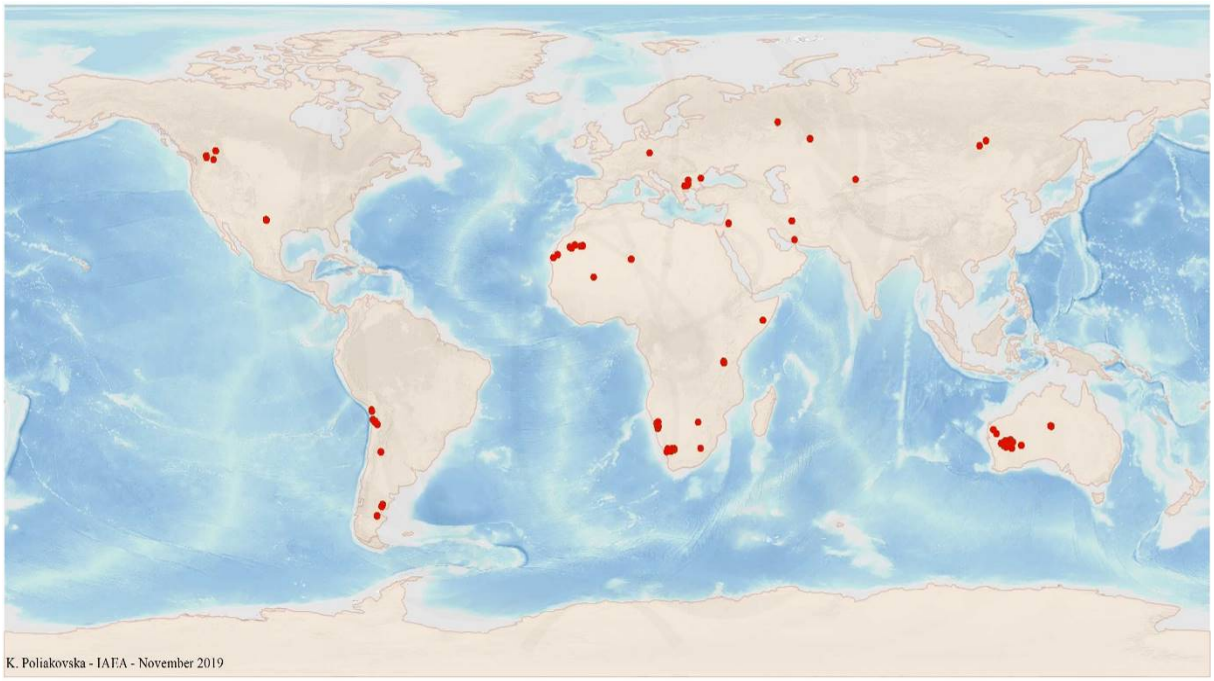

FIG. 11a. World distribution of selected Surficial uranium deposits from the UDEPO database.

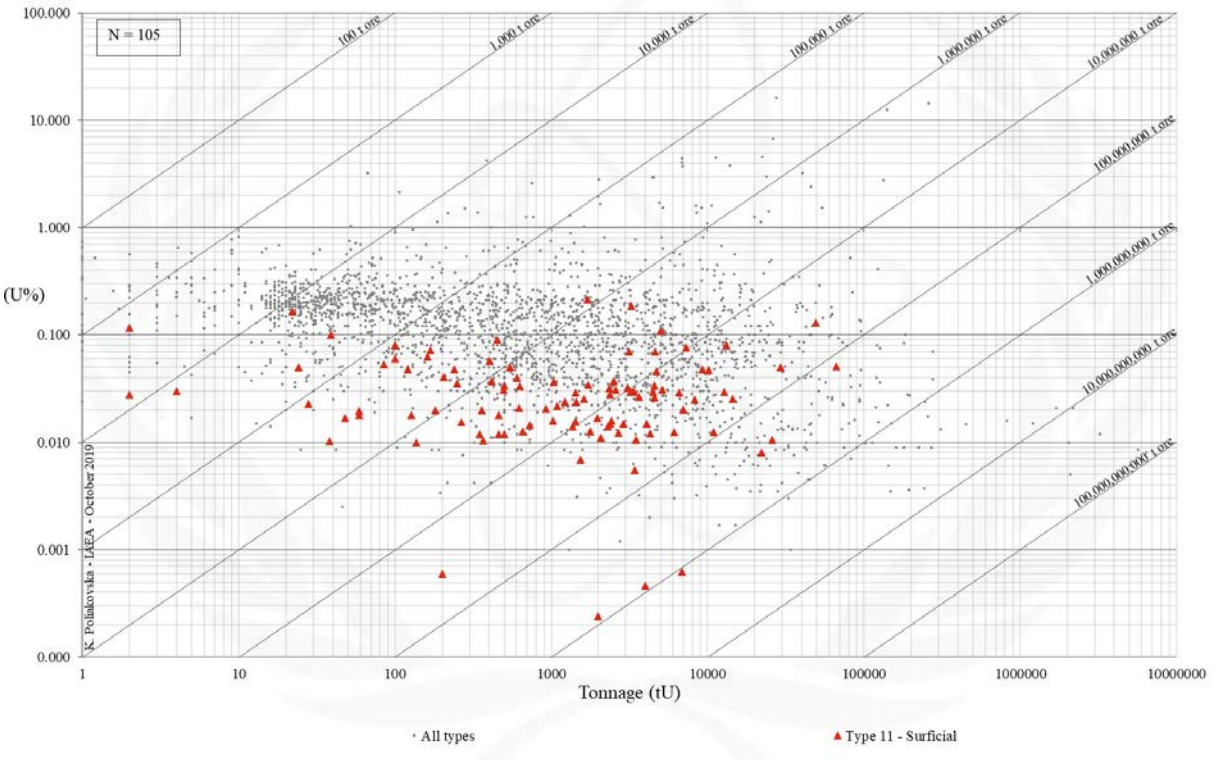

FIG. 11b. Grade and tonnage scatterplot highlighting Surficial uranium deposits from the UDEPO database.

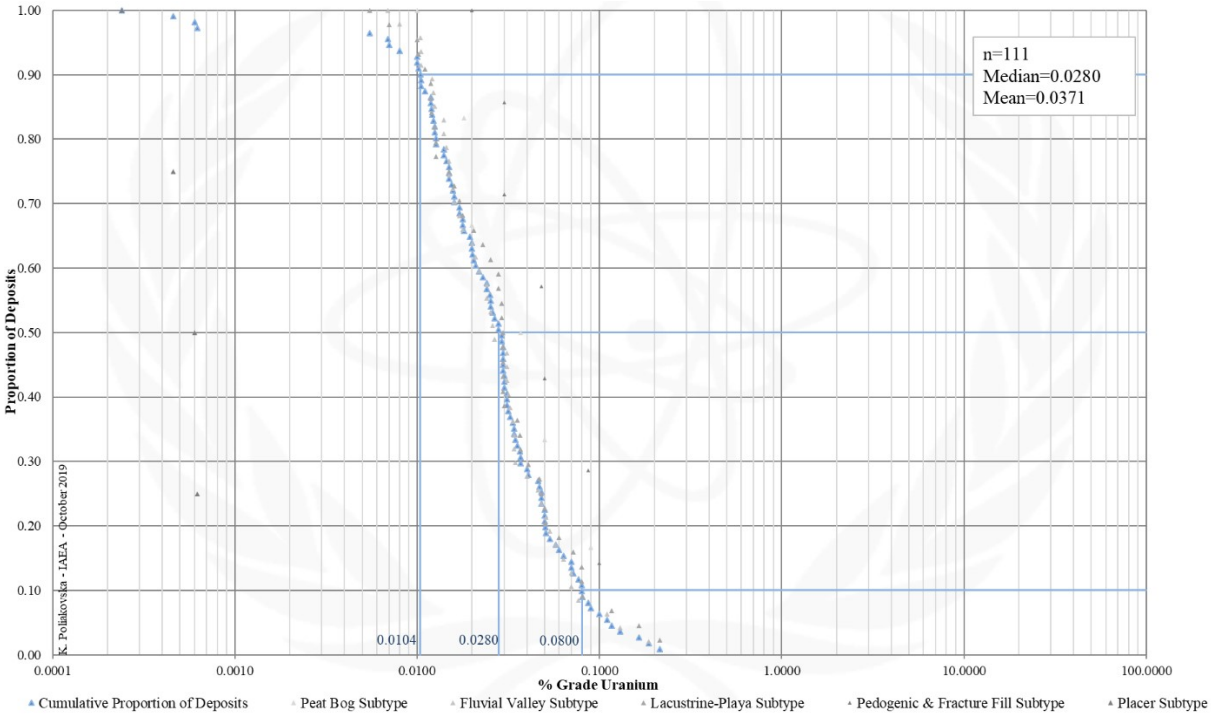

FIG. 11c. Grade Cumulative Probability Plot for Surficial uranium deposits from the UDEPO database.

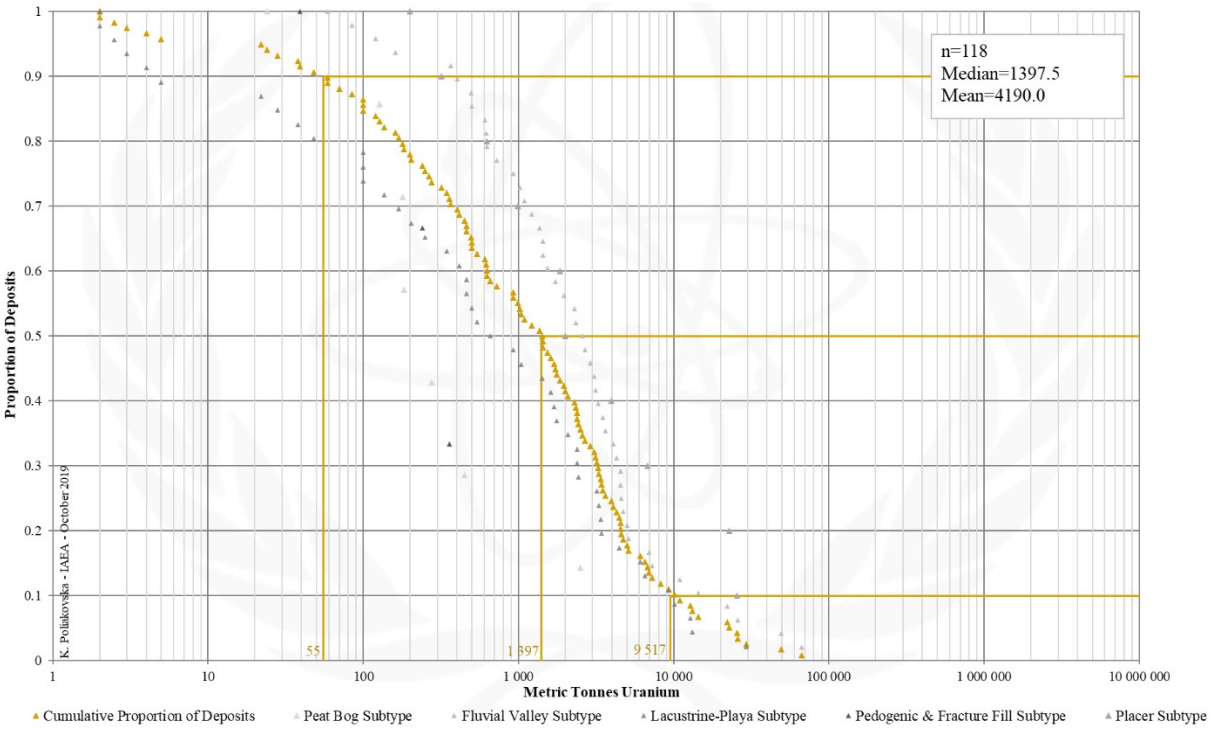

FIG. 11d. Tonnage Cumulative Probability Plot for Surficial uranium deposits from the UDEPO database.

SUBTYPE 11.1. Surficial, Peat Bog

Brief Description
- Surficial deposits cover a diverse group of young (Tertiary to recent), near-surface uranium concentrations in un- or poorly consolidated sediments or soils.
- Peat bog deposits are an uncommon type of uranium deposit and are not known to form accumulations of economic significance.
- They form in intramontane or intracratonic basins adjacent to uranium-enriched source regions.
- The uranium typically accumulates in fluviolacustrine swamps, bogs and muskegs rich in vegetal organic matter.
- No discrete uranium minerals are formed.

Type Examples
- Kamushanovskoye, Kyrgyzstan; Flodelle Creek, USA; Prairie Flats, Canada

Genetically Associated Deposit Types
- Subtype 11.2. Fluvial valley
- Subtype 11.3. Lacustrine-playa
- Subtype 11.4. Pedogenic and fracture fill
- Subtype 11.5. Placer

Principal Commodities
- U

Grades (%) and Tonnages (tU)
- Average: 0.0375, 536.4
- Median: 0.0285, 183.0

Number of Deposits
- Deposits: 8

Provinces (undifferentiated from Surficial Type)
- BC Okanagan Valley, Chile Nth, Chu Basin East, Gascoyne, Gawler Craton, Mayoni Bahi, Namib Desert, Neuquen Basin South, Ngalia Basin, Reguibat Shield, San Jorge Chunut, Texas Southern High Plains, Upington, Volga Ural, Yilgarn North.

Tectonic Setting
- Intermontane basins, intracratonic basins

Typical Geological Age Range
- Tertiary to Recent

Mineral Systems Model

Source

Ground preparation
- Orogenesis; structural preparation (in particular fracturing) of source rocks; actively eroding mountainous terrain; glaciation and deposition of highly permeable till aquifers

Energy
- Steep topographic and hydrological gradients, hydrostatic pressure

Fluids
- Groundwaters
- Surface waters

Ligands
- Ca

Reductants, oxidants and adsorbents
- Organic matter, sulphate reducing bacteria, iron sulphides, ± H_2S, CH_4, clays, reduced groundwaters

Uranium
- Crystalline basement rocks, granitoids, felsic volcanic rocks, pre-existing uranium accumulations, glacial till

Transport

Fluid pathways
- Groundwater aquifers

Trap

Physical
- Low-gradient stream sections
- Stream blockages (e.g., landslides, beaver dams)
- Groundwater mounds, artesian wells
- Fault-fracture zones

Chemical
- Organic ± clay-rich wetland environments (e.g., marshes, bogs, swamps)

Deposition

Change in redox conditions
- Due to interaction between oxidised uranium-bearing groundwaters and reductants

- Due to evapotranspiration promoting changes in groundwater chemistry

Adsorption

- Adsorption of uranium onto organic matter

Preservation

- Tectonic stability
- Climatic stability
- Remobilisation and redeposition
- Location in remote, undeveloped regions (human activity may result in wetland destruction and/or reduction of water availability)

Key Reference Bibliography

INTERNATIONAL ATOMIC ENERGY AGENCY, Geological Classification of Uranium Deposits and Description of Selected Examples. IAEA-TECDOC Series, 1842, 415p (2018).

OTTON, J. K., ZIELINSKI, R. A., JOHNSON, S. Y., The Flodelle Creek surficial uranium deposit, Stevens County, Washington, USA. IAEA TECDOC Series, 500, 241-261 (1989).

TIXIER, K., BECKIE, R., Uranium depositional controls at the Prairie Flats surficial uranium deposit, Summerland, British Columbia. Environmental Geology, 40, 1242-1251 (2001).

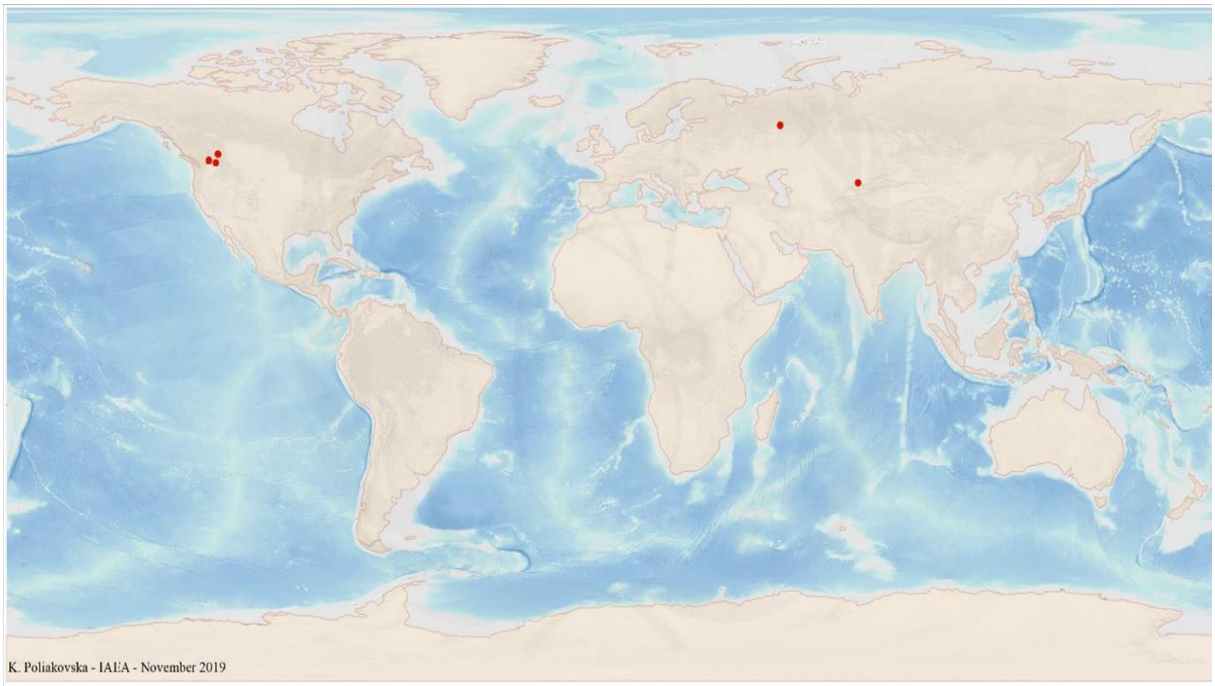

FIG. 11.1a. World distribution of selected Surficial Peat Bog uranium deposits from the UDEPO database.

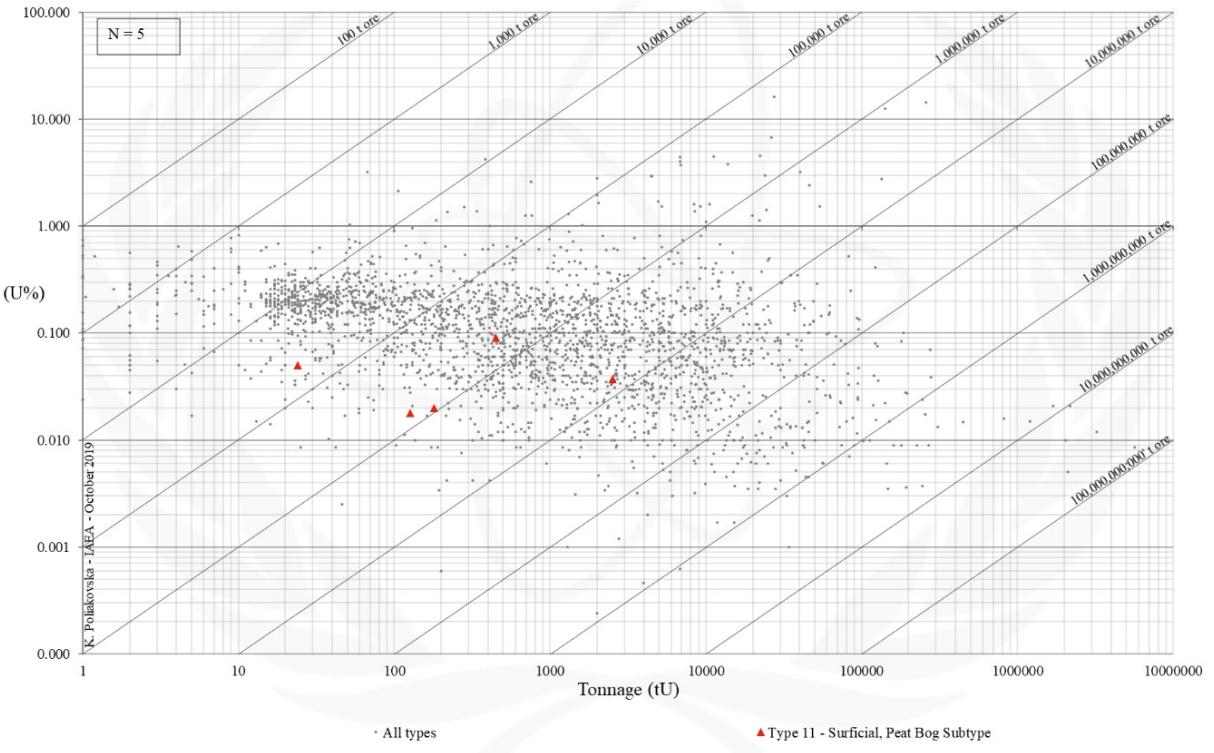

FIG. 11.1b. Grade and tonnage scatterplot highlighting Surficial Peat Bog uranium deposits from the UDEPO database.

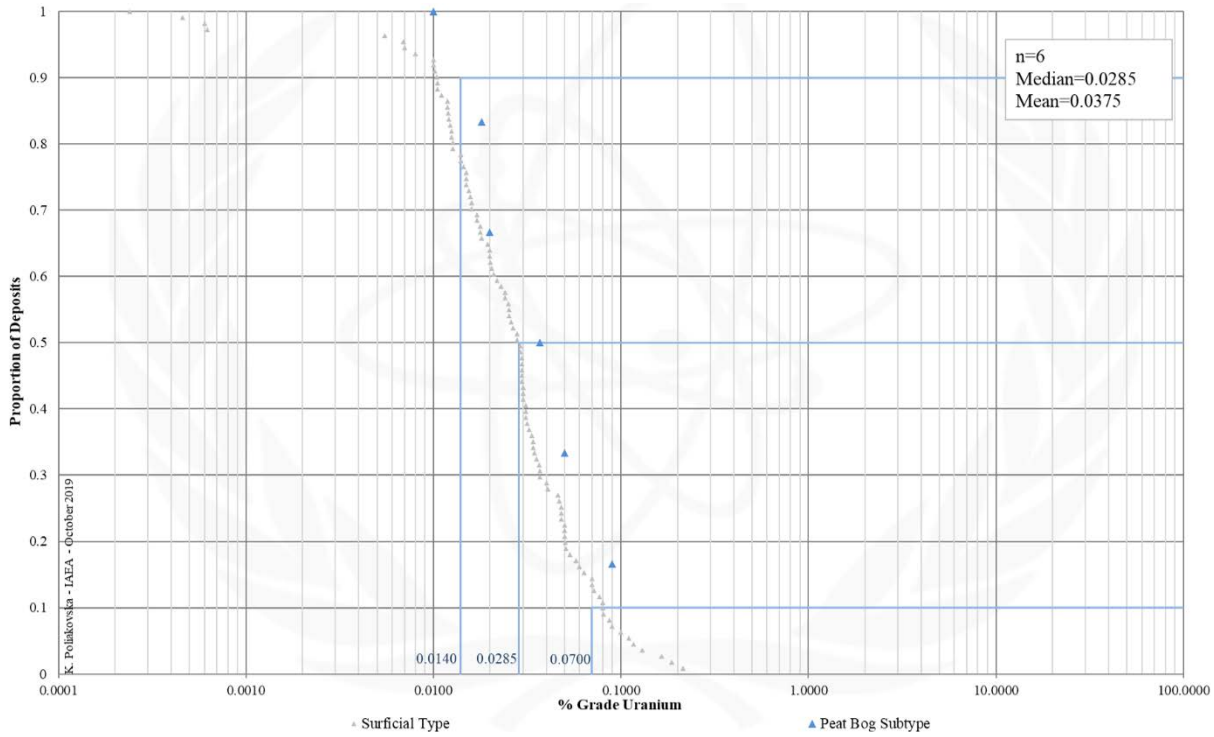

FIG. 11.1c. Grade Cumulative Probability Plot for Surficial Peat Bog uranium deposits from the UDEPO database.

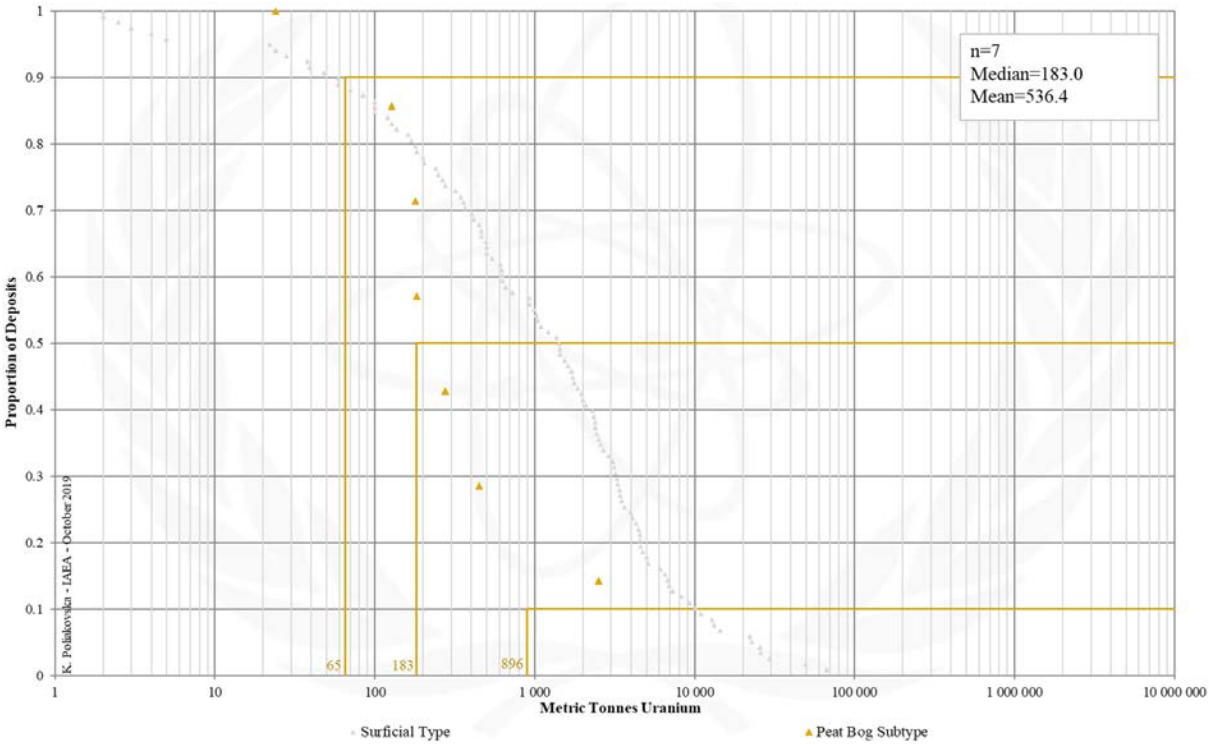

FIG. 11.1d. Tonnage Cumulative Probability Plot for Surficial Peat Boguranium deposits from the UDEPO database.

SUBTYPE 11.2. Surficial, Fluvial Valley

Brief Description

- Surficial deposits cover a diverse group of young (Tertiary to recent), near-surface uranium concentrations in un- or poorly consolidated sediments or soils.
- Fluvial valley uranium deposits occur in palaeovalleys in peneplained cratonic regions in semiarid to arid climate zones.
- The uranium ores take the form of disseminations, vug linings and fracture coatings in calcrete-cemented and non-calcareous conglomerates, silts and sands, gypsiferous sands and associated calcretised conglomerates, or mounded groundwater calcretes and dolocretes and associated fine-grained alluvial sediments.
- Fluvial valley uranium deposits are commonly found within the capillary fringe zone directly above moving groundwater and at or immediately below the local water table.

Type Examples

- Yeelirrie, Thatcher Soak, Dawson-Hinkler, Australia; Langer Heinrich, Trekkopje, Tumas, Namibia

Genetically Associated Deposit Types

- Subtype 11.1. Peat bog
- Subtype 11.3. Lacustrine-playa
- Subtype 11.4. Pedogenic and fracture fill
- Subtype 11.5. Placer

Principal Commodities

- U, V

Grades (%) and Tonnages (tU)

- Average: 0.0363, 6010.0
- Median: 0.0260, 2470.0

Number of Deposits

- Deposits: 48

Provinces (undifferentiated from Surficial Type)

- BC Okanagan Valley, Chile Nth, Chu Basin East, Gascoyne, Gawler Craton, Mayoni Bahi, Namib Desert, Neuquen Basin South, Ngalia Basin, Reguibat Shield, San Jorge Chunut, Texas Southern High Plains, Upington, Volga Ural, Yilgarn North.

Tectonic Setting

- Tectonically stable, peneplained cratonic environments

Typical Geological Age Range

- Tertiary to Recent

Mineral Systems Model

Source

Ground preparation
- Structural preparation (in particular fracturing) of source rocks
- Development of tectonically stable peneplain environments
- Formation and burial of long-lived fluvial river systems
- Climate change from humid to (semi-)arid
- Deep weathering/oxidation

Energy
- Evaporation,
- Low topographic and hydrological gradients
- Hydrostatic pressure

Fluids
- Groundwaters ± surface waters

Ligands
- Ca, S

Reductants, reactants and adsorbents
- Calcrete, clays, organic matter, playa lake chemical deltas

Uranium, vanadium, potassium ± calcium
- Crystalline basement rocks, granitoids, mafic-ultramafic volcanic rocks, banded iron formations, palaeovalley fill

Transport

Fluid pathways
- Groundwater aquifers

Trap

Physical
- Low-gradient palaeovalley sections
- Palaeovalley bends
- Palaeovalley confluences

- Aquifer blockages
- Playa lake entries
- Valley calcretes

Chemical

- Zones of groundwater pooling/upwelling
- Playa lake chemical deltas
- Valley calcretes

Deposition

Change in redox conditions

- Due to interaction between oxidised uranium-bearing groundwaters and reductants
- Due to interaction between oxidised uranium-bearing groundwaters and $CaCO_3$ accumulations
- Due to mixing of oxidised uranium-bearing groundwaters and groundwaters from deeper reservoirs
- Due to mixing of oxidised uranium-bearing groundwaters and highly saline playa lake waters
- Due to changes in pH, Eh and partial pressure of CO_2
- Due to evaporation/evapotranspiration promoting changes in water chemistry
- Due to colloidal precipitation

Adsorption

- Adsorption of uranium onto clays and organic matter

Preservation

- Tectonic stability
- Climatic stability
- Remobilisation and redeposition

Key Reference Bibliography

CHUDASAMA, B., PORWAL, A. K., GONZÁLEZ-ÁLVAREZ, I., THAKUR, S., WILDE, A., KREUZER, O. P., Calcrete-hosted surficial uranium systems in Western Australia: Prospectivity modeling and quantitative estimates of resources. Part 1—Origin of calcrete uranium deposits in surficial environments: A review. Ore Geology Reviews, 102, 906-936 (2018).

CHUDASAMA, B., KREUZER, O. P., THAKUR, S., PORWAL, A. K., BUCKINGHAM, A. J., Surficial uranium mineral systems in Western Australia: Geologically permissive tracts and undiscovered endowment. In: Quantitative and spatial evaluations of undiscovered uranium resources. IAEA-TECDOC Series, 1861, 446-614 (2018).

HALL, S. M., MIHALASKY, M. J., Grade, tonnage, and location data for world calcrete-type surficial uranium deposits. USGS Data Release DR-F7MS3RQS (2017).

INTERNATIONAL ATOMIC ENERGY AGENCY, Geological Classification of Uranium Deposits and Description of Selected Examples. IAEA-TECDOC Series, 1842, 415p (2018).

JAIRETH, S., ROACH, I. C., BASTRAKOV, E., LIU, S., Basin-related uranium mineral systems in Australia: A reviewof critical features. Ore Geology Reviews, 76, 360-394 (2015).

NOBLE, R. R. P., GRAY, D. J., REID, N., Regional exploration for channel and playa uranium deposits in Western Australia using groundwater. Applied Geochemistry, 26, 1956-1974 (2011).

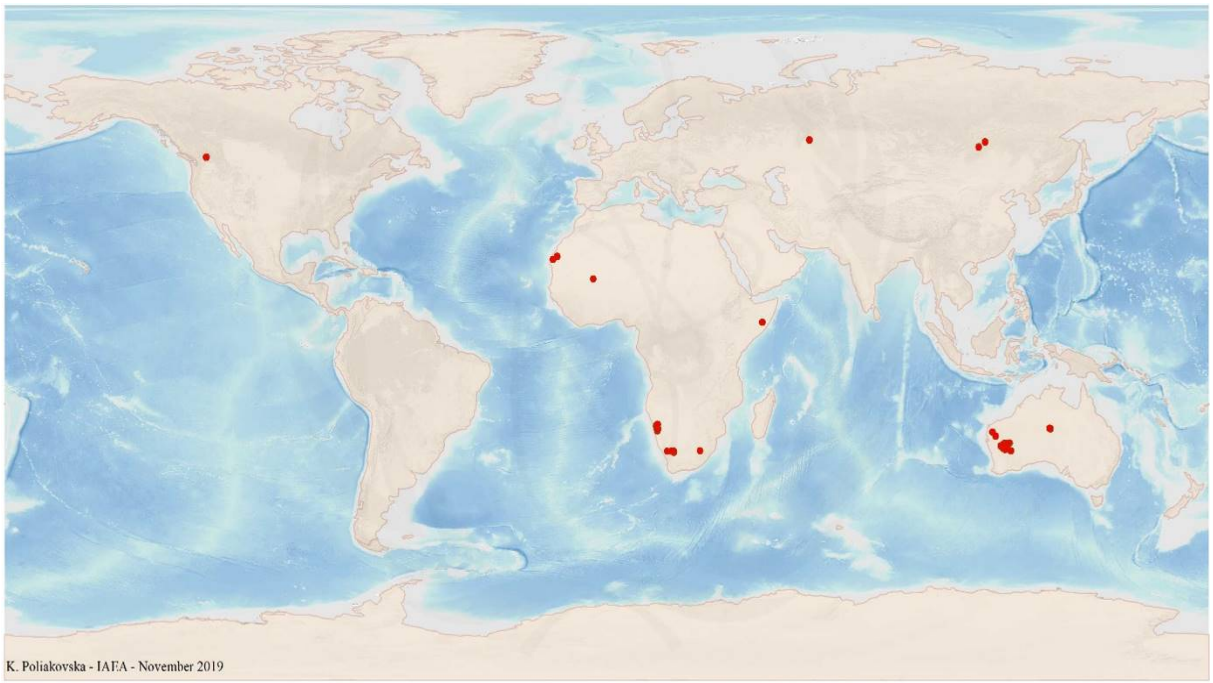

FIG. 11.2a. World distribution of selected Surficial Fluvial Valley uranium deposits from the UDEPO database.

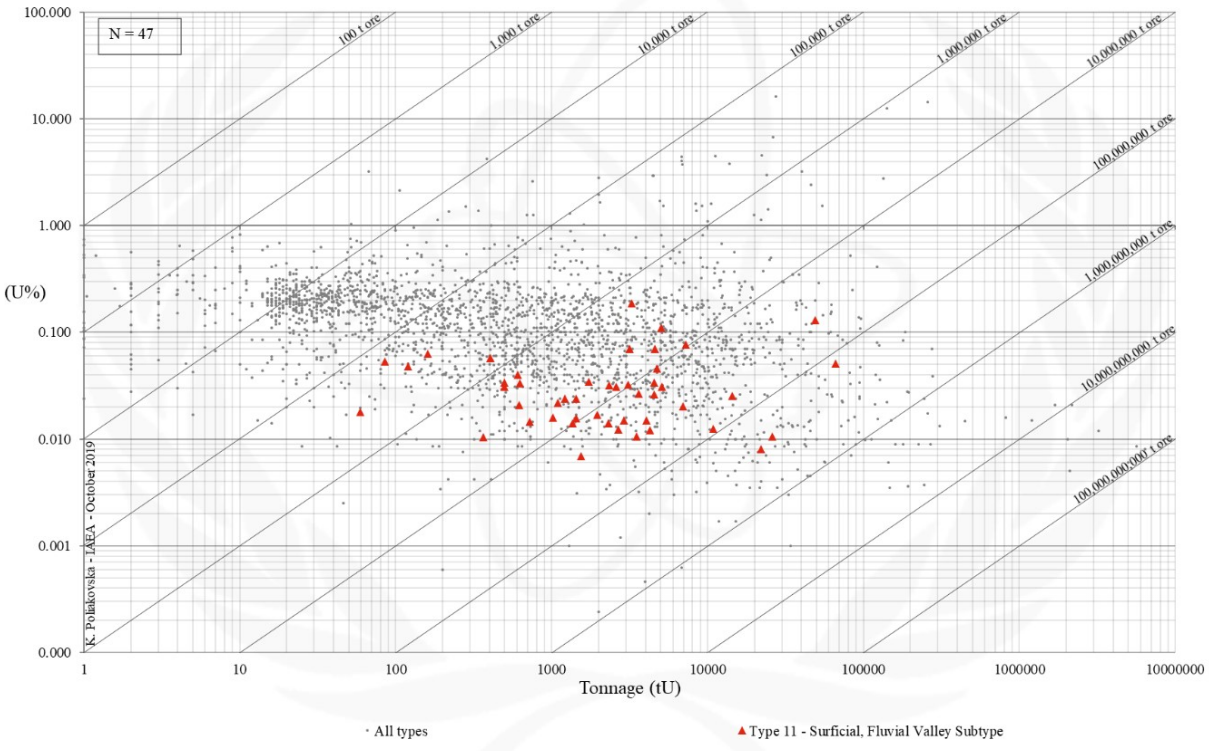

FIG. 11.2b. Grade and tonnage scatterplot highlighting Surficial Fluvial Valley uranium deposits from the UDEPO database.

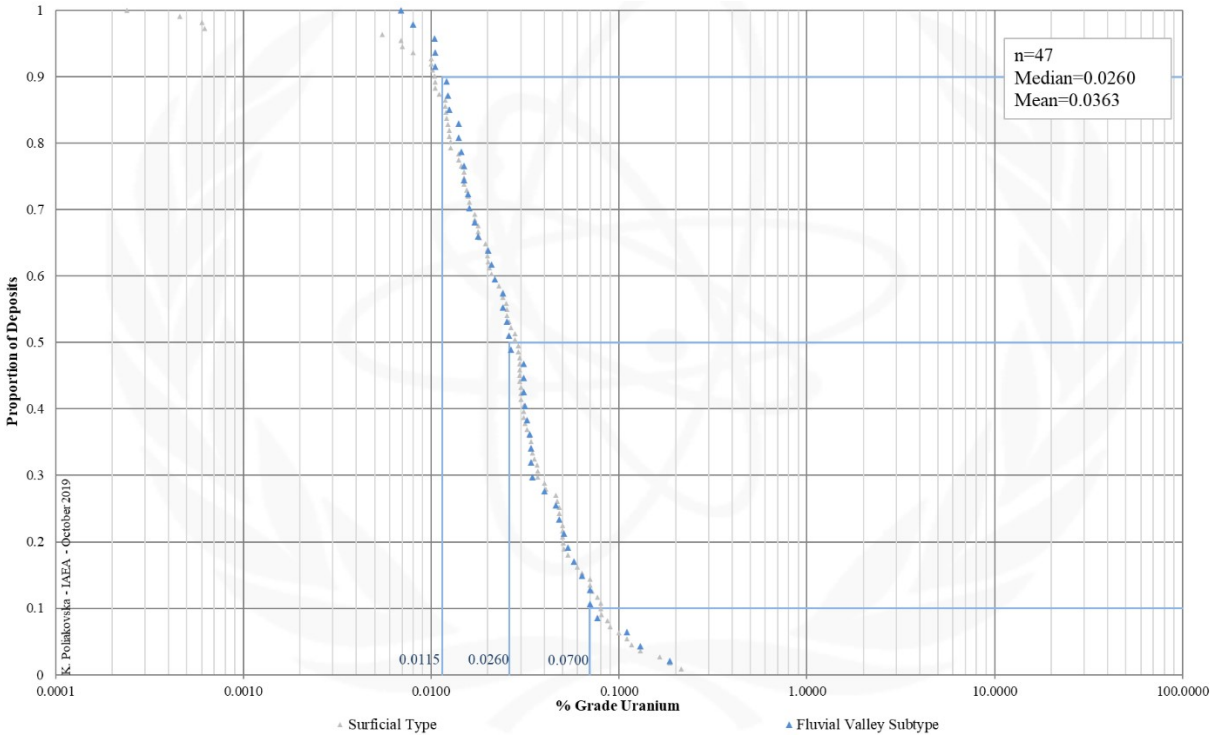

FIG. 11.2c. Grade Cumulative Probability Plot for Surficial Fluvial Valley uranium deposits from the UDEPO database.

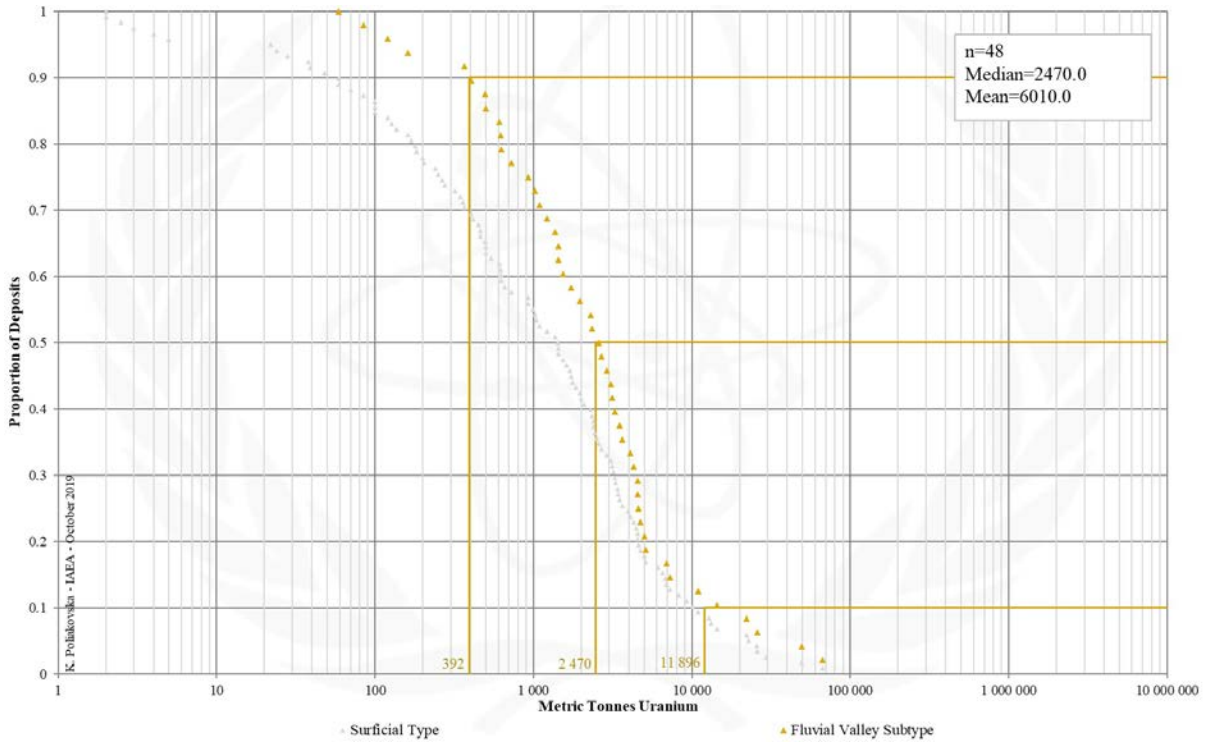

FIG. 11.2d. Tonnage Cumulative Probability Plot for Surficial Fluvial Valley uranium deposits from the UDEPO database.

TYPE 11.3. Surficial, Lacustrine-Playa

Brief Description
- Surficial deposits cover a diverse group of young (Tertiary to recent), near-surface uranium concentrations in un- or poorly consolidated sediments or soils.
- Lacustrine-playa deposits occur in ephemeral lakebeds in peneplained cratonic regions within semiarid to arid climate zones, commonly downstream from fluvial valley uranium deposits with which they are genetically related.
- The uranium ores typically take the form of disseminations and encrustations in evaporitic and alluvial sediments and soft calcrete horizons that accumulated in playa lakes at or near the groundwater table.

Type Examples
- Lake Maitland, Lake Way, Centipede/Millipede, Lakeside, Australia

Genetically Associated Deposit Types
- Subtype 11.1. Peat bog
- Subtype 11.2. Fluvial valley
- Subtype 11.4. Pedogenic and fracture fill
- Subtype 11.5. Placer

Principal Commodities
- U, V

Grades (%) and Tonnages (tU)
- Average: 0.0400, 2773.2
- Median: 0.0292, 599.0

Number of Deposits
- Deposits: 52

Provinces (undifferentiated from Surficial Type)
- BC Okanagan Valley, Chile Nth, Chu Basin East, Gascoyne, Gawler Craton, Mayoni Bahi, Namib Desert, Neuquen Basin South, Ngalia Basin, Reguibat Shield, San Jorge Chunut, Texas Southern High Plains, Upington, Volga Ural, Yilgarn North.

Tectonic Setting
- Tectonically stable, peneplained cratonic environments

Typical Geological Age Range
- Tertiary to Recent

Mineral Systems Model

Source

Ground preparation
- Structural preparation (in particular fracturing) of source rocks
- Development of tectonically stable peneplain environments
- Formation and burial of long-lived fluvial river systems
- Climate change from humid to (semi-)arid
- Deep weathering/oxidation

Energy
- Evaporation,
- Low topographic and hydrological gradients
- Hydrostatic pressure

Fluids
- Groundwaters
- Surface waters

Ligands
- Ca, S

Reductants, reactants and adsorbents
- (Soft) calcrete, clays, organic matter, playa lake chemical deltas

Uranium, vanadium, potassium ± calcium
- Crystalline basement rocks, granitoids, mafic-ultramafic volcanic rocks, banded iron formations, basin fill

Transport

Fluid pathways
- Groundwater aquifers

Trap

Physical
- Playa lake entries
- Soft calcretes and clays

Chemical
- Zones of groundwater pooling/upwelling
- Playa lake chemical deltas

- Soft calcretes
- Organic matter

Deposition

Change in redox conditions
- Due to mixing of oxidised uranium-bearing groundwaters and highly saline playa lake waters
- Due to changes in pH, Eh and partial pressure of CO_2
- Due to evaporation/evapotranspiration promoting changes in water chemistry

Adsorption
- Adsorption of uranium onto clays and organic matter

Preservation

- Tectonic stability
- Climatic stability
- Remobilisation and redeposition

Key Reference Bibliography

CHUDASAMA, B., PORWAL, A. K., GONZÁLEZ-ÁLVAREZ, I., THAKUR, S., WILDE, A., KREUZER, O. P., Calcrete-hosted surficial uranium systems in Western Australia: Prospectivity modeling and quantitative estimates of resources. Part 1—Origin of calcrete uranium deposits in surficial environments: A review. Ore Geology Reviews, 102, 906-936 (2018).

CHUDASAMA, B., KREUZER, O. P., THAKUR, S., PORWAL, A. K., BUCKINGHAM, A. J., Surficial uranium mineral systems in Western Australia: Geologically permissive tracts and undiscovered endowment. In: Quantitative and spatial evaluations of undiscovered uranium resources. IAEA TECDOC Series, 1861, 446-614 (2018).

HALL, S. M., MIHALASKY, M. J., Grade, tonnage, and location data for world calcrete-type surficial uranium deposits. USGS Data Release DR-F7MS3RQS (2017).

INTERNATIONAL ATOMIC ENERGY AGENCY, Geological Classification of Uranium Deposits and Description of Selected Examples. IAEA-TECDOC Series, 1842, 415p (2018).

JAIRETH, S., ROACH, I. C., BASTRAKOV, E., LIU, S., Basin-related uranium mineral systems in Australia: A reviewof critical features. Ore Geology Reviews, 76, 360-394 (2015).

NOBLE, R. R. P., GRAY, D. J., REID, N., Regional exploration for channel and playa uranium deposits in Western Australia using groundwater. Applied Geochemistry, 26, 1956-1974 (2011).

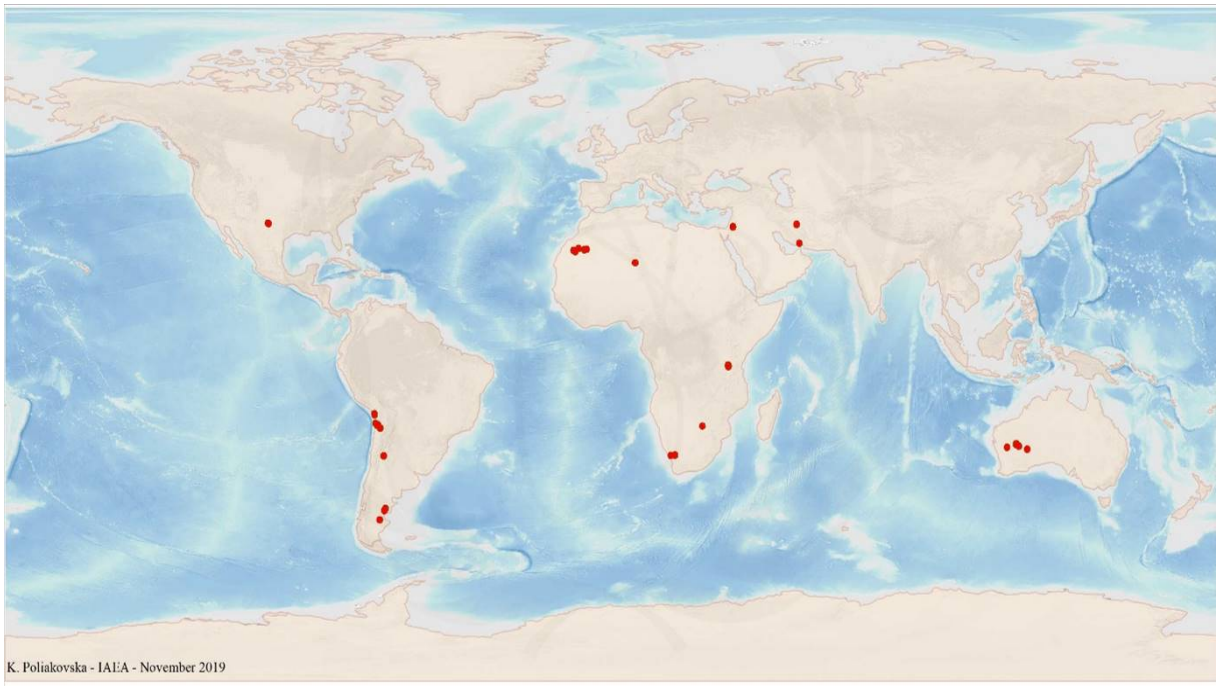

FIG. 11.3a. World distribution of selected Surficial Lacustrine-Playa uranium deposits from the UDEPO database.

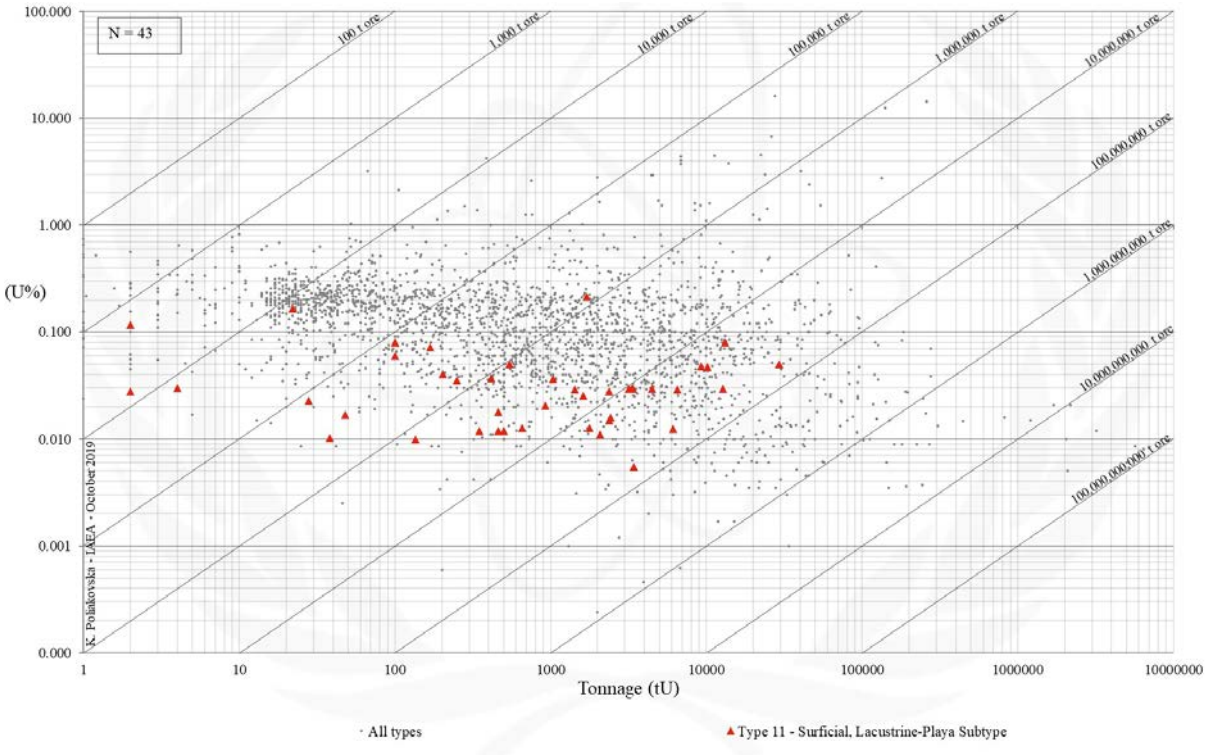

FIG. 11.3b. Grade and tonnage scatterplot highlighting Surficial Lacustrine-Playa uranium deposits from the UDEPO database.

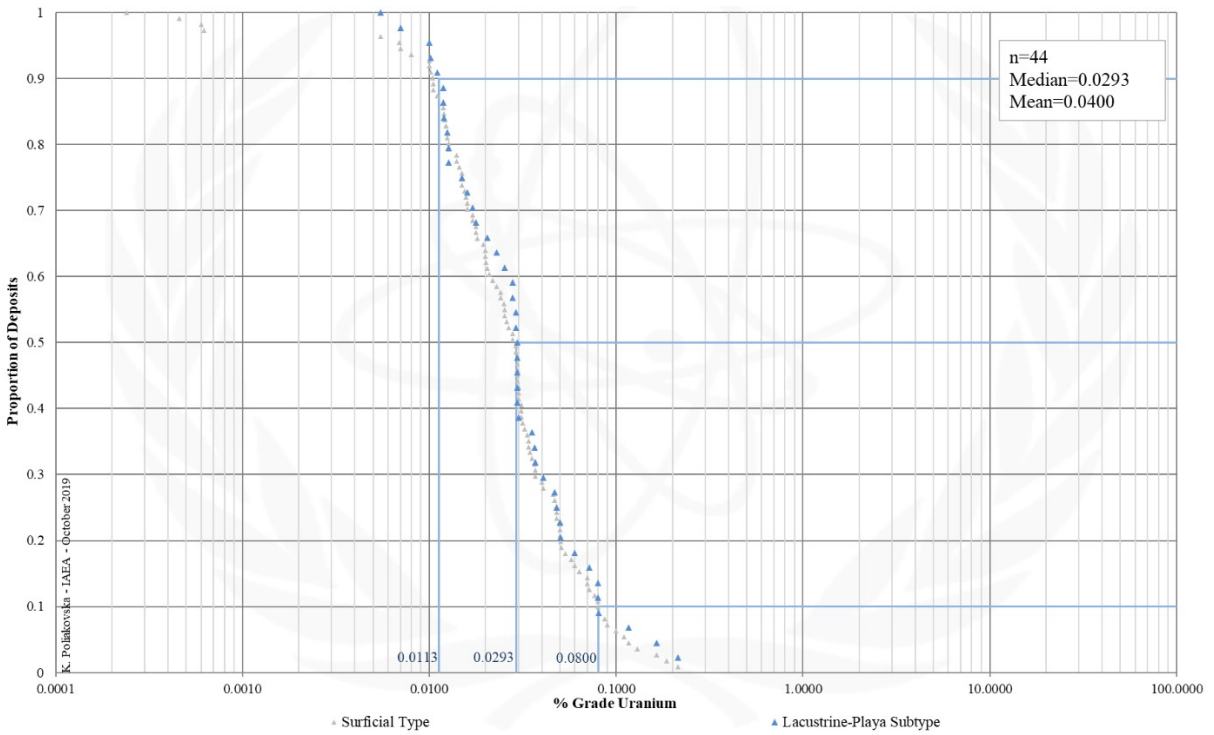

FIG. 11.3c. Grade Cumulative Probability Plot for Surficial Lacustrine-Playa uranium deposits from the UDEPO database.

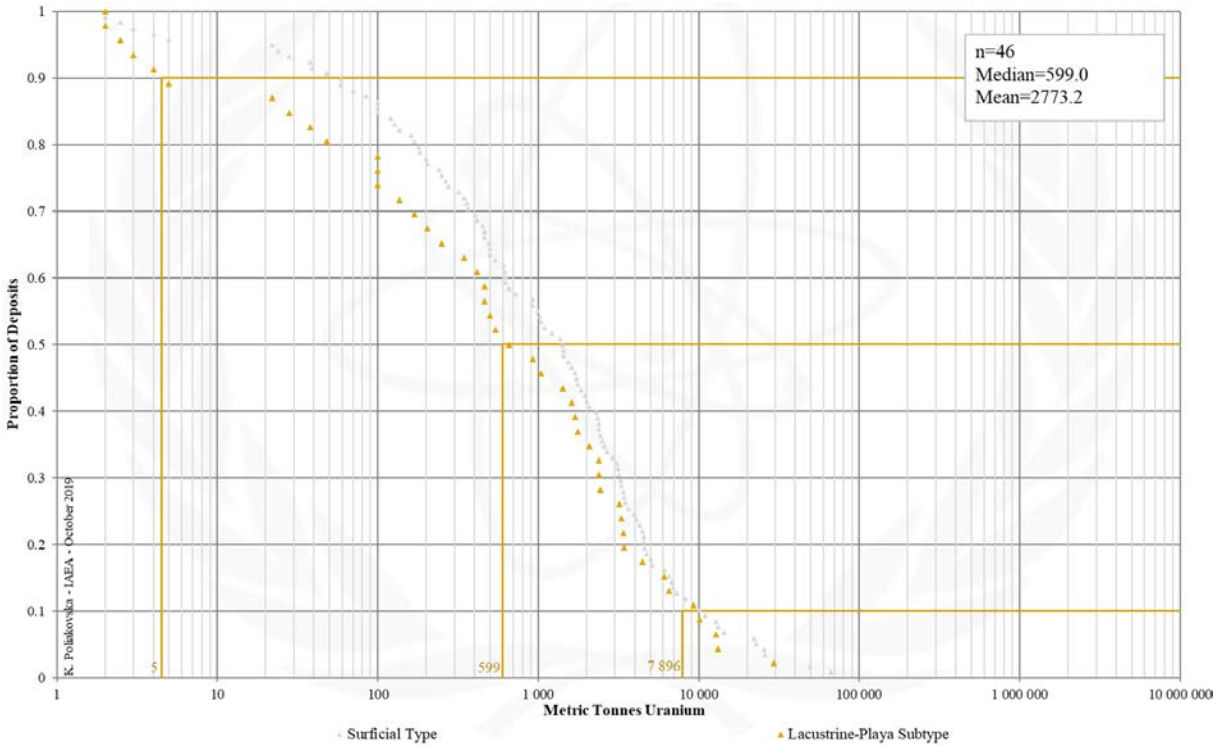

FIG. 11.3d. Tonnage Cumulative Probability Plot for Surficial Lacustrine-Playa uranium deposits from the UDEPO database.

SUBTYPE 11.4. Surficial, Pedogenic & Fracture Fill

Brief Description
- Surficial deposits cover a diverse group of young (Tertiary to recent), near-surface uranium concentrations in un- or poorly consolidated sediments or soils.
- Pedogenic and fracture fill deposits are an uncommon type of uranium deposit and are not known to form accumulations of economic significance.
- The uranium ores, which are hosted in regolith, take the form of disseminations, coatings and fillings in soils and pedogenic encrustations as well as cataclastic zones in deeply oxidised country rocks.

Type Examples
- Beslet, Senokos, Igralishte, Kalatsh Burun and Kara Tepe, Bulgaria; Daybreak Mine, USA

Genetically Associated Deposit Types
- Subtype 11.1. Peat bog
- Subtype 11.2. Fluvial valley
- Subtype 11.3. Lacustrine-playa
- Subtype 11.5. Placer

Principal Commodities
- U

Grades (%) and Tonnages (tU)
- Average: 0.0521, 213.0
- Median: 0.0480, 240.0

Number of Deposits
- Deposits: 7

Provinces (undifferentiated from Surficial Type)
- BC Okanagan Valley, Chile Nth, Chu Basin East, Gascoyne, Gawler Craton, Mayoni Bahi, Namib Desert, Neuquen Basin South, Ngalia Basin, Reguibat Shield, San Jorge Chunut, Texas Southern High Plains, Upington, Volga Ural, Yilgarn North.

Tectonic Setting
- Intermontane basins, intracratonic basins

Typical Geological Age Range
- Tertiary to Recent

Mineral Systems Model

Source

Ground preparation
- Juxtaposition of uraniferous granitoids against young, highly porous sedimentary successions
- Structural preparation (in particular fracturing) of source rocks
- Deep weathering/oxidation

Energy
- Steep topographic and hydrological gradients
- Hydrostatic pressure

Fluids
- Groundwaters
- Surface waters

Ligands
- No information

Reductants, oxidants and adsorbents
- Sulphate reducing bacteria, iron sulphides, clays, organic matter, reduced groundwaters

Uranium, phosphate and calcium
- Granitoids (in particular pegmatites and alaskites), pre-existing uranium accumulations
- Apatite-bearing intrusive and metamorphic rocks

Transport

Fluid pathways
- Shallow ± deeper groundwater aquifers
- Deeply oxidised fault-fracture zones

Trap

Physical
- Artesian wells
- Groundwater mounds
- Deeply oxidised fault-fracture zones

Chemical
- Redox interfaces

Deposition
Change in redox conditions − Due to reduction/oxidation processes controlled by bacterial/microbial activity − Due to mixing of oxidised uranium-bearing groundwaters and reduced groundwaters from deeper aquifers − Due to interaction of oxidised uranium-bearing with wallrock reductants − Due to evapotranspiration promoting changes in groundwater chemistry Adsorption − Adsorption of uranium onto clays
Preservation
− Tectonic stability − Climatic stability − Remobilisation and redeposition

Key Reference Bibliography

DAHLKAMP, F. J., Uranium Deposits of the World: Asia. Springer, Berlin, Heidelberg, 492p (2009).
DAHLKAMP, F. J., Uranium Deposits of the World: USA and Latin America. Springer, Berlin, Heidelberg, 515p (2010).
DAHLKAMP, F. J., Uranium Deposits of the World: Europe. Springer, Berlin, Heidelberg, 792p (2016).
INTERNATIONAL ATOMIC ENERGY AGENCY, Geological Classification of Uranium Deposits and Description of Selected Examples. IAEA-TECDOC Series, 1842, 415p (2018).
LEO, G. W., Autunite from Mt. Spokane, Washington. The American Mineralogist, 45, 99-128 (1960).
UNITED STATES GEOLOGICAL SURVEY, Mineral and water resources of Washington. US Government Printing Office, 436p (1966).

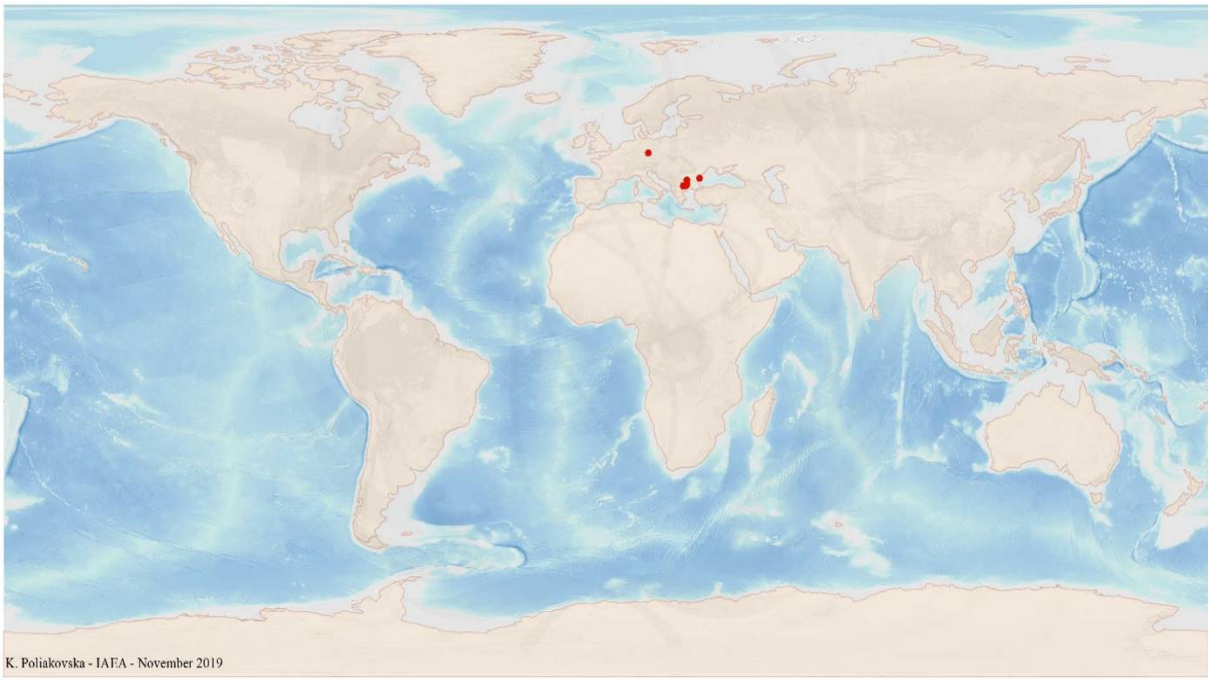

FIG. 11.4a. World distribution of selected Surficial Pedogenic & Fracture Fill uranium deposits from the UDEPO database.

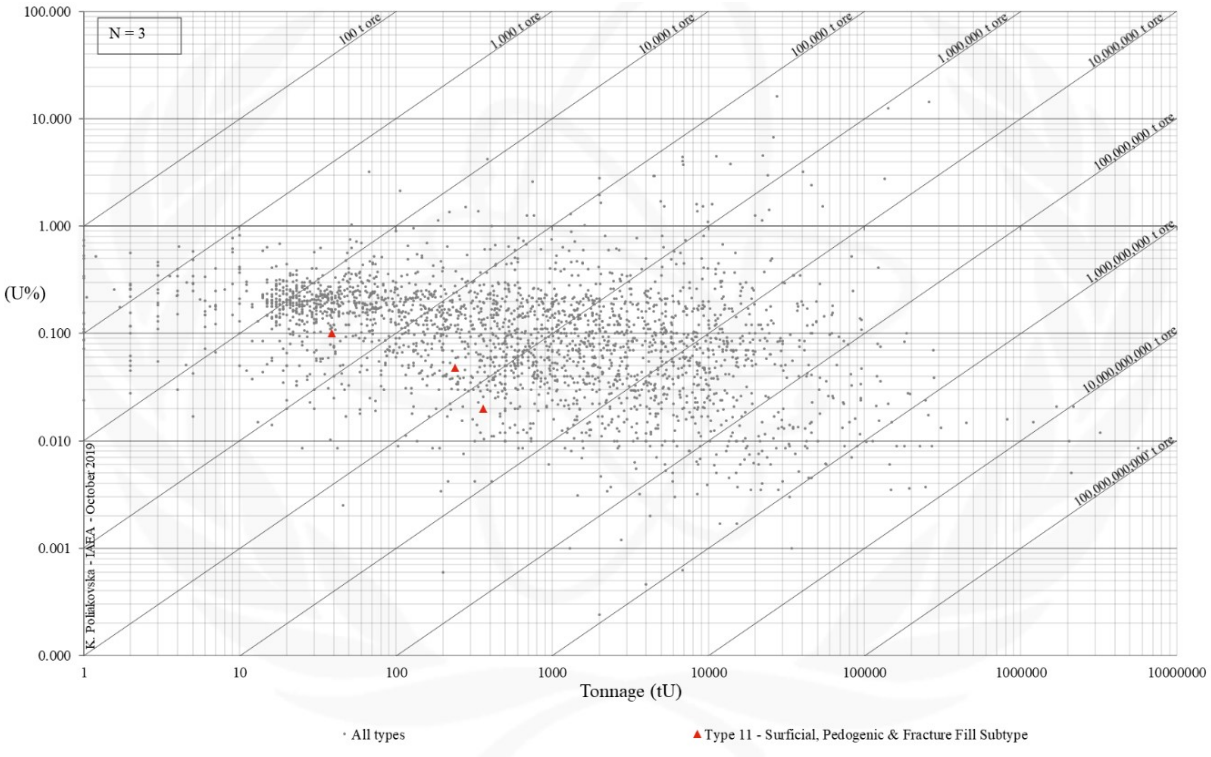

FIG. 11.4b. Grade and tonnage scatterplot highlighting Surficial Pedogenic & Fracture Fill uranium deposits from the UDEPO database.

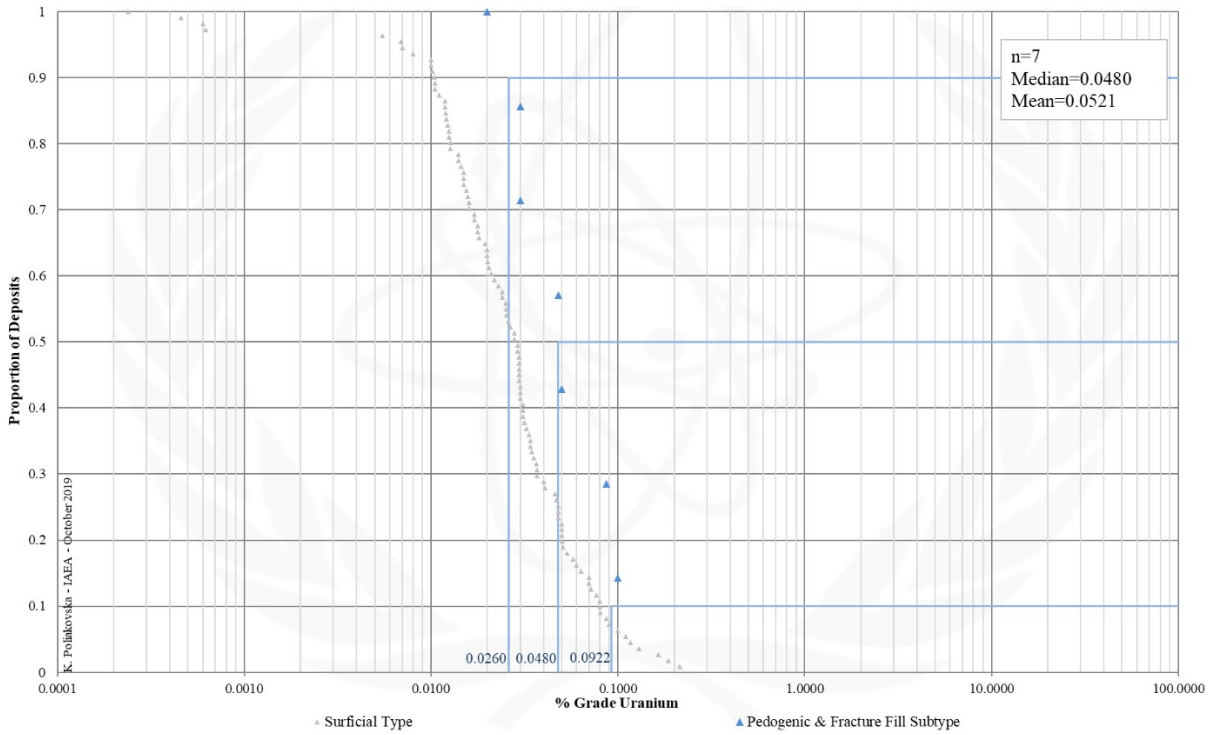

FIG. 11.4c. Grade Cumulative Probability Plot for Surficial Pedogenic & Fracture Fill uranium deposits from the UDEPO database.

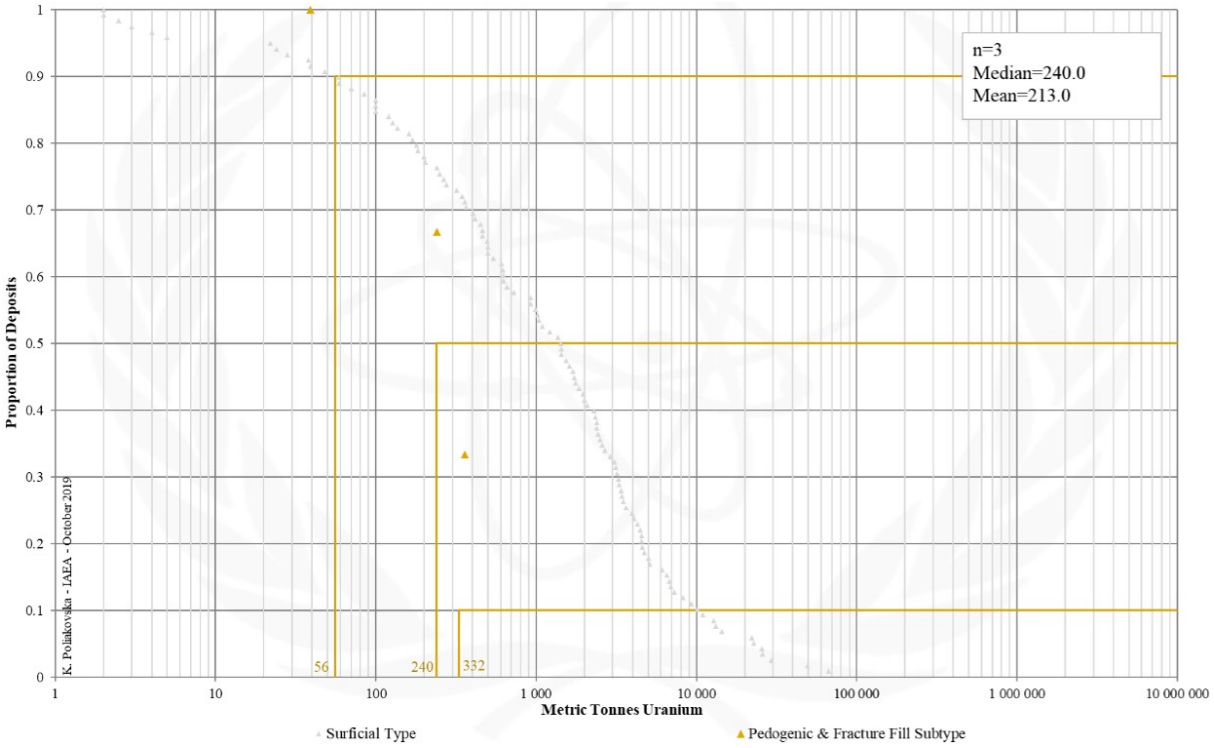

FIG. 11.4d. Tonnage Cumulative Probability Plot for Surficial Pedogenic & Fracture Fill uranium deposits from the UDEPO database.

SUBTYPE 11.5. Surficial, Placer

Brief Description
- Surficial deposits cover a diverse group of young (Tertiary to recent), near-surface uranium concentrations in un- or poorly consolidated sediments or soils.
- Placer deposits are valuable surficial accumulations of dense, hard and chemically stable detrital heavy minerals that form by gravity separation during sedimentary sorting processes in a variety of sedimentary environments.
- Placers can be broadly divided into alluvium, eluvium and beach deposits.
- The principal heavy minerals containing thorium and uranium are zircon, monazite and xenotime. In some cases, the dominant radioactive minerals are uranothorianite, brannerite, euxenite, davidite, betafite and samarskite.

Type Examples
- Alluvial placers: Tash Bulak, Backe, Ottuk, Tunduk, Uzun-Sai, Kyrgyzstan; Bangka Belitung, Semelangan, Indonesia; Red River Valley, USA
- Beach placers: Kerala, India; Coastal Plain Province, USA; Langkawi Islands, Feringghi, Thailand; Ngalia Basin, Australia

Genetically Associated Deposit Types
- Subtype 11.1. Peat bog
- Subtype 11.2. Fluvial valley
- Subtype 11.3. Lacustrine-playa
- Subtype 11.4. Pedogenic and fracture fill

Principal Commodities
- Th, Zr, Ti, P, Fe, REE, U (by- or coproduct only)

Grades (%) and Tonnages (tU)
- Average: 0.0005, 6534.8
- Median: 0.0005, 1925.0

Number of Deposits
- Deposits: 14

Provinces (undifferentiated from Surficial Type)
- BC Okanagan Valley, Chile Nth, Chu Basin East, Gascoyne, Gawler Craton, Namib Desert, Neuquen Basin South, Ngalia Basin, Reguibat Shield, San Jorge Chunut, Texas Southern High Plains, Upington, Volga Ural, Yilgarn North.

Tectonic Setting
- Tectonically stable cratonic/platform environments, stable passive plate margins, intermontane plateaus, accretionary orogenic belts, volcanic arcs and back-arcs

Typical Geological Age Range
- Mesozoic to Recent

Mineral Systems Model

Source

Ground preparation
- Deposition or emplacement of suitable source rocks
- Exposure of source rocks to deep weathering/oxidation
- Formation (± burial) of long-lived fluvial river systems
- Sediment transport along fluvial river systems ± into shallow marine environments

Energy
- Far-field tectonic activity resulting in local uplift and rejuvenation or modification of drainage systems
- (Steep) topographic and hydrological gradients
- Hydrostatic pressure
- Fluvial and ocean currents

Fluids
- Fluvial/ocean waters

Ligands
- Not required

Reductants, oxidants and adsorbents
- Not required

Uranium
- Crystalline basement rocks, granitoids, pre-existing uranium accumulations

Transport

Fluid pathways
- Fluvial channels
- Ocean currents

Trap

Physical
- Abrupt changes in fluvial channel morphology promoting changes in stream energy conditions, including channel

constrictions, enlargements or convergences, migrating channel meanders, bedrock gradient changes, irregular bedrock morphologies and depressions and/or cobbles and boulders
- Morphological barriers affecting ocean wave and wind energy
- Interplay between longshore drift and onshore-offshore currents
- High energy swell/surf/storm wave action driving large sand fluxes onshore and alongshore
- Marine transgressions
- Downwarping of sedimentary basins

Chemical
- Not required

Deposition

Decrease in current velocity
- Decrease in fluvial/shallow marine current velocity below the level required for further transport of heavy detrital minerals, promoting placer deposition
- Repeated sediment reworking, selective sorting of mineral grains by mass and volume and further placer concentration

Preservation

- Tectonic stability
- Climatic stability
- Remobilisation and redeposition

Key Reference Bibliography

ARMSTRONG, F. C., WEIS, P. L., Uranium-bearing minerals in placer deposits of the Red River Valley, Idaho County, Idaho. US Government Printing Office, Geological Survey Bulletin, 1046-C, 36p (1957).

ELS, G., ERIKSSON, P., Placer formation and placer minerals. Ore Geology Reviews, 4, 373-375 (2006).

GARNETT, R. H. T., BASSETT, N. C., Placer deposits. In: HEDENQUIST, J. W., THOMPSON, J. F. H, GOLDFARB, R. J., RICHARDS, J. P. (eds.), Economic Geology 100th Anniversary Volume, 813-843 (2005).

HOATSON, D. M., JAIRETH, S., MIEZITIS, Y., The major rare-earth-element deposits of Australia: geological setting, exploration, and resources. Geoscience Australia, 204p (2017).

HYLAND, S., ULRICH, S., NI 43-101 technical report on the Kyzyl Ompul licence, Kyrgyz Republic, for Powertech Uranium Corporation, Azarga Resources Limited and UrAsia in Kyrgyzstan LLC. Ravensgate Mining Industry Consultants, Unpublished Technical Report, 91p (2014).

LEVSON, V. M., Surficial placers. In: LEFEBURE, D. V., RAY, G. E. (eds.), Selected British Columbia Mineral Deposit Profiles, Volume 1 - Metallics and Coal. British Columbia Ministry of Employment and Investment, Open File Report 1995-20, 21-23 (1995).

NUCLEAR ENERGY AGENCY & INTERNATIONAL ATOMIC ENERGY AGENCY, Uranium 2016: Resources, Production and Demand. OECD Publishing, Paris, 546p (2016).

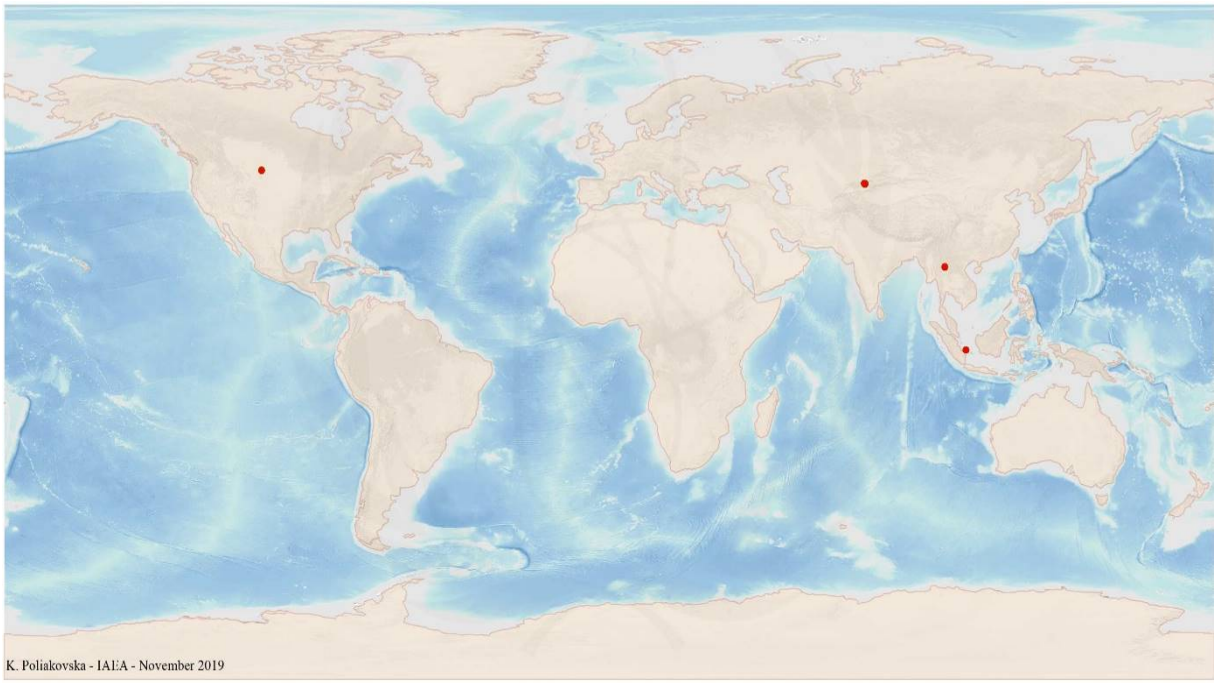

FIG. 11.5a. World distribution of selected Surficial Placer uranium deposits from the UDEPO database.

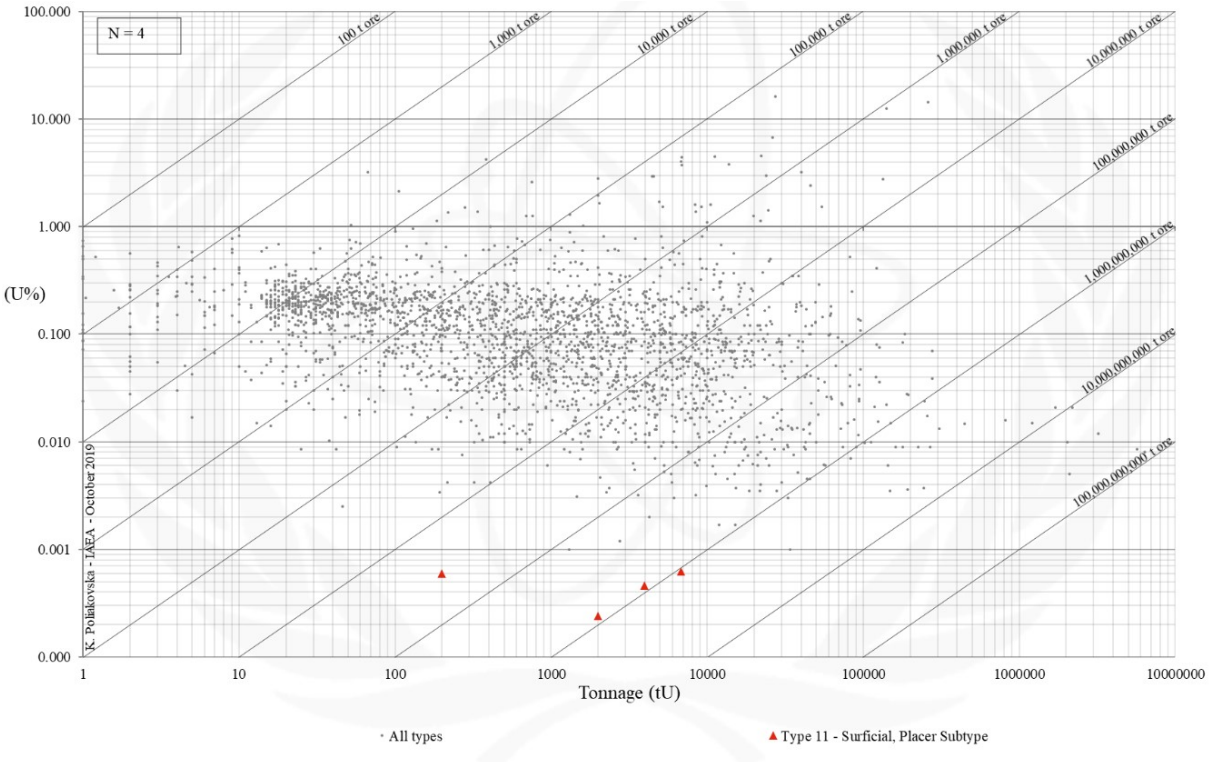

FIG. 11.5b. Grade and tonnage scatterplot highlighting Surficial Placer uranium deposits from the UDEPO database.

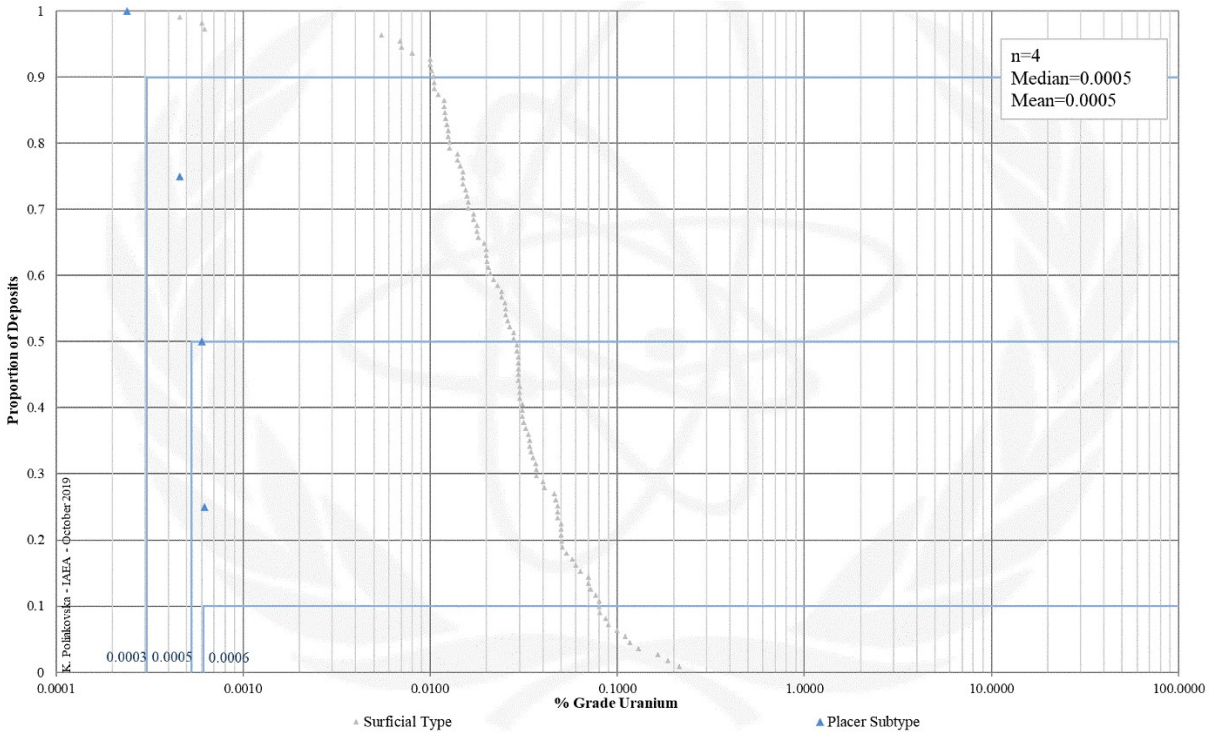

FIG. 11.5c. Grade Cumulative Probability Plot for Surficial Placer uranium deposits from the UDEPO database.

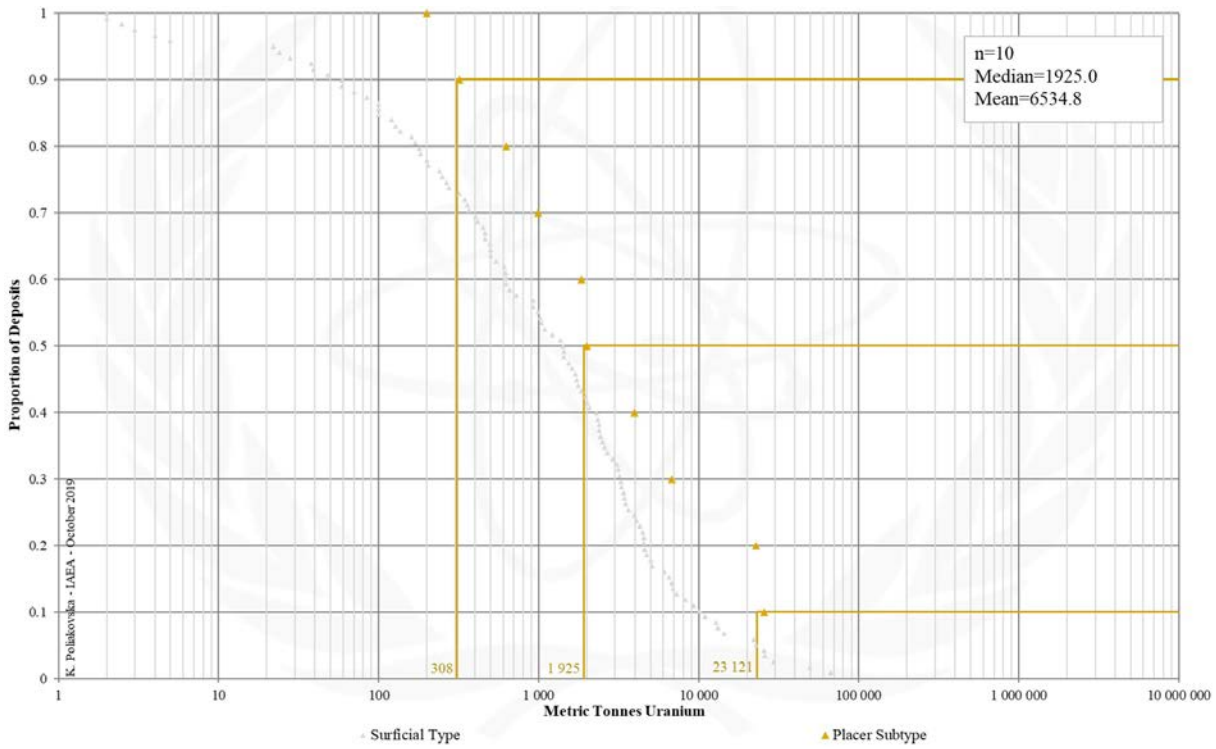

FIG. 11.5d. Tonnage Cumulative Probability Plot for Surficial Placer uranium deposits from the UDEPO database.

Appendix XII

LIGNITE-COAL

Subtype 12. Lignite-Coal

Brief Description
- Lignite-coal deposits typically contain trace uranium up to several parts per million, although some deposits have average concentrations of up to 0.1% U.
- Given the typically very low average grades and metallurgical complexities, few lignite-coal deposits have been mined for uranium and, thus, classify as unconventional uranium resources.
- The uranium in these deposits was most likely sourced from uraniferous crystalline basement rocks, granitoids or pyroclastic sediments that sometimes overly or are intercalated with the lignite-coal seams.
- Two subtypes are recognized: (12.1.) Stratiform and (12.2.) fracture-controlled.

Subtypes
- 12.1. Stratiform
- 12.2. Fracture-controlled

Type Examples
- Subtype 12.1. Koldzhat, Kazakhstan; Williston Basin, USA
- Subtype 12.2. Freital, Germany; Turakavak, Kyrgyzstan

Principal Commodities
- Lignite/coal, U ± As, Be, Cd, Co, Cr, Cu, Ge, Mo, Ni, Pb, REE, Se, Th, Ti, V, W, Y, Zn, Zr

Grades (%) and Tonnages (tU)
- Average: 0.0696, 11773.4
- Median: 0.0500, 2400.0

Number of Deposits
- Deposits: 85

Provinces
- Dnieper Donets, Ebro Basin, Kladno Rakovnik Basin, Min Kush, Moscow Syneclise, Northern Great Plains, Northwest Bohemia, Sogut Issyk Kul, Springbok Flats Coalfield, Volga Ural, West Sudetes, Western Balkhash.

Tectonic Setting
- Intracratonic, foreland and intermontane basins, tectonically stable cratonic (peneplained) environments, coastal plains

Typical Geological Age Range
- Carboniferous to Tertiary

Mineral Systems Model

Source

Ground preparation
- Basin formation
- Deposition of organic matter in paralic, limnic or fluviatile sedimentary environments
- Burial and conversion of organic matter into lignite/coal
- Recurring oxidation (permeability creation) and re-reduction (permeability destruction) events triggered by the decomposition of carbonaceous matter and generation of organic acids and reductants
- Deformation linked to extensional/compressional tectonics and/or salt doming

Energy
- Steep topographic and hydrological gradients
- Hydrostatic pressure
- Salt doming/tectonics
- Far-field tectonic activity or orogenesis resulting in local uplift

Fluids
- Groundwaters

Ligands
- No information

Reductants
- Organic matter (coal, lignite), sulphides, H_2S, CH_4

Uranium
- Igneous rocks (granitoids, felsic volcanics)
- Stratigraphic interbeds (tuffaceous sediments, volcanic ash/pyroclastica)
- Cover sequences (volcanic ash/pyroclastica)

Transport

Fluid pathways
- Groundwater aquifers, palaeovalleys
- Fault-fracture systems (in particular basin growth structures tapping deeper basin sequences, underlying basins or basement, and abutting salt domes)
- Fold hinges
- Regional unconformity surfaces

Trap

Physical
- Lignite/coal seams below massive, highly permeable, coarse sandstone/conglomerate beds
- Gently-dipping strata
- Groundwater interface
- Intraformational unconformities
- Faults, fractures, joints

Chemical
- Lignite/coal seams

Deposition

Change in redox conditions
- Due to interaction of oxidised, uranium-bearing groundwaters with lignite/coal seams
- Due to interaction of oxidised, uranium-bearing groundwaters with extrinsic reductants at/near lignite/coal seams

Adsorption
- Adsorption of U onto clays interbedded with or overlying lignite/coal seams
- Adsorption of U onto clays coating fracture/joint surfaces

Remobilisation and redeposition
- Due to groundwater oscillations
- Due to oxidation of the organic matter and subsequent re-reduction by organic acids and hydrogen, hydrogen sulphide and methane gases

Preservation

- Deep burial and/or downfaulting of lignite/coal seams
- Marine transgression/basin subsidence
- Remobilisation and re-reduction/redeposition
- Capping of mineralised lignite/coal seams by younger flood basalts
- Tectonic stability
- Climatic stability

Key Reference Bibliography

DAHLKAMP, F. J., Uranium Deposits of the World: Asia. Springer, Berlin, Heidelberg, 492p (2009).
DAHLKAMP, F. J., Uranium Deposits of the World: Europe. Springer, Berlin, Heidelberg, 792p (2016).
DENSON, N. M., Uranium in coal in the western United States. US Government Printing Office, Geological Survey Bulletin, 1055, 315p (1959).
DOUGLAS, G. B., BUTT, C. R., GRAY, D. J., Geology, geochemistry and mineralogy of the lignite-hosted Ambassador palaeochannel uranium and multi-element deposit, Gunbarrel Basin, Western Australia. Mineralium Deposita, 46(7), 761-787 (2011).
INTERNATIONAL ATOMIC ENERGY AGENCY, Geological Classification of Uranium Deposits and Description of Selected Examples. IAEA-TECDOC Series, 1842, 415p (2018).
SHUMLYANSKIY, V. A., Two main types of uranium deposit within Phanerozoic formations of Ukraine. IAEA TECDOC Series, 961, 287-295 (1997).

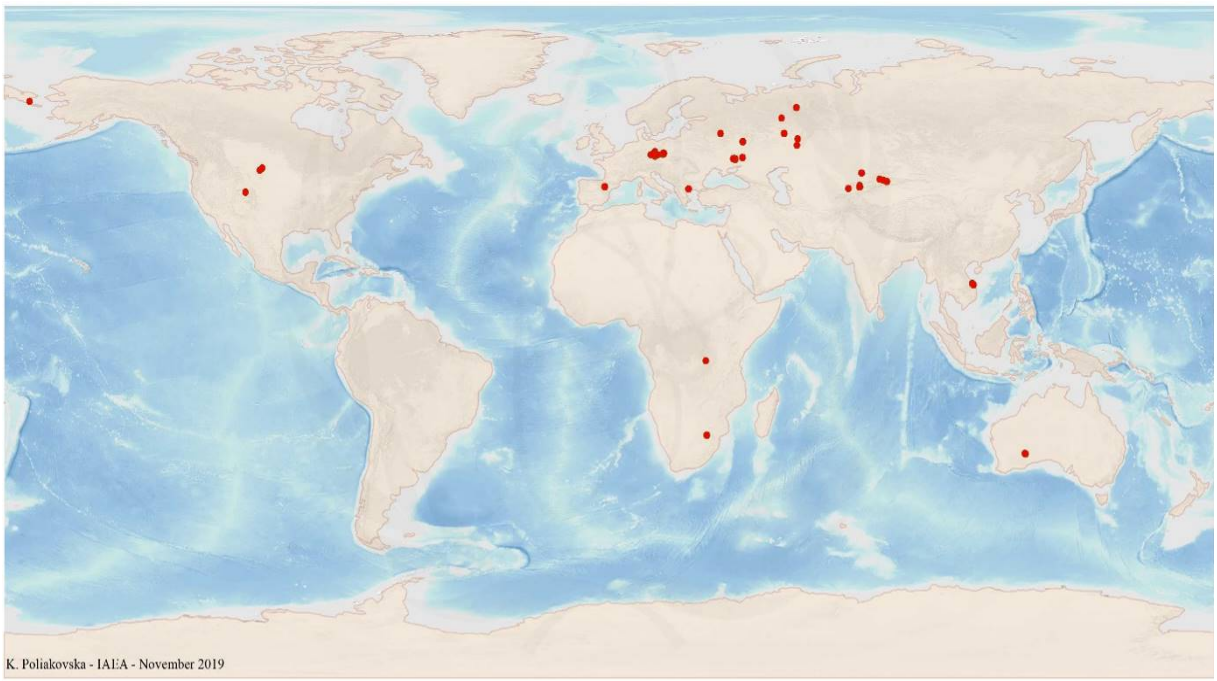

FIG. 12a. World distribution of selected Lignite-Coal uranium deposits from the UDEPO database.

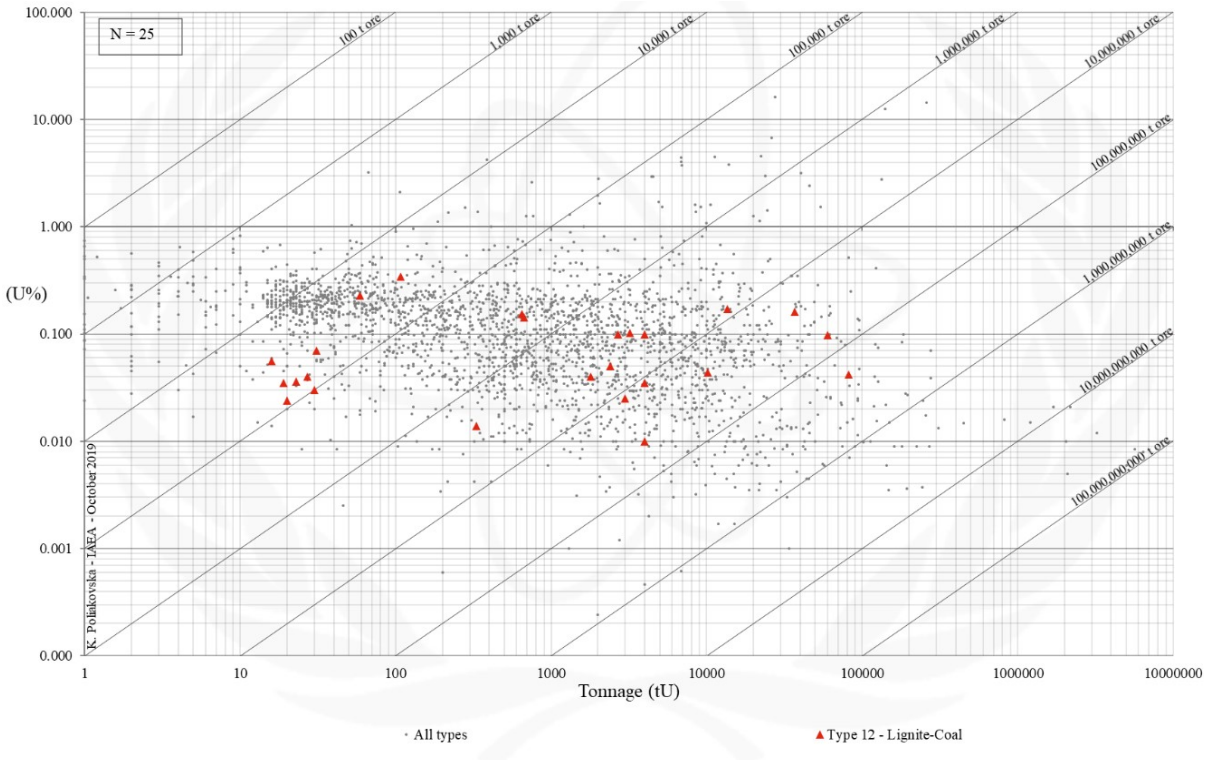

FIG. 12b. Grade and tonnage scatterplot highlighting Lignite-Coal uranium deposits from the UDEPO database.

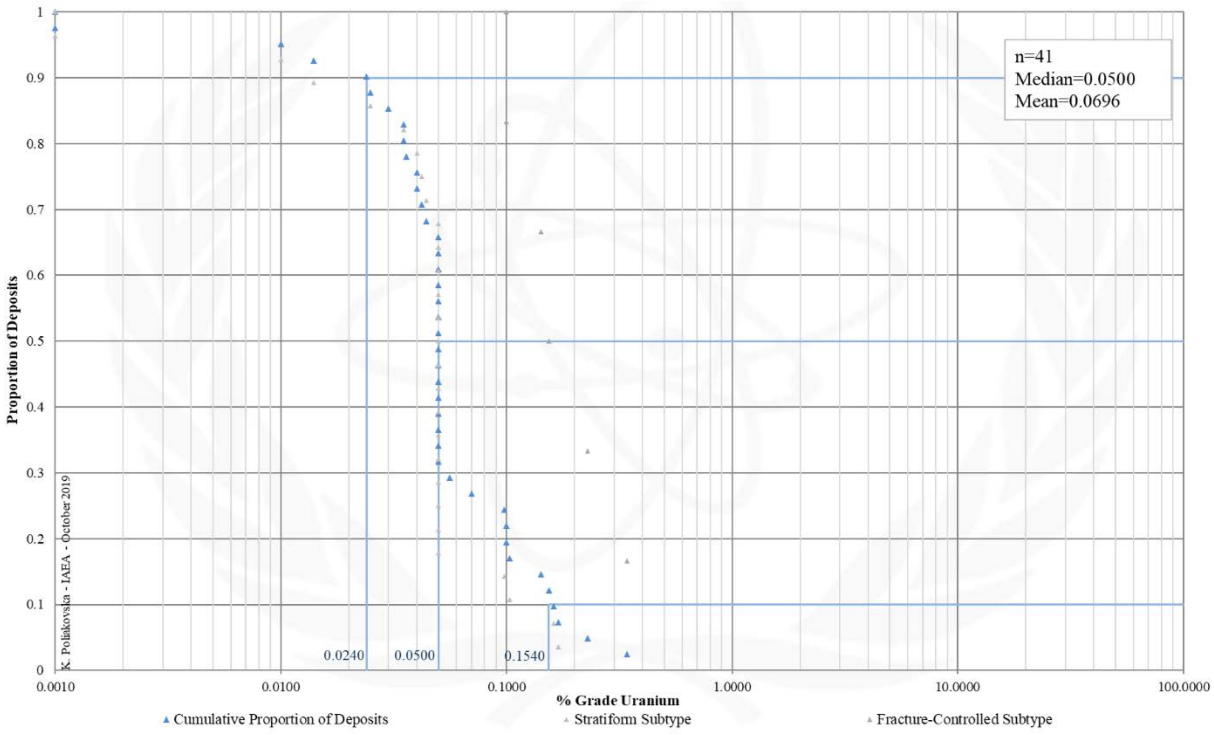

FIG. 12c. Grade Cumulative Probability Plot for Lignite-Coal uranium deposits from the UDEPO database.

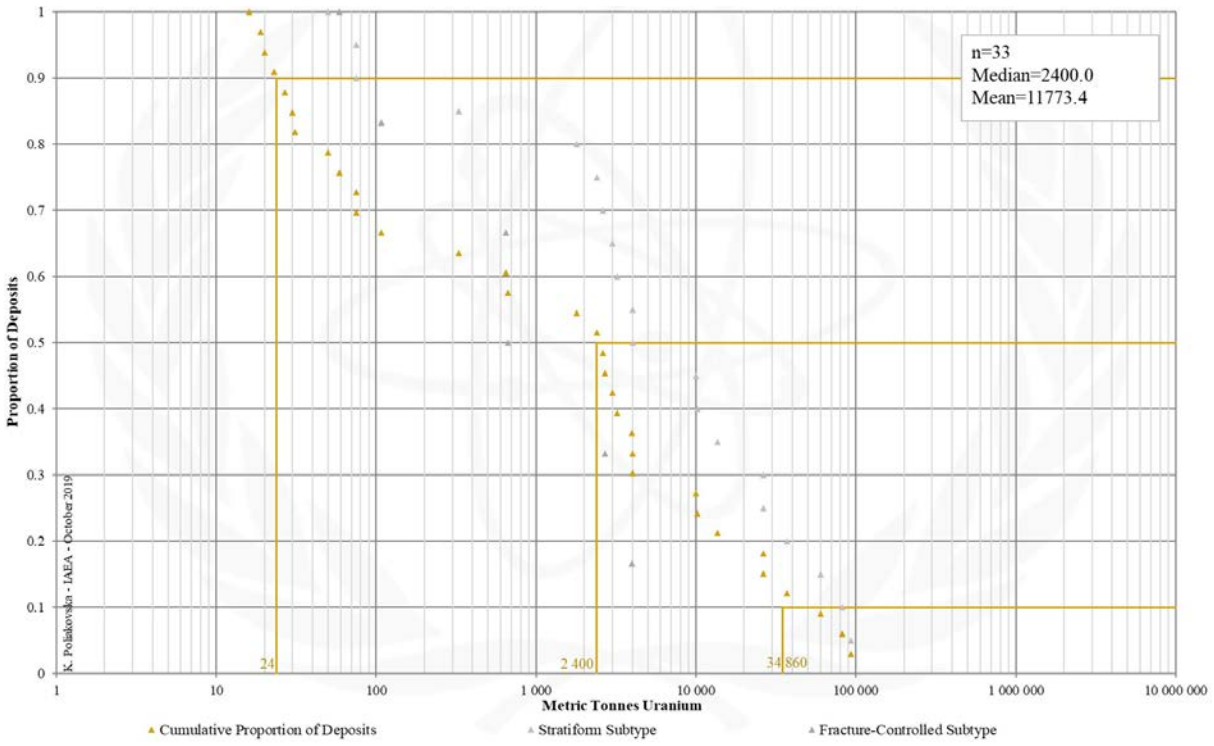

FIG. 12d. Tonnage Cumulative Probability Plot for Lignite-Coal uranium deposits from the UDEPO database.

SUBTYPE 12.1. Lignite-Coal, Stratiform

Brief Description
- Lignite-coal deposits typically contain trace uranium up to several parts per million, although some deposits have average concentrations of up to 0.1% U.
- Given the typically very low average grades and metallurgical complexities, few lignite-coal deposits have been mined for uranium and, thus, classify as unconventional uranium resources.
- The uranium in these deposits was most likely sourced from uraniferous crystalline basement rocks, granitoids or pyroclastic sediments that sometimes overly or are intercalated with the lignite-coal seams.
- Stratiform uranium ores take the form of uniform disseminations in lignite-coal seams with the uranium occurring as mineral phases and adsorbed onto carbonaceous matter.
- Uranium grades are commonly very low but tonnages can be very large.

Type Examples
- Koldzhat, Nizhne Iliskoye, Kazakhstan; Williston Basin, USA; Shogun, Emperor, Ambassador, Australia

Genetically Associated Deposit Types
- Subtype 12.2. Fracture-controlled
- Subtype 9.1. Sandstone, basal channel
- Subtype 9.2. Sandstone, tabular

Principal Commodities
- Lignite-coal, U ± Co, Cu, Ge, Mo, Ni, Pb, REE, Th, Zn

Grades (%) and Tonnages (tU)
- Average: 0.0534, 19009.6
- Median: 0.0500, 4000.0

Number of Deposits
- Deposits: 70

Provinces (undifferentiated from Lignite-Coal Type)
- Dnieper Donets, Ebro Basin, Kladno Rakovnik Basin, Min Kush, Moscow Syneclise, Northern Great Plains, Northwest Bohemia, Sogut Issyk Kul, Springbok Flats Coalfield, Volga Ural, West Sudetes, Western Balkhash.

Tectonic Setting
- Intracratonic, foreland and intermontane basins, tectonically stable cratonic (peneplained) environments, coastal plains

Typical Geological Age Range
- Carboniferous to Tertiary

Mineral Systems Model

Source

Ground preparation
- Basin formation
- Deposition of organic matter in paralic, limnic or fluviatile sedimentary environments
- Burial and conversion of organic matter into lignite/coal
- Recurring oxidation (permeability creation) and re-reduction (permeability destruction) events triggered by the decomposition of carbonaceous matter and generation of organic acids and reductants

Energy
- Steep topographic and hydrological gradients
- Hydrostatic pressure
- (?)Salt doming/tectonics
- (?)Far-field tectonic activity or orogenesis resulting in local uplift

Fluids
- Groundwaters

Ligands
- No information

Reductants
- Organic matter (coal, lignite), sulphides, H_2S, CH_4

Uranium
- Igneous rocks (granitoids, felsic volcanics)
- Stratigraphic interbeds (tuffaceous sediments, volcanic ash/pyroclastica)
- Cover sequences (volcanic ash/pyroclastica)

Transport

Fluid pathways
- Groundwater aquifers, palaeovalleys
- Fault-fracture systems (in particular basin growth structures tapping deeper basin sequences, underlying basins or basement)
- Regional unconformity surfaces

Trap

Physical
- Lignite/coal seams below massive, highly permeable, coarse sandstone/conglomerate beds
- Gently-dipping strata
- Groundwater interface

Chemical
- Lignite/coal seams

Deposition

Change in redox conditions
- Due to interaction of oxidised, uranium-bearing groundwaters with lignite/coal seams

Adsorption
- Adsorption of U onto clays interbedded with or overlying lignite/coal seams

Remobilisation and redeposition
- Due to oxidation of the organic matter and subsequent re-reduction by organic acids and hydrogen, hydrogen sulphide and methane gases

Preservation

- Deep burial and/or downfaulting of lignite/coal seams
- Marine transgression/basin subsidence
- Remobilisation and re-reduction/redeposition
- Capping of mineralised lignite/coal seams by younger flood basalts
- Tectonic stability
- Climatic stability

Key Reference Bibliography

DAHLKAMP, F. J., Uranium Deposits of the World: Asia. Springer, Berlin, Heidelberg, 492p (2009).
DAHLKAMP, F. J., Uranium Deposits of the World: Europe. Springer, Berlin, Heidelberg, 792p (2016).
DENSON, N. M., Uranium in coal in the western United States. US Government Printing Office, Geological Survey Bulletin, 1055, 315p (1959).
DOUGLAS, G. B., BUTT, C. R., GRAY, D. J., Geology, geochemistry and mineralogy of the lignite-hosted Ambassador palaeochannel uranium and multi-element deposit, Gunbarrel Basin, Western Australia. Mineralium Deposita, 46(7), 761-787 (2011).
INTERNATIONAL ATOMIC ENERGY AGENCY, Geological Classification of Uranium Deposits and Description of Selected Examples. IAEA-TECDOC Series, 1842, 415p (2018).

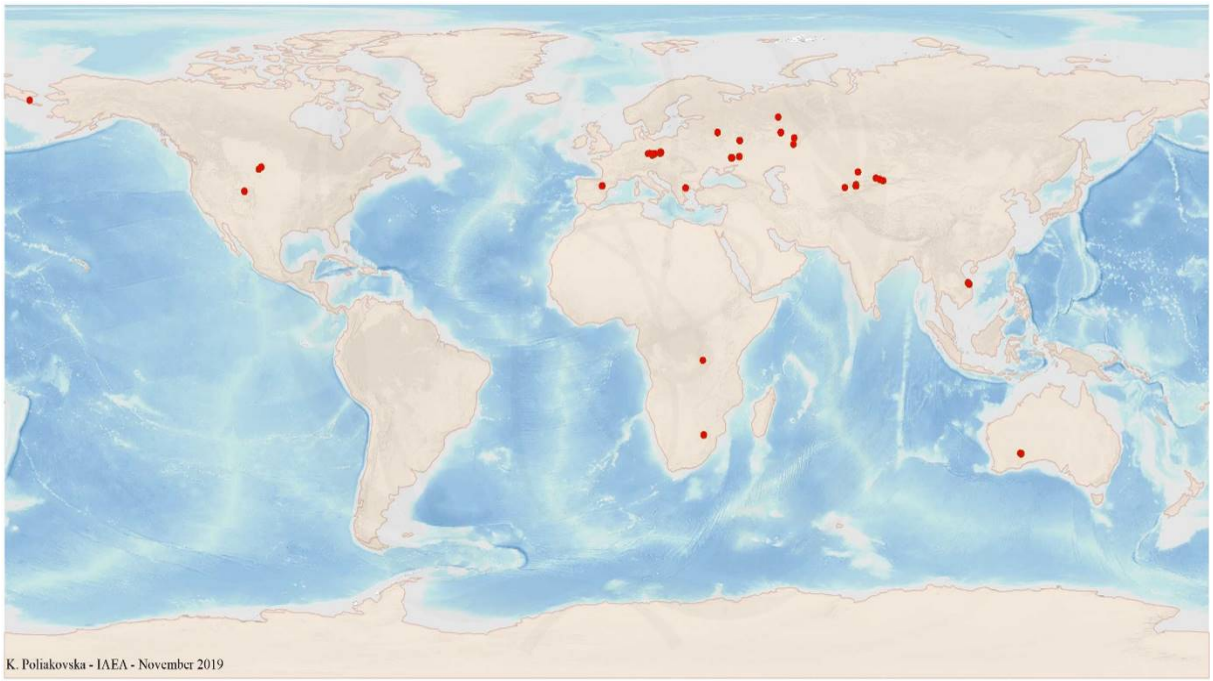

FIG. 12.1a. World distribution of selected Lignite-Coal Stratiform uranium deposits from the UDEPO database.

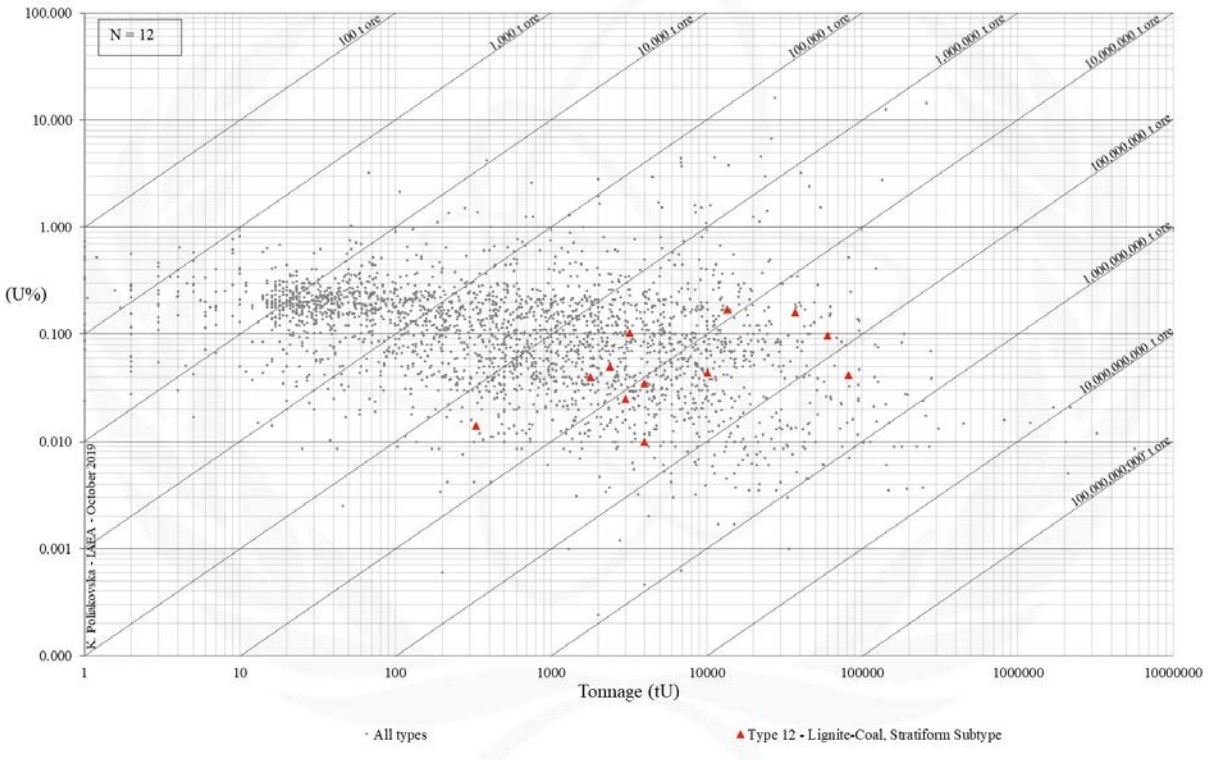

FIG. 12.1b. Grade and tonnage scatterplot highlighting Lignite-Coal Stratiform uranium deposits from the UDEPO database.

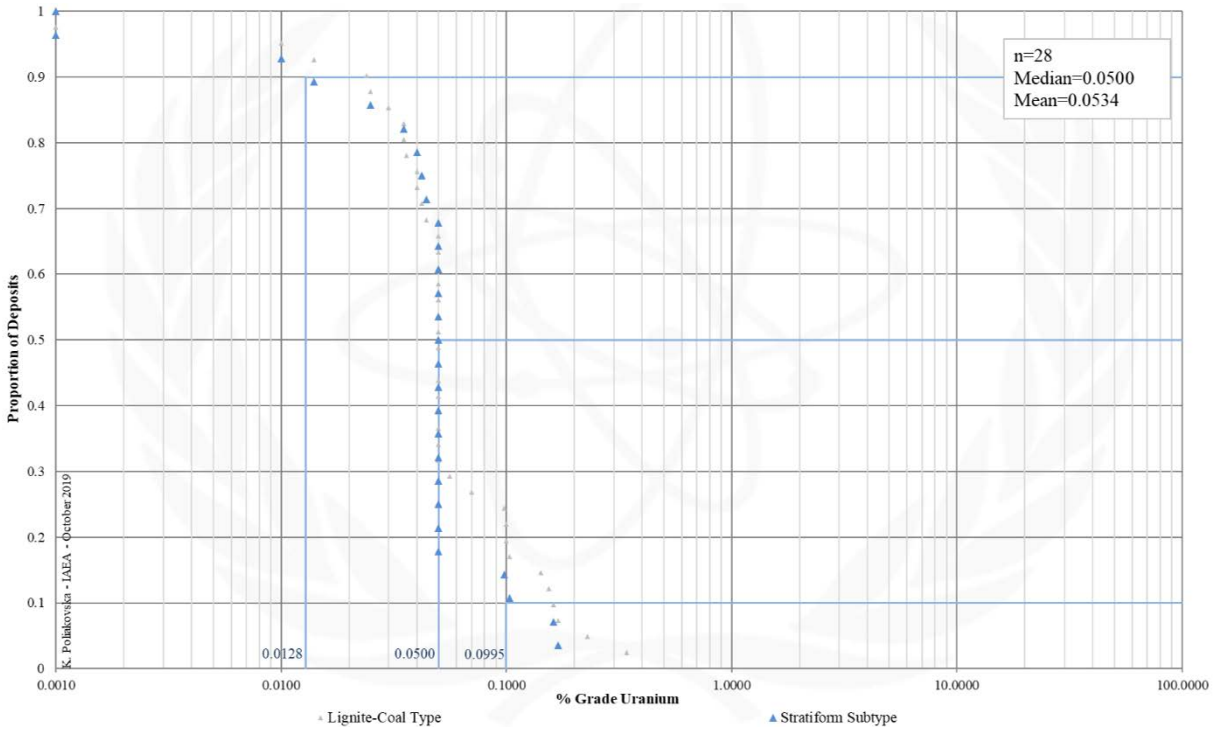

FIG. 12.1c. Grade Cumulative Probability Plot for Lignite-Coal Stratiform uranium deposits from the UDEPO database.

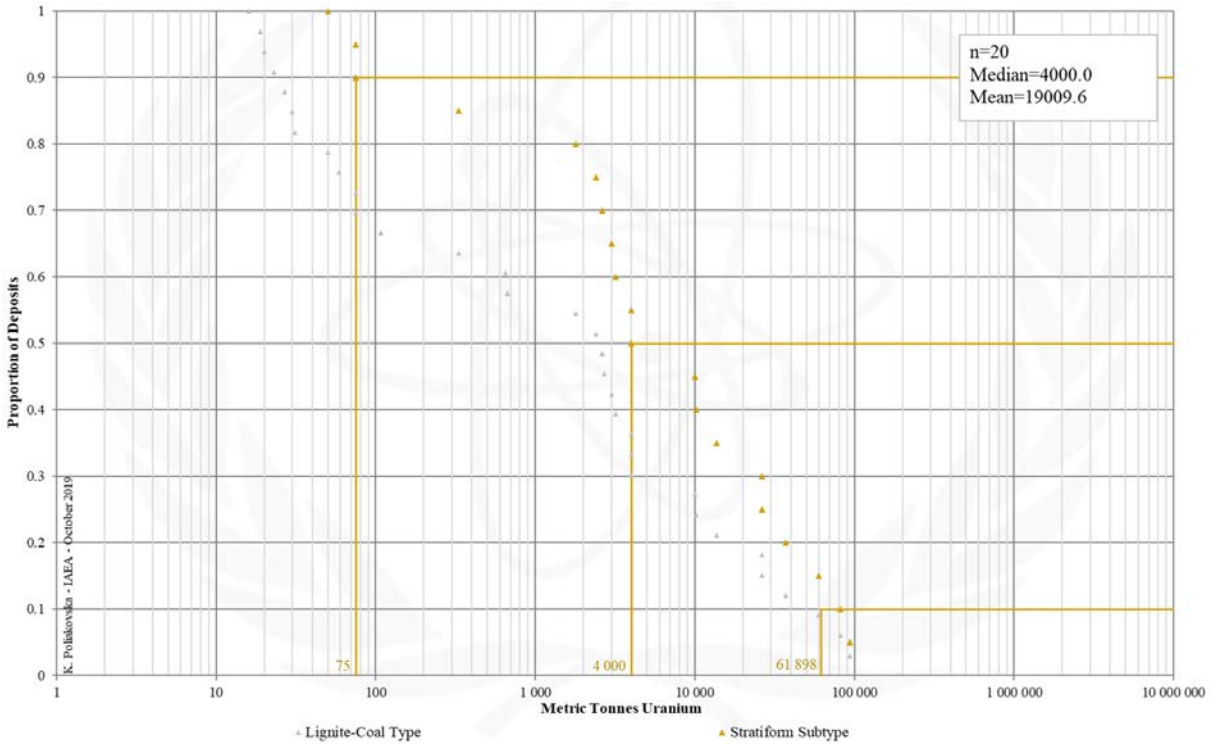

FIG. 12.1d. Tonnage Cumulative Probability Plot for Lignite-Coal Stratiform uranium deposits from the UDEPO database.

SUBTYPE 12.2. Lignite-Coal, Fracture-Controlled

Brief Description

- Lignite-coal deposits typically contain trace uranium up to several parts per million, although some deposits have average concentrations of up to 0.1% U.
- Given the typically very low average grades and metallurgical complexities, few lignite-coal deposits have been mined for uranium and, thus, classify as unconventional uranium resources.
- The uranium in these deposits was most likely sourced from uraniferous crystalline basement rocks, granitoids or pyroclastic sediments that sometimes overly or are intercalated with the lignite-coal seams.
- Fracture-controlled uranium ores take the form of irregularly distributed, structurally-controlled mineralisation that is characterised by strong grade variations.
- No discrete primary uranium mineral phases occur. Rather, the uranium is adsorbed onto carbonaceous matter or bound in organic compounds.
- The host rocks are strongly fractured and jointed.
- Intraformational unconformities often control uranium accumulation.

Type Examples

- Freital, Germany; Turakavak, Kyrgyzstan; Adamovskoe, Ukraine; Cave Hills, Slim Buttes, USA

Genetically Associated Deposit Types

- Subtype 12.1. Stratiform
- Subtype 9.4. Sandstone, tectonic-lithologic

Principal Commodities

- Lignite/coal, U ± As, Be, Cd, Co, Cr, Cu, Ge, Mo, Ni, Pb, REE, Se, Ti, V, W, Y, Zr

Grades (%) and Tonnages (tU)

- Average: 0.1780, 1360.7
- Median: 0.1480, 660.0

Number of Deposits

- Deposits: 7

Provinces (undifferentiated from Lignite-Coal Type)

- Dnieper Donets, Ebro Basin, Kladno Rakovnik Basin, Min Kush, Moscow Syneclise, Northern Great Plains, Northwest Bohemia, Sogut Issyk Kul, Springbok Flats Coalfield, Volga Ural, West Sudetes, Western Balkhash.

Tectonic Setting

- Intracratonic and foreland basins

Typical Geological Age Range

- Carboniferous to (?)Tertiary

Mineral Systems Model

Source

Ground preparation
- Basin formation
- Deposition of organic matter in paralic, limnic or fluviatile sedimentary environments
- Burial and conversion of organic matter into lignite/coal
- Recurring oxidation (permeability creation) and re-reduction (permeability destruction) events triggered by the decomposition of carbonaceous matter and generation of organic acids and reductants
- Deformation linked to extensional/compressional tectonics and/or salt doming

Energy
- Salt doming/tectonics
- Far-field tectonic activity or orogenesis resulting in local uplift

Fluids
- Groundwaters

Ligands
- No information

Reductants
- Organic matter (coal, lignite), sulphides, H_2S, CH_4

Uranium
- Igneous rocks (granitoids, felsic volcanics)
- Stratigraphic interbeds (tuffaceous sediments, volcanic ash/pyroclastica)
- Cover sequences (volcanic ash/pyroclastica)

Transport

Fluid pathways
- Groundwater aquifers, palaeovalleys
- Fault-fracture ± breccia systems (in particular basin growth structures tapping deeper basin sequences, underlying basins or basement, and abutting salt domes)
- Fold hinges and regional unconformity surfaces

Trap

Physical
- Lignite/coal seams below massive, highly permeable, coarse sandstone/conglomerate beds
- Gently-dipping strata
- Groundwater interface
- Intraformational unconformities
- Faults, fractures, joints

Chemical
- Lignite/coal seams

Deposition

Change in redox conditions
- Due to interaction of oxidised, uranium-bearing groundwaters with lignite/coal seams
- Due to interaction of oxidised, uranium-bearing groundwaters with extrinsic reductants at/near lignite/coal seams

Adsorption
- Adsorption of U onto clays interbedded with or overlying lignite/coal seams
- Adsorption of U onto clays coating fracture/joint surfaces

Preservation

- Deep burial and/or downfaulting of lignite/coal seams
- Marine transgression/basin subsidence
- Capping of mineralised lignite/coal seams by younger flood basalts
- Tectonic stability
- Climatic stability

Key Reference Bibliography

DAHLKAMP, F. J., Uranium Deposits of the World: Asia. Springer, Berlin, Heidelberg, 492p (2009).
DAHLKAMP, F. J., Uranium Deposits of the World: Europe. Springer, Berlin, Heidelberg, 792p (2016).
DENSON, N. M., Uranium in coal in the western United States. US Government Printing Office, Geological Survey Bulletin, 1055, 315p (1959).
INTERNATIONAL ATOMIC ENERGY AGENCY, Geological Classification of Uranium Deposits and Description of Selected Examples. IAEA-TECDOC Series, 1842, 415p (2018).
SHUMLYANSKIY, V. A., Two main types of uranium deposit within Phanerozoic formations of Ukraine. IAEA TECDOC Series, 961, 287-295 (1997).

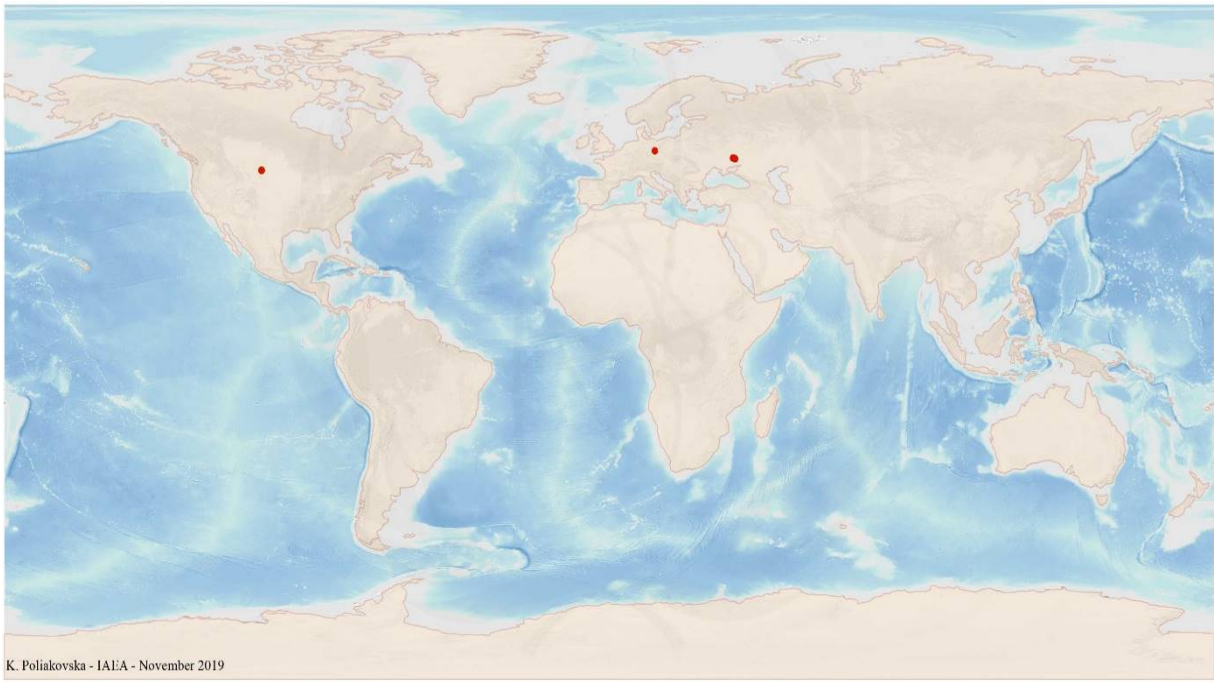

FIG. 12.2a. World distribution of selected Lignite-Coal Fracture-Controlled uranium deposits from the UDEPO database.

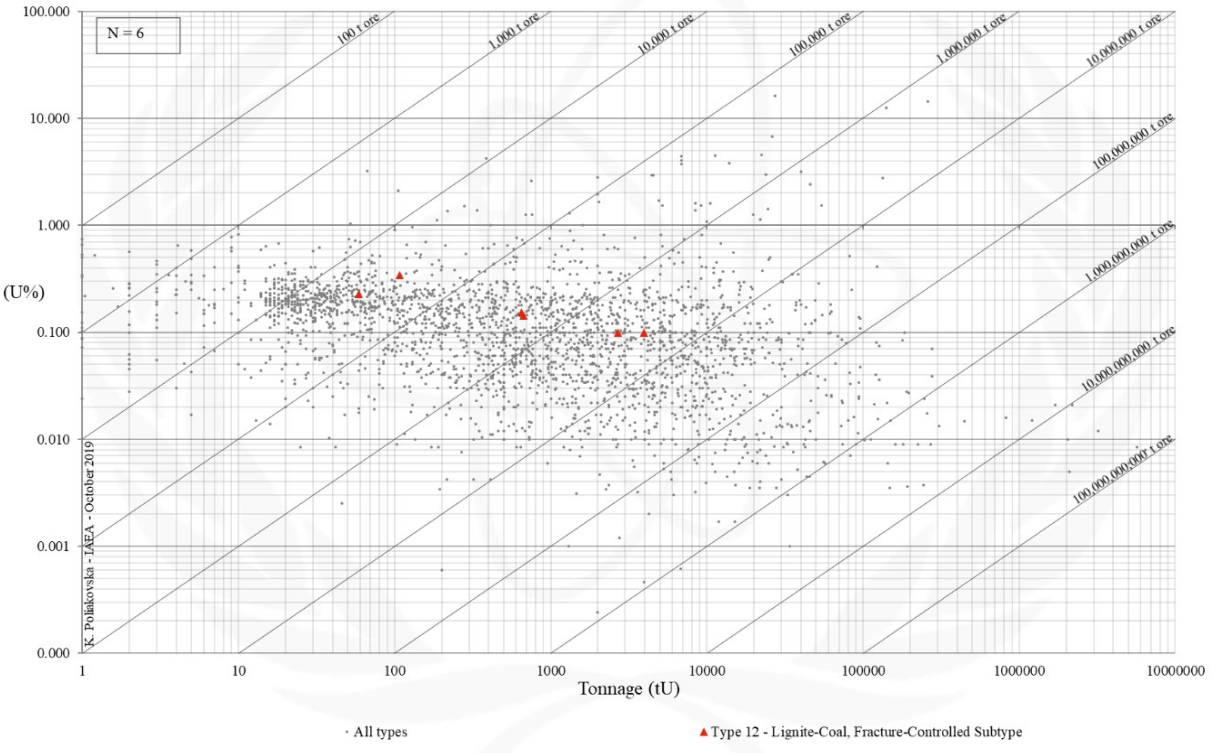

FIG. 12.2b. Grade and tonnage scatterplot highlighting Lignite-Coal Fracture-Controlled uranium deposits from the UDEPO database.

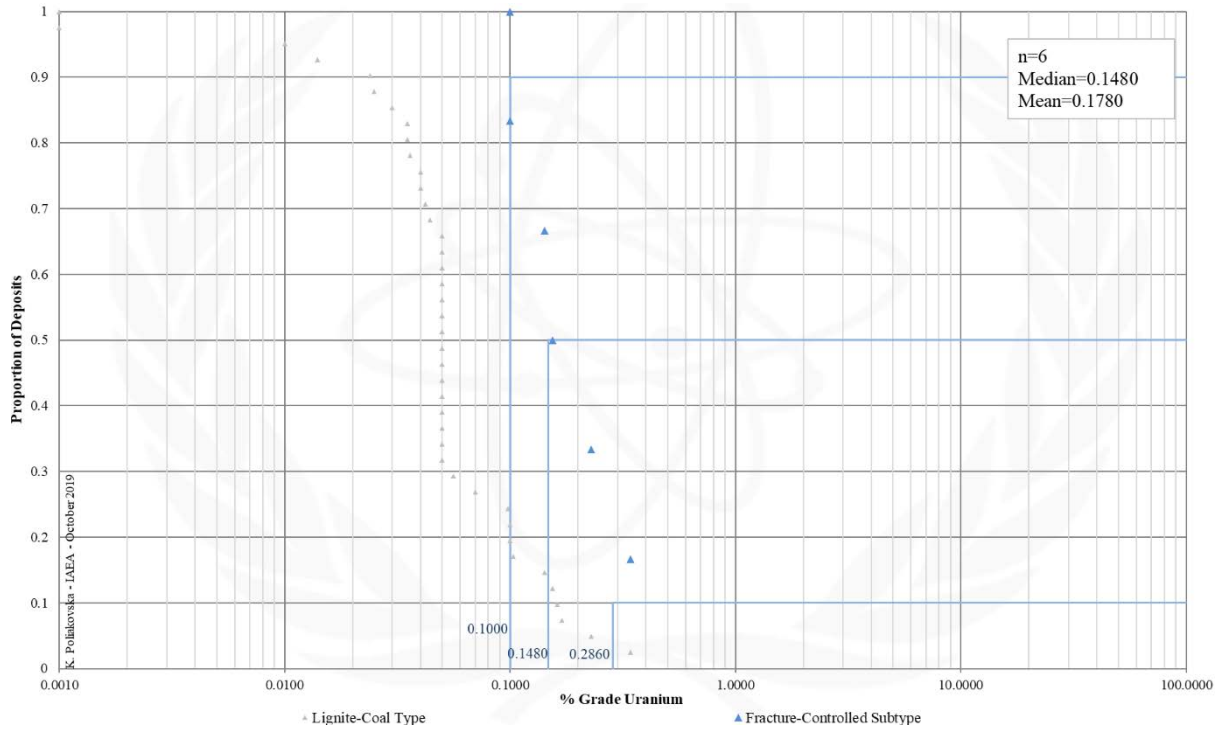

FIG. 12.2c. Grade Cumulative Probability Plot for Lignite-Coal Fracture-Controlled uranium deposits from the UDEPO database.

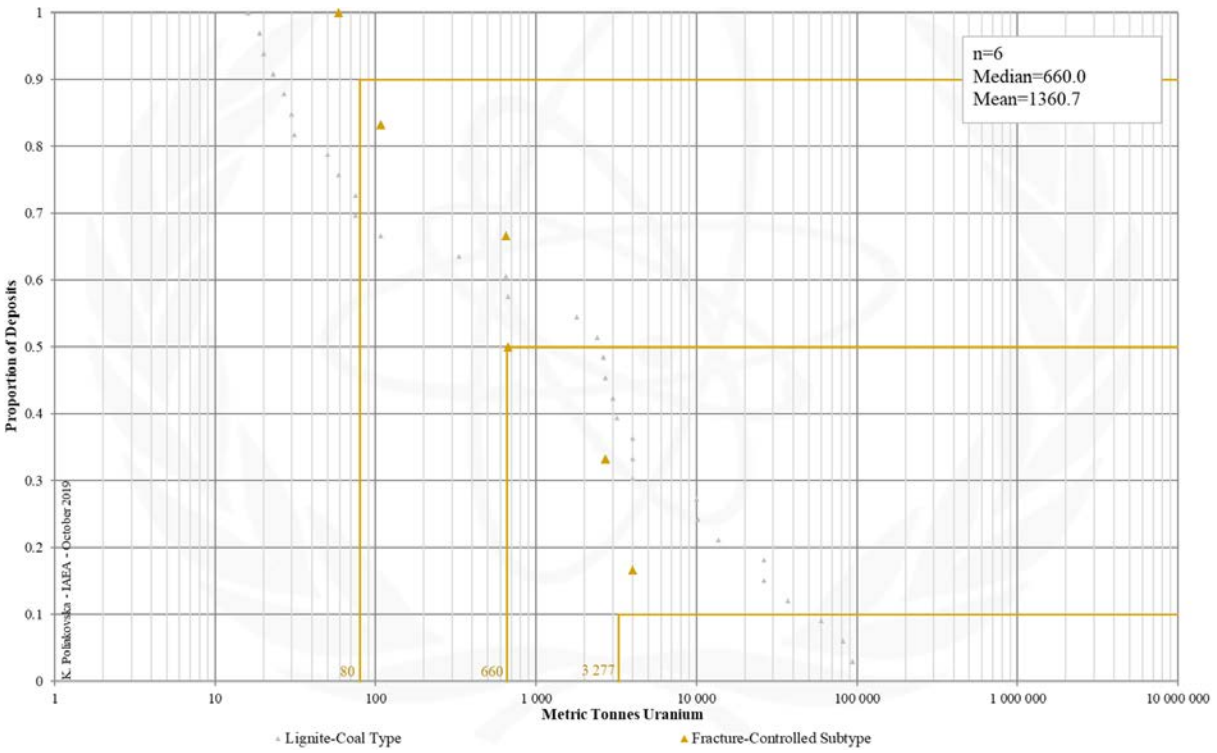

FIG. 12.2d. Tonnage Cumulative Probability Plot for Lignite-Coal Fracture-Controlled uranium deposits from the UDEPO database.

Appendix XIII

CARBONATE

TYPE 13. Carbonate

Brief Description
- Carbonate deposits comprise diverse syn- and epigenetic uranium ores of variable size and grade that formed in a variety of geological settings and at various times in Earth's history.
- The single unifying feature of these ores is their occurrence in calcareous host rocks, which are atypical and commonly unfavourable uranium host rocks given that, by and large, they have low permeability and lack chemical reductants.
- Three subtypes have been described: (13.1.) Stratabound, (13.2.) cataclastic, and (13.3.) palaeokarst.

Subtypes
- 13.1. Stratabound
- 13.2. Cataclastic
- 13.3. Palaeokarst

Type Examples
- Subtype 13.1. Tumalappalle, India
- Subtype 13.2. Mailuu-Suu, Kyrgyzstan; Todilto district, USA
- Subtype 13.3. Sanbaqi, China; Tyuya-Muyun, Kyrgyzstan

Principal Commodities
- Subtype 13.1. U ± P, V
- Subtype 13.2. U, V ± As, Co, Cr, Fe, Mo, Ni, Pb, V
- Subtype 13.3. U ± Ba, Cu, Ra, V

Grades (%) and Tonnages (tU)
- Average: 0.1724, 4803.0
- Median: 0.1750, 75.0

Number of Deposits
- Deposits: 63

Provinces
- Karamazar East, Pryor Mountains, Volga Ural.

Tectonic Setting
- Subtype 13.1. Intracratonic basins
- Subtype 13.2 to 13.3. Collisional orogens

Typical Geological Age Range
- Subtype 13.1. Palaeoproterozoic
- Subtype 13.2. Mesozoic-Tertiary
- Subtype 13.3. Poorly constrained

Mineral Systems Model

Source

Ground preparation
- Subtype 13.1. Intracratonic basin formation and deposition of a thick, laterally extensive succession of impure, phosphatic dolostone
- Subtype 13.2. Orogenesis, metasomatism
- Subtype 13.3. Orogenesis, karstification

Energy
- Subtype 13.1. Marine currents and tides, wave energy, wind energy
- Subtype 13.2. Orogenesis, topography-driven fluid flow and evaporative pumping
- Subtype 13.3. Orogenesis, post-orogenic collapse, far-field tectonic activity

Fluids
- Subtype 13.1. Marine waters
- Subtype 13.2. Groundwaters, hydrothermal fluids
- Subtype 13.3. Groundwaters, connate brines

Ligands
- Subtype 13.1. CO, P
- Subtype 13.2. No information
- Subtype 13.3. Ca

Reductants
- Subtype 13.1. Organic matter (bacteria, algae), phosphate, diagenetic sulphides
- Subtype 13.2. Hydrocarbons
- Subtype 13.3. Diagenetic sulphides, sulfidic breccia, organic matter, sulphate-reducing bacteria, hydrocarbons

Uranium ± phosphate, vanadium
- Subtype 13.1. Granitoids, seawaters
- Subtype 13.2. Felsic igneous and volcaniclastic rocks
- Subtype 13.3. Carbonaceous shales, volcanic rocks, tuffaceous sediments, unknown distal sources
-

Transport

Fluid pathways
- Subtype 13.1. Groundwater aquifers, fluvial channels, marine currents
- Subtypes 13.2. to 13.3. Crustal-scale fault zones and subsidiary fault-fracture systems, regional fold hinges, regional stratigraphic (± karst) aquifers

Trap

Physical
- Subtype 13.1. Inter-tidal and mud-flat environment (sediment sink)
- Subtype 13.2. Fault-fracture systems, fault intersections, zones of high fracture density, folds (limbs, crests), lithological competency contrast (in particular limestone/sandstone), carbonate host rock porosity (stylolites, microfissures, grain interstices, voids, oolite matrix, fossil fragments)
- Subtype 13.3. Karst cavities and voids, solution collapse breccia, ring faults, fault-fracture systems

Chemical
- Subtype 13.1. Inter-tidal and mud-flat environment (habitat for stromatolites/algal mats, favourable setting for iron sulphide and phosphate deposition)
- Subtype 13.2. Pyrobitumen
- Subtype 13.3. Carbonaceous matter

Deposition

Change in redox conditions
- Subtype 13.1. Due to (i) mixing of marine and fresh water in an inter-tidal and mud-flat environment, (ii) evaporation, and/or (iii) interaction of oxidised, uranium-bearing waters with organic matter, iron sulphide and/or phosphate accumulations
- Subtype 13.2. Due to (i) interaction of oxidised, uranium-bearing groundwaters with wallrock reductants, and/or (ii) fluid mixing
- Subtype 13.3. Due to (i) mixing of lateral/downward-flowing, oxidised, uranium-bearing groundwaters and upward-flowing, reducing hydrothermal fluids/brines entering the ring fractures and pipes from below, (ii) interaction of oxidised, uranium-bearing groundwaters with wallrock reductants

Fluid cooling and depressurisation
- Subtype 13.3. Phase separation/CO_2 effervescence

Adsorption
- Subtype 13.1. Absorption of uranyl molecules by organic and inorganic materials

Remobilisation and redeposition
- Subtype 13.1. Diagenetic remobilisation of primary uranium mineralisation and redeposition during burial and under reduced conditions
- Subtype 13.2. Remobilisation of primary uranium mineralisation due to oxidation and redeposition of uranium as hexavalent ores
- Subtype 13.3. Dissolution of primary colloidal uranium and redeposition as secondary hexavalent uranium ores

Preservation

- Deep burial and/or downfaulting
- Infiltration of hydrocarbons
- Relative tectonic stability
- Climatic stability

Key Reference Bibliography

BERGLOF, W. R., MCLEMORE, V. T., Economic geology of the Todilto Formation. New Mexico Geological Society Guidebook, 54, 179-189 (2003).

DAHLKAMP, F. J., Uranium ore deposits. Springer, Berlin, 460p (1993).

DAHLKAMP, F. J., Uranium Deposits of the World: Asia. Springer, Berlin, Heidelberg, 492p (2009).

DOUGLAS, G. B., BUTT, C. R., GRAY, D. J., Geology, geochemistry and mineralogy of the lignite-hosted Ambassador palaeochannel uranium and multi-element deposit, Gunbarrel Basin, Western Australia. Mineralium Deposita, 46(7), 761-787 (2011).

INTERNATIONAL ATOMIC ENERGY AGENCY, Geological Classification of Uranium Deposits and Description of Selected Examples. IAEA-TECDOC Series, 1842, 415p (2018).

MCLEMORE, V. T., The Grants uranium district, New Mexico: update on source, deposition, and exploration. The Mountain Geologist, 48(1), 23-44 (2011).

MIN, M., ZHENG, D., SHEN, B., WEN, G., WANG, X., GANDHI, S. S., Genesis of the Sanbaqi deposit: a paleokarst-hosted uranium deposit in China. Mineralium Deposita, 32, 505-519 (1997).

MOORE-NALL, A. L., Structural controls and chemical characterization of brecciation and uranium vanadium mineralization in the northern Bighorn Basin. Unpublished PhD Thesis, Montana State University, Bozeman, 363p (2016).

RAJARAMAN, H. S., ROY, M., VERMA, M. B., NANDA, L. K., CO Isotope Analysis of dolostone of Vempalle Formation in Dhone-Gudipadu-Korivipalle sector, western part of Papaghni Sub-basin, Andhra Pradesh, and its Impact on uranium mineralization. Journal of the Geological Society of India, 92(2), 134-140 (2018).

SHUMLYANSKIY, V. A., Two main types of uranium deposit within Phanerozoic formations of Ukraine. IAEA TECDOC Series, 961, 287-295 (1997).

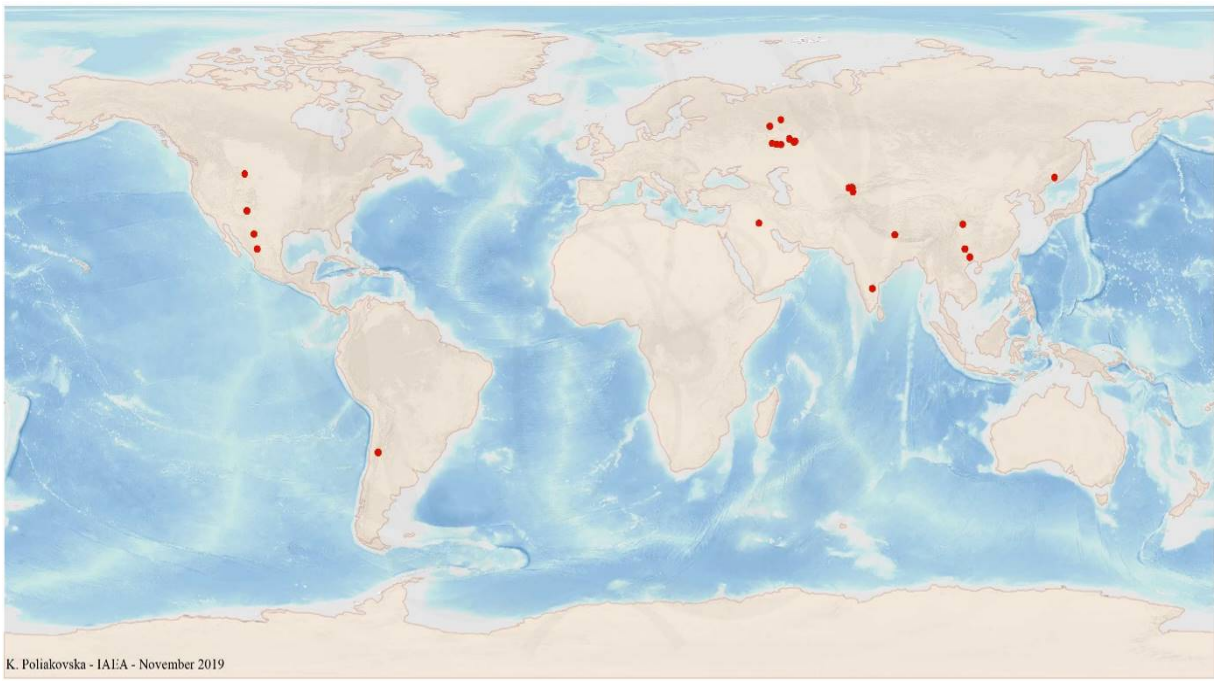

FIG. 13a. World distribution of selected Carbonate uranium deposits from the UDEPO database.

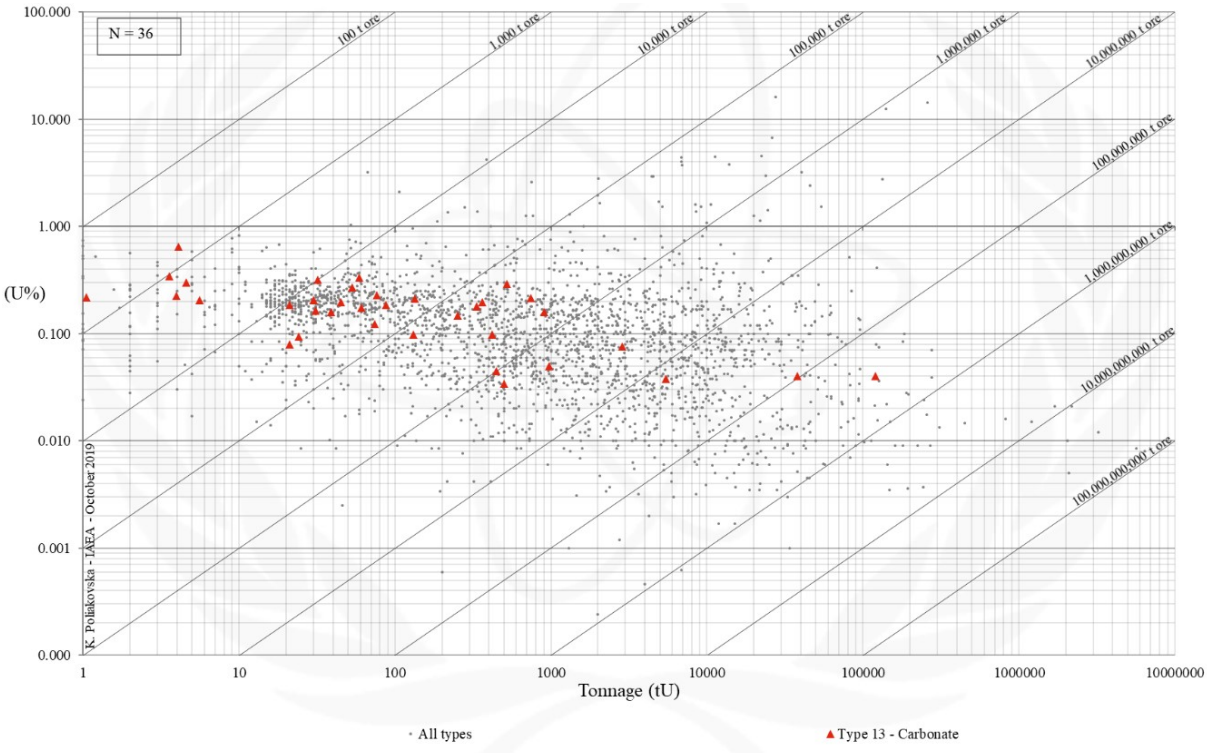

FIG. 13b. Grade and tonnage scatterplot highlighting Carbonate uranium deposits from the UDEPO database.

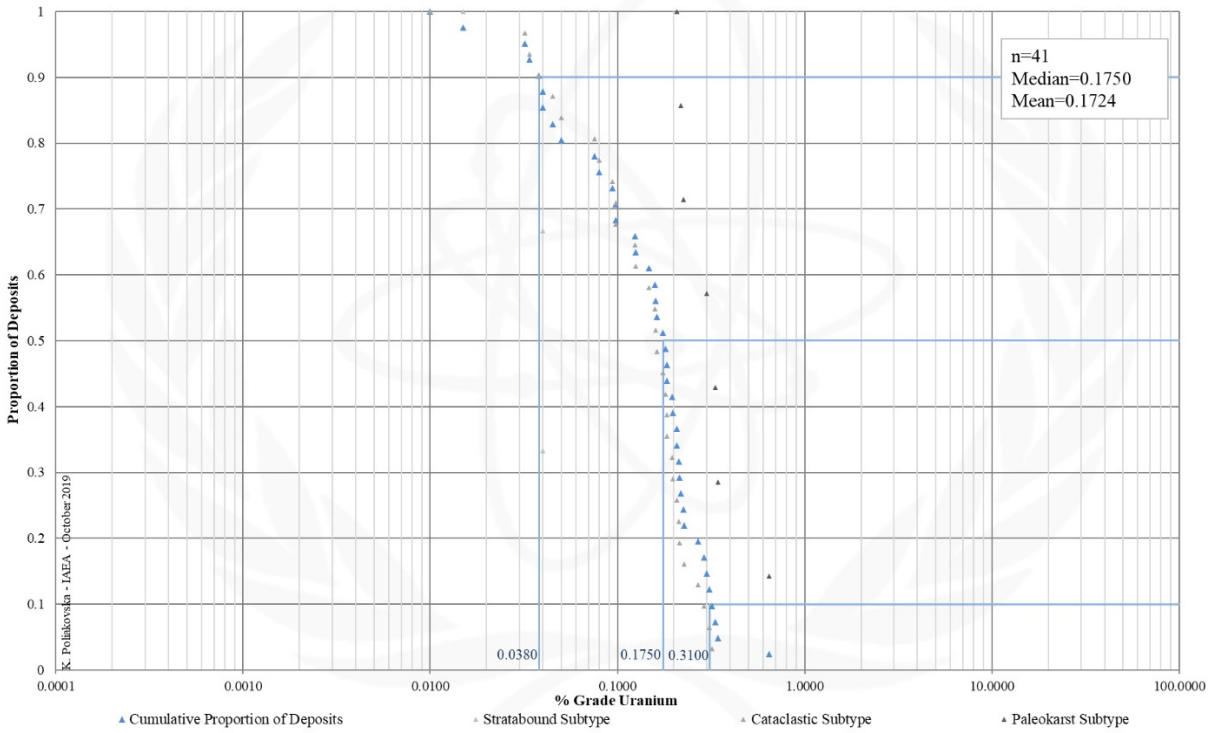

FIG. 13c. Grade Cumulative Probability Plot for Carbonate uranium deposits from the UDEPO database.

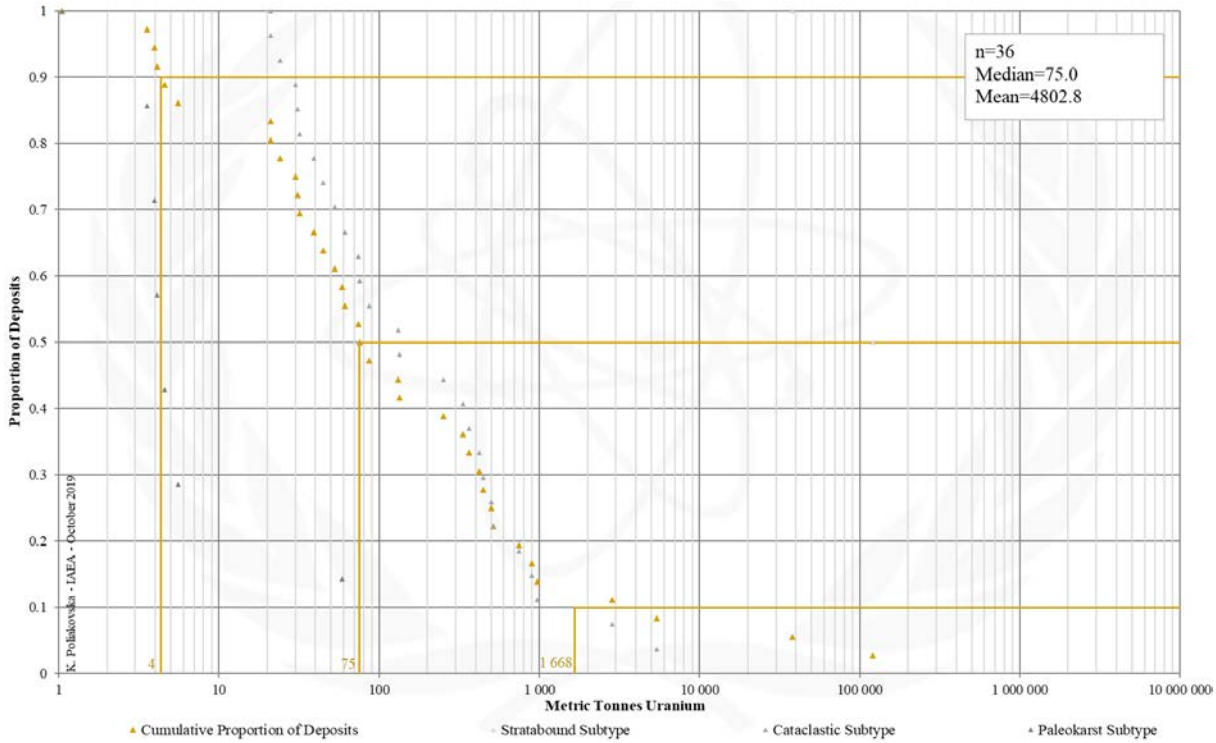

FIG. 13d. Tonnage Cumulative Probability Plot for Carbonate uranium deposits from the UDEPO database.

SUBTYPE 13.1. Carbonate, Stratabound

Brief Description
- Carbonate deposits comprise diverse syn- and epigenetic uranium ores of variable size and grade that formed in a variety of geological settings and at various times in Earth's history.
- Stratabound deposits are known exclusively from the Proterozoic Cuddapah basin of southeastern India.
- The deposits are hosted in impure, phosphatic dolostones deposited in an intertidal and mud flat environment.
- The syngenetic uranium ores take the form of ultrafine disseminations within phosphate-rich dolostone intervals and adsorptions on collophane mineral surfaces.

Type Examples
- Tummalapalle, Rachakuntapalle, Gadankipalle, Chilavaripalle, India

Genetically Associated Deposit Types
- Subtype 13.2. Cataclastic
- Subtype 13.3. Palaeokarst
- Subtype 14.2. Minerochemical phosphorite

Principal Commodities
- U ± P, V

Grades (%) and Tonnages (tU)
- Average: 0.0317, 79114.5
- Median: 0.0400, 79114.5

Number of Deposits
- Deposits: 3

Provinces (undifferentiated from Carbonate Type)
- Karamazar East, Pryor Mountains, Volga Ural

Tectonic Setting
- Intracratonic basins

Typical Geological Age Range
- Palaeoproterozoic

Mineral Systems Model

Source

Ground preparation
- Intracratonic basin formation
- Deposition of a thick, laterally extensive succession of impure, phosphatic dolostone

Energy
- Marine currents and tides
- Wave energy
- Wind energy

Fluids
- Marine waters

Ligands
- CO, P

Reductants
- Organic matter (bacteria, algae), phosphate, diagenetic sulphides

Uranium ± phosphate, vanadium
- Distal granitoids
- Seawaters

Transport

Fluid pathways
- Groundwater aquifers
- Fluvial channels
- Marine currents

Trap

Physical
- Inter-tidal and mud-flat environment (sediment sink)

Chemical
- Inter-tidal and mud-flat environment (habitat for stromatolites/algal mats, favourable setting for iron sulphide and phosphate deposition)

Deposition

Change in redox conditions
- Due to mixing of marine and fresh water in an inter-tidal and mud-flat environment,
- Due to evaporation
- Due to interaction of oxidised, uranium-bearing waters with organics, sulphide and/or phosphate accumulations

Adsorption
- Absorption of uranyl molecules by organic and inorganic materials

Remobilisation and redeposition
- Diagenetic remobilisation of primary uranium mineralisation and redeposition during burial and under reduced conditions

Preservation

- Deep burial and/or downfaulting
- Infiltration of hydrocarbons
- Relative tectonic stability
- Climatic stability

Key Reference Bibliography

DAHLKAMP, F. J., Uranium Deposits of the World: Asia. Springer, Berlin, Heidelberg, 492p (2009).

INTERNATIONAL ATOMIC ENERGY AGENCY, Geological Classification of Uranium Deposits and Description of Selected Examples. IAEA-TECDOC Series, 1842, 415p (2018).

RAJARAMAN, H. S., ROY, M., VERMA, M. B., NANDA, L. K., CO Isotope Analysis of dolostone of Vempalle Formation in Dhone-Gudipadu-Korivipalle sector, western part of Papaghni Sub-basin, Andhra Pradesh, and its Impact on uranium mineralization. Journal of the Geological Society of India, 92(2), 134-140 (2018).

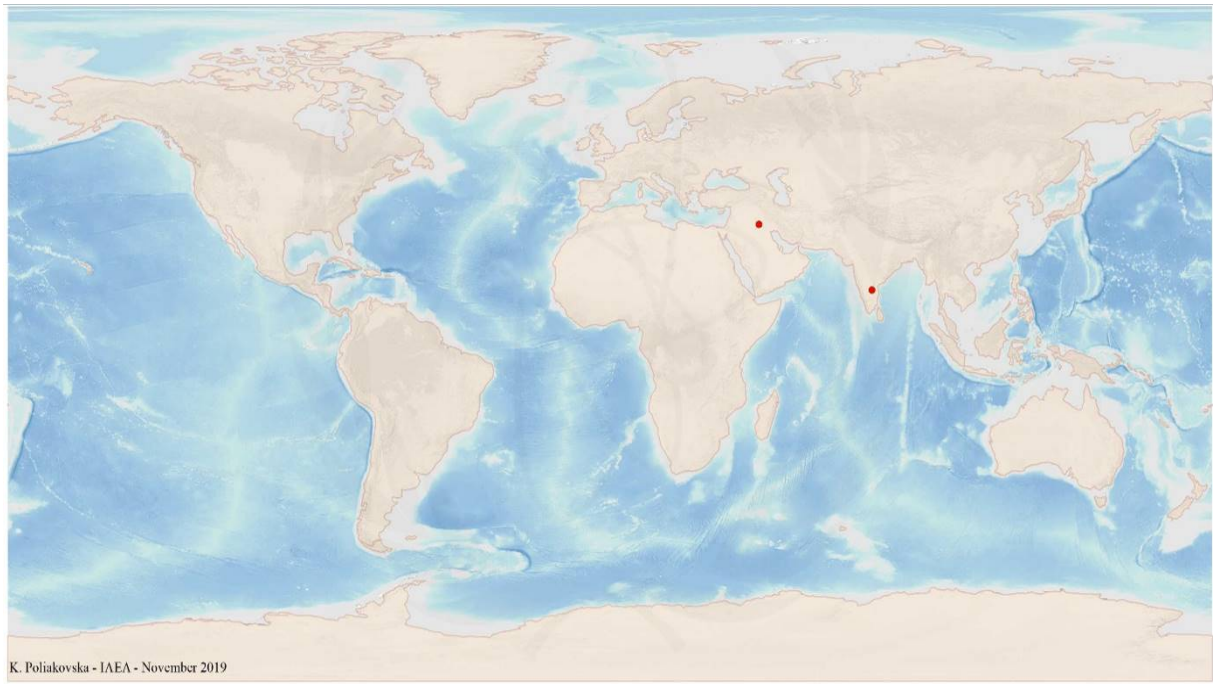

FIG. 13.1a. World distribution of selected Carbonate Stratabound uranium deposits from the UDEPO database.

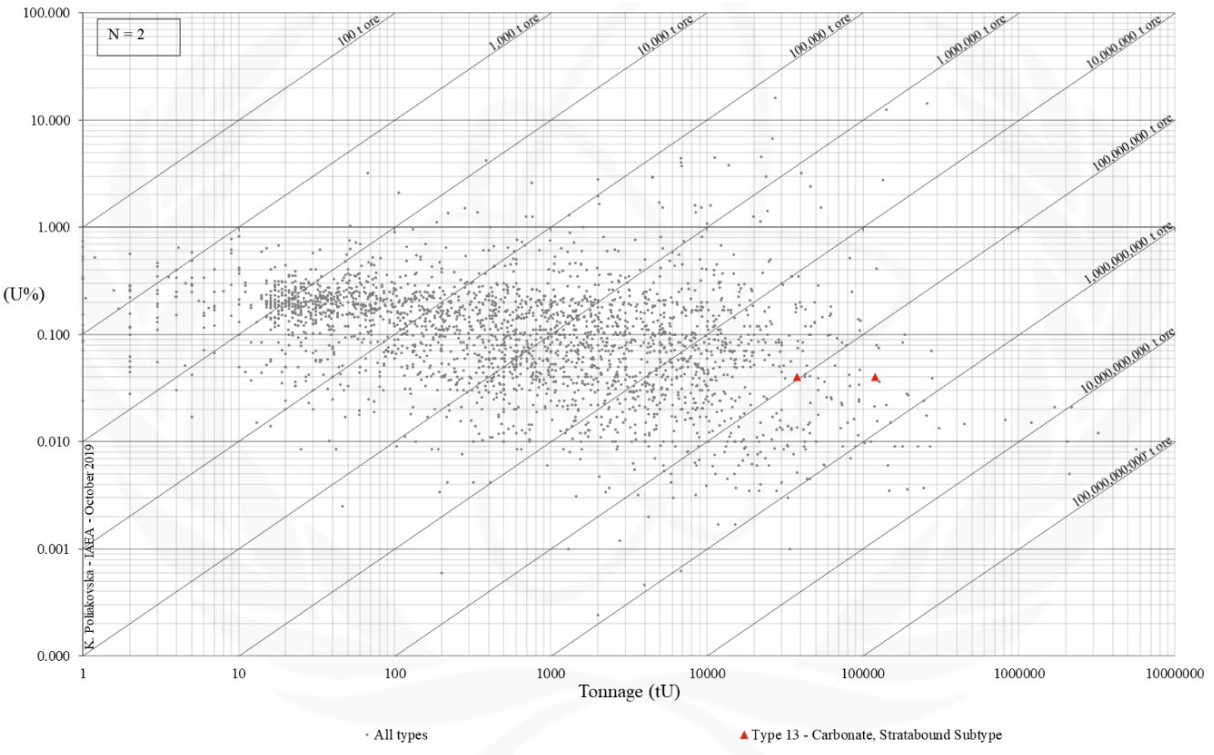

FIG. 13.1b. Grade and tonnage scatterplot highlighting Carbonate Stratabound uranium deposits from the UDEPO database.

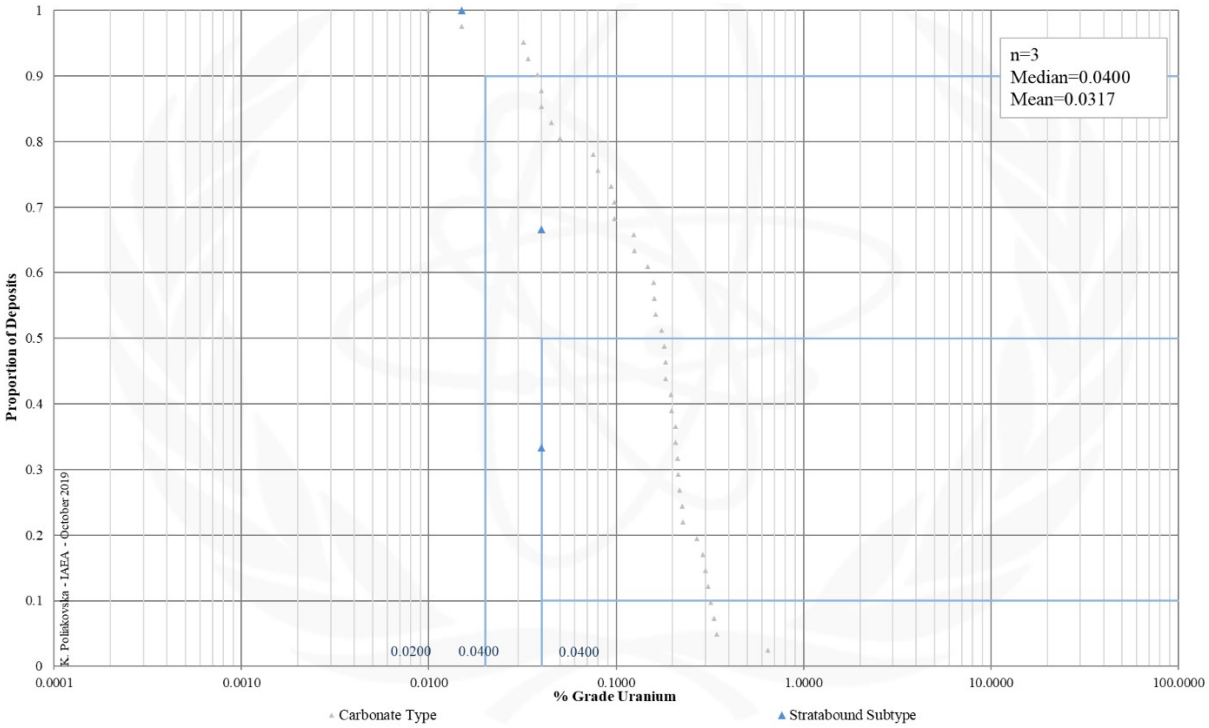

FIG. 13.1c. Grade Cumulative Probability Plot for Carbonate Stratabound uranium deposits from the UDEPO database.

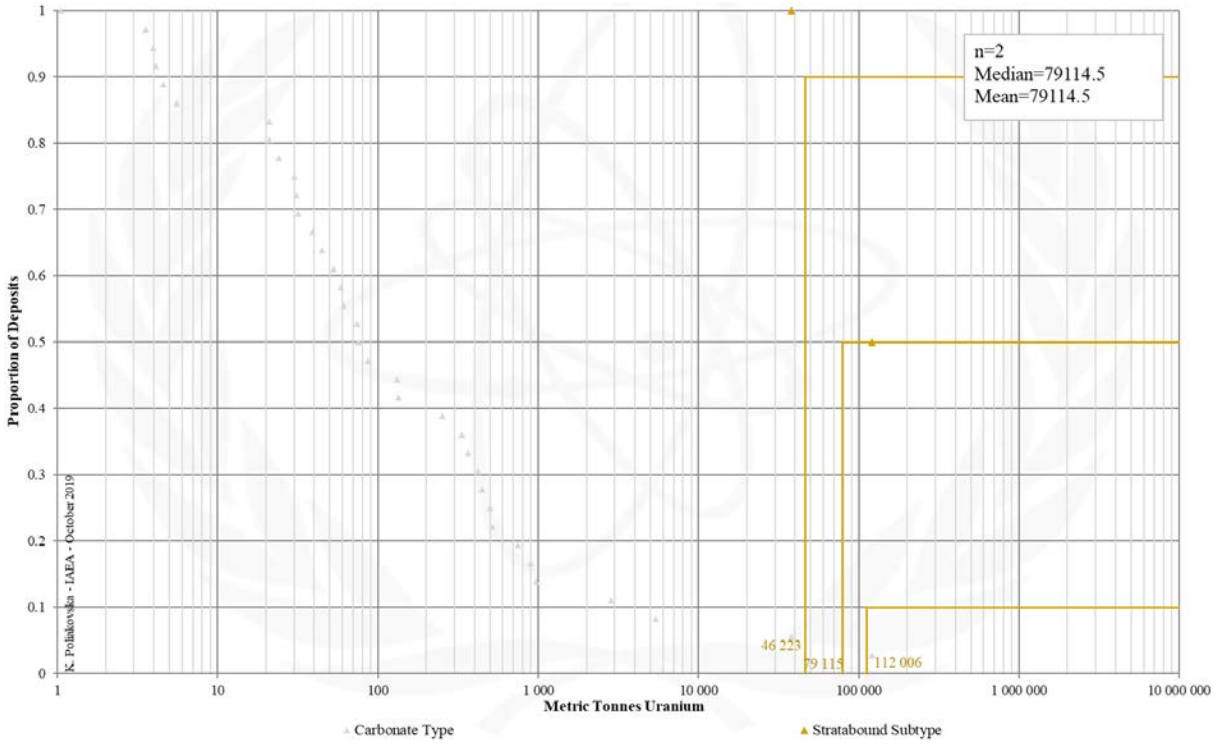

FIG. 13.1d. Tonnage Cumulative Probability Plot for Carbonate Stratabound uranium deposits from the UDEPO database.

SUBTYPE 13.2. Carbonate, Cataclastic

Brief Description
- Carbonate deposits comprise diverse syn- and epigenetic uranium ores of variable size and grade that formed in a variety of geological settings and at various times in Earth's history.
- Cataclastic deposits take the form of structurally-controlled uranium ores associated with fracture zones cutting previously deformed bituminous calcareous sedimentary rocks.

Type Examples
- Mailuu-Suu district, Kyrgyzstan; Todilto district, USA

Genetically Associated Deposit Types
- Subtype 13.1. Stratabound
- Subtype 13.3. Palaeokarst

Principal Commodities
- U, V ± As, Co, Cr, Fe, Mo, Ni, Pb, V

Grades (%) and Tonnages (tU)
- Average: 0.1516, 540.6
- Median: 0.1600, 131.0

Number of Deposits
- Deposits: 51

Provinces (undifferentiated from Carbonate Type)
- Karamazar East, Pryor Mountains, Volga Ural

Tectonic Setting
- Collisional orogens (inverted intermontane and intracratonic basins)

Typical Geological Age Range
- Mesozoic-Tertiary

Mineral Systems Model

Source

Ground preparation
- Orogenesis
- Metasomatism/oxidation

Energy
- Orogenesis
- Topography-driven fluid flow
- Evaporative pumping

Fluids
- Groundwaters
- Hydrothermal fluids/brines

Ligands
- No information

Reductants
- Hydrocarbons (pyrobitumen)

Uranium ± vanadium
- Subtype 13.2. Felsic igneous and volcaniclastic rocks

Transport

Fluid pathways
- Crustal-scale fault zones
- Subsidiary fault-fracture systems
- Regional fold hinges
- Regional stratigraphic aquifers

Trap

Physical
- Fault-fracture systems, fault intersections, zones of high fracture density
- Folds (limbs, crests)
- Lithological competency contrast (in particular limestone/sandstone)
- Carbonate host rock porosity (stylolites, microfissures, grain interstices, voids, oolite matrix, fossil fragments)

Chemical
- Pyrobitumen

Deposition

Change in redox conditions
- Due to interaction of oxidised, uranium-bearing groundwaters with wallrock reductants
- Due to fluid mixing

Remobilisation and redeposition

- Remobilisation of primary uranium mineralisation due to oxidation and redeposition of uranium as hexavalent ores

Preservation

- Deep burial and/or downfaulting
- Infiltration of hydrocarbons
- Relative tectonic stability
- Climatic stability

Key Reference Bibliography

BERGLOF, W. R., MCLEMORE, V. T., Economic geology of the Todilto Formation. New Mexico Geological Society Guidebook, 54, 179-189 (2003).
DAHLKAMP, F. J., Uranium Deposits of the World: Asia. Springer, Berlin, Heidelberg, 492p (2009).
DAHLKAMP, F. J., Uranium Deposits of the World: Europe. Springer, Berlin, Heidelberg, 792p (2016).
INTERNATIONAL ATOMIC ENERGY AGENCY, Geological Classification of Uranium Deposits and Description of Selected Examples. IAEA-TECDOC Series, 1842, 415p (2018).
LUCAS, S. G., KRAINER, K., BERGLOF, W. R., Folding in the Middle Jurassic Todilto Formation, New Mexico-Colorado, USA. Volumina Jurassica, 12(2), 39-54 (2014).
MCLEMORE, V. T., The Grants uranium district, New Mexico: update on source, deposition, and exploration. The Mountain Geologist, 48(1), 23-44 (2011).

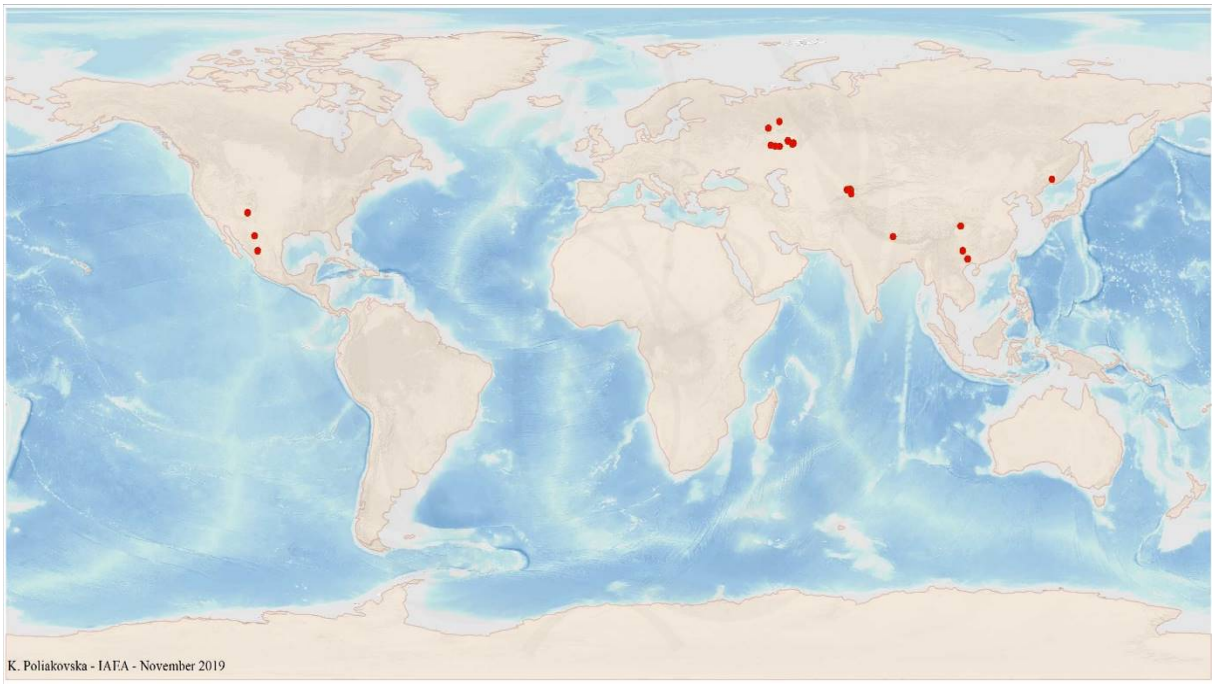

FIG. 13.2a. World distribution of selected Carbonate Cataclastic uranium deposits from the UDEPO database.

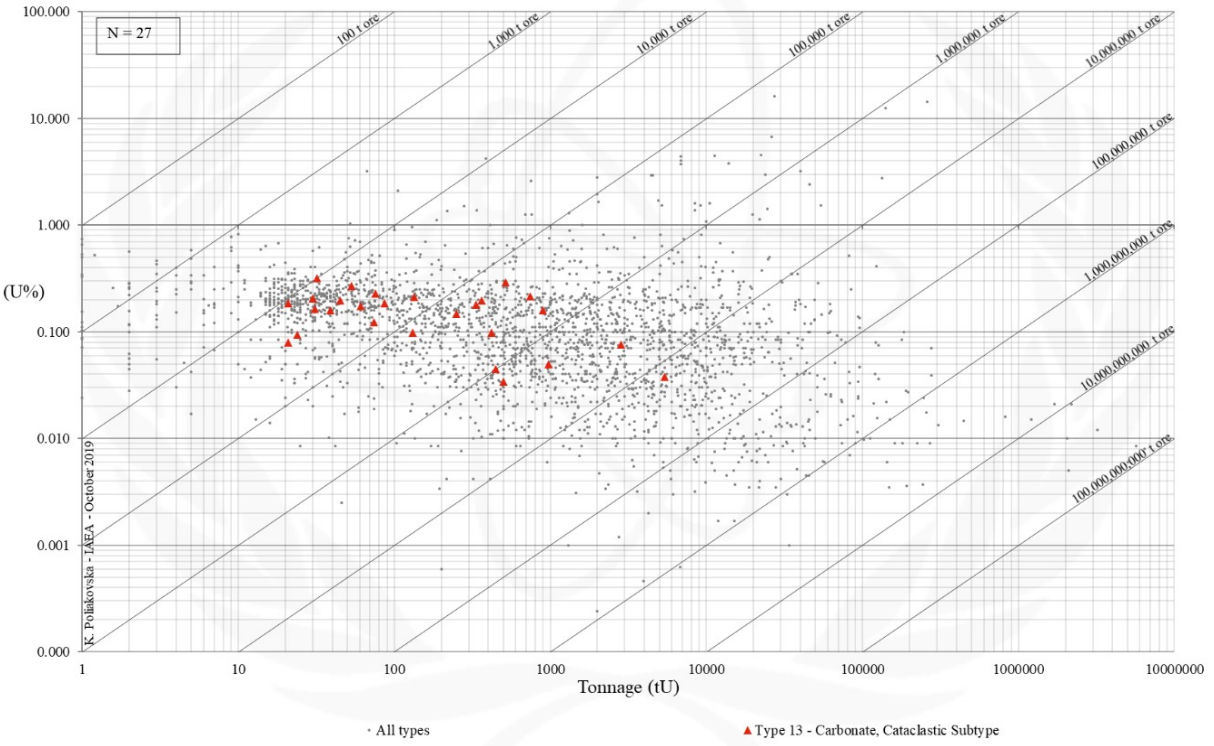

FIG. 13.2b. Grade and tonnage scatterplot highlighting Carbonate Cataclastic uranium deposits from the UDEPO database.

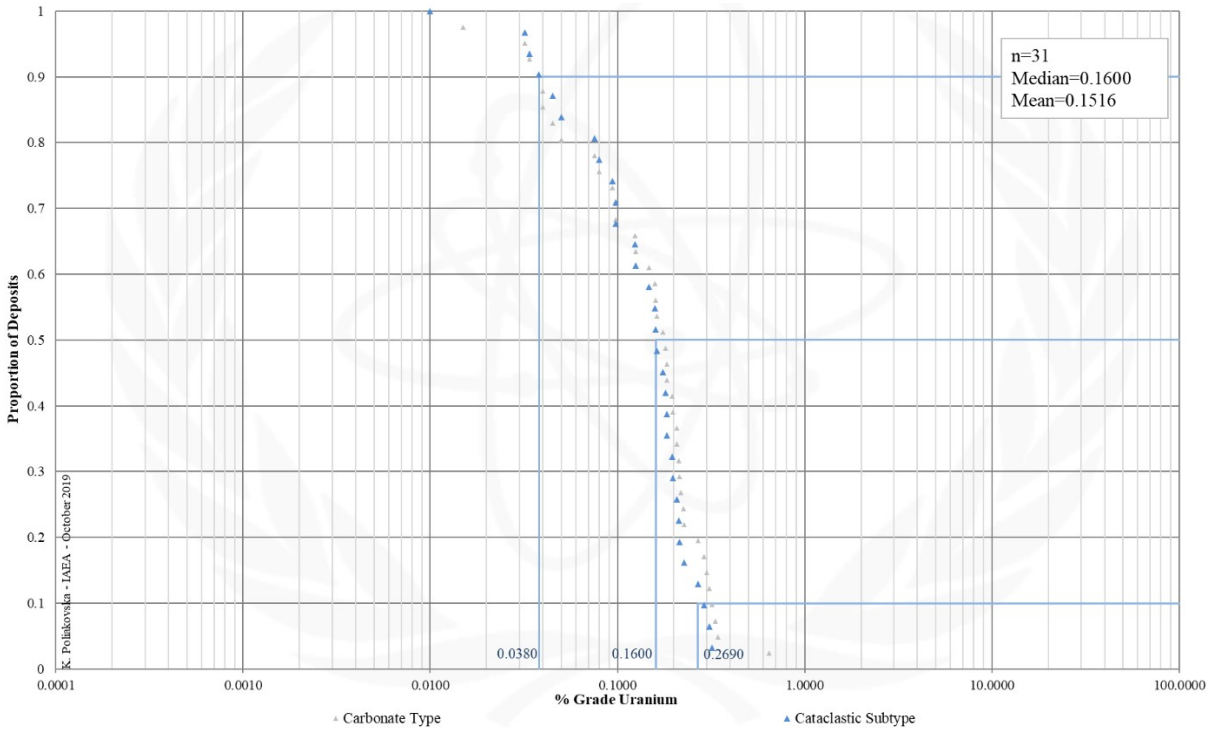

FIG. 13.2c. Grade Cumulative Probability Plot for Carbonate Cataclastic uranium deposits from the UDEPO database.

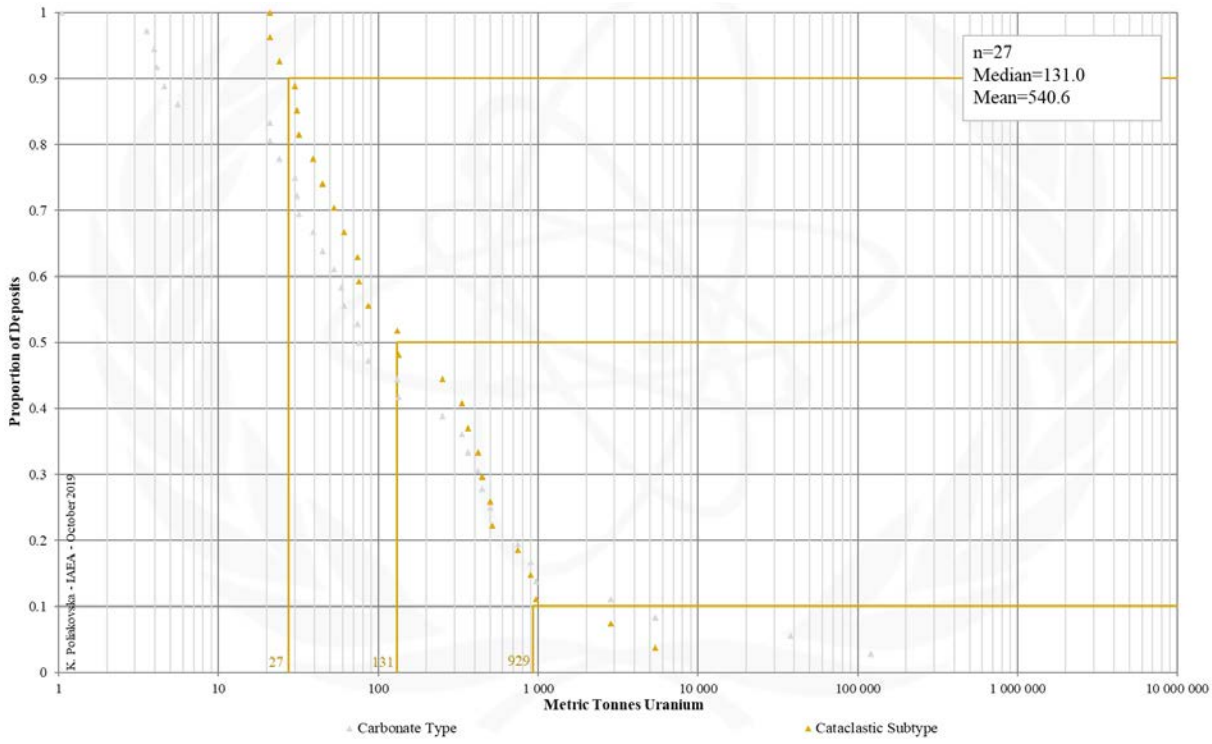

FIG. 13.2d. Tonnage Cumulative Probability Plot for Carbonate Cataclastic uranium deposits from the UDEPO database.

SUBTYPE 13.3. Carbonate, Palaeokarst

Brief Description
- Carbonate deposits comprise diverse syn- and epigenetic uranium ores of variable size and grade that formed in a variety of geological settings and at various times in Earth's history.
- Palaeokarst deposits are hosted by solution collapse breccias and associated ring fracture systems developed in impure, karsted limestone.
- The host breccias vary in size and configuration from small, metre-scale to large bodies that are up to 400 m in diameter and 200 m in vertical extent.

Type Examples
- Pryor-Little Mountains, USA; Sanbaqi, China; Tyuya-Myuyun/Osh district, Kyrgyzstan

Genetically Associated Deposit Types
- Subtype 13.1. Stratabound
- Subtype 13.2. Cataclastic
- Type 8. Collapse breccia pipe

Principal Commodities
- U ± Ba, Cu, Ra, V

Grades (%) and Tonnages (tU)
- Average: 0.3250, 11.7
- Median: 0.2989, 4.1

Number of Deposits
- Deposits: 9

Provinces (undifferentiated from Carbonate Type)
- Karamazar East, Pryor Mountains, Volga Ural

Tectonic Setting
- Collisional orogens

Typical Geological Age Range
- Poorly constrained

Mineral Systems Model

Source

Ground preparation
- Orogenesis
- (Multiple phases of) karstification
- Formation of solution collapse breccias and associated ring fracture systems
- Accumulation of clays and organic matter in karst-related structures

Energy
- Orogenesis
- Post-orogenic collapse
- Far-field tectonic activity

Fluids
- Groundwaters
- Connate brines

Ligands
- Ca

Reductants
- Diagenetic sulphides, sulfidic breccia, organic matter, sulphate-reducing bacteria, hydrocarbons

Uranium ± vanadium
- Carbonaceous shales, volcanic rocks, tuffaceous sediments, unknown distal sources

Transport

Fluid pathways
- Crustal-scale fault zones and subsidiary fault-fracture systems
- Regional fold hinges
- Regional stratigraphic (karst) aquifers

Trap

Physical
- Karst cavities and voids
- Solution collapse breccia
- Ring faults
- Fault-fracture systems

Chemical
- Carbonaceous matter

Deposition

Change in redox conditions
- Due to mixing of lateral/downward-flowing, oxidised, uranium-bearing groundwaters and upward-flowing, reducing hydrothermal fluids/brines entering the ring fractures and pipes from below
- Due to interaction of oxidised, uranium-bearing groundwaters with wallrock reductants

Fluid cooling and depressurisation
- Phase separation/CO_2 effervescence

Remobilisation and redeposition
- Dissolution of primary colloidal uranium due to groundwater oscillations and redeposition as secondary hexavalent uranium ores

Preservation

- Deep burial and/or downfaulting
- Infiltration of hydrocarbons
- Relative tectonic stability
- Climatic stability

Key Reference Bibliography

DAHLKAMP, F. J., Uranium ore deposits. Springer, Berlin, 460p (1993).

DAHLKAMP, F. J., Uranium Deposits of the World: Asia. Springer, Berlin, Heidelberg, 492p (2009).

DAHLKAMP, F. J., Uranium Deposits of the World: Europe. Springer, Berlin, Heidelberg, 792p (2016).

DUBLYANSKY, Y., MICHAJLJOW, W., BOLNER-TAKÁCS, K., HROMAS, J., SZÉKELY, K., HEVESI, A., KRAUS, S., Hypogene karst in the Tyuya-Muyun and the Kara-Tash massifs (Kyrgyzstan). In: KLIMCHOUK, A, PALMER, A. N., DE WAELE, J., AULER, A. S., AUDRA, P. (eds), Hypogene Karst Regions and Caves of the World, Springer, 495-507 (2017).

INTERNATIONAL ATOMIC ENERGY AGENCY, Geological Classification of Uranium Deposits and Description of Selected Examples. IAEA-TECDOC Series, 1842, 415p (2018).

MIN, M., ZHENG, D., SHEN, B., WEN, G., WANG, X., GANDHI, S. S., Genesis of the Sanbaqi deposit: a paleokarst-hosted uranium deposit in China. Mineralium Deposita, 32, 505-519 (1997).

MOORE-NALL, A. L., Structural controls and chemical characterization of brecciation and uranium vanadium mineralization in the northern Bighorn Basin. Unpublished PhD Thesis, Montana State University, Bozeman, 363p (2016).

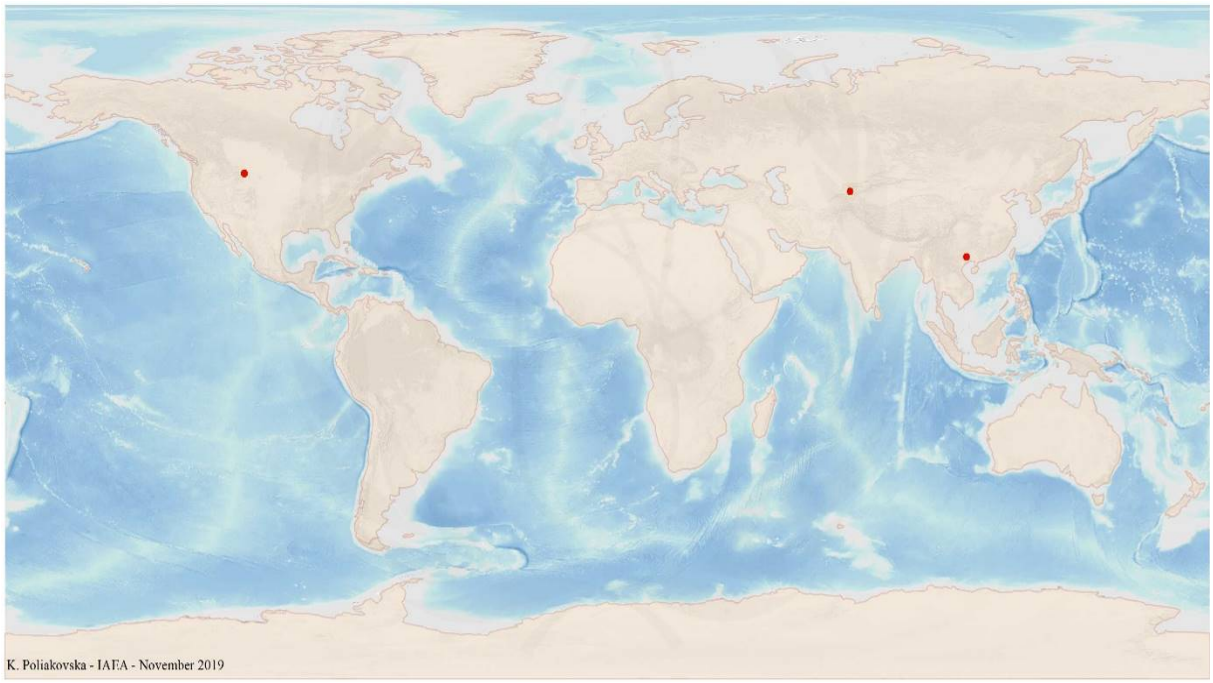

FIG. 13.3a. World distribution of selected Carbonate Palaeokarst uranium deposits from the UDEPO database.

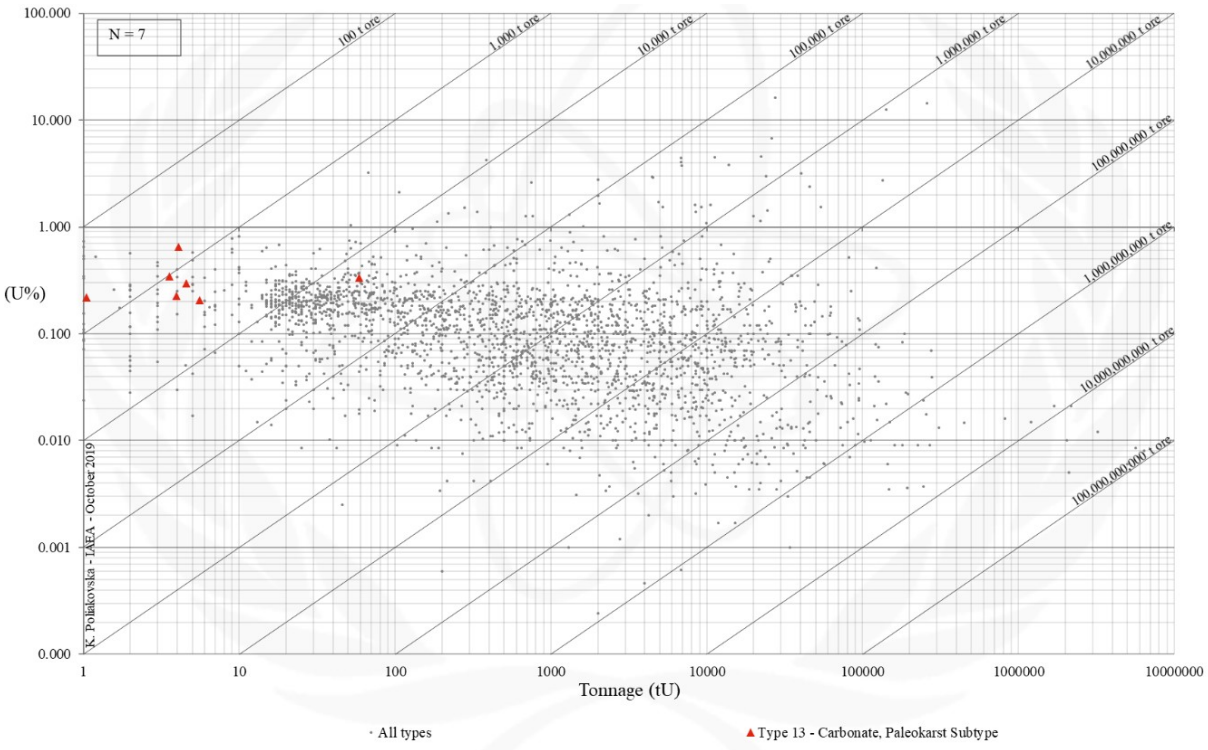

FIG. 13.3b. Grade and tonnage scatterplot highlighting Carbonate Palaeokarst uranium deposits from the UDEPO database.

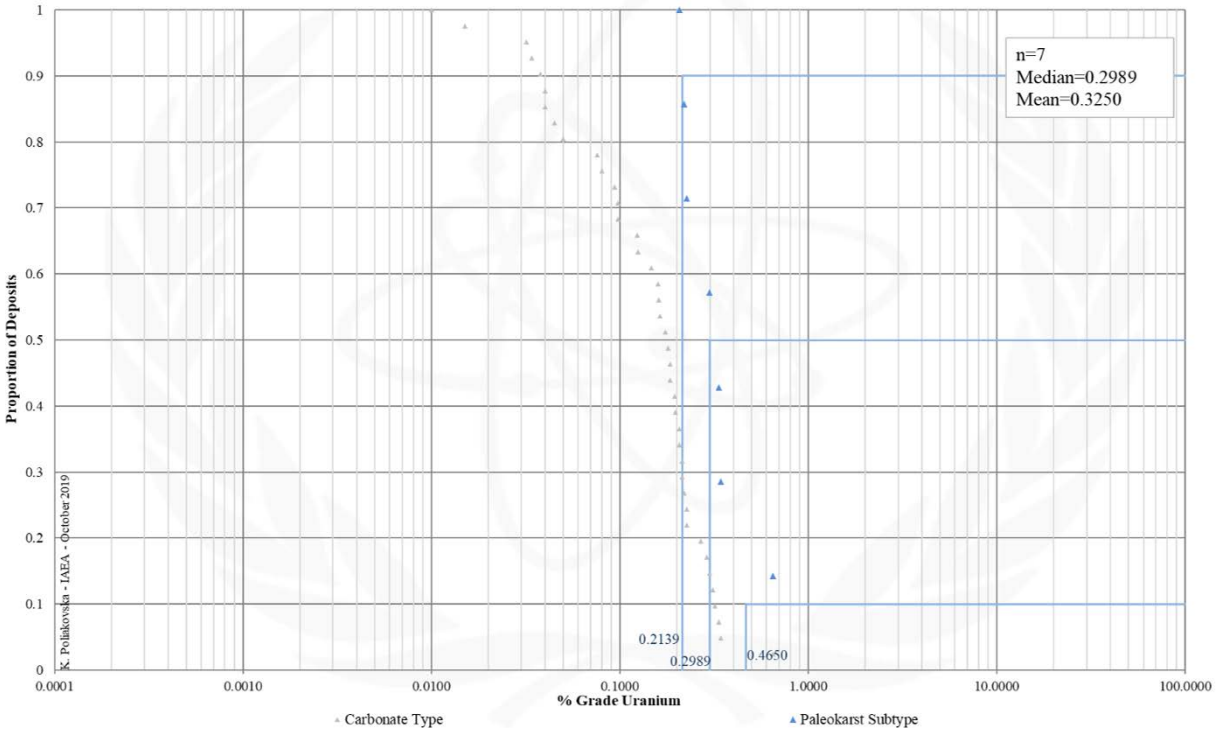

FIG. 13.3c. Grade Cumulative Probability Plot for Carbonate Palaeokarst uranium deposits from the UDEPO database.

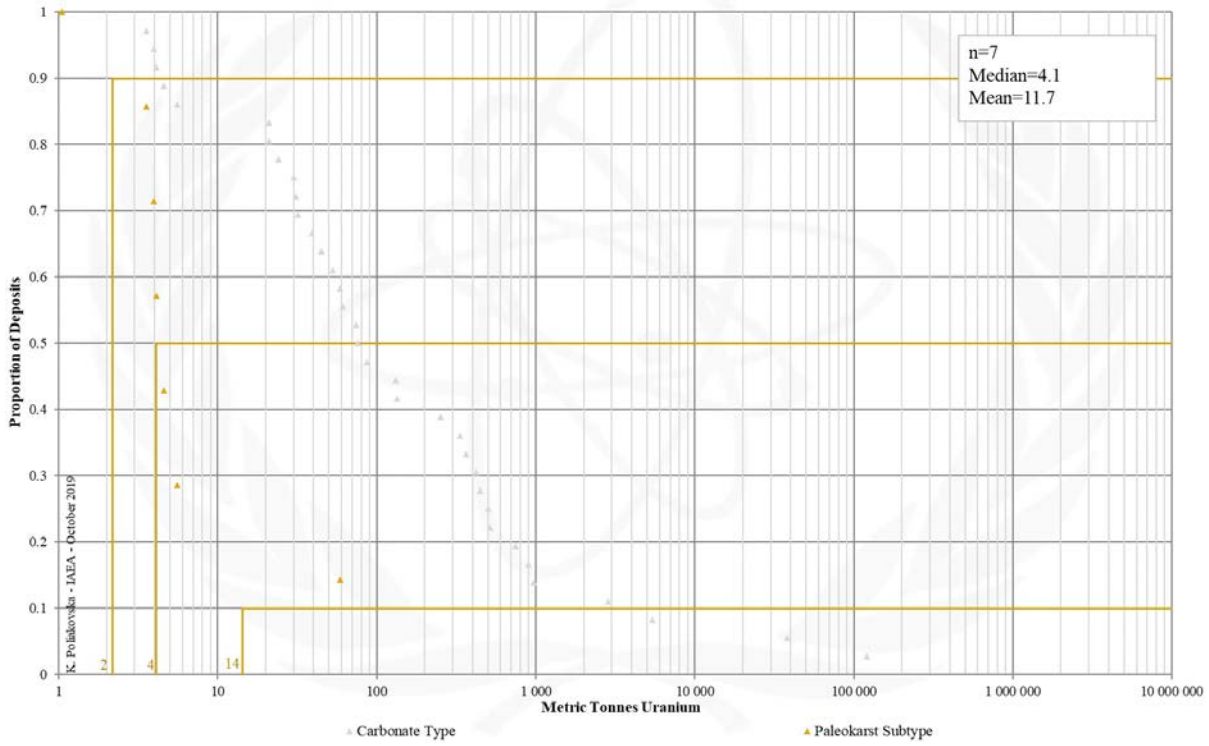

FIG. 13.3d. Tonnage Cumulative Probability Plot for Carbonate Palaeokarst uranium deposits from the UDEPO database.

Appendix XIV

PHOSPHATE

TYPE 14. Phosphate

Brief Description
- Phosphate deposits, the main global source of phosphorus, can host significant uranium resources up to several million tonnes, albeit at very low concentrations.
- The uranium ores take the form of synsedimentary, stratiform, disseminations associated with fine-grained apatite.
- Phosphate deposits are classified as unconventional uranium resources with low grade uranium recoverable as a by-product of phosphate mining.
- Three subtypes have been described: (14.1.) Organic phosphorite, (14.2.) minerochemical phosphorite, and (14.3.) continental phosphate.

Subtypes
- 14.1. Organic phosphorite
- 14.2. Minerochemical phosphorite
- 14.3. Continental phosphate

Type Examples
- Subtype 14.1. Mangyshlak Peninsula, Kazakhstan; Ergeninsky region, Russian Federation
- Subtype 14.2. Phosphoria Formation, USA
- Subtype 14.3. Bakouma district, Central African Republic

Principal Commodities
- Subtype 14.1. P, REE, U (by-product only) ± Co, La, Mo, Ni, Sc, Y
- Subtype 14.2. P ± Cr, Cu, Mo, REE, Se, U (by-product only), Zn
- Subtype 14.3. P, U (by-product only)

Grades (%) and Tonnages (tU)
- Average: 0.0331, 200617.2
- Median: 0.0100, 20300.0

Number of Deposits
- Deposits: 88

Provinces
- Atlas, Baja California, Bakouma Basin, Bofal Gorgol, Chile, East Mediterranean, Egypt Cyrenacia Basin, Ergeninsky, Florida, Mantaro Machay, NW USA srite, Pricaspian, Sechura Basin, Sechura Basin.

Tectonic Setting
- Subtypes 14.1. to 14.2. Continental shelfs and epicontinental (epeiric) platforms
- Subtype 14.3. Intracratonic sag basins

Typical Geological Age Range
- Subtypes 13.1. and 13.3. Tertiary
- Subtype 13.2. Neoproterozoic to Recent

Mineral Systems Model

Source

Ground preparation
- Subtype 14.1. Development of an intricate system of marine troughs and ridges, active tectonism linked to far-field orogenesis, isolation of deep-water troughs due to tectonic uplift and associated eustatic sea-level drops, water stratification and stagnation in a warm, humid climate
- Subtype 14.2. Generation of continental shelf and/or epicontinental (epeiric) platform environments
- Subtype 14.3. Intracratonic basin formation, deposition of a carbonate platform, orogeny, karstification (preferentially along structural discontinuities), formation of karst lakes and deposition of lacustrine phosphatic siltstones

Energy
- Subtype 14.1. Far-field orogeny, tectonic oscillations (uplift and subsidence)
- Subtype 14.2. Seawater currents, wind stress
- Subtype 14.3. Topography (gravity)-driven fluid flow

Fluids
- Subtypes 14.1. to 14.2. Seawaters
- Subtype 14.3. Karstic groundwaters, acidic groundwaters, lake waters

Ligands
- Subtype 14.1. PO
- Subtype 14.2. No information
- Subtype 14.3. Ca

Reductants
- Subtype 14.1. Hydrogen sulphide, phosphatised organic matter (fish bones), sulphidic clays
- Subtype 14.2. No information
- Subtype 14.3. Reduced lake waters, lignite

Uranium ± other metals
- Subtype 14.1. Submarine volcanic centres, reworked organic matter (fish bones)

- Subtype 14.2. Continental sources (felsic igneous rocks)
- Subtype 14.3. Poorly constrained (crystalline basement rocks, limestone, black shales)

Transport

Fluid pathways
- Subtype 14.1. Ocean currents (± controlled by deep troughs with steep slopes)
- Subtype 14.2. Ocean currents, zones of upwelling of deep marine waters, evaporation-driven lagoonal fluid circulation systems
- Subtype 14.3. Stratigraphic aquifers, karst channels, fault-fracture systems tapping into stratigraphic aquifers and/or karst channels

Trap

Physical
- Subtype 14.1. Basement highs/horsts (first-order control on supply and distribution of organic matter)
- Subtype 14.2. Shallow marine continental shelf and epicontinental (epeiric) platform environments, zones of upwelling of deep marine waters, evaporation-driven lagoonal circulation systems
- Subtype 14.3. Karst channels, breccia zones

Chemical
- Subtype 14.1. Fish bone detritus, pyritic clays, H_2S-contamination of bottom waters (anoxic events)
- Subtype 14.2. Organic matter, phosphate
- Subtype 14.3. Organic matter, reducing, strongly alkaline lake waters in karst channels, phosphatic sediments

Deposition

Phosphogenesis
- Subtype 14.2. Phosphogenesis (i) sustained by evaporation-driven lagoonal seawater circulation, or (ii) associated with oxygen minimum zones generated by microbial degradation of accumulating organic matter

Slow sedimentation rates
- Subtype 14.2. Result in longer exposure of apatite grains and enhance their capacity to extract uranium from seawaters

Diagenesis
- Subtype 14.1. Uranium concentration during diagenesis

Adsorption
- Subtype 14.1. Uranium adsorption onto phosphate minerals and phosphatised fish bone detritus
- Subtype 14.2. Uranium adsorption onto (i) organic matter, or (ii) phosphate minerals

Remobilisation and redeposition
- Subtype 14.1. Reworking and redeposition of organic matter and concomitant concentration/upgrading of contained uranium
- Subtype 14.2. Reworking, redeposition and upgrading of contained uranium through (i) repeated marine transgressions promoting re-exposure of phosphate particles to uranium-bearing seawaters and greater uranium uptake thereby producing a high grade regressive lag, (ii) syndepositional winnowing, transport and re-exposure of phosphatic peloids and grains, (iii) storm activity producing thicker and richer phosphate accumulations

Change in redox conditions
- Subtype 14.3. Due to mixing of oxidised (acidic?) groundwaters with reduced lacustrine waters

Preservation
- Deep burial and/or downfaulting
- Establishment or maintenance of anoxic environments
- Laterite caps may act as protective seals
- Relative tectonic stability

Key Reference Bibliography

DAHLKAMP, F. J., Uranium Deposits of the World: Asia. Springer, Berlin, Heidelberg, 492p (2009).
DAHLKAMP, F. J., Uranium Deposits of the World: USA and Latin America. Springer, Berlin, Heidelberg, 515p (2010).
FUCHS, Y., Paleokarst-related uranium deposits. In Developments in Earth Surface Processes, 1, 473-480 (1989).
INTERNATIONAL ATOMIC ENERGY AGENCY, Uranium deposits in Africa: geology and exploration. Proceedings of a regional advisory group meeting, Lusaka, 14-18 November 1977, 262p (1979).
INTERNATIONAL ATOMIC ENERGY AGENCY, Geological Classification of Uranium Deposits and Description of Selected Examples. IAEA-TECDOC Series, 1842, 415p (2018).
PUFAHL, P. K., GROAT, L. A., Sedimentary and igneous phosphate deposits: formation and exploration. Economic Geology, 112(3), 483-516 (2016).
SHARKOV, A. A., Specific features of the structure and evolution of U- and REE-bearing organic phosphate deposits in the southern Mangyshlak region. Lithology and Mineral Resources, 35(3), 252-266 (2000).
STOLYAROV, A. S., IVLEVA, E. I., Upper Oligocene sediments in the Ciscaucasus, Volga–Don, and Mangyshlak regions (central part of the eastern Paratethys): Communication 1. Main compositional and structural features. Lithology and Mineral Resources, 39(3), 252-270 (2004a).
STOLYAROV, A. S., IVLEVA, E. I., Upper Oligocene sediments in the Ciscaucasus, Volga–Don, and Mangyshlak regions (central part of the eastern Paratethys): Communication 2. Facies–paleogeographic sedimentation settings. Lithology and Mineral Resources, 39(4), 359-368 (2004b).

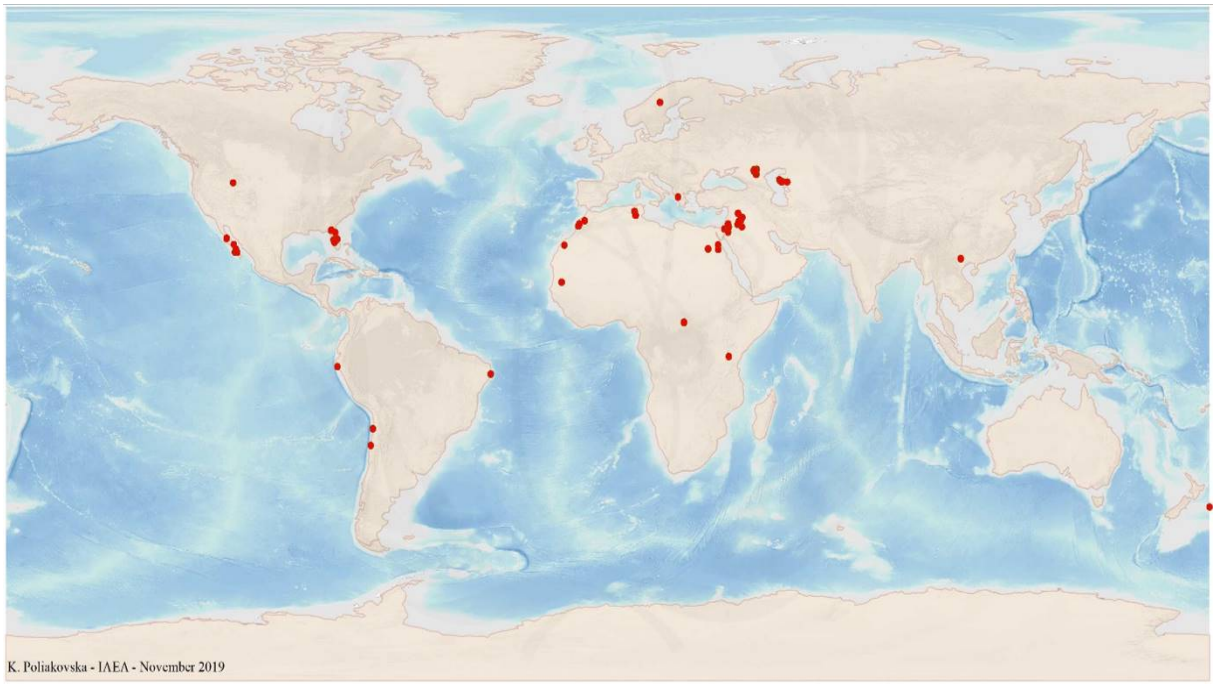

FIG. 14a. World distribution of selected Phosphate uranium deposits from the UDEPO database.

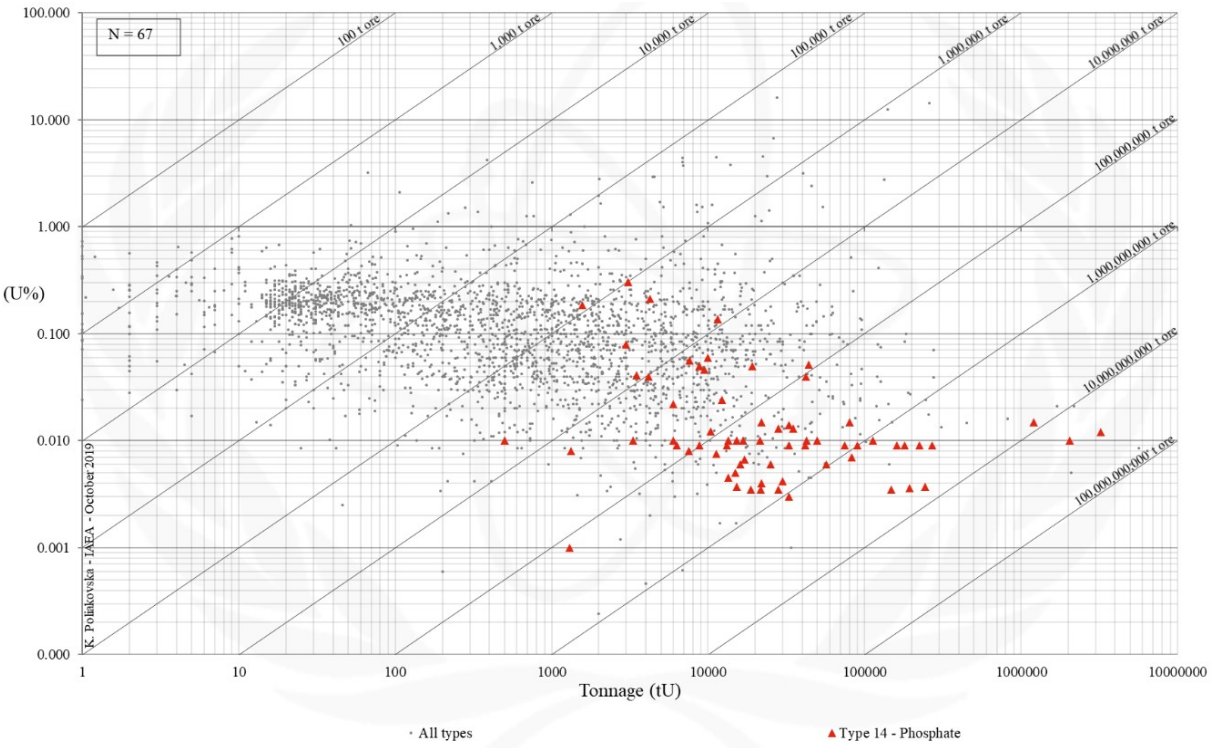

FIG. 14b. Grade and tonnage scatterplot highlighting Phosphate uranium deposits from the UDEPO database.

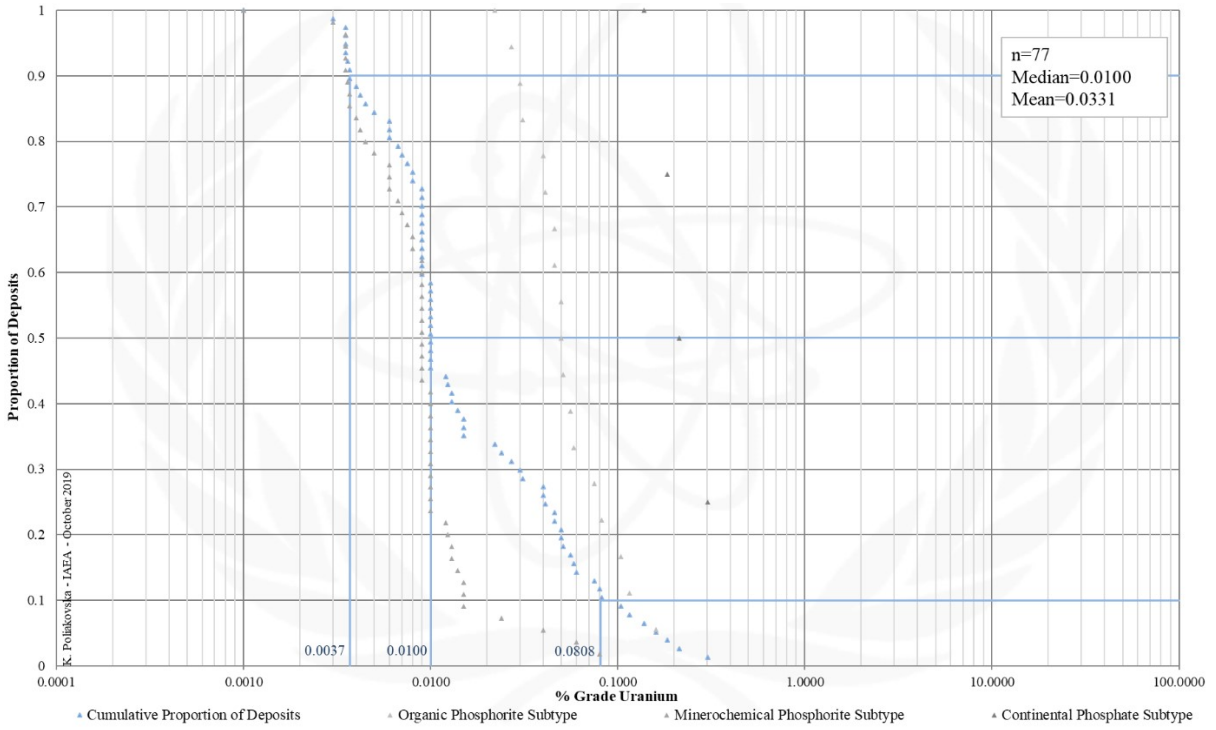

FIG. 14c. Grade Cumulative Probability Plot for Phosphate uranium deposits from the UDEPO database.

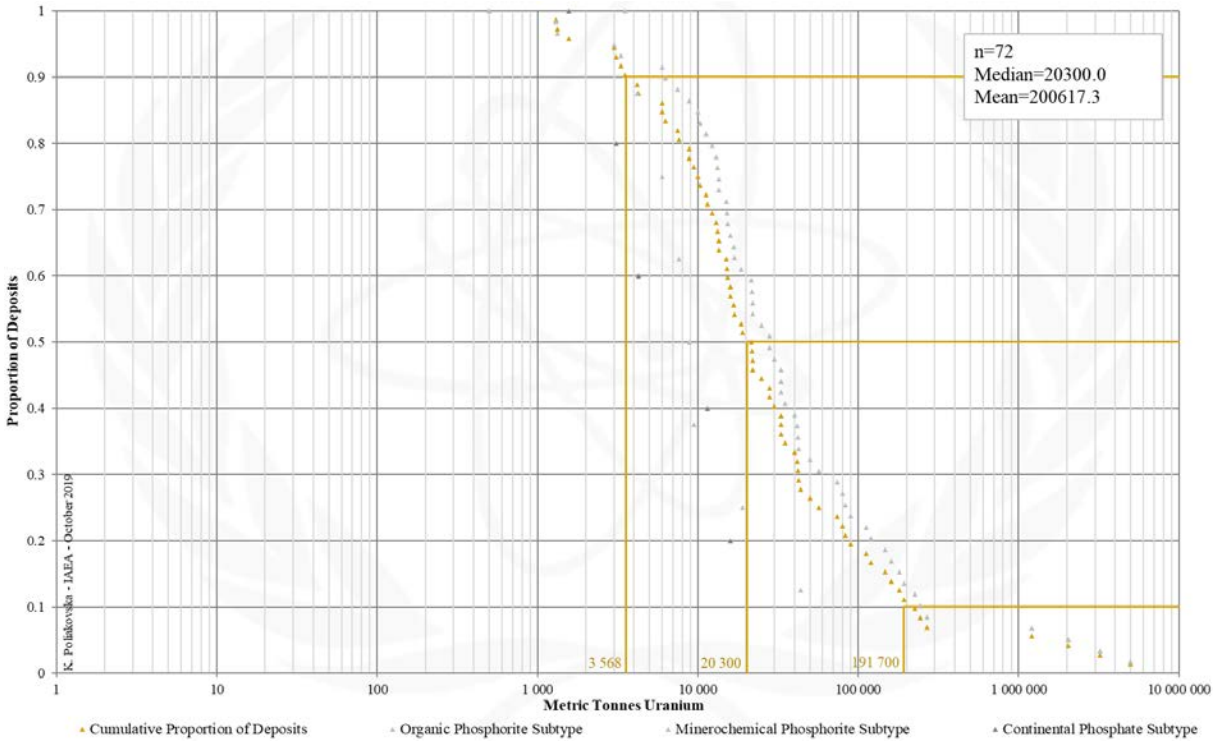

FIG. 14d. Tonnage Cumulative Probability Plot for Phosphate uranium deposits from the UDEPO database.

SUBTYPE 14.1. PHOSPHATE, ORGANIC PHOSPHORITE

Brief Description
- Phosphate deposits, the main global source of phosphorus, can host significant uranium resources up to several million tonnes, albeit at very low concentrations.
- Phosphate deposits are classified as unconventional uranium resources with low grade uranium recoverable as a by-product of phosphate mining.
- Organic phosphorite deposits are known exclusively from Tertiary-age, low-energy, shallow-marine basins in the northern Caspian Sea region.
- The uranium in these deposits is incorporated in phosphatised fish bone detritus in dark clay beds enriched in fish remains and sulphides.

Type Examples
- Mangyshlak Peninsula, Kazakhstan; Ergeninsky district, Russian Federation

Genetically Associated Deposit Types
- Subtype 14.2. Minerochemical phosphorite
- Subtype 14.3. Continental phosphate

Principal Commodities
- P, REE, U (by-product only) ± Co, La, Mo, Ni, Sc, Y

Grades (%) and Tonnages (tU)
- Average: 0.0603, 12808.4
- Median: 0.0500, 8200.0

Number of Deposits
- Deposits 20

Provinces (undifferentiated from Phosphate Type)
- Atlas, Baja California, Bakouma Basin, Bofal Gorgol, Chile, East Mediterranean, Egypt Cyrenacia Basin, Ergeninsky, Florida, Mantaro Machay, NW USA srite, Pricaspian, Sechura Basin, Sechura Basin.

Tectonic Setting
- Continental shelfs and epicontinental (epeiric) platforms

Typical Geological Age Range
- Tertiary

Mineral Systems Model

Source

Ground preparation
- Development of an intricate system of marine troughs and ridges
- Active tectonism linked to far-field orogenesis
- Isolation of deep-water troughs due to tectonic uplift and associated eustatic sea-level drops
- Seawater stratification and stagnation in a warm, humid climate

Energy
- Far-field orogeny
- Tectonic oscillations (uplift and subsidence)

Fluids
- Seawaters

Ligands
- PO

Reductants
- Hydrogen sulphide, phosphatised organic matter (fish bones), sulphidic clays

Uranium ± other metals
- Submarine volcanic centres,
- Reworked organic matter (fish bones)

Transport

Fluid pathways
- Ocean currents (± controlled by deep troughs with steep slopes)

Trap

Physical
- Basement highs/horsts (first-order control on supply and distribution of organic matter)

Chemical
- Fish bone detritus
- Pyritic clays
- H_2S-contamination of bottom waters (anoxic events)

Deposition

Diagenesis
- Uranium concentration during diagenesis

Adsorption
- Uranium adsorption onto phosphate minerals and phosphatised fish bone detritus

Remobilisation and redeposition
- Reworking and redeposition of organic matter and concentration/upgrading of contained uranium

Preservation

- Deep burial and/or downfaulting
- Establishment or maintenance of anoxic environments
- Relative tectonic stability

Key Reference Bibliography

DAHLKAMP, F. J., Uranium Deposits of the World: Asia. Springer, Berlin, Heidelberg, 492p (2009).

INTERNATIONAL ATOMIC ENERGY AGENCY, Geological Classification of Uranium Deposits and Description of Selected Examples. IAEA-TECDOC Series, 1842, 415p (2018).

SHARKOV, A. A., Specific features of the structure and evolution of U- and REE-bearing organic phosphate deposits in the southern Mangyshlak region. Lithology and Mineral Resources, 35(3), 252-266 (2000).

STOLYAROV, A. S., IVLEVA, E. I., Upper Oligocene sediments in the Ciscaucasus, Volga–Don, and Mangyshlak regions (central part of the eastern Paratethys): Communication 1. Main compositional and structural features. Lithology and Mineral Resources, 39(3), 252-270 (2004a).

STOLYAROV, A. S., IVLEVA, E. I., Upper Oligocene sediments in the Ciscaucasus, Volga–Don, and Mangyshlak regions (central part of the eastern Paratethys): Communication 2. Facies–paleogeographic sedimentation settings. Lithology and Mineral Resources, 39(4), 359-368 (2004b).

STOLYAROV, A. S., IVLEVA, E. I., Upper Oligocene sediments in the Ciscaucasus, Volga–Don, and Mangyshlak regions (central part of the eastern Paratethys): Communication. Metal potential and formation conditions of fish bone detritus and iron sulfide deposits. Lithology and Mineral Resources, 39(5), 504-522 (2004c).

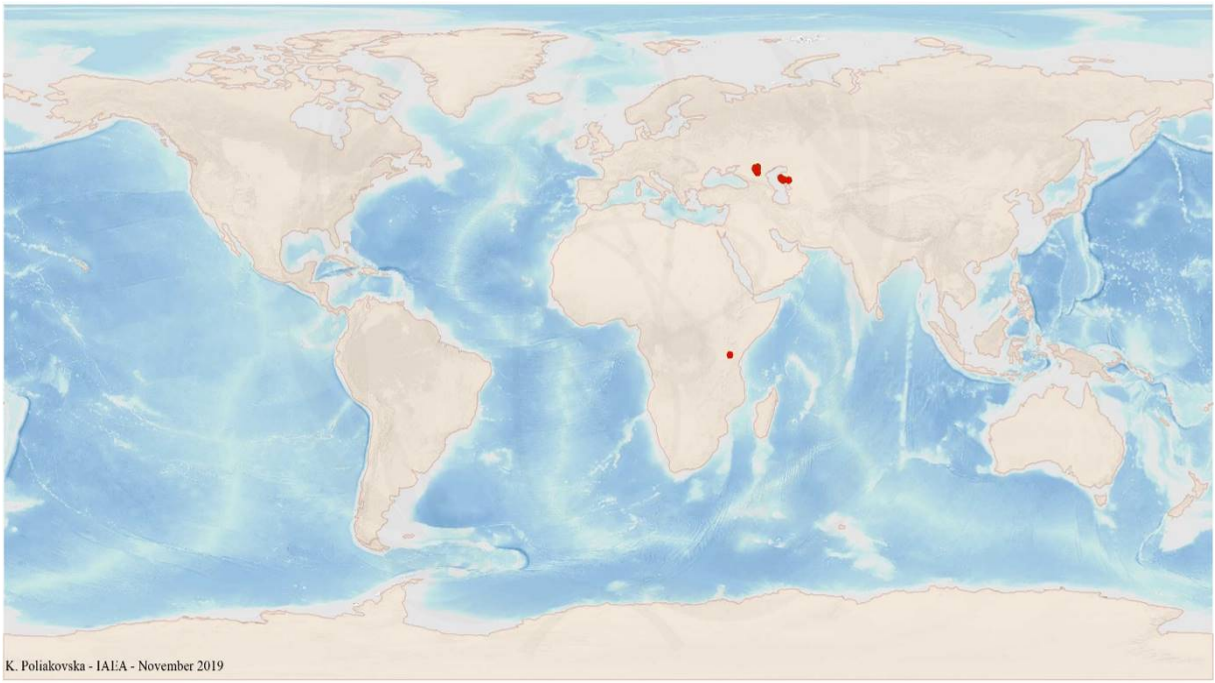

FIG. 14.1a. World distribution of selected Phosphate Organic Phosphorite uranium deposits from the UDEPO database.

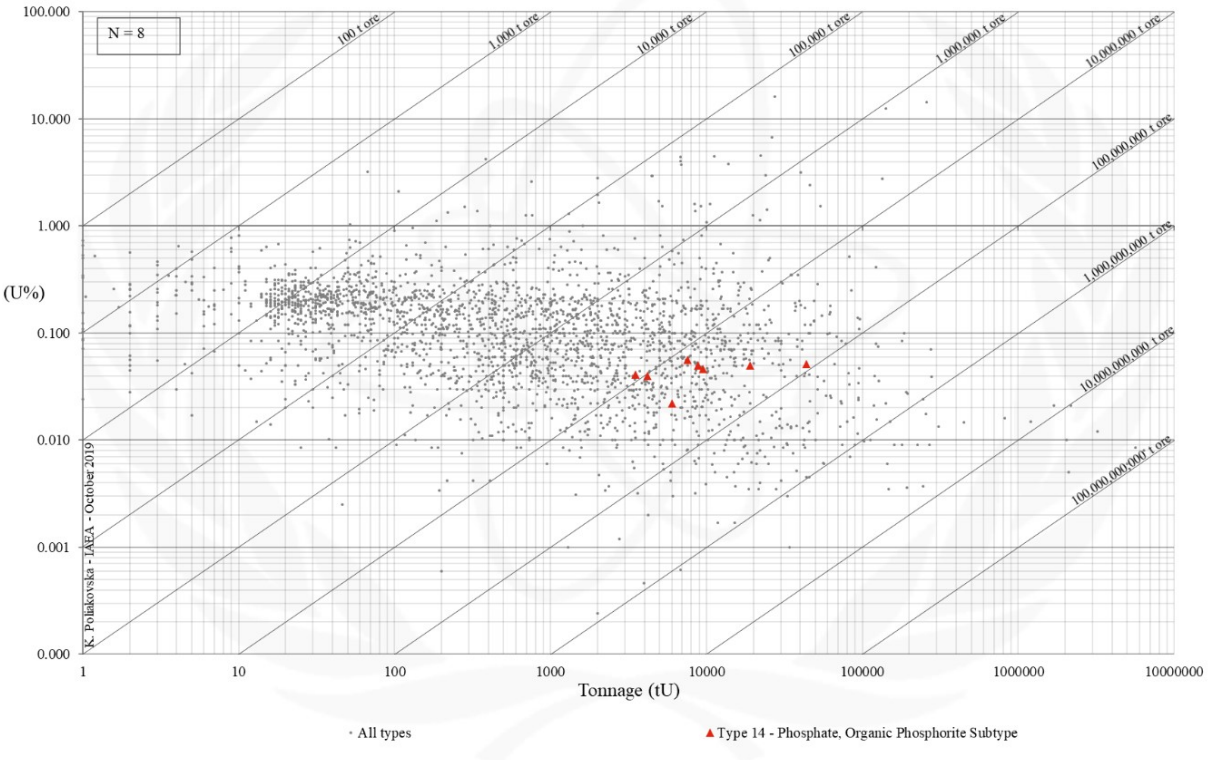

FIG. 14.1b. Grade and tonnage scatterplot highlighting Phosphate Organic Phosphorite uranium deposits from the UDEPO database.

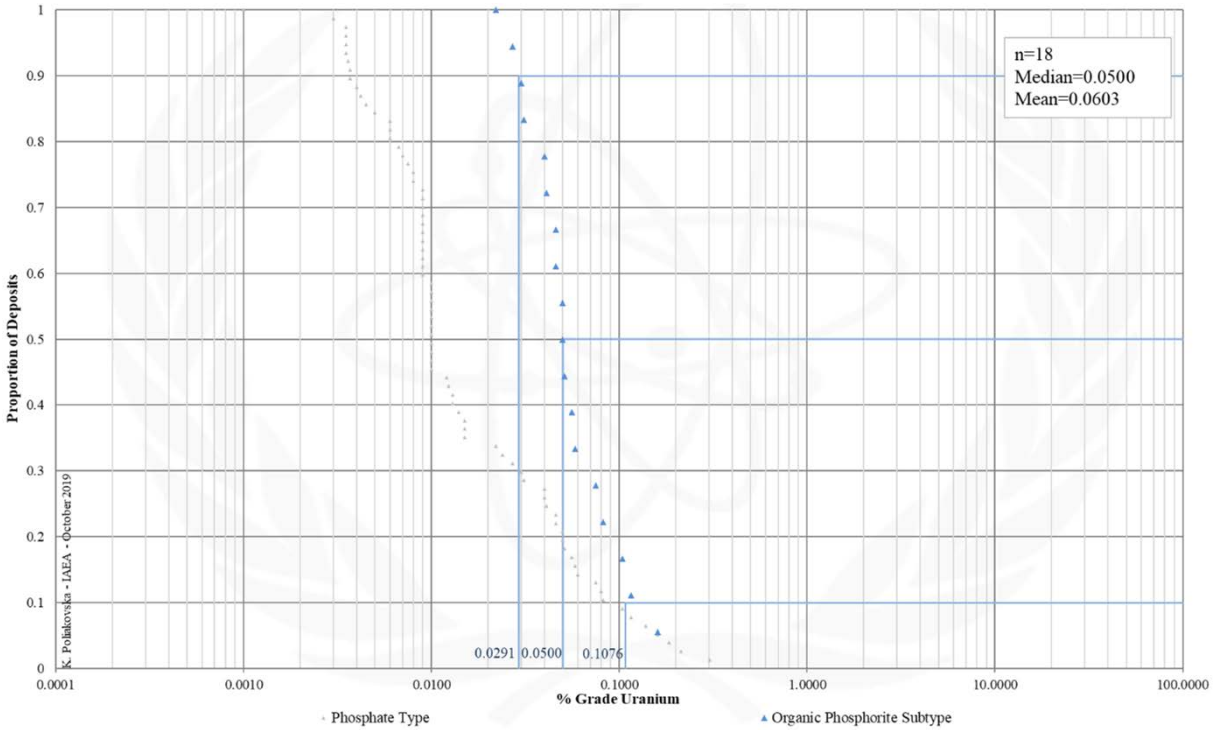

FIG. 14.1c. Grade Cumulative Probability Plot for Phosphate Organic Phosphorite uranium deposits from the UDEPO database.

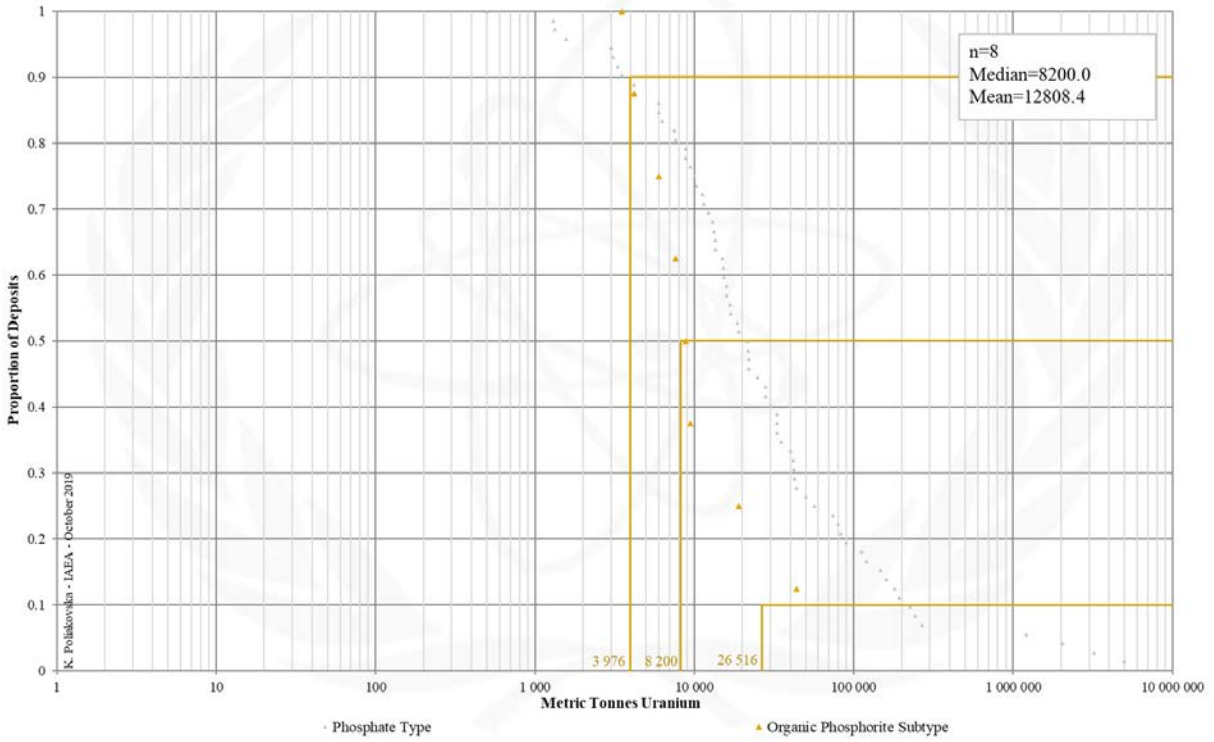

FIG. 14.1d. Tonnage Cumulative Probability Plot for Phosphate Organic Phosphorite uranium deposits from the UDEPO database.

SUBTYPE 14.2. PHOSPHATE, MINEROCHEMICAL PHOSPHORITE

Brief Description
- Phosphate deposits, the main global source of phosphorus, can host significant uranium resources up to several million tonnes, albeit at very low concentrations.
- Phosphate deposits are classified as unconventional uranium resources with low grade uranium recoverable as a by-product of phosphate mining.
- Minerochemical phosphorite deposits are the principal and economically most significant subtype extending over large areas and exhibiting a relatively uniform uranium distribution.
- The uranium ores take the form of stratiform disseminations bound to cryptocrystalline phosphate minerals of marine continental shelf origin.

Type Examples
- Phosphoria Formation, Florida Land Pebble district, USA; Gantour, Morocco

Genetically Associated Deposit Types
- Subtype 14.1. Organic phosphorite
- Subtype 14.3. Continental phosphate
- Subtype 13.1. Carbonate, Stratabound

Principal Commodities
- P ± Cr, Cu, Mo, REE, Se, U (by-product only), Zn

Grades (%) and Tonnages (tU)
- Average:0.0113, 242467.4
- Median: 0.0090, 28000.0

Number of Deposits
- Deposits: 63

Provinces (undifferentiated from Phosphate Type)
- Atlas, Baja California, Bakouma Basin, Bofal Gorgol, Chile, East Mediterranean, Egypt Cyrenacia Basin, Ergeninsky, Florida, Mantaro Machay, NW USA srite, Pricaspian, Sechura Basin, Sechura Basin.

Tectonic Setting
- Continental shelfs and epicontinental (epeiric) platforms

Typical Geological Age Range
- Neoproterozoic to Recent

Mineral Systems Model

Source

Ground preparation
- Generation of continental shelf or epicontinental (epeiric) platform environments

Energy
- Seawater currents
- Wind stress

Fluids
- Seawaters

Ligands
- No information

Reductants
- No information

Uranium ± other metals
- Continental sources (felsic igneous rocks)

Transport

Fluid pathways
- Ocean currents
- Zones of upwelling of deep marine waters
- Evaporation-driven lagoonal fluid circulation systems

Trap

Physical
- Shallow marine continental shelf and epicontinental (epeiric) platform environments
- Zones of upwelling of deep marine waters
- Evaporation-driven lagoonal circulation systems

Chemical
- Organic matter
- Phosphate

Deposition

Phosphogenesis
- Sustained by evaporation-driven lagoonal seawater circulation
- Associated with oxygen minimum zones generated by microbial degradation of accumulating organic matter

Slow sedimentation rates
- Result in longer exposure of apatite grains and enhance their capacity to extract uranium from seawaters

Uranium adsorption
- Onto organic matter
- Onto phosphate minerals

Reworking, redeposition and upgrading of contained uranium
- Through repeated marine transgressions promoting re-exposure of phosphate particles to uranium-bearing seawaters and greater uranium uptake thereby producing a high grade regressive lag
- Through syndepositional winnowing, transport and re-exposure of phosphatic peloids and grains
- Through storm activity producing thicker and richer phosphate accumulations

Preservation

- Deep burial and/or downfaulting
- Relative tectonic stability

Key Reference Bibliography

DAHLKAMP, F. J., Uranium Deposits of the World: Asia. Springer, Berlin, Heidelberg, 492p (2009).

DAHLKAMP, F. J., Uranium Deposits of the World: USA and Latin America. Springer, Berlin, Heidelberg, 515p (2010).

FUCHS, Y., Paleokarst-related uranium deposits. In Developments in Earth Surface Processes, 1, 473-480 (1989).

INTERNATIONAL ATOMIC ENERGY AGENCY, Uranium Deposits in Africa: Geology and Exploration. Proceedings of a Regional Advisory Group Meeting, Lusaka, 14-18 November 1977, 262p (1979).

INTERNATIONAL ATOMIC ENERGY AGENCY, Geological Classification of Uranium Deposits and Description of Selected Examples. IAEA-TECDOC Series, 1842, 415p (2018).

PUFAHL, P. K., GROAT, L. A., Sedimentary and igneous phosphate deposits: formation and exploration. Economic Geology, 112(3), 483-516 (2016).

SHARKOV, A. A., Specific features of the structure and evolution of U- and REE-bearing organic phosphate deposits in the southern Mangyshlak region. Lithology and Mineral Resources, 35(3), 252-266 (2000).

STOLYAROV, A. S., IVLEVA, E. I., Upper Oligocene sediments in the Ciscaucasus, Volga–Don, and Mangyshlak regions (central part of the eastern Paratethys): Communication 1. Main compositional and structural features. Lithology and Mineral Resources, 39(3), 252-270 (2004a).

STOLYAROV, A. S., IVLEVA, E. I., Upper Oligocene sediments in the Ciscaucasus, Volga–Don, and Mangyshlak regions (central part of the eastern Paratethys): Communication 2. Facies–paleogeographic sedimentation settings. Lithology and Mineral Resources, 39(4), 359-368 (2004b).

STOLYAROV, A. S., IVLEVA, E. I., Upper Oligocene sediments in the Ciscaucasus, Volga–Don, and Mangyshlak regions (central part of the eastern Paratethys): Communication. Metal potential and formation conditions of fish bone detritus and iron sulfide deposits. Lithology and Mineral Resources, 39(5), 504-522 (2004c).

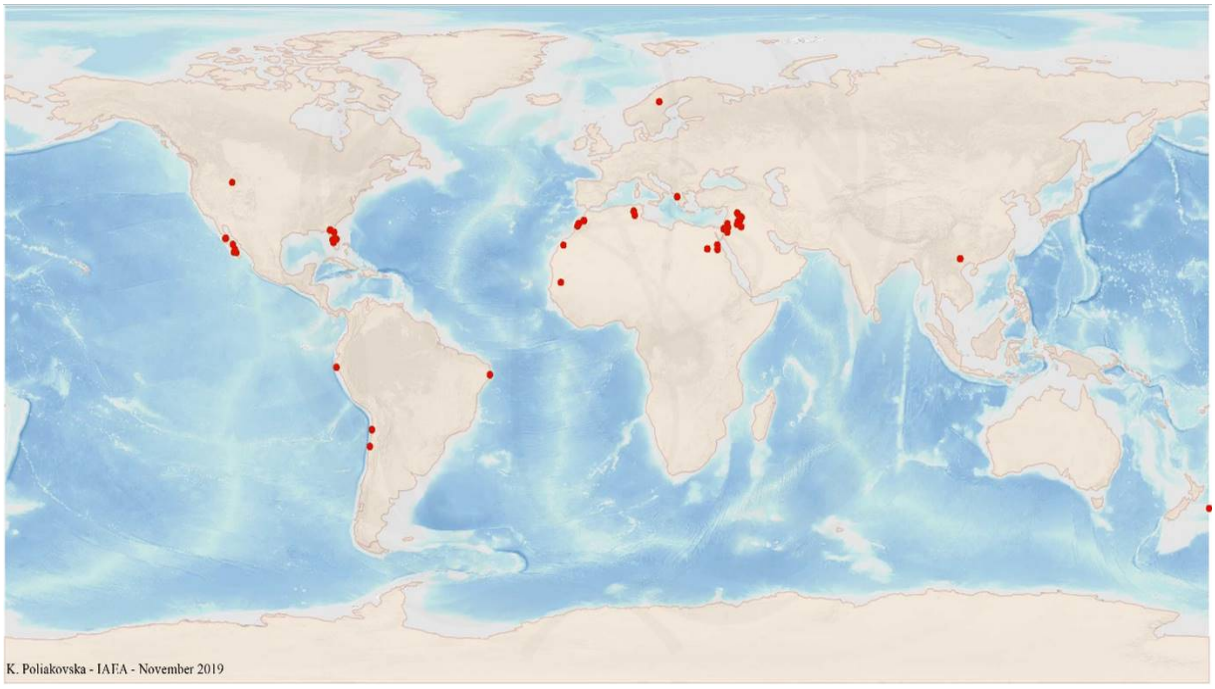

FIG. 14.2a. World distribution of selected Phosphate Minerochemical Phosphorite uranium deposits from the UDEPO database.

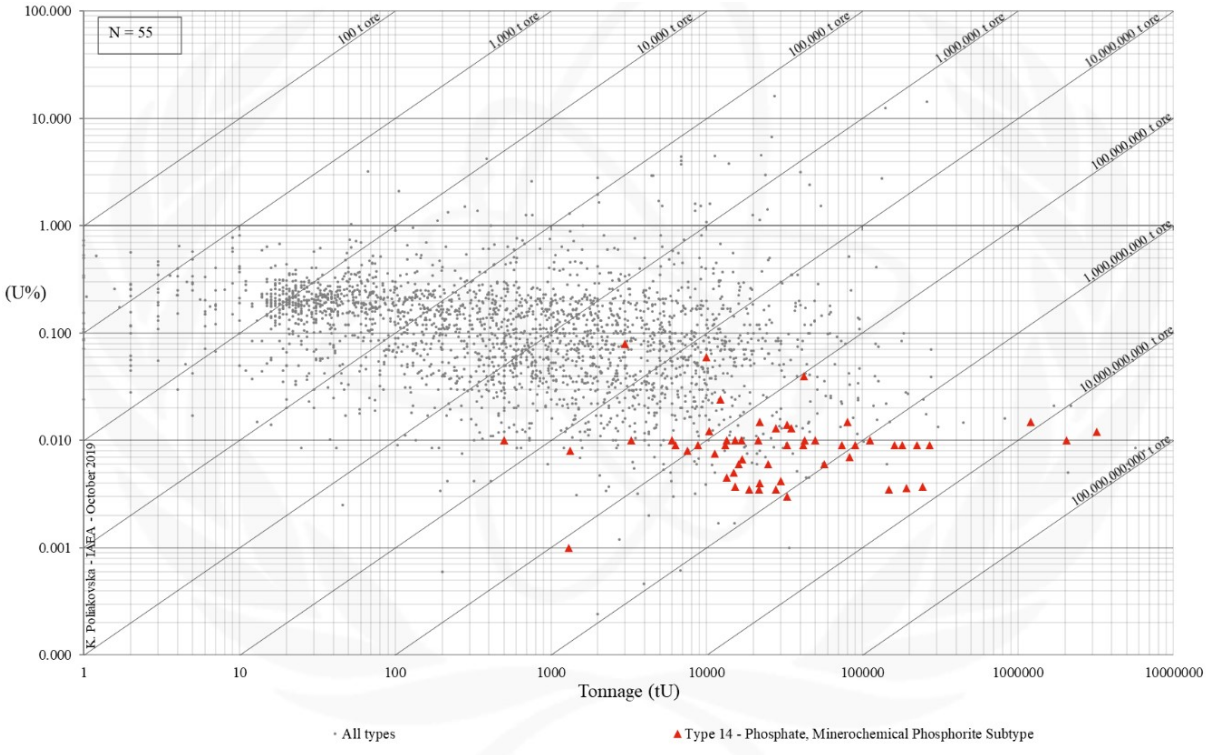

FIG. 14.2b. Grade and tonnage scatterplot highlighting Phosphate Minerochemical Phosphorite uranium deposits from the UDEPO database.

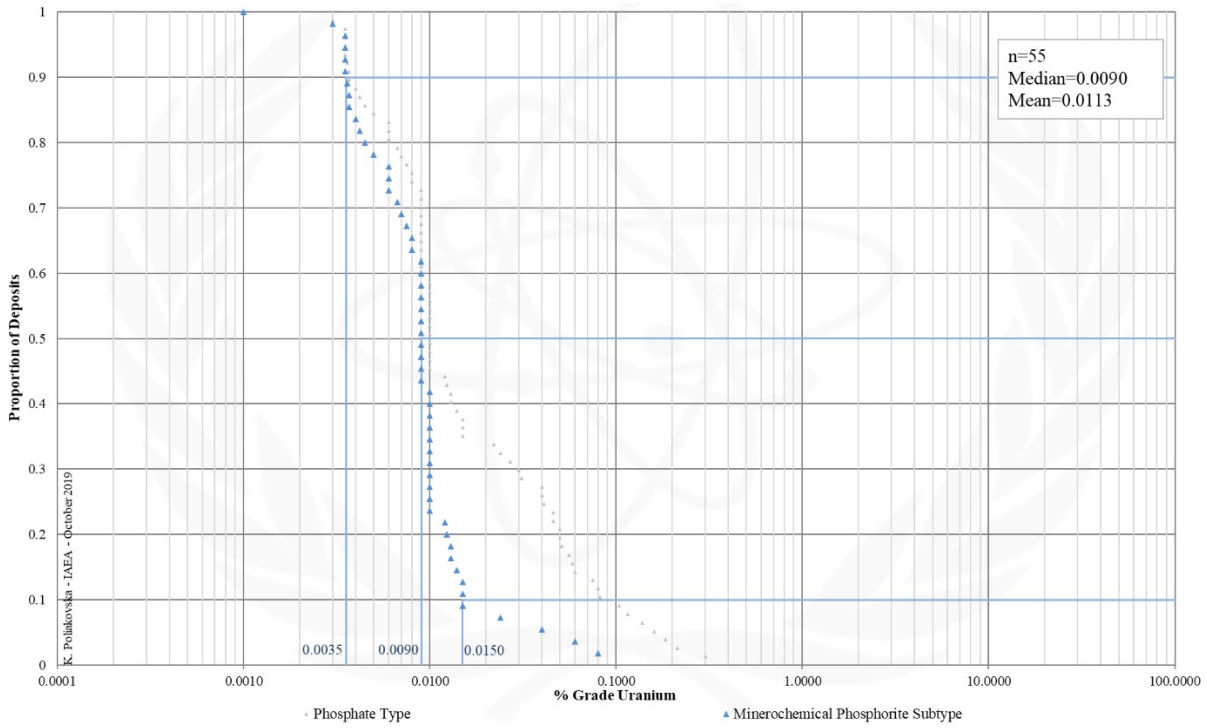

FIG. 14.2c. Grade Cumulative Probability Plot for Phosphate Minerochemical Phosphorite uranium deposits from the UDEPO database.

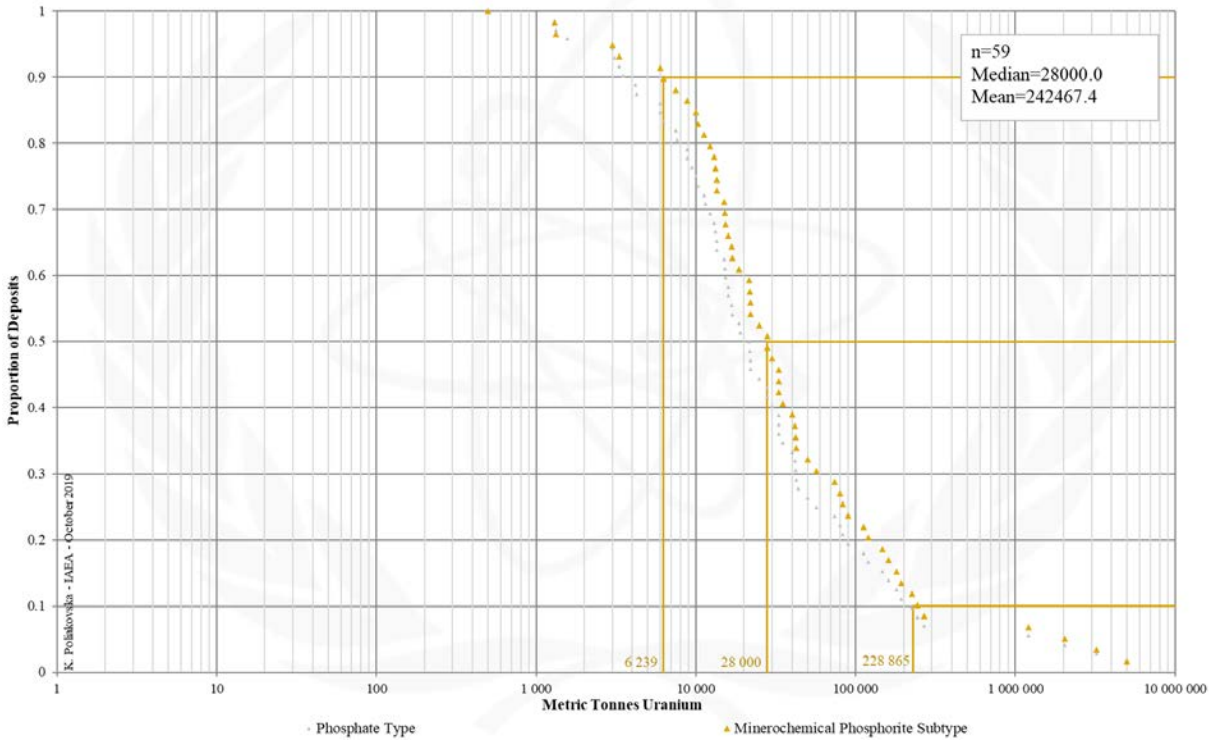

FIG. 14.2d. Tonnage Cumulative Probability Plot for Phosphate Minerochemical Phosphorite uranium deposits from the UDEPO database.

SUBTYPE 14.3. PHOSPHATE, CONTINENTAL PHOSPHATE

Brief Description
- Phosphate deposits, the main global source of phosphorus, can host significant uranium resources up to several million tonnes, albeit at very low concentrations.
- Phosphate deposits are classified as unconventional uranium resources with low grade uranium recoverable as a by-product of phosphate mining.
- Continental phosphate deposits are known exclusively from the Bakouma district (Central African Republic).
- The uranium ores in this district are hosted by phosphatic lacustrine siltstones of Eocene age that were deposited in a fossil karst dissolution channels and depressions preserved in Precambrian limestones and dolomites.

Type Examples
- Bakouma district, Central African Republic

Genetically Associated Deposit Types
- Subtype 14.1. Organic phosphorite
- Subtype 14.2. Minerochemical phosphorite

Principal Commodities
- P, U (by-product only)

Grades (%) and Tonnages (tU)
- Average: 0.2095, 7280.0
- Median: 0.1985, 4250.0

Number of Deposits
- Deposits: 5

Provinces (undifferentiated from Phosphate Type)
- Atlas, Baja California, Bakouma Basin, Bofal Gorgol, Chile, East Mediterranean, Egypt Cyrenacia Basin, Ergeninsky, Florida, Mantaro Machay, NW USA srite, Pricaspian, Sechura Basin, Sechura Basin.

Tectonic Setting
- Intracratonic sag basins

Typical Geological Age Range
- Tertiary

Mineral Systems Model

Source

Ground preparation
- Intracratonic basin formation
- Deposition of a carbonate platform
- Orogeny
- Karstification (preferentially along structural discontinuities)
- Formation of karst lakes and deposition of lacustrine phosphatic siltstones

Energy
- Topography (gravity)-driven fluid flow

Fluids
- Karstic groundwaters, acidic groundwaters, lake waters

Ligands
- Ca

Reductants
- Reduced lake waters, lignite

Uranium
- Poorly constrained (crystalline basement rocks, granitoids, limestone, black shales)

Transport

Fluid pathways
- Stratigraphic aquifers
- Karst caverns/channels
- Fault-fracture systems tapping into stratigraphic aquifers and/or karst channels

Trap

Physical
- Karst channels
- Breccia zones

Chemical
- Organic matter
- Reducing, strongly alkaline lake waters in karst channels
- Phosphatic sediments

Deposition
Change in redox conditions – Due to mixing of oxidised (acidic?) groundwaters with reduced lacustrine waters
Preservation
– Deep burial and/or downfaulting – Laterite caps may act as protective seals – Relative tectonic stability

Key Reference Bibliography

FUCHS, Y., Paleokarst-related uranium deposits. Developments in Earth Surface Processes, 1, 473-480 (1989).
INTERNATIONAL ATOMIC ENERGY AGENCY, Uranium Deposits in Africa: Geology and Exploration. Proceedings of a Regional Advisory Group Meeting, Lusaka, 14-18 November 1977, 262p (1979).
INTERNATIONAL ATOMIC ENERGY AGENCY, Geological Classification of Uranium Deposits and Description of Selected Examples. IAEA-TECDOC Series, 1842, 415p (2018).

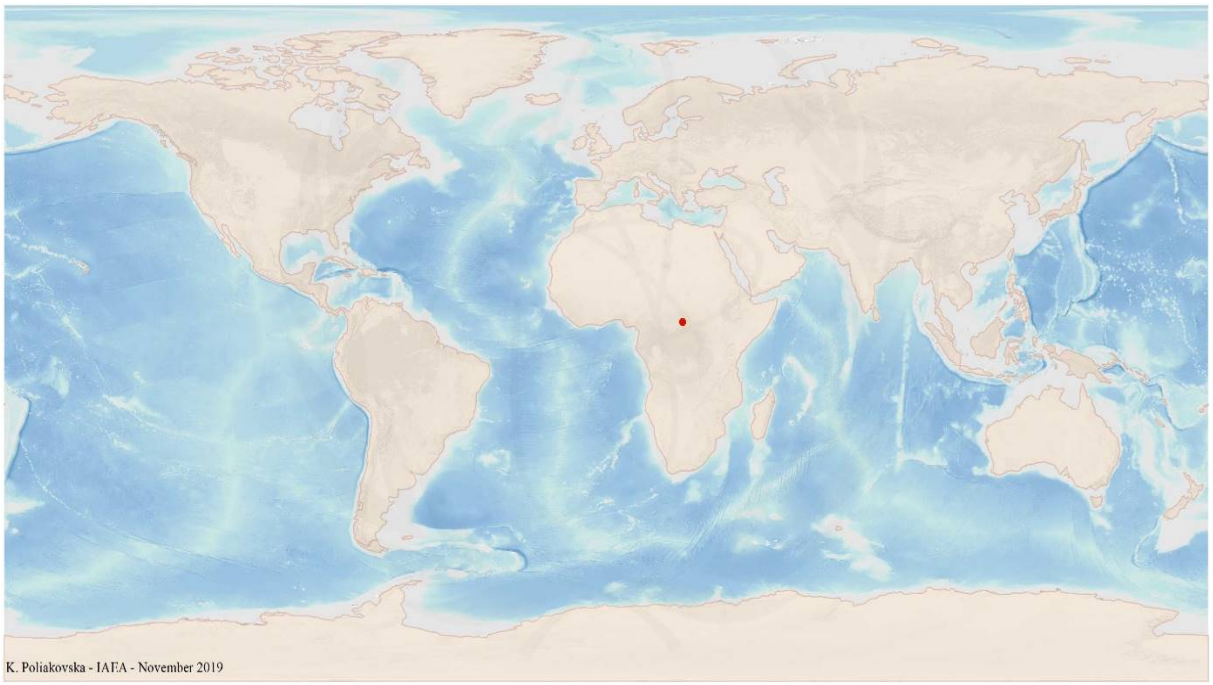

FIG. 14.3a. World distribution of selected Phosphate Continental Phosphorite uranium deposits from the UDEPO database.

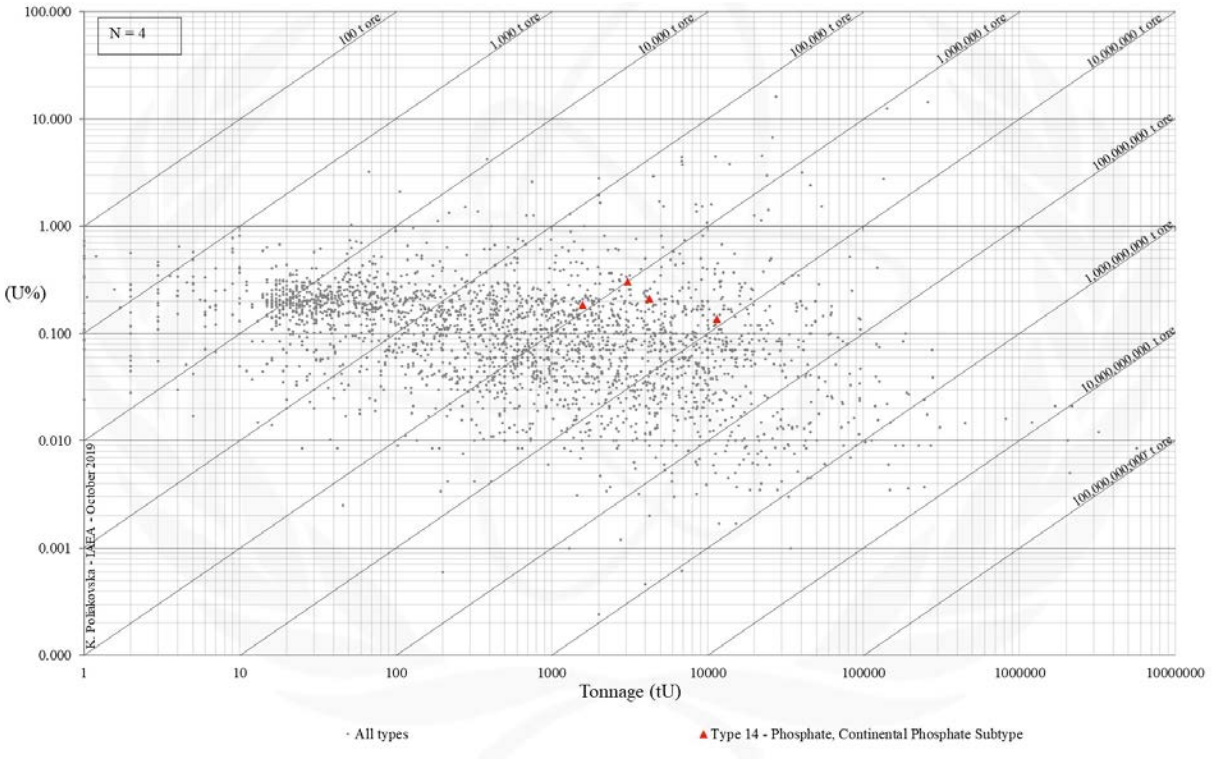

FIG. 14.3b. Grade and tonnage scatterplot highlighting Phosphate Continental Phosphorite uranium deposits from the UDEPO database.

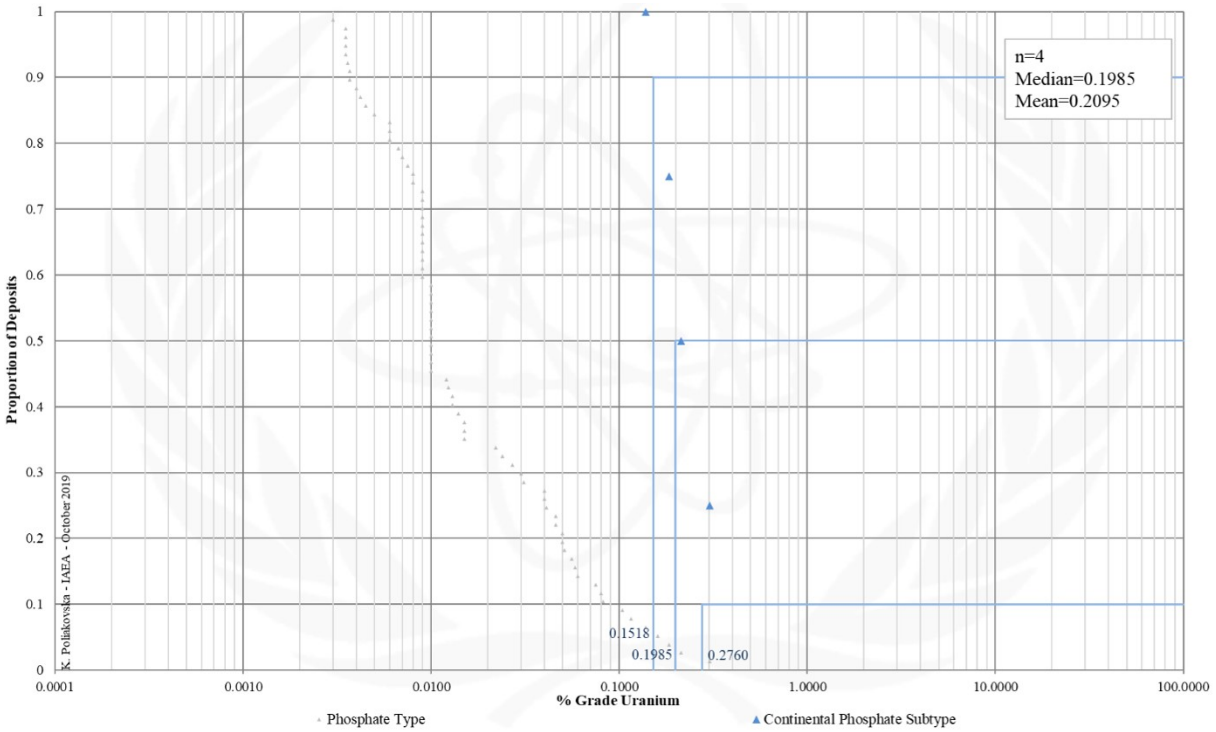

FIG. 14.3c. Grade Cumulative Probability Plot for Phosphate Continental Phosphorite uranium deposits from the UDEPO database.

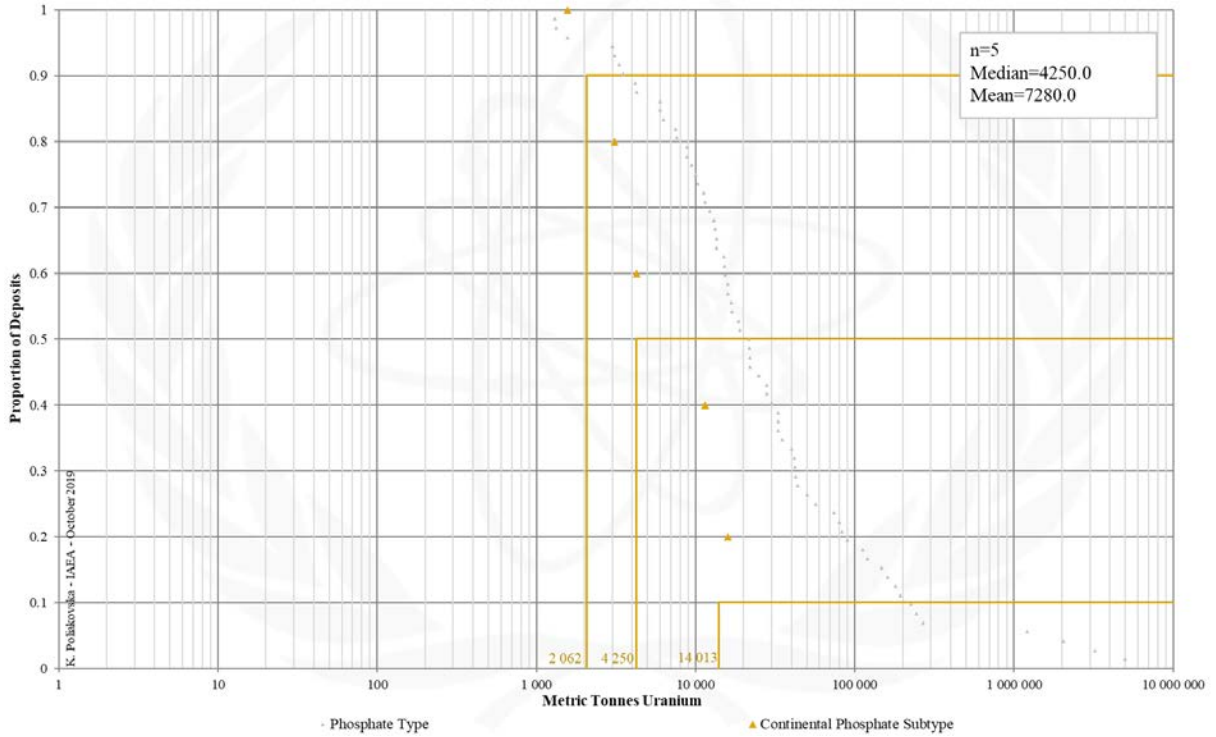

FIG. 14.3d. Tonnage Cumulative Probability Plot for Phosphate Continental Phosphorite uranium deposits from the UDEPO database.

Appendix XV

BLACK SHALE

SUBTYPE 15. BLACK SHALE

Brief Description
- Black shale deposits contain some of the world's largest uranium accumulations albeit at low or very low grades
- They are classified as unconventional uranium resources from which uranium may be produced as a by- or co-product.
- Two subtypes are recognised: (15.1.) Stratiform, and (15.2.) stockwork.
- Stratiform deposits comprise marine, organic–rich shale and coaliferous, pyritic shale, containing synsedimentary, uniformly disseminated uranium adsorbed onto organic material and clay minerals.
- Stockwork deposits take the form of structurally–controlled, stratabound uranium ores in microfracture stockworks developed within or adjacent to black shale horizons.

Subtypes
- 15.1. Stratiform
- 15.2. Stockwork

Type Examples
- Subtype 15.1. Ranstad, Sweden; Chattanooga Shale Formation, USA
- Subtype 15.2. Ronneburg district, Germany; Dzhantuar, Uzbekistan

Principal Commodities
- Subtype 15.1. U (by- or co-product), V ± Cr, Cu, Mn, Mo, P, REE
- Subtype 15.2. U ± Ba, Co, Cu, Mo, Ni, V

Grades (%) and Tonnages (tU)
- Average: 0.0508, 393974.9
- Median: 0.0315, 9692.5

Number of Deposits
- Deposits: 76

Provinces
- Billingen Falbygden, Chattanooga Shale, Estonia North, Kyzylkum, Ogcheon Belt, Ostersund, Saxo Thuringian.

Tectonic Setting
- Subtype 15.1. Epicontinental (rift) basins in tectonically stable cratonic environments
- Subtype 15.2. Collisional orogens

Typical Geological Age Range
- Palaeozoic

Mineral Systems Model

Source

Ground preparation
- Subtype 15.1. Formation of a shallow–marine, barred, epicontinental (rift) basin with low sedimentation rates, brackish to normal marine salinities and anaerobic, strongly reducing conditions
- Subtype 15.2. Deposition of uraniferous black shales, orogenesis

Energy
- Subtype 15.1. Seawater currents, wind stress
- Subtype 15.2. Postorogenic collapse, topography-driven fluid flow

Fluids
- Subtype 15.1. Seawaters
- Subtype 15.2. Meteoric and/or hydrothermal fluids

Ligands
- Subtypes 15.1. and 15.2. No information

Reductants
- Subtype 15.1. Bituminous/sulphidic/phosphatic black shales (incorporate marine plankton, land plant debris)
- Subtype 15.2. Bituminous/sulphidic/phosphatic black shales, dolerites, hydrocarbons, hydrogen

Uranium ± other metals
- Subtype 15.1. Chemical weathering of continental rock
- Subtype 15.2. Oxidised black shales

Transport

Fluid pathways
- Subtype 15.1. Ocean currents
- Subtype 15.2. Crustal-scale fault zones, regional folds, stratigraphic aquifers

Trap

Physical
- Subtype 15.1. Stratified water column with a stable, euxinic bottom layer, low sedimentation rates
- Subtype 15.2. Truncated folds, schistosity/cleavage or faults/fractures at high angles to the regional fabric, fault-fracture systems, zones of high fault/fracture density, fault intersections, breccia, lithological competency contrasts

Chemical
- Subtype 15.1. Anaerobic, strongly reduced seawaters
- Subtype 15.2. Bituminous/sulphidic/phosphatic black shales, dolerites, hydrocarbons, hydrogen

Deposition

Adsorption
- Subtype 15.1. Uranium adsorption onto organic matter, biogenic phosphate and clay minerals

Diagenesis
- Subtype 15.1. Uranium concentration during diagenesis

Change in redox conditions
- Subtype 15.2. Due to (i) interaction of oxidised, uranium-bearing fluids with reduced strata, (ii) to interaction of oxidised, uranium-bearing fluids with liquid and gaseous hydrocarbons or hydrogen that form reactive chemical haloes around permeable structures

Remobilisation and redeposition
- Subtype 15.1. Secondary remobilisation, recrystallisation and upgrading of uranium during metamorphism
- Subtype 15.2. Deep, supergene weathering of uraniferous black shales, leaching and vertical redistribution of uranium and associated metals

Preservation

- Establishment or maintenance of anoxic environments
- Deep burial and/or downfaulting
- Relative tectonic stability

Key Reference Bibliography

BOLONIN, A. V., GRADOVSKY, I. F., Supergene processes and uranium ore formation in the Ronneburg ore field, Germany. Geology of Ore Deposits, 54(2), 122–131 (2012).
DAHLKAMP, F. J., Uranium Deposits of the World: Asia. Springer, Berlin, Heidelberg, 492p (2009).
DAHLKAMP, F. J., Uranium Deposits of the World: USA and Latin America. Springer, Berlin, Heidelberg, 515p (2010).
DAHLKAMP, F. J., Uranium Deposits of the World: Europe. Springer, Berlin, Heidelberg, 792p (2016).
INTERNATIONAL ATOMIC ENERGY AGENCY, Geological Classification of Uranium Deposits and Description of Selected Examples. IAEA-TECDOC Series, 1842, 415p (2018).
LECOMTE, A., CATHELINEAU, M., MICHELS, R., PEIFFERT, C., BROUAND, M., Uranium mineralization in the Alum Shale Formation (Sweden): Evolution of a U-rich marine black shale from sedimentation to metamorphism. Ore Geology Reviews, 88, 71-98 (2017).

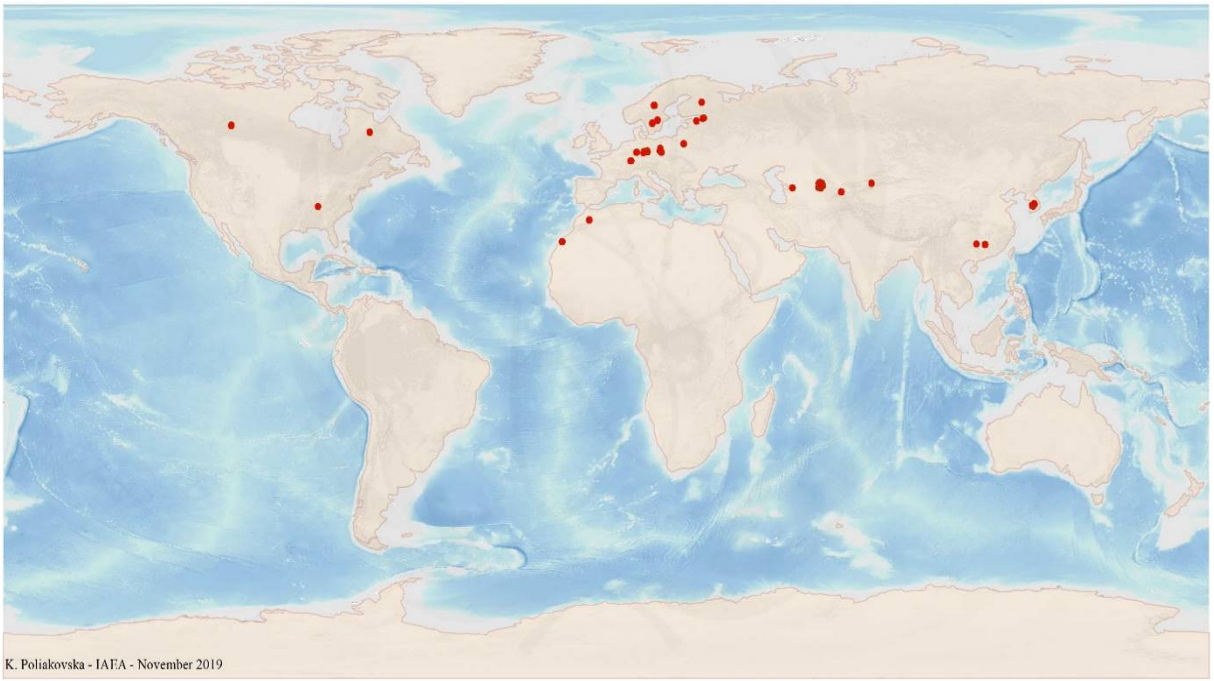

FIG. 15a. World distribution of selected Black Shale uranium deposits from the UDEPO database.

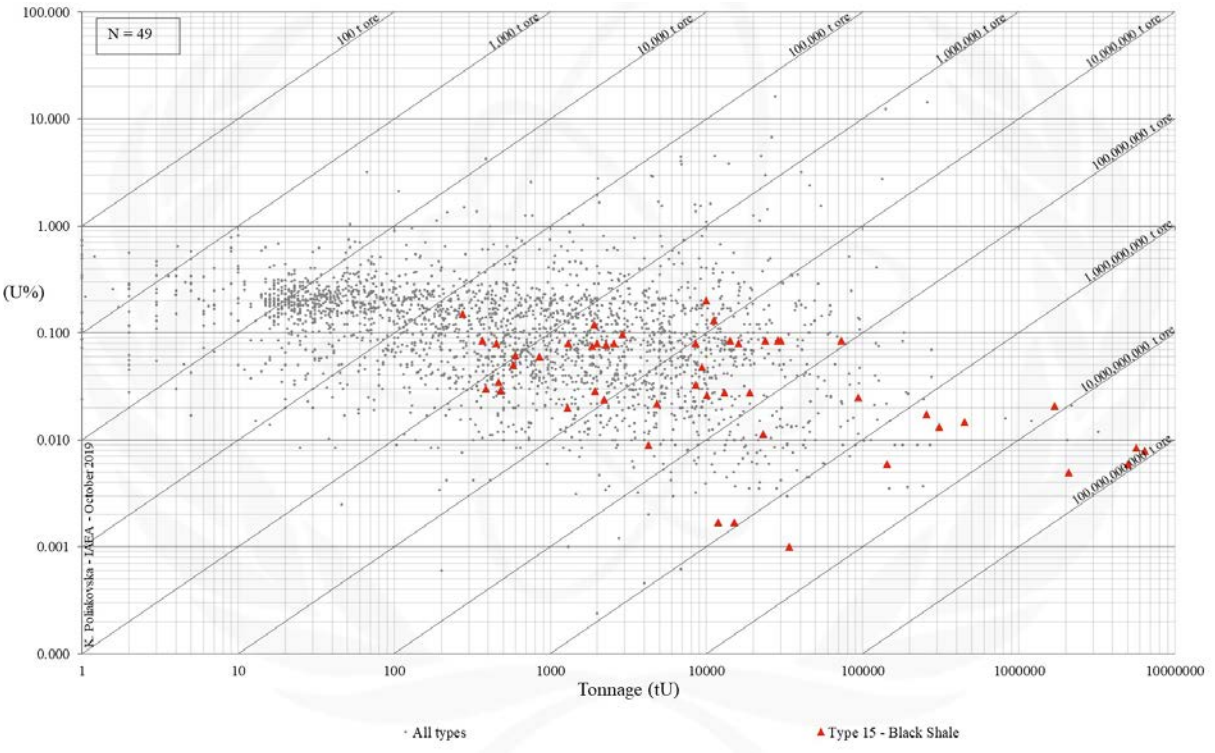

FIG. 15b. Grade and tonnage scatterplot highlighting Black Shale uranium deposits from the UDEPO database.

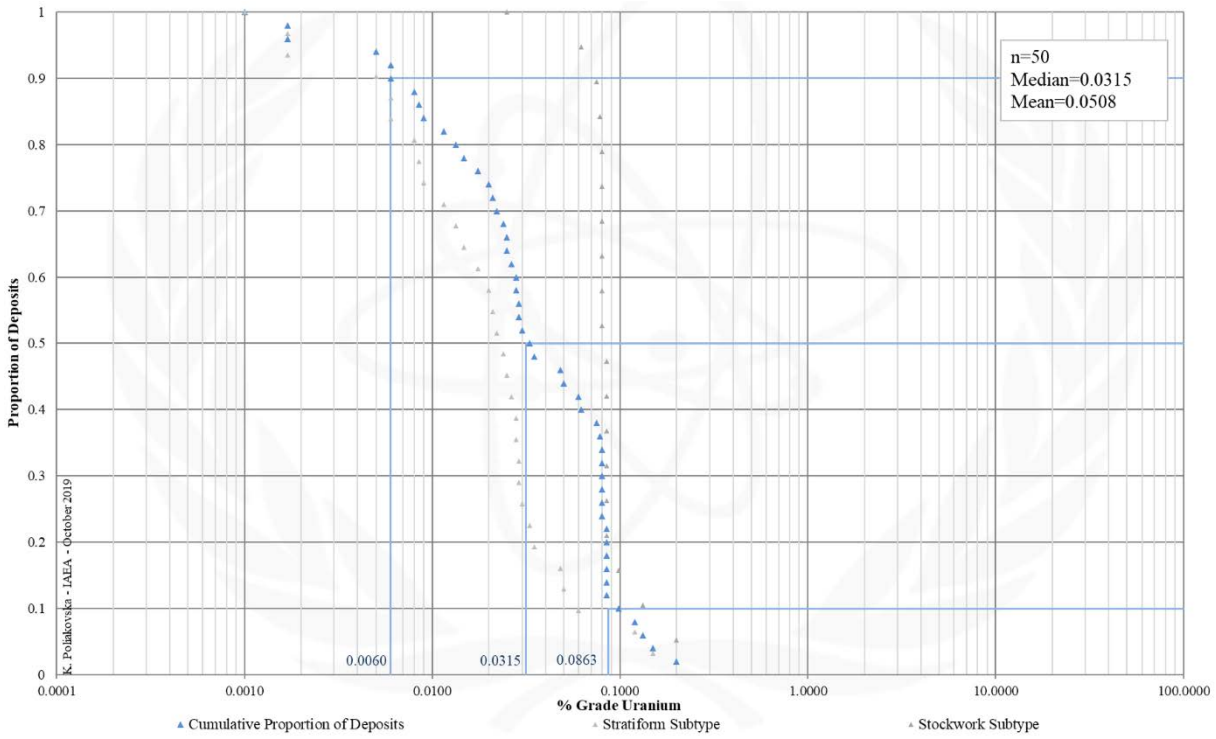

FIG. 15c. Grade Cumulative Probability Plot for Black Shale uranium deposits from the UDEPO database.

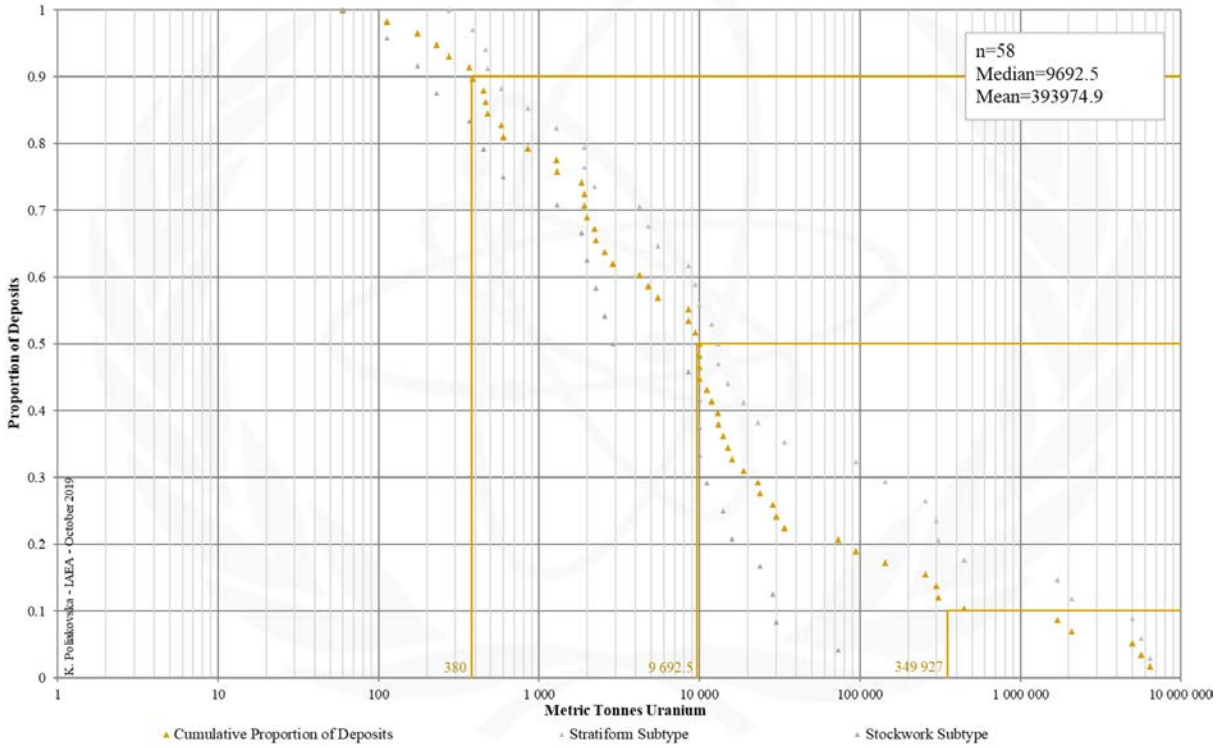

FIG. 15d. Tonnage Cumulative Probability Plot for Black Shale uranium deposits from the UDEPO database.

SUBTYPE 15.1. BLACK SHALE, STRATIFORM

Brief Description
- Black shale deposits contain some of the world's largest uranium accumulations albeit at low or very low grades
- They are classified as unconventional uranium resources from which uranium may be produced as a by- or co-product.
- Stratiform deposits comprise marine, organic–rich shale and coaliferous, pyritic shale, containing synsedimentary, uniformly disseminated uranium adsorbed onto organic material and clay minerals.

Type Examples
- Ranstad, MMS Vicken, Narke, Häggän, Sweden; Chattanooga Shale Formation, USA

Genetically Associated Deposit Types
- Subtype 15.2. Stockwork
- Sedimentary exhalative (SEDEX) deposits

Principal Commodities
- U (by- or co-product), V ± Cr, Cu, Mn, Mo, P, REE

Grades (%) and Tonnages (tU)
- Average: 0.0285, 664704.9
- Median: 0.0220, 12474.5

Number of Deposits
- Deposits 37

Provinces (undifferentiated from Black Shale Type)
- Billingen Falbygden, Chattanooga Shale, Estonia North, Kyzylkum, Ogcheon Belt, Ostersund, Saxo Thuringian.

Tectonic Setting
- Epicontinental (rift) basins in tectonically stable cratonic environments

Typical Geological Age Range
- Palaeozoic

Mineral Systems Model

Source

Ground preparation
- Formation of a shallow–marine, barred, epicontinental (rift) basin with low sedimentation rates, brackish to normal marine salinities and anaerobic, strongly reducing conditions

Energy
- Seawater currents
- Wind stress

Fluids
- Seawaters

Ligands
- No information

Reductants
- Bituminous/sulphidic/phosphatic black shales (incorporate marine plankton, land plant debris)

Uranium ± other metals
- Chemical weathering of continental rock

Transport

Fluid pathways
- Ocean currents

Trap

Physical
- Stratified water column with a stable, euxinic bottom layer
- Low sedimentation rates

Chemical
- Anaerobic, strongly reduced seawaters

Deposition

Adsorption
- Uranium adsorption onto organic matter, biogenic phosphate and/or clay minerals

Diagenesis
- Uranium concentration during diagenesis

Remobilisation and redeposition
- Deep, supergene weathering of uraniferous black shales
- Leaching and vertical redistribution of uranium and associated metals

Preservation
- Establishment or maintenance of anoxic environments
- Deep burial and/or downfaulting with relative tectonic stability

Key Reference Bibliography

DAHLKAMP, F. J., Uranium Deposits of the World: USA and Latin America. Springer, Berlin, Heidelberg, 515p (2010).
DAHLKAMP, F. J., Uranium Deposits of the World: Europe. Springer, Berlin, Heidelberg, 792p (2016).
INTERNATIONAL ATOMIC ENERGY AGENCY, Geological Classification of Uranium Deposits and Description of Selected Examples. IAEA-TECDOC Series, 1842, 415p (2018).
LECOMTE, A., CATHELINEAU, M., MICHELS, R., PEIFFERT, C., BROUAND, M., Uranium mineralization in the Alum Shale Formation (Sweden): Evolution of a U–rich marine black shale from sedimentation to metamorphism. Ore Geology Reviews, 88, 71-98 (2017).

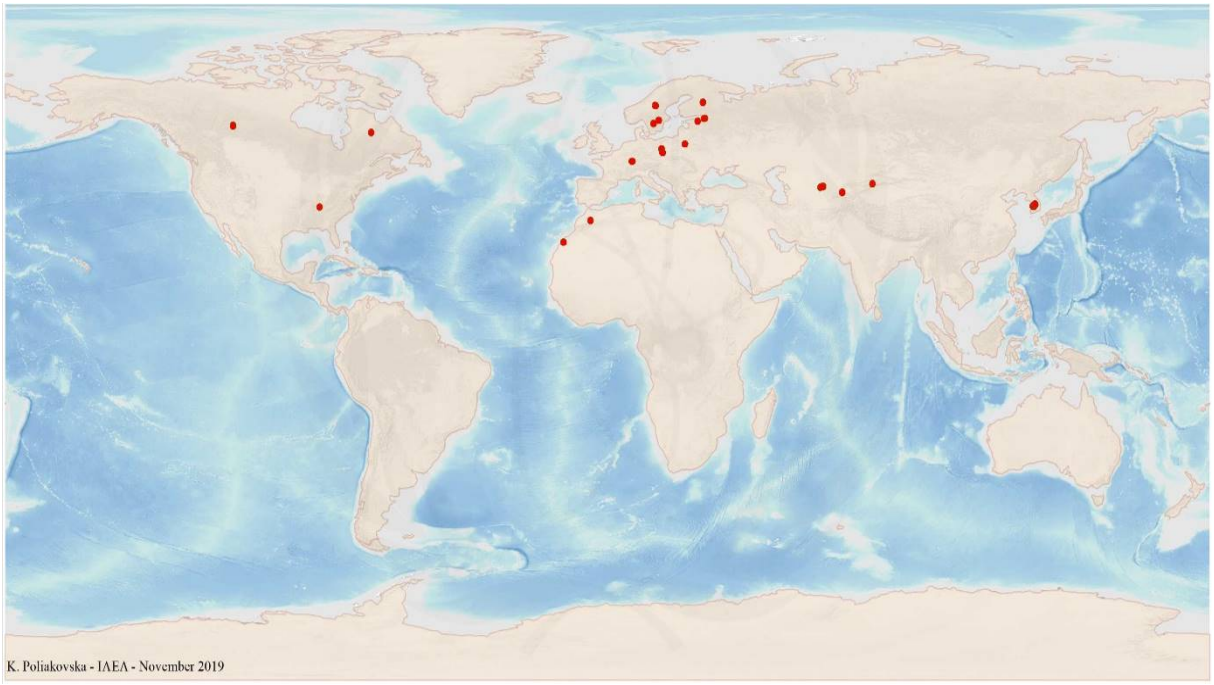

FIG. 15.1a. World distribution of selected Black Shale Stratiform uranium deposits from the UDEPO database.

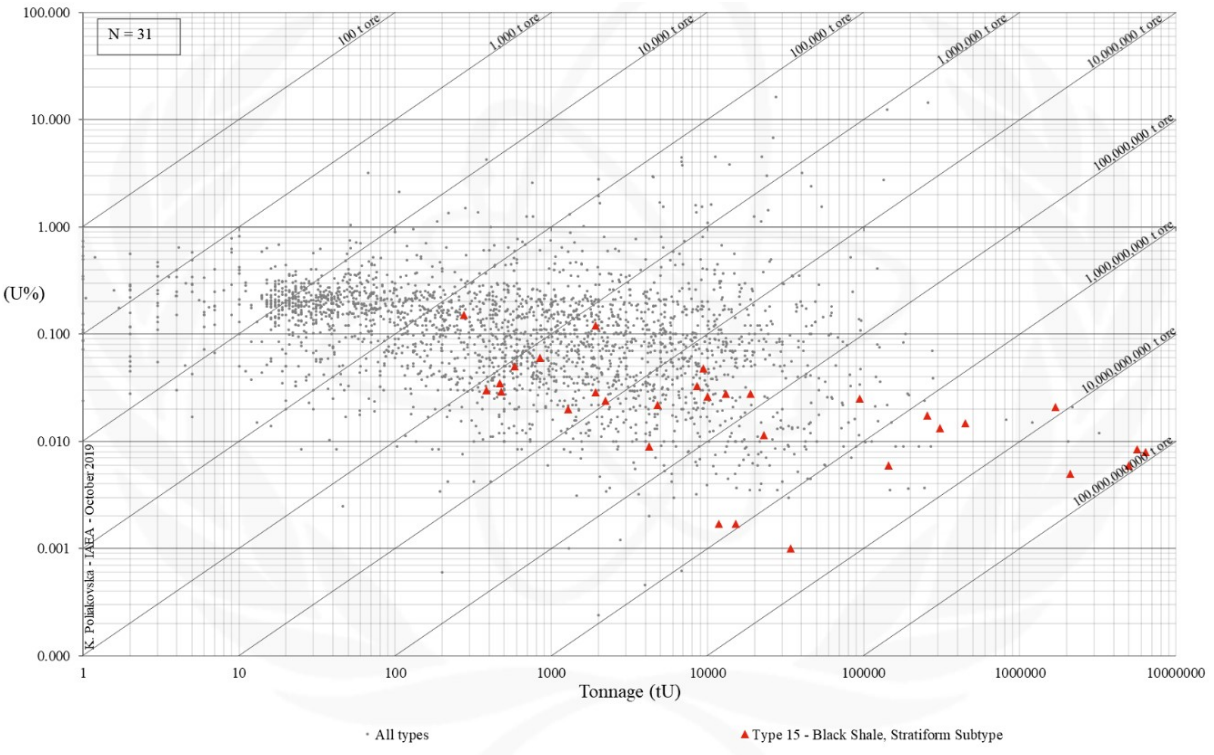

FIG. 15.1b. Grade and tonnage scatterplot highlighting Black Shale Stratiform uranium deposits from the UDEPO database.

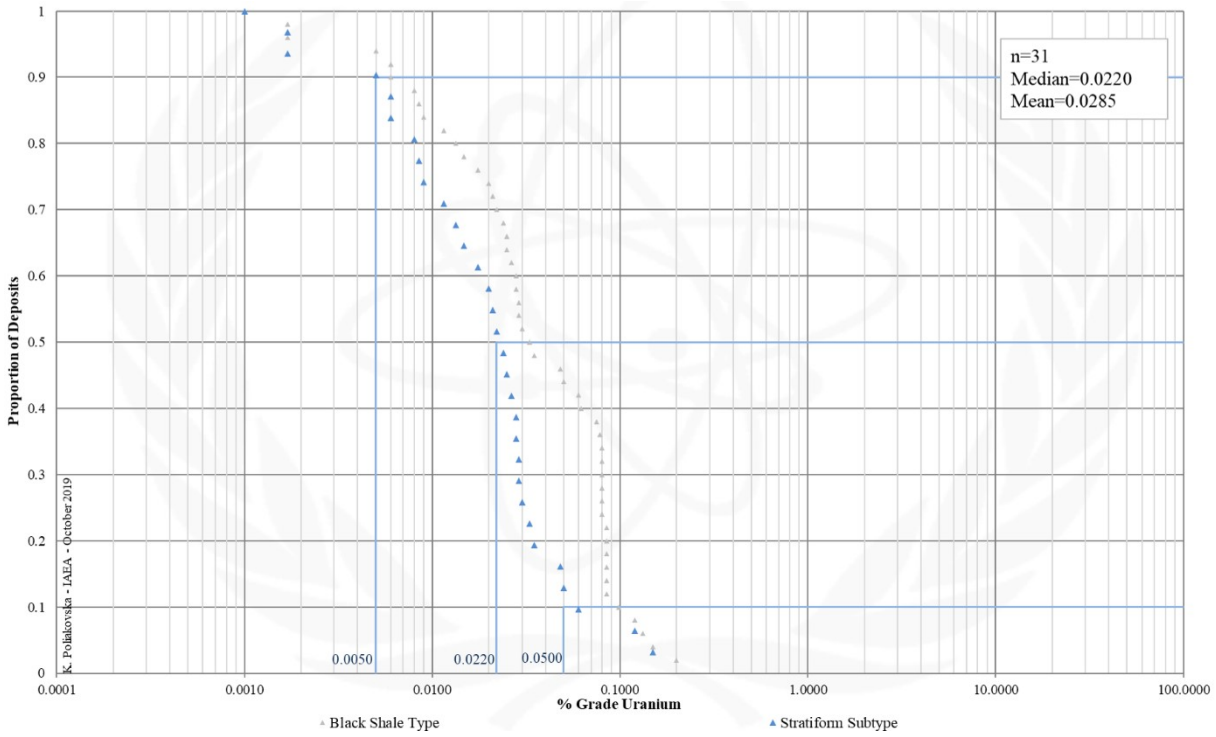

FIG. 15.1c. Grade Cumulative Probability Plot for Black Shale Stratiform uranium deposits from the UDEPO database.

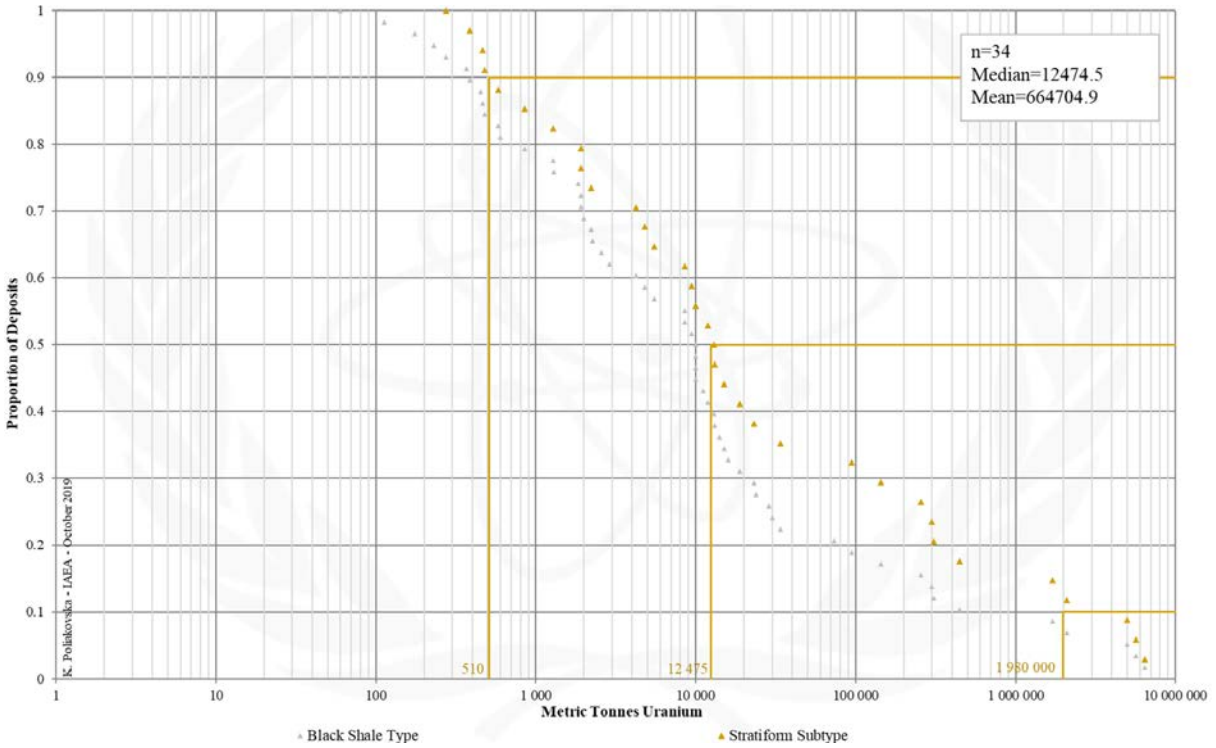

FIG. 15.1d. Tonnage Cumulative Probability Plot for Black Shale Stratiform uranium deposits from the UDEPO database.

SUBTYPE 15.2. BLACK SHALE, STOCKWORK

Brief Description
- Black shale deposits contain some of the world's largest uranium accumulations albeit at low or very low grades
- They are classified as unconventional uranium resources from which uranium may be produced as a by- or co-product.
- Stockwork deposits take the form of structurally-controlled, stratabound uranium ores in microfracture stockworks developed within or adjacent to black shale horizons.

Type Examples
- Gera-Ronneburg, Germany; Dzhantuar, Uzbekistan; Chanziping, China

Genetically Associated Deposit Types
- Subtype 15.1. Stratiform

Principal Commodities
- U ± Ba, Co, Cu, Mo, Ni, V

Grades (%) and Tonnages (tU)
- Average: 0.0874, 10440.7
- Median: 0.0800, 2730.0

Number of Deposits
- Deposits: 38

Provinces (undifferentiated from Black ShaleType)
- Billingen Falbygden, Chattanooga Shale, Estonia North, Kyzylkum, Ogcheon Belt, Ostersund, Saxo Thuringian.

Tectonic Setting
- Collisional orogens

Typical Geological Age Range
- Palaeozoic

Mineral Systems Model

Source

Ground preparation
- Deposition of uraniferous black shales
- Orogenesis

Energy
- Postorogenic collapse
- Topography-driven fluid flow

Fluids
- Meteoric fluid
- Hydrothermal fluids

Ligands
- No information

Reductants
- Bituminous/sulphidic/phosphatic black shales, dolerites, hydrocarbons, hydrogen

Uranium ± other metals
- Oxidised black shales

Transport

Fluid pathways
- Crustal–scale fault zones
- Regional folds
- Stratigraphic aquifers

Trap

Physical
- Truncated folds
- Schistosity/cleavage or faults/fractures at high angles to the regional fabric
- Fault–fracture systems
- Zones of high fault/fracture density
- Fault intersections
- Breccia
- Lithological competency contrasts

Chemical
- Bituminous/sulphidic/phosphatic black shales
- Dolerites
- Hydrocarbons
- Hydrogen

Deposition

Change in redox conditions
- Due to interaction of oxidised, uranium-bearing fluids with reduced strata
- Due to interaction of oxidised, uranium-bearing fluids with liquid and gaseous hydrocarbons or hydrogen that form reactive chemical haloes around permeable structures

Remobilisation and redeposition
- Deep, supergene weathering of uraniferous black shales
- Leaching and vertical redistribution of uranium and associated metals

Preservation

- Deep burial and/or downfaulting
- Relative tectonic stability

Key Reference Bibliography

BOLONIN, A. V., GRADOVSKY, I. F., Supergene processes and uranium ore formation in the Ronneburg ore field, Germany. Geology of Ore Deposits, 54(2), 122–131 (2012).
DAHLKAMP, F. J., Uranium Deposits of the World: Asia. Springer, Berlin, Heidelberg, 492p (2009).
DAHLKAMP, F. J., Uranium Deposits of the World: Europe. Springer, Berlin, Heidelberg, 792p (2016).
INTERNATIONAL ATOMIC ENERGY AGENCY, Geological Classification of Uranium Deposits and Description of Selected Examples. IAEA-TECDOC Series, 1842, 415p (2018).

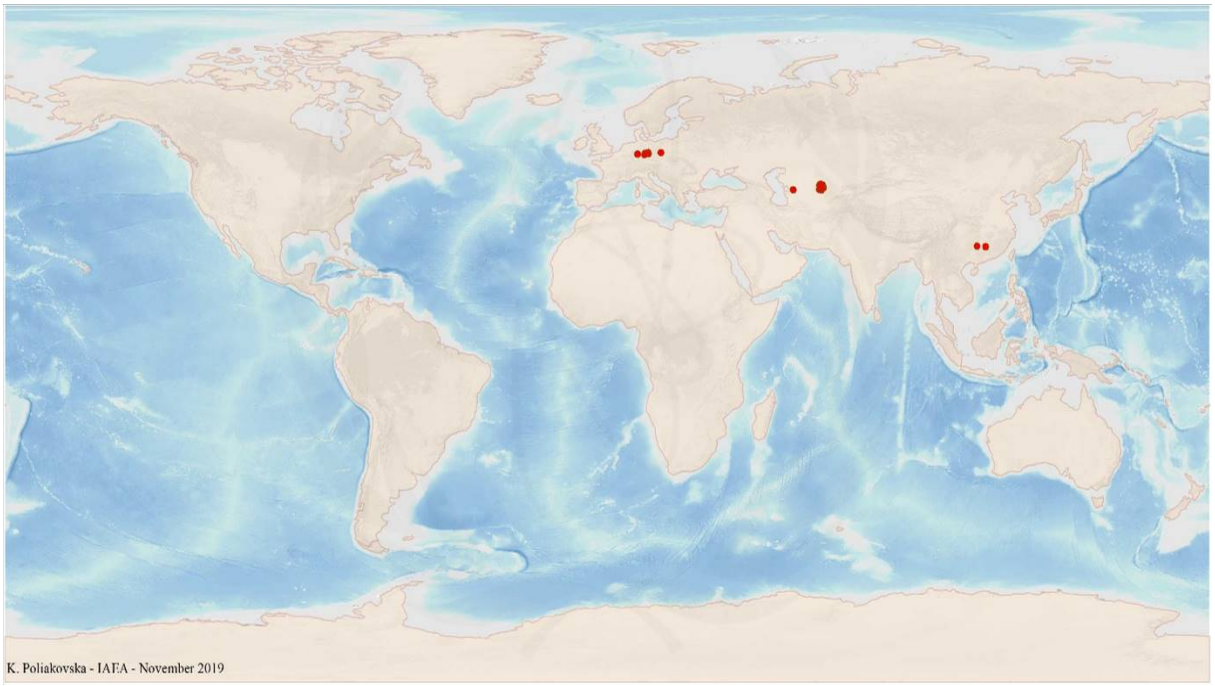

FIG. 15.2a. World distribution of selected Black Shale Stockwork uranium deposits from the UDEPO database.

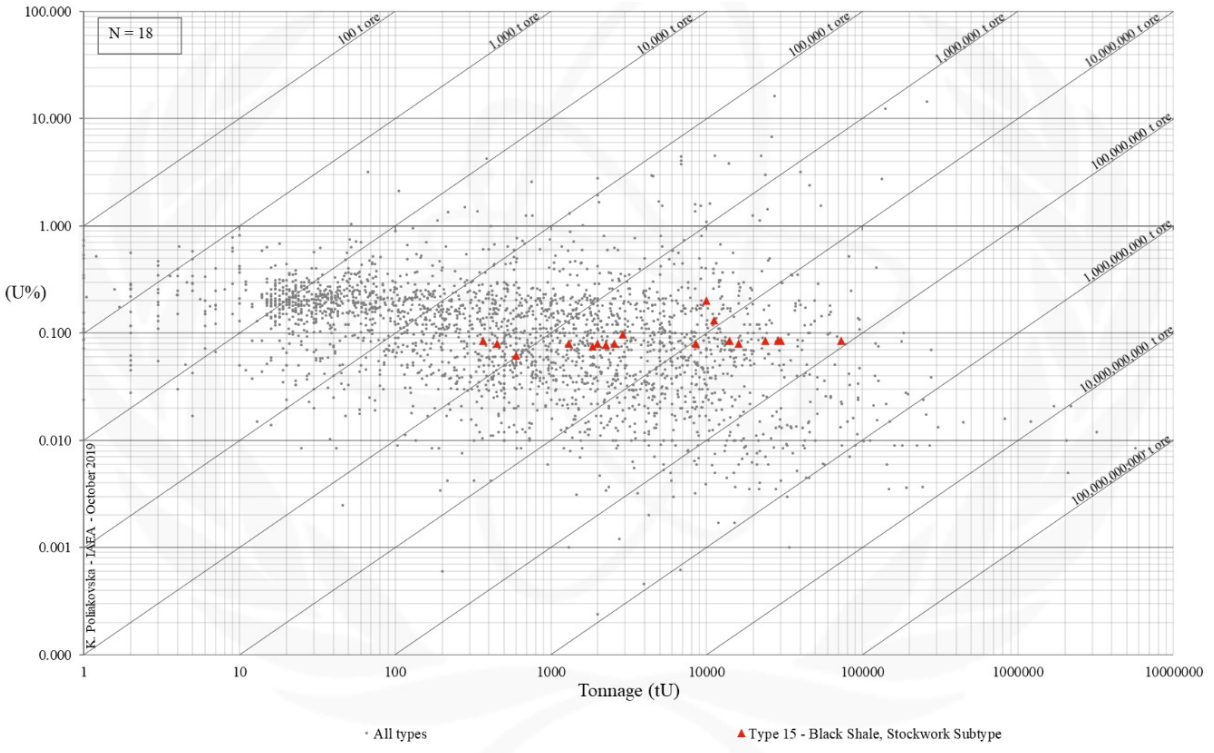

FIG. 15.2b. Grade and tonnage scatterplot highlighting Black Shale Stockwork uranium deposits from the UDEPO database.

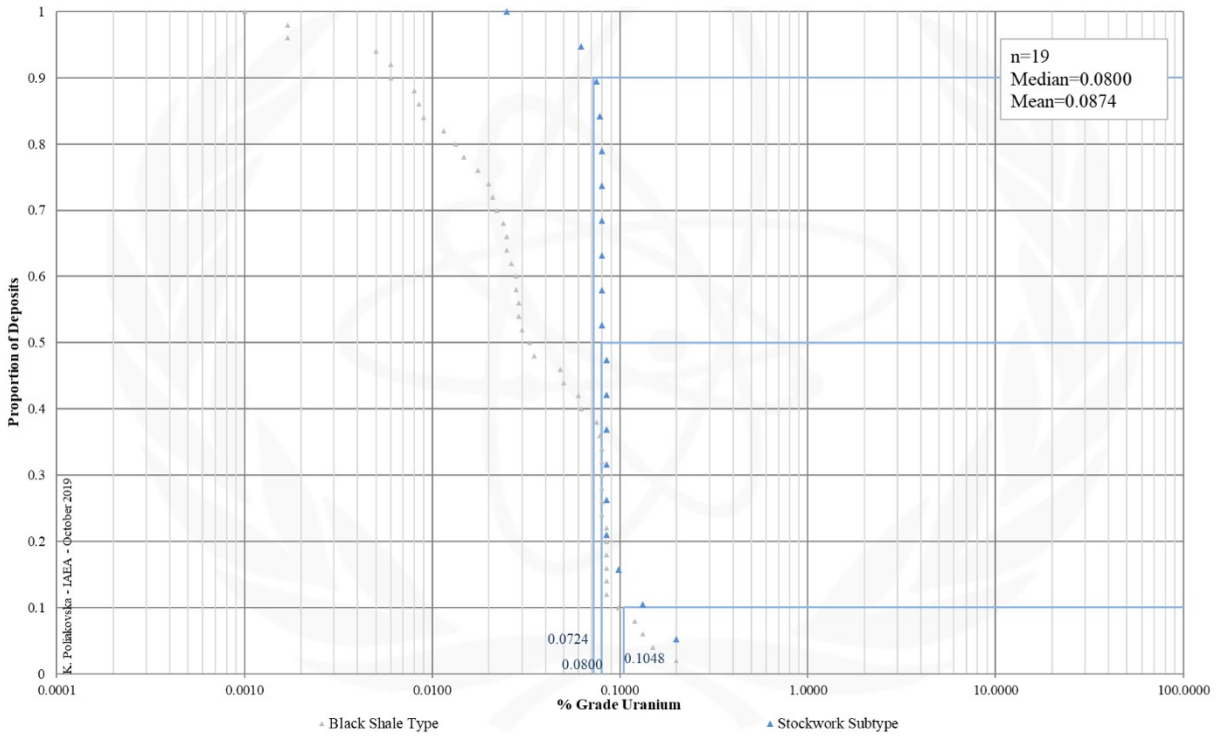

FIG. 15.2c. Grade Cumulative Probability Plot for Black Shale Stockwork uranium deposits from the UDEPO database.

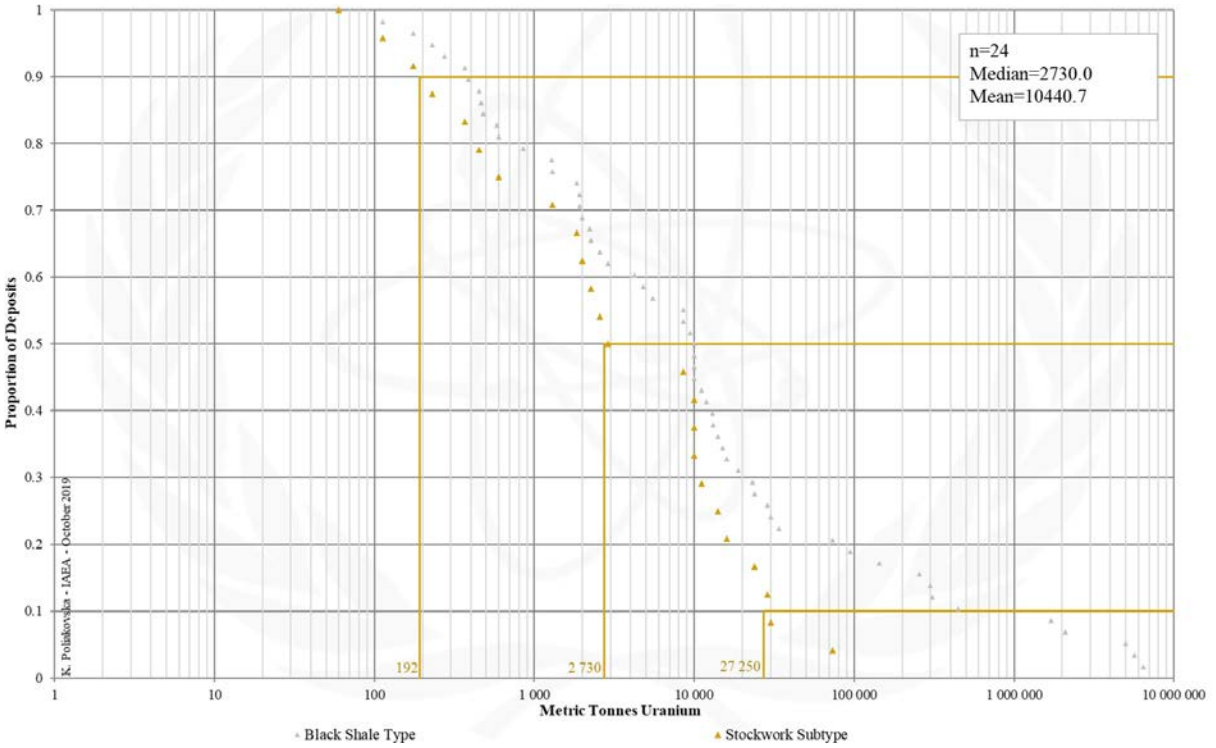

FIG. 15.2d. Tonnage Cumulative Probability Plot for Black Shale Stockwork uranium deposits from the UDEPO database.

REFERENCES

[1] INTERNATIONAL ATOMIC ENERGY AGENCY, World Distribution of Uranium Deposits (UDEPO). IAEA-TECDOC Series, 1843, 247p (2016).

[2] INTERNATIONAL ATOMIC ENERGY AGENCY, World Distribution of Uranium Deposits (UDEPO), 1: 35 000 000 scale map. IAEA-STI/PUB Series, 1800 (2018).

[3] INTERNATIONAL ATOMIC ENERGY AGENCY, World Distribution of Uranium Provinces, IAEA-STI/PUB Series (in prep).

[4] INTERNATIONAL ATOMIC ENERGY AGENCY, Uranium Resources as Co- and By-Products of Polymetallic, Base, Rare Earth and Precious Metal Ore Deposits. IAEA- TECDOC Series, 1849, 157p (2018).

[5] INTERNATIONAL ATOMIC ENERGY AGENCY, Geological Classification of Uranium Deposits and Description of Selected Examples. IAEA-TECDOC Series, 1842, 415p (2018).

[6] INTERNATIONAL ATOMIC ENERGY AGENCY, Unconformity-related Uranium Deposits. IAEA-TECDOC Series, 1857, 295p (2018).

[7] INTERNATIONAL ATOMIC ENERGY AGENCY, Quantitative and Spatial Evaluations of Undiscovered Uranium Resources. IAEA-TECDOC Series, 1861, 627p (2018).

[8] MCCUAIG, T. C., KREUZER, O. P., BROWN, W. M., Fooling Ourselves — Dealing with Model Uncertainty in a Mineral Systems Approach to Exploration. In: Mineral Exploration and Research: Digging Deeper. Proceedings, 9th Biennial SGA Meeting, Dublin, 1435-1438 (2007).

[9] KREUZER, O. P., ETHERIDGE, M. A., GUJ, P., MCMAHON, M. E., HOLDEN, D. J., Linking Mineral Deposit Models to Quantitative Risk Analysis and Decision-Making in Exploration. Economic Geology, 103(4), 829-850 (2008).

[10] KREUZER, O. P., MARKWITZ, V., PORWAL, A. K., MCCUAIG, T. C., A Continent–Wide Study of Australia's Uranium Potential, Part I: GIS–assisted Manual Prospectivity Analysis. Ore Geology Reviews, 38(4), 334-366 (2010).

[11] WYBORN, L. A. I., HEINRICH, C. A., JAQUES, A. L., Australian Proterozoic Mineral Systems: Essential Ingredients and Mappable Criteria. The AusIMM Annual Conference 1994, 109-115 (1994).

[12] KNOX-ROBINSON, C. M., WYBORN, L. A. I., Towards a Holistic Exploration Strategy: Using Geographic Information Systems as a Tool to Enhance Exploration. Australian Journal of Earth Sciences, 44(4), 453-463 (1997).

[13] HRONSKY, J. M., GROVES, D. I., Science of Targeting: Definition, Strategies, Targeting and Performance Measurement. Australian Journal of Earth Sciences, 55(1), 3-12 (2008).

[14] MCCUAIG, T. C., BERESFORD, S., HRONSKY, J., Translating the Mineral Systems Approach into an Effective Exploration Targeting System. Ore Geology Reviews, 38(3), 128-138 (2010).

[15] MCCUAIG, T. C., HRONSKY, J., The Mineral System Concept: The Key to Exploration Targeting. Society of Economic Geologists Special Publication, 18, 153-175 (2014).

[16] MAGOON, L. B., DOW, W. G., The Petroleum System. The Petroleum System — from Source to Trap. AAPG Memoir, 60, 3-24 (1994).

[17] HUSTON, D. L., MERNAGH, T. P., HAGEMANN, S. G., DOUBLIER, M. P., FIORENTINI, M., CHAMPION, D. C., JAQUES, A. L., CZARNOTA, K., CAYLEY, R., SKIRROW, R., BASTRAKOV, E., Tectono-Metallogenic Systems — The Place of Mineral Systems Within Tectonic Evolution, With an Emphasis on Australian Examples. Ore Geology Reviews, 76, 168-210 (2016).
[18] SINGER, D., MENZIE, W. D., Quantitative Mineral Resource Assessments: An Integrated Approach. Oxford University Press, 232p (2010).
[19] DAHLKAMP, F. J., Uranium Deposits of the World: Asia. Springer, Berlin, Heidelberg, 492p (2009).
[20] DAHLKAMP, F. J., Uranium Deposits of the World: USA and Latin America. Springer, Berlin, Heidelberg, 515p (2010).
[21] DAHLKAMP, F. J., Uranium Deposits of the World: Europe. Springer, Berlin, Heidelberg, 792p (2016).

Annex

SUPPLEMENTARY FILES

The supplementary files for this publication can be found on the publication's individual web page at www.iaea.org/publications.

Detailed Deposit Models Spreadsheet

CONTRIBUTORS TO DRAFTING AND REVIEW

Bruce, M.	Australia
Fairclough, M.	International Atomic Energy Agency
Jareith, S.	Australia
Kreuzer, O.	Australia
Mihalasky, M.	United States of America
Poliakovska, K.	International Atomic Energy Agency

Consultancy Meetings

Vienna, Austria 27-29th June 2016 and 23-27th September 2019.

IAEA
International Atomic Energy Agency

No. 26

ORDERING LOCALLY

IAEA priced publications may be purchased from the sources listed below or from major local booksellers.

Orders for unpriced publications should be made directly to the IAEA. The contact details are given at the end of this list.

NORTH AMERICA

Bernan / Rowman & Littlefield
15250 NBN Way, Blue Ridge Summit, PA 17214, USA
Telephone: +1 800 462 6420 • Fax: +1 800 338 4550
Email: orders@rowman.com • Web site: www.rowman.com/bernan

Renouf Publishing Co. Ltd
22-1010 Polytek Street, Ottawa, ON K1J 9J1, CANADA
Telephone: +1 613 745 2665 • Fax: +1 613 745 7660
Email: orders@renoufbooks.com • Web site: www.renoufbooks.com

REST OF WORLD

Please contact your preferred local supplier, or our lead distributor:

Eurospan Group
Gray's Inn House
127 Clerkenwell Road
London EC1R 5DB
United Kingdom

Trade orders and enquiries:
Telephone: +44 (0)176 760 4972 • Fax: +44 (0)176 760 1640
Email: eurospan@turpin-distribution.com

Individual orders:
www.eurospanbookstore.com/iaea

For further information:
Telephone: +44 (0)207 240 0856 • Fax: +44 (0)207 379 0609
Email: info@eurospangroup.com • Web site: www.eurospangroup.com

Orders for both priced and unpriced publications may be addressed directly to:

Marketing and Sales Unit
International Atomic Energy Agency
Vienna International Centre, PO Box 100, 1400 Vienna, Austria
Telephone: +43 1 2600 22529 or 22530 • Fax: +43 1 26007 22529
Email: sales.publications@iaea.org • Web site: www.iaea.org/publications

INTERNATIONAL ATOMIC ENERGY AGENCY
VIENNA
ISBN 978–92–0–109220–5

20-00131